

***In vivo* and *in vitro* studies on docosahexaenoic acid in  
traumatic brain injury**

**Ruth Angus**

**Centre for Neuroscience and Trauma**

**Blizard Institute**

**Barts and The London School of Medicine & Dentistry**

**Queen Mary University of London**

**Thesis submitted to the Queen Mary University of London in  
candidature for the degree of Doctor of Philosophy**

### **Statement of Originality**

I, Ruth Angus, confirm that the research included within this thesis is my own work or that where it has been carried out in collaboration with, or supported by others, that this is duly acknowledged below and my contribution indicated.

I attest that I have exercised reasonable care to ensure that the work is original, and does not to the best of my knowledge break any UK law, infringe any third party's copyright or other Intellectual Property Right, or contain any confidential material.

I confirm that this thesis has not been previously submitted for the award of a degree by this or any other university.

### **Author's Declaration**

The thesis is submitted for the degree of Doctor of Philosophy at Barts and the London School of Medicine and Dentistry, Queen Mary University of London. The research described within this thesis was performed in the Centre for Neuroscience and Trauma within the Blizard Institute. The research was carried out under the supervision of Prof. Adina Michael-Titus, Prof. Gavin Giovannoni and Dr Ping Yip and it is my own work unless stated otherwise.

## Abstract

### Introduction

Traumatic brain injury (TBI) is a devastating disease causing disability and death, and currently there are no effective treatments available. Therefore, there is an utmost need to improve our understanding of the pathophysiology of TBI and to identify potential therapies that can provide neuroprotection after injury. The aims of this thesis were to develop an *in vivo* and *in vitro* model of TBI, in which to assess the potential neuroprotective effects of an omega-3 polyunsaturated fatty acid (PUFAs), docosahexaenoic acid (DHA).

### Method

The controlled cortical impact (CCI) *in vivo* model of TBI was optimized and performed in mice. Both a behavioural (Morris water maze (MWM) for cognitive deficits) and histological endpoints (astrogliosis, lesion size and activated microglia) were used to assess severity and neuroprotective effects of DHA. An *in vitro* model of mechanical TBI was also set up and optimized. This model employed 3D astrocyte cultures obtained from GFP positive rat pups. The CCI impactor from the *in vivo* studies was used to damage the cultures, and at 24 hours, 5 days and 10 days the astrogliosis and cell number was measured.

### Results

The optimization of the *in vivo* studies demonstrated that at impactation depth of 2.2 mm produced an injury that was significantly different to the sham injury, in MWM performance and increased astrogliosis. Interestingly, there was an increase in the amount of astrogliosis on the contralateral side of the brain. A second study performed using the 2.2 mm injury parameters was performed, where an injection of DHA was administered via the tail vein 30 min after injury. The DHA-treated group did not demonstrate any neuroprotection compared to the injury-only group. However, there was an increase in the amount of astrogliosis in the contralateral hippocampus of the DHA-treat group.

In the *fat-1* studies it was shown that older male mice performed worse in the MWM, that the *fat-1* gene did not confer neuroprotection but did lead to increased astrogliosis.

The *in vitro* study revealed that astrocytes in the lesioned gels demonstrated an increase in astrogliosis, there was also an increase in the number of cell in the cultures following the lesion.

### Conclusion

In conclusion, the *in vivo* model of CCI replicated components of the human TBI including a behavioural deficit and pathophysiological changes. Omega-3 PUFAs failed to demonstrate functional neuroprotection in this model, but histologically, promoted an increase in reactive astrogliosis. The development of a novel *in vitro* model of focal injury in a 3D culture system, that elicits reactive astrogliosis, could be used to support further studies of the astrocytic responses to mechanical injury.



## Acknowledgements

I would like to take this opportunity to thank the MRC for funding this work. I would also like to thank my supervisors Prof. Adina Michael-Titus, Prof. Gavin Giovannoni and Dr Ping Yip, particularly Prof. Adina Michael-Titus for her patience and understanding and Dr. Ping Yip for his unwavering support, motivation and for being my loyal surgical assistant.

I would also like to thank colleagues for their support and help during my studies, particularly Sharon, Surinder and Sam. I would like to thank Merion Davies for his help with the tail vein injections of my mice; Dr. James Phillips and his lab group, particularly Caitriona O'Rourke for her help with my 3D cell cultures; Dr. Simon Dyall, for his help with the lipid analysis; all of the BSU staff, particularly Tony for helping me to maintain the *fat-1* colony and for allowing me to have my own behaviour room, and finally my BSc students, Yasser and Tamsin, for contributing to the immunostaining data in this thesis. There are other people I would like to thank for their support and friendship during my PhD studies; Rob Abrehart, Koye Akoni, Matt Brooke, my ladies, Zoe Drymoussi, Louise Adams and my best friend, Yee-man Ching, without whom I really could not have done it, and not forgetting Sam, Gordon, Elis and John.

Finally, I would like to thank my family who have provided amazing support and love, particularly my parents William and Elizabeth Angus, who have shown unbelievable patience, enormous understanding and incredible belief in me, throughout my PhD studies.

## **Poster publications**

1. **Conference:** Annual Meeting of Society for Neuroscience (SFN), San Diego, U.S.A., 2013.

**Title:** A model of traumatic brain injury in the mouse - investigation of an omega-3 fatty acid for acute neuroprotection

**Authors:** R. B. Angus, P. Yip, Y. Al-Omran, G. Giovannoni, A. Michael-Titus.

2. **Conference:** Annual Meeting of the Tissue Cell and Engineering Society (TCES), Southampton, U.K, 2015.

**Title:** Focal mechanical injury induces astrogliosis in a 3D tissue engineered culture model

**Authors:** R. B. Angus, C. O'Rourke, A. Michael-Titus, J.B. Phillips.

## Table of Contents

Abstract .....	3
Acknowledgements.....	5
Poster publications .....	6
Abbreviations .....	15
List of Tables.....	19
List of Figures .....	20
1 General introduction .....	24
1.1 Traumatic Brain Injury .....	24
1.1.1 Epidemiology – Public health.....	24
1.1.2 Management of human TBI .....	25
1.1.3 Early phase management .....	25
1.1.4 Late phase management .....	27
1.1.5 Long-term outcomes of TBI .....	28
1.2 Pathophysiology of TBI .....	29
1.2.1 Biochemical alterations.....	31
1.2.1.1 Glutamate excitotoxicity and intracellular calcium overload .....	31
1.2.1.2 Oxidative stress and free radical production .....	31
1.2.1.3 Lipid peroxidation .....	32
1.2.1.4 Mitochondrial dysfunction.....	32
1.2.1.5 Oedema and changes in intracranial pressure.....	33
1.2.2 Cellular alterations.....	34
1.2.2.1 Blood brain barrier disruption.....	34
1.2.2.2 Necrosis and apoptosis.....	35
1.2.2.3 Neuronal and axonal damage .....	36
1.2.2.4 Cytoskeletal disruption.....	37
1.2.2.5 Glial cell activation .....	38
1.2.2.6 Oligodendrocyte pathology .....	38
1.2.2.7 Microglial activation.....	39
1.2.2.8 Astrogliosis .....	41
1.2.2.9 Inflammatory mediators.....	41
1.3 Potential therapies for TBI .....	42
1.3.1 Surgery .....	42
1.3.2 Neuroprotective strategies.....	42

1.3.2.1	Osmotherapy.....	43
1.3.2.2	Free-radical scavengers.....	44
1.3.2.3	Glutamate receptor antagonists.....	44
1.3.2.4	Calcium channel blockers .....	45
1.3.3	Multifactorial neuroprotective strategies.....	46
1.3.3.1	Hypothermia.....	46
1.3.3.2	Erythropoietin (EPO) .....	46
1.3.3.3	Progesterone .....	47
1.3.3.4	Polyunsaturated Fatty Acids (PUFAs).....	50
1.4	Polyunsaturated fatty acids - General Introduction .....	51
1.4.1	Synthesis, metabolism and transport of fatty acids.....	52
1.5	PUFA in the CNS.....	58
1.5.1	PUFAs and CNS disease .....	58
1.5.1.1	Alzheimer's disease (AD) .....	59
1.5.1.2	Parkinson's disease (PD) .....	59
1.5.1.3	Peripheral nerve injury .....	60
1.5.1.4	Spinal cord injury .....	60
1.5.1.5	Traumatic brain injury.....	61
1.5.2	Brain phospholipids and PUFAs after TBI .....	62
1.5.3	Docosahexaenoic acid.....	62
1.5.4	The roles of DHA in cognition .....	63
1.5.5	DHA and secondary injury mechanisms.....	65
1.6	Failures of TBI therapies .....	66
1.7	In vitro models of TBI .....	68
1.8	Animal modelling of TBI.....	71
1.8.1	Species used in the animal modelling of TBI .....	73
1.8.2	Rodent models of TBI.....	75
1.8.2.1	Fluid percussion model.....	75
1.8.2.2	Marmarou model – impact/acceleration weight drop model .....	76
1.8.2.3	Controlled cortical impact model (CCI) .....	77
1.8.3	Behavioural outcome measures.....	79
1.8.3.1	Open field.....	79
1.8.3.2	The Y-maze.....	83
1.8.3.3	Morris Water Maze .....	84
1.9	Aims.....	86

2	Methods and Materials.....	87
2.1	In vivo studies.....	87
2.1.1	Animals.....	87
2.1.2	Surgery.....	87
2.1.3	DHA preparation and administration.....	89
2.1.4	Behavioural studies.....	91
2.1.4.1	Open field test.....	91
2.1.4.2	Y maze test.....	92
2.1.4.3	Morris water maze test.....	93
2.1.5	Tissue processing.....	95
2.1.5.1	Tissue collection.....	95
2.1.5.2	Tissue sectioning.....	95
2.1.5.3	Toluidine blue staining.....	95
2.1.5.4	Imaging of toluidine blue.....	96
2.1.6	Immunohistochemistry.....	96
2.1.6.1	Microscopy.....	98
2.1.7	Image analysis.....	99
2.1.7.1	Image analysis of GFAP and Iba1.....	99
2.1.7.2	Image analysis of doublecortin staining.....	100
2.1.8	Brain lipid analysis.....	101
2.2	In vitro studies.....	102
2.2.1	Primary cortical astrocyte cultures.....	102
2.2.2	Mechanical lesion of astrocyte cultures.....	103
2.2.3	DHA administration to 3D cultures.....	104
2.2.4	Immunocytochemistry.....	105
2.2.5	Imaging and analysis of 3D cultures.....	105
2.3	Statistical analysis.....	105
3	Characterisation and optimisation of a mouse model of TBI.....	106
3.1	Introduction.....	106
3.1.1	Controlled cortical impact injury model.....	106
3.1.2	Behavioural outcome measures.....	107
3.1.3	Histological endpoints.....	107
3.2	Methods.....	108
3.3	Aims and hypotheses.....	109

3.3.1	Aims.....	109
3.3.2	Hypothesis .....	109
3.4	Results .....	110
3.4.1	The effect of injury severity in the open field test .....	110
3.4.2	The effect of injury severity in the Y-maze test .....	116
3.4.3	The effect of injury severity in the Morris water maze.....	119
3.4.3.1	The effect of injury severity in the Morris water maze test acquisition trial .....	119
3.4.3.2	The effect of injury severity in the Morris water maze - probe trial .....	121
3.4.3.3	The effect of injury severity in the Morris water maze - reverse acquisition trial .....	123
3.4.3.4	The effect of injury severity in the Morris water maze - reverse probe trial .....	125
3.4.3.4.1	Reverse platform.....	125
3.4.3.4.2	Original platform.....	125
3.4.3.4.3	Reverse Probe Trial –Reverse and Original Platform.....	125
3.4.4	Increase in injury severity.....	129
3.4.5	The effect of a 2.2 mm injury severity in the open field test .....	129
3.4.6	The effect of a 2.2 mm injury in the Morris water maze .....	133
3.4.6.1	The effect of a 2.2 mm injury in the Morris water maze - acquisition and probe trial 133	
3.4.6.2	The effect of a 2.2 mm injury severity in the Morris water maze - Reverse acquisition trial 135	
3.4.6.3	The effect of a 2.2 mm injury severity in the Morris water maze - Probe trial.....	135
3.4.6.3.1	Reverse Platform.....	135
3.4.6.3.2	Original Platform.....	135
3.4.7	The effect of injury severity on the ipsilateral hemisphere - cortex and hippocampus.	137
3.4.8	The effect of injury severity on astrocytes in the cortex and the hippocampus .....	140
3.4.9	The effect of injury severity on the microglia in the cortex and the hippocampus .....	143
3.5	Discussion.....	146
3.5.1	Functional outcomes.....	146
3.5.1.1	Open field.....	146
3.5.1.2	Y-Maze .....	147
3.5.1.3	Early behavioural differences after TBI .....	148
3.5.1.4	Morris water maze test .....	149
3.5.2	Pathophysiological changes.....	151
3.5.3	Contralateral glial cell activation.....	153
3.5.4	Impact of sham injury .....	154

3.5.5	The CCI model .....	155
3.5.6	Conclusion.....	155
3.5.7	Main outcomes.....	156
4	The effect of acute DHA administration in a mouse CCI model of TBI.....	157
4.1	Introduction .....	157
4.2	Methods.....	158
4.3	Aims and Hypothesis.....	158
4.3.1	Aims.....	158
4.3.2	Hypothesis .....	159
4.4	Results .....	160
4.4.1	Effect of DHA treatment in the open field.....	160
4.4.2	Effect of DHA treatment in the Morris water maze .....	163
4.4.2.1	The effect of treatment in the first week of Morris water maze – Acquisition trial ..	163
4.4.2.2	The effect of DHA treatment in the first week of the MWM - Probe trial .....	164
4.4.2.3	The effect of DHA treatment in the MWM – Reverse Acquisition trial .....	166
4.4.2.4	The effect of DHA treatment in the Morris water maze – Reverse Probe trial .....	167
4.4.2.4.1	Reverse Platform.....	167
4.4.2.4.2	Original Platform.....	167
4.4.3	The effect of DHA treatment on the ipsilateral hemisphere -cortex and hippocampus	170
4.4.4	The effect of DHA treatment on astrocytes in the cortex and the hippocampus.....	173
4.4.5	The effect of DHA treatment on microglia/macrophages in the cortex and the hippocampus.....	176
4.4.6	Effect of DHA on neurogenesis in the dentate gyrus of the contralateral hippocampus	178
4.5	Discussion.....	179
4.5.1	Effect of DHA treatment on motor function and exploratory behaviour .....	179
4.5.2	Effect of DHA on learning and memory .....	180
4.5.3	Effect of DHA on the brain.....	181
4.5.3.1	Tissue loss .....	181
4.5.3.2	The effect of DHA on microglia and macrophage responses after injury .....	181
4.5.3.3	The effect of DHA on astrogliosis after injury .....	182
4.5.4	DHA treatment does not increase neurogenesis in the dentate gyrus .....	184
4.5.5	Conclusion.....	185
4.5.6	Main outcomes.....	186

5	Controlled cortical impact injury in fat-1 mice .....	187
5.1	Introduction .....	187
5.1.1	Diet and polyunsaturated fatty acids.....	187
5.1.2	The fat-1 transgenic mouse .....	188
5.1.3	The fat-1 mouse in CNS disease .....	191
5.1.4	Aging and TBI.....	191
5.2	Aims and Hypothesis .....	192
5.2.1	Aims.....	192
5.2.2	Hypothesis .....	192
5.3	Methods.....	193
5.3.1	Young and aged male fat-1 mice.....	193
5.3.2	Lipid analysis of brain tissue from young adult female mice.....	193
5.4	Results .....	194
5.4.1	Behavioural response after CCI injury in young adult male fat-1 mice .....	194
5.4.1.1	Morris water maze – Acquisition and Probe trial.....	194
	.....	196
5.4.1.2	Gross tissue loss after CCI injury in young adult male fat-1 mice .....	198
5.4.1.3	Reactive astrogliosis after CCI injury in young adult male fat-1 mice.....	201
5.4.1.4	Activated microglia/macrophages after CCI injury in young adult male fat-1 mice...203	
5.4.2	The effect of CCI in aged male fat-1 mice.....	205
5.4.2.1	Morris water maze – Acquisition and Probe trial.....	205
5.4.2.2	Tissue loss after CCI injury in aged male fat-1 mice.....	208
5.4.2.3	Reactive astrogliosis after CCI injury in aged male fat-1 mice .....	211
5.4.2.4	The effect of CCI in aged fat-1 males – Microglia/macrophage activation.....	214
5.4.3	The effect of CCI on the brain lipid profile in young adult fat-1 females.....	216
5.4.3.1	Effect of the omega-6 enriched diet on the brain lipid profile .....	217
5.4.3.2	Effect of the fat-1 gene on brain lipid profile.....	218
5.4.3.3	Effect of the fat-1 gene on the lipid profile in the brain following a sham injury .....	219
5.4.3.4	Effect of the fat-1 gene had on the lipid profile in the brain following a CCI injury...221	
5.5	Discussion.....	223
5.5.1	The fat-1 gene did not improve cognitive function following a CCI injury.....	223
5.5.2	The fat-1 gene did not prevent gross tissue loss.....	225
5.5.3	The fat-1 gene did not change the microglial/macrophage activation.....	225
5.5.4	The fat-1 gene causes increased reactive astrogliosis following CCI injury .....	226



5.5.5	CCI injury altered the lipid profile of the brain tissue.....	227
5.5.6	Conclusion.....	228
5.5.7	Main outcomes.....	229
6	A novel in vitro model of focal mechanical injury in a 3D astrocytic cell culture .....	230
6.1	Introduction .....	230
6.1.1	Glial cells.....	230
6.1.2	Astrocytes.....	231
6.1.2.1	Morphology.....	231
6.1.2.2	Molecular markers.....	233
6.1.3	The physiological roles of astrocytes.....	235
6.1.3.1	Blood-brain barrier and blood flow .....	235
6.1.3.2	K <sup>+</sup> homeostasis.....	236
6.1.3.3	Neurotransmitter uptake.....	236
6.1.3.4	Synaptic function .....	237
6.1.3.5	Metabolic support.....	238
6.1.4	Brain pathology .....	239
6.1.4.1	Reactive astrogliosis.....	239
6.1.4.2	Glial scar formation.....	241
6.1.4.3	Molecular triggers of astrogliosis .....	241
6.1.4.4	Mechanical triggers of astrogliosis .....	242
6.1.4.5	Time course of reactive astrogliosis.....	243
6.1.4.6	The role of astrocytes following traumatic brain injury.....	243
6.1.5	3D modelling in vitro.....	245
6.1.5.1	Astrocytes in a 3D cell culture.....	246
6.2	Methods.....	247
6.3	Aims and hypothesis .....	249
6.3.1	Aims.....	249
6.3.2	Hypothesis .....	249
6.4	Results .....	250
6.4.1	Effect of a mechanical injury on the cellular volume of astrocytes in the perilesional regions of interest .....	250
6.4.2	Effect of a mechanical injury on the cellular volume of astrocytes in the distal lesion regions of interest .....	252
6.4.3	The number of astrocytes in the perilesional regions of interest.....	254
6.4.4	The number of astrocytes in the regions distal from the lesion site.....	254

6.4.4.1	A summary of the impact injury in 3D gels as an in vitro model of astrogliosis after a mechanical focal injury.....	257
6.4.5	Effect of a mechanical injury on the morphology of astrocytes .....	259
6.4.6	Effect of the lesion on astrocytes at the lesion site.....	261
6.5	Discussion.....	262
6.5.1	A 3D culture as an in vitro model of focal mechanical injury .....	262
6.5.1.1	Astrogliosis .....	262
6.5.1.2	GFAP expression .....	262
6.5.1.3	Changes in morphology .....	263
6.5.1.4	Change in astrocyte number .....	263
6.5.1.5	Topography of the reactive astrocytes.....	264
6.5.1.6	Glial scar formation.....	266
6.5.2	DHA had no effect on GFAP expression or the morphology of astrocytes after impact	266
6.5.2.1	DHA treatment and astrocyte numbers .....	267
6.5.3	Limitations .....	267
6.5.4	Conclusion.....	269
6.5.5	Main outcomes.....	269
7	General discussion.....	270
7.1	Modelling TBI in vivo .....	270
7.2	Effect of DHA and of the fat-1 genotype in CCI.....	273
7.3	In vitro model of TBI.....	276
7.4	Omega-3 PUFAs and their potential in the treatment of TBI.....	278
7.5	Conclusion.....	280
	Appendix 1.1 - The average swim speed during the MWM probe trial for the young and aged fat-1 mice.....	282
	Appendix 1.2 - Standard RM1 chow diet for WT mice with normal diet .....	283
	Appendix 1.3 - A modified AIN-76A diet containing 10% corn oil (high omega-6 PUFAs diet) .....	284
	References .....	285

## Abbreviations

AA	Arachidonic acid
AD	Alzheimer's disease
ADB	Antibody diluting buffer
ADHD	Attention deficit hyperactivity disorder
AIF	Apoptosis-inducing factor
ALA	$\alpha$ -linolenic acid
Aldh1	Aldehyde dehydrogenase 1 family, member 1
ALS	Amyotrophic lateral sclerosis
ANOVA	Analysis of variants
APP	Amyloid precursor protein
AQP4	Aquaporin 4 channel
AQPs	Aquaporins
ATP	Adenosine triphosphate
BBB	Blood brain barrier
BDNF	Brain derived neurotrophic factor
BrdU	5-bromo-2'-deoxyuridine
BSA	Bovine serum albumin
CCI	Controlled cortical impact
CNS	Central nervous system
COX	Cyclooxygenases
CSF	Cerebral spinal fluid
CT	Computerised tomography
DAI	Diffuse axonal injury
DAMPs	Damage-induced molecular patterns
DC	Decompressive craniotomy
DCX	Doublecortin
DG	Dentate gyrus
DHA	Docosahexaenoic acid
Distal-ROI	ROI distal to the lesion

DMEM	Dulbecco's modified Eagle's medium
DPA	Docosapentaenoic acid
DRG	Dorsal root ganglion
DRS	Disability Rating Scale
DTI	Diffusion Tensor Imaging
EAAT	Excitatory amino acid transporters
EAAT1	Excitatory amino acid transporter 1
EAAT2	Excitatory amino acid transporter 2
EPA	Eicosapentaenoic acid
EPO	Erythropoietin
ESA	Erythropoiesis stimulating agent
FA	Fatty acids
FABPs	Fatty-acid binding proteins
FATP	Fatty acid transport protein
FCS	Foetal calf serum
FIM	Functional Independence Measure
GCS	Glasgow Coma Scale
GFAP	Glial fibrillary acidic protein
GFAP-BP	GFAP-breakdown product
GFP	Green fluorescent protein
GLAST	Glutamate aspartate transporter
Gln	Glutamine
GLT-1	Glutamate transporter 1
Glu	Glutamate
GOS	Glasgow Outcome Scale
GOS-E	Glasgow Outcome Scale-Extended
H+	Hydrogen atom
HIT-3	Head Injury Trial-3
HTS	Hypertonic saline
i.p.	Intraperitoneally
i.v.	Intravenously
Iba1	Ionised calcium-binding adapter molecule-1

ICP	Intracranial pressure
IL-12	Interleukin-12
iNOS	Inducible NOS
Kir4.1	Inwardly rectifying K <sup>+</sup> channel
LA	Linoleic acid
LC-PUFAs	Long chain PUFAs
LDL	Low-density lipoprotein
LDLR	LDL receptors
LOX	Lipoxygenases
LPL	Lipoprotein lipase
LTP	Long-term potentiation
mGluRs	Metabotropic glutamate receptors
MIH	Mild induced hypothermia
MRI	Magnetic resonance imaging
MS	Multiple Sclerosis
MWM	Morris water maze
NLRs	NOD-like receptors
NMDA	N-methyl-D-aspartate
NOS	Nitric oxide synthase
NPD1	Neuroprotectin D1
NSCs	Neural stem cells
OCT	Optimal cutting temperature
PAG	Phosphate-activated glutaminase
PAMPs	Pathogen recognition receptors
PBS	Phosphate buffered saline
PC	Phosphatidylcholine
PD	Parkinson's disease
PE	Phosphatidylethanolamine
PEG-SOD	Polyethylene glycol-conjugated superoxide dismutase
Peri-ROI	Perilesional region of interest
PNI	Peripheral nerve injury
PS	Phosphatidylserine

PUFA	Polyunsaturated fatty acids
RNS	Reactive nitrogen species
ROI	Region of interest
ROS	Reactive oxygen species
s.c.	Subcutaneously
S.E.M.	Standard error of the means
SCI	Spinal cord injury
SGZ	Subgranular zone
SVZ	Subventricular zone
TAI	Traumatic axonal injury
TBI	Traumatic brain injury
TLRs	Toll-like receptors
TNF	Tumour necrosis factor
TNF- $\alpha$	Tumour necrosis factor- $\alpha$
VEGFs	Vascular endothelial growth factors
WHO	World Health Organisation
WT	Wild type

## List of Tables

Table 1.1. The Glasgow Coma Scale scoring system.....	26
Table 1.2 Summary of proposed therapeutic strategies for TBI.....	49
Table 1.3 Types of saturated and mono-unsaturated fatty acids.....	52
Table 1.4 Nomenclature of omega-3 and omega-6 PUFAs.....	52
Table 1.5. Summary of in vitro models of TBI.....	69
Table 1.6 Summary of different cell culture systems.....	70
Table 1.7 The various in vivo models of TBI.....	72
Table 1.8 Species used in various in vivo models of TBI.....	73
Table 1.9 Example of behavioural tests used as outcome measures in animal TBI models.....	81
Table 2.1 Summary of primary antibodies used.....	98
Table 5.1 Disease models that have utilised the <i>fat-1</i> mice.....	190
Table 6.1. Subtypes of astrocytes based on their location, morphology and structural characteristics. .....	232
Table 6.2. Molecular markers for the identification of astrocytes and astrocytic subtypes.....	234
Table 6.3. A summary of the potentially beneficial or damaging roles of astrocytes following TBI.....	244

## List of Figures

Figure 1.1 Schematic showing the evolution of the primary injury to the secondary injury following TBI. ....	30
Figure 1.2 Schematic representation of the activation of microglial cells in response to neuronal injury, and the different microglial phenotypes. ....	40
Figure 1.3 Fatty acid structures. ....	51
Figure 1.4 Synthesis of long-chain omega-3 and omega-6 PUFAs in the liver. ....	54
Figure 1.5 Transport and processing of LC-PUFAs into the brain. ....	57
Figure 1.6 Schematic demonstrating the differences in brain aspect between species; Mouse, Cat and Human. ....	74
Figure 1.7 Equipment used in the fluid percussion model of TBI. ....	75
Figure 1.8 Equipment used in the Marmarou model of TBI. ....	76
Figure 1.9 Equipment used in the controlled cortical impact model of TBI. ....	77
Figure 1.10 Open field test. ....	80
Figure 1.11 Y-maze test. ....	83
Figure 1.12 Morris water maze test. ....	85
Figure 2.1 Surgical setup for the controlled cortical impact injury (CCI) in mice. ....	90
Figure 2.2 Open field test. ....	91
Figure 2.3 . Y maze test. ....	92
Figure 2.4 Training and testing schedule for the Morris water maze. ....	94
Figure 2.5 Morris water maze test. ....	94
Figure 2.6 Brain regions examined after toluidine blue staining. ....	96
Figure 2.7 Schematic representation of the brain sections used for immunohistochemical analysis. ...	97
Figure 2.8 Schematic representation of the regions of interest (ROI) used for analysis at each coronal brain level. ....	99
Figure 2.9 Quantification of GFAP immunolabelling using ImageJ analysis in mouse cortical brain tissue. ....	100
Figure 2.10 Quantification of Iba1 and doublecortin staining. ....	101
Figure 2.11 Timeline of the in vitro studies. ....	103
Figure 2.12 Mechanical injury to the 3D astrocyte gels. ....	104
Figure 3.1 Timeline for the administration of the behavioural tests after surgery. ....	108
Figure 3.2. Effect of injury severity on open field performance. ....	112
Figure 3.3. Effect of injury severity on the distance travelled and line crossings in the first week. ....	113
Figure 3.4 The total distance travelled after injury in the open field. ....	113



Figure 3.5 The number of line crossings after injury in the open field. ....	114
Figure 3.6 The effect of injury severity on the time spent immobile within the open field test. ....	115
Figure 3.7. Effect of injury severity on Y-maze performance. ....	117
Figure 3.8. Effect of injury severity on the Y-maze performance on day 3 and day 8. ....	118
Figure 3.9. Effect of injury severity on acquisition training in the Morris water maze. ....	120
Figure 3.10. Effect of injury severity on the probe trial performance in the Morris water maze. ....	122
Figure 3.11. Effect of injury severity on the reverse acquisition training in the Morris water maze. ....	124
Figure 3.12 Effect of injury severity on reverse probe trial performance in the second week of Morris water maze testing. ....	126
Figure 3.13. Effect of injury severity on original platform measures during the reverse probe trial. ....	127
Figure 3.14 Reverse probe trial. ....	128
Figure 3.15. Timeline for the execution of the behavioural tests after surgery. ....	129
Figure 3.16 Effect of a 2.2 mm injury on the open field performance. ....	130
Figure 3.17 Open field testing of a 2.2 mm injury versus a sham injury at day 1, 7, 14, 21 and 28 post-injury. ....	131
Figure 3.18 Open field testing of a 2.2 mm injury versus a sham injury. ....	132
Figure 3.19. Effect of a 2.2 mm injury vs. sham control on acquisition training and probe trial in the first week of the Morris water maze. ....	134
Figure 3.20 Effect of a 2.2 mm injury vs sham control on the reverse acquisition training. ....	136
Figure 3.21. Brain sections stained with toluidine blue. ....	138
Figure 3.22. The effect of injury severity on the ipsilateral brain regions as compared to the contralateral side. ....	139
Figure 3.23. The effect of injury severity on the GFAP expression. ....	141
Figure 3.24. The effect of injury severity on the reactive astrogliosis in the cortex and hippocampus. ....	142
Figure 3.25. Microglia with Iba1 labelling at various injury severities. ....	144
Figure 3.26. The effect of injury severity on the number of microglia/macrophages in the cortex and hippocampus. ....	145
Figure 4.1. Timeline for the i.v. administration of DHA and the behavioural tests after CCI. ....	158
Figure 4.2 Effect of DHA treatment after CCI injury on the open field performance. ....	161
Figure 4.3. Effect of DHA treatment in CCI injury on the open field performance at day 1, 7, 14, 21 and 28 of the study. ....	162
Figure 4.4 Effect of DHA treatment on acquisition training in the Morris water maze. ....	164
Figure 4.5. Effect of DHA Treatment on Acquisition training and Probe trial Performance In the first week of the Morris Water Maze. ....	165

Figure 4.6. Effect of DHA Treatment on Acquisition training in the second week of the Morris Water Maze.....	168
Figure 4.7. Effect of DHA Treatment on Probe trial Performance in the second week of the Morris water maze.....	169
Figure 4.8. Lesion size after CCI and DHA treatment.....	171
Figure 4.9. The effect of DHA treatment post-injury on the ipsilateral brain regions as compared to the contralateral side.....	172
Figure 4.10 The effect of DHA treatment on GFAP expression.....	174
Figure 4.11. The effect of DHA treatment on reactive astrogliosis post-injury in the cortex and hippocampus.....	175
Figure 4.12. The effect of DHA treatment post-injury on Iba1+ cells.....	176
Figure 4.13. The effect of DHA treatment on the number of microglia/macrophages in the cortex and hippocampus.....	177
Figure 4.14. The effect of DHA treatment on the number of DCX+ cells in the Dentate Gyrus. ....	178
Figure 5.1 Timeline for the testing in the Morris water maze following CCI in the fat-1 mice. ....	193
Figure 5.2. Effect of the fat-1 gene in young males on the performance in the Morris water maze.....	196
Figure 5.3. Effect of the fat-1 gene in young males on the performance in the Morris water maze Acquisition and Probe trial. ....	197
Figure 5.4. Brain sections from young wild type and fat-1 mice stained with toluidine blue.....	199
Figure 5.5. The effect the fat-1 gene has in young males on tissue loss after CCI.....	200
Figure 5.6. The effect of the fat-1 gene on GFAP expression in young males. ....	201
Figure 5.7 The effect the fat-1 gene has in on reactive astrogliosis in the cortex and hippocampus in young males.....	202
Figure 5.8. The effect of fat-1 gene on the Iba1 expression in young males.....	203
Figure 5.9. The effect the fat-1 gene has on the number of Iba1+ cells in the cortex and hippocampus in young males.....	204
Figure 5.10. Effect of the fat-1 gene in aged males on the performance in the Morris water maze.....	206
Figure 5.11 Effect of the fat-1 gene in aged males on the performance in the Morris water maze Acquisition and Probe trial. ....	207
Figure 5.12 Brain sections from aged wild type and fat-1 mice stained with Toluidine blue. ....	209
Figure 5.13. The effect the fat-1 gene has in aged males on tissue loss after CCI.....	210
Figure 5.14 The effect of fat-1 gene on GFAP expression. ....	212
Figure 5.15. The effect the fat-1 gene had on reactive astrogliosis in the cortex and hippocampus of aged males. ....	213
Figure 5.16. The effect of fat-1 gene on the no. of Iba1+ cells in aged fat-1 males.....	214

Figure 5.17. The effect of the fat-1 gene in aged males on the number of microglia/macrophages in the cortex and hippocampus. ....	215
Figure 5.18 Representative gas chromatogram. ....	216
Figure 5.19. The effect a high omega-6 PUFA diet has on the lipid profile of the brain tissue. ....	217
Figure 5.20. The effect of the fat-1 gene has on the lipid profile of the brain tissue. ....	218
Figure 5.21 The effect the sham injury has on the lipid profile of the brain tissue. ....	220
Figure 5.22. The effect the CCI injury has on the lipid profile of the brain tissue. ....	222
Figure 6.1. Schematic representation of protoplasmic and fibrous astrocyte morphology. ....	231
Figure 6.2. Schematic of the blood brain-barrier (BBB). ....	235
Figure 6.3. Schematic representation of the glutamate-glutamine shuttle at a glutamatergic synapse. ....	237
Figure 6.4. Schematic representations of the gradations of reactive astrogliosis. ....	240
Figure 6.5. Examples of main triggers of reactive astrogliosis. ....	242
Figure 6.6. Schematic representation of cells in in vitro cultures. ....	246
Figure 6.7 Timeline of the in vitro studies. ....	247
Figure 6.8. Experimental setup for the 3D astrocytic culture. ....	248
Figure 6.9 The effect of lesion and DHA treatment on GFP expression and GFAP immunostaining in the perilesional ROI. ....	251
Figure 6.10. The effect of lesion and DHA treatment on GFP expression and GFAP immunostaining in the ROI distal to the lesion. ....	253
Figure 6.11. Effect of Impact and DHA treatment on the number of astrocytes in the perilesional ROI at 1 day, 5 days and 10 days post-lesion. ....	255
Figure 6.12. Effect of Impact and DHA treatment on the number of astrocytes in the distal to the lesion ROI at 1 day, 5 days and 10 days post lesion. ....	256
Figure 6.13. Effect of impact on a 3D astrocyte culture in the perilesional and away from lesion ROI, at 1 day, 5 days and 10 days post-impact. ....	258
Figure 6.14. Population analysis of the effect of impact on the number of processes per astrocyte in the perilesional and away from lesion ROI. ....	260
Figure 6.15. Glial scar formation in 3D astrocytic culture. ....	261

# **1 General introduction**

## **1.1 Traumatic Brain Injury**

Traumatic brain injury (TBI) describes damage caused to the brain parenchyma either from direct impact or as a result of indirect external forces (Werner and Engelhard, 2007). Patients can suffer from a wide variety of symptoms, including cognitive, motor and sensory dysfunction as well as mood, sleep and speech problems. The World Health Organisation (WHO) estimates that by 2020 TBI will be the largest cause of death worldwide (WHO, 2006). This global increase in TBI means that there is high demand for resources, ranging from intensive care units during the acute stage to rehabilitation during the recovery stage, and to social care and housing. There is a personal cost to the patients and their family as well as a societal cost due to the loss of future earnings to patients. TBI has recently been quoted to cost Europe a staggering £23.9 billion. The UK cost alone is £4.1 billion, for direct (e.g. hospital stay, drugs, brain scans) and indirect costs (e.g. loss of earning, loss of productivity, crime) associated with TBI (Gustavsson et al., 2011).

### **1.1.1 Epidemiology – Public health**

TBI is the largest cause of death and disability in males under 50 years of age (Maas et al., 2008). There are numerous ways in which a patient will receive a head injury. The most common causes of a TBI are motor vehicle accidents, sporting injuries, as a result of violence or during combat within a war zone. These causes are the main reason for the high prevalence of TBI in the young male population. However, there have been changes in the epidemiology of TBI due to the ageing population. In recent years, there has been an increase in the percentage of TBI sufferers over the age of 60, both male and female (Rozenbeek et al., 2013, Stocchetti et al., 2012). This aging population mainly suffer from TBI due to falls. Although there are more co-morbidities in the older age group, there is a greater direct and indirect cost to support a younger patient, since they will suffer from lifelong disabilities as a result of a TBI. As well as a change in the age range of patient populations that suffer a TBI, there has also been a shift in the geographical epidemiology of TBI, linked to economic development. An increase in

the number of motor vehicles in the developing world has seen countries such as India experience increasing numbers of TBI (WHO, 2006).

The large population of TBI patients and the substantial cost of care, both of which are set to rise in the coming years, make the treatment of TBI a priority. A greater understanding of the pathophysiology of TBI will assist in patient care and help find an effective therapy for TBI.

### **1.1.2 Management of human TBI**

There is currently no successful therapy for TBI, so clinicians can only provide supportive and palliative care. Several factors have contributed to this absence of treatment. One of the biggest obstacles to an efficacious treatment is the heterogeneous nature of the disease. TBI is extremely heterogeneous between patients; they differ in severity, brain region affected and may present with various additional poly-trauma complications. There are guidelines and protocols for treatment in the immediate and acute phase of the injury, and for the ongoing treatment in the chronic phase of the injury (NICE, 2014). Despite these guidelines, treatment of each patient's injury will need to be tailored to the individual's symptoms (NICE, 2014).




### **1.1.3 Early phase management**

When patients first arrive at the hospital after a serious incident a doctor will be expected to treat the greatest threat to life, which is not always the brain per se that is injured. This may mean that trauma surgeons are initially there first to prevent further blood loss, to intubate and help ventilation of the lungs and to treat any internal organ damage, which may be prioritised over the TBI. Nevertheless, there will still be an initial evaluation of the TBI, conducted by the emergency room staff or the paramedics.

The initial assessment used is scored using a neurological scale called the Glasgow Coma Scale (GCS), which awards a score out of 15 that correlates with the severity of a patient's TBI (Table 1.1). The GCS criteria are grouped into three categories: eye movement, verbal response and motor response. The patient is assessed for all three criteria and awarded a score. Scores below 8 are classified as severe

injuries, those between 9-12 are considered to reflect moderate TBI and those equal to or above 13 are referred to as mild injuries.

**Table 1.1. The Glasgow Coma Scale scoring system.**

<p><b><u>Best Eye Response</u></b></p> 	Spontaneous – blinking at baseline	4
	Opens to verbal command	3
	Opens to pain	2
	None	1
<p><b><u>Best Verbal Response</u></b></p> 	Oriented	5
	Confused, but able to answer questions	4
	Inappropriate answers, words discernible	3
	Incomprehensible speech	2
	None	1
<p><b><u>Best Motor Response</u></b></p> 	Obeys commands to movement	6
	Purposeful movement in response to painful stimulus	5
	Withdraws from pain	4
	Abnormal (spastic) flexion	3
	Extensor (rigid) response	2
	None	1

If the GCS is less than 13 on the initial assessment in the emergency room, a patient will receive a computerised tomography (CT) scan. The CT scan is used to assess any bleeding or swelling within the brain. A neurosurgeon may be called if something on the CT scan is a concern, such as a subarachnoid haemorrhage, haematoma or skull fracture. A neurosurgeon may also be called if the patient's condition worsens, i.e. a deterioration in the GCS score since the admission or a persisting coma. As well as ongoing assessment of the patient using the GCS, the patient will be observed for any additional or changing symptoms, such as seizures or vomiting. The patient's intracranial pressure will also be monitored for any changes using an electronic device that is inserted between the skull and the brain or directly into the brain via a bolt, given that raised intracranial pressure is one of the main causes of death (Reilly and Bullock, 1997). Depending upon all of these factors, a patient may receive neurosurgery or be admitted straight on the intensive care or high dependency units within the hospital, until there are signs of improvement. It is important to note that the GCS has limitations, as the scale can be ineffective when the patient is intoxicated, sedated or intubated.

#### **1.1.4 Late phase management**

During the late phase (3 months post-injury), a patient will continue to be monitored in order to track the progression of the secondary injury and to monitor symptoms. Follow-up rehabilitation is unique to the specific patient's symptoms and can include one or more of the following: physiotherapy, occupational therapy, psychotherapy, and speech therapy. Depending on the injury, a patient may have to take medication for ongoing pain, spasticity, hormone replacement and psychiatric reasons (NHS, 2016).

The GCS is used for the initial assessment of the level of consciousness of a TBI patient. There are more neurological scales, that are used to assess the ongoing symptoms during a patient's rehabilitation and they can be used to measure the efficacy of new therapies. Three examples of these neurological scales include: The Functional Independence Measure (FIM), the Glasgow Outcome Scale (GOS) and the Disability Rating Scale (DRS) (Pangilinan, 2015). These tests have been shown to be useful in the prediction of the long term outcome for patients, particularly the GOS, when taken at 3 months post-injury (King et al., 2005). While being useful to monitor a patient's progress, these tests can be subjective, with a patient reporting their own progress.

Tracking the evolution of the secondary injury can be done using various imaging techniques. As mentioned earlier, CT scans are routinely used in the acute phase after the injury, but are also used to monitor the progression of the disease. However, CT scans cannot detect diffuse axonal injury (DAI) (Pangilinan, 2015). Magnetic resonance imaging (MRI) is a more sensitive anatomical imaging method, most useful at detecting delayed haematomas and assessing damage to the deep brain structures (e.g. basal ganglia and thalami). However, MRI imaging is a more expensive option compared to a CT scan and up until 72 hours after injury is no more sensitive than a CT scan at determining anatomical changes in the brain after TBI. Other imaging techniques such as single photon emission computed tomography (SPECT) and positron emission tomography (PET) imaging are more rarely used, but can be employed to analyse cerebral blood flow and DAI (Lee and Newberg, 2005).

After monitoring of the injury via imaging, the brain pathology can only really be fully characterised by a post-mortem examination of the brain. As many patients, particularly those with mild to moderate brain injuries, live for years after their injury, our knowledge of the immediate pathology that follows a TBI in the human brain is limited. To understand more about the pathology after injury, animal models of TBI have been developed. These models help with the investigation of the pathology post-injury and in the development of novel therapies for the treatment of TBI.

### **1.1.5 Long-term outcomes of TBI**

As a result of a TBI, patients may suffer from persistent and long-term consequences. These may include physical impairments (both motor and sensory), sleep disorders, endocrinopathies, cognitive dysfunction, psychiatric disorders, pain, seizures and the development of neurodegenerative diseases such as dementia (Stocchetti and Zanier, 2016). These long-term consequences require further and pro-longed clinical care, observation and treatment. A potential link between TBI and the development of dementia, particularly Alzheimer's disease, has been studied in mild to severe TBI patients, with conflicting outcomes (Dams-O'Connor et al., 2013, Rapoport et al., 2008, Lee et al., 2013). In a recent retrospective epidemiological study conducted by Gardner and colleagues, they found that those patients with a moderate to severe TBI aged 55 years or older had an increased risk of developing dementia when compared to non-TBI trauma patients (Gardner et al., 2014).

In younger TBI patients, repeated exposure to head trauma can cause a progressive neurodegenerative disorder known as Chronic traumatic encephalopathy (CTE). This is a relatively new diagnosis, first described by Dr. Bennet Omalu in 2005. His seminal paper details the histopathological characteristics and the premortem symptoms of a retired American football player (Omalu et al., 2005). It suggests that there is a link between the repetitive concussions as suffered by athletes playing high-impact contact sports such as rugby and American football, and the development of neuropsychiatric symptoms including depression, psychosis, aggression and dementia (DeKosky et al., 2013). The pathology of CTE patients includes diffuse neocortical A $\beta$  plaques and neurofibrillary tangles, this is identical to the pathology of the neurodegenerative disease that afflicts boxers, known



as dementia pugilistica, the aetiology being the difference between the two (Omalu et al., 2005, DeKosky et al., 2013).

## **1.2 Pathophysiology of TBI**

The pathophysiology of TBI can be divided into two phases: the primary injury and the secondary injury.

The primary injury is defined as the damage caused during the moment of injury/impact. This is the direct damage to the brain parenchyma. The primary injury results in cell death that is caused by the impact to the brain, whether it is a shock wave, direct mechanical contact with an object or damage to the skull impacting upon the brain tissue. The primary injury phase causes immediate death of the cells and tissue beneath the site of impact, which can be associated with skull fractures, haematomas, haemorrhage and blood brain barrier (BBB) breakdown.

The initial cell death leads to a cascade of biochemical, molecular and cellular mechanisms that lead to the expansion of the primary area of injury. This evolution of the primary injury site is known as the secondary injury and occurs in the minutes, weeks and years following the TBI. This secondary injury is the cause of many of the behavioural symptoms suffered by patients and is also the main target for potential TBI therapy. The secondary injury phase encompasses numerous different and complex processes including: glutamate excitotoxicity, lipid peroxidation, oxidative stress, changes in intracranial pressure, apoptosis, further necrosis, neuronal and axonal damage, activation of the glial cells and release of inflammatory mediators (Fig.1.1) (Werner and Engelhard, 2007).

One main focus area for TBI research is to target these processes individually or together as a way of limiting the expansion of the secondary injury, thereby limiting the symptoms suffered by the TBI patient. There is currently no way of targeting the death caused by the primary injury, which can only be via preventative measures such as using seatbelts, protective headgear and airbags.

		<u>Injury</u> Focal, Diffuse, Shockwave					
		Systemic Impact		Local Impact			
Primary Injury	Seconds to Minutes	Skull Fracture	Vascular Changes -Hemorrhage -Hemotoma -Blood Brain Barrier Dysfunction	Diffuse Axonal Injury -Axonal Shearing	Cellular Injury -Depolarization -Calcium Influx -Glutamate Excitotoxicity	Necrosis	
	Secondary Injury	Hours to Days	Ischemia -Decreased Cerebral Blood Flow	Oedema -Increased ICP	Glial Cell Activation -Microglia activation -Reactive Astrogliosis	Cellular Dysfunction -Neuronal Loss -Axonal Degeneration	Mitochondrial Dysfunction  Oxidative Stress -Free Radical Production Lipid Peroxidation
		Weeks to Months		Inflammation -Increased Pro-inflammatory Cytokine Release -Infiltration of Leukocytes	Cell Death/Apoptosis		Glial Scar Formation
		Months to Years	Neurobehavioural Consequences -Motor Dysfunction -Cognitive Dysfunction	Tissue Remodelling -Neuroplasticity -Tissue Remodelling		Hypothalamic-Pituitary Dysfunction -Hormonal Dysfunction	

**Figure 1.1 Schematic showing the evolution of the primary injury to the secondary injury following TBI.** Adapted from (Reifschneider et al., 2015, Xiong et al., 2013, Schaar et al., 2010, Buccafusco JJ, 2009)

### **1.2.1 Biochemical alterations**

#### **1.2.1.1 Glutamate excitotoxicity and intracellular calcium overload**

The process of glutamate excitotoxicity occurs almost immediately after the primary injury has been sustained. There are 3 main reasons for the large amounts of excitatory amino acid glutamate to be released into the extracellular space after TBI. Firstly, the destruction of cell membranes during the primary mechanical damage causes the intracellular glutamate to be released into the extracellular space. Secondly, large membrane depolarizations, caused by injury, increase the vesicular release of glutamate and, thirdly, post-injury energy diminution causes the glutamate transporters of the astrocytes to fail, thereby resulting in high levels of glutamate to be left in the synaptic cleft (Walker and Tesco, 2013, Yi and Hazell, 2006).

Glutamate excitotoxicity leads to an increase in intracellular  $Ca^{2+}$ , neuronal injury and ultimately neuronal cell death. Glutamate activates ionotropic glutamatergic receptors, which leads to an influx of  $Na^+$  and  $Ca^{2+}$  ions; this leads to membrane depolarization and subsequent opening of voltage-dependent calcium channels and N-methyl-D-aspartate (NMDA) receptors (Mark et al., 2001). Further  $Ca^{2+}$  influx leads to mitochondrial dysfunction, oxidative stress and apoptosis (Walker and Tesco, 2013).

#### **1.2.1.2 Oxidative stress and free radical production**

Oxidative stress describes the harm caused by free radicals, which can include damage to the cell membrane, proteins and DNA, as well as lipid peroxidation and inhibition of the mitochondrial electron transport chain (Abdul-Muneer et al., 2015). Free radicals are molecules with unpaired electrons. These unpaired electrons make them highly reactive and, in an attempt to gain an electron, they cause damage. There are two main families of free radicals: reactive oxygen species (ROS: e.g. superoxide, hydroxyl radical and hydrogen peroxide) and reactive nitrogen species (RNS: e.g. peroxynitrite and nitrogen dioxide) (Abdul-Muneer et al., 2015). In normal brain function these free radicals are largely neutralised by the endogenous antioxidant system (e.g. superoxide dismutase and

glutathione peroxidase). TBI causes an increase in intracellular  $\text{Ca}^{2+}$  which activates numerous enzymes including phospholipase  $\text{A}_2$  and nitric oxide synthase (NOS), which in turn increases the production of ROS and RNS (Lewén et al., 2000). This large production of free radicals causes the antioxidant system to become overwhelmed, causing damage and contributing to the secondary injury pathophysiology.

#### **1.2.1.3 Lipid peroxidation**

Lipid peroxidation describes the oxidative damage caused to polyunsaturated fatty acids (PUFA) such as linoleic acid (LA), eicosapentaenoic (EPA) acid and docosahexaenoic acid (DHA) as a result of attack by free radicals. Lipid peroxidation is initiated by a ROS-induced hydrogen atom ( $\text{H}^\bullet$ ) which gains an electron from the PUFA, turning it into a lipid radical which goes on to turn adjacent lipids into lipid radicals, thereby propagating a chain reaction of lipid peroxidation (Bains and Hall, 2012). The termination step in lipid peroxidation occurs when there is a depletion of substrates and the lipid radical reacts with another lipid radical or radical scavenger system (Bains and Hall, 2012). The damage to cellular membrane lipids can cause the cell membrane to become irrevocably damaged and the products of lipid peroxidation can lead to cell death.

#### **1.2.1.4 Mitochondrial dysfunction**

Oxidative stress and the accumulation of  $\text{Ca}^{2+}$  after TBI lead to mitochondrial dysfunction and subsequently a reduction in adenosine triphosphate (ATP) production. The excessive influx of  $\text{Ca}^{2+}$  triggered by glutamate excitotoxicity overwhelms the  $\text{Ca}^{2+}$  buffering performed by the  $\text{Na}^+$ - $\text{Ca}^{2+}$  exchanger of the mitochondria. This leads to loss of the mitochondrial membrane potential, an increase in ROS production and consequent oxidative damage, to which mitochondrial DNA is particularly vulnerable (Prins et al., 2013, Walker and Tesco, 2013, Cheng et al., 2012). Mitochondrial dysfunction, in particular permeabilization of the mitochondrial membrane, can trigger cell death mechanisms, both necrosis and apoptosis. Mitochondria can trigger the apoptotic pathway either by releasing cytochrome c into the cytosol, which causes caspase activation and therefore apoptosis, or in a caspase-independent manner, through the release of apoptosis-inducing factor (AIF) (Cheng et al.,

2012, Lemasters et al., 1998, Lewén et al., 2001). In addition, mitochondrial dysfunction can indirectly amplify the extrinsic apoptotic pathway. This extrinsic pathway is discussed in section 1.2.2.2.

Oxidative stress can cause mitochondrial dysfunction in several ways through the action of ROS. They can inhibit the electron transport chain and decrease energy production, cause mutations within the mitochondrial DNA, instigate lipid peroxidation on the inner membrane and promote the caspase-dependent apoptotic pathway (Murphy, 2009). In turn mitochondrial dysfunction can contribute to oxidative stress by producing ROS. This leads to a cycle of mitochondrial dysfunction and ROS production that ultimately ends up in cell death (Starkov, 2008, Lin and Beal, 2006).

#### **1.2.1.5 Oedema and changes in intracranial pressure**

Brain oedema plays a significant role in the secondary injury of TBI. Two types of oedema have been characterized within the brain: vasogenic oedema and cellular oedema (Kempski, 2001, Unterberg et al., 2004). Vasogenic oedema refers to the accumulation of water in the extracellular spaces due to the breakdown of the BBB. Cellular brain oedema describes the accumulation of intracellular water, which occurs due to the failure of cellular membrane ion pumps, causing osmotic movement of water into cells. Both vasogenic and cellular oedema lead to an increase in brain volume, thereby increasing ICP. Increased ICP adds to the deleterious effect of the secondary injury by reducing cerebral blood flow, causing further hypoxia, which in turn leads to impaired neuronal function and potentially neuronal cell death (Michinaga and Koyama, 2015).

Marmarou and colleagues have shown with MRI that the oedema in patients with severe head trauma is predominantly intracellular in nature, but have concluded that both extra- and intracellular oedema can lead to increased ICP (Marmarou et al., 2006, Marmarou et al., 2000). Raised ICP is the most common cause of death in patients with severe TBI and monitoring of ICP is part of standard aftercare for TBI patients (Romner and Grände, 2013). Currently, oedema in the clinic is treated using osmotic diuretics including mannitol or hypertonic saline. These work by drawing fluid into the intravascular space via the osmotic gradient, however, due to the systemic nature of these drugs they have several

serious side effects including systemic hypotension and renal failure (Walcott et al., 2012). This has led to investigations for novel targets to treat oedema.

Several molecules are involved in the pathogenesis of TBI-induced oedema, including factors that affect cellular or BBB permeability such as vascular endothelial growth factors (VEGFs), water channel proteins called aquaporins (AQPs) and ion channels including the cation channel SUR1/TRPM4 which is upregulated after TBI, leading to cellular oedema (Walcott et al., 2012, Michinaga and Koyama, 2015, Zweckberger et al., 2014). Targeting these molecules to treat oedema has been shown to be efficacious in animal models of ischaemia and TBI (Michinaga and Koyama, 2015). Antagonism of VEGF reduced oedema in mice that received an ischaemia/reperfusion injury, as assessed by MRI (van Bruggen et al., 1999). The predominant AQP channel in the brain is the subtype AQP4, found largely on the astrocytic endfeet. Igarashi and colleagues found that mice pre-treated with a AQP4 inhibitor exhibited less oedema following a focal ischaemia (Igarashi et al., 2011). Thirdly, an existing anti-diabetic drug, a sulfonylurea inhibitor called glibenclamide, inhibits SUR1, which may inhibit cellular oedema (Zweckberger et al., 2014). This range of targets reflects the complex nature by which oedema is caused following a TBI.

## **1.2.2 Cellular alterations**

### **1.2.2.1 Blood brain barrier disruption**

Mechanical damage to the BBB occurs in the primary injury phase, and disruption of the BBB contributes to the secondary injury pathophysiology. The BBB is made up of cerebrovascular endothelial cells, joined together by tight junctions, whose role is to safeguard the brain by restricting the molecules that can and cannot enter the brain, creating a highly selective and specialised environment for normal brain function. However, disruption to the BBB following TBI causes the immediate increase in the permeability of this barrier, and otherwise excluded blood borne molecules can enter the brain in a uncontrolled manner (Chodobski et al., 2011). In addition to increasing the permeability of the BBB, disruption to the brain vasculature initiates the coagulation cascade, causing the aggregation of platelets and clotting factors within the vessels surrounding the contusion area and

reducing the pericontusional blood flow (Stein et al., 2002). This reduced cerebral blood flow in the pericontusional area mimics that seen in stroke patients; this ischaemia contributes to the secondary injury pathology (von Oettingen et al., 2002).

The disruption of the BBB can both contribute to the secondary injury and be further increased by the action of other secondary injury mechanisms such as glutamate excitotoxicity and oxidative stress. Glutamate excitotoxicity (as discussed in section 1.2.1.1) describes the rapid release of the neurotransmitter glutamate into the extracellular space after TBI. The metabotropic glutamate receptors (mGluRs); mGluR1, mGluR4 and mGluR5 have been shown to be expressed by human cerebrovascular endothelial cells and activation of these mGluRs by mGluR group I or III agonists increased the permeability of these endothelial cells in vitro (Collard et al., 2002). Glutamate excitotoxicity can indirectly propagate the damage to the BBB by inducing oxidative stress, through activation of NMDA receptors, thereby causing an increase in intracellular  $Ca^{2+}$  and subsequent production of large numbers of free radicals (Mark et al., 2001, Lewén et al., 2000). Dempsey and colleagues showed that NMDA receptor antagonists reduced the permeability of the BBB in rats at 6 hours after TBI (Dempsey et al., 2000). Oxidative stress can cause further damage to the BBB. ROS such as superoxide ions and hydrogen peroxide, have been shown to increase the permeability of endothelial cells (Schreibelt et al., 2007, Pun et al., 2009). This continued disruption to BBB contributes to the secondary injury pathophysiology and further expansion of the primary contusion area.

#### **1.2.2.2 Necrosis and apoptosis**

There are two main types of cell death that occur following a TBI: necrosis and apoptosis. Necrosis describes the rapid and uncontrolled cell death that occurs following a severe focal mechanical injury, ischaemia and glutamate excitotoxicity (Werner and Engelhard, 2007). Cells undergoing necrosis lose membrane integrity and the nucleus shrinks. The cell membrane ruptures and provokes an inflammatory response whereby the cell detritus is cleared. In contrast, apoptosis is a programmed cell death mechanism and is highly regulated. The hallmark changes that occur in a cell when undergoing apoptosis include membrane budding, chromatin condensation and nuclear fragmentation (Stoica and

Faden, 2010). Apoptosis can be initiated by extrinsic pathways, including activation of tumour necrosis factor (TNF) and Fas receptors or by intrinsic pathways that involve permeabilization of the mitochondrial outer membrane and subsequent release of cytochrome c into the cytosol (Stoica and Faden, 2010, Lewén et al., 2001). Both the intrinsic and extrinsic pathways lead to the activation of the cysteine acid-protease caspase 3. It is the caspase-dependent cleavage of specific substrates that induces apoptosis (Yakovlev and Faden, 2001). Necrosis is the predominant mechanism of cell death immediately following a TBI. Apoptosis follows during the secondary injury and causes the death of neurones and glial cells in the perilesional area (Walker and Tesco, 2013, Raghupathi et al., 2000).

### **1.2.2.3 Neuronal and axonal damage**

In the primary injury, neurones are damaged through direct severing of the axon or through shearing forces that cause the axons to stretch. These initial injuries progress during the secondary injury phase and can result in further neuronal damage and extensive lesions within the brain. Severing the axon immediately halts axonal transport and causes release of all intracellular contents into the extracellular space: a main consequence of this is glutamate excitotoxicity (see section 1.2.1.1). Diffuse axonal injury (DAI) is a term used to describe the human widespread axonal injury following TBI, whereby vulnerable axons, most often the white matter tracts, undergo stretch injury and eventual degeneration (Johnson et al., 2013b). The term Traumatic axonal injury (TAI) is used to describe this same phenomenon within *in vitro* or *in vivo* models of stretch injury (Hill et al., 2016). DAI is typically associated with diffuse TBI causes, such as acceleration/deceleration injuries or rotational injuries. Both of these occur as a result of motor vehicle accidents or blast trauma. It has been suggested that DAI is directly responsible for the loss of consciousness or coma seen in TBI patients (Gennarelli et al., 1982).

The shearing force can cause axons to stretch, become undulated and misaligned due to microtubules becoming disorganised and buckling (Tang-Schomer et al., 2010). This leads to an impediment of axonal transport, subsequent axonal swelling, secondary disconnection and finally to Wallerian degeneration (Povlishock, 1992, Johnson et al., 2013b). Besides the initial shearing or mechanical



forces, secondary injury cascades can also cause damage to the neurones. The secondary cascades that can have a detrimental effect on neurones include mitochondrial dysfunction, oxidative stress and lipid peroxidation, inflammation and glial cell activation.

DAI can occur even in mild TBI, but can only be diagnosed with post-mortem histology. The novel neuroimaging technique, diffusion tensor imaging (DTI), may make it possible to examine the extent of DAI in a TBI patient. DTI is a type of MRI that measures changes in the speed or direction of the diffusion of water molecules within the white matter tracts. DTI measures can provide information on tract disorganisation, axonal swelling, loss of neurones, quality of downstream nerve terminals, so therefore provide information on connectivity changes in TBI (Irimia et al., 2012, Johnson et al., 2013b). If combined with MRI, these measures could provide information on the functional connectivity of the large networks within the brain, such as those that support cognition, thereby allowing for more accurate diagnosis and outcome prediction following TBI (Ham and Sharp, 2012).

#### **1.2.2.4 Cytoskeletal disruption**

The cytoskeleton is a complex network of proteins that provide the cell with structural support, organisation of intracellular contents, and helps to establish the cell's morphology (Fletcher and Mullins, 2010). Underpinning the axonal injury as described above (see section 1.2.2.3) is the degeneration of important components required in the axonal cytoskeleton. Cytoskeleton disruption following TBI does not exclusively affect neuronal cells but can also affect the glial cells. As cytoskeletal proteins are usually absent from the extracellular space, their presence in plasma or cerebrospinal fluid (CSF) has been identified as a potential biomarker for TBI.

The main cytoskeletal proteins in neuronal cells include neurofilaments and microtubules. Neurofilaments are a type of intermediate filament that provide structure and stability to the axons of neurones, they are heteropolymers that are made from three polarized sidearm subunits attached to a central unit that helps to keep the neurofilaments equally spaced apart (Fournier et al., 2015). This equal spacing is reduced following neurotrauma, when they become 'compacted', due to either altered phosphorylation or proteolysis of the sidearm subunits, which has been suggested to lead to

collapse of the neurofilament network (Pettus and Povlishock, 1996, Siedler et al., 2014). Microtubules on the other hand, are involved in the transport of proteins along the length of the axon, they are larger in diameter than neurofilaments and more rigid (Fletcher and Mullins, 2010). Under shearing forces (section 1.2.2.3), microtubules breakage causes undulations in the axon and eventual disassembly of the microtubules (Tang-Schomer et al., 2010). Disruption of the neurofilament and microtubule networks has been linked to the continued, secondary axotomy in the white matter tracts, which is part of the DAI cascade (Fournier et al., 2015).

The intermediate filaments in other CNS cell types are also affected by TBI and change during the secondary injury phase. One example that we will focus on within this thesis is the intermediate filament glial fibrillary acidic protein (GFAP), which is found predominantly in the glial cell type, astrocytes. Following injury astrocytes exhibit a change in their morphology, they undergo hypertrophy as well as proliferation, and in doing so they increase the amount GFAP they express (Yang and Wang, 2015). This phenomenon is known as 'reactive astrogliosis' and is described in more detail in chapter 6.

#### **1.2.2.5 Glial cell activation**

The glial cells in the brain are more numerous than neuronal cells. The main glial cell populations include oligodendrocytes, microglia and astrocytes. These glial cells have several roles in brain function including trophic support, mediation of inflammation, myelination and maintenance of the extracellular environment. These glial cells present with particular pathophysiological changes following TBI, which are summarised below.

#### **1.2.2.6 Oligodendrocyte pathology**

Oligodendrocytes are the cells within the CNS that are responsible for the myelination of axons. TBI induces apoptosis of oligodendrocytes, which subsequently leads to a decrease in myelination and therefore a reduction in axonal saltatory conduction. This demyelination can also leave axons exposed to harmful effects of the secondary injury, as well as producing symptoms in TBI patients similar to

those seen in demyelinating diseases such as multiple sclerosis (MS), including problems with learning and cognition (Fields, 2008).

Damage to the oligodendrocytes occurs as a result of several of the secondary injury cascades including hypoxia, oxidative stress, excitotoxicity and energy deprivation due to mitochondrial dysfunction (Dewar et al., 2003, Underhill and Goldberg, 2007, Lyons and Kettenmann, 1998). Oligodendrocytes are prone to the apoptotic cell death pathway. In a study conducted by Lotocki and colleagues, the apoptotic marker caspase-3 was present in oligodendrocytes in rats as early as 6 hours after injury (Lotocki et al., 2011). It has also been suggested that within the glial cell populations, oligodendrocytes are most vulnerable to cell death following TBI, as opposed to astrocytes and microglia (Lyons and Kettenmann, 1998).

#### **1.2.2.7 Microglial activation**

Microglia are the resident immune cells of the brain and share characteristics with other immune cells of the body, including phagocytosis of foreign bodies and cellular debris, as well as having antigen-presenting capabilities (Hickey and Kimura, 1988). The microglia are the main instigators of the inflammatory cascades that occur after a TBI. Following TBI microglia become 'activated' and in doing so change from a ramified morphology to a hypertrophic or bushy morphology (Tambuyzer et al., 2009).

Microglia in the mature brain become 'activated' in response to many molecules or changes in the extracellular environment, often signals that suggest the CNS is under threat from an invading pathogen or that the brain tissue has become damaged. Microglia are able to become 'activated' by a wide array of signals, due to the wide range of receptors that they express. These include pathogen recognition receptors such as toll-like receptors (TLRs) and NOD-like receptors (NLRs), which recognise pathogen-associated molecular patterns (PAMPs) and detect the endogenously produced damage-induced molecular patterns (DAMPs), also known as alarmins, that are released by damaged and stressed cells (Hanisch and Kettenmann, 2007, Loane and Kumar, 2016). Other factors such as ATP,

glutamate and cytokines are released by cells damaged due to TBI can also ‘activate’ microglia (Domercq et al., 2013).

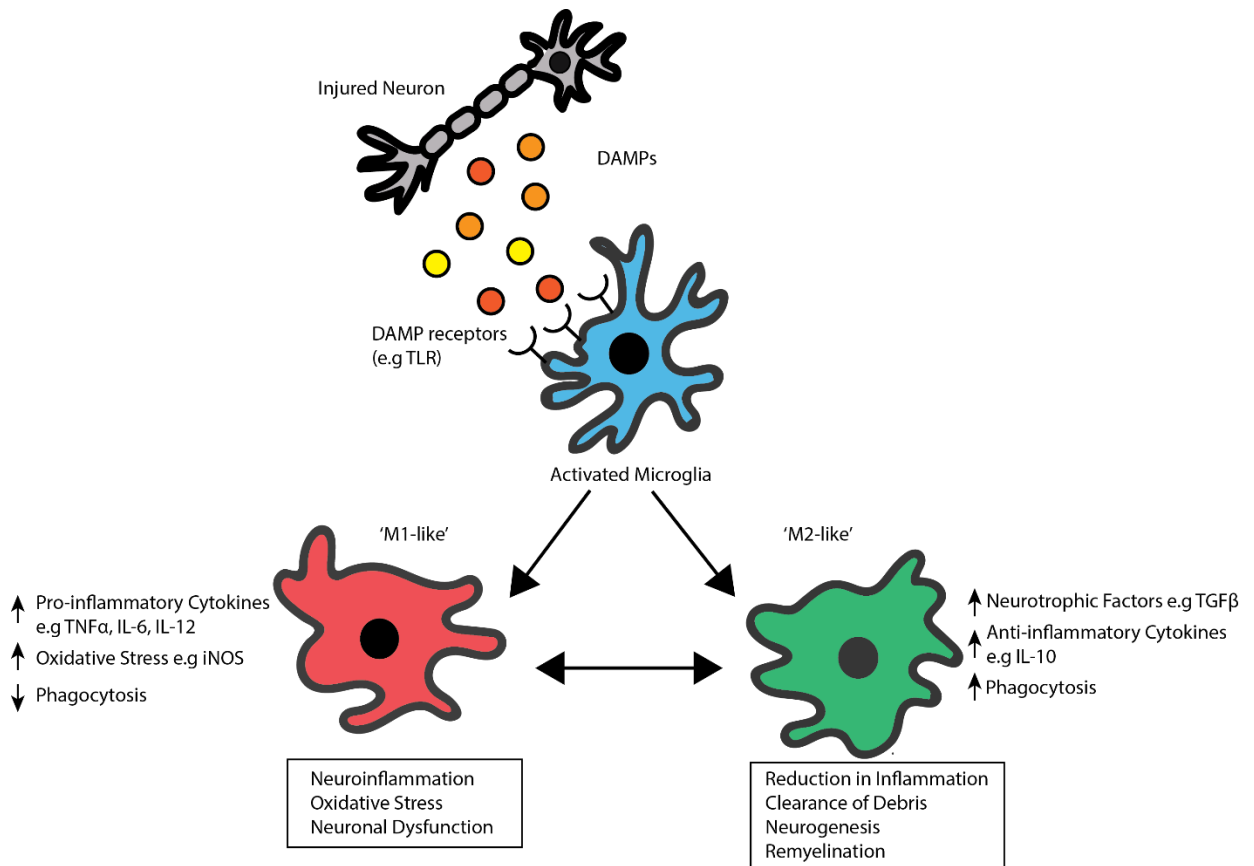


**Figure 1.2 Schematic representation of the activation of microglial cells in response to neuronal injury, and the different microglial phenotypes.** Damage-induced molecular patterns (DAMP); Tumour necrosis factor- $\alpha$  (TNF- $\alpha$ ); Interleukin-6 (IL-6); Interleukin-12 (IL-12); inducible Nitric oxide synthase (iNOS); Transforming growth factor- $\beta$  (TGF- $\beta$ ); Interleukin-10 (IL-10). (Loane and Kumar, 2016)

Similarly to other glial cell types in the brain, there are different phenotypes of microglia. These become apparent upon activation, when they will adopt either an ‘M1-like’ or ‘M2-like’ phenotype (Fig. 1.2). These various phenotypes are believed to have opposing roles in the aftermath of a TBI (Karve et al., 2016). The ‘M1’ microglia phenotype is considered to have detrimental effects on the surrounding tissue, as they produce pro-inflammatory cytokines such as interleukin-12 (IL-12), express inducible NOS (iNOS) and have reduced phagocytosing abilities. In contrast, the ‘M2’ phenotype is traditionally seen as the neuroprotective phenotype, due to its production of anti-inflammatory cytokines (IL-10) and growth factors (e.g. tumour growth factor - $\beta$ ; TGF- $\beta$ ) (Wang et al., 2013). There is evidence to suggest that the ‘M2-like’ microglia may even promote regeneration and repair within the

CNS, by promoting neurogenesis of neural stem cells (NSCs) and remyelination (Butovsky et al., 2006, Miron et al., 2013). Despite the 'M2-like' phenotype exhibiting beneficial effects, it is not always the dominant microglial phenotype in the lesion site following TBI. At different time-points post-TBI, the predominant microglia phenotype varies. There is evidence to suggest that there is an initial increase in the 'M2' phenotype with a peak at 5-7 days, followed by a dominant 'M1' phenotype in the longer term (Karve et al., 2016, Jin et al., 2012). The 'M1-like' phenotype has been shown to be dominant in patients in the months and years following TBI (Johnson et al., 2013a).

#### **1.2.2.8 Astrogliosis**

Astrocytes have a marked reaction following TBI. This response is referred to as 'reactive astrogliosis' and reflects changes to the astrocyte morphology, increased proliferation and increased expression of the intermediate filament glial fibrillary acidic protein (GFAP) (Sofroniew and Vinters, 2010). Astrocytes also migrate towards the lesion site after TBI and are the main cell type to contribute to the formation of the glial scar. The glial scar describes a thick border of cells that surrounds the lesion site and acts as a physical barrier, which may although protect the surrounding healthy tissue from the damaged necrotic tissue of the primary injury site, but can also act as a barrier to regenerating neurones after injury (Sofroniew, 2009). Similar to the microglia, reactive astrocytes are capable of having both detrimental and protective roles following a TBI (Laird et al., 2008, Karve et al., 2016). The roles of astrocytes following TBI are covered in greater detail in the introduction to chapter 6.

#### **1.2.2.9 Inflammatory mediators**

Several mediators of inflammation are involved in the secondary injury pathophysiology, including cytokines, chemokines and growth factors, which are released by numerous cell types. Two pro-inflammatory cytokines that are increased after TBI include IL-1 $\beta$  and tumour necrosis factor- $\alpha$  (TNF- $\alpha$ ) (Abdul-Muneer et al., 2015). IL-1 $\beta$  and TNF- $\alpha$  both contribute to the progression of the tissue damage and encourage the recruitment of immune cells and infiltration of peripheral leukocytes, including macrophages and T-cell lymphocytes (Lucas et al., 2006, Werner and Engelhard, 2007). In normal brain function TNF- $\alpha$  has important roles in ionic homeostasis and synaptic plasticity. Following TBI

there is an increase in the activity of TNF- $\alpha$ , which has been associated with tissue damage and neurobehavioral deficits (Longhi et al., 2013, Feuerstein et al., 1994).

### **1.3 Potential therapies for TBI**

Currently, there are very few treatment options for TBI patients. With the increasing patient population, the substantial cost both socially and economically, there has been a real effort to find a therapy suitable for the treatment of TBI. A summary of potentially neuroprotective therapeutic strategies are presented in Table 1.2.

#### **1.3.1 Surgery**

Neurosurgical interventions can be one of the first courses of action that may minimise the damage to the brain during the secondary injury phase. Surgical interventions are most commonly used to monitor or reduce increased ICP. Increased ICP can be caused by hematomas and haemorrhages, which can be removed or drained surgically. If the brain tissue has become swollen and increased ICP has not been brought under control through alternative therapies, a decompressive craniectomy or hemicraniectomy may be performed (Haddad and Arabi, 2012). All the surgical efforts to reduce the ICP can help to reduce the negative contribution raised ICP has to the secondary injury cascade, and therefore improve the outcome of the patient. However, a study conducted by Cooper and colleagues showed that although patients who had undergone decompressive craniectomy surgery saw a reduction in ICP, they also scored much lower on the GOS at 6 months (Cooper et al., 2011).

#### **1.3.2 Neuroprotective strategies**

As discussed in section 1.2, the brain tissue destroyed by the primary injury cannot be rescued. However, the multiple secondary injury mechanisms detailed above provide several therapeutic targets for the treatment of TBI. Through the prevention of the progression of some of these secondary mechanisms, the expansion of the primary injury area can be limited or halted and this could lead to a decrease in neurobehavioral symptoms in TBI patients. This strategy of targeting the secondary injury mechanisms, can be referred to as neuroprotection. Neuroprotective strategies can

be defined as any therapeutic that results in the salvage, recovery or regeneration of the nervous system, its cells, structure and function (Vajda, 2002).

The strategy of neuroprotection is the basis of several therapies that have been used and clinically tested for the treatment of several neurodegenerative diseases such as Parkinson's disease, Alzheimer's disease and amyotrophic lateral sclerosis (ALS). In the case of TBI, there are several secondary injury mechanisms that if halted may be able to confer neuroprotection. There have been many therapeutics designed to have neuroprotective effects following TBI, but very few have made it to clinical trials and currently none have demonstrated significant efficacy in improving neurological outcomes following TBI. Several factors may contribute to this lack of success, including clinical trial design, the heterogeneity of the TBI patient population and treatment protocols. Also it is worth noting that there are multiple contributors to the secondary injury, which might suggest that therapeutically targeting just one mechanism may not be enough to confer significant beneficial outcomes.

#### **1.3.2.1 Osmotherapy**

Potential neuroprotective agents targeted at specific secondary injury mechanisms are described here and summarised in Table 1.2. Many therapies have been used to target increased ICP, including neurosurgery (e.g. decompressive craniectomy). However, neurosurgery is dangerous and is only used in patients where death is imminent (Haddad and Arabi, 2012). Raised ICP can cause compression and even occlusion of cerebral blood vessels. This can lead to a reduction of cerebral blood flow, which can cause hypoxia, neuronal dysfunction and eventually cell death (Michinaga and Koyama, 2015). Osmotically active substances have been used to target increased ICP. Osmotherapy works by increasing the osmolality of the serum, by introducing a hyperosmolar substance such as hypertonic saline (HTS) or mannitol intravenously. These substances cause water from the cells of the brain to pass into the vasculature along the osmotic gradient, thereby reducing the fluid in the brain and decreasing the ICP.

HTS has a high concentration of salt, whereas mannitol is a sugar alcohol solution. Both have been shown to reduce ICP following TBI, with neither substance being more efficacious than the other (Ichai et al., 2009, Jagannatha et al., 2016, Boone et al., 2015). However, despite these agents reducing ICP, neither have been able to improve neurological outcome or reduce mortality in TBI patients in the long term (Wakai et al., 2007, Burgess et al., 2016, Walcott et al., 2012, Boone et al., 2015).

### **1.3.2.2 Free-radical scavengers**

Targeting free radical species is another strategy by which neuroprotection could be obtained following TBI. Free radicals contain an unpaired electron that can cause oxidative stress leading to lipid peroxidation and mitochondrial dysfunction. In normal brain function there are molecules that target free radicals in order to control the oxidative stress level, but this system is overwhelmed in TBI. By therapeutically increasing the amount of free radical scavenging within the brain, oxidative stress could be reduced and the impact of the secondary injury minimised. Polyethylene glycol-conjugated superoxide dismutase (PEG-SOD), is an example of such therapy. PEG-SOD converts the oxygen free radical, superoxide ion ( $O_2^-$ ) into an oxygen molecule ( $H_2O$ ) or hydrogen peroxide ( $H_2O_2$ ), thereby limiting oxidative stress (Broxton and Culotta, 2016). PEG-SOD was taken to phase II and phase III clinical trials, but failed to demonstrate any statistically significant benefit, in improving outcome or preventing mortality following TBI (Muizelaar et al., 1993, Narayan et al., 2002).

### **1.3.2.3 Glutamate receptor antagonists**

Within minutes of the primary injury, glutamate excitotoxicity is triggered, and this secondary injury event goes on to trigger several other cascades and eventually leads to cell death. Therefore, antagonists targeting post-synaptic glutamate receptors may be able to suppress the damage caused by excessive glutamate release. The NMDA receptor is a glutamate receptor and ion channel, when activated by glutamate and glycine binding, the ion channel opens to allow positive ions (e.g.  $Ca^{2+}$  ions) into the post-synaptic neurone and thereby propagate excitotoxicity. Dexanabolol is a non-competitive NMDA glutamate receptor antagonist, that prevents the NMDA-R ion channel from opening in response to glutamate binding, thereby preventing the influx of  $Ca^{2+}$  ions and depolarisation



(Feigenbaum et al., 1989). Dexanabinol has been taken to clinical trials for the treatment of TBI. In a phase II clinical trial, dexanabinol appeared to reduce the amount of time severe TBI patients experienced increased ICP and showed a trend at improving neurological outcome, using the GCS at 3 and 6 months post-injury (Knoller et al., 2002). However, in a large multicentre phase III clinical trial, no difference in ICP or neurological outcome (as measured by the GOS at 6 months) was seen in patients with severe TBI (Maas et al., 2006).

#### **1.3.2.4 Calcium channel blockers**

One of the main consequences of glutamate excitotoxicity is a large influx of  $Ca^{2+}$  ions into cells. As discussed above, the antagonists of the NMDA-R prevent the influx of  $Ca^{2+}$  by preventing activation of the ion channel by glutamate. Calcium channel blockers are an alternative to glutamate receptor antagonists. Two drugs that block calcium channels are ziconotide (SNX-111 an N-type calcium channel blocker) and nimodipine (an L-type calcium channel blocker), both of which have been trialled as neuroprotective agents in TBI.

In experimental head injury in rats, ziconotide reduced mitochondrial dysfunction and appeared to have a wide time-window for administration, 15 minutes to 6 hours post-injury (Verweij et al., 2000). However, a clinical trial of 160 patients had to be terminated due to the high incidence of mortality in the ziconotide-treated group when compared to the placebo group, due to the side effect of hypotension in these patients (Xiong et al., 2009).

Nimodipine is an antagonist for the L-type calcium channel blocker that originally appeared to demonstrate some improvement in patients with subarachnoid haemorrhage in three randomised controlled trials, as reported by a large Cochrane review (Towart and Kazda, 1979, Langham et al., 2003). Also, results from the Head Injury Trial-3 (HIT-3) trial conducted in 123 patients suggested that nimodipine treatment significantly lowered the risk of mortality and disability (Narayan et al., 2002). However, the combined results of the clinical trials HIT-1, HIT-2 and HIT-4, showed that nimodipine failed to have any beneficial effect in the subgroup of TBI patients that had suffered a subarachnoid haemorrhage (Vergouwen et al., 2006).

### **1.3.3 Multifactorial neuroprotective strategies**

As highlighted in the previous sections, many therapeutics with a single mechanism of action against one component of the secondary injury cascade, have failed to be efficacious in clinical trials. For this reason, many other neuroprotective strategies which have several proposed mechanisms of action, have been trialled in TBI.

#### **1.3.3.1 Hypothermia**

Mild induced hypothermia (MIH) is when a patient's body temperature is maintained at 32°C-35°C. Although MIH has been repeatedly tested for efficacy in TBI in the clinic to reduce ICP, meta-analysis of large randomised controlled trials has found that hypothermia has no effect on TBI patient outcome and can also cause adverse side effects (Lazaridis and Robertson, 2016, Zhang et al., 2015).

The hypothesis that underpins hypothermia as a neuroprotective therapeutic strategy, is that many of the cellular and molecular cascades that are part of the secondary injury are temperature-sensitive (Sahuquillo and Vilalta, 2007). Hypothermia is believed to affect many of the secondary injury mechanisms in order to confer neuroprotection. These include reducing the metabolic rate, decreasing ICP, reducing oedema formation, suppressing the inflammatory response, reducing glutamate excitotoxicity and calcium influx (Sahuquillo and Vilalta, 2007). Recently, it has been suggested that MIH can induce neuroprotective cold-shock proteins (Wu et al., 2016b).

Eurotherm3235 was a large multicentre randomized controlled trial that recruited 387 patients from 2009 through to 2014, in 47 centres, across 18 countries (Andrews et al., 2013). The study focused on the effect hypothermia had on reducing ICP after TBI. Preliminary data from this study, suggested that MIH reduced ICP in a sample of 17 patients (Flynn et al., 2015). The conclusion from the Eurotherm3235 trial was that ICP was reduced with hypothermia, but did not result in improved outcomes, when compared to patients that received standard care (Andrews et al., 2015).

#### **1.3.3.2 Erythropoietin (EPO)**

EPO is a hematopoietic growth factor that controls erythropoiesis and is produced endogenously by the kidneys (Foley, 2008). EPO is believed to have a neuroprotective effect in TBI due to its activity in

several molecular mechanisms involved in the secondary injury (Ponce et al., 2013). EPO has demonstrated an antioxidant effect in an *in vitro* model of neurodegenerative disease, as well as attenuating lipid peroxidation in foetal rats (Wu et al., 2007). It has also been suggested that EPO exhibits a neuroprotective effect by protecting against glutamate excitotoxicity and reducing oedema (Morishita et al., 1997, Kawakami et al., 2000, Gatto et al., 2015).

EPO has demonstrated efficacy in animal models of TBI, including an improvement in the novel object recognition (NOR) cognitive behavioural test in rats after traumatic axonal and hypoxic injury (Hellewell et al., 2013). Schober and colleagues also found improvement with EPO treatment in a rat model of CCI, whereby EPO-treated rat pups had improved cognition and improved neuronal survival and inhibition of caspase-dependent apoptosis (Schober et al., 2014).

A recent retrospective study investigating the effect of an erythropoiesis stimulating agent (ESA) that acts like EPO, found that treatment with ESA was associated with improved in-hospital survival in severe TBI patients (Talving et al., 2010). However, two clinical trials designed to test the efficacy of EPO in the treatment of TBI failed to show any efficacy, with the larger of the trials (EPO-TBI) being conducted in 27 centres, over 7 countries in 596 patients (Robertson et al., 2014, Nichol et al., 2015a).

### **1.3.3.3 Progesterone**

As with hypothermia and EPO, progesterone has been tested as a therapeutic for TBI due to its multifactorial targets for neuroprotection. Progesterone is a hormone involved in the regulation of the menstrual cycle and pregnancy, that like EPO, is produced endogenously. The basis for the administration of the female sex hormone progesterone stems from observations that females recover better after experimental TBI (Stein, 2011, Stein, 2015). There is controversy in the literature whether gender has an impact on the outcome of TBI (Roof et al., 1993, Groswasser et al., 1998, Farace and Alves, 2000).

In models of rat TBI, progesterone treatment appeared to reduce glutamate excitotoxicity, lipid peroxidation and inflammation (Roof et al., 1996, Roof et al., 1997, Shear et al., 2002, Stein, 2011). It is also suggested to reduce oedema through changes in the expression of cell membrane water channels,

specifically the aquaporin 4 channel (AQP4) (Guo et al., 2006). A functional study has shown that progesterone improves rats' performance in the Morris water maze test following TBI (Shear et al., 2002). Importantly, progesterone has also shown efficacy in TBI models of larger species, as well as in other injury models, resulting in progesterone being taken to clinical trials in human TBI patients (Stein, 2011).

In a phase II clinical trial of 100 patients, entitled ProTECT, TBI patients that received the progesterone treatment had a reduced mortality rate at 30 days, with moderate TBI patients more likely to have a moderate to good outcome, as measured by the GOS-E (Wright et al., 2007). Based on the data from this trial and other phase II trials, in which progesterone treatment had a positive impact on TBI patient outcome, phase III clinical trials on progesterone treatment went forward despite having incomplete understanding of progesterone's mechanism of action (Xiao et al., 2008, Vandromme et al., 2008). Two large multicentre phase III clinical trials went forward with optimistic hopes for the efficacy of progesterone treatment. However, the SyNAPSe phase III trial which was completed in 2014 failed to show that progesterone treatment had any impact on patients' GOS-E score 6 months post-injury (Skolnick et al., 2014). Another larger phase III clinical trial that was conducted in parallel with the SyNAPSe trial, entitled ProTECT III, was terminated on the basis of not exhibiting any positive results (Skolnick et al., 2014, Wright et al., 2014, Goldstein et al., 2016).

**Table 1.2 Summary of proposed therapeutic strategies for TBI. (Xiong et al., 2009)**

<b>Therapeutic Strategy</b>	<b>Mechanism of Action</b>	<b>Conclusions</b>	<b>References</b>
Nimodipine	Calcium channel blocker	Potentially beneficial effects in subarachnoid haemorrhage. Systematic review did not confirm benefits.	(Langham et al., 2003, Vergouwen et al., 2006)
SNX-111	N-type calcium channel blocker	Improved mitochondrial function, however increased mortality due to hypotension.	(Verweij et al., 2000)
Methyl-prednisolone/ dexamethasone	Corticosteroids – anti-oxidative/anti-inflammatory	Results of large scale CRASH trial demonstrated that treatment with corticosteroids led to a higher risk of death.	(Edwards et al., 2005)
Mannitol	Reduces ICP Reduces Inflammation	Randomised trials have given insufficient data on the effectiveness of pre-hospital mannitol treatment.	(Wakai et al., 2007)
Hypertonic saline	Reduces ICP	Randomised trials show no differences in mortality, neurological outcomes, and ICP reduction with hypertonic saline.	(Burgess et al., 2016)
Decompressive craniotomy (DC)	Reduces ICP	A phase III randomised trial DECRA showed that DC decreased intracranial pressure but was associated with more unfavourable outcomes.	(Cooper et al., 2011)
Dexanabinol	NMDA receptor antagonist	A phase III randomised trial showed dexanabinol to be safe but not efficacious in TBI.	(Maas et al., 2006)
Polyethylene	Anti-oxidant, free	In Phase II and Phase III trials	(Muizelaar et al., 1993,

glycol-conjugated superoxide dismutase (PEG-SOD)	radical scavenger	PEG-SOD showed no statistical improvement in GOS, or difference in mortality rate in severe TBI.	Young et al., 1996, Hamm et al., 1996)
Hypothermia	Multifactorial ↓ Oedema ↓ Metabolic rate Calcium antagonism ↓ Excitotoxicity ↓ Inflammation	The Eurotherm3235 phase III trial concluded that treatment with hypothermia showed no improvement in TBI patients when compared to standard care.	(Peterson et al., 2008, Andrews et al., 2013, Zhang et al., 2015, Flynn et al., 2015, Andrews et al., 2015)
Erythropoietin (EPO)	Multifactorial <ul style="list-style-type: none"> <li>• Antioxidant</li> <li>• ↓ Inflammation</li> <li>• ↓ Excitotoxicity</li> <li>• ↓ Oedema</li> </ul>	The phase III trial, EPO-TBI concluded that EPO treatment failed to show any efficacy in TBI patients.	(Ponce et al., 2013, Nichol et al., 2015b)
Progesterone	Multifactorial <ul style="list-style-type: none"> <li>• ↓ Oedema</li> <li>• ↓ Inflammation</li> <li>• ↓ Excitotoxicity</li> <li>• Antioxidant</li> </ul>	In two large phase III trials (SyNAPSe and PROTECT III) progesterone treatment did not provide any benefit on the neurological recovery in moderate or severe TBI.	(Skolnick et al., 2014, Meyfroidt and Taccone, 2015, Schumacher et al., 2015, Wright et al., 2014)

#### 1.3.3.4 Polyunsaturated Fatty Acids (PUFAs)

Several of the potential therapeutics that have been taken to clinical trials have multiple mechanisms of action. Another type of compound that has shown to have some therapeutic potential in neurological disorders and neurotrauma, whilst being safe and tolerable in humans, are the omega-3 polyunsaturated fatty acids (Dyall and Michael-Titus, 2008). The omega-3 PUFAs are the neuroprotective compounds under investigation in this thesis.

## 1.4 Polyunsaturated fatty acids - General Introduction

Fatty acids (FA) are carboxylic acids with long unbranched aliphatic tails, that can be saturated or unsaturated. The level of saturation and the various functional groups determine the family to which each fatty acid belongs. Saturated fatty acids contain no double bonds and mono-unsaturated fatty acids contain one carbon-carbon double bond (Table 1.3). Fatty acids that contain more than one double bond are known as polyunsaturated fatty acids (Fig.1.3 and Table 1.4).

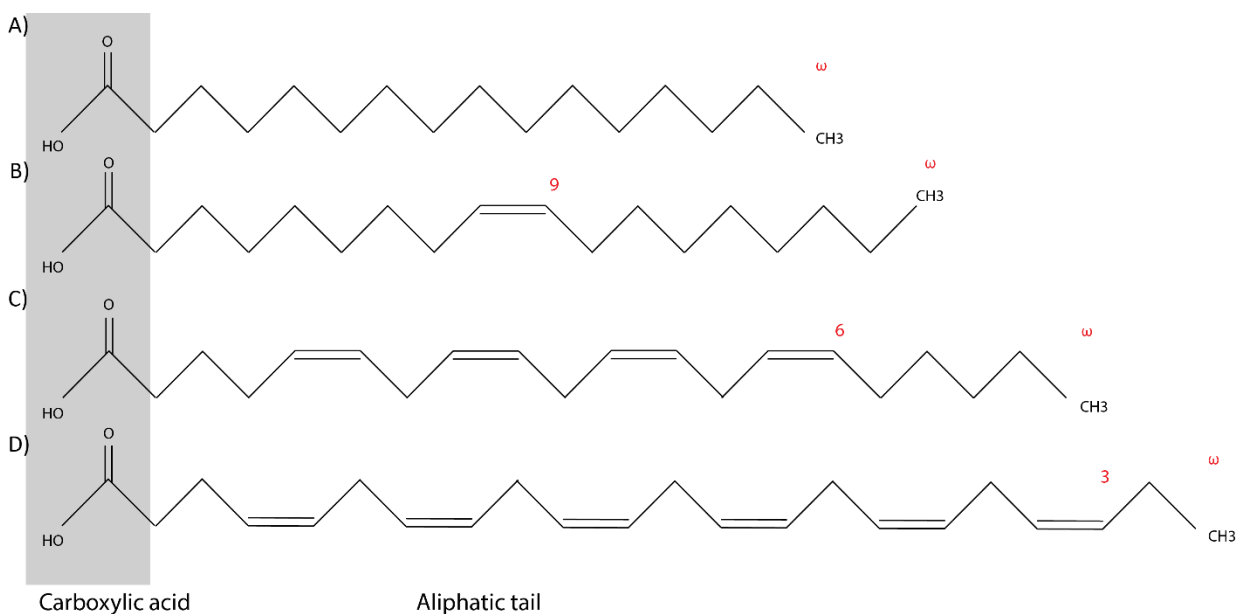


**Figure 1.3 Fatty acid structures.** A) The saturated FA; Palmitic acid, (B) omega-9 monounsaturated FA; Oleic acid, (C) omega-6 poly-unsaturated FA; Arachidonic acid, (D) omega-3 poly-unsaturated FA; Docosahexaenoic acid.

PUFAs (Table 1.4) can be further divided into sub-groups according to the position of the first double bond from the methyl end of the chain (Fig. 1.3). The two main groups are the omega-3 PUFAs, where the first carbon-carbon double bond from the methyl end of the carboxylate is found at the omega-3 position, and the omega-6 PUFAs, where the position of the first double bond is at the omega-6.

**Table 1.3 Types of saturated and mono-unsaturated fatty acids**

Type	Common Name	Abbreviation	No. of Carbon Atoms	No. of Double Bonds	Numerical Designation
Saturated	Palmitic acid	PA	16	0	16:0
	Stearic acid	SA	18	0	18:0
Mono - unsaturated Omega-9	Oleic acid	OA	18	1	18:1 n-9

**Table 1.4 Nomenclature of omega-3 and omega-6 PUFAs.**

Type	Common Name	Abbreviation	No. of Carbon Atoms	No. of Double Bonds	Numerical Designation	
Polyunsaturated	Omega-6	Linoleic acid	LA	18	2	18:2 n-6
		$\gamma$ -linoleic acid	GLA	18	3	18:3 n-6
		Dihomo- $\gamma$ -linoleic acid	DGLA	20	3	20:3 n-6
		Arachidonic acid	AA	20	4	20:4 n-6
		Docosatetraenoic acid	DTA	22	4	22:4 n-6
		Docosapentaenoic acid	DPA n-6	22	5	22:5 n-6
	Omega-3	$\alpha$ -linolenic acid	ALA	18	3	18:3 n-3
		Stearidonic acid	SDA	18	4	18: n-3
		Eicosatetraenoic acid	ETA	20	4	20:4 n-3
		Eicosapentaenoic acid	EPA	20	5	20:5 n-3
		Docosapentaenoic acid	DPA n-3	22	5	22:5 n-3
		Docosahexaenoic acid	DHA	22	6	22:6 n-3

#### 1.4.1 Synthesis, metabolism and transport of fatty acids

Both the saturated and monounsaturated fatty acids can be synthesised de novo in the brain (Bazin et al and Layé, 2014). The PUFAs, however, cannot be synthesised in the human brain due to the lack of the necessary desaturase enzymes, so these fatty acids have to be obtained through the diet. Omega-6 fatty acids can be found in ready supply in vegetable oils, whereas cold-water oily fish are a rich source of omega-3 fatty acids. Long chain PUFAs (LC-PUFA) (20-22 carbon chain) can be obtained directly from the diet or can be metabolised from the shorter chain (18 carbon) PUFAs linoleic acid (LA) and  $\alpha$ -linolenic acid (ALA). The conversion of the 18 carbon PUFAs ALA and LA into the 20-22 carbon omega-3 PUFAs DHA, EPA and the omega-6 PUFA AA, occurs in the liver, through a series of desaturation and



elongation steps, detailed in figure 1.4 (Rapoport et al., 2007, Nakamura and Nara, 2003). Once synthesised in the liver long chain PUFAs (LC-PUFAs) are released into the bloodstream, from which uptake can occur by the CNS. LC-PUFAs can also gain access to the bloodstream via lipolysis from adipocytes, or from the small intestine, where dietary LC-PUFAs are absorbed. Once in the bloodstream LC-PUFAs bind to the protein albumin.

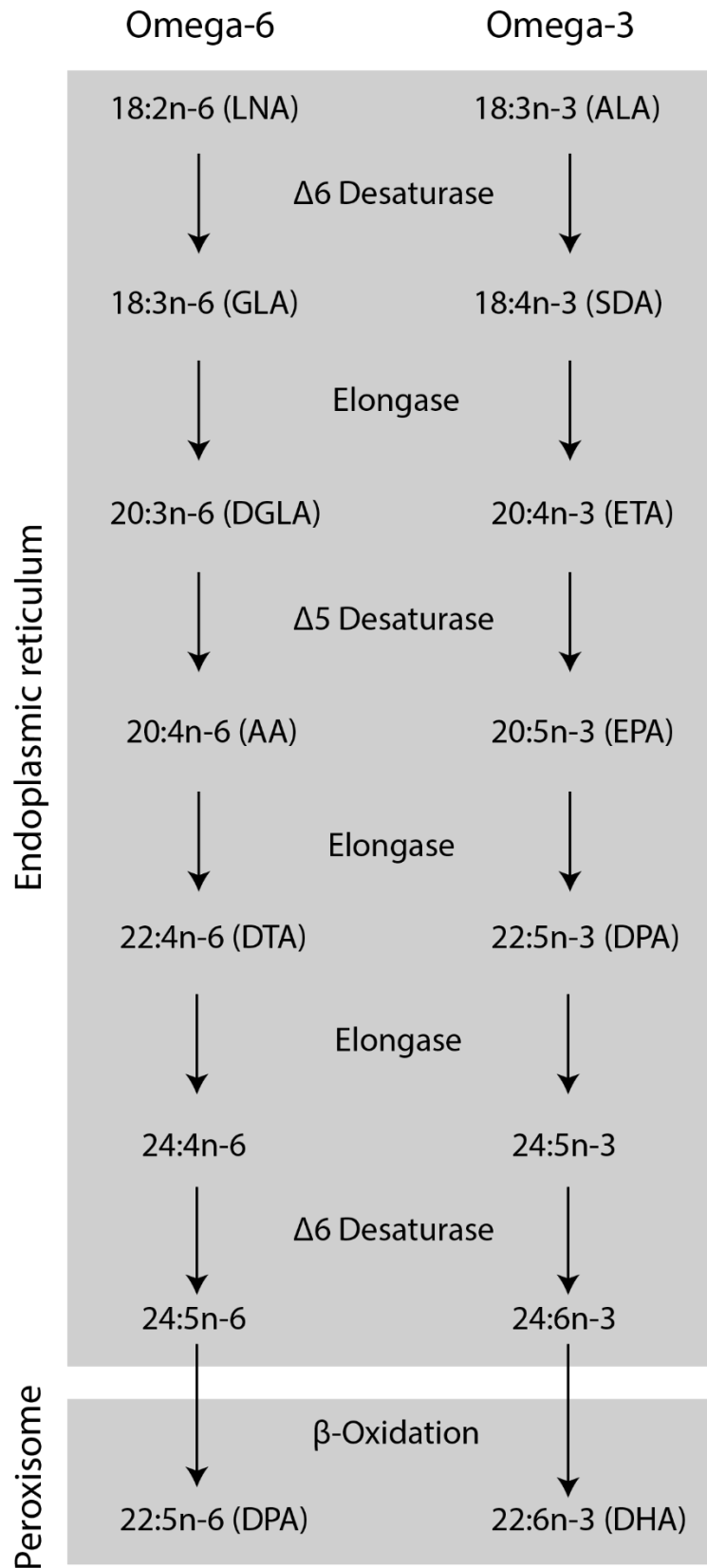


Figure 1.4 Synthesis of long-chain omega-3 and omega-6 PUFAs in the liver.

In order to gain access to cells, PUFAs have to un-bind (dissociate) from albumin or be separated from the lipoprotein via hydrolysis by lipoprotein lipases. The unbound LC-PUFAs can be absorbed into the outer leaflet of the plasma membrane. Following absorption, the PUFA must then traverse the plasma membrane (Fig. 1.5). There are 3 main ideas as to how this occurs. Firstly, by passive diffusion across the membrane, a process known as “flip—flop”, where upon the dissociation of the PUFA from the lipoprotein or albumin, it is absorbed into the outer layer and then flip-flopped to the inner membrane where it quickly dissociates and is then released into the cytosol. Other proposed methods of plasma membrane transport suggest that the FA is helped across by membrane-associated proteins. Either through a transmembrane protein (acting as a channel) or by binding the FA to aid their diffusion through the membrane, these proteins are known as fatty-acid binding proteins (FABPs) and may include the protein CD36. Recent studies have suggested that CD36 may not be a FA transporter but instead aids in the metabolism of FA and transports cholesteryl esters instead (Xu et al., 2013). Figure 1.5 illustrates the mechanisms by which LC-PUFAs cross the BBB to enter the brain. Recent studies have identified the transporter Mfsd2a as a major form of transport of DHA into the brain (Nguyen et al., 2014).

After crossing the BBB (for a detailed description of the BBB and its composition see section 6.1.3.1) into the brain, the PUFAs can be activated by the enzyme acyl-CoA synthase to fatty acyl-CoA (Watkins, 2008). PUFAs then bind to cytosolic FABPs, which guide the PUFAs to different pathways, either for esterification or metabolism (Furuhashi et al., 2011). Activated PUFAs, esterified by acyl-transferase become incorporated into the phospholipids of the plasma membrane; the LC-PUFAs most commonly involved in this way are DHA and AA (Bazinet and Layé, 2014). Different PUFAs are associated with different phospholipids with varying degrees of preference; the half-lives of PUFAs are also dependent on the phospholipids to which they are bound (Rapoport, 2001, Rapoport, 1999). The composition of the PUFAs in the phospholipid membrane is important as it can affect the signalling pathways within the cell (Graber et al., 1994). PUFAs hydrolysed from the phospholipids of the cell membrane by the action of phospholipases (e.g. PLA<sub>2</sub>), are then available to be converted into the oxygenated PUFA derivatives, called eicosanoids and docosanoids. Cyclooxygenases (COX) and

lipoygenases (LOX) are responsible for converting the free LC-PUFAs into eicosanoids (these include prostaglandins, thromboxanes, lipoxins and leukotrienes) and docosanoids (neuroprotectins and resolvins) (Tassoni et al., 2008).

The metabolism of PUFAs, in particularly LNA, ALA and EPA involves undergoing  $\beta$ -oxidation in the mitochondria, where they are converted to acetyl-CoA, which can then enter the tricarboxylic acid (TCA) cycle. Interestingly, the ATP produced by the  $\beta$ -oxidation of FAs is relatively small compared to that generated by the oxidation of glucose. This low ATP yield and the high amount of oxidative stress caused by the process of  $\beta$ -oxidation may be the reason for the low level of brain FA  $\beta$ -oxidation (Schönfeld and Reiser, 2013).

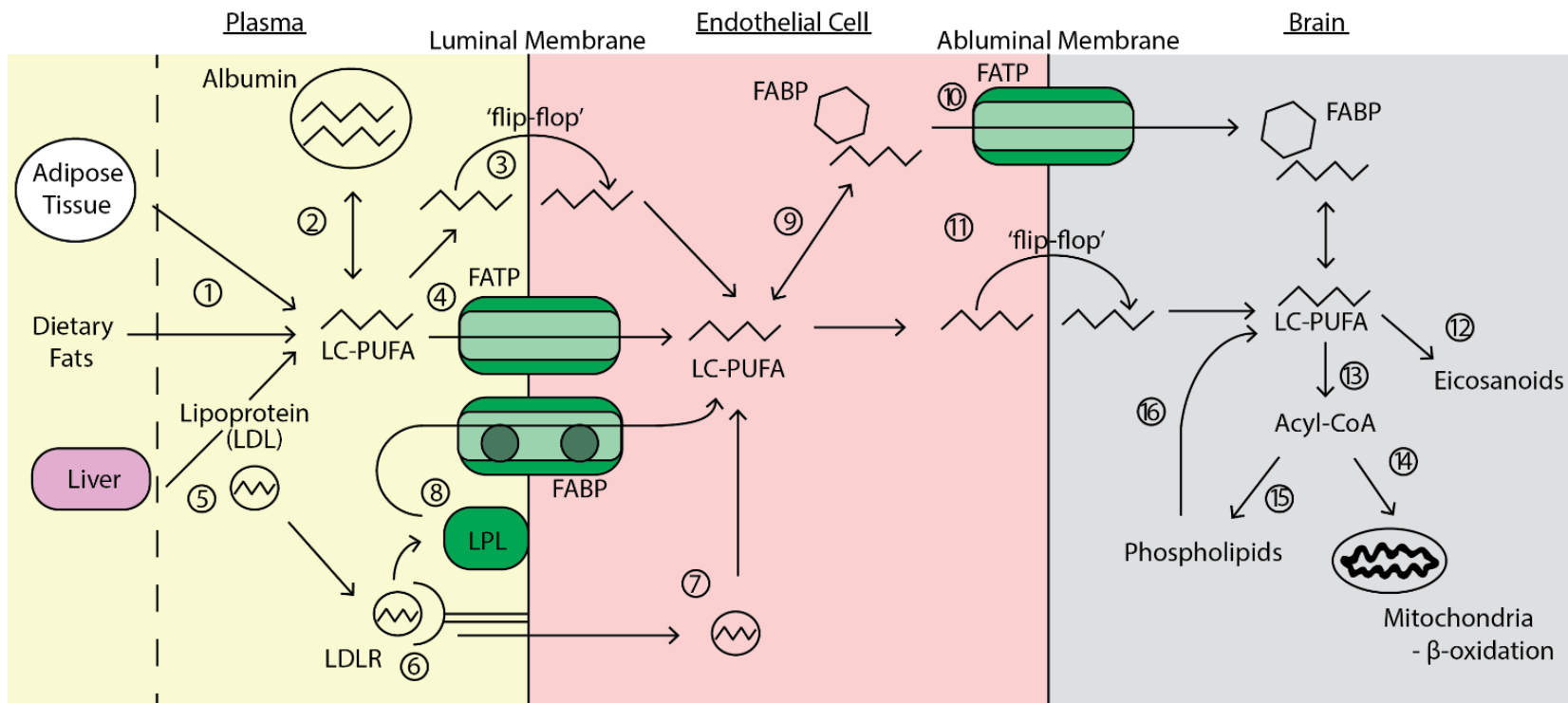


**Figure 1.5 Transport and processing of LC-PUFAs into the brain.**

LC-PUFA enter the plasma through dietary intake, as a result of metabolism in the liver or release from the adipose tissue (1). In the plasma some PUFAs are bound to albumin (2), then become unbound in order to cross the luminal plasma membrane of the endothelial cells of the blood brain barrier, either through passive diffusion via the 'flip-flop' (3) or via facilitated diffusion through a membrane fatty acid protein (FATP) (4). Other PUFAs travel to the brain in the plasma as lipoproteins, such as low-density lipoprotein (LDL) (5). LDL can bind to specific LDL receptors (LDLR), which can induce endocytosis and cross the plasma membrane (6). Once transferred across the plasma membrane, LDLs can be hydrolysed to release PUFAs (7). Alternatively, LDL interacts with a lipoprotein lipase (LPL) to produce a lysophospholipid, which can cross the plasma membrane via facilitated diffusion (8). After crossing the luminal plasma membrane the LC-PUFAs can become associated with fatty-acid binding proteins (FABP) (9) and cross the neuronal plasma membrane via facilitated diffusion (10) or passive transport (11). Once inside the cell, LC-PUFAs can be converted into eicosanoids by the enzymes, cyclooxygenase (COX) or lipoxygenase (LOX) (12). Other LC-PUFAs are activated by the enzyme acyl-CoA synthase, to become Acyl-CoA (13). From here they can enter the mitochondria and undergo  $\beta$ -oxidation, where it can then enter the TCA cycle (14), or more commonly Acyl-CoA undergoes esterification by the enzyme acyltransferase and is then incorporated into the phospholipids (15). These LC-PUFAs can be released back into the free fatty acid pool by the action of phospholipases (e.g. PLA<sub>2</sub>) (16).

## **1.5 PUFA in the CNS**

The brain tissue has one of the highest percentages of lipids in the body, second to adipose tissue (Tassoni et al., 2008). PUFAs have several roles in the brain which include modulating the function of the neuronal membrane, providing lipid mediators for cell signalling and affecting neuroplasticity. As mentioned above, PUFAs are incorporated into the phospholipids of the cell membrane. The composition of PUFAs within the membrane can affect the membrane fluidity, permeability and composition of lipid rafts (Stillwell and Wassall, 2003, Stillwell et al., 2005, Yehuda et al., 2005). The lipid mediators eicosanoids and docosanoids, which are produced by oxygenation of PUFAs by COX and LOX enzymes, can activate several signalling pathways in the brain (Dyall, 2015). Lipoxins, which are derived from AA as well as resolvins, which are derived from DHA, are both known to promote the resolution of inflammation (Farooqui et al., 2007). Neuroplasticity is affected by PUFAs hydrolysed from the membrane phospholipids; these can influence endocannabinoid signalling and synaptic plasticity. A deficiency in PUFAs in the diet has been shown to alter neuroplasticity and has been linked to impaired emotional behaviours (Lafourcade et al., 2011).

### **1.5.1 PUFAs and CNS disease**

Dietary deficiencies in LC-PUFAs, particularly omega-3 PUFAs, have been associated with several diseases, including coronary heart disease, stroke, cancers (i.e. breast, colon and prostate), autoimmune diseases (e.g. lupus) as well as CNS disorders (i.e. Alzheimer's disease and Parkinson's disease) (Connor, 2000, Janssen and Kiliaan, 2014). Due to their multiple important roles in normal brain function, dietary deficiencies in PUFAs leading to a reduction in brain PUFA levels, can lead to neurobehavioral deficits in learning and increased risk of anxiety and depression (Larrieu et al., 2012, Lafourcade et al., 2011). This link between dietary intake of PUFAs and neurodevelopmental and neuropsychiatric disorders has also been seen in the clinic, including a correlation between low intake of omega-3 PUFAs and attention deficit hyperactivity disorder (ADHD) (Hibbeln and Davis, 2009, Antalis et al., 2006). Modern day Western diets include a high amount of omega-6 PUFAs, with a corollary decrease in the amount of omega-3 PUFAs. This has led to a suggestion that Western diets

are deficient in omega-3 PUFAs (Simopoulos, 2006). Therefore, those who consume this diet are at risk of the diseases associated with a dietary deficiency in omega-3 PUFAs, as mentioned above.

As PUFA deficiency may contribute to many neurological diseases, it is thought that oral treatment with omega-3 PUFAs could be beneficial. Furthermore, acute treatment with omega-3 PUFA has also been reported to have therapeutic potential. Studies have shown that there may be some benefit in treatment with omega-3 PUFAs in Alzheimer's disease (AD), Parkinson's disease (PD), peripheral nerve injury (PNI) and spinal cord injury (SCI) (Zhao et al., 2011, de Lau et al., 2005, Gladman et al., 2012, Liu et al., 2015). These examples will be discussed below.

#### **1.5.1.1 Alzheimer's disease (AD)**

Alzheimer's disease (AD) is a progressive neurodegenerative disease that is characterised by the formation of amyloid beta plaques in the brain tissue and intraneuronal fibrillary tangles and by cognitive dysfunction, predominantly memory loss. In aging the amount of omega-3 and omega-6 PUFAs decreases and this is seen even more so in AD patients (Yehuda et al., 2002). This decrease in PUFAs is seen predominantly in the area of the brain responsible for learning and memory, including the hippocampus (Yehuda et al., 2005). In a transgenic mouse model of AD, whereby mice develop amyloid-beta plaques, a diet enriched in the omega-3 PUFA DHA helped to reduce beta-amyloid production (Lim et al., 2005). Many clinical trials have evaluated the treatment with omega-3 supplements or diets enriched in omega-3 PUFAs. A Cochrane study published this year failed to find any efficacy of the treatment with omega-3 supplementation in AD. However, it still remains unclear as to whether omega-3 supplementation may improve non-AD dementia patients (Burckhardt et al., 2016).

#### **1.5.1.2 Parkinson's disease (PD)**

Parkinson's disease (PD) is a neurodegenerative disease in which, the dopaminergic neurones of the substantia nigra progressively die, causing dysfunction of the brain's basal ganglia system and leading to the symptoms of PD (e.g. tremor, rigidity and bradykinesia). Models of PD in rodents or primary neuronal cell cultures can be created by administration of the neurotoxin methylphenylpyridinium

(MPP+), which can selectively damage dopaminergic neurones. In an *in vitro* model, the administration of the omega-3 DHA derivative NPD1 rescued primary neuronal cells from MPP+ induced apoptosis (Calandria et al., 2015). In humans, the 'Rotterdam study' was a large study that aimed to see if there was a link between dietary intake of PUFAs and reduced risk of PD. The study suggested that diets rich in monounsaturated FA and PUFAs were associated with significantly lower risk of PD (de Lau et al., 2005). More studies are required in order to elucidate whether omega-3 supplementation has any potential efficacy in the treatment of PD.

#### **1.5.1.3 Peripheral nerve injury**

Peripheral nerve injury (PNI) may be caused by trauma including compression, crush or transection of axons in the peripheral nervous system, resulting in the loss of either/or both motor and sensory function. Although, peripheral nerves are able to regenerate, unlike axons in the central nervous system (CNS), this is dependent on the distance regeneration has to occur over, as demonstrated by work done previously in our lab, by Gladman and colleagues (Gladman et al., 2012). *In vitro* omega-3 PUFAs have been shown to encourage neurite growth in primary neuronal cultures (Robson et al., 2010). From our own laboratory group, *in vitro* and *in vivo* studies with the *fat-1* transgenic mouse, a genetic mouse model that produces endogenously high levels of omega-3 PUFAs, provided evidence that omega-3 PUFAs aid recovery after PNI, possibly via neuroprotection (Gladman et al., 2012).

#### **1.5.1.4 Spinal cord injury**

The treatment of spinal cord injury (SCI) with omega-3 PUFAs has also been investigated by colleagues in our laboratory. SCI, much like TBI, has no adequate treatment at present, and affects millions of people worldwide. In our group, acute treatment with intravenous DHA injection at 30 minutes post injury promoted functional recovery and induced neuronal plasticity in rats with a cervical hemisection SCI (Liu et al., 2015). It was also previously shown that in a compression model of SCI in rats, an acute intravenous dose of DHA combined with a diet enriched in DHA reduced lipid peroxidation, macrophage infiltration, increased neuroplasticity and improved locomotor function (Huang et al., 2007). However, in a small randomised controlled trial, SCI patients were given oral DHA and EPA supplements for 14 months, a year after the initial SCI, and this supplementation failed to improve



their outcomes (Norouzi Javidan et al., 2014). This suggests that omega-3 PUFA treatment might be of benefit in SCI, if given in the acute phase.

#### **1.5.1.5 Traumatic brain injury**

The beneficial effects observed with omega-3 treatment in some diseases, especially in SCI, contribute to the hypothesis that omega-3 treatment may improve outcomes in TBI. There is also recent evidence that suggests low levels of omega-3 PUFAs in the diet impairs recovery from TBI (Desai et al., 2014). Desai and colleagues, showed that mice with a 70% deficiency in brain levels of DHA had a worse outcome when compared to the TBI only mice; they had reduced cognitive and motor function as well as an increased lesion size (Desai et al., 2014).

*In vitro* studies (as detailed in Figure 1.5) suggest that omega-3 PUFA treatment may be beneficial in TBI, due to its effects on secondary injury pathways. The omega-3 PUFA DHA has been shown *in vitro* to promote neuronal survival, prevent apoptosis, reduce inflammation and oxidative stress (Akbar et al., 2005, Chen et al., 2005, German et al., 2006, Bazan, 2005).

Further evidence that omega-3 PUFAs may be beneficial in TBI comes from a patient case study published by Lewis and colleagues. The case study describes a patient that suffered a severe head trauma and was in a vegetative state, as a result of a motor vehicle accident. At day 10 post TBI the patient started to receive very high levels of the omega-3 PUFAs (EPA and DHA), through enteral feeding, and by day 21 the patient came off the ventilator and gradually began to show physical and cognitive improvements, eventually being discharged at 4 months (Lewis et al., 2013).

The many important roles of omega-3 PUFAs in the brain, the evidence that omega-3 PUFAs may aid in the treatment of other neurological disorders and the neuroprotective effects omega-3 PUFAs have demonstrated in *in vitro* studies as well as in the SCI and PNI models in our laboratory, contributed to the hypothesis of this thesis, that omega-3 PUFAs may confer neuroprotection in TBI.

### **1.5.2 Brain phospholipids and PUFAs after TBI**

PUFAs are structural components of phospholipids and they also have signalling roles, as reviewed earlier. The phospholipids in the brain are altered following TBI and the changes correlate with patient outcome, as suggested by observations on the CSF from patients with TBI. Pasvogel and colleagues found that when compared to TBI patients that survived, TBI patients that died had higher concentrations of the phospholipids, phosphatidylethanolamine (PE) and phosphatidylcholine (PC) in their CSF, on day 1 after TBI, suggesting that the integrity of neuronal and glia cell membranes was highly disrupted after injury (Pasvogel et al., 2010). In rodent models of TBI, the composition of the phospholipid classes, as well as the level of individual PUFAs within plasma have been found to be altered. Emmerich and colleagues recently reported that at 24 hours after TBI mice had an increase in PE in plasma, and a reduction in all classes of phospholipids that contained the PUFAs AA and DHA, in the chronic stages (3, 6, 12 and 24 months) (Emmerich et al., 2016). It has also been shown that levels of AA and DHA are reduced in the cortex and cerebellum of injured mice, and a reduction in hippocampal DHA levels following TBI correlates with impaired learning ability at 3 months post injury, in the Barnes maze test (Abdullah et al., 2014).

### **1.5.3 Docosahexaenoic acid**

Docosahexaenoic acid (DHA) is found in high amounts in retinal tissue, sperm cells, synaptosomes and cortical tissue (Stillwell and Wassall, 2003, Breckenridge et al., 1972, Neill and Masters, 1973, Tinoco, 1982, Brenna and Diau, 2007). It is the most common long chain omega-3 PUFA found in the brain, and is almost 300 times more concentrated in the central nervous system than the omega-3 PUFA EPA (Chen et al., 2009). DHA enters the brain from plasma through mechanisms described in the general introduction (Fig. 1.5). Very little DHA is synthesised in the brain tissue itself via  $\beta$ -oxidation, therefore most of the DHA found in the brain comes from the diet or metabolism in the liver (Demar et al., 2005). Plasma DHA exists as non-esterified and esterified pools, and recent pharmacokinetic studies in adult rats show that the plasma non-esterified DHA is the major pool supplying the brain (Chen et al., 2015).

Phospholipids are the main components of the cell membranes and their composition can affect synaptic structure, membrane fluidity and cell signalling pathways (Wellner et al., 2011, Dyall and Michael-Titus, 2008). The different PUFAs in the CNS are preferentially incorporated into specific phospholipid classes. DHA is primarily incorporated into the phospholipid phosphatidyl ethanolamine (PE), less so into phosphatidyl choline (PC) and even less into the other classes of phospholipids at the *sn*-2 position (Stillwell and Wassall, 2003). DHA is more enriched in the inner leaflet of the cell membrane, particularly when incorporated into the phospholipid PE or phosphatidylserine (PS) (Stillwell and Wassall, 2003).

The unique structure of DHA means that when it is incorporated into phospholipids, it can alter cell membrane properties, including permeability, fluidity and cell signalling (Stillwell et al., 2005, Stillwell and Wassall, 2003). DHA has 6 double bonds which are locked in their *cis*-orientation, making them rigid and suggesting that they have limited flexibility; however, studies employing nuclear magnetic resonance spectroscopy (NMR) have produced evidence that DHA has extremely high conformational flexibility (Feller, 2008, Everts and Davis, 2000, Gawrisch et al., 2003). In a study conducted by Gawrisch and colleagues, NMR data revealed that the flexibility of the DHA chain increases from the carbonyl head group to the terminal methyl group, as the carbon-carbon bonds act like flexible 'hinges' (Gawrisch et al., 2003). When bound to membrane phospholipids, DHA is able to be in several different conformations by bending, tilting and folding. This extensive flexibility of the DHA chain can cause the phospholipid bilayers of the cell membrane to be flexible (Gawrisch et al., 2003).

#### **1.5.4 The roles of DHA in cognition**

Studies have shown that diet composition can have an impact on cognitive function. Mice fed on a diet with low levels of omega-3 PUFAs exhibit poorer performance in cognitive tests (Fedorova et al., 2007). Conversely, rats fed on a diet enriched with DHA improve their performance in cognitive behavioural tests including the radial-arm maze (Gamoh et al., 1999, Gamoh et al., 2001). In a model of impact/acceleration TBI in rats, pre-injury dietary supplementation with DHA improved performance in the MWM test (Mills et al., 2011).

The effect DHA has on cognitive performance is likely to be at least partly related to the roles DHA has within the regions of the brain responsible for learning and memory, such as the hippocampus. DHA supports hippocampal function by promoting neurogenesis. The hippocampus and the subventricular zone (SVZ) of the lateral ventricle wall are the only areas of the human adult brain able to display neurogenesis continuously, whereas the olfactory bulb in lower mammals also displays continuous neurogenesis (Eriksson et al., 1998, Ernst and Frisé, 2015). DHA promotes neurogenesis *in vivo* and *in vitro*, as demonstrated by the increase in the immunohistochemical marker of proliferating cells, 5-bromo-2'-deoxyuridine (BrdU) (Kawakita et al., 2006). It is unclear how DHA promotes neurogenesis, but suggestions include: (i) DHA increases the proliferative activity of neural stem cells (NSC) thereby increasing the number of newborn neurons, (ii) DHA encourages NSCs to exit the cell cycle to become differentiated neuronal cells, or (iii) DHA confers neuroprotection, thereby increasing the survival of newborn neurons (Kawakita et al., 2006, Insua et al., 2003, Akbar et al., 2005). The improved performance of aged rats in a spatial memory test was correlated with an increased level of neurogenesis seen in the hippocampus, and a DHA-enriched diet has been shown to up-regulate the expression of genes (e.g. *c-fos*) in the hippocampus, associated with long-term potentiation (LTP) (Drapeau et al., 2003, Tanabe et al., 2004). LTP is a model for the reinforcement of synapses through increased stimulation, which is believed to underlie synaptic plasticity and learning and memory (Bliss and Collingridge, 1993).

DHA also contributes to hippocampal function through promotion of synaptogenesis and by strengthening synaptic plasticity (Su, 2010). DHA supplementation increases the level of the growth factor brain derived neurotrophic factor (BDNF), which plays a key role in the promotion of synaptogenesis (Wu et al., 2008, Cunha et al., 2010). With an increase in the number of synapses, there is an increase in synaptic proteins such as synapsin-1, expressed at higher levels after dietary DHA supplementation (Cao et al., 2009). Through the promotion of neurogenesis and synaptogenesis, DHA supplementation can support hippocampal-based learning and memory.

As well as dietary supplementation, acute injection of DHA or of emulsions containing DHA has also been shown to confer neuroprotection. Although an acute injection cannot alter the composition of

the phospholipids in cell membranes, it has been shown to improve outcome in animals models of SCI, epilepsy and stroke (Liu et al., 2015, Trépanier et al., 2015, Williams et al., 2013, Taha et al., 2010, Hong et al., 2014, Hong et al., 2015). Our group has shown that an acute injection of DHA 30 minutes after SCI (and up to 2 hours after injury) can promote neuroplasticity, increase neuronal and glial cell survival, improve locomotor function and reduce lesion size (Liu et al., 2015, King et al., 2006). In a model of epilepsy, the subcutaneous injection of DHA an hour before pentylenetetrazol (PTZ) administration, increased the latency to seizure activity in rats, and this effect correlated with an increase in unesterified levels of DHA in the serum, without affecting brain phospholipid DHA levels (Taha et al., 2010, Trépanier et al., 2012). In models of stroke, Hong and colleagues, have shown that an i.v. dose of DHA 3 hours post-occlusion of the middle cerebral artery (MCA) improves motor function, cognition and reduces tissue loss up to 3 weeks after injury, and in the acute phase reduces BBB permeability as demonstrated by decreased Evans blue extravasation (Hong et al., 2014, Hong et al., 2015). Omega-3 PUFAs can be incorporated into emulsions and administered via injection of such emulsions. The benefit of using an emulsion for the delivery of omega-3 PUFAs is the reduction in FA oxidation and the slower release of the omega-3 PUFAs. Emulsions containing omega-3 PUFAs, particularly DHA, have also been reported to induce neuroprotection and reduction of brain tissue loss in a hypoxic-ischaemic injury in neonate animals (Williams et al., 2013).

#### **1.5.5 DHA and secondary injury mechanisms**

The mechanisms that contribute to the secondary injury after TBI include oxidative stress and neuroinflammation, which can lead to enhanced cell death via apoptosis. Neuroprotectin D1 (NPD1) is a docosanoid derived from DHA and it has been shown to have anti-inflammatory, anti-oxidative and anti-apoptotic effects (Bazan, 2005, Mukherjee et al., 2004, Bazan, 2009a, Bazan, 2009b). In a model of stroke, NPD1 infused during reperfusion down-regulated DNA damage caused by oxidative stress and reduced apoptosis through the regulation of pro- and anti-apoptotic proteins. NPD1 down-regulates the pro-apoptotic protein Bax and up-regulates the anti-apoptotic protein Bcl-2 (Bazan, 2009b). DHA

supplementation has also been shown to increase superoxide dismutase (SOD) and the silent information regulator 2 (Sir2) after TBI, which are known to have anti-oxidant effects (Wu et al., 2011).

Glial cell activation is an important part of the secondary injury inflammatory pathways. In our model of CCI, astrogliosis and microglial cell activation was induced by the injury and reflected as an up-regulation of GFAP and increase in the number of Iba1+ cells. DHA acute treatment following SCI in our laboratory and in other groups has been shown to reduce glial cell activation, by reducing microglia/macrophage number and GFAP staining (Paterniti et al., 2014, Lim et al., 2013b). DHA may modulate glial cells by reducing the amount of pro-inflammatory cytokines released from glial cells (e.g. TNF- $\alpha$  and IL-6) that would otherwise go on to further activate additional microglia and cause astrogliosis (Heras-Sandoval et al., 2016, Gupta et al., 2012).

## **1.6 Failures of TBI therapies**

After the failures of the progesterone SyNAPSe and PROTECT III trials as well as the Eurotherm3235 and EPO-TBI clinical trials, questions surrounding the reasons for these failures have been raised. The reasons, as suggested in a 2015 review by Stein are as follows (Stein, 2015):

- **Heterogeneous patient population** – The heterogeneous nature of TBI means that recruitment of a uniform patient population is impossible. Between patients, the cause, location and severity of the injury differ. Other factors are the time to hospital, post-injury complications and the patients' underlying resilience to the trauma or any pre-existing conditions.
- **Appropriate outcome measure** – Although the GOS is the most commonly used outcome measure, it has been suggested that it may not be sensitive enough. Other composite scores used to assess outcome also rely on the patient's own reporting which can be subjective. Screening for biomarkers of injury in the cerebrospinal fluid (CSF) or blood serum may be a more effective and sensitive outcome measure. Several potential biomarkers have been identified including the S100-B and glial fibrillary acidic protein (GFAP), both markers of

astroglial injury, as well as neurofilament light polypeptide, which is a marker of axonal damage (Zetterberg et al., 2013). Combining outcome scores with biomarker analysis and advanced brain imaging may produce a clearer assessment of patient outcome.

- **Ineffective dosing** – Failure of these large clinical trials may be down to sub-optimal dose or ineffective dosing schedule. There have been very few large trials comparing single dosing to sustained dosing. Also there may be failure in the translation of the preclinical doses to the clinical trial dose (Narayan et al., 2002). It is also worth remembering that at the preclinical testing phase several potential treatments are given before the injury or close to the time of injury, which does not reflect the common clinical situation.
- **Inadequate pre-clinical testing** – There could be several factors at the preclinical phase causing failures down the line in clinical trials, including false positives, anaesthesia, drug interactions, simplistic injury models, translation of drugs from animals to humans assuming trans-species validity of targets, the relevance of outcome measures and the use of genetically identical animals.

These points further reiterate the complexity, the heterogeneity and the difficulty of translation from bench to bedside of TBI. Particularly important are the potential problems with the pre-clinical testing. If another therapeutic strategy is to make it to a large scale clinical trial and prove to be efficacious, the preclinical testing needs to be of a high standard and take into consideration the points raised (Loane and Faden, 2010). The different *in vitro* and *in vivo* models of TBI used for preclinical screening are discussed below.

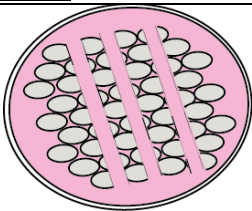
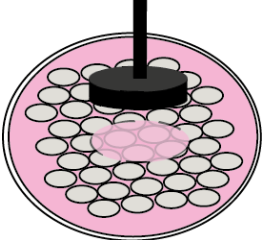
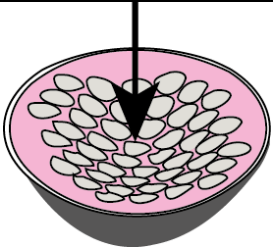
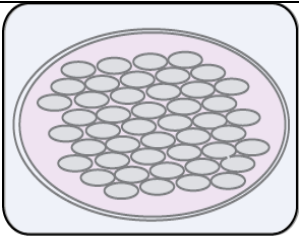
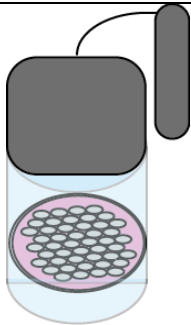
## **1.7 In vitro models of TBI**

*In vitro* models have been developed to reflect different types of TBI. There are models that mimic focal lesions by causing direct injury to tissue or cells: these include transection and weight-drop models. There are also *in vitro* models designed to reflect the shearing that neuronal cells undergo in a diffuse injury, which include a shear strain model and a shockwave blast injury model (Morrison et al., 1998). Changes in the environment *in vitro* allow the study of the response to a particular environmental change that occurs following a TBI. Such manipulations of the environment can be the modification of the glucose concentration within the media to produce hypoglycaemic conditions, or reduction in the available oxygen within the incubator, to mimic hypoxia. These models are summarised in the table below (Table 1.5).

*In vitro* models can be modified by the selection of the cell culture system. Immortalized cell lines, primary cell cultures and organotypic tissue preparations can all be subjected to any of the TBI *in vitro* models described. There are advantages and limitations to each of these culture systems, concerning viability, longevity, similarity to CNS cell types and behaviour within a culture system.



**Table 1.5. Summary of in vitro models of TBI.**

<u>Injury Model</u>	<u>Description of Injury</u>	<u>Schematic</u>	<u>References</u>
<p><u>Stylet transection/Scratch assay</u> A plastic stylet or Barkan goniotomy knife is used to create a cell free lesion along the coverslip.</p>	<p>Transected cells release intracellular glutamate and K<sup>+</sup> to mimic glutamate excitotoxicity and disruption of ion homeostasis.</p>		<p>(Tecoma et al., 1989) (Brizuela et al., 2015) (Xu et al., 2014a)</p>
<p><u>Weight-drop</u> Similar to the <i>in vivo</i> weight drop model. A known weight is dropped onto a layer of cells or onto an organotypic tissue slice.</p>	<p>The weight drop causes compression to the cells or tissue beneath it to produce axonal compression-like axonal injury.</p>		<p>(Siege et al., 1999) (Krassioukov et al., 2002)</p>
<p><u>Shear strain injury</u> Cells grown on a specialised flexcell material. The material can then be manipulated and deformed to cause a shear injury to the cells.</p>	<p>Strain injury causes cell rupture and death. Increase in axonal damage that can be changed by the duration and extent of the strain.</p>		<p>(Gladman et al., 2010, Ellis et al., 1995)</p>
<p><u>Hypoxia-Ischaemia</u> A glucose free medium is used to induce an ischaemic reaction in the cells. Cells are incubated in a low oxygen incubator to cause hypoxia.</p>	<p>Hypoglycemia causes neuronal cell death. Hypoxia causes a decrease in neurite growth and eventually cell death in neurones as well as other CNS cells.</p>		<p>(Gladman et al., 2010)</p>
<p><u>Blast Injury</u> Cells are placed in a water filled tube. A shock wave is generated through a column powered by compressed gas.</p>	<p>Shockwave injury causes cell death and indicates BBB injury in a culture of endothelial cells. Organotypic cultures also show high levels of cell death.</p>		<p>(Effgen et al., 2012)</p>

**Table 1.6 Summary of different cell culture systems.**

Cell culture system	Examples	Advantages	Limitations	References
Immortalized Cell Lines	PC12 cells, SHSY5Y cells, Glioblastoma cell lines	<ul style="list-style-type: none"> <li>• Commercially available</li> <li>• Ready supply -Can be frozen and passaged</li> <li>• Robust</li> </ul>	<ul style="list-style-type: none"> <li>• Most are not derived from neuronal cells, usually cancerous cells.</li> <li>• Not representative of CNS cells</li> </ul>	(Wang et al., 2014a) (Xu et al., 2014b)
Primary Cells	DRG cell, Astrocytes, Microglia, Cortical and Hippocampal neurones	<ul style="list-style-type: none"> <li>• CNS specific cells from targeted tissue</li> <li>• Single cell type populations can be isolated or co-cultured</li> </ul>	<ul style="list-style-type: none"> <li>• Harvesting of cells can cause damage and be a complex process</li> <li>• Short-term experiments as they cannot be passaged</li> <li>• Behaviour of cells may change ex vivo</li> </ul>	(Gladman et al., 2010) (Si et al., 2014)
Organotypic Tissue Preparations	Spinal cord, Brain slices and Hippocampal slices	<ul style="list-style-type: none"> <li>• The complex tissue is maintained ex vivo</li> <li>• Three-dimensional</li> </ul>	<ul style="list-style-type: none"> <li>• Very short-term studies</li> <li>• Tissue preparations must be thin to avoid tissue necrosis and hypoxia</li> </ul>	(Effgen et al., 2014) (Pohland et al., 2015)

The benefits of *in vitro* models make them a useful tool for the screening of potentially neuroprotective therapies for TBI. They are also useful for the investigation of the cellular and molecular secondary injury pathways that contribute to the pathophysiology following TBI. A novel *in vitro* model of TBI, which employs the use of a pneumatic impactor to create a focal injury in 3D tissue culture is described in chapter 6 of this thesis.

## 1.8 Animal modelling of TBI

Clinical TBI is very heterogeneous, and this had led to the development of several animal models that reflect different aspects of human TBI symptoms and pathologies. The two types of injury modelled most extensively in animals are focal and diffuse injuries (Xiong et al., 2013). Models that mimic focal and diffuse injuries are described below and the advantages and disadvantages of these models are detailed in Table 1.7.

- Focal injury describes a localised impact, where direct penetration of the brain tissue occurs. This causes destruction of the skull, brain parenchyma and blood vessels at the site of impact. The models that result in a focal injury include the **controlled cortical impact (CCI) model**, the **fluid percussion model** and the **weight drop model**. The CCI model causes a direct injury to the brain parenchyma with a pneumatically driven rigid impactor. **The fluid percussion model** employs a high pressure fluid bolus to cause focal destruction of the brain parenchyma. This model also induces some diffuse damage. The **weight drop model**, is where a weight is dropped directly onto the exposed brain tissue to cause a focal injury.
- Diffuse injury describes the damage caused to brain tissue, in particular neurons, when it is stretched and sheared. The animal models that mimic this type of injury include **blast injury models**, whereby animals (predominantly swine) are exposed to the shockwaves caused by an explosive blast. Diffuse injury can also be modelled in a **closed head model of rotational injury**, where animals receive rapid axial head rotations with a pneumatic actuator. The previously described **weight drop model** can be adapted to cause diffuse injury, if the weight is dropped onto a flat disk attached to the skull in order to distribute the energy across the entire brain.

**Table 1.7 The various in vivo models of TBI.** (Cernak, 2005, Xiong et al., 2013, Marklund and Hillered, 2011)

	<b>Species</b>	<b>Type of injury</b>	<b>Advantages</b>	<b>Limitations</b>
<b>Fluid Percussion Midline</b>	Swine Sheep Dog Cat Rabbit <b>Rat</b> <b>Mouse</b>	Focal and diffuse	<ul style="list-style-type: none"> <li>• Reproducible</li> <li>• No skull fracture</li> <li>• Severity easily adjusted</li> </ul>	<ul style="list-style-type: none"> <li>• Craniotomy</li> <li>• High mortality rate</li> </ul>
<b>Lateral</b>	Swine <b>Rat</b> <b>Mouse</b>	Focal and diffuse	<ul style="list-style-type: none"> <li>• Reproducible</li> <li>• Severity easily adjusted</li> </ul>	<ul style="list-style-type: none"> <li>• Craniotomy</li> <li>• High mortality rate</li> </ul>
<b>Marmarou/ Impact-acceleration</b>	<b>Rat</b> <b>Newly developed for mice</b>	Diffuse	<ul style="list-style-type: none"> <li>• Produces prolonged unconsciousness</li> </ul>	<ul style="list-style-type: none"> <li>• High mortality rate</li> <li>• Variability (between animals and centres)</li> <li>• Creates widespread diffuse injury</li> </ul>
<b>Controlled cortical impact</b>	Monkey Swine Sheep Ferret <b>Rat</b> <b>Mouse</b>	Focal	<ul style="list-style-type: none"> <li>• Injury parameters can be tightly controlled</li> <li>• Injury severity can be altered</li> <li>• Highly reproducible (between animals and centres)</li> <li>• Long lasting behavioural deficits</li> <li>• Low mortality rate</li> </ul>	<ul style="list-style-type: none"> <li>• Craniotomy</li> </ul>
<b>Weight drop</b>	<b>Rat</b> <b>Mouse</b>	Focal	<ul style="list-style-type: none"> <li>• Injury severity can be altered</li> <li>• Behavioural deficits</li> </ul>	<ul style="list-style-type: none"> <li>• Craniotomy</li> <li>• Parameters not so tightly controlled</li> <li>• Similar to the Marmarou model, but creates a localised focal injury</li> </ul>
<b>Blast injury</b>	Swine <b>Rat</b> <b>Mouse</b>	Diffuse	<ul style="list-style-type: none"> <li>• Closely mimics the injury mechanism in human TBI</li> </ul>	<ul style="list-style-type: none"> <li>• Standardised</li> </ul>

### 1.8.1 Species used in the animal modelling of TBI

The TBI models that represent focal and diffuse injuries have been conducted in a wide variety of species. Most commonly used species are rodent, but there are several models that have been adapted to use larger species, such as swine and cats. All of the species used are able to mirror some of either the neurobehavioral consequences or pathophysiological tissue changes observed in the human condition (Table 1.8).

**Table 1.8 Species used in various in vivo models of TBI.**

Species	TBI models	Pathophysiology similar to humans	References
Non-human primates	Controlled cortical Impact (CCI)	<ul style="list-style-type: none"> <li>• ↑ICP</li> </ul>	(King et al., 2010)
Swine	Closed head rotational injuries CCI Blast injury	<ul style="list-style-type: none"> <li>• Axonal injury</li> <li>• Subarachnoid haemorrhage</li> <li>• Cortical lesion</li> </ul>	(Sullivan et al., 2013) (Manley et al., 2006) (Bauman et al., 2009)
Cat	Lateral fluid percussion	<ul style="list-style-type: none"> <li>• Subarachnoid haemorrhage</li> <li>• Haematomas</li> </ul>	(Hayes et al., 1987) (Carey et al., 1990)
Rat	CCI Fluid percussion Weight drop models Blast Injury	<ul style="list-style-type: none"> <li>• Hypotension</li> <li>• Axonal Injury</li> <li>• Cortical contusion</li> <li>• Haemorrhage</li> </ul>	(Dixon et al., 1991) (Cernak et al., 2004)
Mouse	CCI Fluid percussion Weight drop models	<ul style="list-style-type: none"> <li>• BBB breakdown</li> <li>• Cortical tissue loss</li> <li>• Axonal injury</li> </ul>	(Smith et al., 1995) (Flierl et al., 2009) (Carbonell et al., 1998)

There are clear advantages and disadvantages to using a particular species in which to model TBI. The larger species have a neuroanatomy that is more representative of the human brain. Pigs and cats, like humans have a gyrencephalic cortical structure and a similar white-to-grey matter ratio (Gennarelli, 1994). Despite the clear benefits of using an animal that has neuroanatomical similarities to humans, there are limitations that need to be considered when using larger species. Firstly, the high cost of housing and maintaining larger species. Secondly, the life span of these animals make long term studies more time consuming, and therefore not suitable for a high-throughput screening of potential therapies. Thirdly, there are more substantial ethical concerns when larger species are used (Marklund and Hillered, 2011).

Rodents are the main animals used in models of TBI. Unlike the larger species, the rodents' neuroanatomy has some very obvious differences to that of a human's neuroanatomy ( Fig. 1.6). The cortices in a rodent's brain are lissencephalic. Also, the ratio of white-to-grey matter is very different (less white matter) and the olfactory bulbs make up a larger proportion of the brain than that in human (Gennarelli, 1994). Despite these differences, rodents are a much more viable option for the initial screening of a novel therapeutics due to their relative cost, size and life span. There is one other main benefit to using rodent species, in particular mice, over the larger species, and that is the ability to manipulate the genetics of a mouse to produce a desired transgenic breed (Xiong et al., 2013). Transgenic mice enable a researcher to look much more in depth at the processes contributing to the secondary injury and at novel therapies.

It could be suggested that the high number of studies conducted in rodents, as opposed to larger species, may be one of the major reasons leading to the failure of therapies for TBI. The positive neuroprotective effects of therapies seen in rodents may not be translational to human patients due to the neuroanatomical differences stated above.

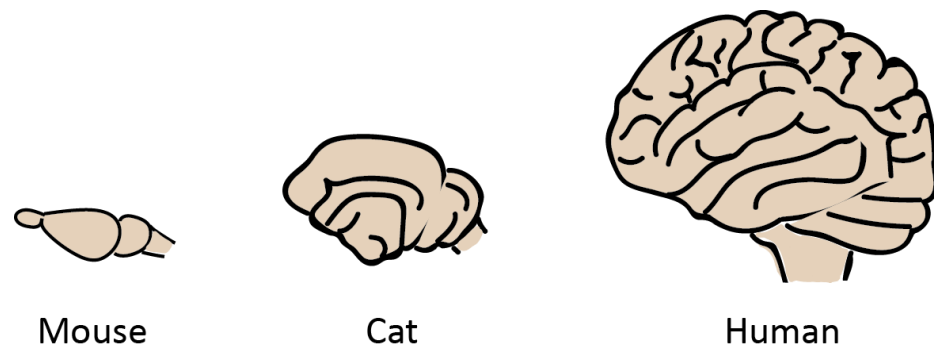


**Figure 1.6 Schematic demonstrating the differences in brain aspect between species; Mouse, Cat and Human.**

## 1.8.2 Rodent models of TBI

The model of TBI that is characterised in this thesis will be in a rodent species. Three of the most popular models of TBI conducted in rodent species include the fluid percussion model, the Marmarou model (a weight-drop model) and the controlled cortical impact model (CCI). These three models are described in detail here.

### 1.8.2.1 Fluid percussion model

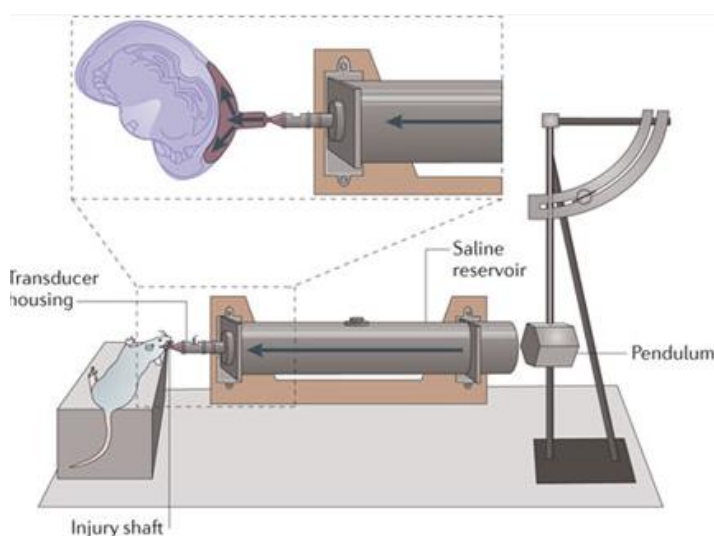


**Figure 1.7** Equipment used in the fluid percussion model of TBI. (Xiong et al., 2013).

The fluid percussion model is first mentioned in the literature in 1989 (McIntosh et al., 1989). This model causes both focal and diffuse injuries and has been adapted to mimic different types of TBI, by altering the location of the injury from a lateral location to the midline (Cortez et al., 1989, Thompson et al., 2005). The fluid percussion model employs a large piece of equipment made up of a pendulum and a saline reservoir (Fig. 1.7).

The injury is caused by the release of a pendulum onto one end of a saline reservoir (fluid filled tube), while the other end sits next to the exposed intact dura through a craniotomy. The force of the pendulum impact on one end of the tube causes a pressure wave of fluid within the tube, and this results in a fluid bolus being forced into the brain, causing a deformation of the brain tissue (Marklund

and Hillered, 2011, McIntosh et al., 1989). The severity of the injury can also be altered by increasing the pressure wave of the fluid within the tube via increasing the angle of the pendulum.

Nonetheless, the design of the equipment does allow for some errors to occur. Firstly, the dropping of the pendulum by the tester as a means of initiating the injury is not a precise method and allows for some tester error. Secondly, after the pendulum has been released and impacted the reservoir tube, it still has some momentum force. The tester should be aware of this and make sure to be prepared to catch the pendulum, before it rebounds and causes a second injury.

### **1.8.2.2 Marmarou model – impact/acceleration weight drop model**

The impact-acceleration weight drop model, was presented first by Marmarou in 1994, five years after the fluid percussion model, and is often referred to as the Marmarou model (Foda and Marmarou, 1994).

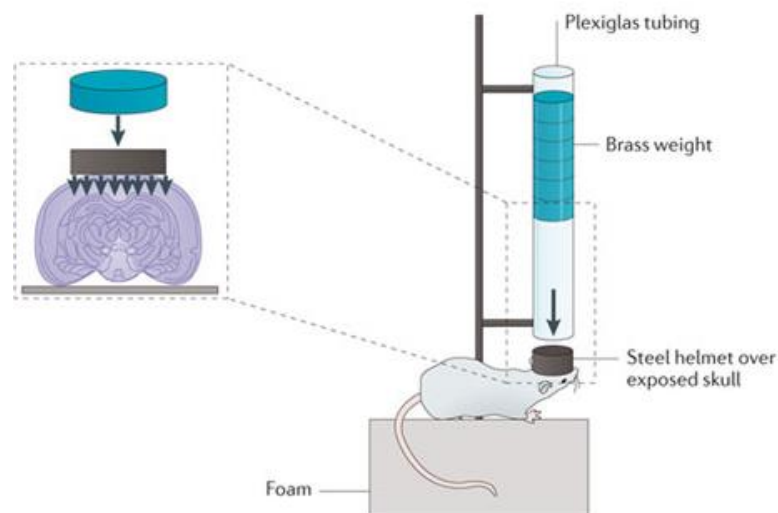


**Figure 1.8 Equipment used in the Marmarou model of TBI. (Xiong et al., 2013)**

This model creates a global diffuse injury throughout the rodent's brain. It does this by having a weight falling onto a steel disc that is glued to the skull of the rodent. The head of the rodent rests on a piece of foam, with a defined 'spring constant', to allow a controlled movement of the head after impact (Marmarou, 1994; Morales, 2005). The injury causes widespread axonal injury, due to the steel disc distributing the energy of the impact over the whole brain (Morales et al., 2005).



This model is able to replicate the diffuse injury without causing a focal lesion, similar to the injury observed from a motor vehicle accident. The diffuse injury occurs because of acceleration and deceleration forces causing the brain to move within the skull (Foda and Marmarou, 1994). Consequently, the axons shear and become damaged, which leads to Wallerian degeneration and eventually neuronal cell death. The main advantage of this model is the ability to isolate the diffuse injury and investigate the diffuse pathophysiology alone. This model is also able to achieve prolonged unconsciousness in rodents, an aspect of TBI that most models do not replicate (Marmarou, 1994)

The Marmarou model, much like the fluid percussion model relies on the impact of a falling weight (or pendulum), so important to prevent a rebound injury. Another similarity is the complexity of the equipment used to initiate the injury. These problems may be overcome with the increased use of the equipment.

### **1.8.2.3 Controlled cortical impact model (CCI)**

The controlled cortical impact (CCI) model is an example of a model that causes a focal injury by direct brain deformation (Fig. 1.9) (Lighthall, 1988).

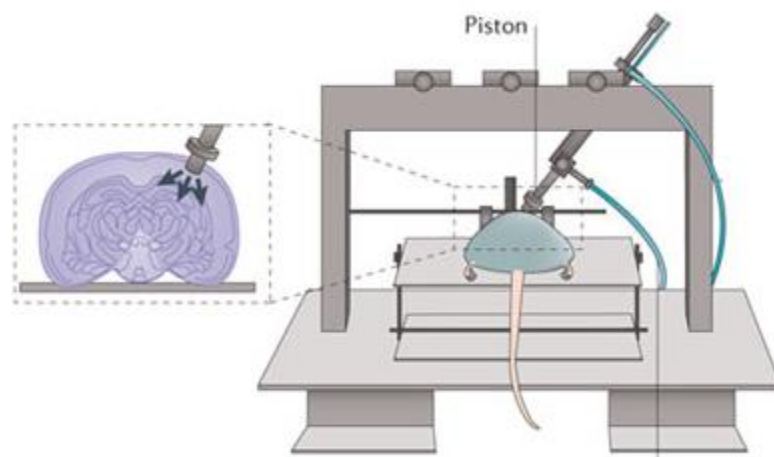


**Figure 1.9 Equipment used in the controlled cortical impact model of TBI. (Xiong et al., 2013)**

This model was first developed in ferrets, but then later in rats and mice (Dixon et al., 1991, Smith et al., 1995). To deliver CCI to a rodent, a craniotomy is performed over one hemisphere. Then, a

pneumatically driven rigid impactor strikes the intact dura mater to cause deformation of the brain tissue (Marklund and Hillered, 2011). The pathophysiology following CCI has been shown to include brain oedema, elevated intracerebral pressure, reduced cortical perfusion, decreased cerebral blood flow, as well as neuroendocrine and metabolic changes, which are hallmarks of clinical TBI (Baskaya, 1997; Cherian, 1994; Bryan, 1995; Prasad, 1994).

The pneumatically driven rigid impactor is operated via a computer, and the parameters can therefore be tightly controlled. These parameters include impactor velocity, depth of impact and dwell time (O'Connor et al., 2011). The ability to stringently control the various parameters limits the variability between each injury conducted for each rodent. This high reproducibility between injuries is very important in the early stages of pharmacological screening in order to determine the efficacy of a new therapeutic agent.

The equipment needed to perform this model is relatively simple and its design means that there is no risk of rebound injury (O'Connor et al., 2011). This model can offer high reproducibility of injury between animals and between centres due to the parameters of the injury being digitally controlled. Despite the technical advantages of this model over the fluid percussion and Marmarou model, the CCI model does have some disadvantages that are worth considering. Firstly, the lesion size caused by the impactor is relatively large. This large lesion size is not comparable to that of the injuries seen in human patients that survive a TBI. Secondly, and similarly to the fluid percussion model, a craniotomy needs to be performed prior to the injury. A craniotomy obviously does not reflect the usual pathology of a human TBI and may attenuate secondary brain swelling if the bone flap is not replaced (Zweckberger, 2006; De Bonis, 2010). Nonetheless, a craniotomy does mean that there is no risk of skull fracture in the rodent, which would cause further damage, leading to a more heterogeneous injury between animals, lowering the reproducibility and negating the model's use as a therapeutic screening tool. Overall, this model has high reproducibility, is good as a therapeutic screening tool and is technically relatively simple to operate.

### **1.8.3 Behavioural outcome measures**

The symptoms suffered by TBI patients vary depending on the type, location and severity of the TBI. After a TBI, complex cognition and personality changes may develop. Due to the significant impact that neurobehavioural symptoms have on a patient's quality of life, a key outcome measure for *in vivo* models of TBI must be a deficit in relevant behavioural tests. Behavioural analysis in rodents includes many established tests that assess different aspects of behaviour, and monitor anxiety, learning, memory and motor function. The most common neurobehavioural outcome assessed in rodent models of TBI are cognitive and motor dysfunction. These commonly used behavioural tests are reviewed below and in Table 1.9.

#### **1.8.3.1 Open field**

The open field test measures the exploratory behaviour of a rodent within a confined space, e.g. a Perspex box. The behaviour of the rodent within the box can be used as an index of general locomotor activity and has also been interpreted to reflect the anxiety of the animal exposed to a new environment. The open field has been used to test these behaviours in a variety of models of neurological conditions, including TBI. TBI patients can experience symptoms including anxiety and motor dysfunction and therefore this behavioural test would be a relevant outcome measure in the assessment of a TBI rodent model. With reference to anxiety, rodents that spend a reduced amount of time in the central zone and an increased amount of time next to the walls of the open field are indicating anxiety-related behaviours (Jones et al., 2008). In a lateral fluid percussion model, rats that received a severe injury spent less time in the central zone, suggesting that they were more anxious than the control groups (Jones et al., 2008). Using this test as a measure of anxiety is contested, as noted in a review of the literature, as mice treated with certain anxiolytic drugs did not exhibit reduced anxiety-related behaviours in the open field (Prut and Belzung, 2003).

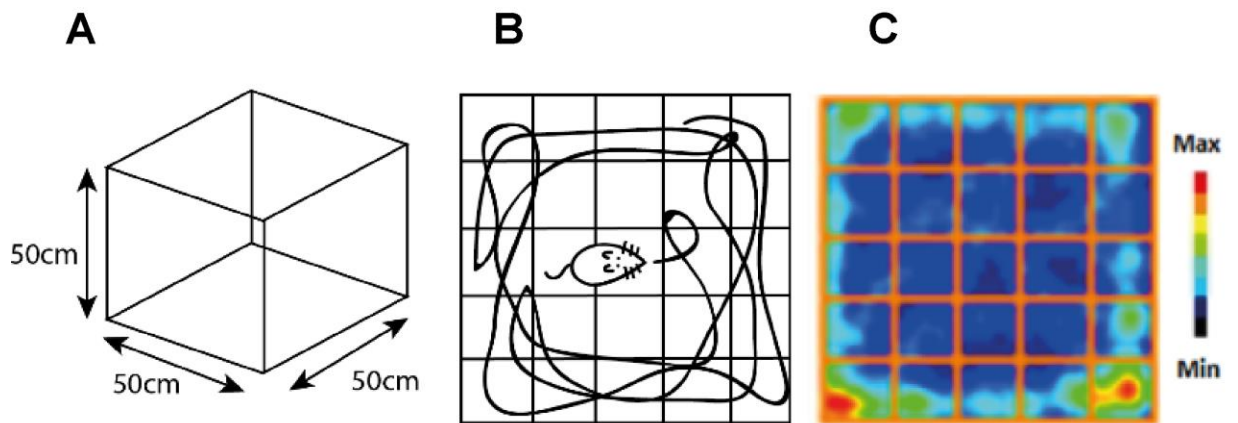


**Figure 1.10 Open field test.** Dimensions of Perspex box (A), behaviour of rodent during the test (B) and an illustrated outcome measure of the open field test (C).

The distance travelled within the open field is an outcome measure that can be used to assess the locomotor activity of the rodent. After a CCI injury, mice that received a severe injury showed a decrease in the distance travelled and therefore exhibited reduced locomotor activity (Zhao et al., 2012b). Reduced locomotor activity may also reflect other symptoms induced by the CCI injury, including anxiety, depression, habituation to the test apparatus or motor dysfunction. It would take further behavioural testing to decipher the precise cause of the reduced locomotor activity.

**Table 1.9 Example of behavioural tests used as outcome measures in animal TBI models.** (Armario and Nadal, 2013, Xiong et al., 2013, Schaar et al., 2010)

Behavioural Test	Behavioural outcome						Test Paradigm	Strengths of the Test	Limitations of the Test
	Learning	Memory	Gross Motor Function	Anxiety-related	Sensorimotor	Mood Disorder			
Morris Water Maze	+	+	-	-	-	-	An acquisition phase of 2-4 swimming trials a day for 4 days, in which the animal should learn to locate the hidden platform. At 24 hours after the last acquisition trial, a probe trial (with the platform removed) is performed.	<ul style="list-style-type: none"> <li>-Gold standard test for memory deficits</li> <li>-Tests for deficits in the animal's ability to learn</li> <li>-Tests spatial memory</li> <li>-No pre-test starvation</li> <li>-Paradigm is adaptable</li> </ul>	<ul style="list-style-type: none"> <li>-Results can be affected by a number of factors including water temperature, home cage environment, testing room environment.</li> </ul>
Y-Maze	+	+	-	-	-	-	An acquisition trial (5– 15 minutes), in which one arm is blocked. After an interval time of up to 2 hours there is a retrieval trial. The animal is allowed to explore all 3 arms of the maze.	<ul style="list-style-type: none"> <li>-Tests for deficits in the animal's ability to learn</li> <li>-Tests spatial memory</li> <li>-No pre-test starvation</li> <li>-Paradigm is adaptable – spontaneous arm alternation.</li> </ul>	<ul style="list-style-type: none"> <li>-Results can be affected by testing environment.</li> <li>-Time consuming</li> <li>-Habituation</li> </ul>
Elevated Plus-Maze	-	-	-	+	-	-	Animals are allowed to explore the open and enclosed arms for a 5 minute trial.	<ul style="list-style-type: none"> <li>-No pre-test starvation</li> <li>-Short testing period</li> <li>-No pre-training required</li> </ul>	<ul style="list-style-type: none"> <li>-Results can be affected by exposure to previous behavioural tests, previous handling, testing environment</li> <li>-Intra-lab variability</li> </ul>

Novel Object Recognition	+	+	-	-	-	-	Animals are exposed to 2 identical objects within an open-field. After a 24 hour interval time, the animals are placed back in the test with 1 familiar object and 1 unfamiliar object.	-No pre-test starvation -Paradigm is adaptable	-Results can be affected by exposure to previous behavioural tests, olfactory stimuli, testing environment.
Neurological Severity Score	-	-	+	-	+	-	Animals are given a score on the completion of 10 tasks including – beam balance, beam walking, startle reflex, paresis and seeking behaviour. These tasks can be repeated every 24 hours.	-No pre-test starvation -Simple to administer	-Composite score may mask individual deficits -Results can be affected by exposure to previous behavioural tests, olfactory stimuli, testing environment .
Forced Swim Test	-	-	-	-	-	+	Mice are forced to swim in a narrow beaker of water for 6 minutes.	-No pre-test starvation -Simple, low cost	-Swimming performance between tests can be markedly different, due to adaptation rather than depressed behaviour.
Open-Field Test	-	-	+	+	-	-	Animals are allowed to explore an open field test environment for a 5 – 30 minute trial. These trials can be repeated throughout the study.	-No pre-test starvation -Paradigm is adaptable -Measures multiple behaviours.	-Results can be affected by olfactory stimuli and testing environment.

### 1.8.3.2 The Y-maze

The Y-maze has been used to test memory function by exploiting rodents' natural exploratory behaviour. There are two main protocols for the Y-maze in which one of the three arms is blocked, in order to create an arm within the maze that will be novel to the test rodent (Sarnyai et al., 2000). Once exposed to the novel arm, the amount of time the animal spends in the novel arm is indicative of the rodent's memory function, as the rodent recognises its novelty and spends time exploring it. Mice that received a hippocampal lesion failed to recognise the novel arm, thereby providing evidence that the Y-maze is a useful test for memory (Sanderson et al., 2007). As with other cognitive behavioural tests, results from the Y-maze can be misinterpreted for a number of reasons, for example if the locomotor activity is altered, the time spent exploring the novel arm may be lessened (Sanderson et al., 2010).

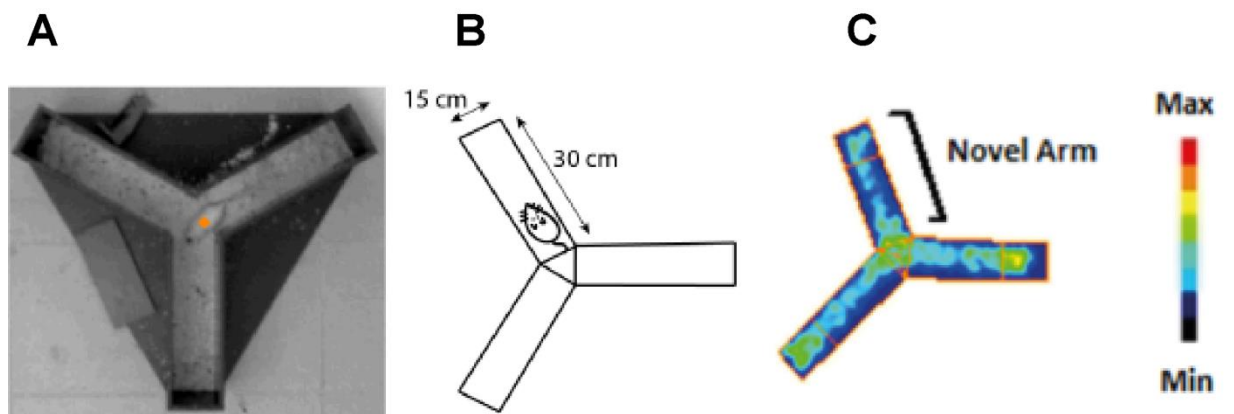


**Figure 1.11 Y-maze test.** Actual image of the apparatus in use (A), behaviour of rodent during the test (B) and illustrate the outcome measure of the Y-maze test (C).

### **1.8.3.3 Morris Water Maze**

The most regularly used test for learning and memory dysfunction is the Morris water maze (MWM). This test has been used to evaluate memory deficits in neurodegenerative disease models such as AD models, as well as for discriminating between young and aged rodents (Buccafusco JJ, 2009, D'Hooge and De Deyn, 2001). It has also been used to distinguish between experimental brain lesion severities in mice (Washington et al., 2012, Smith et al., 1991).

The MWM test is a complex task that requires the rodent to employ a range of neurological processes. The aim of the task is to locate the hidden platform within the water tank, therefore escaping the water. It is the impetus to escape the water that motivates the animal to locate the platform. During the acquisition phase, the rodent is required to learn to navigate its way to the platform by using the visual cues that surround the tank. In order to complete this task the rodent must employ place learning and spatial memory (Buccafusco JJ, 2009, Morris, 1984). The brain region essential for these processes is the hippocampus. Bilateral and unilateral hippocampal lesions in rats and mice have resulted in complete or severely impaired performance in the MWM task (D'Hooge and De Deyn, 2001, Clark et al., 2005). The hippocampus is one of the main brain regions damaged by a TBI, independent of the location and severity of the TBI (Kotapka et al., 1994).

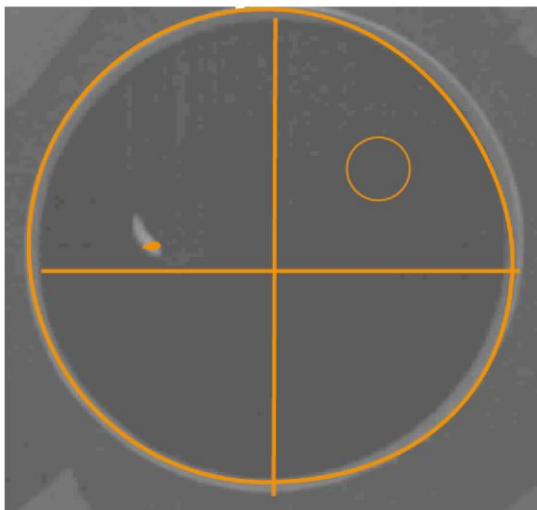
This test is useful for assessing both the animal's ability to learn during the acquisition phase and its memory in the probe trial. The dual outcome measures allow the evaluation of the cognitive aftermath of a TBI without pre-injury training and without pre-test food deprivation. Despite the multiple useful outcome measures this test provides, it does have limitations. These include the size of the test equipment, the time taken to perform this test and the substantial effect external environmental factors have on the performance of the animals within the test (Vorhees and Williams, 2006). As with the Y-maze test, the locomotor function of the animal can impact upon the animal's performance in the test. Therefore, additional outcome measures, such as average speed as well as concurrently running locomotor activity testing are of benefit.



The limitations of the MWM may not be restricted to the operation of the test, but may include the misinterpretation of the outcome measures. An increased latency to the platform zone is interpreted as impaired memory function, and this assumes that the animal is attempting to employ a cognitive strategy to locate the platform and failing. However, it does not take into consideration the likelihood that an animal may be using a non-cognitive strategy such as thigmotaxis, that may be lengthening their latency time, thus leading to the mistaken assumption that these animals are memory-impaired (Wolfer et al., 1998).

The MWM may have its limitations, but as one of the most frequently used and widely accepted cognitive tests, it is a good and accessible behavioural tool for the evaluation of memory impairment in *in vivo* models of TBI. Notwithstanding the benefits of behavioural testing for preclinical screening of novel therapeutics, assessment of some of the subtle changes in cognitive and psychiatric behaviour (e.g. speech and mood disorders) following TBI cannot be carried out.

**A**



**B**



**Figure 1.12 Morris water maze test.** Actual image of apparatus in use (A) and representative trace of route to the platform (B).

## 1.9 Aims

The main aims of this thesis are as follows:

- 1) To optimise and characterise a mouse model of TBI with behavioural and histological endpoints.
- 2) To investigate whether treatment with the omega-3 fatty acid docosahexaenoic acid improves outcome in a mouse model of TBI.
- 3) To investigate whether a sustained high level of endogenous omega-3 fatty acids in the transgenic *fat-1* mouse can lead to an improved outcome after TBI.
- 4) To set up and characterise an in vitro model of mechanical injury for the study of the effects of docosahexaenoic acid on specific cell populations.

## **2 Methods and Materials**

### **2.1 In vivo studies**

#### **2.1.1 Animals**

All animal procedures were approved by the Animal Welfare and Ethics Committee of Queen Mary University of London, in accordance with the United Kingdom Animals (Scientific Procedures) Act 1986 and with international guidelines on the ethical use of animals. All animals were maintained on a 12 hour light/dark cycle with ad libitum access to food and water and at a temperature of  $21 \pm 1^\circ\text{C}$ .

Mice used were either male CD1 mice at 10-12 weeks old or transgenic *fat-1* mice with aged and sex matched C57BL/6 mice as control, as indicated in the corresponding chapters.

The original *fat-1* breeders were provided by Dr J.X. Kang (Harvard University, Massachusetts, USA) and the colony was maintained in house by mating heterozygous *fat-1* mice with wild type C57BL/6 mice purchased from Charles River UK, Ltd (Margate, UK). Heterozygous male mice 49-53 weeks old (aged), male mice 10-12 weeks old (young adult) and female mice aged 10-12 weeks old (young adult) and wild-type littermates were used in the studies. The genotypes of these mice were verified by PCR analysis of ear punches, provided by Charles River Laboratories (Margate, UK).

The phenotype of the *fat-1* mice was also reliant on the mice being fed on an omega-6 PUFA rich diet (Kang et al., 2004). The special omega-6 PUFA rich diet was fed to both *fat-1* and wild-type littermates (AIN-76A diet containing 10% corn oil, TestDiet UK, Product no. 1812592; Appendix 1.2) and animals were allowed access to the diet and water ad libitum. The diet was changed daily and stored at  $-20^\circ\text{C}$  to prevent oxidation of the omega-6 PUFAs in the diet. Aged and gender matched C57BL/6 mice bought from Charles River Laboratories (Margate, UK) were used as controls and were fed on a standard diet (RM1, Special Diets Services, Lillico Biotechnology, Surrey; Appendix 1.3).

#### **2.1.2 Surgery**

The CCI model was chosen due to the reasons discussed in section 1.8.2.3, the model is reproducible between animals and centres, unlike several other TBI animal models. It was also chosen because the

CCI equipment in was already being employed in a contusion model of spinal cord injury with our lab group.

All the controlled cortical impact (CCI) surgeries in mice were performed by the author. Mice were anaesthetized with a mixture of ketamine (50 mg/kg) and medetomidine (10 mg/kg) intraperitoneally (i.p.) and given pre-emptively analgesia buprenorphine (0.05 mg/kg) subcutaneously (s.c.). Surgical anaesthesia was confirmed by loss of the tail pinch reflex and corneal reflex. Anaesthesia depth was monitored throughout the surgery by monitoring the respiration rate.

Mice were placed into a stereotaxic frame and secured with mouse teeth bar and guinea pig ear bars. A midline incision was made to expose the skull and a 3.5 mm craniotomy was made over the right parietal bone (central point was at -2.0 mm bregma, 2.5 mm lateral) using a 0.5 mm diameter burr bit connected to a hand held dental drill. Care was taken so that the dura mater was undisturbed during the drilling and the removal of the skull flap.

The contusion was carried out using the Hatteras PinPoint controlled cortical impactor (Hatteras Instruments, USA) (Fig. 2.1). The parameters used were: 3.0 m/s velocity, 100 ms dwell time, and 20° angle. The injury severity (based on behavioural tests) was determined by the impact depth; 1.5 mm (very mild), 2.0 mm (mild), and 2.2 mm (moderate). Sham injury mice received a craniotomy only. After the injury, the skull bone flap was replaced, the skin sutured and the animal placed into a warm incubator (27-28°C) to recover. In certain studies, agents were administered intravenously (i.v.) at 30 min post-injury. Approximately 45 min after the anaesthesia of the animal, atipamezole (Antisedan, 2 mg/kg, s.c.) and sterile saline (100 ml/kg, s.c.) were administered to reverse the anaesthetic effect and provide rehydration, respectively. Each mouse was housed separated after surgery to prevent fighting and the interference with the surgery site such as removal of sutures. Post-operative care involved daily weight monitoring and twice daily administration of buprenorphine (0.05 mg/kg, s.c.) until there was weight gain.

### **2.1.3 DHA preparation and administration**

Stock solutions of the free fatty acid DHA (Sigma, Dorset, UK) were made up in ethanol under 100% nitrogen. Each 5  $\mu$ l 1 M stock aliquots were kept in light sensitive, airtight glass containers (Agilent, Stockport, UK) and were stored at -20°C until required. An aliquot of the stock solution was diluted initially with 50  $\mu$ l 100% ethanol and then to a final concentration providing the dose required (500 nmol/kg) with sterile saline (NaCl 0.9%). DHA or vehicle (Veh) was administered intravenously via a tail vein 30 minutes post-injury in a volume of 5 ml/kg. The injections were administered by Mr Meirion Davies, another member of the laboratory, to keep the experimenters blinded to the treatment received.

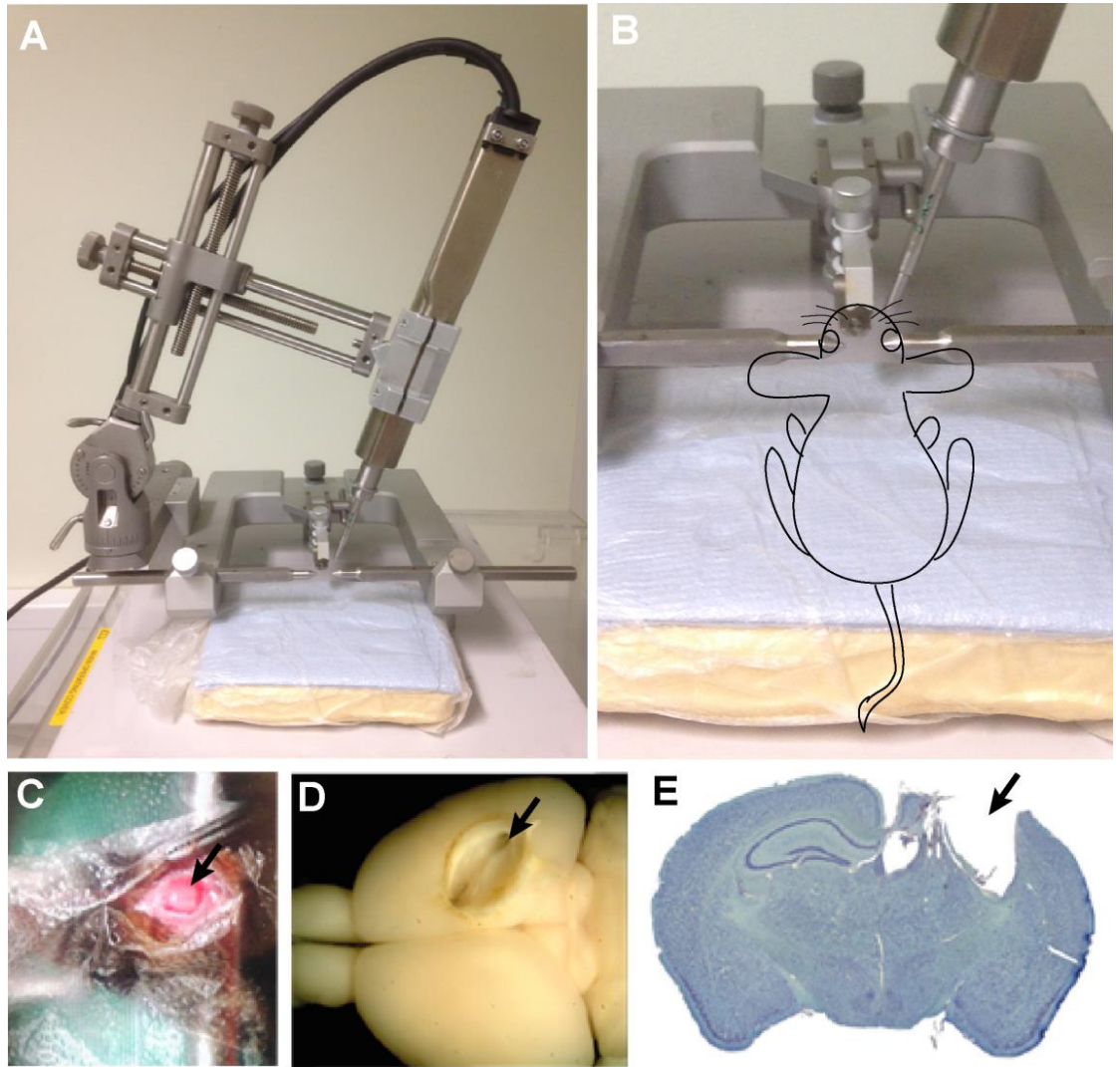


**Figure 2.1 Surgical setup for the controlled cortical impact injury (CCI) in mice.** (A) Apparatus used to carry out the cortical impact using the computer controlled pneumatic device. (B) Positioning of the mouse during the surgery. (C) Mouse covered in a sterile plastic surgical drape with a craniotomy (arrow). (D) Macroimage of the unilateral CCI injury (arrow) in a mouse brain at 28 days post injury. (E) Toluidine Blue stained coronal brain section with a unilateral CCI injury (arrow) at 28 days post injury.

## 2.1.4 Behavioural studies

### 2.1.4.1 Open field test

The open field test was conducted on day 1, 7, 14, 21 and 28 post-injury. The mice were placed in a 50 cm x 50 cm black box in low lighting and were allowed to explore for 5 minutes (Fig. 2.2). The base of the box was divided into 25 (10 cm x 10 cm) square zones. The distance travelled, the speed, time spent immobile and the number of line crossings made by the mice was recorded and tracked using the software ANYmaze (San Diego Instruments, USA).

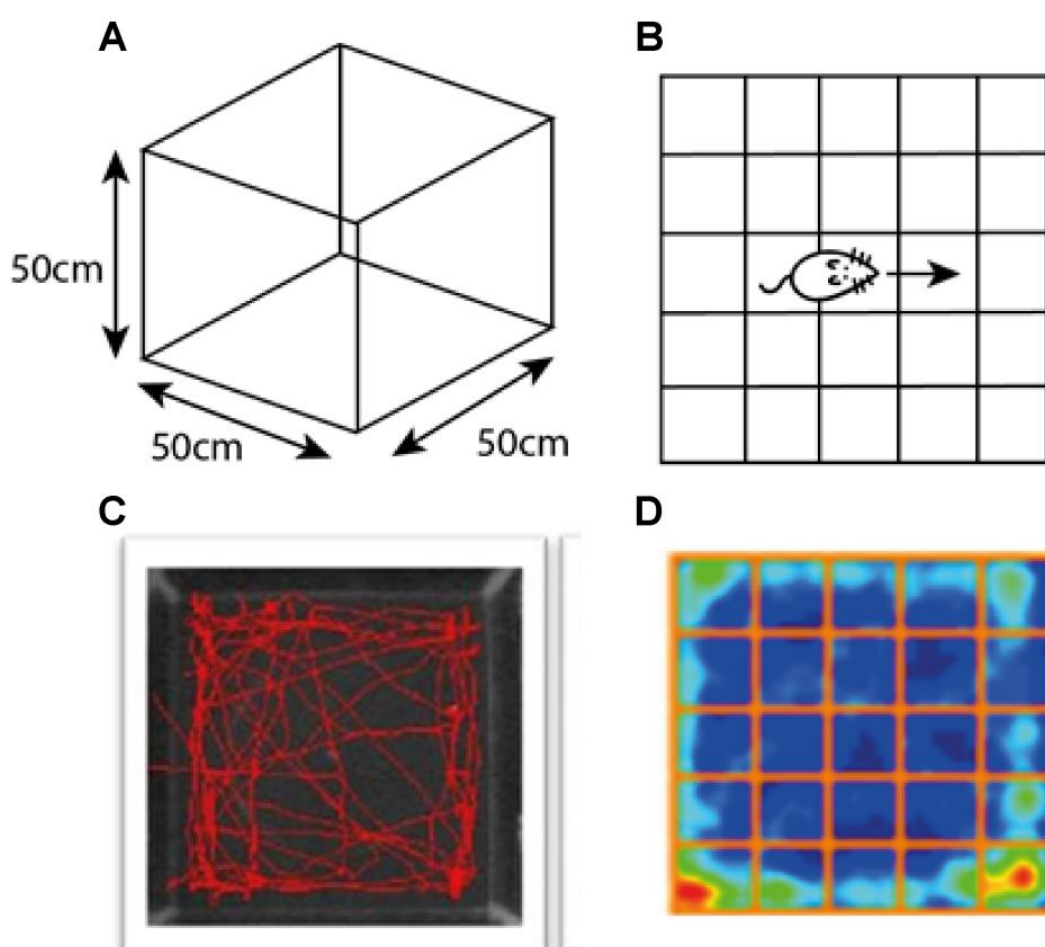


**Figure 2.2 Open field test.** (A) Dimensions of the open field. (B) Division of the base into 10 x 10 cm square zones (C) An example of an exploration trace created by the ANYmaze software (D) An example of an occupancy plot showing the frequency of the mouse at a particular region observed during the testing period.

### 2.1.4.2 Y maze test

The maze comprises of three arms (30 cm x 15 cm) at an angle of 120° from each other, with a different visual cue at the end of each arm. One arm was selected as the start arm and one arm was selected to be blocked off, to later become the novel arm. The animal was placed in the start arm and was allowed to explore the two open arms of the maze for 5 minutes. The animal was then removed; 2 hours later it was placed back into the maze. During this time, all three arms were open and available to explore for 5 minutes. It is expected that the 'novel' unexplored arm would encourage longer exploration in healthy mice (Wright and Conrad, 2005, Sanderson et al., 2009). This 'retention' trial used the ANYmaze software (San Diego Instruments, USA) to record the amount of time the animal spent in the novel arm (Fig. 2.3).

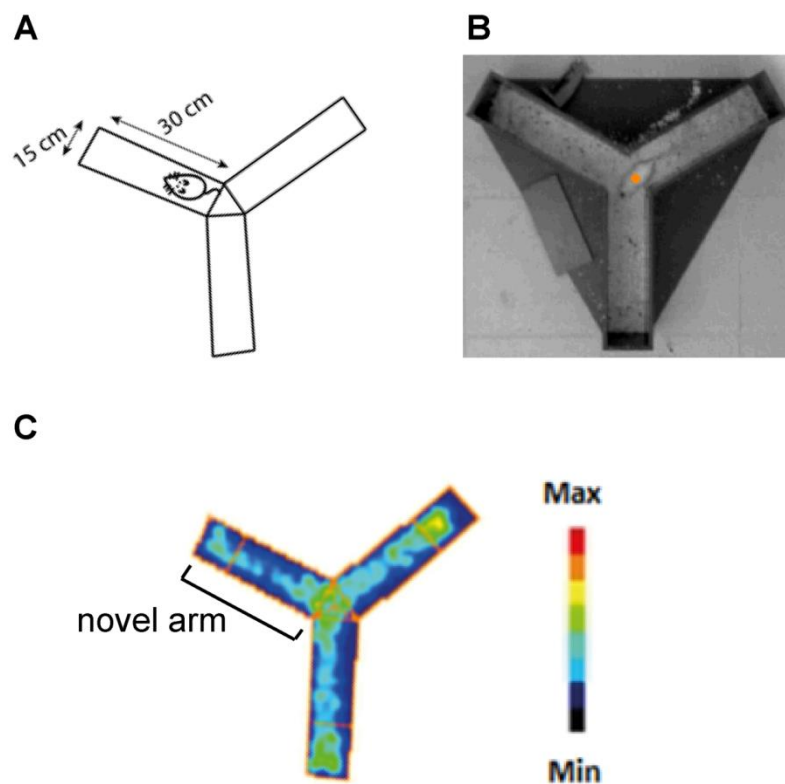


**Figure 2.3 . Y maze test.** (A) Dimensions of the Y maze. (B) A screen capture of a mouse marked with an orange dot, during the Y maze test (C) An example of an occupancy plot showing the frequency of presence of the mouse in different arms of the Y maze, observed during the testing period.



### **2.1.4.3 Morris water maze test**

The protocol for the Morris water maze test (MWM) used was adapted from (Washington et al., 2012). It was conducted in very low lighting and mice were allowed to acclimatise to the room for 4 hours prior to testing. The MWM test was performed on days 15-19 and 22-26 after CCI injury (Fig. 2.4). The water maze tank was 100 cm in diameter and filled with water that was maintained at 26°C and made opaque using black or white water-based paint (dependent on mouse strain) (Fig. 2.5). Extra-maze spatial cues were hung on the walls of the tent in which the tank was located. The platform was 10 cm in diameter and was submerged 1 cm below the surface of the water. The initial training of the mice took place on days 15-18 (initial acquisition phase) and consisted of 4 trials per day. The mice were placed into the tank at one of the four entry points, each entry point was located in the middle of each compass-related quadrant (NE, SE, SW & NW), and each of these entry points was used by each mouse on every day of the acquisition phase. The interval time between each trial for each mouse was 20 minutes. The location of the platform stayed the same throughout the initial training. The mice were given 90 seconds to locate the platform within the tank and remained on the platform for 10 seconds before they were removed. Mice that did not find the platform in the 90 seconds were placed on the platform for 10 seconds before being removed. The tracking software ANYmaze (San Diego Instruments) was used to record the latency to reach the platform. On day 19 after injury (24 hours after the last trial of the training phase), a probe trial was conducted in which the platform was removed and the animal was tracked over a 90 second trial. The latency to enter the zone where the platform used to be located was measured, as well as the number of times this zone was crossed and the time spent within the platform quadrant (NE). This training phase and probe trial was then repeated from day 22 onward, and the platform was repositioned in the opposite quadrant (reverse platform; SW) to the one in which the original platform was located. During the probe trial on day 26, the latency to the platform zone, the line crossings and time spent in the various quadrants were recorded, for both the original platform and the reverse platform zone. This protocol was shortened to just one week of acquisition training (day 15 – 18) and one probe trial (day 19), and no reverse protocol, for the studies conducted with the transgenic *fat-1* mice.

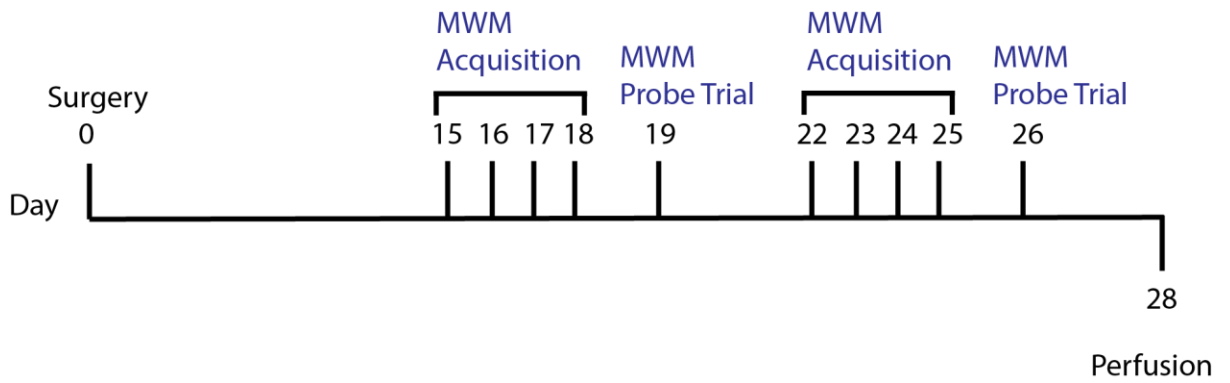


**Figure 2.4 Training and testing schedule for the Morris water maze.** Studies were stopped after the first probe trial (day 19) and animals perfused at day 21, while some other trials continued with another set of training and probe trial (day 26) and animals perfused at day 28.

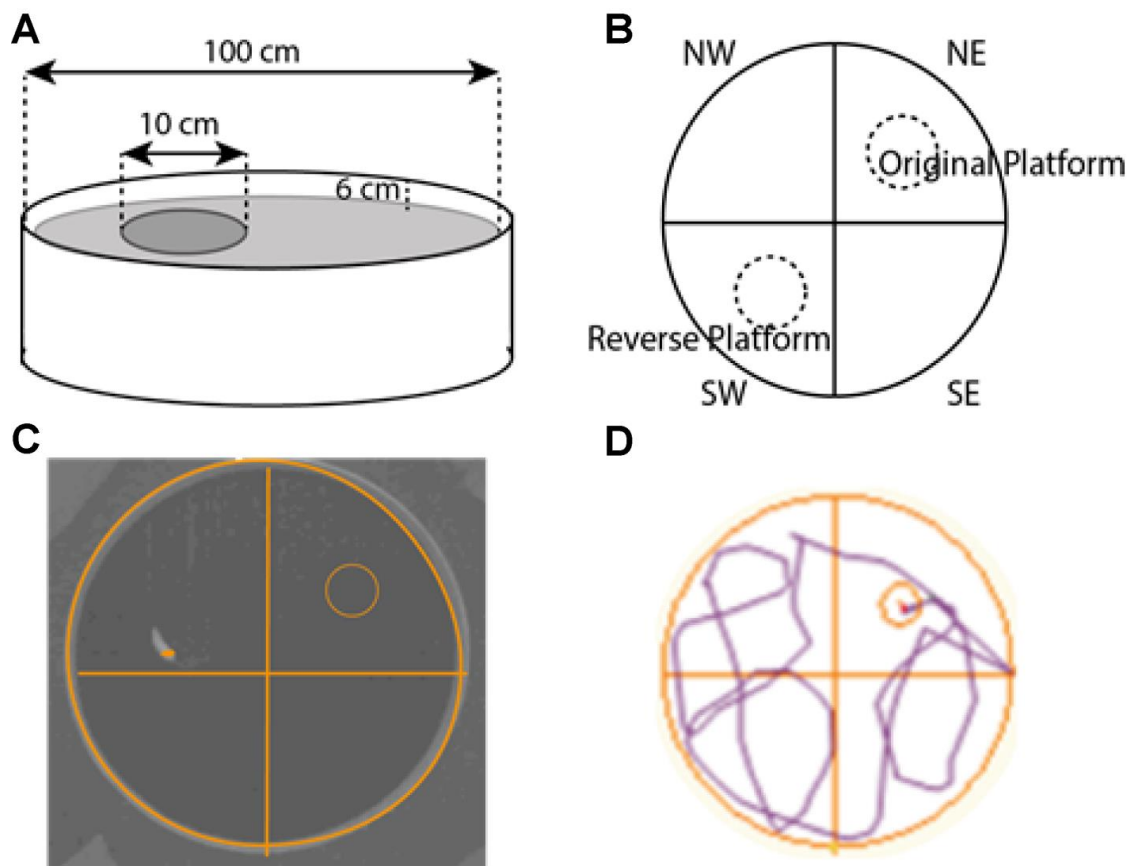


**Figure 2.5 Morris water maze test.** (A) Dimensions of the Morris water maze. (B) The compass-related quadrants and the positioning of the platform during different tests. (C) A screen capture of a mouse marked with an orange dot during the Morris water maze test (D) An example of a trace showing the movement of the mouse heading to the platform observed during the testing period.

## **2.1.5 Tissue processing**

### **2.1.5.1 Tissue collection**

Mice were culled at 1, 21 or 28 days post-injury by inducing deeply anaesthesia with sodium pentobarbital (50 mg/kg, i.p), then were transcardially perfused with saline followed by 4% paraformaldehyde (in 0.1 M phosphate buffer). The entire brain was dissected out and post fixed in 4% paraformaldehyde at 4°C for 24 hours, then cryoprotected in 20% sucrose (in 0.01 M PBS) at 4°C until further processed. A 2 mm coronal segment surrounding the lesion site was dissected out of the brain and embedded in OCT embedding medium (VMR, Lutterworth) and stored at -80°C until further processing.

For tissue collected for brain lipid analysis, the mice were deeply anaesthetised with sodium pentobarbital, then transcardially perfused briefly with saline. Each brain was rapidly removed, separated into selected brain regions and frozen on dry ice. The brain regions were stored at -80°C until further processed.

### **2.1.5.2 Tissue sectioning**

Serial 20 µm coronal sections throughout the lesion epicentre and the length of the hippocampus were cut using the cryostat and collected on Superfrost Plus glass microscope slides (VWR, Lutterworth, UK). The slides were allowed to dry at room temperature prior to storage in slide boxes at -20°C until further processed.

### **2.1.5.3 Toluidine blue staining**

Selected slides were removed from the -20°C, allowed to warm up to room temperature and become dry. Slides received a 5 minute wash in 0.01 M PBS to remove OCT embedding medium. A solution of 0.1% toluidine blue (Sigma, UK) in 70% ethanol was applied to the slides for 5 minutes. The slides were washed 3 times in 0.01 M PBS and then mounted in PBS glycerol (1:9) and imaged immediately.

#### 2.1.5.4 Imaging of toluidine blue

Bright field images of the brain sections stained with toluidine blue were taken with a 4X objective using a stereology microscope (Fig. 2.6). Images were merged together using the ImageJ software (National Institutes of Health, USA). The lesion areas were measured using ImageJ software.

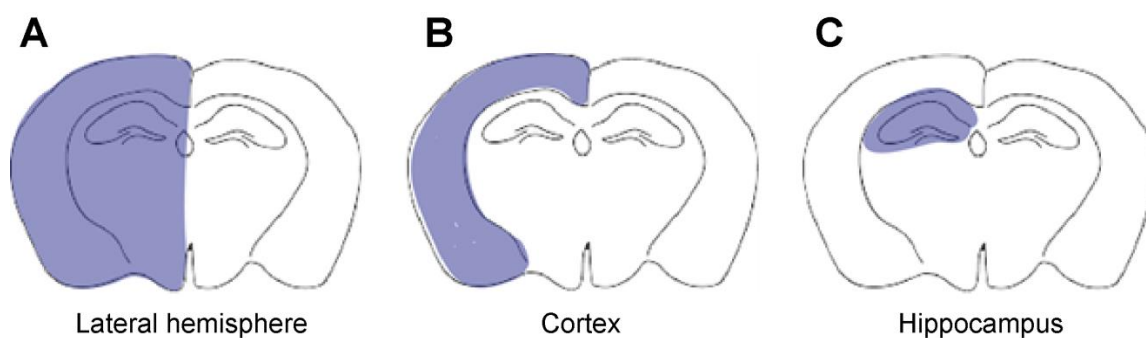


**Figure 2.6 Brain regions examined after toluidine blue staining.** Areas shaded in blue were regions used to compare the ipsilateral and contralateral regions.

#### 2.1.6 Immunohistochemistry

Slides with the frozen sections were removed from  $-20^{\circ}\text{C}$  and allowed to return to room temperature. Slides were then washed 3 times in 0.01 M PBS for 5 minutes each time. During the immunohistochemistry protocol, positive controls of injured mouse spinal cord and negative primary antibody omitted controls were analysed alongside the test mouse brain tissue, as appropriate.

For the antigen retrieval procedure, after the initial PBS washes the slides were placed in an  $80^{\circ}\text{C}$  water bath for 30 minutes with antigen unmasking solution (Vector labs, H-3300) and then incubated with 10% goat or donkey serum for an hour at room temperature. Primary antibody diluted in antibody diluting buffer (ADB, comprised of 0.01M PBS, 0.2% Triton X-100 and 0.1 sodium azide), was incubated with the tissue overnight at  $4^{\circ}\text{C}$ . The sections were washed 3 times with 0.01 M PBS for 5 minutes each and then the corresponding secondary antibody conjugated with Alexa Fluor-488 or Alexa Fluor-594 (diluted in ADB; Molecular Probes, UK) was incubated with the tissue for 2 hours at room temperature. Washes in 0.01 M PBS were repeated three times and then sections were counterstained with the fluorescent nuclear dye Hoechst (0.2mg/100 ml, Sigma UK) for 5 minutes.

Slides were washed again and mounted in PBS glycerol (1:9) and stored at 4°C in the dark until ready for microscope imaging.

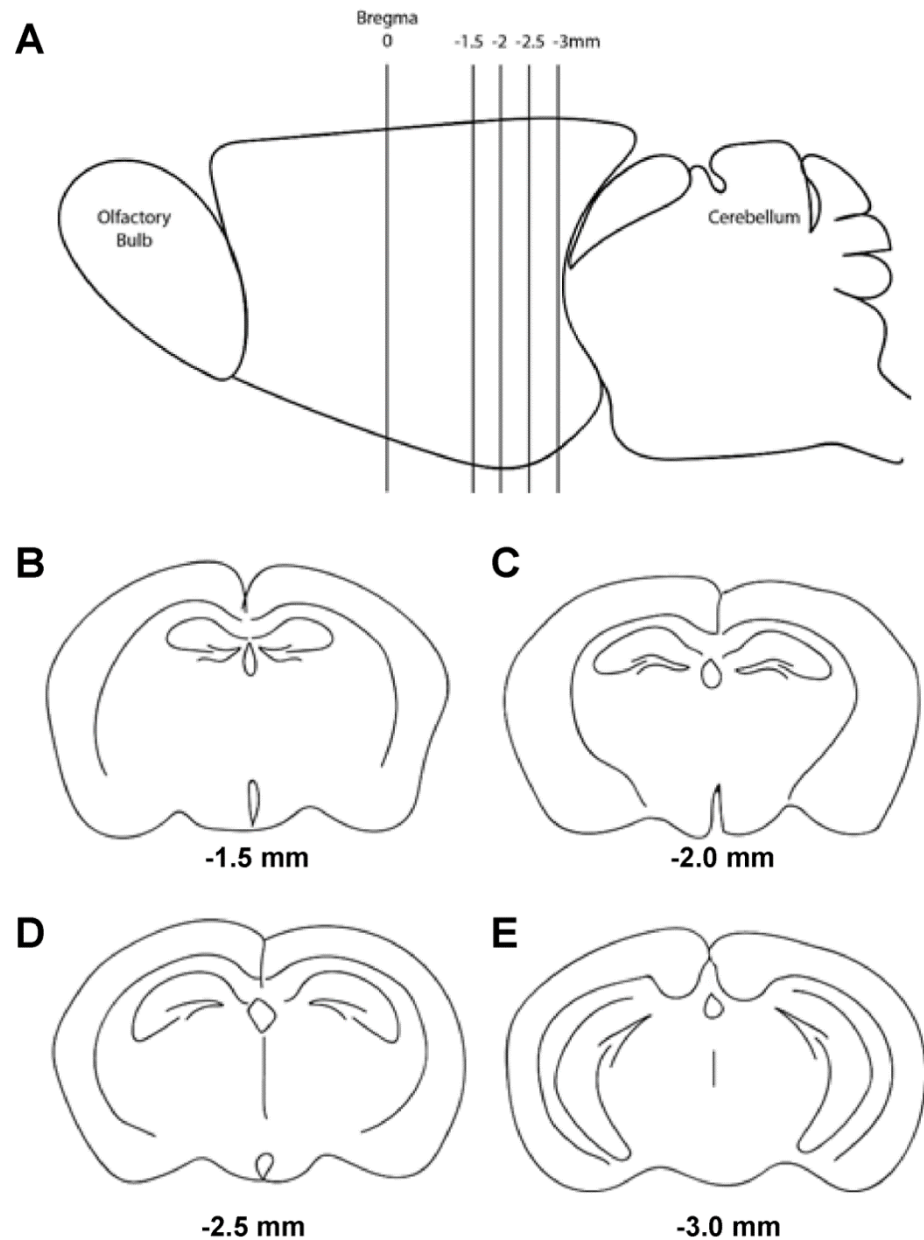


**Figure 2.7 Schematic representation of the brain sections used for immunohistochemical analysis.** A) Sagittal view of a mouse brain with the locations of the coronal sections used for analysis in relation to the bregma landmark. A representation of the coronal slices (levels), using the hippocampus as the main landmark at (B) -1.5 mm, (C) -2 mm, (D) -2.5 mm and (E) -3 mm in reference to bregma.

**Table 2.1 Summary of the primary antibodies used.**

<b>Primary Antibody</b>	<b>Concentration</b>	<b>Antibody host</b>	<b>Supplier</b>	<b>Protein specificity</b>
GFAP - Glial fibrillary acidic protein	1:1000	Polyclonal Rabbit	Dako (Denmark)	The intermediate filament glial fibrillary acidic protein specific to astrocytes.
Iba1 - Ionized calcium binding adapter molecule-1	1:1000	Polyclonal Rabbit	Wako (Japan)	Calcium binding protein expressed by macrophages/microglia
DCX – Doublecortin	1:100	Polyclonal Guinea Pig	Merck Millipore (Germany)	Microtubule-associated protein expressed by immature neurons

#### **2.1.6.1 Microscopy**

Fluorescent microscopy was conducted using the Leica epifluorescence microscope (Wetzlar, Germany). Regions of interest (ROI) identified using a 20X objective were chosen for analysis. These included 4 from the cortex and 4 from the contralateral hippocampus, and from each of the 4 coronal brain levels chosen for analysis (-1.5 mm, -2 mm, -2.5 mm and -3 mm posterior from bregma) (Fig. 2.7). Cortical images included 2 ROI from the ipsilateral cortex surrounding the lesion site and 2 ROI matching the location in the contralateral cortex. The ROI imaged in the contralateral hippocampus were in 4 distinct hippocampus locations; the dentate gyrus (DG), CA1, CA2 and CA3 regions. The staining in each region was measured or counted and expressed as mean  $\pm$  standard error to the mean (S.E.M.) (Fig. 2.8)

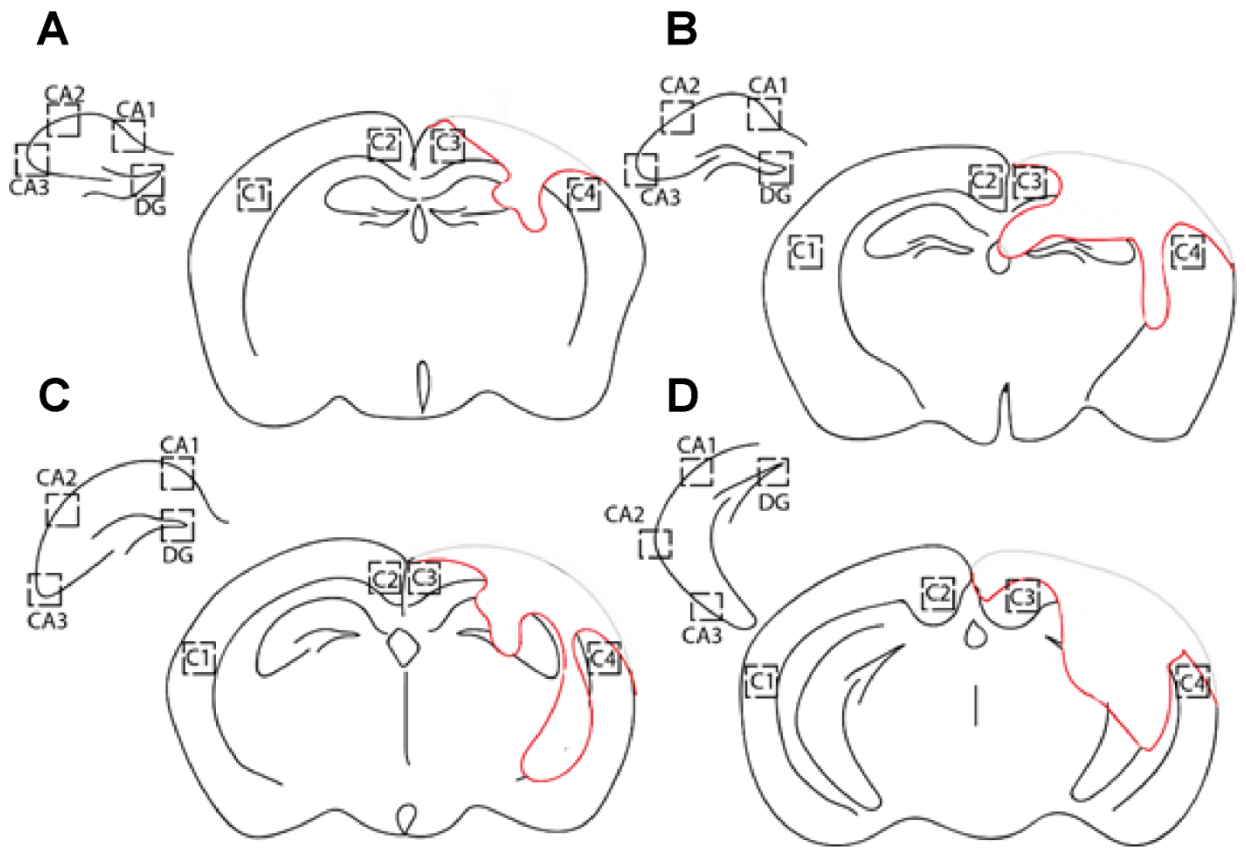


**Figure 2.8 Schematic representation of the regions of interest (ROI) used for analysis at each coronal brain level.** (A) -1.5 mm, (B) -2 mm, (C) -2.5 mm and (D) -3 mm, posterior from bregma. The ROI from the cortex include C1 and C2 from the contralateral cortex and C3 and C4 from the ipsilateral cortex, surrounding the lesion site (marked in red). There are 4 ROI within the contralateral hippocampus used for analysis; the dentate gyrus (DG), CA1, CA2 and CA3 regions. The size of the ROI was the view taken using a x10 objective.

## 2.1.7 Image analysis

### 2.1.7.1 Image analysis of GFAP and Iba1

To determine the amount of reactive astrogliosis, GFAP immunoreactivity was analysed using the ImageJ software. In the cortical and hippocampal ROIs, a measuring frame of 250  $\mu\text{m}$  x 250  $\mu\text{m}$  was placed on the image and an appropriate threshold level was set to allow for the finer processes of the GFAP-positive astrocytes to be identified. The level of immunoreactivity was expressed as a percentage of the measuring frame and compared to the control group. This method was used as the reactive astrocytes in injured tissue can overlap considerably and therefore cell counts were not suitable.

The number of Iba1-positive microglia was counted within a measuring frame of 250  $\mu\text{m}$  x 250  $\mu\text{m}$  that was placed on the ROI images. ImageJ software was then used to count the number of Iba1-positive

cells and expressed as the mean  $\pm$  S.E.M. This method was chosen as the microglia maintained their individual domains and the Iba1 immunolabeling is weaker in the finer microglia processes, making accurate thresholding difficult.

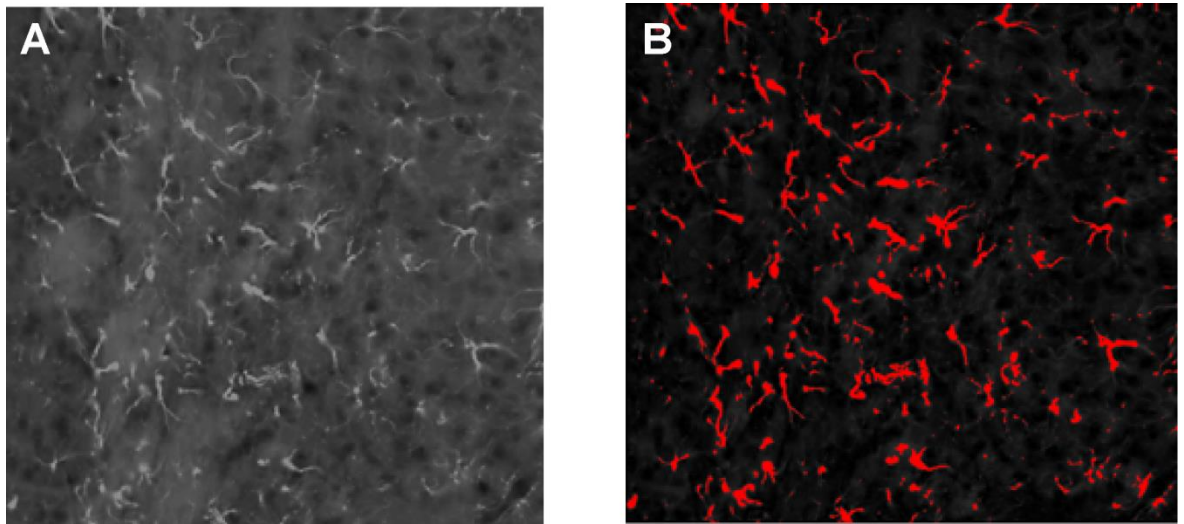


**Figure 2.9 Quantification of GFAP immunolabelling using ImageJ analysis in mouse cortical brain tissue.** (A) ImageJ software was used to convert images at a set threshold (B) where the processes of astrocytes could be detected. The level of immunoreactivity was expressed as a percentage of the measuring frame and compared to the control group.

#### **2.1.7.2 Image analysis of doublecortin staining**

Representative images of the dentate gyrus (DG) in the contralateral hippocampus were taken using the Leica epifluorescence microscope (Wetzlar, Germany), using a X20 objective. The number of Hoechst and doublecortin-positive cells along the DG were counted using a hand held cell counter at each of the 4 coronal levels (-1.5 mm, -2 mm, -2.5 mm and -3 mm posterior from bregma).



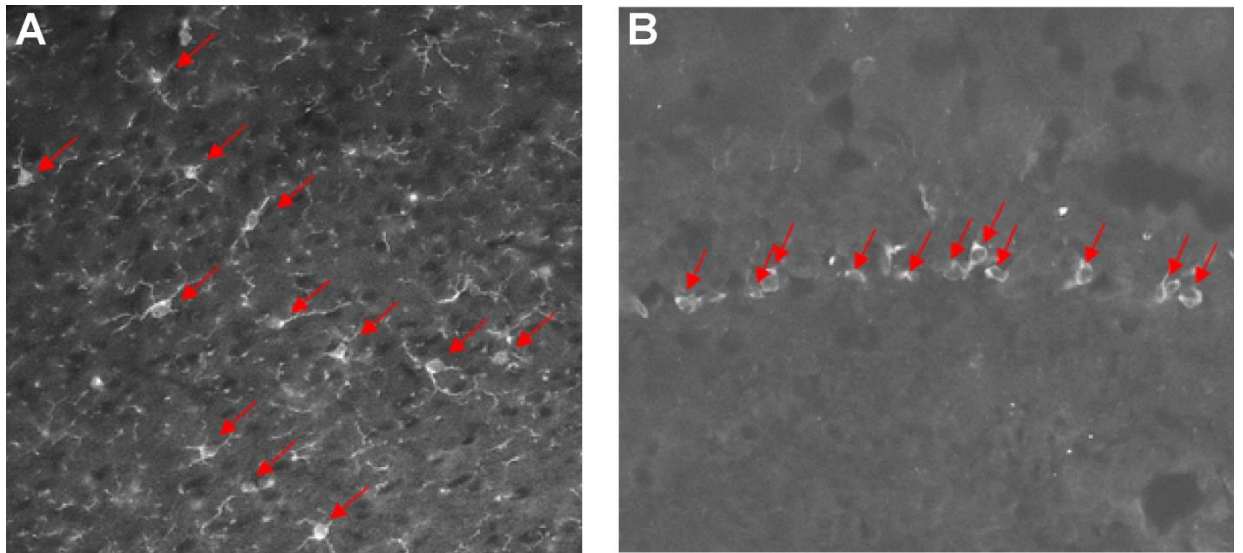


**Figure 2.10 Quantification of Iba1 and doublecortin staining.** (A) Iba1-immunolabelled cells and (B) Doublecortin-labelled cells in the hippocampus. Labelled cells are indicated with red arrows and were counted using ImageJ analysis.

### **2.1.8 Brain lipid analysis**

Lipid analysis was performed using the same method as previously reported and was performed in the laboratory of Dr Simon Dyll at Roehampton university (Gladman et al., 2012, Dyll et al., 2007).

Brain tissue (excluding cortex and hippocampus) of wild-type (WT) mice, *fat-1* mice and naïve C57BL/6 female mice was harvested at 24 hours after CCI and stored at  $-80^{\circ}\text{C}$  until lipid analysis. Lipids were extracted from the brain tissue using the method described by Folch et al. (1957), with 0.01% w/v 2,6-di-tert-butyl-p-cresol (butylated hydroxytoluene; BHT) added as an antioxidant (FOLCH et al., 1957). The total phospholipids were isolated using thin layer chromatography (Manku et al., 1983). Transesterification of the lipids was carried out by the addition of 14% boron trifluoride in methanol at  $100^{\circ}\text{C}$  for 20 minutes. The fatty acid composition was then measured and the individual fatty acids within each tissue sample were identified using gas chromatography coupled to mass spectrometry (Agilent 6890 gas chromatograph connected to an Agilent 5973 mass selective detector; Agilent Technologies) using a Supelcowax 10 capillary column (30 m x 0.25 mm x 0.25 mm; Sigma) (Dyll et al., 2007). Lipid identity was confirmed by retention times compared to known standards and mass spectra comparison to the National Institute of Standards and Technology database. Quantification

was performed on selected ion peak area by ChemStation software (Agilent Technologies, U.S.A). Corrections were made for variations in the detector response and values of detected fatty acids were normalised to 100% and expressed as mol%.

## **2.2 In vitro studies**

### **2.2.1 Primary cortical astrocyte cultures**

All in vitro studies were carried out at the Eastman Dental Institute, University College London in collaboration with Dr James Phillips and with help from Dr Caitriona O'Rourke. The protocol used was adapted from (East et al., 2009).

The primary astrocyte cultures were prepared from the cortices of transgenic green fluorescent protein (GFP) postnatal 2 day-old rat pups. Following decapitation, the cortices were dissected out and the meninges and associated blood vessels removed with fine forceps. The tissue was cut up and placed in 250 µg/ml trypsin in 10 ml disaggregation medium [containing: 4 mM glucose (Sigma, UK), 3 mg/ml bovine serum albumin (BSA; Sigma), 1.5 mM MgSO<sub>4</sub> (VWR, UK) in Ca<sup>2+</sup>- and Mg<sup>2+</sup>-free Earle's balanced salt solution (Gibco, Invitrogen, UK)] for 15 min at 37°C, and agitated. A dilute solution of soya bean trypsin inhibitor (21 µg/ml SBTI; Sigma) and deoxyribonuclease 1 (6 µg/ml DNase; Sigma) was then added and the cell suspension was centrifuged for 2 min at 250 ×g. The supernatant was removed and the pellet resuspended in 500 µl concentrated solution of SBTI (133 µg/ml) and DNase (40 µg/ml). The solution was triturated and a further 500 µl concentrated SBTI and DNase solution was added to the suspension. The material at the top of the suspension was removed to a separate 15 ml tube. This trituration procedure was repeated twice more. The resulting cell suspension was then underlain with 4 % w/v BSA, which was then centrifuged at 250 ×g for 5 min. The supernatant was gently removed and the pellet resuspended in Dulbecco's modified Eagle's medium (DMEM; Gibco) supplemented with penicillin/streptomycin (100 U/ml and 100 µg/ml respectively; Sigma) and with 10 % v/v foetal calf serum (FCS). This cellular suspension was dispensed into 75 cm<sup>2</sup> flasks (Greiner, Stonehouse, UK) which had been pre-coated with poly-D-lysine (Sigma) at an approximate density of

1–2 cortices/flask containing 20 ml of DMEM. The cultures were stored in an incubator at 37°C with 5% CO<sub>2</sub>.

Astrocytes were expanded in culture for 10 - 14 days to reach confluence. Once confluent, the medium was removed and 7 ml trypsin–EDTA solution (Sigma) was added to each flask for 15 min at 37°C. The trypsin was neutralized by the addition of 13 ml DMEM (penicillin, streptomycin, 10% FCS).

The astrocytes were placed into 3D cultures 24 hours prior to the mechanical injury. Astrocytes seeded into gels at 1 million/ml (500,000 per well of a 24-well plate) were used. The preparation of the gels involved mixing a 10 % cell suspension in DMEM, 10 % 10x minimum essential medium (MEM; Sigma) and 80 % rat tail collagen (2 mg/ml in 0.6% acetic acid; First Link, UK), then neutralized using sodium hydroxide. Once the gel was gently mixed with the cell suspension, it was transferred into 24-well plates (0.5 ml per well, resulting in gels approximately 3 mm thick). Gels were then placed into the incubator (37°C, 5% CO<sub>2</sub>) to set for 10 minutes. Once set, 1 ml of DMEM (penicillin, streptomycin, 10% FCS) was added to the well and gels were placed back into the incubator for 24 hours before lesion (Fig. 2.11).

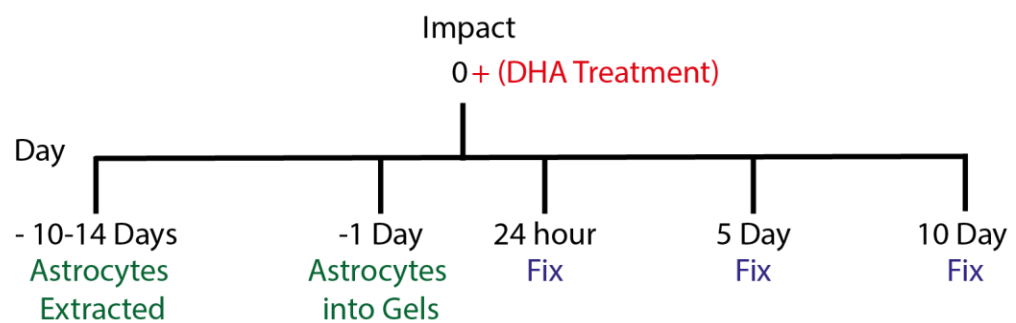


**Figure 2.11 Timeline of the in vitro studies.** Astrocytes were extracted 10-14 days prior to lesion and were placed in a 3D collagen gel 24 hours before lesion. DHA or vehicle was added to the gel directly after the lesion. Astrocytes in 3D gels were fixed 1 day, 5 days and 10 days post lesion.

### **2.2.2 Mechanical lesion of astrocyte cultures**

To administer the lesion injury to the gel, the medium was first removed from the gel and then the corresponding well was aligned under the Hatteras PinPoint impactor device. The impactor tip was 3 mm in diameter and the parameters used for the impact were; velocity, 3.0 m/s; dwell time, 100 ms

and impact depth of 2 mm. After all the impacts had been administered, 1 ml of DMEM (penicillin, streptomycin, 10% FCS) was added to each gel and returned back to the incubator (Fig. 2.12).

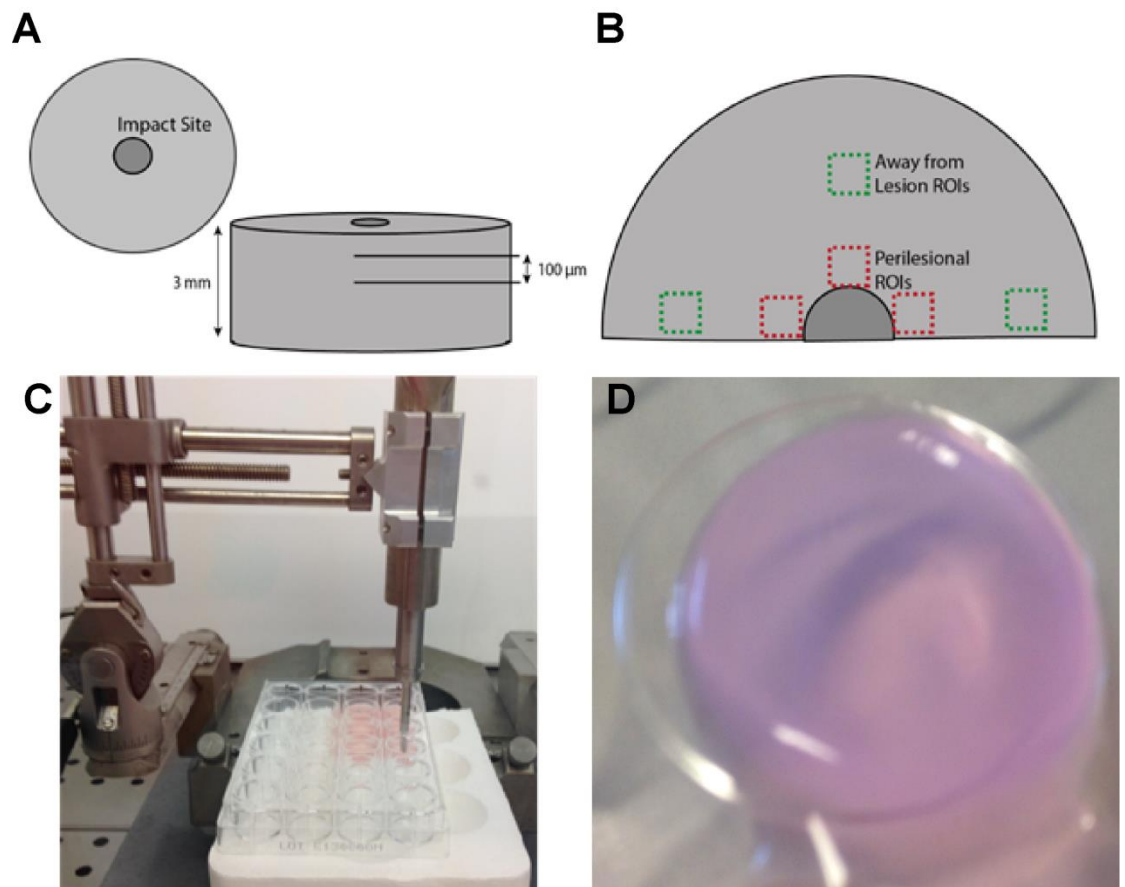


**Figure 2.12 Mechanical injury to the 3D astrocyte gels.** (A) Schematic of the gel from above and from the side showing the height of the gel and the 100 µm z-stack imaged region chosen for analysis. (B) Schematic showing the regions of interest (ROI) imaged for analysis, perilesional ROIs (red) and away from lesion ROIs (green). (C) The Hatteras™ PinPoint impactor equipment and (D) the impact caused an indentation to the middle of the 3D gel.

### **2.2.3 DHA administration to 3D cultures**

Stock solutions of the free fatty acid DHA (Sigma, Dorset, UK) were made up in ethanol under 100% nitrogen. The 5 µl 1 M stock aliquots were kept in light sensitive, airtight glass containers (Agilent, Stockport, UK) and were stored at -20°C until required. An aliquot of the stock solution was diluted to the final concentration (1 µM) with the DMEM (penicillin, streptomycin, 10% FCS) and added to each gel immediately after the impact.

#### **2.2.4 Immunocytochemistry**

At 24 hours, 5 days and 10 days post-impact the gels were washed in 0.01 M PBS and then fixed in 4% paraformaldehyde for 24 hours. The gels were cut into halves for staining and image analysis. Cells were permeabilized with 0.5% Triton X-100 (Sigma, UK) for 30 minutes and then washed 3 times with 0.01 M PBS, before being incubated with 5% normal goat serum in 0.01 M PBS for 30 minutes. After repeating the washes gels were incubated with rabbit polyclonal antibody (1:300; DAKO) overnight at 4°C. The next day after incubation with the primary antibody, washes were repeated and the gels were then incubated with the secondary antibody (1:300; Goat anti-rabbit Dylight 549; Vectorlabs, USA). The gels were washed and stored in 0.01 M PBS at 4°C.

#### **2.2.5 Imaging and analysis of 3D cultures**

Fluorescence microscopy was performed on the gels using a Leica Confocal DMIRB fluorescence microscope with LaserShape2000 software and Volocity analysis software. There were 3 images taken in the perilesional area and 3 taken away from the lesion, as shown in Fig. 2.12. Each field was 1 x 1 mm x 100 µm (xyz), with 100 slices per stack in the Z dimension. Using the Volocity software the volume of GFP or GFAP staining per field was measured, the numbers of cells were counted and the staining per cell was calculated. The numbers of processes per cell were counted using ImageJ software and the distribution of the number of processes presented as a histogram.

### **2.3 Statistical analysis**

All testing and analysis was performed blinded. All statistical analyses were performed using Graph Pad Prism 5.0 (GraphPad, USA). For the open field and the MWM acquisition trial tests, a two-way repeated measures ANOVA with post-hoc Bonferroni testing was used. One-way or two-way ANOVA testing or Kruskal-Wallis tests were used to compare experimental groups in all other behavioural tests and in the histological analysis. Data was presented as mean with standard error of the means (S.E.M.) and differences were considered statistically different at  $p < 0.05$ .

## **3 Characterisation and optimisation of a mouse model of TBI**

### **3.1 Introduction**

There is a strong and immediate need for novel therapies in the treatment of TBI. Potential novel therapies for TBI need to be screened for efficacy *in vivo* before being brought to the clinic. At the beginning of this thesis work there was no established *in vivo* model of TBI at Queen Mary University of London.

As previously discussed in the main introduction (section 1.8) there are many experimental TBI models which can be carried out in mice and rats, including the fluid percussion model, the weight drop/Marmarou model and the controlled cortical impact (CCI) injury model (Xiong et al., 2013). This chapter presents data from studies designed and performed to optimize a CCI injury in mice within our group. The CCI model was chosen due to it being a widely used model for creating a focal TBI in mice, its high reproducibility, and also because our group has already set up an established model of SCI contusion injury. The impactor used to set up this CCI model was the same used to cause spinal cord contusion injury in rats and mice. The aim of the work presented in this chapter was to establish a human TBI equivalent and reproducible CCI model in mice, with behavioural endpoints and related histopathological changes. The optimisation of a CCI mouse model in our laboratory would then allow us to evaluate potential TBI therapies and their impact in terms of functional outcome and tissue protection.

#### **3.1.1 Controlled cortical impact injury model**

There are several parameters that need consideration when setting up the CCI model of injury. The parameters were chosen with regards to the technical specifications of the Hatteras PinPoint Impactor equipment and to reflect the most often used parameters in the literature, as detailed in section 2.1.2 (Romine et al., 2014, Chen et al., 2014, Pleasant et al., 2011, Whalen et al., 1999, Smith et al., 1995, Jin et al., 2012, Kabadi et al., 2012, Saatman et al., 2006, Susarla et al., 2014, Washington et al., 2012). This is so that the results obtained in our CCI model could be compared to those reported by other groups, and thus allow us to ascertain the validity of our observations. In particular, the impact depth

parameter was the independent variable (depths of 1.5 mm, 2 mm and 2.2 mm from surface of the brain) being assessed. It is important to establish an injury severity with defined endpoints, so that this model can be used as a screening tool for novel TBI therapies. The behavioural and histological outcomes of these impact depths helped determine the impact depth parameter to be used in all the subsequent TBI studies shown within this thesis.

### **3.1.2 Behavioural outcome measures**

One of the major symptom complaints made by TBI patients is memory loss (Paniak et al., 2002, Gasquoin, 1997). Memory loss is frequently assessed after CCI injury in rodents using the MWM test and this test was therefore selected to assess the memory deficits in our mice. As the MWM is most commonly performed two weeks after the injury was induced, we decided to employ the Y-Maze as another test to assess memory and learning deficits earlier in our protocol. Unlike the MWM, the Y-Maze does not require any stress-induced motivation and could therefore assess baseline learning and memory function of the mice after injury. The open field test was also included in our behaviour testing protocol, to ensure that any deficits seen in the cognitive behaviour tests are due to poor cognition and not motor dysfunction.

### **3.1.3 Histological endpoints**

As discussed in the introduction, there are several cellular cascades that form part of the secondary injury. Glial cells in particular have a pronounced response during the secondary injury. The astrocytes and microglia change their morphology and express injury-induced proteins that correlate with injury severity. A hallmark of injury-induced astrogliosis is the increase in the expression of the intermediate filament GFAP. This is seen in post-mortem brain tissue of TBI patients (Harish et al., 2015). Activated microglia can be identified by the expression of calcium-binding protein Iba1 (Ito et al., 2001). Another key feature of the primary and secondary injury is cell death, which underlies tissue loss. Several groups have reported substantial tissue loss after CCI directly below the site of impact, using gross histological assessment (Berpohl et al., 2006, Onyszchuk et al., 2007, Zhao et al., 2012a). In order for our CCI model to be comparable to other studies in the literature, we focussed on the evidence of increased GFAP and Iba1 staining, as well as the amount of gross tissue loss.

## 3.2 Methods

The animals used in this chapter were CD1 male mice aged 10-12 weeks. The CCI injury model used to cause a unilateral injury is described in section 2.1.2. The behavioural tests in this chapter include the open field test (section 2.1.4.1), Y-maze test (section 2.1.4.2) and the MWM acquisition and probe trial tests (section 2.1.4.3), and the reverse MWM paradigm. The general protocol used for the execution of these behavioural tests is detailed in figure 3.1. After perfusion on day 28 post-injury, brain tissue was stained using the toluidine blue method (section 2.1.5.1) and immunostained for GFAP and Iba1 (section 2.1.5.2).

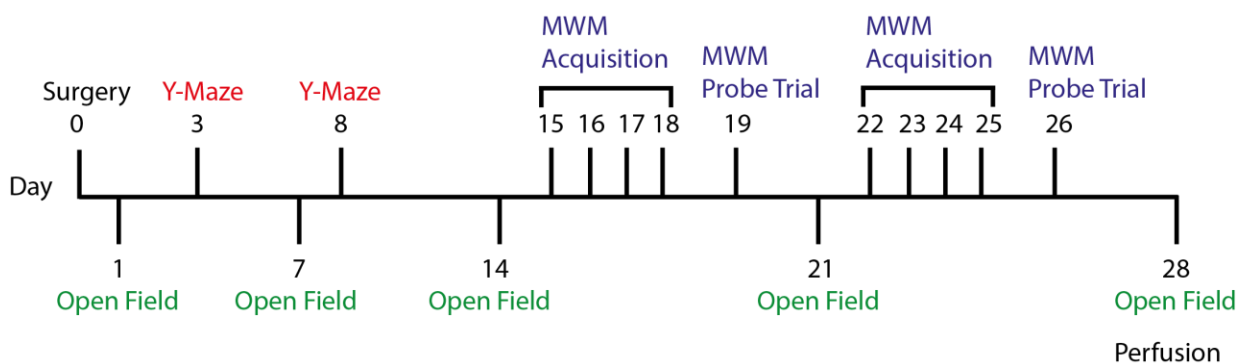


**Figure 3.1 Timeline for the administration of the behavioural tests after surgery.** Including the open field, Y-maze and the first MWM acquisition (day 15-18) and probe trial (day 19), and the second week reversal MWM acquisition (day 22-25) and reverse probe trial (day 26).



### **3.3 Aims and hypotheses**

#### **3.3.1 Aims**

The aim of the work presented in this chapter was to characterise a CCI mouse model of TBI with long-term behavioural and histological endpoints including:

- Transient and long lasting deficits in learning and memory as assessed by the Y-maze and the MWM acquisition and probe trials, respectively.
- Persistent tissue damage and reactivity around the site of the impact; tissue loss and glial cell activation

#### **3.3.2 Hypothesis**

The hypothesis for this work is that CCI injury at graded depths will produce graded neurological deficits which can be assessed using the Y-maze test, open field test, and Morris water maze (MWM) test. We also hypothesized that histological changes would show a positive correlation with the severity of the injury, as reflected in the neurological outcome.

### **3.4 Results**

The results document the characterisation of a CCI mouse model of injury that produces a lesion that creates a sufficient, but, potentially, rescuable deficit in a memory-based behavioural test. The parameter that was used to alter the severity of the CCI injury was the depth of the penetration of the impactor tip into the brain. In the first study, we used impact depths of 1.5 mm and 2.0 mm. In the second study, the impact depth was increased to 2.2 mm. We also assessed the histopathological changes in the brain tissue of these mice at 28 days post CCI injury, using immunohistochemistry.

#### **3.4.1 The effect of injury severity in the open field test**

The open field test was used to assess gross locomotor function, anxiety-related behaviour (thigmotaxis), habituation and hyperactivity (section 1.8.3.1). To assess the potential gross and persistent deficits caused by a CCI injury, control and injured mice were exposed to the open field test chamber for 5 minutes at 5 time points post-injury; 1, 7, 14, 21 and 28 days.

The zones in which the mice spend their time during the 5 minute open field test can be indicative of both anxiety-related behaviour as well as habituation to the open-field chamber. All 4 groups (naïve uninjured controls, sham-craniotomy, 1.5 mm and 2.0 mm impact depth) exhibited similar behavioural profiles in terms of the amount of time they spent in the outer zone against the walls of the open field chamber (thigmotaxis) (Fig. 3.2B), the time they spent in the inner zone (Fig. 3.2C) and the number of entries to the central zone during the test (Fig. 3.2D). All groups spent less time in the inner zone and more time in the outer zone over the course of the study.

On day 1 post-injury the 4 groups (naïve, sham-injured, 1.5 mm and 2.0 mm CCI injured) showed no significant difference to each other in the distance they travelled and the number of line crossings they made during the five minute trial. However, at day 7 post-injury the naïve group behaviour was different compared to the injured groups. Between day 1 and day 7 the naïve group reduced the distance travelled from  $28.9 \pm 1.6$  m to  $20.1 \pm 1.3$  m, whereas the distance travelled by the 3 injured groups remained above 25 metres on both day 1 and day 7 (Fig. 3.3A).

The naïve group also showed a difference in the number of line crossings on day 7, when compared to the 3 injured groups (Fig. 3.3B). The number of line crossings the naïve group made on day 1 ( $234.5 \pm 18.3$ ) and day 7 ( $228.8 \pm 9.0$ ) were similar, whereas the 3 injured groups increased the number of line crossings from day 1 to day 7. The differences exhibited between the behaviour of the naïve group and the injured groups during the first week disappeared in the subsequent open field tests on days 14, 21 and 28 (Fig. 3.5).

All 4 injury groups spent less than 30 seconds immobile on day 1 post injury ( Fig. 3.6). At the end of the first week, the naïve group spent almost 3 fold as much time immobile when compared to the sham, 1.5 mm and 2.0 mm injury groups. The naïve group continued to spend the most time immobile when compared to the other groups over the course of the study.

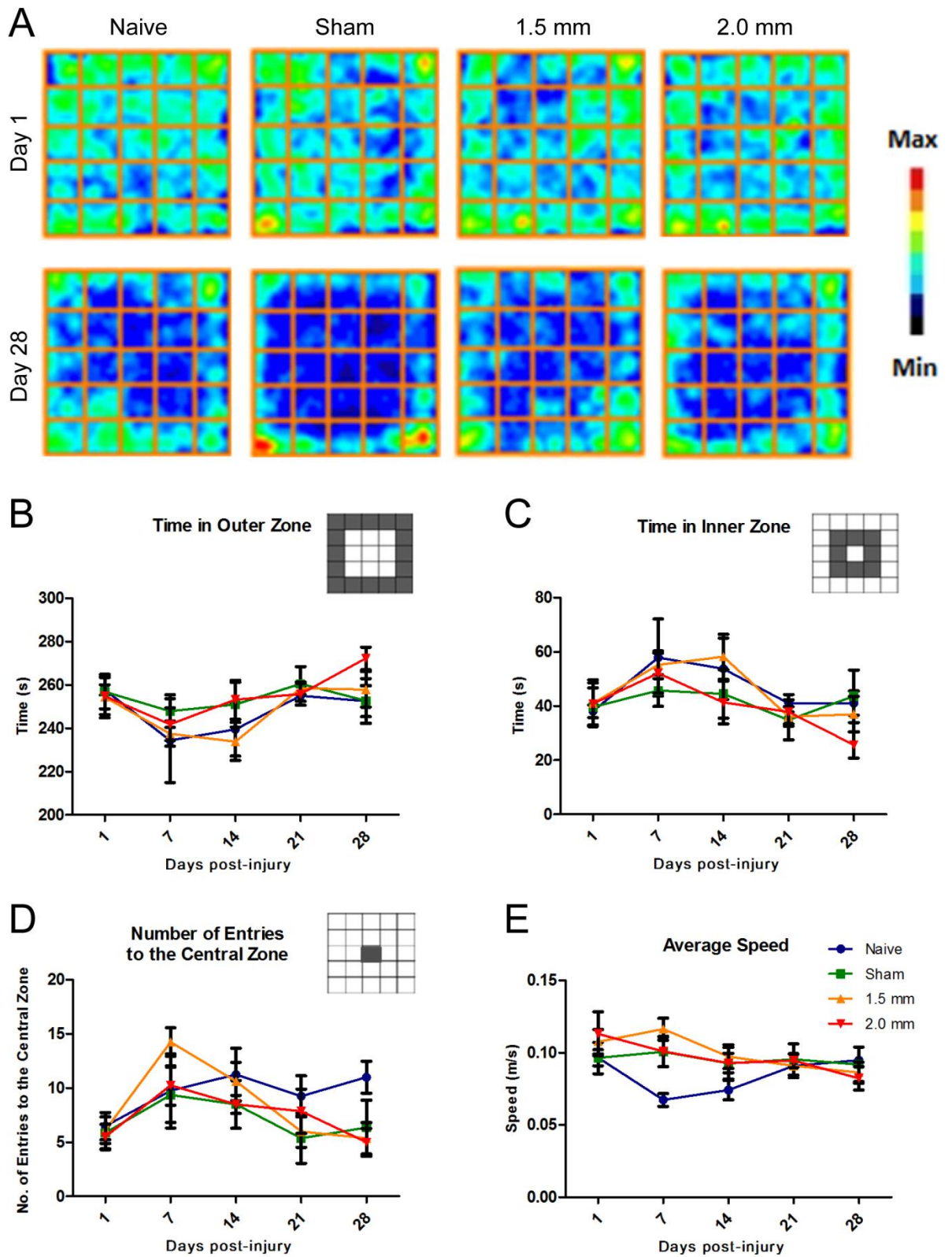


**Figure 3.2. Effect of injury severity on open field performance.** (A) Representative occupancy plots from open field testing on day 1 and day 28 from each experimental group. (B, C) The average time spent by each group in the outer perimeter and the inner zone. (D) The average number of entries to the central zone. (E) The average speed in the open field. Mean  $\pm$  S.E.M. N = 4-8 animals per group.

### Open Field – Day 1 and Day 7

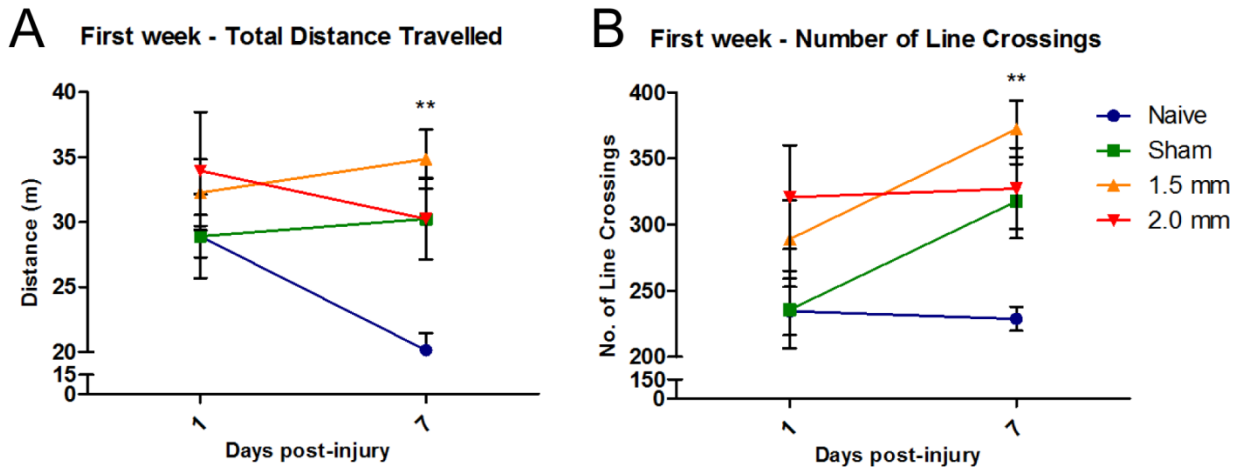


**Figure 3.3. Effect of injury severity on the distance travelled and line crossings in the first week.** (A) total distance travelled and (B) the number of line crossings on days 1 and 7 of testing. On day 7 the naïve vs. 1.5 mm injury group showed statistically significant differences (\*\* $p < 0.01$ ) using a two way ANOVA with post-hoc Bonferroni testing. Mean  $\pm$  S.E.M. N = 4-8 animals per group.

### Open Field - Total Distance Travelled

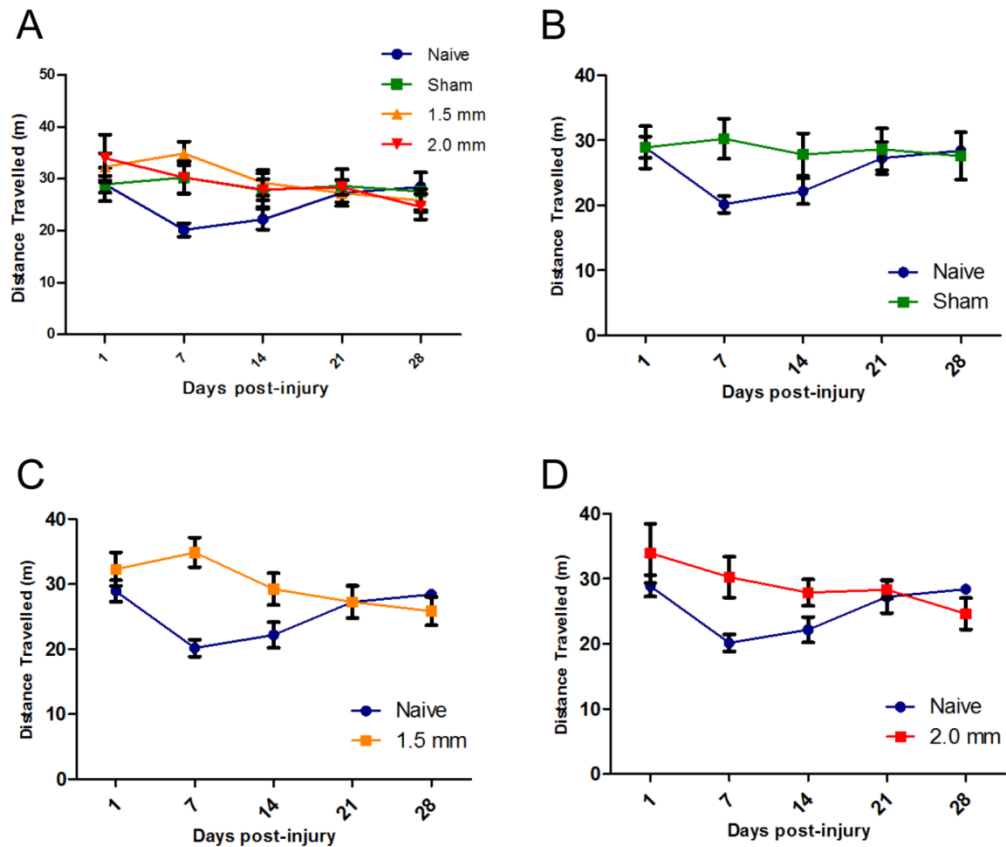


**Figure 3.4 The total distance travelled after injury in the open field.** (A) all 4 groups, (B) naïve vs. Sham, (C) naïve vs. 1.5 mm and (D) naïve vs. 2.0 mm, at day 1, 7, 14, 21 and 28 post-injury. Mean  $\pm$  S.E.M. N = 4-8 animals per group.

**Open Field – Number of Line Crossings**

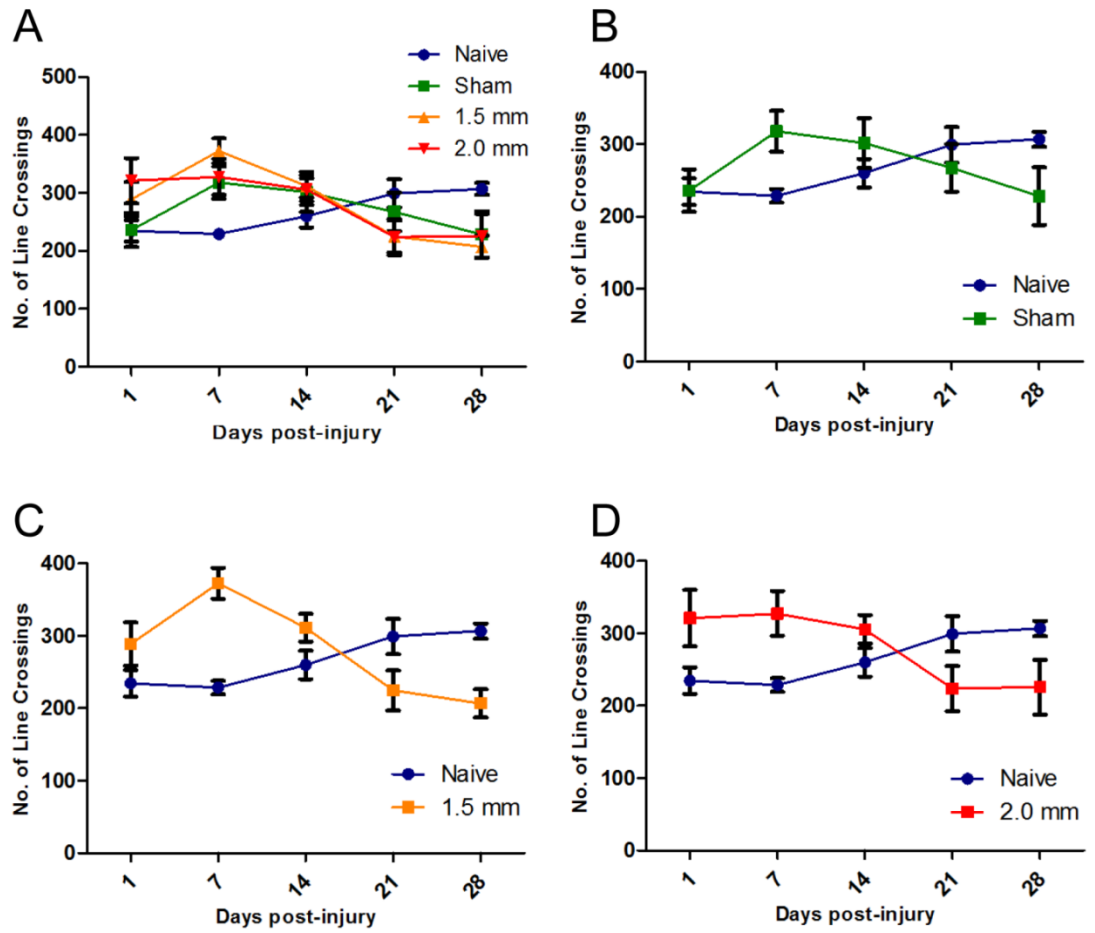


**Figure 3.5** The number of line crossings after injury in the open field. (A) all 4 groups, (B) naïve vs. sham, (C) naïve vs. 1.5 mm and (D) naïve vs. 2.0 mm, at day 1, 7, 14, 21 and 28 post-injury. Mean  $\pm$  S.E.M. N = 4-8 animals per group.

### Open Field – Time Spent Immobile

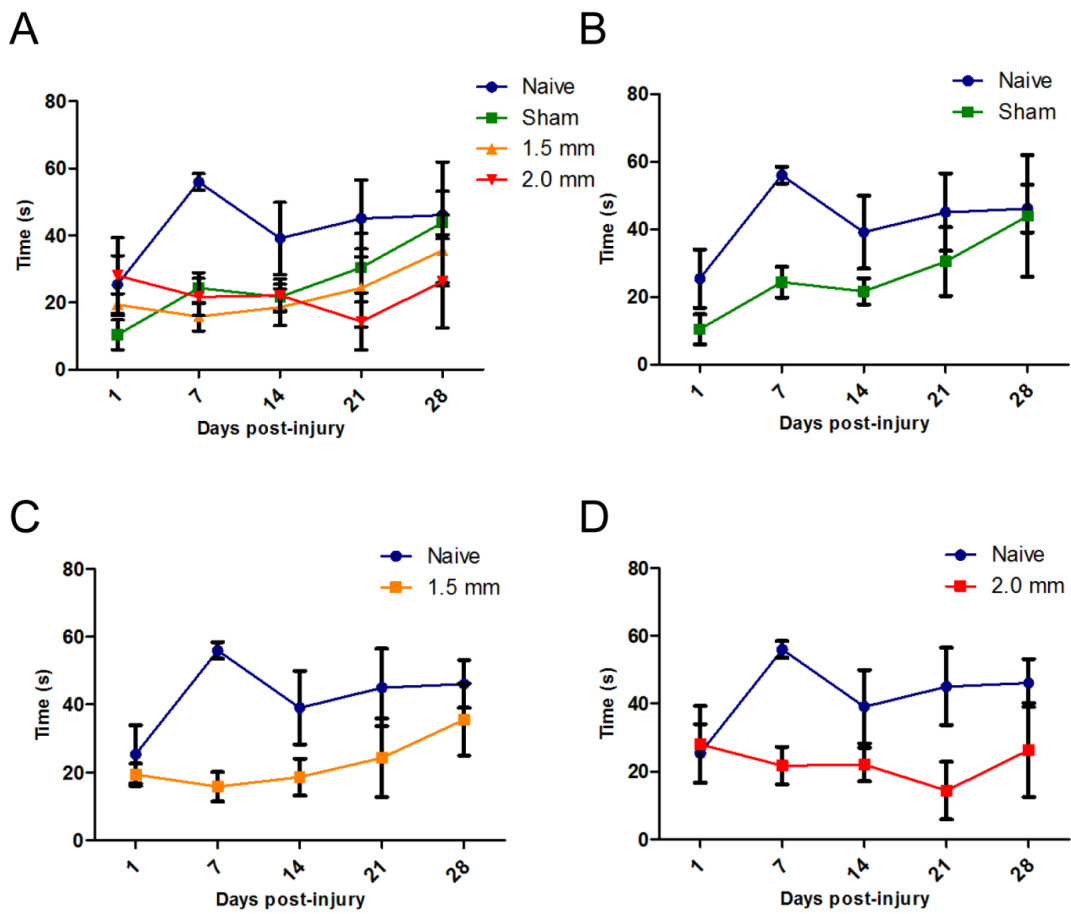


**Figure 3.6** The effect of injury severity on the time spent immobile within the open field test. (A) All 4 groups, (B) naïve vs. sham, (C) naïve vs. 1.5 mm and (D) naïve vs. 2.0 mm, at day 1, 7, 14, 21 and 28 post-injury. Mean  $\pm$  S.E.M. N = 4-8 animals per group.

### **3.4.2 The effect of injury severity in the Y-maze test**

The Y-maze novel arm protocol was used in this study to assess memory deficits (sections 1.8.3.2, 2.1.4.2). On day 3 and day 8 post-injury the mice received two trials, an acquisition trial and a retention trial with a 2 hour inter-trial time. Increased attention towards the novel arm in the retention trial suggests that the mice retain their memory function.

On day 3, mice in the 1.5 mm and 2.0 mm injury groups spent less time in the novel arm than the naive and sham-injured groups (Fig. 3.7B). Mice exposed to the novel arm for the first time should spend more than a third of the retention trial time (5 minutes) in the novel arm, therefore mice spending longer than 100 seconds in the novel arm are exhibiting normal exploratory behaviour and reaction to novelty. Both the naïve and sham-injured groups spent more than 100 seconds in the novel arm: naive group ( $123.6 \pm 9.7$  s) and the sham-injured group ( $115.3 \pm 10.5$  s).

At day 8 post-injury all the groups spent more than 100 seconds in the novel arm (Fig. 3.7D). The naive group spent the longest time in the novel arm. The mice in the 3 injury groups spent more time in the novel arm at day 8 than they had during the earlier Y-maze test on day 3 (Fig. 3.8A). The 2.0 mm CCI group made the most entries to the novel arm during the day 3 retention trial (Fig. 3.7C). At day 8 the naive and 1.5 mm CCI group made more entries than the sham and 2.0 mm CCI groups. Statistical analysis revealed no group was significantly different compared to the others in either measurement, i.e. on day 3 or day 8.



### Y-Maze – Day 3 and 8 post injury

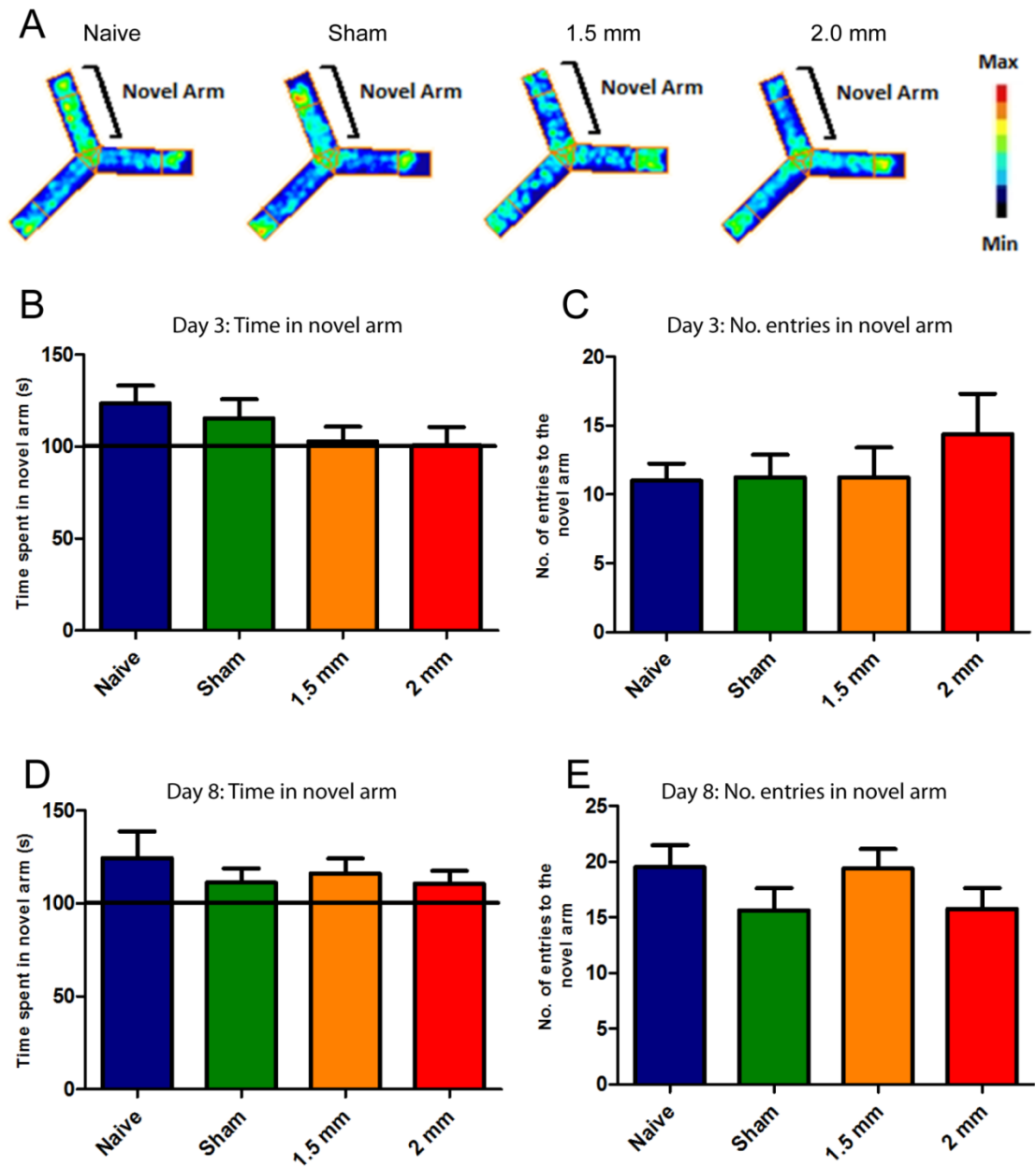


**Figure 3.7. Effect of injury severity on Y-maze performance.** (A) Representative occupancy plots from the day 3 retention trials for each experimental group. (B) Time spent exploring the novel arm and (C) the number of entries into the novel arm during the 5 minute retention trial on day 3 post-injury. Mean  $\pm$  S.E.M. N = 4- 8 animals per group.

### Y-Maze – Day 3 and Day 8

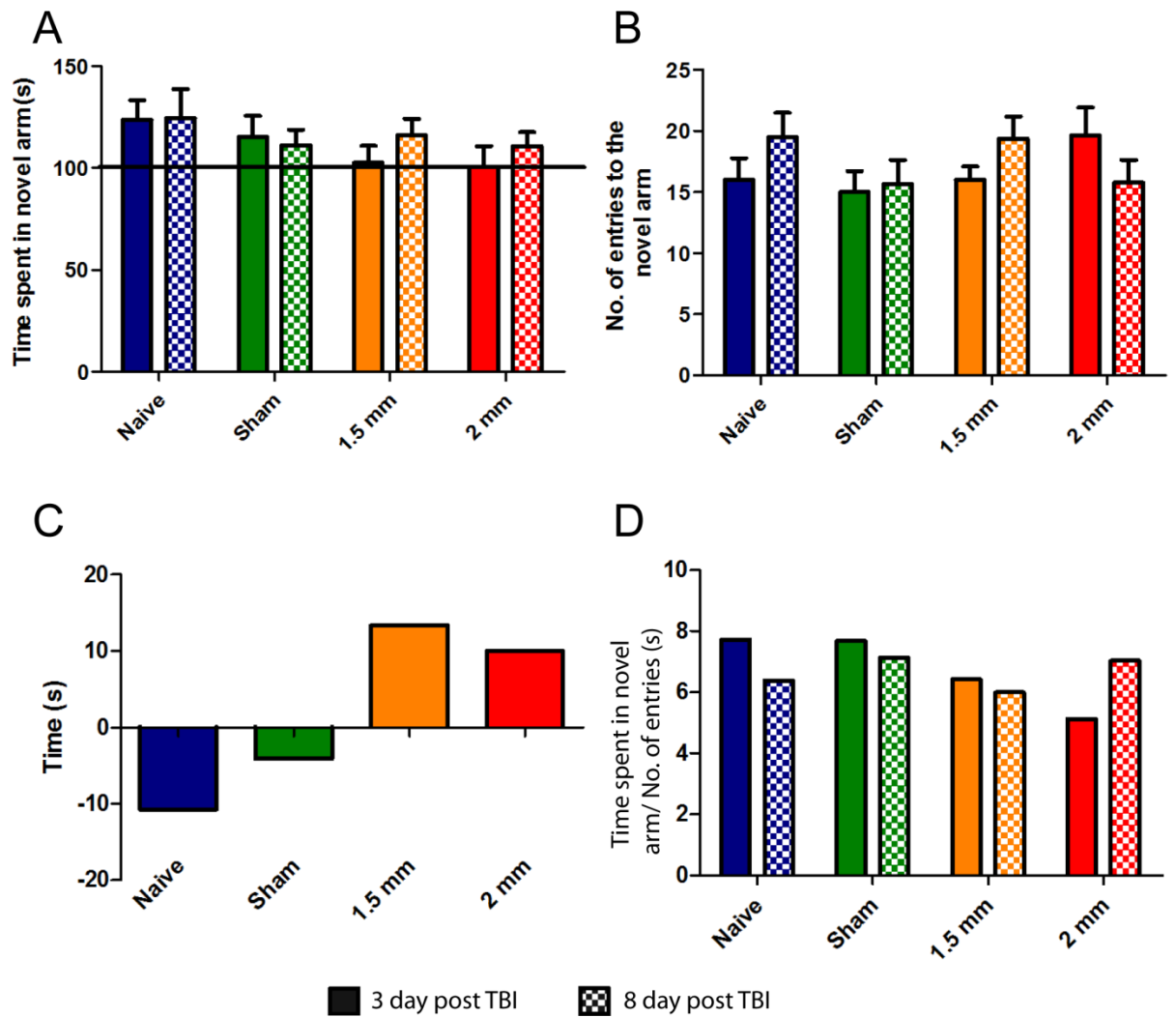


**Figure 3.8. Effect of injury severity on the Y-maze performance on day 3 and day 8.** (A) The time spent in the novel arm and (B) Number of entries to the novel arm on day 3 and day 8. (C) The difference in time spent in the novel arm between day 3 and day 8. (D) The time spent in the novel arm divided by the number of entries to the novel arm, on day 3 and day 8. Mean  $\pm$  S.E.M. N = 4- 8 animals per group.

### **3.4.3 The effect of injury severity in the Morris water maze**

#### **3.4.3.1 The effect of injury severity in the Morris water maze test acquisition trial**

The acquisition phase of the MWM is designed to test the capacity of the mice to learn. Over the course of the 4 testing days during the acquisition phase, all of the groups became faster at locating the hidden platform and escaping the water (Fig. 3.9B). The naïve group had the steepest decrease in escape latency over the acquisition trial period (naive day 15 vs. day 18; \*\*\* $p < 0.001$ ), suggesting that they had the best learning capacity.

The naïve group ( $15.2 \pm 5.2$  s) showed a significant decrease in escape latency when compared to all 3 other groups (sham  $32.7 \pm 3.8$  s, \* $p < 0.05$ ; 1.5 mm  $38.9 \pm 4.4$  s, \*\* $p < 0.01$ ; 2.0 mm  $48.9 \pm 6.9$  s, \*\*\* $p < 0.001$ ) at day 17 post-injury.

The naïve group demonstrated a faster escape latency than the sham-injury group at day 17 (Fig. 3.9C), and the difference was statistically significant (\* $p < 0.05$ ). The naïve group ( $12 \pm 2.4$  s) still had a faster escape latency than the sham-injured group ( $26.7 \pm 5.7$  s) on day 18 post-injury, but the difference was not statistically significant.

On day 18 post-injury the naïve group showed a significant difference in escape latency when compared to the 1.5 mm (\* $p < 0.05$ ) and 2.0 mm injury (\*\* $p < 0.01$ ) groups. The average escape latency of the 4 trials conducted on day 18 for the naïve group ( $12 \pm 2.4$  s) was almost 4-fold lower than that of the 2.0 mm injury group ( $44 \pm 5.7$  s).

The sham-injured group did not show any significant differences compared to the 1.5 mm and 2.0 mm injury groups, on any day during the acquisition phase (Fig. 3.9F - G).

### Acquisition Trial

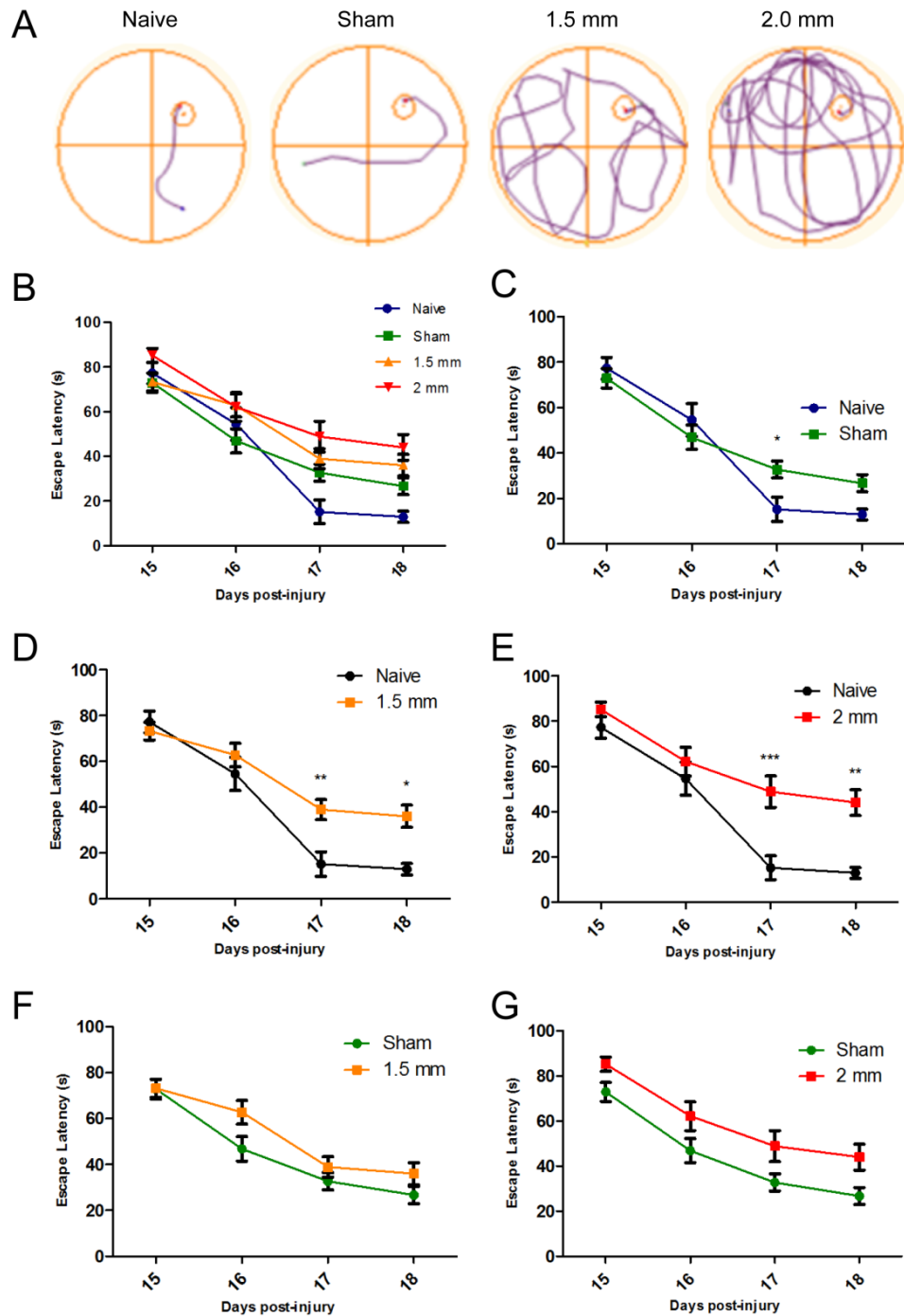


**Figure 3.9. Effect of injury severity on acquisition training in the Morris water maze.** The average escape latency of the 4 trials conducted on each day of the acquisition phase. (A) Representative traces from a trial on day 18 post-injury during the acquisition phase. (B) Escape latencies for all 4 experimental groups during the acquisition phase. (C) Acquisition phase showing naïve vs. sham-injury; the naïve group shows a significant difference to the sham group (\* $p < 0.05$ ) on day 17 post-injury. (D) naïve vs. 1.5 mm injury group; there is a significant difference in escape latencies on day 17 and 18 post-injury (\* $p < 0.05$ , \*\* $p < 0.01$ ). (E) naïve vs. 2.0 mm injury group, with significant differences at day 17 and 18 post-injury (\*\* $p < 0.01$ , \*\*\* $p < 0.001$ ). (F) sham-injured vs. 1.5 mm injury group and (G) sham vs. 2.0 mm injury group, with no significant differences between them. Repeated measures two-way ANOVA with post-hoc Bonferroni test was used for statistical analysis. Mean  $\pm$  S.E.M. N = 4–8 animals per group.

### **3.4.3.2 The effect of injury severity in the Morris water maze - probe trial**

At 24 hours after the last trial of the acquisition phase, the probe trial was conducted. The platform was removed from the tank and the mouse was allowed to swim and explore the tank for 90 seconds. Mice that can recall the location of the platform from the 4 days of acquisition training are expected to spend more time in the target quadrant that used to contain the platform, have a short latency to the platform zone and revisit the platform zone more frequently.

If a mouse spends more than a quarter of the trial time in the target quadrant, it can be proposed that the mouse has a preference for spending time in that quadrant, thus remembers the location of the platform. The naïve group was the only group to spend more than 25 % of the probe trial in the target quadrant, whereas the 2.0 mm group spent only 20.2 % of time in the target quadrant (Fig. 3.10B).

The naïve, sham-injured and 1.5 mm injury group had a short latency to entry to the platform zone (Fig 3.10C). In contrast, the mean average latency of the mice in the 2.0 mm injury group was almost double that seen in the 3 other groups. Despite this difference, there was no statistically significant difference between the 4 groups, overall.

The number of platform crossings did not vary much between the naïve ( $8.3 \pm 2.8$ ), sham-injured ( $8.4 \pm 3.0$ ) and 1.5 mm ( $7.4 \pm 2.3$ ) injured groups, whereas the 2.0 mm group ( $5 \pm 2.4$ ) made fewer platform crossings during the probe trial. The two other outcome measures which were the 'total distance travelled' (Fig. 3.10E) and the 'average speed' (Fig. 3.10F) of each group were similar to each other.

### Probe Trial

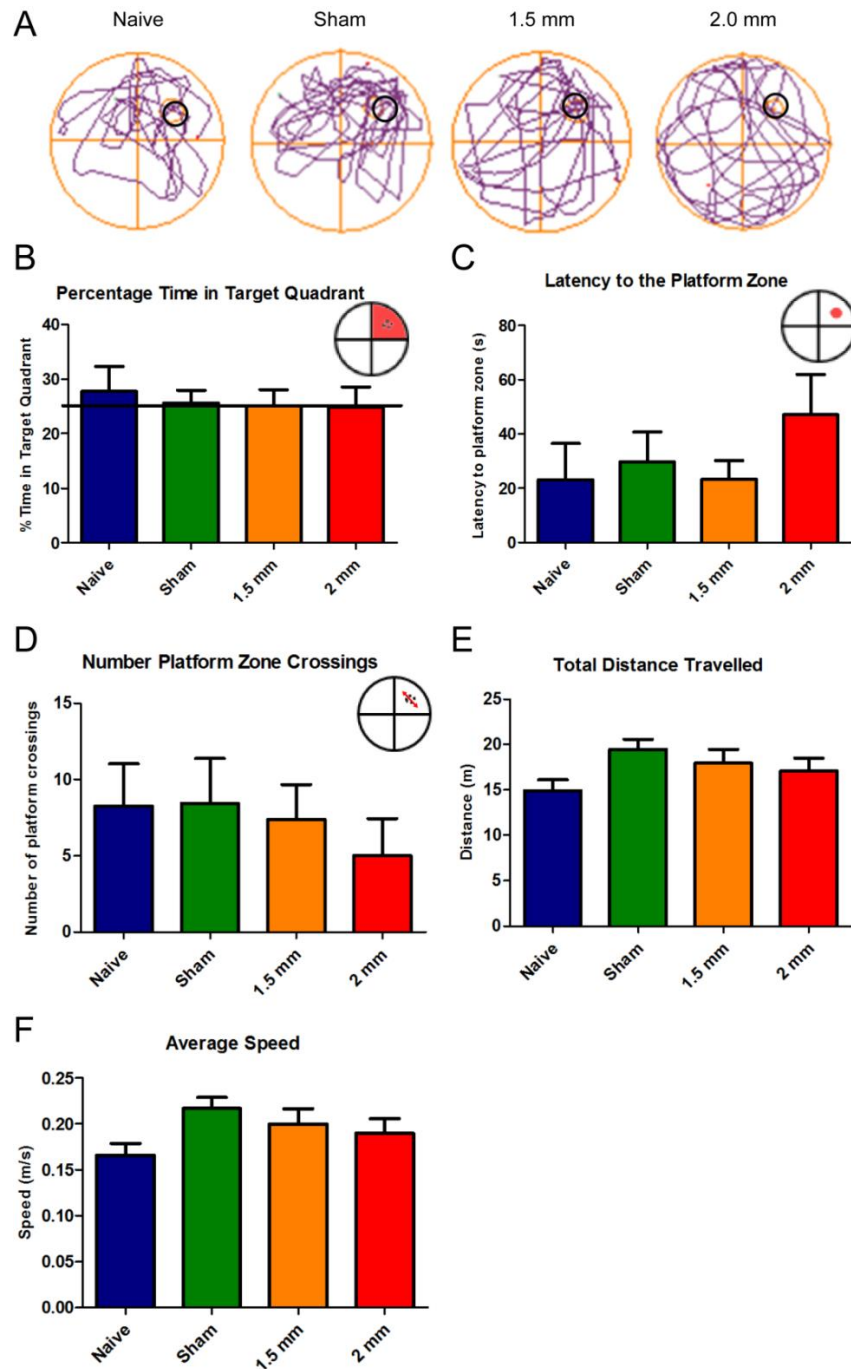


**Figure 3.10. Effect of injury severity on the probe trial performance in the Morris water maze.** (A) Representative track plots of a mouse from each experimental group. (B) The percentage time the mice spent in the target quadrant (where the platform used to be situated). (C) The latency to the zone where the platform used to be situated. (D) The number of crossings of the platform zone. (E) The total distance travelled during the probe trial. (F) The average speed during the probe trial. Mean  $\pm$  S.E.M. N = 4-8 animals per group.

### **3.4.3.3 The effect of injury severity in the Morris water maze - reverse acquisition trial**

It was decided that due to the lack of significant difference between the sham group and the injury groups in the rate of learning in the first week of acquisition phase trial, a second week of acquisition training should be performed, as demonstrated in a protocol used by Washington and colleagues (Washington et al., 2012). In this second week of training the platform is moved to the quadrant opposite the initial location (from north-east quadrant to the south-west quadrant). This reverse acquisition training can be used to expose possible subtler deficits in learning between the injury groups.

Using this new paradigm, the sham and the 1.5 mm injury groups showed no difference in escape latency in the reverse acquisition trial when compared to the naïve group (Fig. 3.11). The 2.0 mm injury group showed a significantly different (\* $p < 0.05$ , \*\*\* $p < 0.001$ ) escape latency when compared to the naïve group on all 4 days of the acquisition phase of the reversal training (Fig. 3.11D). When compared to the sham-injured group, the 2.0 mm group also showed a significant deficit (\* $p < 0.05$ ) in escape latency on the 2<sup>nd</sup> and 3<sup>rd</sup> training days of the second week reversal acquisition trial (Fig. 3.11F). The 1.5 mm group showed no significant difference to the sham-injured group (Fig. 3.11E).

### Reverse Acquisition Trial

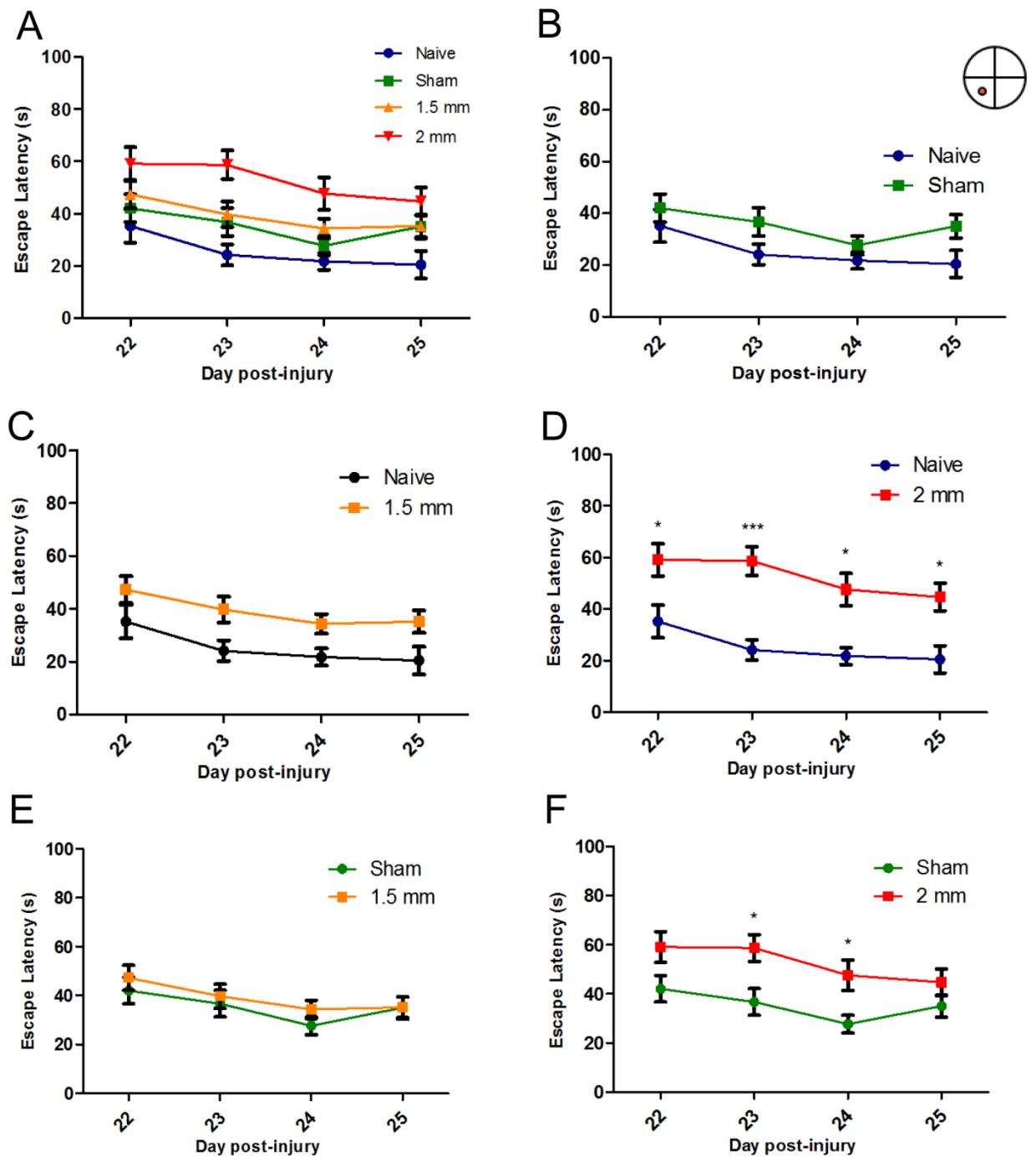


**Figure 3.11. Effect of injury severity on the reverse acquisition training in the Morris water maze.** The average escape latency of the 4 trials conducted on each day of the acquisition phase. (A) escape latencies for all 4 injury groups, (B) acquisition phase showing naïve vs. sham-injury, (C) naïve vs. 1.5 mm injury group, (D) naïve vs. 2.0 mm injury group, with significant differences on all trial days post-injury (\* $p < 0.05$ , \*\*\* $p < 0.001$ ). (E) sham-injured vs. 1.5 mm injury group and (F) sham vs. 2.0 mm injury group, with a significant difference between them at days 23 and 24 post-injury (\* $p < 0.05$ ). Repeated measures two way ANOVA with post-hoc Bonferroni testing used for statistical testing. Mean  $\pm$  S.E.M. N = 4–8 animals per group.



#### **3.4.3.4 The effect of injury severity in the Morris water maze - reverse probe trial**

##### **3.4.3.4.1 Reverse platform**

At 24 hours after the completion of the second week of the MWM, i.e. the reverse acquisition trial, a probe trial was conducted (Fig. 3.12). In the reversal probe trial the sham, 1.5 mm and 2.0 mm groups were slower at getting to the reverse platform zone than the naïve group (Fig. 3.12B). The naïve group took under half of the time ( $12.8 \pm 5.0$  s) to get to the reverse platform zone than the sham group ( $26.3 \pm 6.3$  s), the 1.5 mm ( $23.7 \pm 4.6$  s) and 2.0 mm ( $24.0 \pm 6.8$  s) injury groups. The naïve group also showed a higher number of reverse platform zone crossings ( $6.3 \pm 1.4$ ), when compared to the sham group ( $4.7 \pm 0.9$ ), the 1.5 mm ( $4.6 \pm 0.8$ ) and the 2.0 mm ( $4.8 \pm 1.0$ ) injured groups (Fig 3.12C).

##### **3.4.3.4.2 Original platform**

During the day 26 probe trial, outcome measures relating to the location of the original platform (first week of MWM testing; NW quadrant) were also measured. These included: 'Time in the original platform quadrant', 'latency to the original platform zone' and the 'number of original platform zone crossings' (Fig. 3.13).

The naïve and sham control groups displayed different behaviours when compared to the 1.5 mm and 2.0 mm injury groups with regard to the original platform measures. The naïve ( $33.5 \pm 10.9$  s) and sham ( $40.2 \pm 11.2$  s) groups took longer to visit the original platform zone than the 1.5 mm ( $14.2 \pm 7.4$  s) and 2.0 mm ( $16.7 \pm 7.6$  s) injury groups. The naïve and sham groups exhibited a higher number of original platform zone crossings in comparison to the CCI injury groups, although the naïve group ( $4.75 \pm 1.4$ ) visited the zone almost twice as much as the sham group ( $2.6 \pm 1.1$ ). In the probe trial after the second week of MWM testing, neither of the 1.5 mm or 2.0 mm injury groups demonstrated any significant differences compared to the sham or naïve groups.

##### **3.4.3.4.3 Reverse Probe Trial –Reverse and Original Platform**

The naïve and sham groups exhibited different behaviours compared to the 1.5 mm and 2.0 mm injury groups with regard to the original platform zone, during the day 26 probe trial. The naïve and sham

groups took longer to get to the original platform zone, but then visited the original platform more often and spent more time in the quadrant in which the original platform was located (Fig. 3.14).

The two injured groups (1.5 mm and 2.0 mm) made statistically significantly ( $*p<0.05$ ) fewer entries to the original platform zone than the reverse platform zone in the day 26 probe trial. The 1.5 mm group visited the reverse platform  $4.6 \pm 0.8$  times and the original platform  $1.0 \pm 0.6$  times. The 2.0 mm group visited the reverse platform  $4.9 \pm 1.1$  times and the original platform  $1.2 \pm 0.7$  times. This suggests that the injured groups had more difficulty recalling the location of the original platform.

### Reverse Probe Trial – Reverse Platform

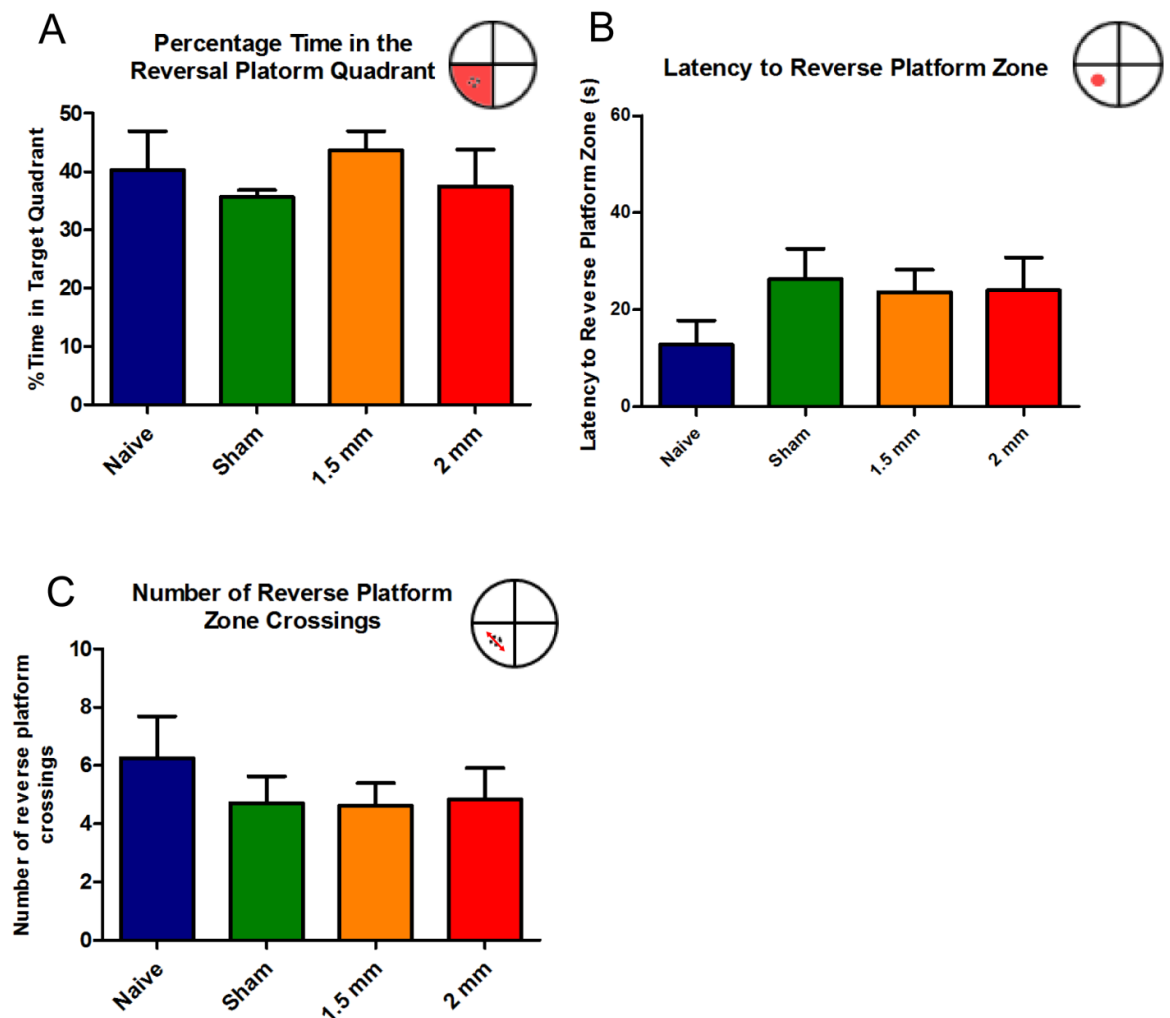


**Figure 3.12 Effect of injury severity on reverse probe trial performance in the second week of Morris water maze testing.** (A) The percentage time the mice spent in the target quadrant (where the platform used to be situated). (B) The latency to the zone where the platform used to be situated. (C) The number of crossings of the reverse platform zone. No statistical differences using one-way ANOVA. Mean  $\pm$  S.E.M. N = 4-8 animals per group.

### Reverse Probe Trial –Original Platform

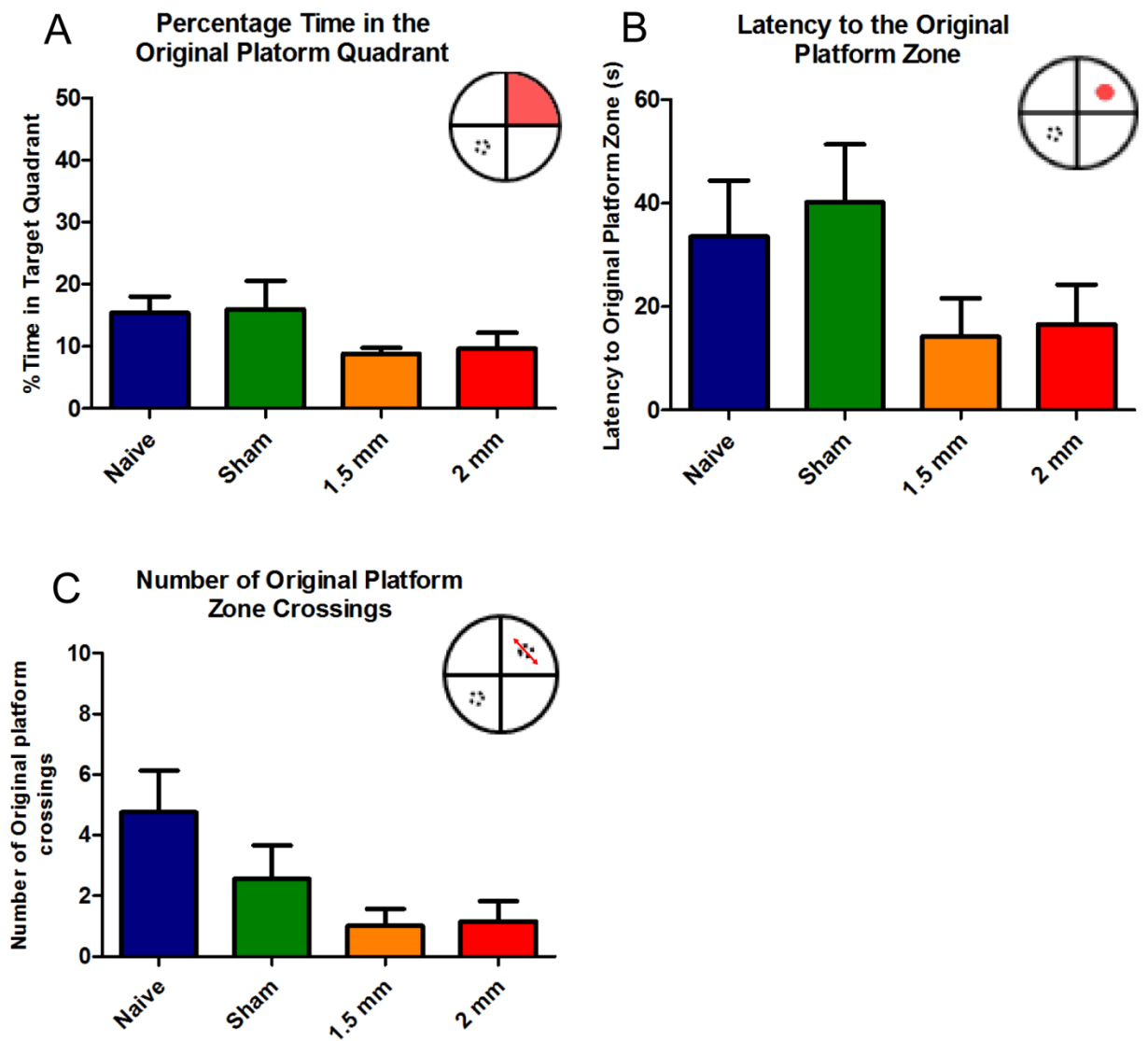


**Figure 3.13. Effect of injury severity on original platform measures during the reverse probe trial.** (A) The percentage time the mice spent in the original platform quadrant (where the original platform used to be situated). (B) The latency to the original platform zone. (C) The number of crossings of the original platform zone. No statistical differences using one-way ANOVA. Mean  $\pm$  S.E.M. N = 4-8 animals per group.

### Reverse Probe Trial –Reverse and Original Platform

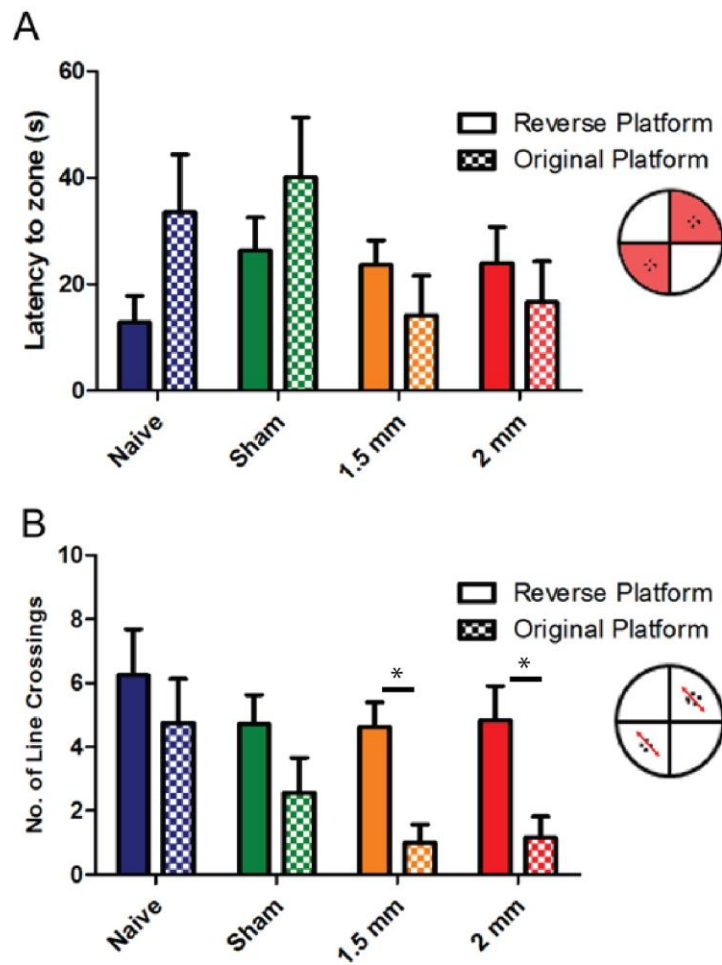


**Figure 3.14 Reverse probe trial.** (A) The latency to the reverse and original platform zones and (B) the number of crossings of the reverse and original platform zones by all four groups during the day 26 probe trial. The 1.5 mm (\* $p < 0.05$ ) and 2.0 mm (\* $p < 0.05$ ) injury group made statistically significantly fewer crossings of the original platform than the reverse platform. Two-way ANOVA with post-hoc Bonferroni testing was used. Mean  $\pm$  S.E.M. N = 4-8 animals per group.

### 3.4.4 Increase in injury severity

The 1.5 mm and 2.0 mm injury groups showed no significant differences to the naïve and sham control groups in the probe trials, after the first and second week of the acquisition trials. As the most severe injury depth of 2.0 mm failed to show statistically significant and robust differences compared to the sham craniotomy group, another optimisation study was conducted with an increased impact depth of 2.2 mm, tested against a group of sham injured animals. This study also included open field testing and the two-week MWM protocol including the reverse acquisition and probe trial (Fig. 3.15).

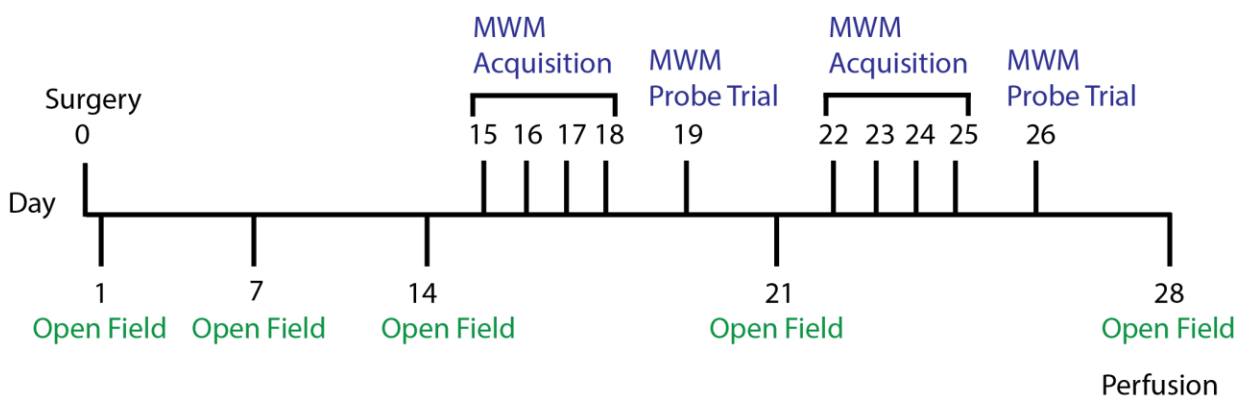


**Figure 3.15. Timeline for the execution of the behavioural tests after surgery.** The open field and the first MWM acquisition (day 15-18) and probe trial (day 19), and the second week reversal MWM acquisition (day 22-25) and reverse probe trial (day 26).

### 3.4.5 The effect of a 2.2 mm injury severity in the open field test

The open field test was conducted using the same protocol as in the previous study (Fig. 3.15). The time spent in the outer and inner zones, the time spent immobile, total distance travelled and the number of line crossings were measured, as demonstrated in the occupancy plots (Fig. 3.16).

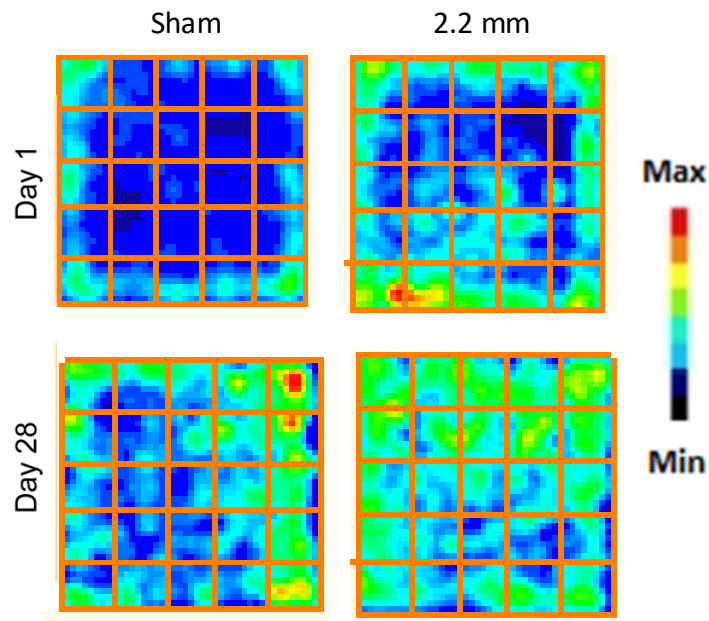


**Figure 3.16 Effect of a 2.2 mm injury on the open field performance.** Representative occupancy plots from open field testing on day 1 and day 28 from each experimental group.

There was no difference between the 2.2 mm injury and sham group in the time they spent in the inner or outer zone (Fig. 3.17A - B). Both the sham and 2.2 mm group spent the same amount of time immobile on day 1 post-injury. Over the course of the study the sham group spent an increasing amount of time immobile, while the time spent immobile by the 2.2 mm injury group remained constant (Fig. 3.18C). On day 28 post-injury the sham group ( $52.6 \pm 7.6$  s) spent almost twice as much time immobile as the 2.2 mm injury group ( $23.6 \pm 5.6$  s). At this time point the difference was found to be statistically different ( $*p < 0.05$ ), using a two-way ANOVA with post-hoc Bonferroni test.

The total distance travelled (Fig. 3.18C) and the number of line crossings (Fig. 3.18D) made by mice in the 2.2 mm injury group and sham group showed no statistically significant differences on any of testing days. However, between day 1 and day 7 the 2.2 mm injury group increased the distance travelled and the number of line crossings made (Fig. 3.18A - B). In contrast, the sham group decreased the distance they travelled and the number of line crossings made between day 1 and day 7 (Fig. 3.18A - B).

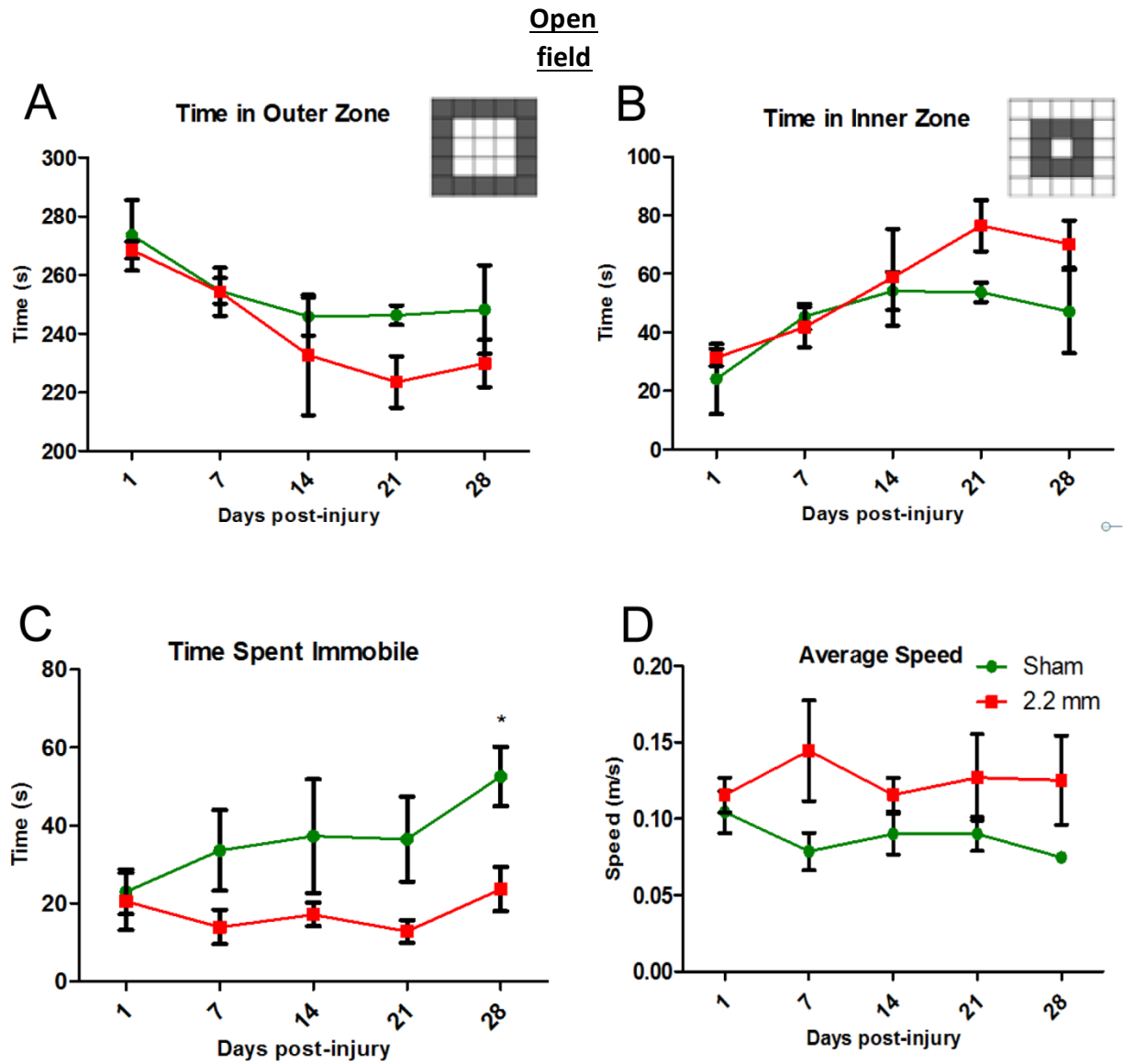


**Figure 3.17 Open field testing of a 2.2 mm injury versus a sham injury at day 1, 7, 14, 21 and 28 post-injury.** (A) The time spent in the outer zone and (B) the time spent in the inner zone. (C) The total time spent immobile; there is a significant difference between the sham and 2.2 mm injury group at day 28 post-injury ( $*p < 0.05$ ), using a two-way ANOVA with post-hoc Bonferroni testing. (D) The average speed of the animals. Mean  $\pm$  S.E.M. N = 4-7 animals per group.

### Open Field

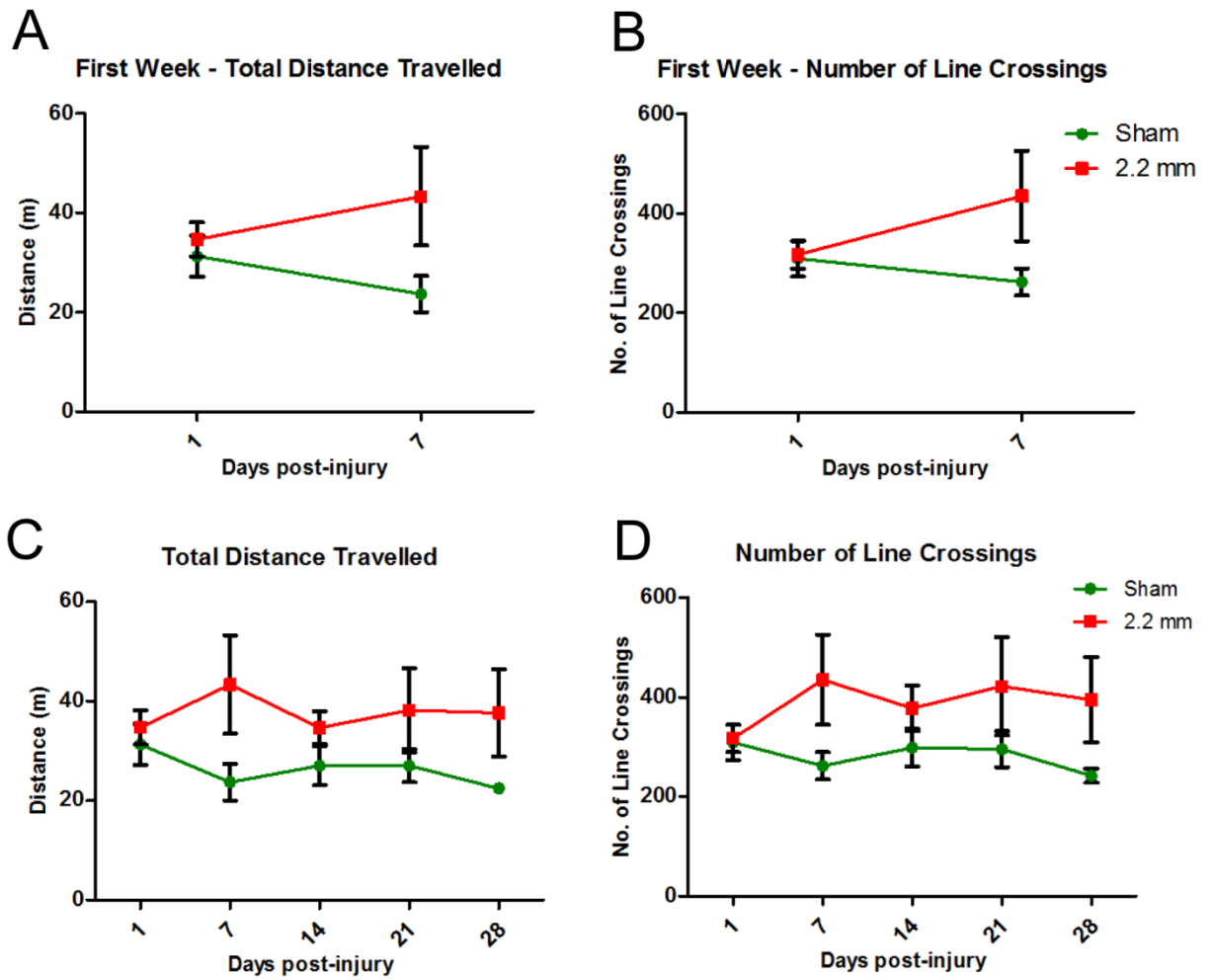


**Figure 3.18 Open field testing of a 2.2 mm injury versus a sham injury.** (A) The total distance travelled and (B) the number of line crossings made by the mice on day 1 and 7 in the first week post—injury. (C) Total distance travelled and (D) the number of line crossings at day 1, 7, 14, 21 and 28 post-injury. Mean  $\pm$  S.E.M. N = 4-7 animals per group.



### **3.4.6 The effect of a 2.2 mm injury in the Morris water maze**

#### **3.4.6.1 The effect of a 2.2 mm injury in the Morris water maze - acquisition and probe trial**

As in the previous study, the acquisition trial of the MWM is designed to test the capacity of the mice to learn. The mice in the 2.2 mm injury group had a longer escape latency time on each of the acquisition training days, compared to the sham group (Fig. 3.19A, B). The 2.2 mm group did reduce their escape latency from the first day of training (day 15) to the last day of the acquisition trial (day 18), from  $72.2 \pm 7.0$  s to  $41.5 \pm 6.0$  s. Despite this reduction in escape latency, the sham group was still statistically significantly ( $***p < 0.001$ ) faster at locating the platform on all four days of the acquisition trial.

During the probe trial held on day 19 (Fig. 3.19C - D), the sham group first entered the platform zone significantly ( $*p < 0.05$ ) faster than the 2.2 mm injury group. The sham group also entered the platform zone more often than the 2.2 mm group, although there was no statistically significant difference vs. the 2.2 mm group.

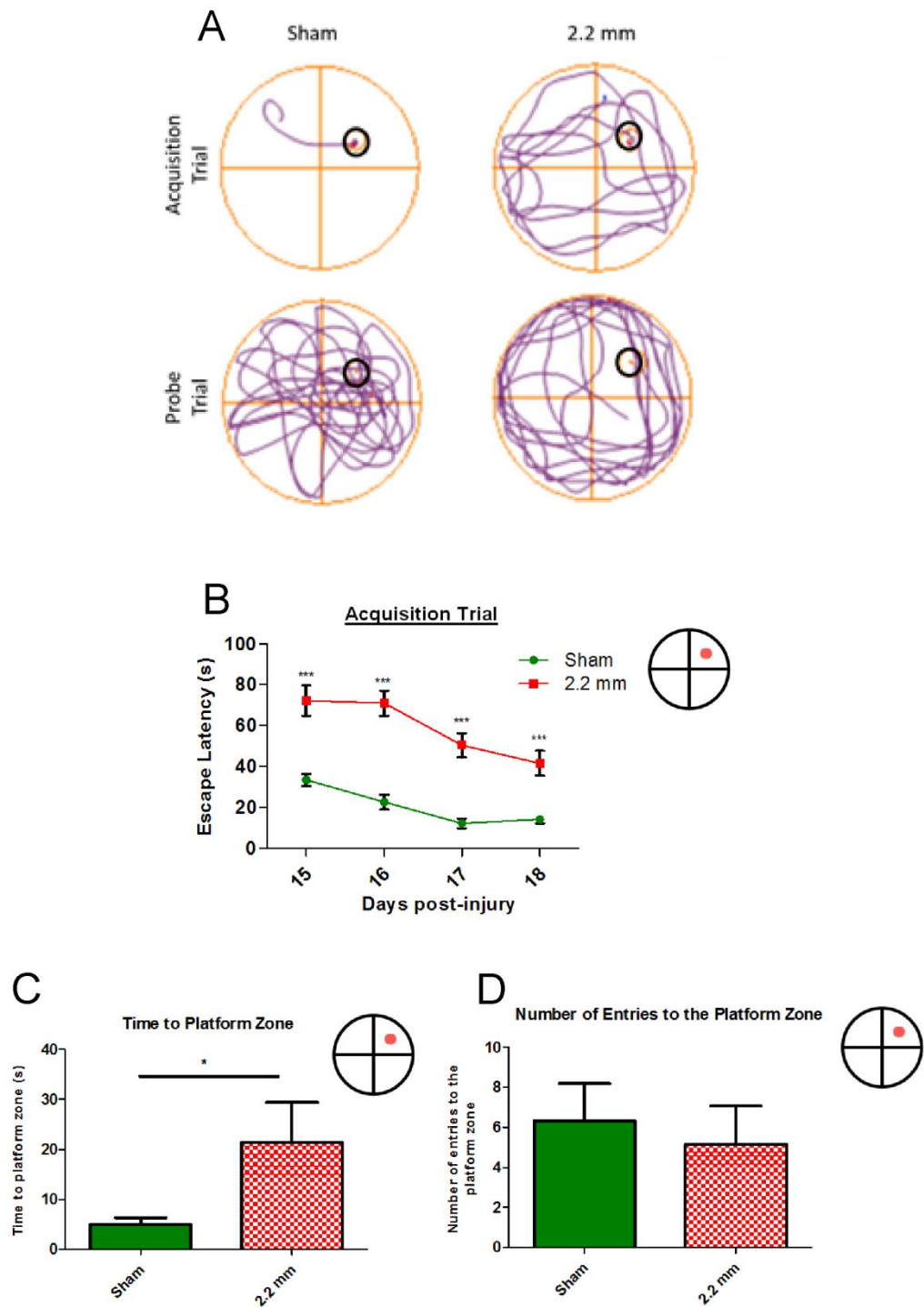


**Figure 3.19. Effect of a 2.2 mm injury vs. sham control on acquisition training and probe trial in the first week of the Morris water maze.** (A) Representative traces from a trial on day 18 post-injury during the acquisition training and probe trial. (B) The average escape latency of the 4 trials conducted on days 15 – 18 post-injury during the acquisition training. On all days of the acquisition training the 2.2 mm injury groups had a slower escape latency when compared to the sham group ( $***p<0.001$ ). Statistical significance was determined using a two-way repeated measures ANOVA with post-hoc Bonferroni test. On day 19 a probe trial was conducted. (C) The time to the platform zone. The 2.2 mm injury group was slower than the sham group ( $*p<0.05$ ). (D) The number of entries to the platform zone during the probe trial on day 19 post-injury. Mean  $\pm$  S.E.M. N = 4–7 animals per group.

#### **3.4.6.2 The effect of a 2.2 mm injury severity in the Morris water maze - Reverse acquisition trial**

As in the previous study, a reverse acquisition and probe trial was performed. The platform was moved from its original location to the quadrant opposite (from north-east quadrant to the south-west quadrant). The 2.2 mm injury group had a longer escape latency when compared to the sham group, on every day of the reverse acquisition training (Fig. 3.20A). The difference in escape latencies was not as large as in the first week of acquisition training, but was still statistically significant ( $*p < 0.05$ ), when using a two-way repeated measures ANOVA with post-hoc Bonferroni test.

#### **3.4.6.3 The effect of a 2.2 mm injury severity in the Morris water maze - Probe trial**

A second probe trial was conducted on day 26, 24 hours after the last training trial of the acquisition phase. The platform was removed from the pool and outcome measures relating to the reverse platform zone and the original platform location were recorded during the 90 second trial (Fig. 3.20B, C, D & E).

##### **3.4.6.3.1 Reverse Platform**

In the probe trial the 2.2 mm injury group entered the reverse platform zone slower than the sham group ( $*p < 0.05$ ) (Fig. 3.20B). The sham group first entered the reverse platform zone in  $5.4 \pm 1.5$  s, whereas the 2.2 mm injury group first entered the zone in  $27.0 \pm 8.0$  s. The sham group also entered the reverse platform zone more frequently than the 2.2 mm injury group ( $4.7 \pm 0.7$  vs.  $3.0 \pm 0.9$  entries), although this difference was not statistically significant.

##### **3.4.6.3.2 Original Platform**

During the probe trial outcome measures relating to the original platform zone were also measured (Fig. 3.20D, E). The time taken for the 2.2 mm injury group and the sham group to visit the original platform zone was very similar and did not show any significant differences. This was also the case for the number of visits to the original platform zone.

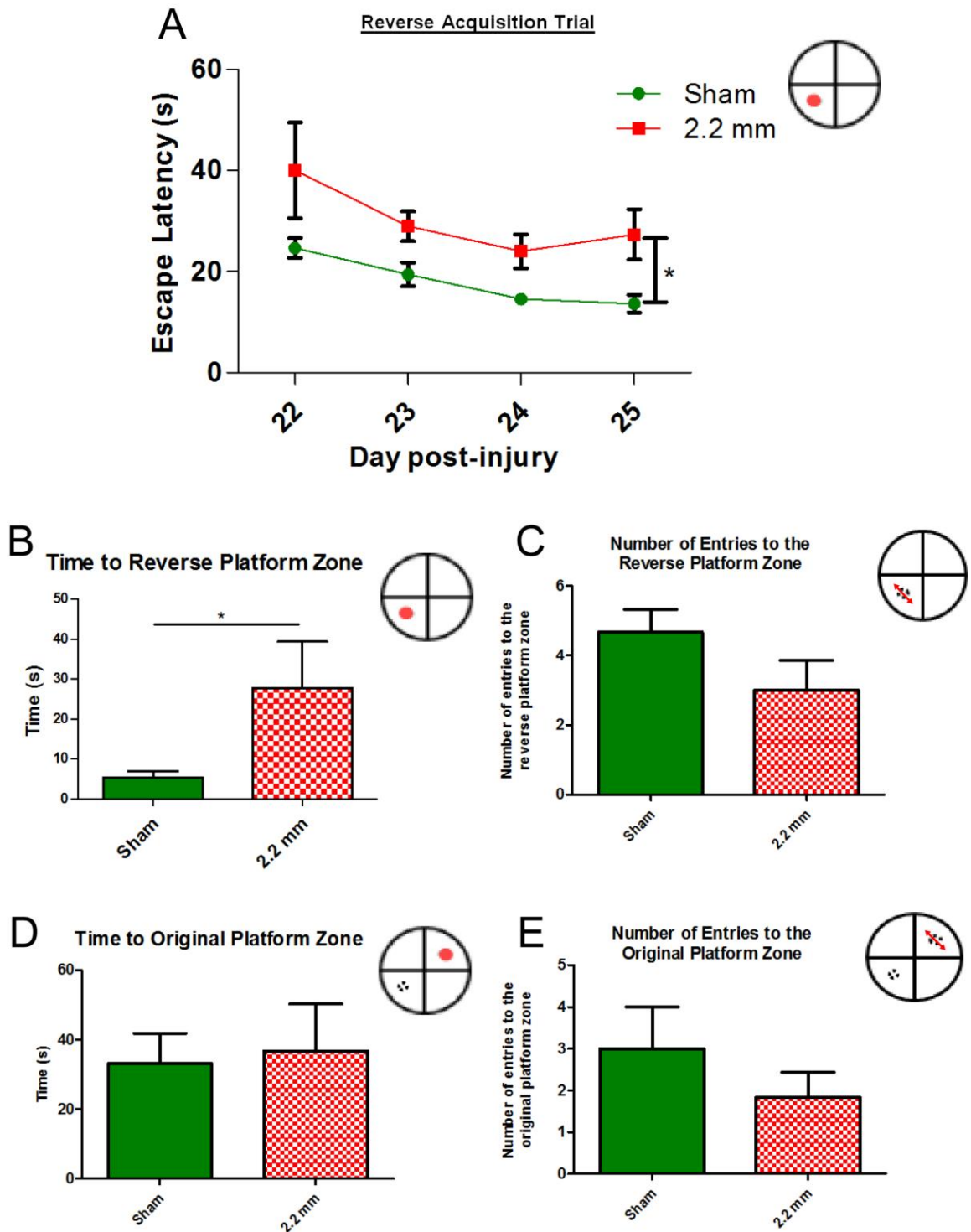


**Figure 3.20 Effect of a 2.2 mm injury vs sham control on the reverse acquisition training.** The average escape latency of the 4 trials conducted on days 22 – 25 post-injury in the reverse paradigm. On all days of the reverse acquisition training the 2.2 mm injury groups had a slower escape latency when compared to the sham group (\* $p < 0.05$ ). Statistical significant was determined using a two-way repeated measures ANOVA with post-hoc Bonferroni test. Mean  $\pm$  S.E.M. N = 4-7.

### **3.4.7 The effect of injury severity on the ipsilateral hemisphere - cortex and hippocampus**

After perfusion of the mice on day 28, the brain tissue was cut into coronal sections. Sections from 4 locations (-1.5, -2, -2.5 and -3 mm posterior to bregma) spanning the area of the lesion were analysed using a general histological stain (toluidine blue; a blue dye that has a high affinity for acidic cell components, such as nucleic acids), to assess the extent of tissue lost after injury (Fig. 3.21).

The increased injury depth and severity resulted in an increased tissue loss at 28 day post-injury on the ipsilateral side of the brain compared to the contralateral side (Fig. 3.22). The size of the ipsilateral hemisphere, cortex and hippocampus were measured as a percentage of the equivalent contralateral brain region, on selected sections. All three injury groups (1.5, 2.0, 2.2 mm) lost over 20 % of the ipsilateral cortical area (Fig. 3.22B).

The 1.5 mm injury group had a 20 % loss in ipsilateral cortical tissue, but no loss in ipsilateral hippocampal tissue. In contrast, the 2.0 mm and 2.2 mm injured groups lost over 50% of the hippocampus on the ipsilateral side (Fig. 3.22C). Qualitatively, the ipsilateral hippocampal tissue in the 1.5 mm group maintained a normal structure, while the remaining hippocampal tissue in the 2.0 mm and 2.2 mm injury groups had a much distorted structure, with some regions of the hippocampus being compressed or absent entirely (Fig. 3.21).

The sham injury group showed no significant tissue loss in any of the three measurements, however toluidine blue staining revealed damage to the surface of the cortex beneath the site of the craniotomy (Fig 3.21).

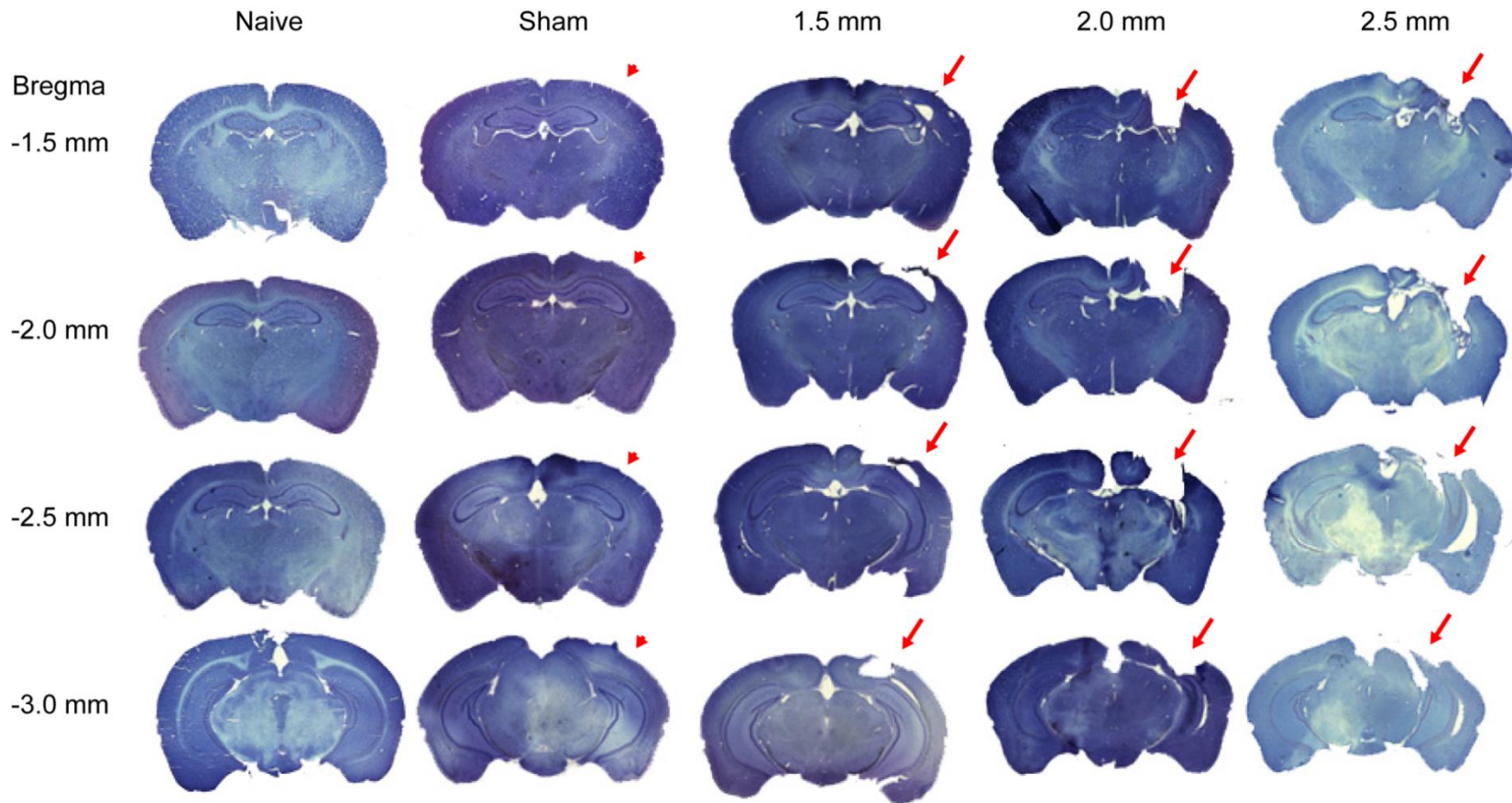


**Figure 3.21. Brain sections stained with toluidine blue.** Coronal brain sections (20  $\mu$ m) posterior from the naïve, sham, 1.5 mm, 2.0 mm and 2.2 mm injury groups. The brain sections were taken from the following location posterior to bregma skull landmark: -1.5 mm, - 2.0 mm, -2.5 mm and - 3.0 mm. The red arrowheads indicate the region of craniotomy and the red arrows indicate the location of the injury site.

## Ipsilateral hemisphere, cortex and hippocampal changes

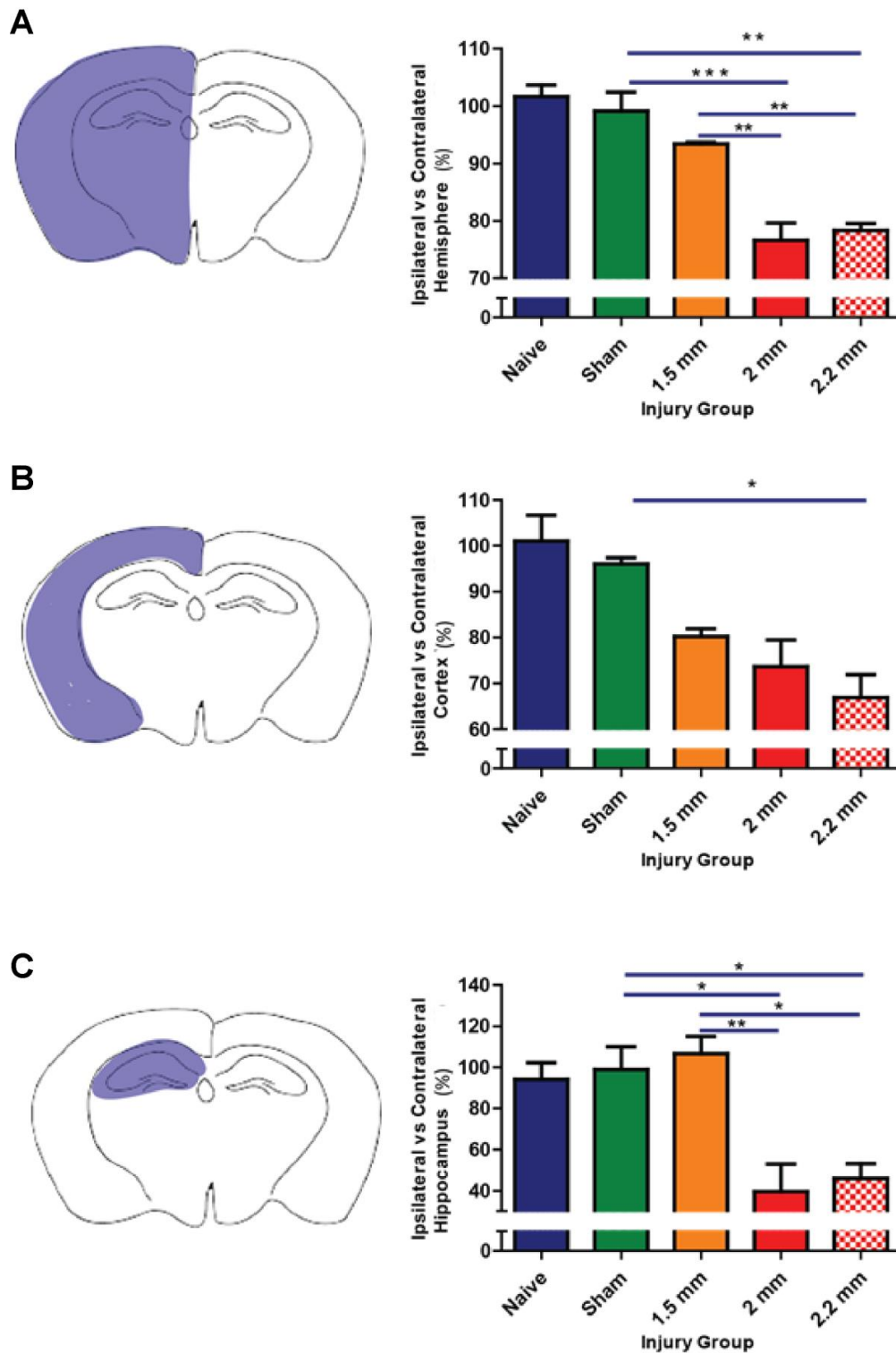


**Figure 3.22.** The effect of injury severity on the ipsilateral brain regions as compared to the contralateral side. (A) hemisphere, (B) cortex and (C) hippocampus. Statistical significance was found using one-way ANOVA and post-hoc Bonferroni testing (\*p<0.05, \*\*p<0.01, \*\*\*p<0.001). Mean ± S.E.M. N = 3 animals per group.

### **3.4.8 The effect of injury severity on astrocytes in the cortex and the hippocampus**

Following TBI, the glial cells, such as astrocytes and microglia in the area surrounding the lesion site, can become 'activated' (section 1.2.2.7). When 'activated', these glial cells change their morphology and phenotype. In particular, when astrocytes become 'activated' they begin to undergo a process called 'reactive astrogliosis', and become hypertrophic, highly ramified and upregulate the intermediate filament protein GFAP (Sofroniew, 2009). Brain tissue collected from the mice was immunolabelled with an anti-GFAP antibody, to assess the extent of reactive astrogliosis induced in the different injury groups, within the cortex and the contralateral hippocampus. The amount of GFAP staining was measured by the percentage increase in staining compared to the naïve control group.

Four regions of interest (ROI) within the cortex were chosen for the analysis of the GFAP immunofluorescence. Two ROI from the border of the lesion site (Fig. 3.24A; C3 - C4) in the ipsilateral cortex were analysed and two ROI in the equivalent locations on the contralateral side (Fig. 3.24A; C1 - C2). The amount of GFAP immunofluorescence was calculated as a percentage increase when compared to the naïve group GFAP staining within the same ROI.

Within the contralateral cortex (Fig. 3.24B), the sham, 1.5 mm and the 2.0 mm injury groups all showed an increase in GFAP staining compared to the equivalent area in the naïve group. The 2.2 mm injury group had a much higher increase ( $486.5 \pm 155$  %) in the amount of GFAP staining compared to the naïve group. Despite this increase there was no statistically significant difference overall.

In the ipsilateral cortex (Fig. 3.24C) the sham group showed no increase in GFAP labelling compared to the naïve group. The 1.5 mm and 2.0 mm injury groups both showed an increase in GFAP staining by 3-fold, while the 2.2 mm group showed an increase in GFAP staining of over 600 % compared to the naïve group. The 2.2 mm injury group showed a statistically significant (\*\* $p < 0.01$ ) difference compared to the sham group.

Due to the destruction of the ipsilateral hippocampus, ROI in the contralateral hippocampus were analysed for GFAP staining. Four ROI in the contralateral hippocampus, including the dentate gyrus (DG), and areas CA1, CA2 and CA3 were analysed (Fig 3.24A). The four ROI showed a graded



percentage increase in GFAP vs. the equivalent areas in the control group, correlating with the severity of the injury (Fig. 3.24D), sham ( $121.6 \pm 39\%$ ), 1.5 mm ( $152.3 \pm 19.1\%$ ), 2.0 mm ( $192.9 \pm 19.1\%$ ) and the 2.2 mm injury group ( $270.4 \pm 73.8\%$ ). The analysis of the DG ROI showed that the sham, 1.5 mm and 2.0 mm injury groups all displayed a similar percentage increase in GFAP labelling compared to the naïve group (Fig. 3.24E). However, the 2.2 mm injury group, showed a much higher increase in GFAP labelling compared to naïve, of almost 400%, with increased astrogliosis nearer the lesion.

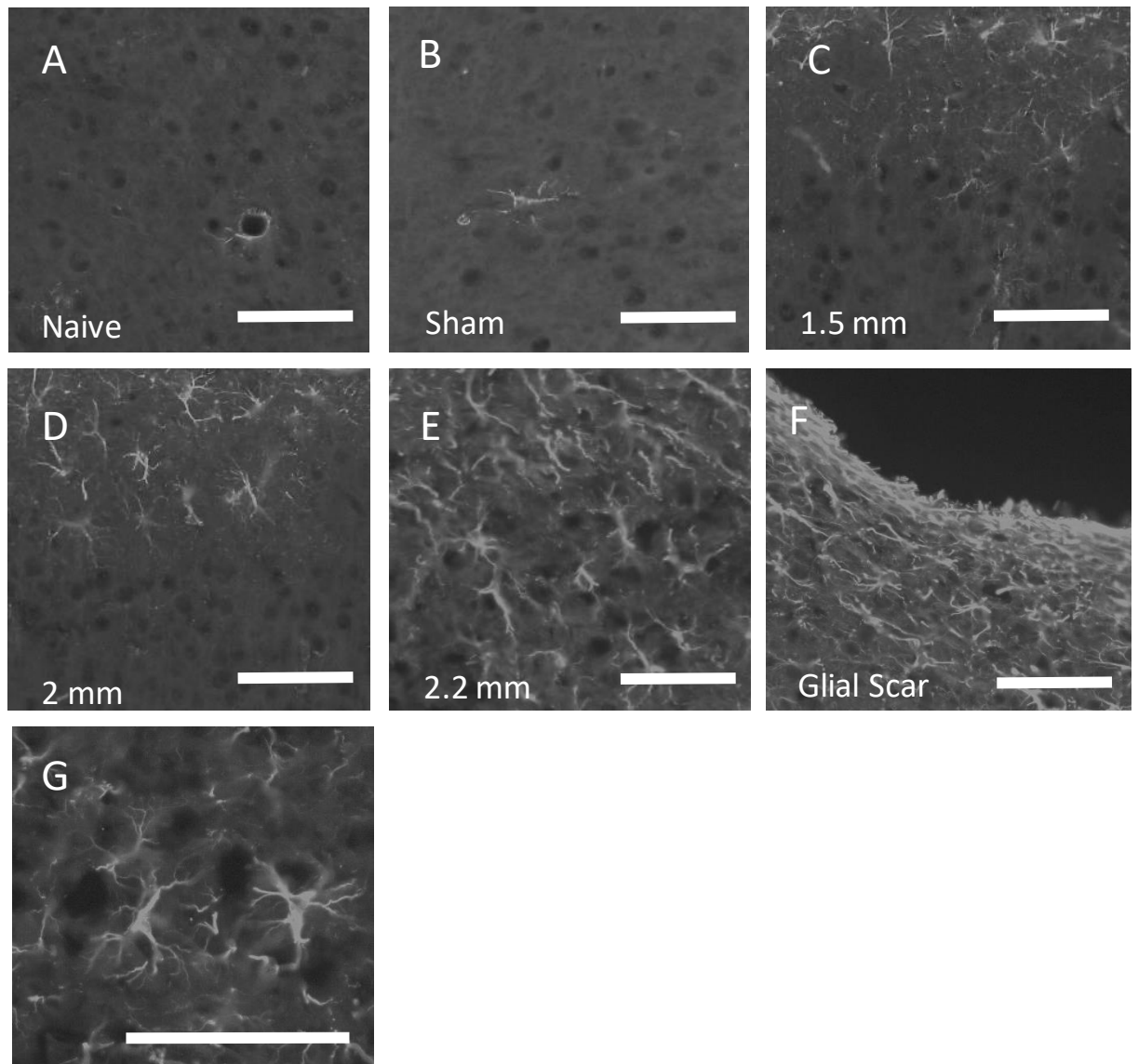


**Figure 3.23. The effect of injury severity on the GFAP expression.** Immunolabelling of reactive astrocytes with GFAP in the ipsilateral cortex in the (A) naïve, (B) sham-injured, (C) 1.5 mm, (D) 2.0 mm, (E) 2.2 mm injury groups in tissue adjacent to the lesion (top of image), (F) the glial scar in a 2.0 mm group and (G) astrocytes in the contralateral hippocampus. Scale bar = 100  $\mu\text{m}$ .

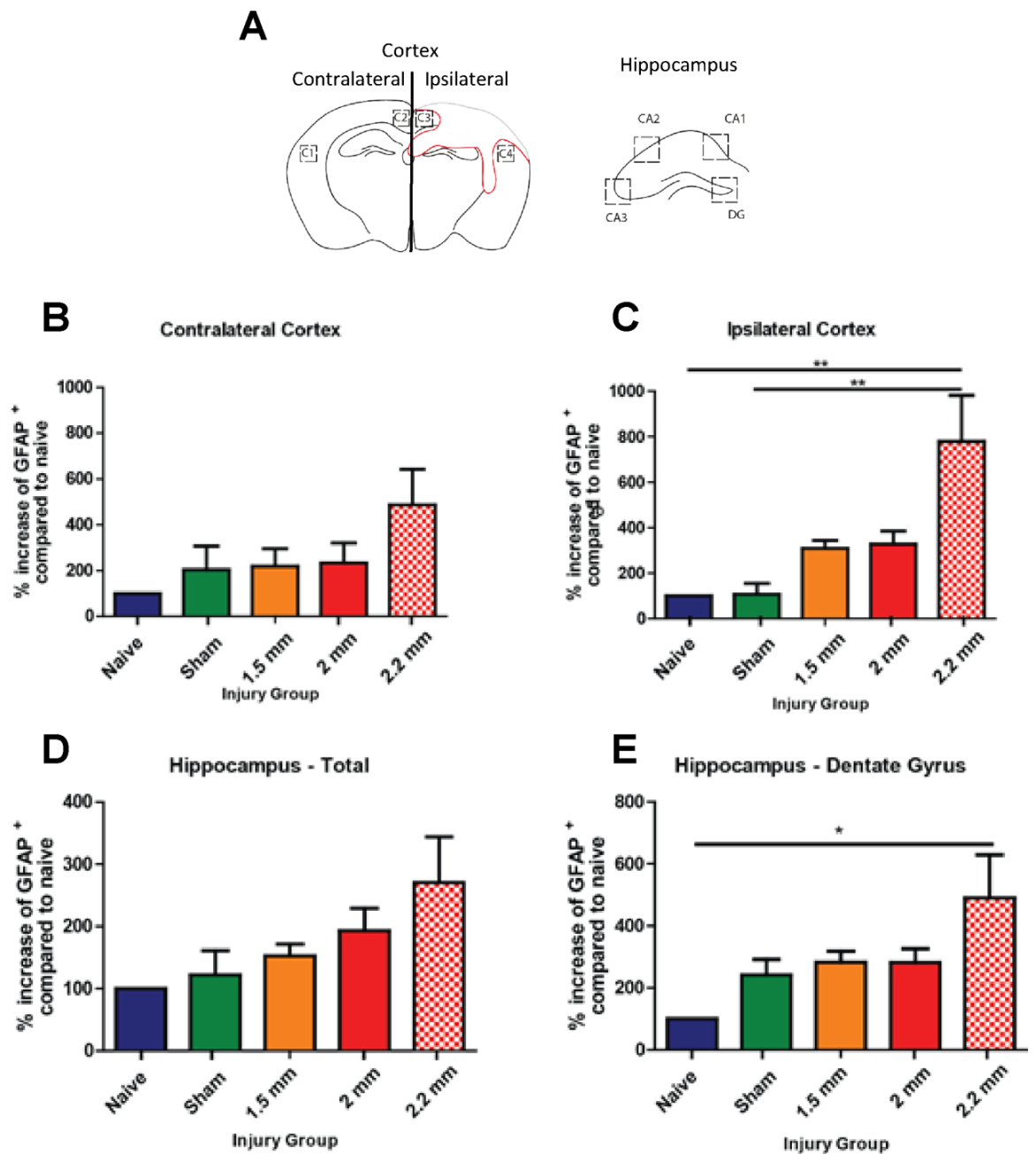


**Figure 3.24. The effect of injury severity on the reactive astrogliosis in the cortex and hippocampus.** (A) Schematic showing the ROI in the cortex and hippocampus that were analysed for GFAP labelling (GFAP<sup>+</sup>). The percentage increase in GFAP labelling compared to the naïve group in (B) the contralateral cortex, (C) the ipsilateral cortex, (D) the contralateral hippocampus and (E) the dentate gyrus of the hippocampus. Statistical significance was determined using one-way ANOVA and post-hoc Bonferroni test (\* $p < 0.05$ , \*\* $p < 0.01$ ). Mean  $\pm$  S.E.M. N=4-6 animals per group.

### **3.4.9 The effect of injury severity on the microglia in the cortex and the hippocampus**

In the same ROI, the microglia cells were labelled using an anti-Iba1 antibody. Iba1 is a calcium-binding protein that is up-regulated in microglia after injury and indicates activation of these cells (Ito et al., 2001). However, Iba1 also labels cells of monocytic lineage including infiltrating macrophages, which are more likely to be present in injured brain tissue due to the breakdown of the BBB. Differentiating between the two cell types is difficult due to them both being labelled by Iba1, as well as sharing similar morphology. Therefore, the number of Iba1-positive (Iba1+) cells in each ROI was counted as a measure of the presence of microglia/macrophages post-injury (Fig. 3.25).

In the contralateral cortex (Fig. 3.26B) the number of Iba1+ cells was significantly increased in all of the injury and sham groups compared to the naïve group (naïve vs sham \*\* $p < 0.01$ ; 1.5 mm, \*\*\* $p < 0.001$ ; 2.0 mm, \*\*\* $p < 0.001$ ; 2.2 mm, \*\*\* $p < 0.001$ ). The 1.5 mm, 2.0 mm and 2.2 mm injury groups all showed a significant increase (sham vs. 1.5 mm, #  $p < 0.05$ ; 2.0 mm, ###  $p < 0.001$ ; 2.2 mm, ###  $p < 0.001$ ) in the number of Iba1+ cells compared to the sham group, with the 2.0 mm ( $61 \pm 4$ ) and 2.2 mm ( $60 \pm 4$ ) groups exhibiting double the number of Iba1+ cells than the sham group ( $31 \pm 5$ ) group.

In the ipsilateral cortex (Fig. 3.26C) the sham, 1.5 mm, 2.0 mm and the 2.2 mm injury groups all showed a significant increase in the number of Iba1+ cells compared with the naïve group (naïve vs. sham, \*\*  $p < 0.01$ ; 1.5 mm, \*\*\*  $p < 0.001$ ; 2.0 mm, \*\*\*  $p < 0.001$ ; 2.2 mm, \*\*\*  $p < 0.001$ ). The 2.2 mm group had a significantly higher number of Iba1+ cells ( $122 \pm 13$ ) than all of the other injury groups (2.2 mm vs sham, ####  $p < 0.001$ ; 1.5 mm, &&  $p < 0.01$ ; 2.0 mm, \$\$  $p < 0.01$ ).

In the hippocampus, the naïve group ( $57 \pm 8$ ) again exhibited the lowest number of Iba1+ cells, with all of the other injury groups showing a statistically significant (naïve vs. sham, \*\*  $p < 0.01$ ; 1.5 mm, \*\*  $p < 0.01$ ; 2.0 mm, \*\*\*  $p < 0.001$ ; 2.2 mm, \*\*\*  $p < 0.001$ ) higher number of Iba1+ cells: sham ( $117 \pm 2$ ), 1.5 mm ( $114 \pm 8$ ), 2.0 mm ( $131 \pm 9$ ) and 2.2 mm group ( $184 \pm 8$ ). The 2.2 mm group had a significantly higher number of Iba1+ cells compared to all of the other groups (2.2 mm vs. sham, ####  $p < 0.001$ ; 1.5 mm, &&&  $p < 0.001$ , 2.0 mm, \$\$  $p < 0.01$ ). Within the DG ROI, the naïve group ( $22 \pm 3$ ) had the lowest number of Iba1+ cells and the 2.2 mm group ( $57 \pm 2$ ) had the highest number, showing significance

against the naïve (2.2 mm vs. naïve, \*\*\*  $p < 0.001$ ), sham (2.2 mm vs. sham, #  $p < 0.05$ ) and 2.0 mm groups (2.2 mm vs. 2.0 mm, &  $p < 0.05$ ).

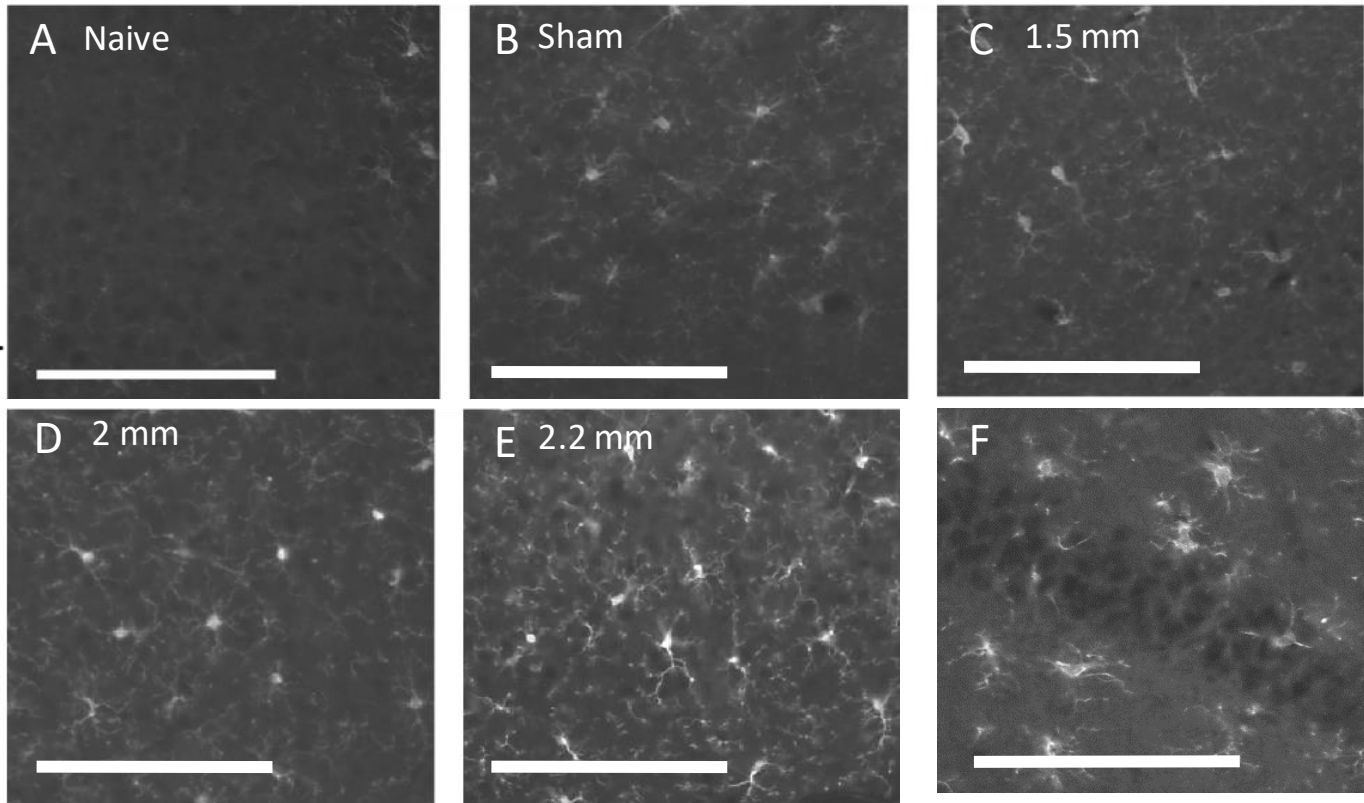


**Figure 3.25. Microglia with Iba1 labelling at various injury severities.** Iba1 immunolabelling in the ipsilateral cortex in the (A) naïve, (B) sham-injured, (C) 1.5 mm, (D) 2.0 mm, (E) 2.2 mm injury groups and (F) microglia in the contralateral hippocampus. Scale bar = 100  $\mu\text{m}$ .

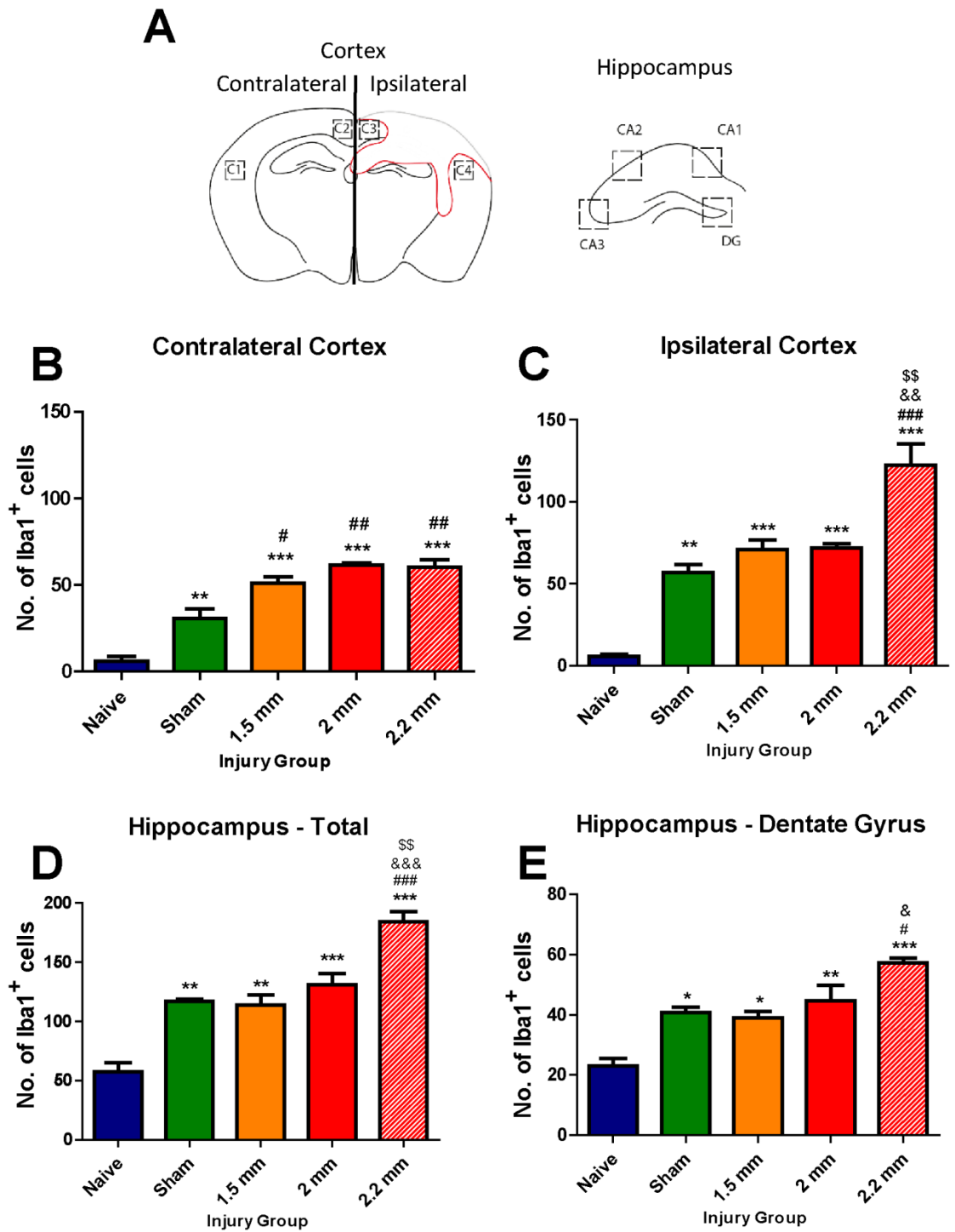


**Figure 3.26. The effect of injury severity on the number of microglia/macrophages in the cortex and hippocampus.** (A) The ROI in the cortex and hippocampus that were analysed for Iba1<sup>+</sup> cell numbers. The number of Iba1<sup>+</sup> cells in the (B) contralateral cortex, (C) the ipsilateral cortex, (D) the contralateral hippocampus and (E) the dentate gyrus of the hippocampus. Statistical significance was determined using one-way ANOVA and post-hoc Bonferroni testing (\*  $p < 0.05$ , \*\*  $p < 0.01$ , \*\*\*  $p < 0.001$  vs. the naïve group; #  $p < 0.05$ , ###  $p < 0.01$ , ####  $p < 0.001$  vs. the sham group; &  $p < 0.05$ , &&  $p < 0.01$  vs. the 1.5 mm group; \$\$\$  $p < 0.01$  vs. the 2.0 mm group). Mean  $\pm$  S.E.M. N=3 animals per group.

### **3.5 Discussion**

The primary aim of these studies presented in this section of the thesis was to optimise a CCI mouse model of TBI, with the aim to characterise a behavioural deficit that mirrors relevant human TBI neurological consequences, specifically the cognitive deficit of memory loss. Injury severity in patients has been shown to correlate with their long-term neurobehavioural outcome (Rapoport et al., 2002). For our model to be valid as a screening tool for potential TBI therapeutics, we expected the injury severity to correlate with a significant and robust cognitive behavioural deficit. In our studies, the injury severity was increased by increasing the impact depth, thereby increasing the extent of the tissue damage. A variety of behavioural tests were used to identify neurobehavioural deficits. The MWM test distinguished more clearly between the different injury severities. The injury severity which caused a robust deficit in the MWM test was the 2.2 mm impact depth. The 2.2 mm group had a significant deficit in the acquisition and probe trials of the MWM test when compared to the sham group. Histologically, there was also a graded increase in the reactive astrogliosis and microglia activation in the cortex and hippocampus, which correlated with injury severity.

#### **3.5.1 Functional outcomes**

Three behavioural tests were conducted in order to assess any severity dependent deficits in the gross locomotor function, the anxiety and cognitive ability of mice after TBI. The tests used were the open field, Y-Maze and the MWM test.

##### **3.5.1.1 Open field**

The primary purpose for conducting the open field test was to ensure that the locomotor function of the injury groups was comparable, therefore any deficits seen in the cognitive tests involving active motor performance (i.e. the MWM test) were due to cognitive and not motor dysfunction. The outcome measures 'distance travelled' and 'number of line crossings' confirmed that there was no difference between injury groups over the course of the studies. We did note, however, that the injured animals had a lower immobility score over time compared to naïve or sham injured mice – indicating a slight hyperactivity. The overall lack of difference in the various parameters considered,

between the injury groups within the open field test reflects similar results as those produced by Washington and colleagues, which showed that the open field test demonstrated no deficit in mice at 21 days after moderate CCI, using similar parameters to our study (Washington et al., 2012).

As discussed in section 1.8.3.1, the open field test has been used to assess other behaviours, such as anxiety. Spending a large amount of time in the outer zone of the open field apparatus, a phenomenon termed “thigmotaxis”, is suggested to be indicative of anxiety-like behaviour. There is conflicting data in the literature as to whether the CCI model does in fact cause a deficit in anxiety behaviour. Some groups suggest that CCI injury causes anxiety, a study performed by Yu and colleagues showed that thigmotaxis is increased in mice following a CCI injury (Yu et al., 2012, Chauhan et al., 2010). Others however, demonstrate no difference in anxiety (Sierra-Mercado et al., 2015), or suggest that CCI mice actually exhibit reduced anxiety behaviour (Washington et al., 2012) and may thus show disinhibition. Due to the complexities of testing rodents for anxiety, the conflicting data may relate to the sensitivity of the anxiety-based behavioural assay administered (Tucker et al., 2016). Our data did not show any difference in anxiety behaviours as assessed using the open field test over the time scale of the experiment.

### **3.5.1.2 Y-Maze**

The Y-maze test was conducted only in the first part of the study and not continued thereafter, due to the lack of a sufficient behavioural deficit between control and injury groups. There was some non-significant difference observed on day 3, when the naïve and sham group spent more time in the novel arm than the 1.5 mm and 2.0 mm injury groups. However, this difference in trend was not maintained on day 8 post-injury, suggesting that this deficit may be transient if at all significant.

The paradigm used in this study (section 2.1.4.2) was to measure time spent within the novel arm of the maze in the retrieval trial. Time spent in the novel arm and the number of entries into the novel arm is interpreted in this paradigm as indicators that the mouse views the novel arm as ‘un-explored’ and therefore chooses to spend more time exploring it. However, this outcome measure may be prone

to misinterpretation. As previously mentioned (section 1.6.3.2), differences between the groups' locomotor function could result in an invalid interpretation of the results in this test.

One of the main benefits of this type of assessment is that it does not require food deprivation or involves stress, as observed in tests such as the dig task or the Porsolt forced swim test (Martens et al., 2013, Can et al., 2012). The absence of any food reward or stress motivation may be affecting the results of this test. In some TBI patients, it is reported that cognitive symptoms such as deficits in decision making or memory function are only obvious in stressful situations (Gouvier et al., 1992). This could explain the absence of notable differences between the injury groups in the Y-Maze test when compared to the MWM results. The lack of any significant deficit might also be due to the earlier time points at which this test was administered (day 3 and day 8). Due to the progressive nature of this disease, a significant deficit in cognitive function may not yet have been fully developed. However, Smith and colleagues were able to see a deficit between CCI-injured mice compared to sham-injured mice in the MWM test only 48 hours after injury (Smith et al., 1995). This provides further support to the notion that a stress-inducing motivator may be needed in order to reveal a cognitive deficit.

### **3.5.1.3 Early behavioural differences after TBI**

It is worth noting that despite there being an absence of differences in the Y-maze and open field test outcome measures over the course of the 4-week study, there is an indication that there may be some transient differences within the first week after injury. As previously mentioned, the 1.5 mm and 2.0 mm injury groups failed to spend more time in the novel arm at day 3 post-injury compared to the control groups. Correspondingly, within the open field test, the sham, 1.5 mm and the 2.0 mm groups travelled further and made more line crossings than the naïve group at day 7 post-injury. However, these differences disappeared after 7 days post injury. Transient deficits are not uncommon in rodent models of neurotrauma; for example, in SCI models rodents spontaneously recover some motor function early, following injury (Creed et al., 2011, Scherbel et al., 1999, Bareyre et al., 2004, You et al., 2003). It is also possible that the changes in these behaviours over time may not be due to any



transient component of the secondary injury pathology, or lag time in compensatory function, but could be due to habituation of the mouse to the testing environment.

#### **3.5.1.4 Morris water maze test**

The MWM test is used to assess hippocampal-dependent spatial learning and memory function in rodents. In the studies presented in this chapter, the MWM test revealed differences in memory function between the injury groups, and thereby helped to determine an injury severity level (2.2 mm impactor depth) to use in subsequent studies. Initially, a 4-day acquisition paradigm followed by a single probe trial was used (section 2.1.4.3). In the first study the acquisition trial revealed differences between the naïve group and the other injury groups (1.5 mm and 2.0 mm). However, in the first week probe trial (day 19) the differences in memory function between the injury groups were less notable. As previously mentioned, Washington et al. demonstrated clearer differences between the different severity groups when employing a second week reversal MWM test (Washington et al., 2012). In the study paradigm, this is where the acquisition and probe testing protocol remain the same, but the location of the platform is changed. The data from our second week probe trial (day 26) supported what was shown by Washington and colleagues: our 1.5 mm and 2.0 mm injury groups headed towards the location of the original platform zone as opposed to the reverse platform zone (Washington et al., 2012). This might indicate that the cognitive function of the injured mice in the first week of acquisition training is superior to their cognitive function in the second week. This could be due to the progressive nature of the TBI pathology, whereby cognitive ability declines as the impact of the secondary injury pathology increases. With regards to the results of the second week acquisition trial, the 2.0 mm group exhibited some deficit compared to the sham group, but this was not significant throughout the acquisition trial. The fluctuation of the 2.0 mm injury group's cognitive ability may suggest that the injury in this paradigm is too mild, to see a consistent deficit. This has been seen in the clinic as well, where cognitive deficit in TBI patients categorised as mild or moderate is fluctuating (Satz et al., 1998). In order for our CCI model to be robust, the injury group needs to have a reproducible and significant cognitive deficit when compared to the sham injury group. Considering

this, it was decided to repeat the study with an increased impactor depth of 2.2 mm and compare its effect to a sham-injury group only.

It is important for the deficit to be significant against the sham group, as the sham group undergoes the same surgical procedures and aftercare regimen as in the impacted groups, but without the actual brain injury. Mice undergoing surgery receive anaesthesia such as ketamine, which has been shown to have neuroprotective and neuroregenerative properties that can cause beneficial outcomes in mice following TBI (Himmelseher and Durieux, 2005). Therefore, it is important that any influence these peri-operative compounds have on the baseline performance of the mice, is matched in the control group. Conversely, a craniotomy can have a detrimental impact on the behavioural outcome of mice, as seen in the first week acquisition trial in the first study (Fig. 3.9). Therefore, it is important that any baseline negative effect the craniotomy has on the mice is matched by the control group.

In the second study, during the first week of MWM testing the 2.2 mm injury group exhibited a significant deficit in learning in the acquisition trial, as well as a significant deficit in memory function in the first week probe trial, when compared to the sham group. The 2.2 mm group continued to have a significant deficit during the reversal MWM acquisition and probe trial. The outcomes of the MWM test in this second study demonstrated that an impactor depth of 2.2 mm causes an injury level sufficient enough to produce significant cognitive dysfunction in the mice and is therefore an appropriate impact depth for our CCI mouse model of TBI.

It was important for the continuation of this study and its relevance, that there was a deficit in the MWM, as it is an established behavioural test for memory function. As mentioned in the introduction to this chapter, memory loss is one of the main complaints of TBI patients. It is also a common test used when screening transgenics as a model for neurodegenerative diseases, or as a screening tool for therapeutics that may reverse or diminish memory loss (Bromley-Brits et al., 2011). Several lab groups that employ the mouse CCI model of TBI, use the MWM as a behavioural test (Washington et al., 2012, Xuan et al., 2014, Su et al., 2015, Kabadi et al., 2012, Zhang et al., 2012). Our MWM data shows that

our CCI model reproduces the changes seen by other groups in the same field of research, using the same model of injury.

### **3.5.2 Pathophysiological changes**

It was hypothesised that the tissue loss would increase with the severity of the injury, as the impactor extends further into the brain tissue, thereby causing more damage. Studies have shown that the lesion size and tissue loss correlates with impactor depth and thereby injury severity (Saatman et al., 2006). This correlation was also observed in the tissue from our studies. Neither the naïve or sham group exhibited any significant tissue loss. The 1.5 mm injury group exhibited some ipsilateral tissue loss, however, it still had more tissue preservation when compared to the other 2.0 mm and 2.2 mm groups, particularly in ipsilateral the hippocampus region. This may explain why the 1.5 mm injury group performed so well in the hippocampal-dependent MWM test. The 2.0 mm and 2.2 mm injury groups did not show any statistical significance between each other in the percentage of tissue lost within each of the locations (ipsilateral hemisphere, cortex and hippocampus). The 2.0 mm and 2.2 mm injury groups did exhibit a huge loss in ipsilateral hippocampal tissue, of almost 50%, with any remaining ipsilateral hippocampal tissue appearing misshapen or squashed. This loss, while considerable, was not significant enough to cause complete failure in the MWM acquisition trial. The data suggest that the intact contralateral hippocampus and/or the remaining ipsilateral hippocampal tissue are providing some compensatory effect. It is worth noting that the deficits in the MWM test were observed several days before this tissue was collected and that the tissue loss at the time of the testing may not be as great. In future studies it may be worth sacrificing earlier to establish a pattern of pathophysiological changes across a time course. But the main focus of these studies was to observe behavioural differences.

The literature does not accurately define specific impactor depths as mild, moderate or severe injuries. Unlike human TBI where the GCS is used to define the severity of the injury, there is no universal score or behavioural test that defines the severity of the injury in animals. Due to the differences between laboratory set ups and protocols (e.g. impactor equipment, rodent species and strain, different

outcome measures) the severity of the injury may pertain to the unique set up within individual laboratories (Xiong et al., 2013). Therefore, it has been up to the individual laboratory to define a set of outcomes as a mild, moderate or severe injury, when optimising their model, as was carried out in this first chapter. Due to the inter-laboratory discrepancy, our injury (2.2 mm), which we have defined as 'moderate', may not relate to the moderate severity of other research groups modelling TBI. Furthermore, it may also not be the equivalent of a moderate human TBI as defined by the GCS. The differences between human and rodent brains are discussed in the general introduction of this thesis; these differences may make the translation of TBI severity between mouse and human even more difficult.

In addition to the tissue loss, we hypothesized that glial cell activation would show a positive correlation with the injury severity. The extent of astrogliosis has been shown to correlate with TBI severity (Sofroniew, 2009). One of the main indicators of reactive astrogliosis is an up-regulation of the intermediate filament GFAP, and this up-regulation was positively correlated with the severity of the response. As hypothesised, there was an increase in the expression of GFAP with the increase in injury severity. Unlike the tissue loss data, there was a marked difference between the 2.0 mm and 2.2 mm injury group, with the 2.2 mm injury group eliciting more reactive astrogliosis within the cortex (both ipsilateral and contralateral) and the hippocampus. This increase in reactive astrogliosis correlated with the poorer MWM behavioural outcomes of the 2.2 mm group. The amount of reactive astrogliosis may be more indicative of injury severity than the amount of tissue loss, as there is a clearer step-wise increase in GFAP expression.

Human TBI is characterised by astrogliosis, where increased GFAP immunostaining in post-mortem brain tissue at the site of contusion is seen, with decreasing astrogliosis distally from the injury site (Harish et al., 2015, van Landeghem et al., 2006). Due to the difficulty in obtaining human brain tissue for analysis of astrogliosis, GFAP has been looked at as a serum biomarker for determining injury

severity. Several studies have shown an increase in GFAP serum levels that corresponds to clinical outcome and severity of TBI (Pelinka et al., 2004, Nylén et al., 2006, Vos et al., 2010).

As with the astrocytes, the microglial response was increased in the injured groups. Activated microglia and infiltrating macrophages identified by the expression of Iba1 were counted within the same ROI as the astrocyte analysis. The 2.2 mm group had the highest number of Iba1+ cells in the ipsilateral cortex, as well as the contralateral hippocampus. Unlike the astrocytic response, the sham, 1.5 mm and 2.0 mm injury groups all had comparable increased numbers of Iba1+ cells in all ROI. An increase in microglia activation following a TBI has been seen in other CCI mouse models of TBI and post-mortem human TBI brain tissue, which is reflected by our results (Loane et al., 2014, Chen et al., 2014). Microglia are known to migrate to the site of injury; this is reflected in our data by the increase in the number of Iba1+ cells in the ipsilateral ROI (Hernandez-Ontiveros et al., 2013). However, we should also consider that the increase in the number of Iba1+ cells could also be due to microglia proliferation (Gómez-Nicola et al., 2013). Interestingly, as with the astrocytic response, there was an increase in the number of Iba1+ cells in the contralateral ROI.

### **3.5.3 Contralateral glial cell activation**

An unexpected outcome that was observed in the glial analysis by immunohistochemistry was the increase in immunostaining of the activated glial cells in the contralateral cortex. Originally, the purpose of analysing the homologous contralateral cortex areas was to use them as a control for the impacted ipsilateral side. However, our study shows that an ipsilateral CCI injury can cause widespread response throughout other brain regions. This phenomenon has been seen in the stroke literature, where there is increased GFAP expression in the hemisphere contralateral to the focal occlusion (Patience et al., 2015, Bidmon et al., 1998, Takatsuru et al., 2013). There could be several reasons for this increase in contralateral glial response. Firstly, the contralateral cortex may experience injury due to compression against the skull during the initial swelling of the ipsilateral side caused by the impaction (Xiong et al., 2013, Cole et al., 2011). Secondly, the glial cells on the contralateral side may

have been activated through chemotaxic signalling (Domercq et al., 2013, Ohsawa et al., 2007). Thirdly, glial cell migration, as it has been shown that populations of astrocytes from various regions such as the subventricular zone, migrate towards the site of the injury (Benner et al., 2013). Fourthly, they may be due to the interhemispheric functional connectivity of large brain networks, whereby damage caused to neurones on the ipsilateral side is communicated to the corresponding neurones on the contralateral side, thereby inciting glial activation (Marquez de la Plata et al., 2011, Mayer et al., 2011). Using diffusion MRI tractography, Crofts and colleagues found that in stroke patients there was a decrease in connectivity not only ipsilaterally, but also in the contralateral regions homologous to the lesioned ipsilateral side (Crofts et al., 2011). Furthermore, on both sides, there were also regions with *increased* connectivity.

#### **3.5.4 Impact of sham injury**

Interestingly, the sham group displayed deficits in behaviour and altered histology despite not being exposed to the direct impact of brain injury. The craniotomy that the sham group undergoes is an invasive surgery that can result in a pathological response, including oedema, inflammation and vascular disruption (Cole et al., 2011). The craniotomy surgery, despite appearing to cause no disruption to the dura macroscopically, may have caused some microscopic structural damage to the underlying brain tissue, as seen in the histological analysis. This damage may be the result of disruption of fine blood vessels and nerve fibres that connect the brain to the skull. Also, the hand held drill used in this method causes friction during drilling, so therefore heat could cause further damage to the brain tissue. Furthermore, the drilling procedure can produce fine bone powder which may cause irritation to the dura and provoke an inflammatory response. Another point raised in the paper published by Cole and colleagues, is that the swelling caused by the changed ICP due to the craniotomy may cause the contralateral hemisphere to undergo compression, and this may account for some of the contralateral glial cell activation (Cole et al., 2011). As witnessed in our model, the sham-injured group in the study conducted by Cole and colleagues, displayed some behavioural deficits compared to naïve animals, however these were not statistically significant. This suggests that the sham injury is in itself a unique injury to the brain, distinct from the direct injury caused by the

impactor to the brain tissue, which was worth noting and became the basis for using a sham group as a control group, rather than a naïve group.

### **3.5.5 The CCI model**

The CCI model as described in the general introduction is a widely used model for rodent TBI due to the high reproducibility of the injury, low variability in injuries between samples and the relative ease of administration. It also mimics several key aspects of the human TBI including neurobehavioral and pathophysiological consequences.

The data in this chapter provides evidence that this model causes cognitive dysfunction, as learning impairment and memory loss was seen in the MWM test, thus being relevant to some of the human cognitive symptoms of TBI. In our model the impact depth needed to produce a behavioural deficit was larger than we anticipated, as others in the literature have reported that shallower impact depths had elicited behavioural deficits (Washington et al., 2012, Brody et al., 2007, Xiong et al., 2008, You et al., 2003, Bermpohl et al., 2006, Fox et al., 1998). This difference could be due to differences in impact parameters (such as dwell time or velocity of impact) or as discussed earlier, could be due to the inter-laboratory variability in injury severity definitions. Furthermore, it could be due to the control group by which the injured groups are compared to, in order to assess deficit significance.

Our model was also able to replicate some of the secondary injury pathophysiology seen in other animal models and in human TBI, including hallmark severity-dependent astrogliosis, increased number of Iba1+ cells and tissue loss at the contusion site.

### **3.5.6 Conclusion**

The aim of this first chapter was to optimize and characterize a CCI mouse model of TBI that had behavioural as well as histological endpoints that reflected aspects of the human pathology and was

similar to the CCI mouse models of other groups. The data in this chapter has met these criteria, which allows it to be used as a tool for exploration of novel therapeutics for neuroprotection in TBI.

### **3.5.7 Main outcomes**

- A CCI injury of 2.2 mm impact depth causes a deficit in the learning and memory behaviour of mice as test by the MWM test, but no deficit in gross locomotor function.
- This same injury caused significant ipsilateral tissue loss, astrogliosis and microglia activation.
- Glial cell activation was observed in the contralateral cortex.
- The sham-injury does produce some deficit in behaviour and glial cell activation.



## **4 The effect of acute DHA administration in a mouse CCI**

### **model of TBI**

#### **4.1 Introduction**

As discussed in the general introduction, the omega-3 PUFAs have many roles in the CNS. They may be potentially useful in the treatment of several CNS disorders and may confer neuroprotection in TBI. In our laboratory, the acute administration of the omega-3 PUFA DHA improved functional and histological outcomes in a variety of SCI models in both mice and rats (Huang et al., 2007, Liu et al., 2015, Paterniti et al., 2014, Ward et al., 2010, King et al., 2006, Lim et al., 2013b). The effect was seen when DHA was administered intravenously 30 minutes post injury and was further improved by a diet enriched by DHA (Huang et al., 2007). In these studies, administration of DHA reduced inflammation, astrogliosis and the microglial/macrophage activation, as well as improved motor function after SCI. As SCI and TBI pathophysiology have many similarities (Rowland et al., 2008, Anderson and Hall, 1993, Kwon et al., 2004), we hypothesised that DHA may be efficacious in the treatment of TBI. In this chapter we investigated the effect of an acute dose of DHA post-injury, on the performance of the animals in the MWM, and on astrocyte and microglial activation in our model of mouse CCI.

The beneficial effect of DHA supplementation and DHA acute treatment in models of injury to the central nervous system, suggest that DHA may have beneficial effects following TBI, which was the hypothesis on which we based the work presented in this chapter.

## 4.2 Methods

The animals used in this chapter were CD1 male mice aged 10-12 weeks. The CCI injury model used to cause a unilateral injury is described in section 2.1.2. An intravenous (i.v.) injection of DHA (500 nmol/kg) or vehicle (Veh) was given in the tail vein 30 minutes after the injury. The behavioural tests in this chapter include the open field test (section 2.1.4.1) and the MWM acquisition and probe trial (section 2.1.4.3), including the reverse MWM paradigm. The protocol used for the execution of these behavioural tests is detailed in figure 4.1. After perfusion on day 28 post-injury, the brain tissue was dissected out and cut into sections which were stained using the toluidine blue method and immunostained for GFAP, Iba1 and doublecortin (DCX) (as described in section 1.1.6).

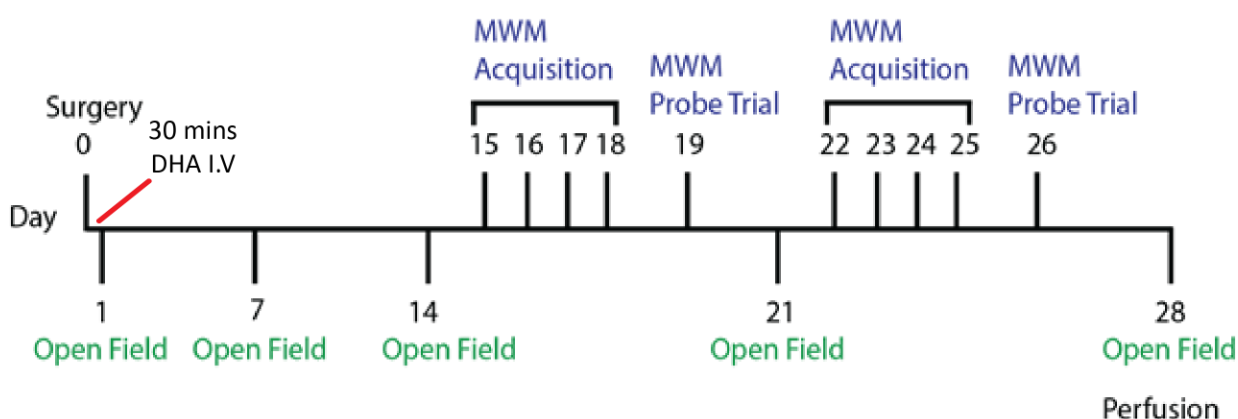


**Figure 4.1. Timeline for the i.v. administration of DHA and the behavioural tests after CCI.** The open field, Y-maze and the first MWM acquisition (day 15-18) and probe trial (day 19), and the second week reversal MWM acquisition (day 22-25) and reverse probe trial (day 26).

## 4.3 Aims and Hypothesis

### 4.3.1 Aims

The aim of the chapter was to investigate the effects of an acute treatment with DHA in a CCI mouse model of TBI and assess long-term behavioural and histological correlates including:

- Learning and memory as assessed by the MWM acquisition and probe trials

- Persistent tissue damage and alterations under the site of the impact; tissue loss and glial cell activation
- Effect on neurogenesis

#### **4.3.2 Hypothesis**

Based on the results reported after acute DHA administration in various models of injury, it was expected that DHA treatment would reduce the lesion size, the astrogliosis and microglial activation, and would enhance neurogenesis, in parallel with an improvement in cognitive behavioural outcome.

## **4.4 Results**

The work in this chapter documents the effect of an acute dose of DHA (500 nmol/kg, i.v.) 30 minutes post-injury in a CCI mouse model. We assessed the effect DHA had on learning and memory in the MWM. We also assessed the effect DHA had on astrogliosis, microglial activation, lesion size and neurogenesis in the brain tissue of these mice at 28 days post-CCI.

### **4.4.1 Effect of DHA treatment in the open field**

The open field paradigm was used to measure the locomotor function of the mice, to confirm that any differences seen in MWM test were not due to changes in motor function.

The total distance travelled and the number of line crossings made by the mice during their 5 minute exposure to the test was measured as an indicator of their motor ability. All 3 groups travelled over 20 metres and made over 200 line crossings during all of their tests, over the course of the study. However, the sham group maintained the same distance travelled and number of line crossings throughout the study, whereas the 2 groups that received an injury (with either vehicle treatment or DHA treatment) increased the distance travelled and the line crossings made over the course of the study. Despite there being no statistically significant differences between the groups, there were still differences seen between the groups. On day 21, the DHA-treated group travelled  $38.9 \pm 7.7$  m, which was 10 metres more than the sham group, which travelled  $29.7 \pm 1.9$  m. However, the vehicle-treated group travelled over 20 metres more than the sham group, at  $53.6 \pm 11.6$  m. In the model development chapter, we had seen that the 2.2 mm injury group consistently had higher number of line crossings and travelled further throughout the study compared to the sham group. Thus, overall, the injury seemed to make animals hyperactive over time (a trend we had noticed before), and this tendency was reduced by DHA treatment.

There was no significant difference seen in the amount of time any of the groups spent in the middle or outer zones during the study. However, on day 1 post-injury, the vehicle treated ( $273.0 \pm 3.0$  s) group spent more time in the outer zone and less time in the inner zone when compared to the DHA-treated ( $246.1 \pm 11.2$  s) and sham ( $246.6 \pm 12.1$  s) groups.

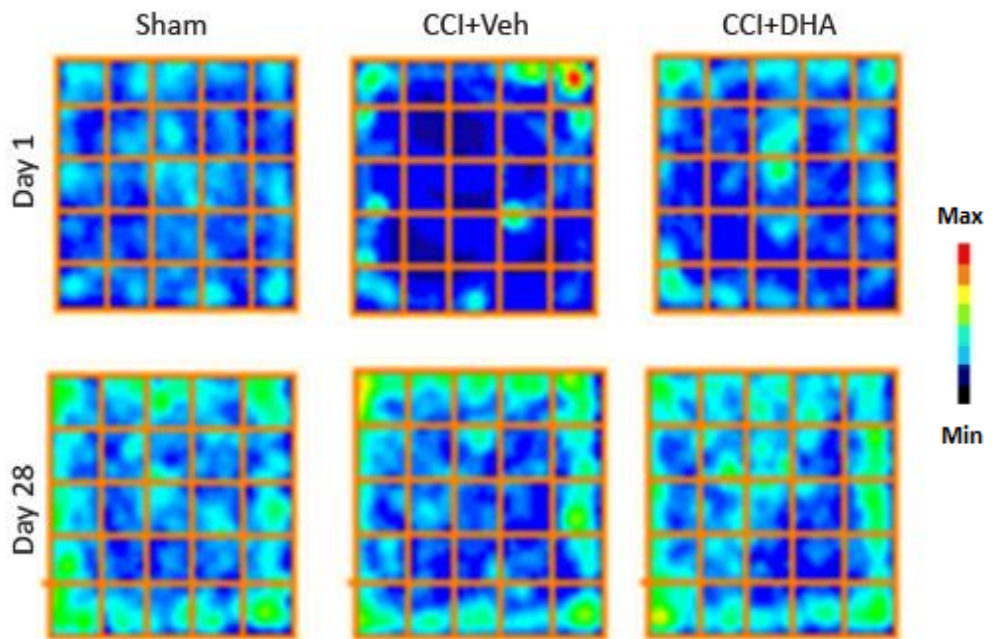


**Figure 4.2** Effect of DHA treatment after CCI injury on the open field performance. Representative occupancy plots from open field testing on day 1 and day 28 from each experimental group.

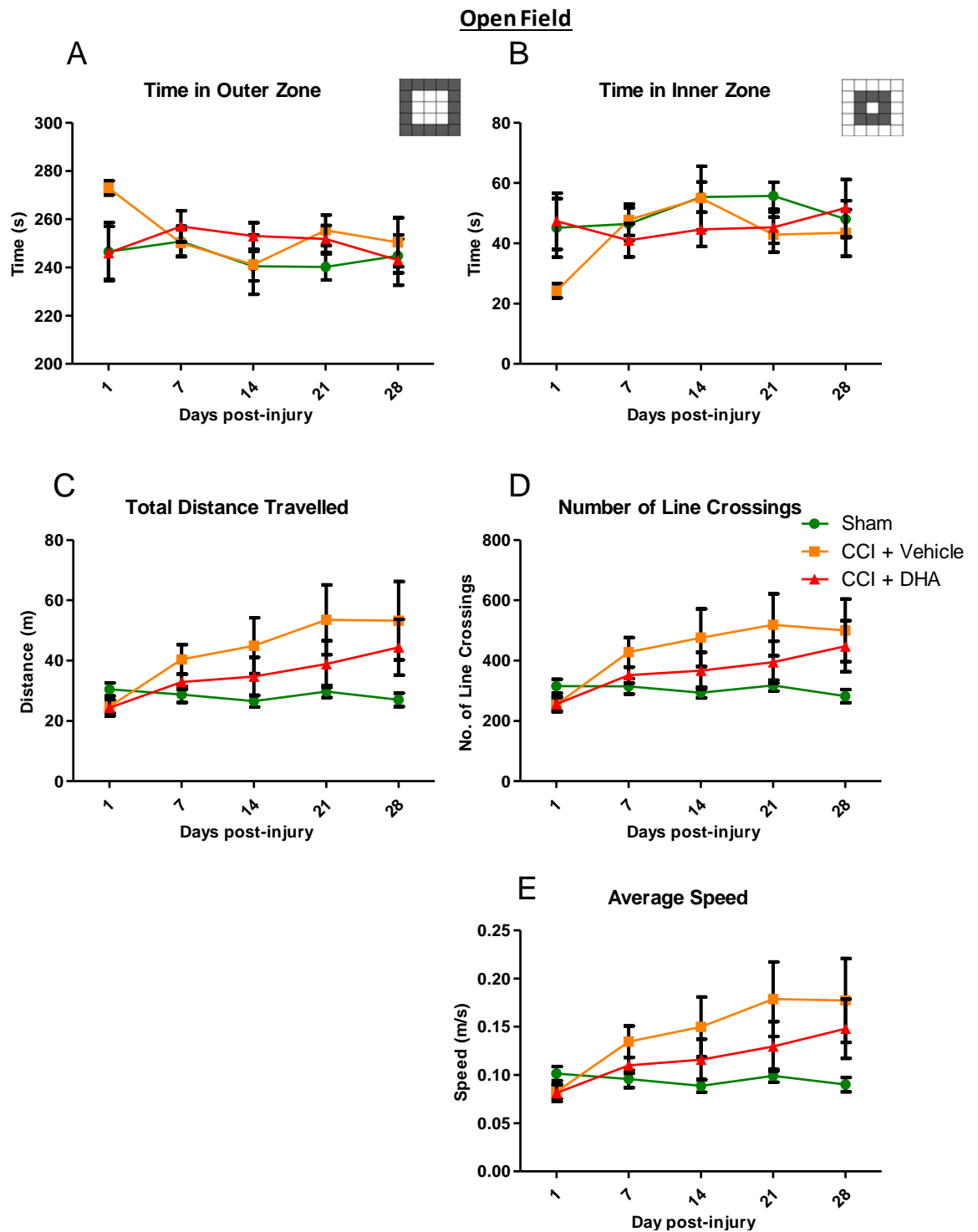


**Figure 4.3. Effect of DHA treatment in CCI injury on the open field performance at day 1, 7, 14, 21 and 28 of the study.** (A) The time spent in the outer zone and (B) the time spent in the inner zone. (C) The total distance travelled, (D) the number of line crossings and (E) the average speed of the animals. Mean  $\pm$  SEM. N = 7-12 animals per group.

## **4.4.2 Effect of DHA treatment in the Morris water maze**

### **4.4.2.1 The effect of treatment in the first week of Morris water maze – Acquisition trial**

The two-week MWM protocol that was used in the model development chapter was also used in this study, to assess learning and memory function in these mice. The first week of acquisition testing took place on days 15 – day 18 post-injury, with four trials per day (Fig. 4.4A; Fig. 4.5A). The sham group in this study had the fastest escape latencies throughout the acquisition trial when compared to the 2 groups that received a CCI. The sham mice reduced their average escape latency from  $42.8 \pm 3.4$  s on day 15 to  $16.7 \pm 1.3$  s on day 17, which was the third day of the acquisition trial. On the final day of the acquisition training (day 18), the sham group still had the fastest escape latency at  $20.1 \pm 2.4$  s.

Both of the CCI groups reduced their escape latencies over the 4 days of training, but showed no differences between them. Both the CCI + Veh (CCI + Veh vs. Sham; day 16, <sup>#</sup> $p < 0.05$ ; day 17, <sup>###</sup> $p < 0.00$ ; day 18, <sup>#</sup> $p < 0.05$ ) and CCI + DHA (CCI + DHA vs. Sham; day 15, <sup>&</sup> $p < 0.05$ ; day 16, <sup>&</sup> $p < 0.05$ ; day 18, <sup>&&</sup> $p < 0.01$ ) were significantly slower at locating the platform when compared to the sham group. The CCI + Veh group had an average escape latency of  $56.9 \pm 6.9$  s on day 15, that was reduced to  $43.9 \pm 4.1$  s on day 18. The CCI + DHA group reduced its escape latency from  $60.9 \pm 5.1$  s on day 15, to  $40.5 \pm 5.7$  s on day 18. Like the sham group, the CCI + DHA group had its quickest average escape latency on day 17 (the third day of the acquisition training) at  $31.6 \pm 4.6$  s; due to this latency the CCI + DHA group showed no statistical difference when compared to sham.

#### 4.4.2.2 The effect of DHA treatment in the first week of the MWM - Probe trial

On day 19 post injury, 24 h after the last trial of the first week of acquisition training, the mice were given a probe trial.

In this probe trial (Fig. 4.4B), the sham group had the shortest latency time to the platform zone of  $11.2 \pm 2.9$  s, followed by the CCI + DHA group  $26.2 \pm 8.4$  s and then the CCI + Veh  $37.2 \pm 10.5$  s (Fig. 4.5B). The difference between the latter two was not statistically significant.

The sham group also made the most entries to the platform zone, on average  $5.4 \pm 0.8$  entries, whereas the CCI + DHA group made only  $3.9 \pm 0.5$  entries and the CCI + Veh group made  $2.5 \pm 0.6$  entries (Fig. 4.5C). The number of entries made by the CCI + Veh group were statistically significantly lower than the sham group ( $*p < 0.05$ ). The CCI + DHA group however did not show any statistically significant difference either to the sham or CCI + Veh groups. In both of the probe trial measures, the CCI + DHA group did not appear to perform as poorly as the CCI + Veh group, but still did not perform as well as the sham group.

#### Morris water maze

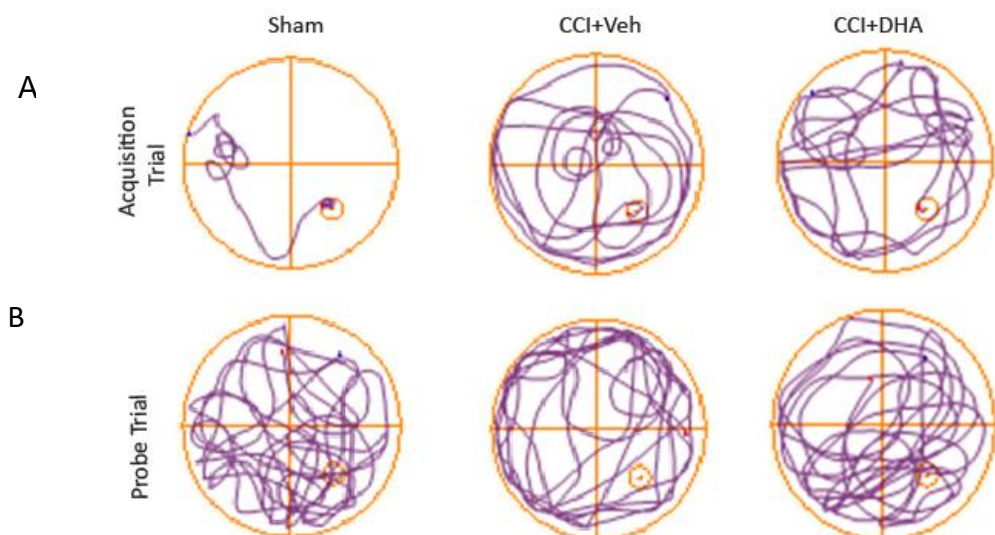


**Figure 4.4 Effect of DHA treatment on acquisition training in the Morris water maze.** Representative traces from a trial on (A) day 18 post-injury during the acquisition training and the (B) day 19 probe trial.



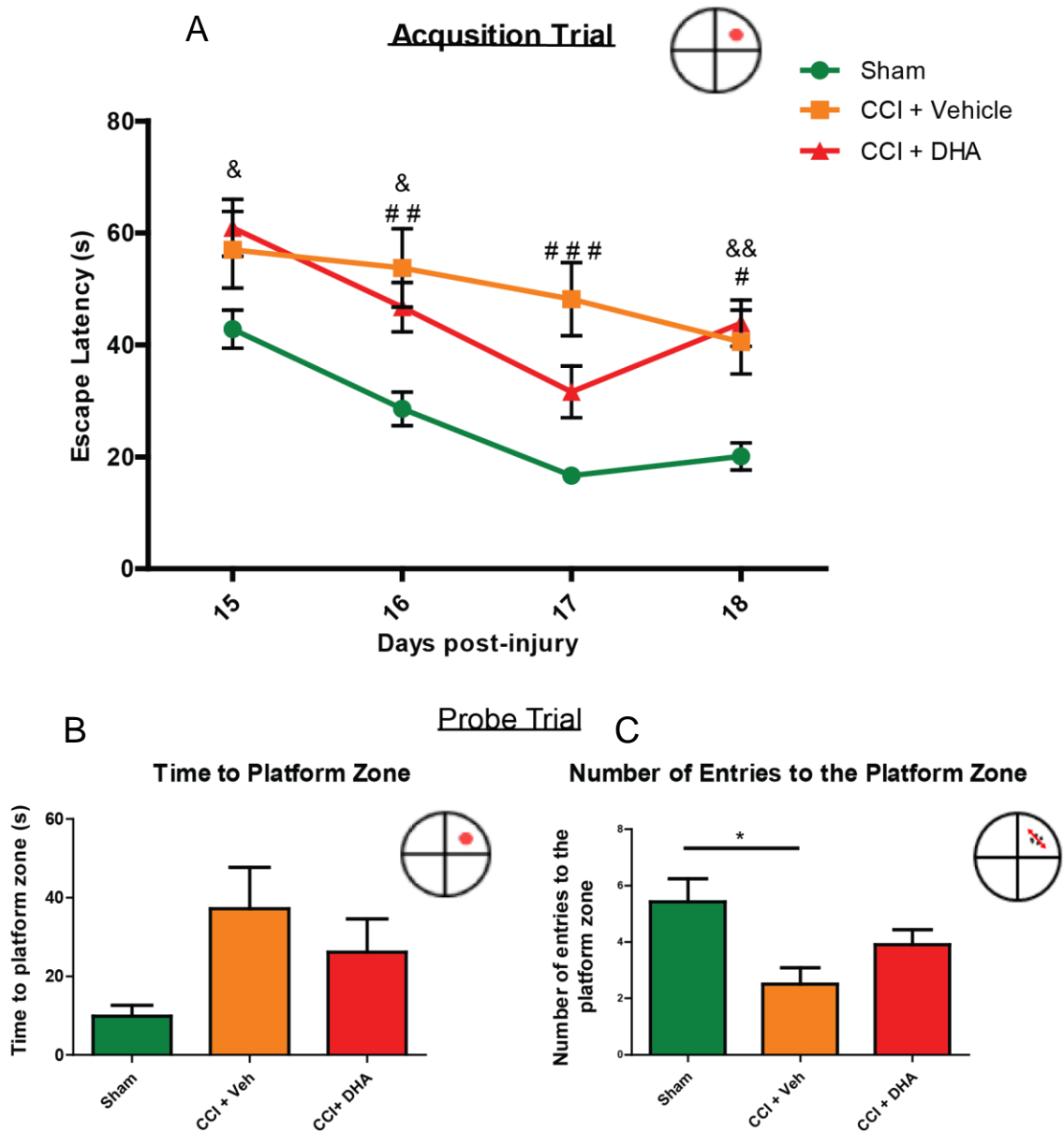


**Figure 4.5. Effect of DHA Treatment on Acquisition training and Probe trial Performance In the first week of the Morris Water Maze.** (A) The average escape latency of the 4 trials conducted on days 15 – 18 post-injury during the acquisition training. The CCI + Veh group had statistically significantly slower escape latencies compared to the sham group on day 16 (###  $p < 0.01$ ), day 17 (####  $p < 0.001$ ) and day 18 (#  $p < 0.05$ ). The CCI + DHA group were also statistically slower compared to the sham group on day 15 (&  $p < 0.05$ ), day 16 (&  $p < 0.05$ ) and day 18 (&&  $p < 0.01$ ). There was no statistically significant difference on any day of the acquisition training between the CCI + Veh group and the CCI + DHA group. Statistical significance was determined using a two-way repeated measures ANOVA with post-hoc Bonferroni test. On day 19 the probe trial was conducted; (B) the time taken to the platform zone and (C) the number of entries to the platform zone, where the CCI + Veh group made fewer entries compared to the sham group (\*  $p < 0.05$ ). Mean  $\pm$  S.E.M. N= 7-12 animals per group.

#### **4.4.2.3 The effect of DHA treatment in the MWM – Reverse Acquisition trial**

On day 22 post-injury, the MWM second week of reverse acquisition training was initiated. In the second week of the MWM the platform was located in the opposite quadrant to the first week of MWM training (from the north-east quadrant to the south-west quadrant). The mice were exposed to a 4-day acquisition training phase and another probe trial 24 hours later (Fig. 4.1).

As seen in the model development chapter, the second week of reverse acquisition training (Fig. 4.6; day 22-25) did not show the same steep decrease in escape latency over the 4-days of training compared to that seen in the first week of training (day 15-18). This may be due to the mice becoming acclimatised to the MWM paradigm.

During the reverse acquisition training the sham group had the statistically fastest escape latency compared to the two CCI groups. At the start of the reverse acquisition training the sham group located the platform in  $25.1 \pm 2.5$  s (day 22), which was reduced to  $12.2 \pm 1.3$  s by the end of the training (day 25).

The CCI groups showed no significant differences to each other during the second week reverse acquisition training. Both CCI + Veh group (CCI + Veh vs. Sham; day 22, #### p<0.001; day 23, ## p<0.01; day 24, ## p<0.01; day 25, #### p<0.001) and the CCI + DHA group (CCI + DHA vs. Sham; day 22, &&& p<0.001; day 23, &&& p<0.001; day 24, &&& p<0.001) had statistically significantly slower escape latencies when compared to the sham group. However, on the final day of training the average escape latency of the CCI + DHA group decreased from  $42.0 \pm 3.5$  s to  $29.6 \pm 3.9$  s; this sizable decrease in escape latency resulted in the CCI + DHA group no longer exhibiting a statistically significant difference to the sham group.

#### **4.4.2.4 The effect of DHA treatment in the Morris water maze – Reverse Probe trial**

On day 26 post-injury and 24 hours after the last trial of the second week reverse acquisition training, a probe trial was performed. Outcome measures pertaining to the original location of the platform zone (north-east quadrant) and the reverse platform location (south-west quadrant) were measured.

##### **4.4.2.4.1 Reverse Platform**

During the probe trial on day 26, the time taken to enter the reverse platform zone was measured (Fig. 4.7A), the sham group entered the reverse platform zone in the quickest time of  $10.4 \pm 7.2$  s. Both the CCI + Veh and the CCI + DHA group took almost twice as long to enter the reverse platform zone,  $24.4 \pm 7.4$  s and  $27.5 \pm 8.8$  s respectively. Despite these different values, there was no statistically significant difference between the groups.

The number of entries to the reverse platform zone was also measured (Fig. 4.7B), with the sham group making the most visits to the reverse platform zone, i.e.  $5.9 \pm 1.0$  entries. The CCI + Veh group made on average  $3.6 \pm 0.8$  entries to the reverse platform zone. The CCI + DHA group made the fewest entries to the reverse platform zone,  $2.3 \pm 0.5$ , which was statistically significantly lower than the sham group ( $p < 0.05$ ), using the one-way ANOVA test with post-hoc Bonferroni testing.

##### **4.4.2.4.2 Original Platform**

The time taken to the original platform zone in the south-west quadrant and the number of entries to the original platform zone were also measured in the day 26 probe trial.

The three groups showed no statistical difference between them, in the time taken to enter original platform zone (Fig. 4.7C; Sham  $35.8 \pm 9.9$  s; CCI + Veh  $41.4 \pm 8.7$  s; CCI + DHA  $29.9 \pm 7.7$  s). The same was true for the number of entries to the original platform zone (Fig. 4.7D; Sham  $2.0 \pm 0.5$ ; CCI + Veh  $2.2 \pm 0.5$ ; CCI + DHA  $3.4 \pm 0.6$ ).

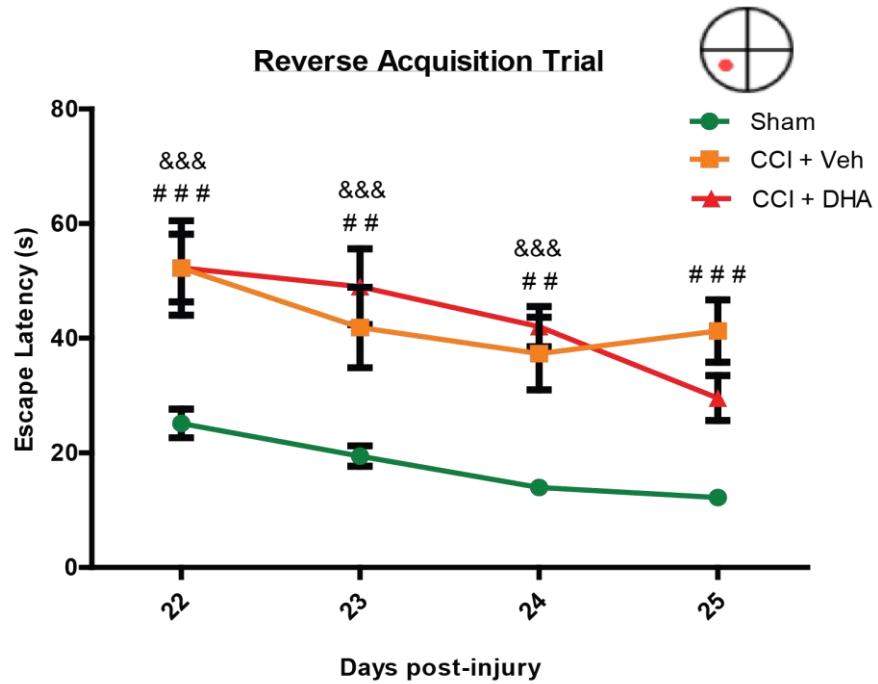


**Figure 4.6. Effect of DHA Treatment on Acquisition training in the second week of the Morris Water Maze.** The average escape latency of the 4 trials conducted on days 22 –25 post-injury during the acquisition training. The CCI + Veh group had statistically significantly lower escape latencies compared to the sham group on day 22 (####  $p < 0.001$ ), day 23 (###  $p < 0.01$ ), day 24 (##  $p < 0.01$ ) and day 25 (####  $p < 0.001$ ). The CCI + DHA group were also slower compared to the sham group on day 22 (&&&  $p < 0.001$ ), day 23 (&&&  $p < 0.001$ ) and day 24 (&&&  $p < 0.001$ ). There were no statistically significant differences on any day of the acquisition training between the CCI + Veh group and the CCI + DHA group. Statistical significance was determined using a two-way repeated measures ANOVA with post-hoc Bonferroni test. Mean  $\pm$  S.E.M. N= 7-12 animals per group.

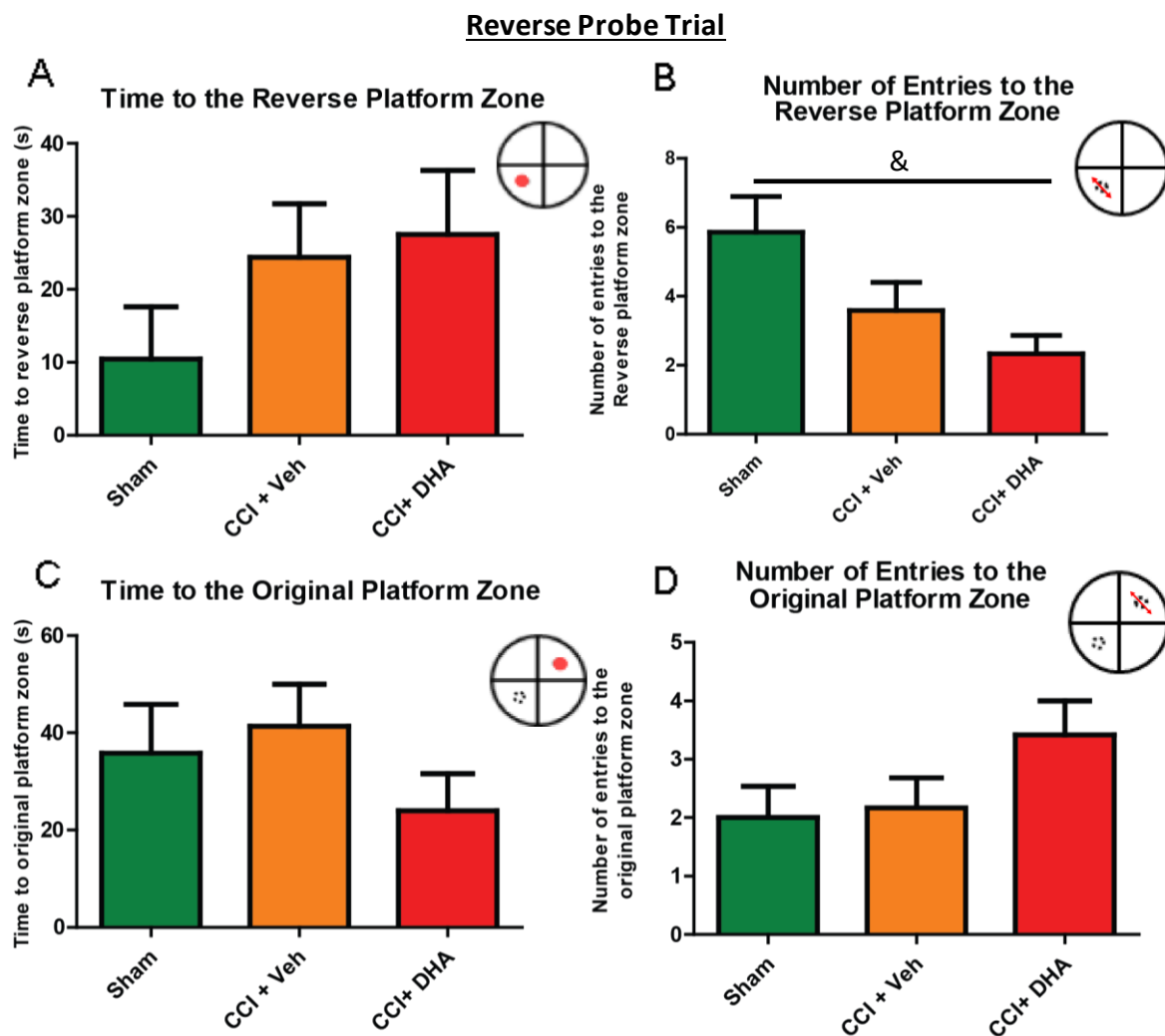


**Figure 4.7. Effect of DHA Treatment on Probe trial Performance in the second week of the Morris water maze.** On day 26 the probe trial was conducted; (A) the time taken to the reverse platform zone, (B) the number of entries to the reverse platform zone. The CCI + DHA group visited the reverse platform statistically fewer times than the sham injured group (&  $p < 0.05$ ), when using a one-way ANOVA with post-hoc Bonferroni test. (C) The time taken to the original platform and (D) the number of entries to the original platform zone. Mean  $\pm$  S.E.M. N= 7-12 animals per group.

#### **4.4.3 The effect of DHA treatment on the ipsilateral hemisphere -cortex and hippocampus**

After perfusion of the mice on day 28, the brain tissue was cut into coronal sections; selected sections from 4 locations (-1.5, -2.0, -2.5 and -3.0 mm posterior from bregma) spanning the area of the impact lesion were analysed using toluidine blue staining.

The CCI + Veh and CCI + DHA group had substantial tissue loss in all three of the measurements, including the ipsilateral hemisphere, ipsilateral cortex and hippocampus, when compared to the contralateral side (Fig. 4.8; Fig. 4.9A, B, C). The Sham group did not show any tissue loss on the ipsilateral side. Both the CCI + Veh and CCI + DHA showed a statistically significant loss of tissue compared to the Sham group in the ipsilateral hemisphere (\*\*  $p < 0.01$ ), the ipsilateral cortex (\*\*\*)  $p < 0.001$ ) and the ipsilateral hippocampus (\*\*\*)  $p < 0.001$ ). The DHA treatment did not prevent any tissue loss after CCI, and failed to show any statistically significant difference to the CCI + Veh group.

The ipsilateral hippocampus in both CCI groups was almost entirely absent at the 1.5 mm, -2.0 mm and -2.5 mm coronal levels, and was still only partially present at -3.0 mm level (Fig. 4.8). The CCI + Veh group had  $21.9 \pm 7.5\%$  of the ipsilateral hippocampus remaining at 28 days post-injury (Fig. 4.9C). The CCI + DHA group had a similarly low percentage of ipsilateral hippocampus remaining,  $25.6 \pm 2.0\%$  (Fig. 4.9C). Overall, the analysis of the sections from injured animals revealed that the tissue was very fragile, and at times it was difficult to assess whether some of the missing tissue was due to the expansion of the injury or to the loss of tissue due to the fragility of tissue sections placed on slides, especially during the tissue processing and staining steps.

As observed in the model development chapter, the Sham group did not lose any ipsilateral tissue, but did display some damage to the surface of the cortex on the ipsilateral side, beneath the craniotomy site (Fig. 4.8).

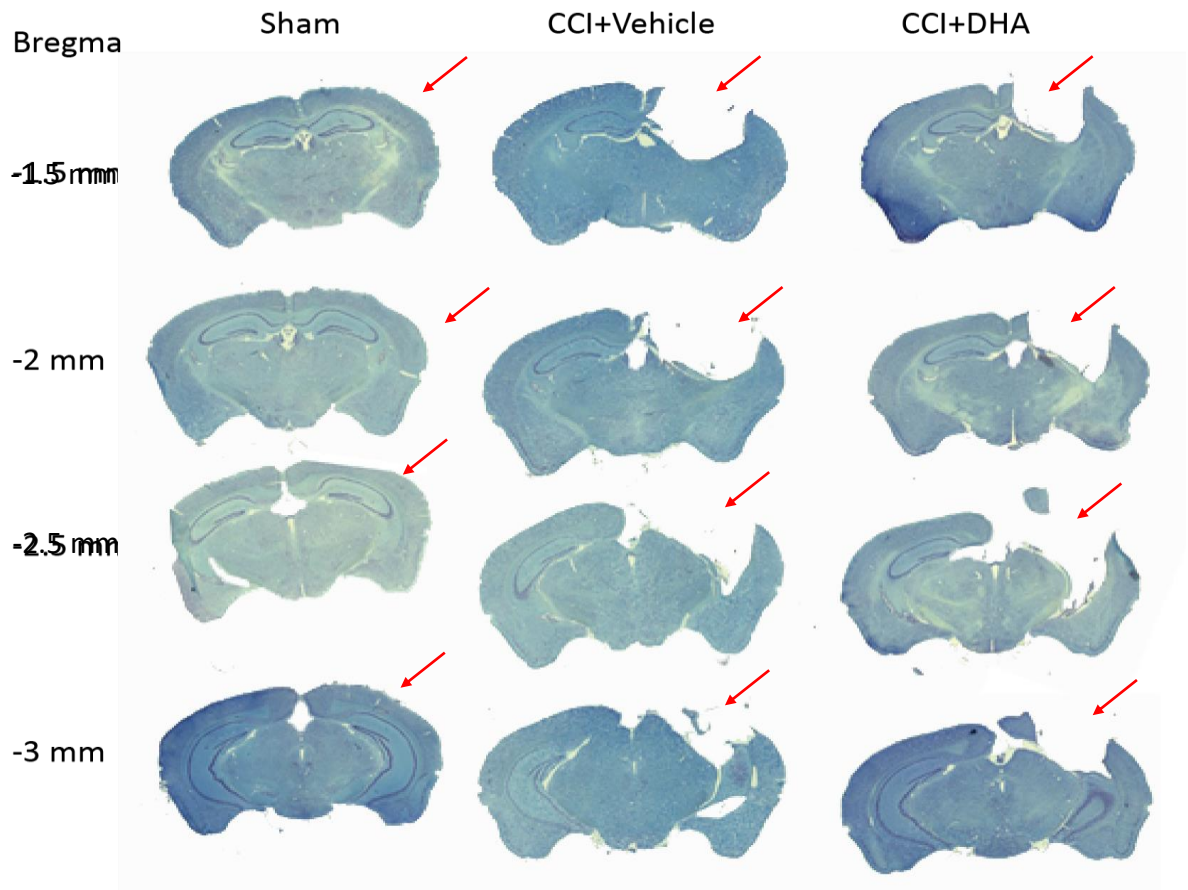


**Figure 4.8. Lesion size after CCI and DHA treatment.** Coronal brain sections from the sham, CCI + Veh and CCI + DHA groups. The brain sections were taken from the following locations posterior to bregma: -1.5 mm, - 2.0 mm, -2.5 mm and -3.0 mm. The red arrow heads indicate the region of craniotomy.

## Ipsilateral hemisphere, cortex and hippocampal changes

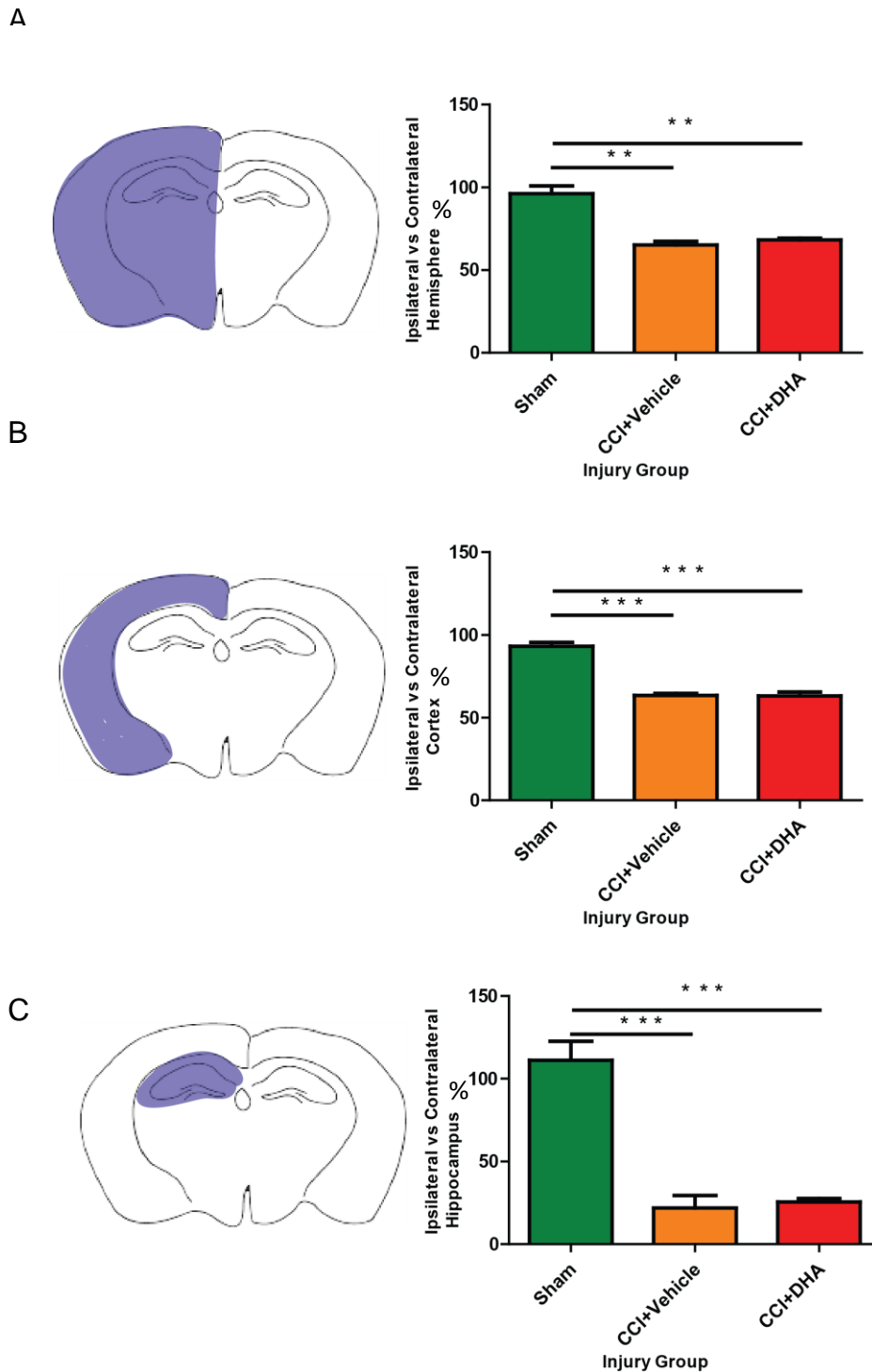


**Figure 4.9.** The effect of DHA treatment post-injury on the ipsilateral brain regions as compared to the contralateral side. (A) hemisphere, (B) cortex and (C) hippocampus. Statistical analysis using one-way ANOVA and post-hoc Bonferroni testing (\*\* $p < 0.01$ , \*\*\* $p < 0.001$ ). Mean  $\pm$  S.E.M. N = 3 animals per group.



#### **4.4.4 The effect of DHA treatment on astrocytes in the cortex and the hippocampus**

Reactive astrogliosis is a hallmark of the secondary injury that follows TBI. In the model development chapter of this thesis, the amount of reactive astrogliosis correlated with the injury severity. The amount of astrogliosis was measured by the percentage increase in the immunolabelling for the marker GFAP, within the ipsilateral and contralateral cortex, as well as the contralateral hippocampus (Fig. 4.10).

The increase in contralateral GFAP staining was reported in the previous chapter on model development. This phenomenon was also seen in the CCI groups in this chapter, but the DHA treatment did not have any impact on the contralateral cortex GFAP staining when compared to the vehicle-treated group (Fig. 4.11 B). The CCI + Veh group and the CCI + DHA group had an increase in the amount of contralateral cortex GFAP staining of  $549.4 \pm 240.5 \%$  and  $554.0 \pm 80.9 \%$  respectively, when compared to the Sham group. The Sham group did not show any increase in contralateral GFAP staining compared to the naïve group.

There was an increase in the amount of GFAP labelling surrounding the impact site on the ipsilateral cortex in the CCI groups. (Fig. 4.11B). The Sham group had a percentage increase compared to naïve animals of  $343.7 \pm 209.7 \%$ . The increase in the percentage of GFAP staining in the CCI groups compared to the Sham group was almost 7x fold higher (CCI + Veh,  $2245.1 \pm 484 \%$ ; CCI + DHA,  $2424.2 \pm 836.3 \%$ ). The CCI + DHA group did not show any difference in ipsilateral cortical GFAP staining compared to that seen in the CCI + Veh group. The GFAP staining in the CCI + DHA and CCI + Veh groups, in both the ipsilateral and contralateral cortices showed increased levels, but also large variability as evidenced by the large error bars.

In the total hippocampus ROI (Fig. 4.11C), the CCI + Veh group had an increase in GFAP compared to the Sham group ( $266 \pm 55.3 \%$ ). Interestingly, in the hippocampus the CCI + DHA group showed an increase in GFAP staining ( $709.3 \pm 220.6 \%$ ) that was over double that seen in the CCI + Veh group, although this was not statistically significant.

In the dentate gyrus ROI of the hippocampus (Fig. 4.11D) the CCI + DHA group ( $675.9 \pm 135.0\%$ ) had a statistically significantly ( $*p < 0.05$ ) higher amount of GFAP immunolabelling compared to the Sham group ( $130.3 \pm 60.0\%$ ). The CCI+DHA group had almost twice as much GFAP immunolabelling as the CCI+Veh group ( $360.8 \pm 119.6\%$ ), but this was not statistically significant.

The DHA treatment did not affect the GFAP immunolabelling in the cortical ROI; however, the DHA treatment appeared to cause an increase in the reactive astrogliosis in the contralateral hippocampus, although this increase was not statistically significant.

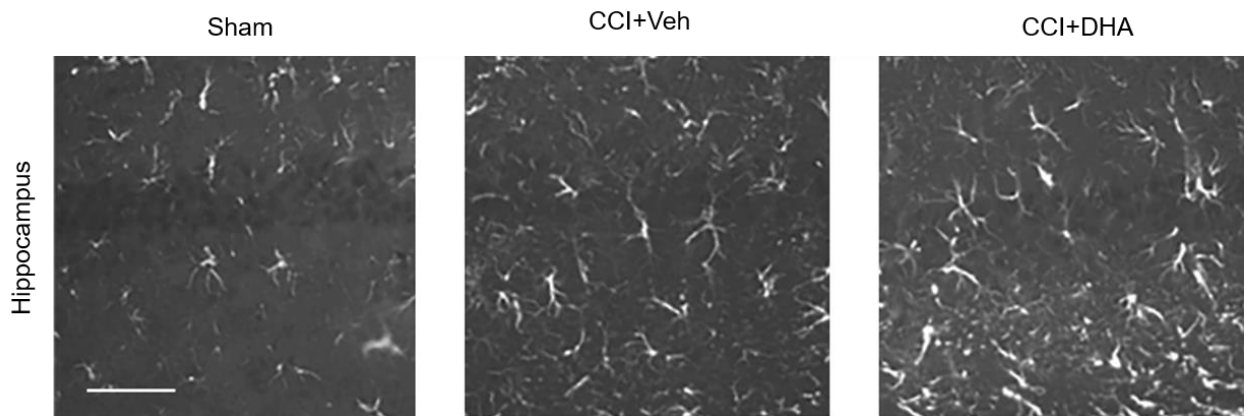


**Figure 4.10 The effect of DHA treatment on GFAP expression.** Immunolabelling of reactive astrocytes with GFAP in the contralateral hippocampus in the sham, CCI + Veh and CCI + DHA groups. Scale bar = 100  $\mu\text{m}$ .

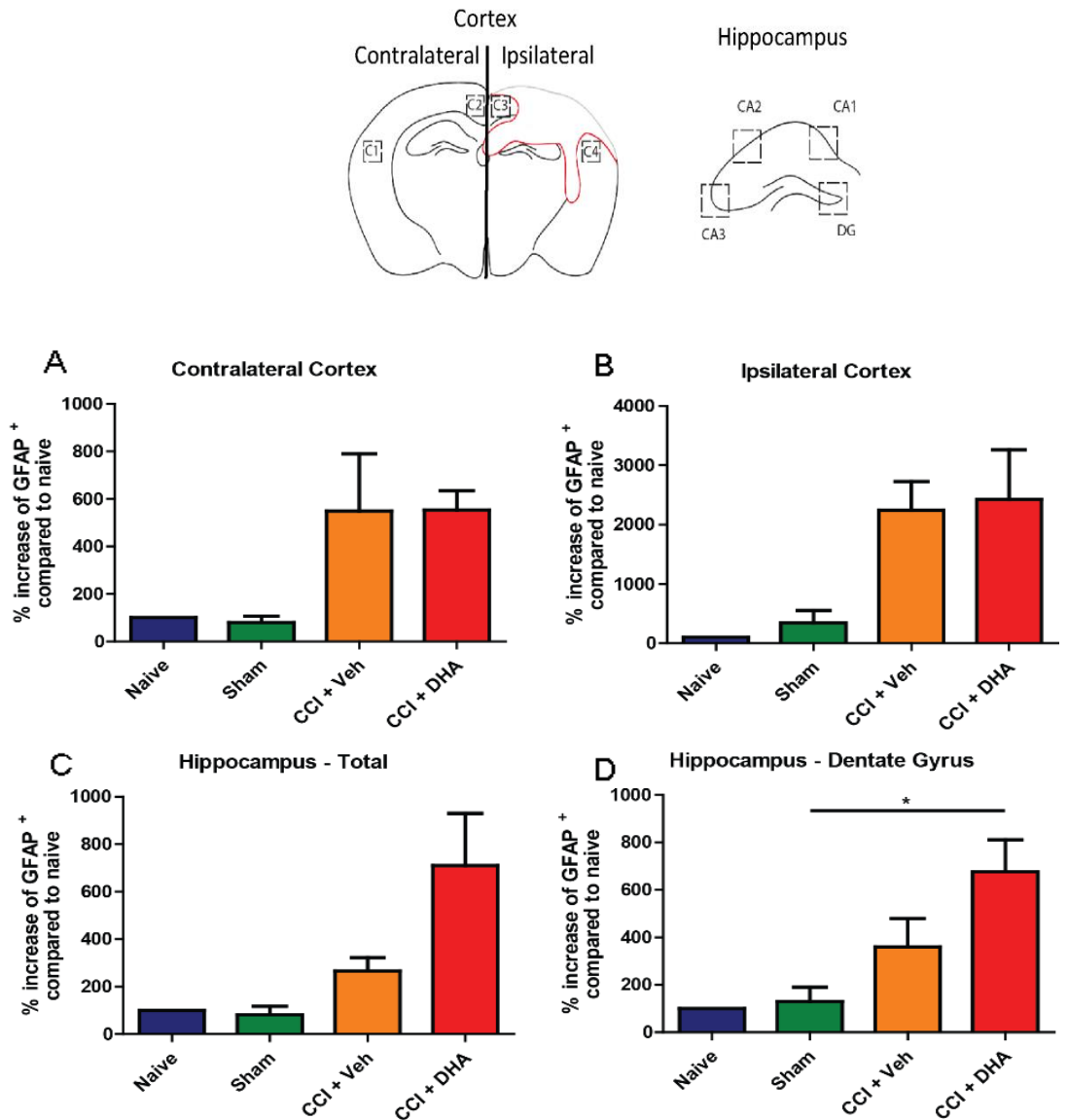


**Figure 4.11. The effect of DHA treatment on reactive astrogliosis post-injury in the cortex and hippocampus.** Schematic showing the ROI in the cortex and hippocampus that were analysed for GFAP labelling (GFAP<sup>+</sup>). The percentage increase in GFAP labelling compared to naïve tissue in (A) the contralateral cortex, (B) the ipsilateral cortex, (C) the contralateral hippocampus and (D) the dentate gyrus of the hippocampus. The CCI + DHA group displayed a statistically significant increase in GFAP<sup>+</sup> compared to the sham group (\* $p < 0.05$ ) in the dentate gyrus. Statistical significance was determined using one-way ANOVA and post-hoc Bonferroni test. Mean  $\pm$  S.E.M. N=6 animals per group.

#### 4.4.5 The effect of DHA treatment on microglia/macrophages in the cortex and the hippocampus

The numbers of activated microglial/macrophage cells were counted within the same regions of interest used to measure astrogliosis; these were identified using labelling for Iba1 (Fig. 4.12).

In the contralateral cortex and the ipsilateral cortex there was no difference in the number of Iba1+ cells between the CCI + Veh and CCI + DHA groups (Fig. 4.13A, B). In the contralateral cortex the CCI + Veh ( $110 \pm 11$ ) and the CCI + DHA ( $108 \pm 11$ ) groups had an increase in the number of Iba1+ cells compared to the Sham group ( $77 \pm 21$ ), but there was no statistical significance. This was also the case for the ipsilateral cortex; the CCI + Veh ( $163 \pm 20$ ) and the CCI + DHA ( $153 \pm 16$ ) groups had a higher number of Iba1+ cells than the Sham group ( $146 \pm 18$ ), with no statistical significance seen between groups.

As in the cortical ROI, there were no statistically significant differences between the Sham ( $197 \pm 9$ ), CCI + Veh ( $261 \pm 1$ ) and CCI + DHA ( $236 \pm 22$ ) groups in the values measured in the total hippocampal ROI (Fig. 4.13C, D).

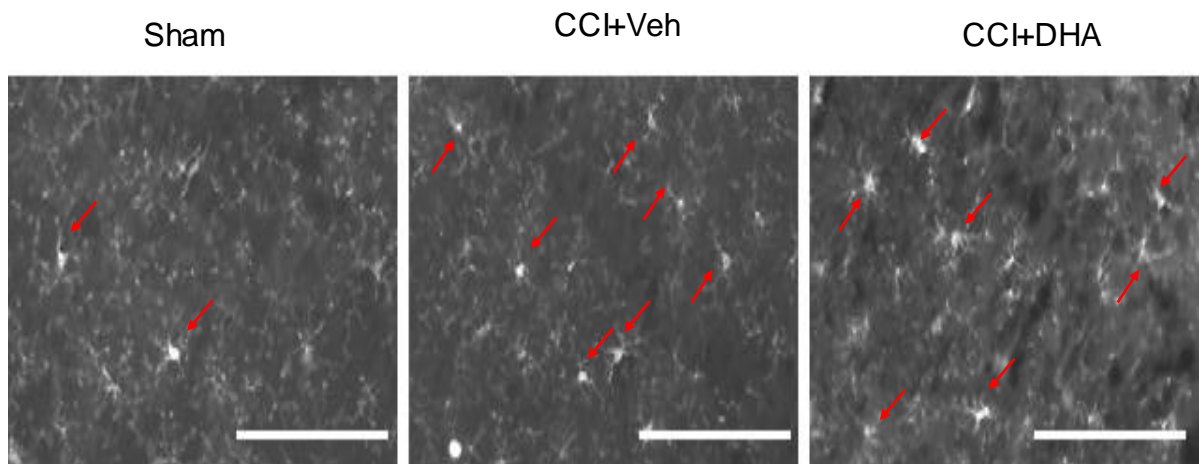


**Figure 4.12.** The effect of DHA treatment post-injury on Iba1+ cells. Immunolabelling of activated microglia/macrophages with Iba1, identified with red arrows, in the contralateral hippocampus (CA2 ROI) in the sham, CCI + Veh and CCI + DHA groups. Scale bar = 150  $\mu$ m.

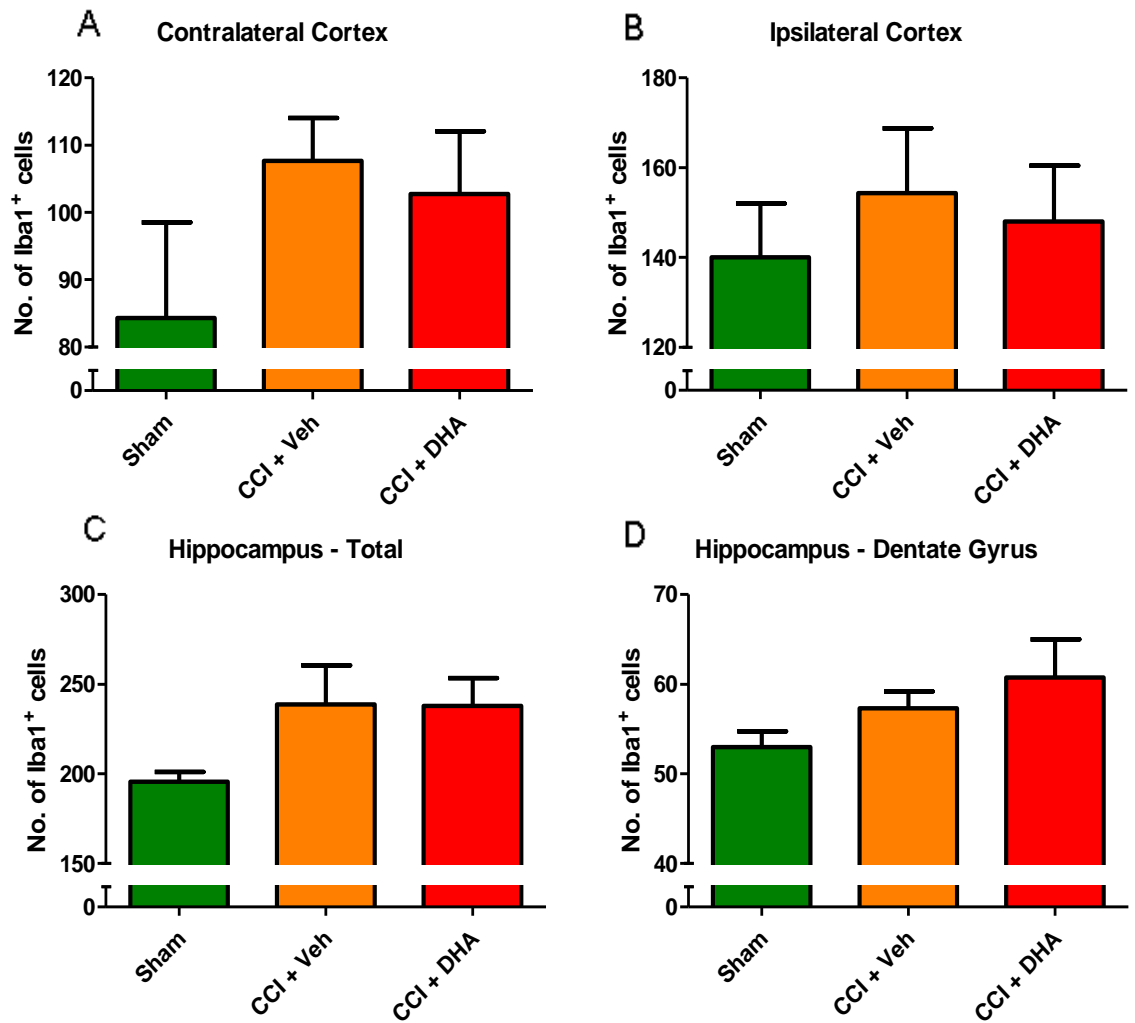


**Figure 4.13.** The effect of DHA treatment on the number of microglia/macrophages in the cortex and hippocampus. The number of Iba1<sup>+</sup> cells in (A) the contralateral cortex, (B) the ipsilateral cortex, (C) the contralateral hippocampus and (D) the dentate gyrus of the hippocampus. Mean ± S.E.M. N=6 animals per group.

#### 4.4.6 Effect of DHA on neurogenesis in the dentate gyrus of the contralateral hippocampus

The number of immature neurones were counted in the dentate gyrus region of the contralateral hippocampus. These immature neurones were identified using co-labelling of the nuclear marker DAPI and doublecortin (DCX) (Fig. 4.14), indicative of neurogenesis (Xuan et al., 2014).

There was no difference in the number of DCX+ cells in the dentate gyrus between the CCI + Veh group ( $210 \pm 50$ ) and the CCI + DHA group ( $181 \pm 8$ ). The groups that received a CCI injury did have an increased number of DCX+ cells in the dentate gyrus, when compared to the Sham group ( $90 \pm 25$ ). There were no statistically significant differences between any of the groups.

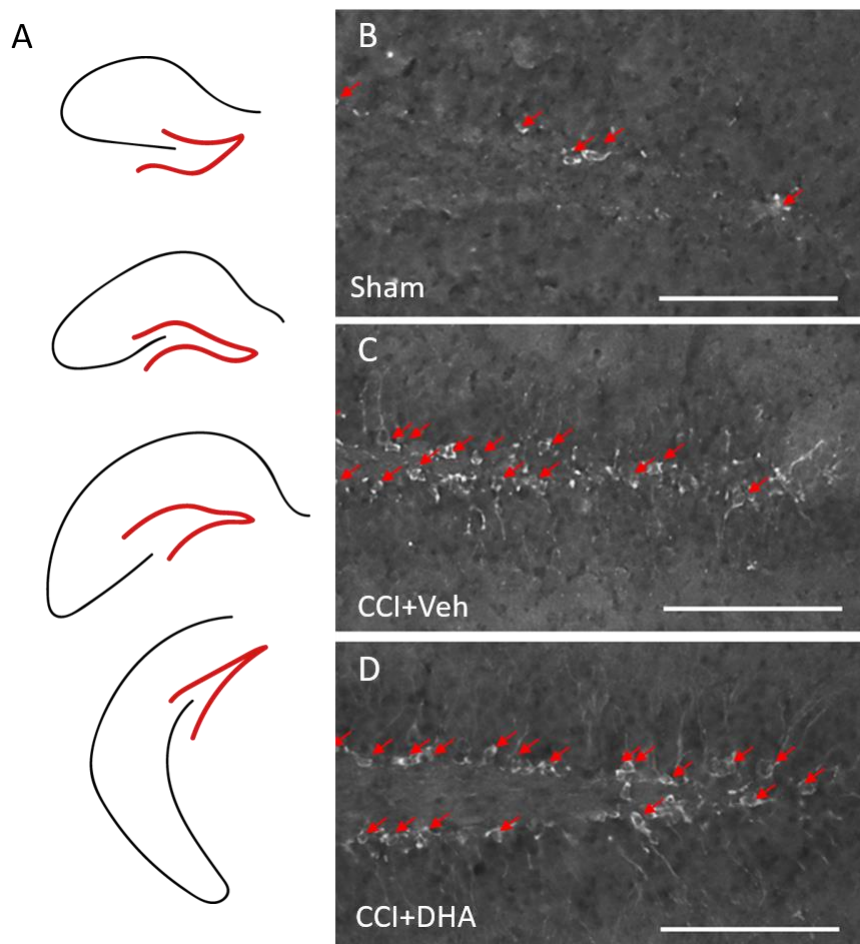


**Figure 4.14. The effect of DHA treatment on the number of DCX+ cells in the Dentate Gyrus.** (A) Schematic of the contralateral hippocampus with the dentate gyrus highlighted in red, in each of the four coronal slices analysed. Immunolabelling with DCX, identified with red arrows in the (B) sham group, (C) CCI+Veh and the (D) CCI+DHA group. Scale bar = 100  $\mu$ m.

## **4.5 Discussion**

The results presented in this chapter did not support the hypothesis formulated in the introduction of this part of the work. Acute treatment with DHA post-TBI failed to significantly improve outcome in the MWM, reduce lesion size or prevent microglial activation. Instead of reducing reactive astrogliosis as seen in the SCI models studied previously, acute DHA treatment appeared to increase GFAP immunolabelling in the contralateral hippocampus. Although there was an increase in the number of immature neurones in the dentate gyrus of the contralateral hippocampus in the DHA-treated group compared the sham operated group, this increase was equal to that seen post-injury in the injured control group, suggesting that there was no modulation by DHA of the increase in neurogenesis due to the CCI injury.

### **4.5.1 Effect of DHA treatment on motor function and exploratory behaviour**

The predominant aim of the open field testing was the same as it was in the previous chapter, to highlight any significant locomotor deficits that may confound the cognitive dysfunction assessed in the MWM. The three groups did not show any statistically significant differences from each other in the distance travelled and the number of line crossings made over the course of the study. Despite there being no statistical differences, there was a trend for the groups that received a CCI to increase the distance they travelled and the number of line crossings made over the course of the study. This may be indicative of the CCI injury causing some form of hyperactive behaviour, which has been seen in rats following CCI injury (Lewén et al., 1999). It may also be a TBI consequence in human patients; akathisia has been reported following TBI and a recent population study has linked paediatric TBI to attention deficit hyperactivity disorder (ADHD) (Desai et al., 2010, Silver and Yablon, 1996, Yang et al., 2016). Overall, the DHA treatment had no major impact on the behaviour of the CCI injured mice within the open field, thus any behaviours displayed in the MWM maze would not have been due to a deficit in gross locomotor function.

#### **4.5.2 Effect of DHA on learning and memory**

The same two-week MWM protocol that was used in the model development chapter was used to assess the effect of acute DHA treatment (Fig. 4.1). The acute DHA treatment did not induce any long-term benefit in this test after CCI. DHA-treated mice failed to demonstrate any sustained increased learning capability over the control injured in the first week (day 15-18) or second week (day 22-25) of acquisition training – although in the first week, the DHA-treated animals performed transiently better. In the probe trials (day 19 and day 26), the CCI + DHA group did not show any improvement over the CCI + Veh group, although in the first probe trial, there was a tendency to perform better.

Diets deficient in DHA cause animals with no injury to become impaired in cognitive tests, such as the Barnes maze (Fedorova et al., 2007, Desai et al., 2014). In a study performed by Moriguchi and colleagues, rats fed on an omega-3 deficient diet had slower escape latencies and reduced memory function in the MWM. In a subsequent study, the authors found that this dietary-induced impairment could be rescued with omega-3 PUFA supplementation (Moriguchi et al., 2000, Moriguchi and Salem, 2003). Dietary deficiency in DHA also proved to worsen cognitive outcome assessed with the novel object recognition test, 7 days following a CCI injury in mice (Desai et al., 2014). This suggests that deficiency in DHA may be related to a worse cognitive outcome. However, these are studies which assess dietary manipulations, whereas our study used the acute injection of a very small amount of DHA, which is transient in the circulation, so should not affect phospholipid composition. Soon after our studies with DHA in TBI were initiated, reports on the effect of the administration of DHA by repeated injections in rats with TBI were published (Begum et al., 2014, Harvey et al., 2015). Both of these recent studies failed to show any long-term (>7 days) behavioural benefits of DHA administration in rat TBI. The only reported neurological benefit was observed in the first week post-injury in the performance on the animals on beam tasks, which reflect sensorimotor coordination (Begum et al., 2014).



### **4.5.3 Effect of DHA on the brain**

The histology data from the model development chapter showed that with increased severity there was increased tissue loss and glial activation. This would suggest that treatments that reduced the severity of the injury would also be linked to a reduced tissue loss and/or reactive gliosis.

#### **4.5.3.1 Tissue loss**

The DHA treatment did not appear to reduce tissue loss following the CCI injury in the ipsilateral hemisphere, cortex or hippocampus, as assessed 4 weeks post-injury. By this time post-injury, the lesion in the ipsilateral hemisphere has become extensive, and the fixed frozen tissue sections were fragile, making very accurate determinations of lesion size difficult. Interestingly, in recent work done in our group, the analysis on tissue collected one week post-CCI and processed in thin paraffin-embedded sections, which were more robust, showed a significant reduction in the lesion size after treatment with DHA (Orli Thau-Zuzhman, personal communication). In a SCI model, we recently showed that a DHA-enriched dietary preparation (also containing other nutrients) improved functional outcome and protected the tissue (Pallier et al., 2015), and in a stroke model, DHA acute treatment combined with a fish oil-enriched diet preserved tissue (Pallier et al., 2015, Pu et al., 2016), suggesting that longer-term or combined DHA treatments may be more beneficial at reducing tissue loss post-injury. The effect of high chronic levels of omega-3 PUFAs are investigated in more detail in the following chapter.

#### **4.5.3.2 The effect of DHA on microglia and macrophage responses after injury**

TBI is associated with a complex response of the microglia/macrophages, which has been studied in various experimental models. As discussed in the general introduction (section 1.2.2.7) microglial activation is a hallmark of TBI secondary injury and these glia can adopt different phenotypes that exhibit both detrimental and beneficial effects. The heterogeneity of the microglia extends beyond the 'M1-like' and 'M2-like' phenotypes, and microglia can vary in their morphology and also tissue distribution (Loane and Kumar, 2016, Loane and Byrnes, 2010, Lawson et al., 1990, Hanisch, 2013). Harnessing the microglia response to provide a neuroprotective effect (i.e. release of growth factors such as BDNF, anti-inflammatory cytokines, IL-10 and reduce phagocytosis) or to reduce the

detrimental effects (i.e. release of pro-inflammatory cytokines, TNF $\alpha$  and ROS) could provide a potential treatment for TBI (Loane and Byrnes, 2010, Loane and Faden, 2010).

Treatment with DHA has been shown to alter the microglia response to injury; in our group DHA reduced microglia activation 4-6 weeks following SCI (Lim et al., 2013b). In an organotypic hippocampal culture DHA administration reduced the microglia activation following lipopolysaccharide (LPS)-induced inflammation (Chang et al., 2015).

In our CCI model, DHA treatment did not appear to change the microglia/macrophage response, measured by the Iba1 staining 4 weeks post-injury. However, our late time point of 4 weeks may be missing potential effects DHA may have on microglia following TBI in the acute phase, since the microglia peak response has been suggested to be at 7 days post-injury (Loane and Byrnes, 2010). However, Harvey and colleagues have recently found that DHA treatment following CCI in rats did not lead to a reduction in Iba1+ staining at 3, 7 or 21 days post-injury (Harvey et al., 2015). The difference between the outcome of DHA treatment in SCI and TBI models on microglia, highlights the subtle differences that may exist between the two disease pathologies in terms of microglia response and its modulation by the fatty acid.

#### **4.5.3.3 The effect of DHA on astrogliosis after injury**

There was an increase in the amount of reactive astrogliosis in the CCI injured mice, when compared to the animals receiving craniotomy only. As mentioned in the first chapter, this latter group did demonstrate some GFAP-labelling of reactive astrocytes in the ipsilateral cortex. The reasons for this were discussed in the previous chapter (section 1.5.4) and support the concept that a craniotomy is a unique injury itself, separate from the direct focal injury to the brain parenchyma (Cole et al., 2011).

The CCI injured groups also demonstrated an increase in the reactivity of astrocytes in the contralateral cortex, as reported in the previous chapter and similar to observations reported in the stroke literature (Patience et al., 2015). There may be multiple explanations for this contralateral activation. As discussed previously (section 1.5.3), this could be due to compression of the contralateral cortex during impactation, chemotaxic signalling and interhemispheric communication.

The DHA treatment did not reduce the amount of reactive astrogliosis in the ipsilateral or contralateral cortex. This is in contrast to results seen with DHA in SCI models in our laboratory and others, where acute DHA treatment reduced the amount of GFAP immunolabelling surrounding the lesion site in the injured cord (Paterniti et al., 2014). Figueroa and colleagues found that DHA *pre-treatment* in SCI improved locomotor function, was associated with tissue sparing and promoted anti-apoptotic pathways, without causing a reduction in astrocyte or microglia activation (Figueroa et al., 2012). They suggest that the neuroprotective effect of DHA is independent of its anti-inflammatory effects.

Interestingly, there was an increase in reactive astrogliosis in the contralateral hippocampus of the DHA treated mice. The contralateral hippocampus was analysed due to the absence of the hippocampus in the ipsilateral hemisphere in the CCI injured mice, but also because the main behavioural outcomes measured in our studies are learning and memory, which is predominantly controlled by the hippocampus region in the brain (Jarrard, 1993).

A reduction in reactive astrogliosis is traditionally believed to be indicative of neuroprotection. However, more recently the idea that the role of astrocytes following neurotrauma is exclusively a detrimental one has been questioned. Astrocytes are involved in several processes in the CNS under normal conditions, including maintenance of the BBB, ion homeostasis and synaptic function. Under pathological conditions astrocytes can cause further damage through the prevention of axonal regeneration and inducing neuroinflammation, but they may also have a beneficial role including BBB repair and removal of damaged tissue (discussed further in chapter 6) (Sofroniew and Vinters, 2010, Pekny and Pekna, 2016). Myer and colleagues suggested that astrocytes may have an essential protective role in neurotrauma, after they found that mice which had all of their astrocytes ablated immediately following TBI, had a poorer outcome (Myer et al., 2006). Also a study performed in a rat model of stroke injury reported an increase in reactive astrogliosis, cell survival and improved outcome following treatment with DHA (Eady et al., 2012a), further suggesting that a DHA associated increase in reactive astrogliosis may be potentially beneficial.

Astrocytes of the hippocampus may have a different role than those in the cortex. In a study performed by Estrada and colleagues in glucose deprived rats, reported an increase in reactive astrogliosis in the hippocampus and this was correlated with an increase in the amount of neurogenesis seen in the hippocampus (Estrada et al., 2009). As discussed in the introduction, increased neurogenesis correlates with improved memory outcome (Kawakita et al., 2006, Drapeau et al., 2003, Tanabe et al., 2004). However, in our MWM protocol the CCI+DHA group did not show an improved learning or memory function in the MWM performance in the 4 weeks after injury.

#### **4.5.4 DHA treatment does not increase neurogenesis in the dentate gyrus**

The dentate gyrus (DG) is one of the only locations in the adult mammalian brain able to display neurogenesis, apart from the subventricular zone (SVZ) (Drew et al., 2013). Neurogenesis in the dentate gyrus is essential for memory function, as proven in studies in which neurogenesis in mice has been ablated using irradiation, thereby worsening their performance in the radial arm maze (a spatial memory test) (Clelland et al., 2009). The CCI injured mice in our study showed an increase in the number of immature neurones in the dentate gyrus of the contralateral hippocampus. Despite this increase in neurogenesis, both CCI injured groups performed poorly in the MWM, suggesting that the increased neurogenesis of the contralateral hippocampus did not compensate for the loss of approximately 75% of the ipsilateral hippocampal tissue.

The increase in neurogenesis following injury is a phenomenon also seen in stroke models (Türeyen et al., 2004, Kuge et al., 2009). Following experimental stroke and TBI, neurogenesis is increased in both the subgranular zone (SGZ) of the dentate gyrus and the SVZ (Parent, 2003). The data from these studies and our own suggest that increased neurogenesis is a common response to insult to the brain tissue. Endogenous neural stem cells (NSCs) of the SGZ may differentiate into neurons to replace those lost or damaged following TBI and then incorporate themselves into existing neural circuits (Sun, 2014). This endogenous neurogenesis following TBI can be manipulated exogenously by intraventricular infusion of various growth factors including bFGF, EGF and VEGF and may offer an

avenue for potential neuroprotective therapies (Sun et al., 2009, Sun et al., 2010, Lee and Agoston, 2010).

The neurogenesis seen in the SGZ of the dentate gyrus in our CCI-injured mice, may indicate an attempt of the NSCs of the DG to replace the hippocampal neurones lost as a result of the trauma (Kernie and Parent, 2010, Sun, 2014). The hippocampal neurones are particularly vulnerable to cell death following TBI and therefore their replacement by neurogenesis might explain the increased number of DCX+ cells in the hippocampus in both of the CCI groups, in the absence of an improved performance in the MWM (Royo et al., 2006)

DHA treatment has been shown to increase neurogenesis in both *in vivo* and *in vitro* studies (Kawakita et al., 2006). In our study however, DHA failed to increase the number of immature neurones in the contralateral hippocampus when compared to the vehicle treated group, suggesting that in this dosing regimen DHA did not promote further neurogenesis compared to the insult-induced neurogenesis.

#### **4.5.5 Conclusion**

The data produced in this chapter suggest that a single acute DHA treatment at the dose of 500 nmol/kg, at 30 min after TBI, does not improve outcome following CCI injury in mice. The treatment does not reduce tissue loss, or exert anti-inflammatory effects as measured by microglial/macrophage activation and reactive astrogliosis one month after injury. The CCI injury does induce neurogenesis in the hippocampus, which reflects the brain insult-induced neurogenesis reported in the literature, but this is unaffected by DHA treatment (Parent, 2003). DHA appears to increase the reactive astrocyte response induced by injury in the contralateral hippocampus. This indicates that the fatty acid had some impact on injury –related events, and raises the issue of the regime/dose administered. We hypothesise that further studies could explore a range of doses, to establish if at higher levels of acute exposure, the fatty acid displays more effects, in particular more impact on neurological outcome. Subsequent studies in this thesis will investigate the effect of prolonged endogenous production of higher omega-3 PUFAs on outcome following CCI and the effect the DHA treatment has directly on astrocytes in an *in vitro* model of focal mechanical injury.

#### 4.5.6 **Main outcomes**

- Acute DHA treatment does not confer tissue protection in moderate CCI injury
- Acute DHA treatment amplifies hippocampal reactive astrogliosis
- Acute DHA does not modulate the CCI-induced contralateral neurogenesis

## **5 Controlled cortical impact injury in fat-1 mice**

### **5.1 Introduction**

As discussed in the main introduction (section 1.4), evidence obtained in various models and using various paradigms of administration, suggests that omega-3 PUFAs may have a role in neuroprotection. As seen in the previous chapter, an acute injection of the omega-3 PUFA DHA post-injury does not appear to improve outcome in mice following CCI. This suggests that the single i.v. administration of DHA at the 500 nmol/kg dose is not efficacious as an acute treatment strategy. A chronic treatment with DHA or mixtures of omega-3 fatty acids containing DHA (such as fish oil) may have beneficial effects in the treatment of TBI. This was suggested by the early studies carried out by Bailes and his collaborators; thus, they were the first to show that oral supplementation for a month post-injury with DHA at the dose of 10 mg/kg/day or 40 mg/kg/day, reduced the axonal dysfunction after impact acceleration injury in rats (Bailes and Mills, 2010). In a subsequent publication, a supplementation with a similar dose of DHA contained in fish oil, also showed a reduction in caspase-3 expression after injury (Mills et al., 2011). Our group has recently conducted studies using a transgenic mouse line, the *fat-1* mice, which have high levels of endogenous omega-3 fatty acids in their body tissues (Kang et al., 2004). Our previous studies in spinal cord injury (SCI) and peripheral nerve injury (PNI) models employing these *fat-1* transgenic mice have shown that higher levels of endogenous omega-3 PUFAs conferred neuroprotection in these models of traumatic injury (Gladman et al., 2012, Lim et al., 2013a). In this chapter, *fat-1* transgenic mice were used in our CCI model of TBI, to determine whether an endogenous high level of omega-3 PUFAs can confer neuroprotection and improve neurobehavioral outcomes after TBI.

#### **5.1.1 Diet and polyunsaturated fatty acids**

Diet composition has an important effect on a person's health, with fats being vital to a balanced diet. Mammals are unable to make sufficient omega-3 and omega-6 PUFAs *de novo*, therefore PUFAs must be obtained from the diet and are referred to as essential fatty acids (as discussed in section 1.4.1) (Lee et al., 2016). An essential omega-6 PUFA is linoleic acid (LA), and from this 18-carbon chain PUFA

the longer chain n-6 PUFA arachidonic acid (AA) can be synthesised. An essential omega-3 PUFA is the 18-carbon chain alpha-linolenic acid (ALA), from which the longer chain omega-3 PUFAs eicosapentaenoic acid (EPA) and docosahexaenoic acid (DHA) can be synthesised ( Fig. 1.4) (Gómez Candela et al., 2011). In the past 150 years the ratio of omega-6/omega-3 fatty acids in our diets has changed from 1:1 to a ratio of 20-25:1 (Simopoulos, 2006, Simopoulos, 2011). Thus, the western diet contains an excessive amount of omega-6 PUFAs and is deficient in omega-3 PUFAs. Evolutionarily, humans are not genetically adapted to convert these excess omega-6 PUFAs to omega-3 PUFAs, due to the absence of the appropriate fatty acid desaturase enzymes. This excessive amount of omega-6 PUFAs has been linked with several pathologies, including chronic cardiovascular disease, diabetes, cancer and rheumatoid arthritis (Simopoulos, 2006). Concurrently, low intake of omega-3 PUFAs has been correlated with many disorders and has been linked to cognitive decline in the elderly (Stangland Thuret, 2009, Freemantle et al., 2006). Dietary supplementation is an effective approach that is used to study the effects of different PUFAs on lipid profiles *in vivo*. There are several limitations to the dietary supplementation approach that may lead to conflicting data and inaccurate results. The aim of dietary supplementation is to increase the amount of PUFAs within the tissues of the animals. In order to assess the effect of supplementation, a control group has to be put on a diet which is identical but lacking the active ingredient. It is often difficult or impossible to match a control diet with the same composition and calorific content as the test diet. Therefore, variations seen between test and control may not be due to the active ingredient alone. This has been seen particularly in the testing of omega-3 fatty acid diet supplementation (Kang, 2007). A further limitation pertaining particularly to the testing of the effects of dietary PUFAs is that they are very unstable compounds and can oxidise very quickly.

### **5.1.2 The fat-1 transgenic mouse**

To solve the problems caused by omega-3 dietary supplementation, Kang and colleagues have produced a transgenic mouse that is able to produce high endogenous omega-3 PUFAs from omega-6 PUFAs (Kang et al., 2004). As previously mentioned, mammals do not have the capacity to convert



omega-6 PUFAs into omega-3 PUFAs. However, some lower species such as the round worm *Caenorhabditis elegans* are able to carry out this process, because they express the *fat-1* gene which encodes the enzyme omega-3 fatty acid desaturase (Lee et al., 2016). It is this *fat-1* gene that Kang and colleagues have cloned into mice, resulting in the *fat-1* transgenic mice (Kang et al., 2007). When heterozygous *fat-1* mice mate, litters born will contain both heterozygous/homozygous transgenic mice and wild-type mice. As these littermates are housed together and fed on the same diet, they will generate different fatty acid profiles within their tissues. When fed on a diet containing a high concentration of omega-6 fatty acids, the *fat-1* mice expressing the omega-3 fatty acid desaturase can convert large amounts of the omega-6 fatty acids to omega-3 fatty acids and therefore will have high concentration of omega-3 fatty acids and low concentrations of omega-6 fatty acids within their tissues. In contrast, their wild-type littermates that do not express the *fat-1* gene, will express within their tissues low levels of omega-3 fatty acids and high concentrations of omega-6 fatty acids, when fed on the same omega-6 rich diet (Kang et al., 2004, Kang, 2007).

This model of *fat-1* transgenic mice has been of great benefit in the field of omega-3 PUFA research. Firstly, it eliminates the several difficulties associated with dietary supplementation of omega-3 PUFAs such as diet manufacturing, control diet composition, inadequate diet storage and separate housing of mice. Secondly, this model shortens the length of feeding time that is usually required in dietary supplementation to obtain a change in the fatty acid composition of the tissues. Conversion from omega-6 to omega-3 fatty acids can occur as early as the embryonic stage and lasts for the duration of the animal's life. Thirdly, this model creates two distinctly different fatty acid profiles (high omega-3/6 and low omega-3/6 PUFA ratio) within the same litter. The high levels of omega-3 fatty acids seen in *fat-1* mice are similar to those seen in mice fed on an omega-3 PUFA enriched diet (Kang et al., 2004). Additionally, this model can be genetically crossed with other transgenic lines to evaluate the effect omega-3 PUFAs have in a variety of disease states, such as in recent studies in the Swedish mutation human amyloid precursor protein 695 isoform (APP695) mouse used to model Alzheimer's disease pathology (Kang, 2007, Wu et al., 2016a).

Since the production of the *fat-1* transgenic mouse in 2004, several groups worldwide have utilised this model to study the effect that high levels of endogenous omega-3 PUFAs have in a variety of diseases including skin and colon cancer, liver disease, rheumatoid arthritis and traumatic injury and more recently, stroke (Table 5.1).

**Table 5.1 Disease models that have utilised the *fat-1* mice.**

<b><u>Disease Model</u></b>	<b><u>Key Findings</u></b>	<b><u>Reference</u></b>
Skin cancer – Malignant melanoma	Fat-1 mice had a reduction in the growth rate of melanoma	(Yin et al., 2016)
Colon cancer - colitis-associated cancer	Increased apoptosis of tumour cells, reduced colonic inflammation and decreased ulceration	(Han et al., 2016, Jia et al., 2008)
Alcohol-induced liver disease	Down-regulation of: hepatic lipogenesis, inflammatory response and oxidative stress	(Huang et al., 2015)
Rheumatoid arthritis	Decrease in: inflammation, ankle swelling, bone erosion and cartilage degradation	(Woo et al., 2015)
Stroke	Improved long-term behaviour outcomes. Reduced infarct volume. Increased revascularization and angiogenesis and neurogenesis following stroke	(Wang et al., 2014b, Hu et al., 2013)
Alzheimer’s disease	Less severe cognitive deficits and sensorimotor dysfunction and a reduction in astrogliosis	(Wu et al., 2016a)
Parkinson’s disease	Positive correlation between higher tissue levels of DHA and dopaminergic markers	(Bousquet et al 2011)
Peripheral nerve injury	Accelerated functional recovery, reduced muscle atrophy and increased axonal survival	(Gladman et al., 2012)
Spinal cord injury	Improved locomotor function. Increased neuronal survival and a reduction in microglia activation	(Lim et al., 2013a)

### **5.1.3 The fat-1 mouse in CNS disease**

*Fat-1* mice have recently been studied in several models of CNS disease (Table 5.1) with results that indicate that high levels of endogenous omega-3 PUFAs confer neuroprotection and improved behavioural outcomes (Wang et al., 2014b, Hu et al., 2013, Wu et al., 2016a, Gladman et al., 2012, Lim et al., 2013a).

In models of stroke, Alzheimer's disease and SCI, *fat-1* mice showed a better outcome compared to their wild-type littermates. In stroke models, the *fat-1* mice had increased revascularisation following cerebral ischemia caused by occlusion of the left middle cerebral artery, as well as improved motor function as measured by the rotarod and cylinder behavioural tests (Wang et al., 2014b). In an Alzheimer's disease model, where the Swedish mutation APP transgenic mouse line was crossed with the *fat-1* mouse, the *APP/fat-1* had improved cognitive function, reduced amyloid aggregation, reduced neuronal cell death and a decrease in reactive astrogliosis (Wu et al., 2016a). Recently, our group conducted compression SCI in *fat-1* mice. Following SCI, the *fat-1* mice had improved locomotor function, decreased microglia activation and a reduction in pro-inflammatory cytokines (e.g. IL-6) (Lim et al., 2013a). These beneficial outcomes seen in the *fat-1* mouse suggested that the *fat-1* mice might have an improved neurological outcome after a CCI. If so, this would indicate that prophylactically high omega-3 PUFAs may confer neuroprotection in TBI.

### **5.1.4 Aging and TBI**

In western populations, there has been a shift in the epidemiology of TBI. Generally, the most common TBI population are younger men aged < 45 years old. However, due to the increasing aging population, a large majority of TBI patients are now much older, with patients over 75 years old having the highest incidence of TBI-related hospitalisations (Roozenbeek et al., 2013). Elderly TBI patients are more likely to die as a result of their TBI, are more likely to have pre-trauma co-morbidities, and take a range of medications which may increase risk of haematomas (Parekh and Barton, 2010, Roozenbeek et al., 2013). For example, many elderly patients take the anti-coagulant drug warfarin, which has been

linked to severe TBI, a worse outcome and a higher incidence of death (Lavoie et al., 2004). In elderly patients, the risk of worse outcome following TBI is also increased due to cerebrovascular atherosclerosis, reduced free radical clearance and moderate cerebral atrophy, associated with aging brain tissue (Thompson et al., 2006). Despite some controversy in the literature, there is also evidence to suggest that there is a link between TBI and the risk of developing dementia and specifically Alzheimer's disease (Gardner et al., 2014, Fleminger et al., 2003, Helmes et al., 2011).

Cognitive decline correlates with aging and can therefore slow recovery after TBI (Mahncke et al., 2006). Elderly patients with pre-trauma dementia or age-related cognitive decline can have additional complications for outcome measures, such as the GOS following TBI (Thompson et al., 2006). Interestingly, there is evidence to suggest that those individuals whose diets have contained high levels of omega-3 PUFAs throughout their life, have reduced cognitive decline in older age (Pusceddu et al., 2016, Cederholm et al., 2013). Given that an older age at the time of injury is a factor that leads to a worse outcome following TBI, we have also included a study in this chapter to investigate the impact of a CCI injury in old *fat-1* mice and their wild-type littermates.

## **5.2 Aims and Hypothesis**

### **5.2.1 Aims**

- To investigate the effect of high endogenous omega-3 PUFAs in young and aged mice following a CCI injury. The behavioural outcome was measured using the MWM and histological outcomes included tissue loss, microglial activation and reactive astrogliosis.
- To investigate the changes in the brain lipid profile of *fat-1* mice in the acute phase following CCI injury.

### **5.2.2 Hypothesis**

Based on the positive data produced in our group in *fat-1* mice in PNI and SCI models, it was hypothesised that there would be an improved outcome in *fat-1* mice following CCI injury, including reduced tissue loss, microglial activation, reactive astrogliosis and improved cognitive function.

## 5.3 Methods

### 5.3.1 Young and aged male fat-1 mice

The animals in this chapter were produced by mating heterozygous *fat-1* mice with wild type C57BL/6 mice. Heterozygous male mice 10-12 weeks old (young adult) and 49-53 weeks old (aged) were fed on a high omega-6 PUFA enriched diet in order to maintain the high omega-3: omega-6 ratio of the *fat-1* mice and the high omega-6: omega-3 ratio of the wild-type littermates. The same CCI injury was administered to these mice as described in the model development chapter and in methods section 2.1.2. A one week MWM protocol was used, with a 4-day acquisition trial (day 15 – 18) and a probe trial administered 24 hours following the last acquisition trial (day 19) (Fig. 5.1). After perfusion on day 21 post-injury, brain tissue was stained using toluidine blue and immunostained for GFAP (astrocytic marker) and Iba1 (microglia/macrophage marker). Age-matched naïve C57BL/6 male mice were used as controls for behavioural and histological testing.

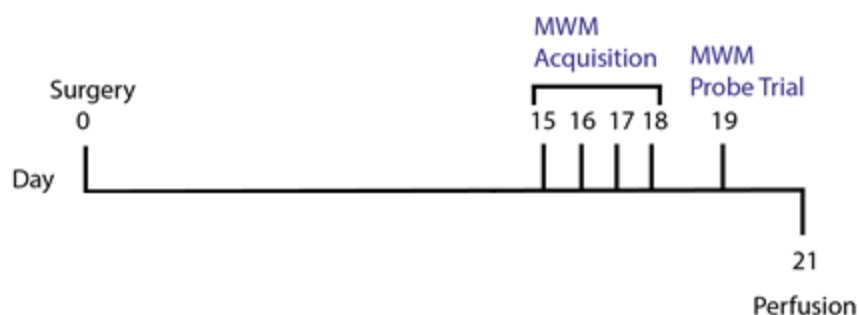


**Figure 5.1 Timeline for the testing in the Morris water maze following CCI in the *fat-1* mice.**

### 5.3.2 Lipid analysis of brain tissue from young adult female mice

The animals used for lipid analysis were female mice aged 10-12 weeks old, their wild-type littermates and naïve controls. CCI injury was conducted and then 24 hours later, the brain tissue was collected for lipid analysis. The analysis was carried out using thin layer chromatography and gas liquid chromatography (methods 2.1.1).

## 5.4 Results

*Fat-1* mice were used to investigate the potential neuroprotective effect high levels of endogenous omega-3 PUFA in tissues had on the outcome following a CCI injury. Young adult (10 -12 weeks) male *fat-1* mice and their wild type (WT) littermates were matched with naïve C57BL/6 controls. We assessed the effect of the *fat-1* gene on cognitive function using the Morris water maze (MWM) and on histological markers, i.e. tissue loss, microglial activation and reactive astrogliosis, using toluidine blue staining and immunolabelling. The same outcome measures were also used to assess the effect the *fat-1* gene had in aged (49 – 53 weeks) male mice following CCI.

In this chapter we also investigated the effect the *fat-1* gene had on the lipid profile of the brain tissue following CCI injury in young female mice 24 hours following injury. We used thin layer chromatography and gas liquid chromatography to establish the changes in fatty acids, with emphasis on the omega-6 fatty acids linoleic acid (LA 18:2n-6) and arachidonic acid (AA), and the omega-3 fatty acids docosapentaenoic acid (DPA) and docosahexaenoic acid (DHA).

### 5.4.1 Behavioural response after CCI injury in young adult male fat-1 mice

The male mice in this study which were considered young adults were 12-13 weeks old at the time of the injury. CCI injury was conducted on mice that expressed the *fat-1* gene (termed *fat-1*+CCI group) and their wild-type (WT) littermates (termed WT+ CCI group), which were all fed on a high omega-6 PUFA diet. For behavioural and histological testing, they were matched with naïve 12 week-old C57BL/6 male mice, to act as the control naïve group.

#### 5.4.1.1 Morris water maze – Acquisition and Probe trial

During the one-week acquisition training protocol (Fig. 5.1), that began on day 15 post-injury, all groups demonstrated a decrease in their escape latency (Fig. 5.2; Fig. 5.3A). The naïve group, which acted as our control group for this study, had the steepest learning curve. On day 15 the naïve group took an average of  $53.9 \pm 9.6$  s to find the platform over the 4 trials, which was reduced to  $18.8 \pm 7.6$  s on the final day of the acquisition training on day 18.

The *fat-1* transgenic and WT groups that received a CCI injury also reduced their escape latencies over the acquisition training. The WT + CCI group had an average escape latency of  $74.0 \pm 4.3$  s on day 15, which decreased to  $40.7 \pm 5.4$  s on day 18. The *fat-1* + CCI group had an average escape latency of  $64.3 \pm 3.2$  s on day 15, which decreased to  $36.1 \pm 4.9$  s on day 18. Despite this decrease in escape latencies over the acquisition training, the WT + CCI and *fat-1* + CCI animals were still statistically significantly slower than the naïve group (day 15: Naïve vs. WT + CCI, \*\*\* $p < 0.001$ ; day 16: Naïve vs. WT + CCI, \* $p < 0.05$ ; day 17: Naïve vs. WT + CCI, \*\*\* $p < 0.001$ ; Naïve vs. *fat-1* + CCI, \*\*\* $p < 0.001$ ; day 18: Naïve vs. WT + CCI, \*\*\* $p < 0.001$ ; Naïve vs. *fat-1* + CCI, \*\*\* $p < 0.001$  -statistical significance was determined using a two-way repeated measures ANOVA with post-hoc Bonferroni tests).

The probe trial was conducted on day 19, 24 hours after the last acquisition training day trial. The outcome measures from the probe trial were the same as in previous chapters, in which the time taken to the platform zone and the number of entries to the platform zone were analysed (Fig. 5.3B, C). The *fat-1* gene did not appear to affect locomotor performance as assessed by the analysis of the average swim speed of the young mice in the day 19 MWM probe trial (see appendix 1.1).

As expected, the naïve control group was the quickest to enter the platform zone during the probe trial ( $18.5 \pm 5.9$  s). The WT + CCI group ( $43.8 \pm 9.9$  s) and the *fat-1* + CCI group ( $32.0 \pm 6.3$  s) were both slower. However, the *fat-1* group had over a 10 s improvement in the latency to enter the platform zone – but this difference compared to the WT + CCI group was not statistically significant (Fig. 5.3B). Compared to naïve control animals, the WT + CCI animals had a decreased number of entries into the platform zone. The *fat-1* group had a performance which was similar to the naïve control animals, but overall the effect was not statistically significant (Fig. 5.3C).

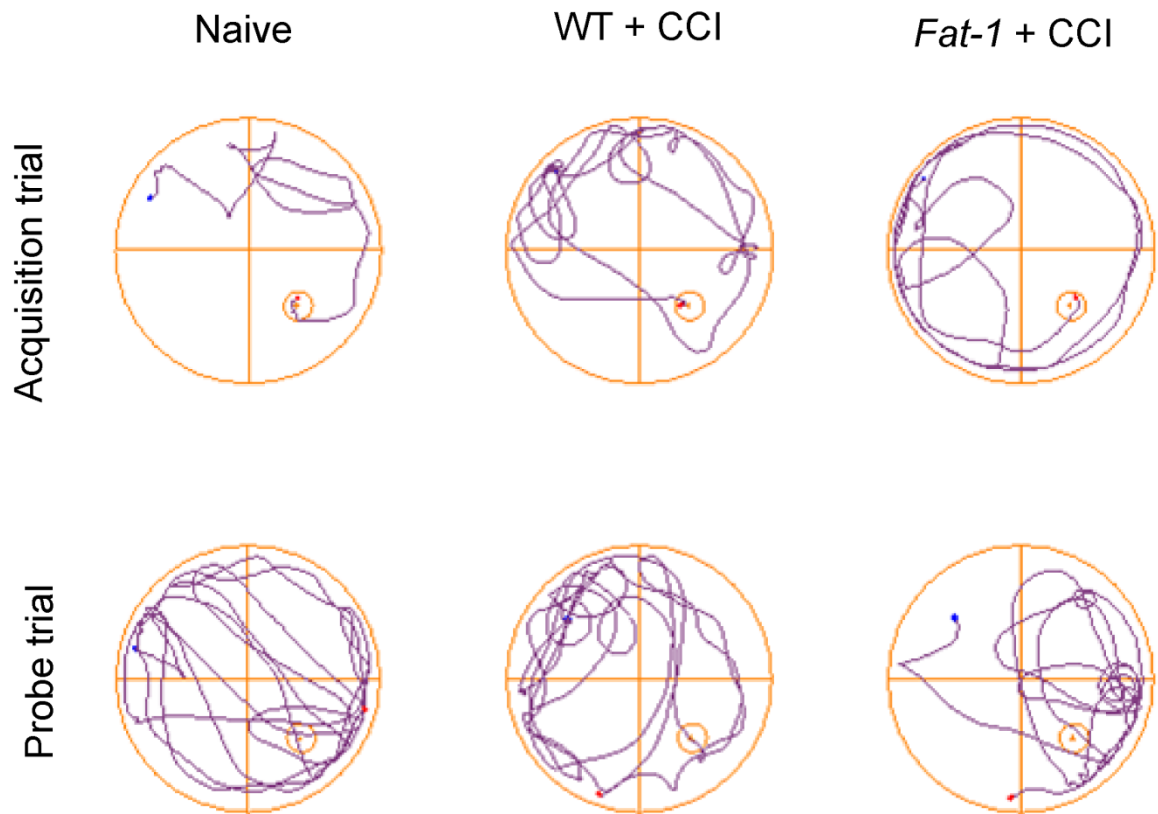


**Figure 5.2. Effect of the *fat-1* gene in young males on the performance in the Morris water maze.** Representative traces from the day 18 post-injury during the acquisition training and the day 19 probe trial.



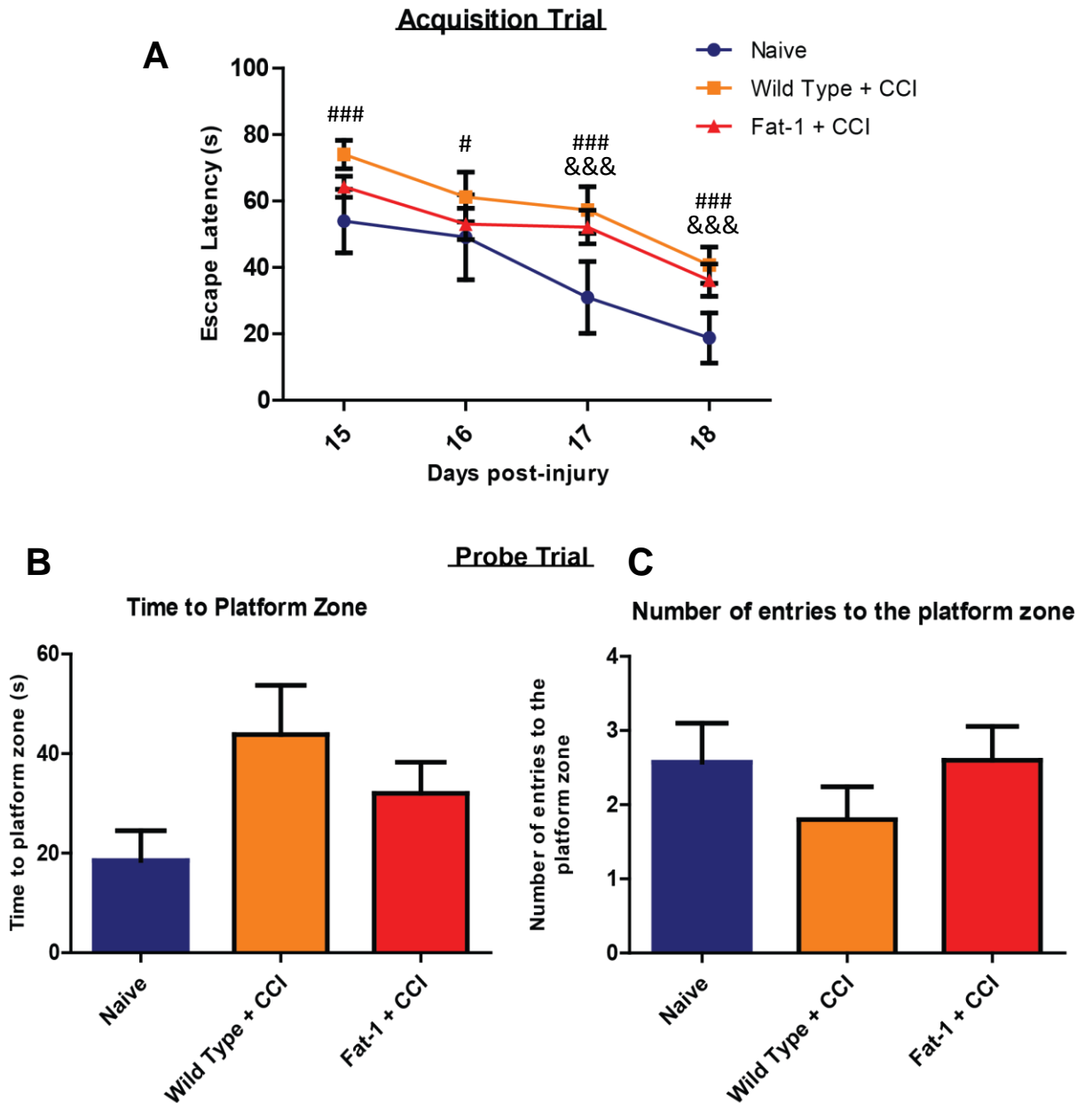


**Figure 5.3. Effect of the fat-1 gene in young males on the performance in the Morris water maze Acquisition and Probe trial.** (A) The average escape latency of the 4 trials conducted on days 15- 18 post injury during the acquisition training. The WT+CCI had significantly slower escape latencies compared to the naïve group on day 15 (### $p < 0.001$ ), day 16 (# $p < 0.05$ ), day 17 (### $p < 0.001$ ) and day 18 (### $p < 0.01$ ). The *fat-1* + CCI were also statistically slower than the naïve group on day 17 (&&& $p < 0.001$ ) and day 18 (&&& $p < 0.001$ ). There were no statistical differences between the WT + CCI and the *fat-1* + CCI groups during the acquisition training. On day 19 the probe trial was conducted; (B) the time taken to the platform zone and (C) the number of entries to the platform zone. There were no statistical differences between any of the groups in the probe trial measures. Statistical analysis of the acquisition training was conducted using a two-way repeated measures ANOVA with post-hoc Bonferroni tests. Mean  $\pm$  SEM. Naïve, N=6; WT+CCI, N=10; Fat-1+CCI, N=19.

#### **5.4.1.2 Gross tissue loss after CCI injury in young adult male fat-1mice**

After perfusion of the mice on day 21, the brain tissue was collected and cut into coronal sections. Sections from 4 locations (-1.5, -2.0, -2.5 and -3.0 mm posterior to bregma) spanning the area of the lesion were analysed using toluidine blue staining.

The WT + CCI and *fat-1* + CCI groups had substantial tissue loss in all three of the measurements carried out; the ipsilateral hemisphere, ipsilateral cortex and hippocampus, when compared to the contralateral side (Fig. 5.4; Fig. 5.5A-C). The naïve group represented the baseline. The WT + CCI and *fat-1* + CCI groups had a statistically significant loss of tissue compared to the naïve group in the ipsilateral hemisphere (\* $p < 0.05$ ), the ipsilateral cortex (\*\* $p < 0.01$ ) and the ipsilateral hippocampus (\*\* $p < 0.001$ ). The presence of the *fat-1* gene did not prevent the tissue loss after CCI as there were no statistically significant differences in comparison to the WT + CCI group.

The ipsilateral hippocampus in both of the CCI groups had the biggest reduction in size, when compared to the contralateral hippocampus. The WT + CCI group only had  $26.3 \pm 3.2$  % ipsilateral hippocampal tissue intact compared to the *fat-1* + CCI group, with  $28.3 \pm 3.2$  % remaining (Fig. 5.5C).

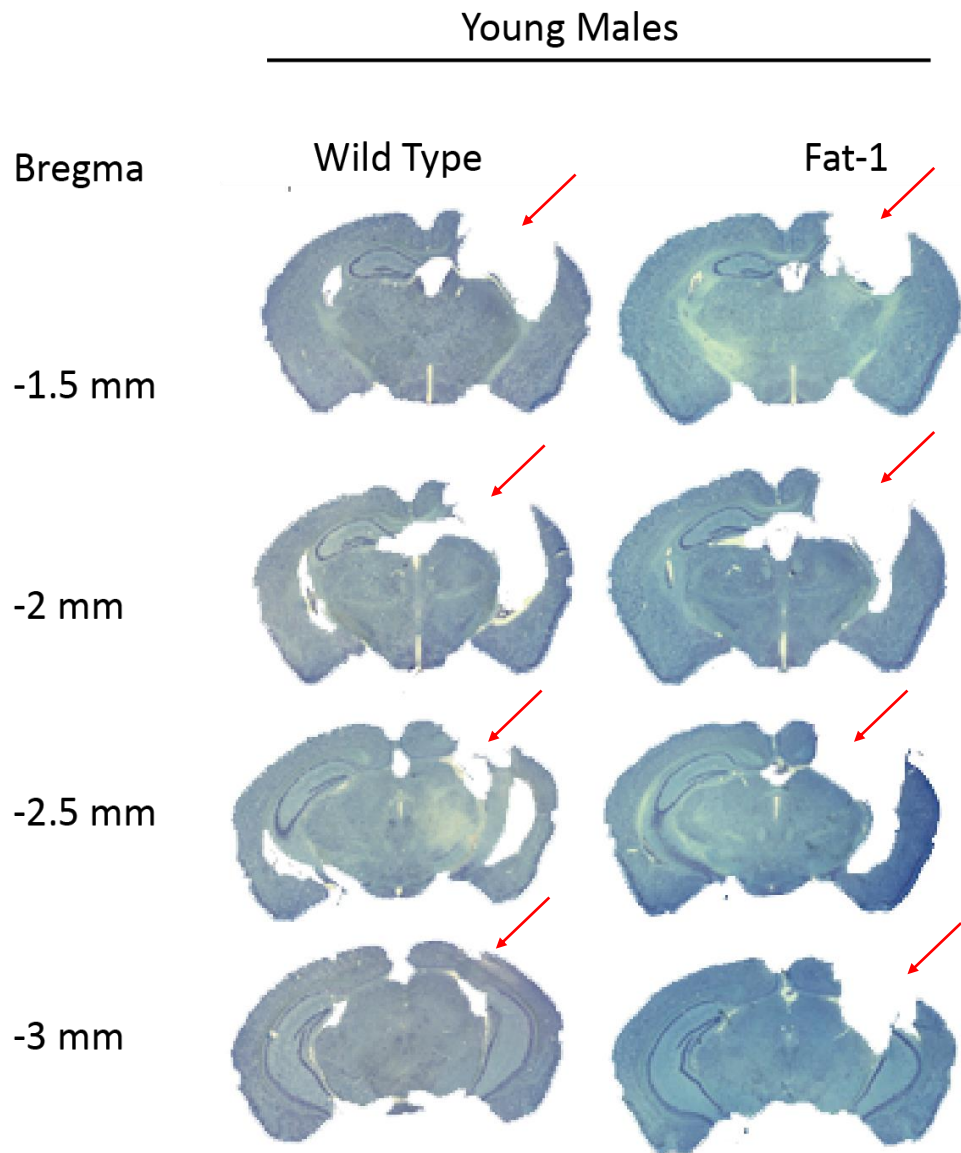


**Figure 5.4. Brain sections from young wild type and fat-1 mice stained with toluidine blue.** 20  $\mu$ m coronal brain sections from WT + CCI and *fat-1* + CCI groups, taken from the following locations posterior to bregma: -1.5 mm, -2.0 mm, -2.5 mm and -3.0 mm. The red arrows indicate the region of the injury site.

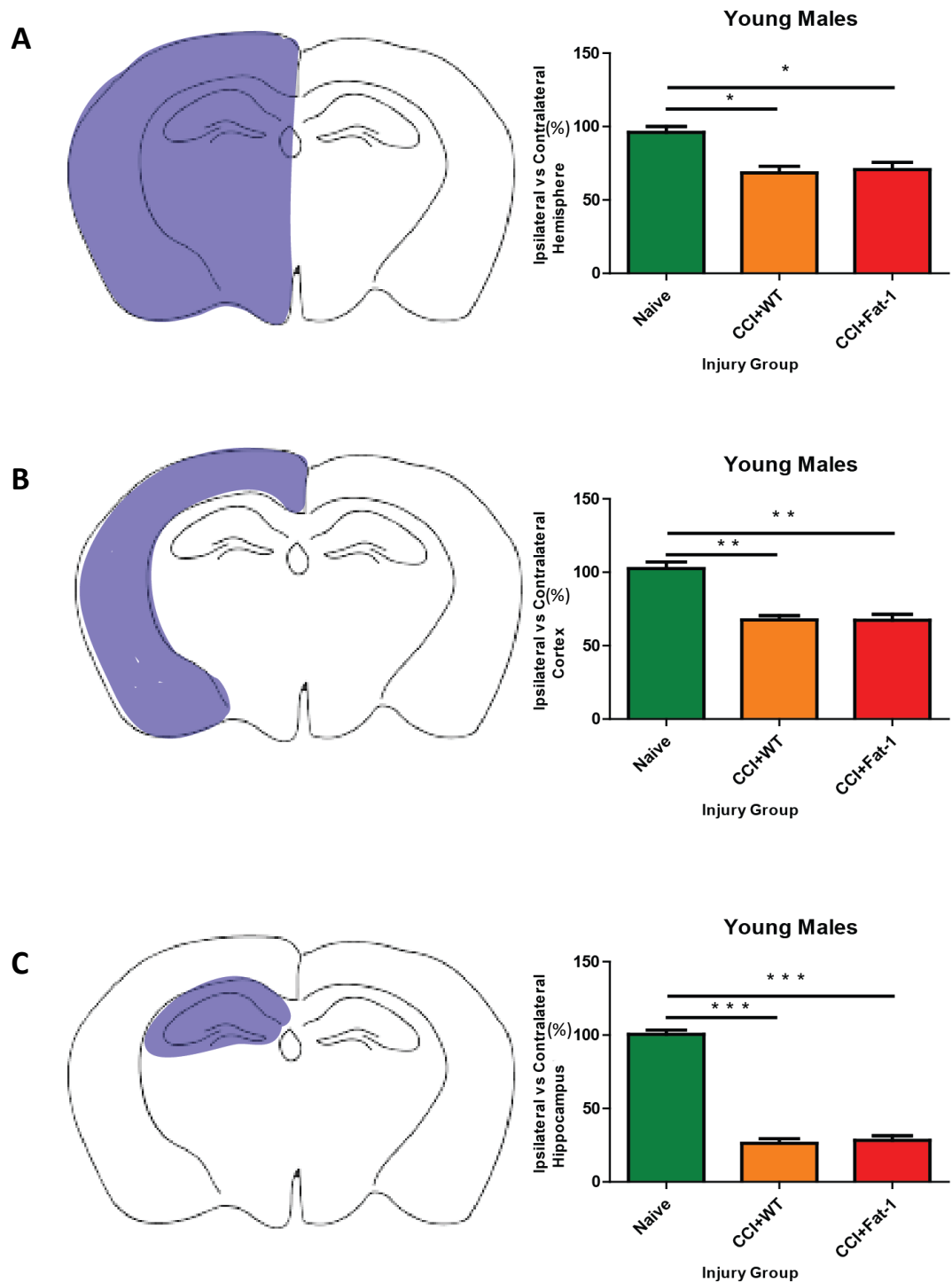


**Figure 5.5. The effect the fat-1 gene has in young males on tissue loss after CCI.** (A) hemisphere, (B) cortex and (C) hippocampus. Statistical significance determined using one-way ANOVA and post-hoc Bonferroni testing (\* $p < 0.05$ , \*\* $p < 0.01$ , \*\*\* $p < 0.001$ ). Mean  $\pm$  S.E.M. N= 3 animals per group.

#### 5.4.1.3 Reactive astrogliosis after CCI injury in young adult male *fat-1* mice

The percentage area covered by GFAP immunolabelling was measured in the same ROI as in previous chapters, to determine the level of reactive astrocytosis (Fig. 5.6; Fig. 5.7). The CCI injured groups showed increased GFAP immunolabelling when compared to the naïve controls. The WT + CCI (\*\* $p < 0.001$ ) and the *fat-1* + CCI (\*\* $p < 0.001$ ) showed a statistically significant increase in the amount of GFAP immunolabelling in the ipsilateral cortex when compared to the naïve group (Fig. 5.7B). There was also an increase in the GFAP immunolabelling in the *fat-1* + CCI group ( $p < 0.05$ ) compared to the WT + CCI in the ipsilateral cortex. In the contralateral cortex, the *fat-1* + CCI mice (\*\* $p < 0.01$ ) had increased GFAP immunolabelling when compared to the naïve group (Fig. 5.7A). The WT + CCI group had a higher percentage of GFAP immunolabelling compared to the naïve control, but this was not statistically significant.

There was increased GFAP immunolabelling in the hippocampus in the *fat-1* + CCI group compared to the naïve ( $p < 0.05$ ) and WT + CCI ( $p < 0.05$ ) groups (Fig. 5.7C). There were no significant differences between the naïve and the WT + CCI groups. There were no differences between the three groups in the GFAP immunolabelling in the dentate gyrus (Fig. 5.7D).

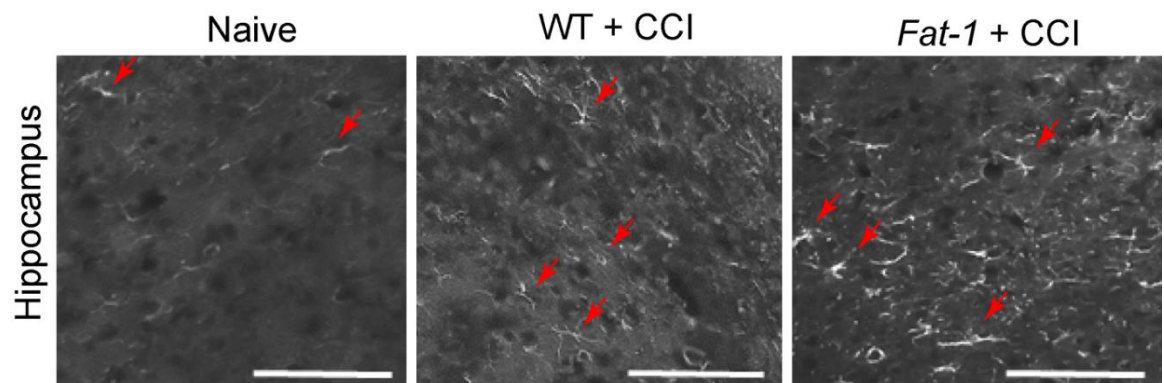


**Figure 5.6. The effect of the *fat-1* gene on GFAP expression in young males.** Immunolabelling of reactive astrocytes with GFAP in the ipsilateral cortex in the naïve, WT + CCI and *fat-1* + CCI groups. Red arrows indicate a GFAP+ cell. Scale bar = 100 μm.

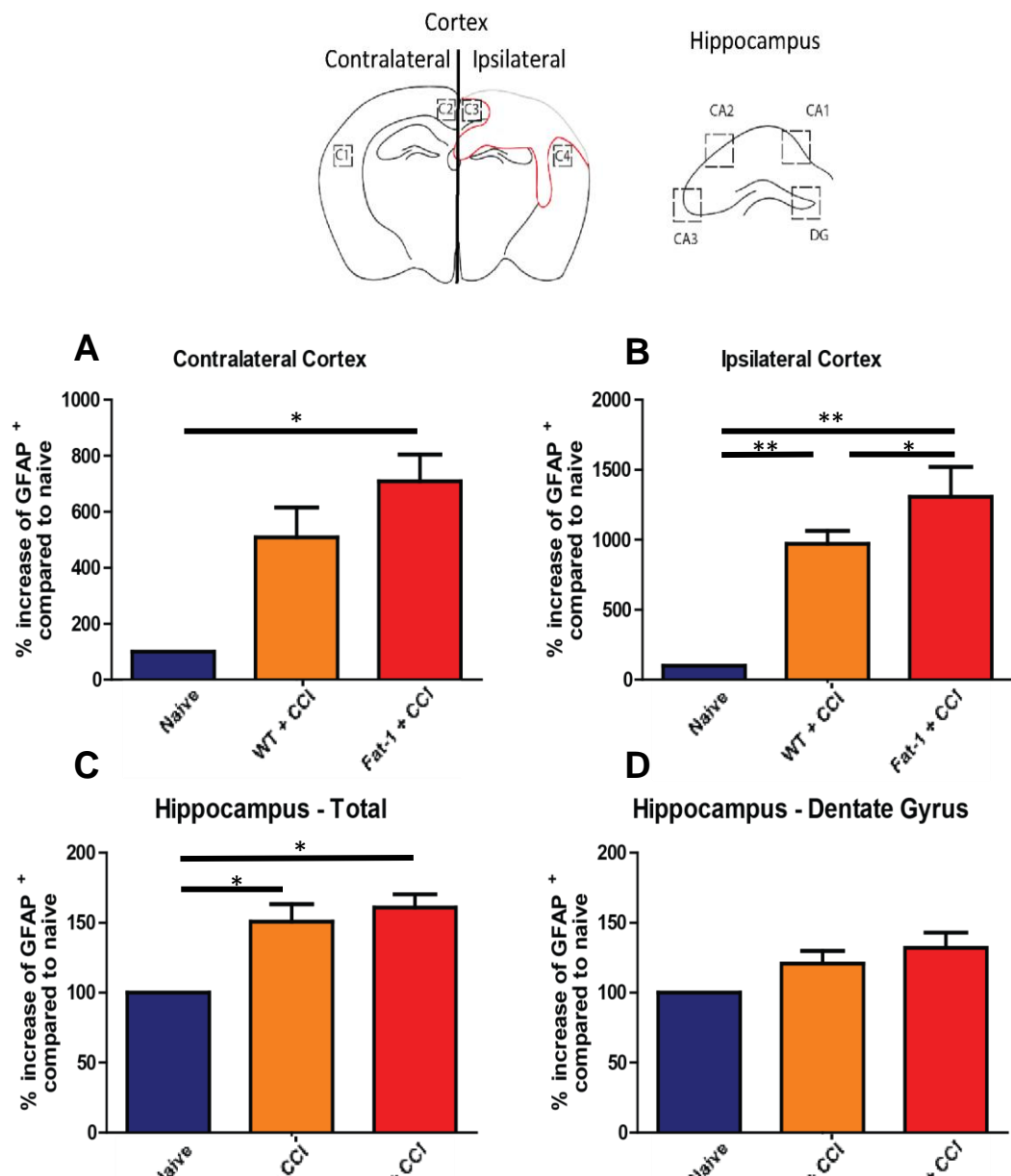


**Figure 5.7 The effect the *fat-1* gene has in on reactive astrogliosis in the cortex and hippocampus in young males.** Schematic showing the ROI in the cortex and hippocampus that were analysed for GFAP labelling (GFAP+). The percentage increase in GFAP labelling in the WT + CCI and *fat-1* + CCI groups was compared to young naïve tissue. (A) In the contralateral cortex the *fat-1* + CCI (\*\* $p < 0.01$ ) group had an increased amount of GFAP+ labelling compared to the naïve group. (B) In the ipsilateral cortex there was increased GFAP+ labelling in the CCI groups (WT + CCI vs. Naïve, \*\*\* $p < 0.001$ ; *fat-1* + CCI vs. Naïve, \*\*\* $p < 0.001$ ; *fat-1* + CCI vs. WT + CCI, \* $p < 0.05$ ). (C) In the contralateral hippocampus the *Fat-1* + CCI showed increased GFAP+ labelling compared to the naïve group (\* $p < 0.05$ ) the WT+CCI group also had increased GFAP+ labelling vs. the naïve group (\* $p < 0.05$ ). (D) There was no difference in GFAP+ labelling between groups in the dentate gyrus of the hippocampus. Statistical significance was determined using one-way ANOVA and post-hoc Bonferroni test. Mean  $\pm$  S.E.M. N=4-5 animals per group.

#### 5.4.1.4 Activated microglia/macrophages after CCI injury in young adult male *fat-1* mice

The same ROI used to analyse reactive astrogliosis in the cortex and contralateral hippocampus, were used to analyse the number of activated microglia/macrophages in these mice (Fig. 5.8). The lowest number of Iba1+ cells was found in the naïve group, in all ROI. In the contralateral cortex the naïve group had  $20 \pm 5$  Iba1+ cells, which was statistically fewer than the WT + CCI group  $60 \pm 12$  (\* $p < 0.05$ ) and the *fat-1* + CCI group  $57 \pm 6$  (\* $p < 0.05$ ) (Fig. 5.9A). In the ipsilateral cortex the *fat-1* + CCI ( $80 \pm 17$ ) and the WT + CCI ( $65 \pm 7$ ) groups had a higher number of Iba1+ cells compared to the naïve group ( $29 \pm 4$ ) (Fig. 5.9B). Only the WT + CCI group showed a statistically significant increase in the number of Iba1+ cell vs. the naïve group (\* $p < 0.05$ ).

In the contralateral hippocampus, the two injury groups had a higher number of Iba1+ cells than the naïve group (Fig. 5.9C). The WT + CCI group had  $201 \pm 14$  Iba1+ cells and the *fat-1* + CCI group had  $224 \pm 26$  Iba1+ cells, both of these had a statistically significant increased number of Iba1+ cells compared to the naïve group which had  $125 \pm 8$  (WT + CCI vs naïve, \* $p < 0.05$ ; *fat-1* + CCI vs naïve, \*\* $p < 0.01$ ).

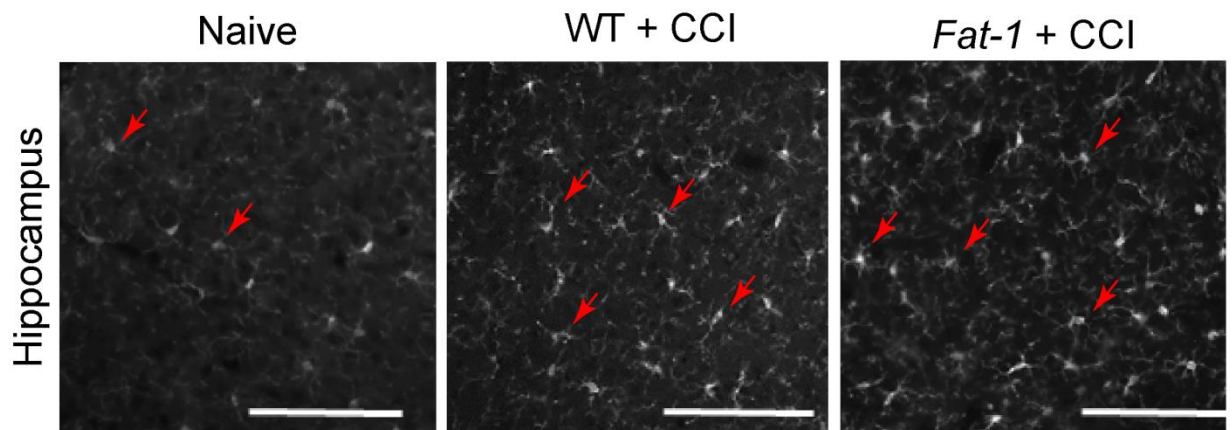


**Figure 5.8. The effect of *fat-1* gene on the Iba1 expression in young males.** Immunolabelling of activated microglia/macrophages with Iba1, in the contralateral cortex in the naïve, WT + CCI and *fat-1* + CCI groups. Red arrows indicate Iba1+ cells. Scale bar = 100  $\mu\text{m}$ .

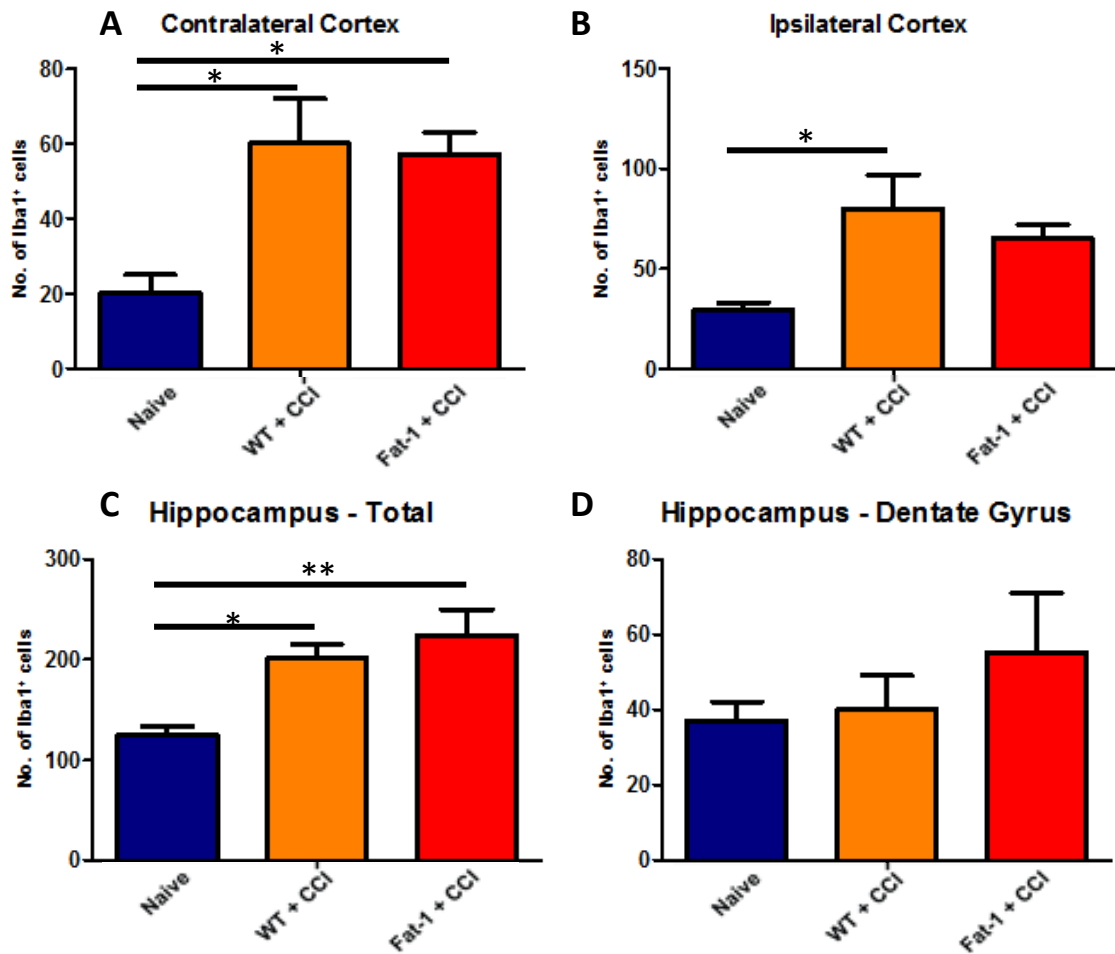


**Figure 5.9. The effect the *fat-1* gene has on the number of Iba1+ cells in the cortex and hippocampus in young males.** The numbers of activated microglia/macrophages were identified with Iba1+ immunolabelling in the WT + CCI and *Fat-1* + CCI groups and was compared to young male naïve tissue. (A) In the contralateral cortex the *fat-1* + CCI group (\* $p < 0.05$ ) and the WT + CCI group (\* $p < 0.05$ ) had an increased no. of Iba1+ cells compared to the naïve group. (B) In the ipsilateral cortex there was increased no. of Iba1+ cells in WT + CCI group (\* $p < 0.05$ ) vs naïve group. (C) In the contralateral hippocampus the CCI injured groups had increased no. of Iba1+ cells, *fat-1* + CCI vs naïve, \*\* $p < 0.01$ ; WT + CCI vs naïve, \* $p < 0.05$ ). (D) In the dentate gyrus of the hippocampus, there was no statistically significant difference between the groups. Statistical significance was determined using one-way ANOVA and post-hoc Bonferroni test. Mean  $\pm$  S.E.M. N= 4- 5 animals per group.



#### **5.4.2 The effect of CCI in aged male fat-1 mice**

The males in this study were 49-53 weeks old at the time of the injury. Mice that expressed the *fat-1* gene and their WT littermates received a CCI injury and were fed on a high omega-6 PUFA diet. For behavioural and histological testing, they were matched with naïve 52 week-old C57BL/6 male mice, which acted as the control group.

##### **5.4.2.1 Morris water maze – Acquisition and Probe trial**

The acquisition training protocol (Fig. 5.1; Fig.5.10) began on day 15 post-injury. The naïve group was the only group that demonstrated learning ability (Fig. 5.11A). The naïve group on day 15 had an average escape latency of  $81.3 \pm 5.3$  s on day 15, that was reduced to  $22.4 \pm 4.6$  s on day 18. The aged WT + CCI group and the aged *Fat-1* + CCI group failed to show a significant reduction in escape latency over the 4 days of the acquisition training. On day 15 the WT + CCI group had an escape latency of  $66.6 \pm 6.5$  s and on day 18 it had an escape latency of  $54.2 \pm 3.7$  s. The *Fat-1* + CCI group on day 15 had an escape latency of  $68.4 \pm 6.3$  s and on day 18 it had an escape latency of  $55.9 \pm 13.2$  s.

The probe trial was conducted on day 19 post-injury, 24 hours after the last acquisition training trial (Fig. 5.10; Fig.5.11B, C). The *fat-1* gene did not appear to affect locomotor performance as assessed by the analysis of the average swim speed of the aged mice in the day 19 MWM probe trial (see appendix 1.1). The naïve group was able to reach the platform zone quickest with a latency of  $29.9 \pm 16.2$  s, whereas the two CCI injured groups took on average over a minute to reach the platform zone (WT + CCI,  $63.0 \pm 16.7$  s; *Fat-1* + CCI,  $75.9 \pm 14.1$  s).

The number of entries made to the platform zone during the probe trial was higher in the naïve mice than in the mice that received a CCI injury (Fig. 5.11C). There was no difference between the WT + CCI and *Fat-1* + CCI groups in the number of visits to the platform zone, which for both groups was fewer than 1 visit, meaning that some mice in those groups did not enter the platform zone at all during the 90 s probe trial.

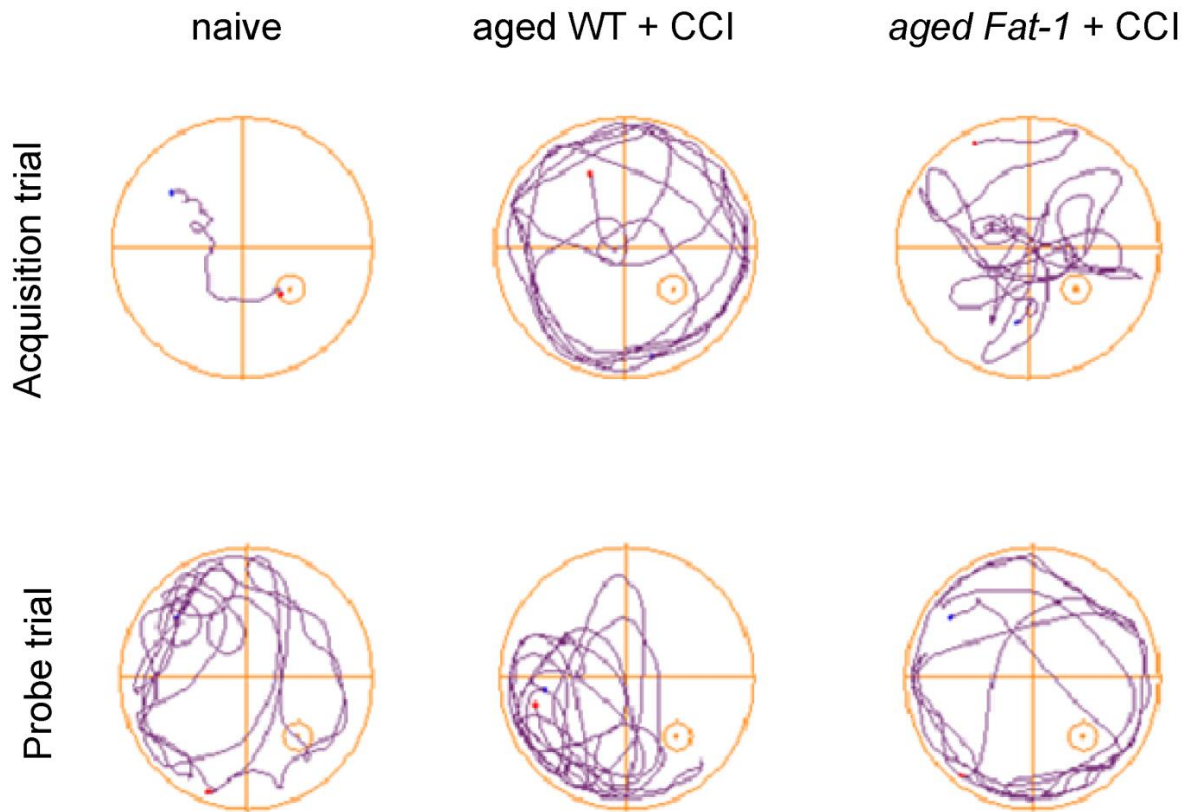


**Figure 5.10. Effect of the *fat-1* gene in aged males on the performance in the Morris water maze.** Representative traces from the day 18 post-injury during the acquisition training and the day 19 probe trial.

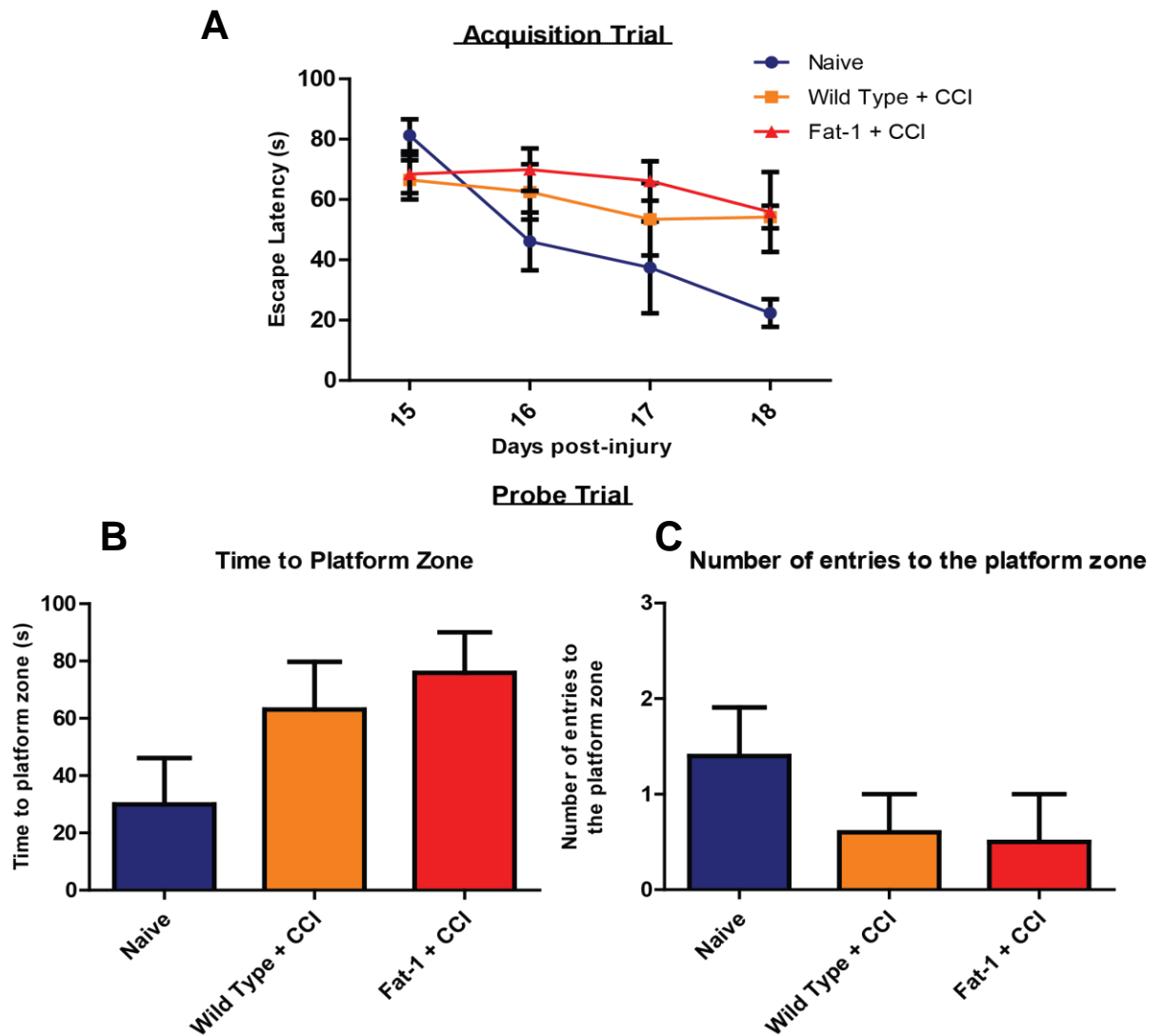


**Figure 5.11 Effect of the *fat-1* gene in aged males on the performance in the Morris water maze Acquisition and Probe trial.** (A) The average escape latency of the 4 trials conducted on days 15- 18 post injury during the acquisition training. The WT + CCI and the *Fat-1* + CCI groups had slower escape latencies than the naïve group, but it was not statistically significant. On day 19 the probe trial was conducted; (B) the time taken to the platform zone and (C) the number of entries to the platform zone. There were no statistical differences between any of the groups in the probe trial measures. Mean  $\pm$  SEM. Naïve, n=5; WT + CCI, n=5; *Fat-1* + CCI, n=4.

#### **5.4.2.2 Tissue loss after CCI injury in aged male *fat-1* mice**

After perfusion of the aged mice on day 21, the brain tissue was cut into 20  $\mu\text{m}$  thick sections (Fig. 5.12). Coronal brain slices from 4 locations (-1.5, -2.0, -2.5 and -3.0 mm in reference to bregma) spanning the area of the impact lesion and were analysed using toluidine blue staining.

The aged WT + CCI and aged *fat-1* + CCI group had substantial tissue loss in all three of the measurements, the ipsilateral hemisphere, ipsilateral cortex and hippocampus, when compared to the contralateral side (Fig. 5.13A-C). The aged naïve group did not show any tissue loss on the ipsilateral side. The aged WT + CCI and aged *fat-1* + CCI groups had a statistically significant loss of tissue compared to the naïve group in the ipsilateral hemisphere (\*\* $p < 0.01$ ), the ipsilateral cortex (\*\* $p < 0.01$ ) and the ipsilateral hippocampus (\*\* $p < 0.01$ ). The presence of the *fat-1* gene did not prevent any tissue loss after CCI, and therefore failed to show any statistical difference to the aged WT + CCI group.

The ipsilateral hippocampus in both of the aged CCI groups had the biggest reduction in hippocampal size when compared to the contralateral hippocampus. The aged WT + CCI group only had  $16.7 \pm 3.8\%$  ipsilateral hippocampal tissue remaining and the aged *fat-1* + CCI group only had  $31.5 \pm 10.5\%$  remaining (Fig. 5.13C).

Old Males

---

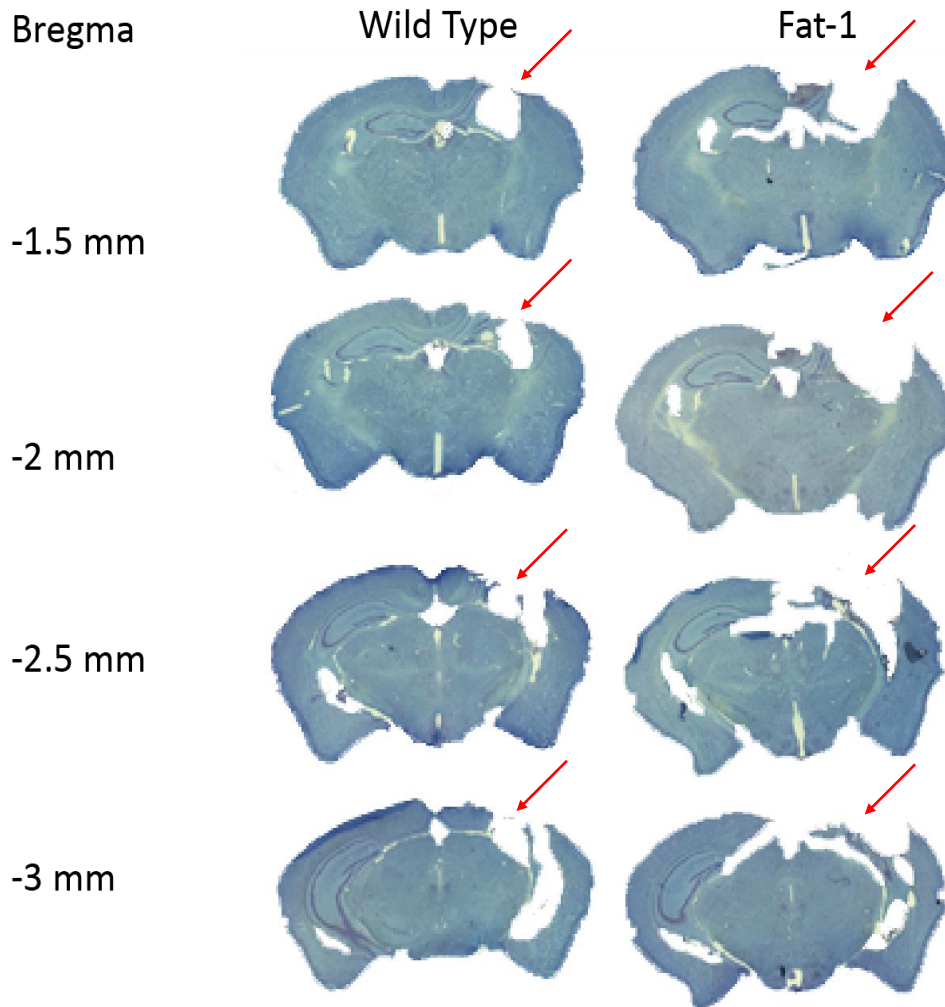


**Figure 5.12 Brain sections from aged wild type and *fat-1* mice stained with Toluidine blue.** 20  $\mu$ m coronal brain sections from WT + CCI and *Fat-1* + CCI groups. The brain sections were taken from the following location back from the bregma reference: -1.5 mm, - 2.0 mm, -2.5 mm and- 3.0 mm. The red arrow heads indicate the location of the injury site.

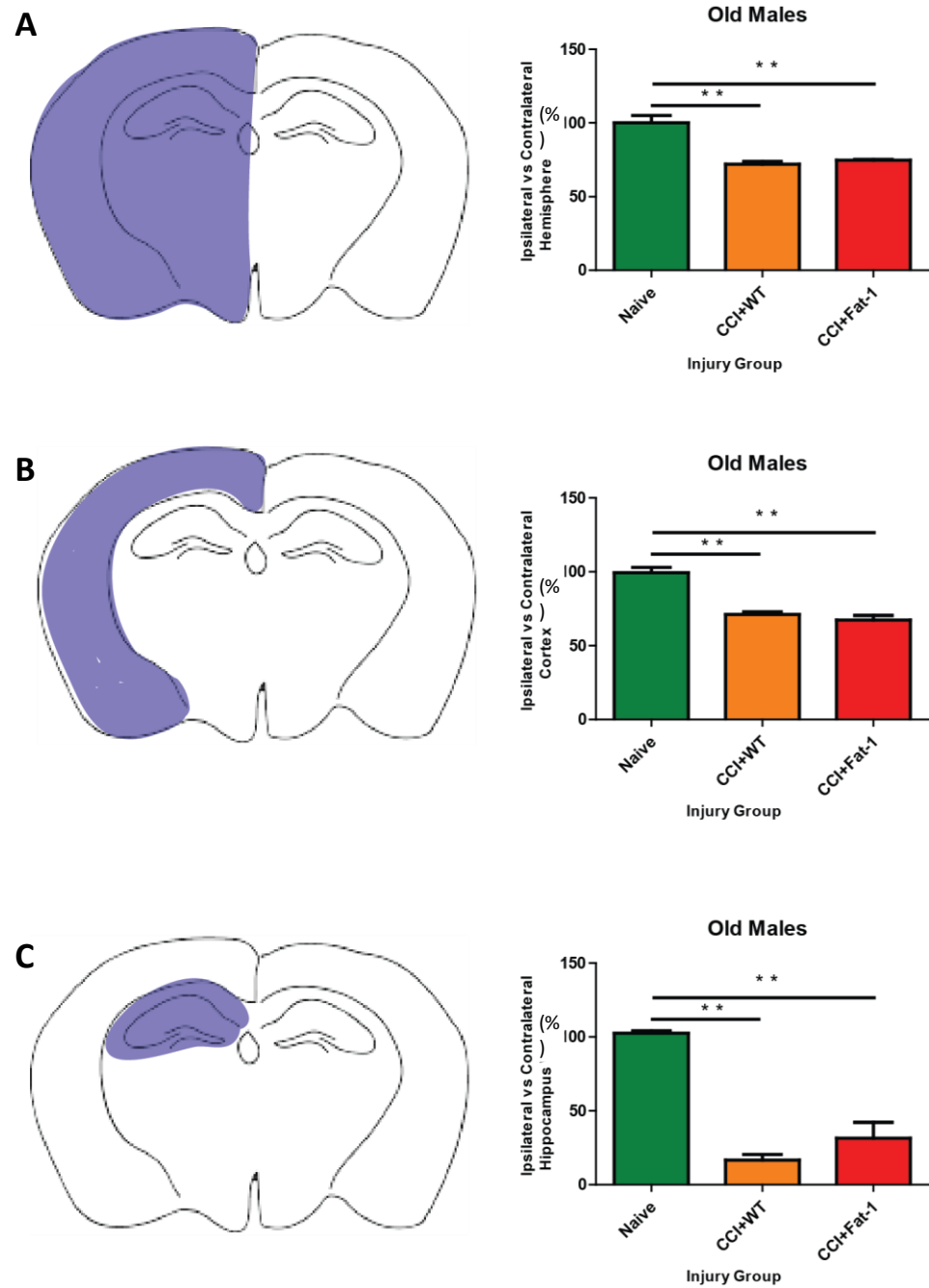


**Figure 5.13. The effect the *fat-1* gene has in aged males on tissue loss after CCI.** (A) Hemisphere, (B) cortex and (C) hippocampus. Statistical significance was found using one-way ANOVA and post-hoc Bonferroni testing (\*\* $p < 0.01$ ). Mean  $\pm$  SEM. N= 3 animals per group.

#### **5.4.2.3 Reactive astrogliosis after CCI injury in aged male fat-1 mice**

The percentage area covered by GFAP labelling was measured in the same ROI as in previous chapters, to determine the reactive astrocytosis (Fig. 5.14). The aged naïve group had very little GFAP labelling in the contralateral and ipsilateral cortices when compared to the two aged CCI injury groups (Fig.5.15A,B). The WT + CCI (\*p<0.05) and *fat-1* + CCI groups (\*\*p<0.01) showed a statistically significant increase in GFAP immunolabelling in the ipsilateral cortex when compared to the naïve group. The two aged CCI injury groups did not show any statistically significant differences to each other, although the aged *fat-1* + CCI mice had almost 1.5 times as much GFAP labelling ( $1454.1 \pm 268.2$  %) compared to the aged WT + CCI ( $880.1 \pm 44.7$  %) GFAP labelling in the ipsilateral cortex.

The contralateral cortex had a smaller increase in GFAP immunolabelling than the ipsilateral cortex. In the contralateral cortex (Fig. 5.15A) the aged *fat-1* + CCI group had statistically increased GFAP immunolabelling compared to both the naïve (\*\*p<0.001) and aged WT + CCI group (\*\*p<0.01). The aged WT + CCI group also had increased GFAP immunolabelling when compared to the naïve group (\*\*p<0.001).

There was increased GFAP immunolabelling in the hippocampus (Fig. 5.15C) in the aged *fat-1* + CCI injured group compared to the aged naïve (\*p<0.05) and the aged WT + CCI (\*p<0.05) groups. There were no significant differences between the aged naïve and the aged WT + CCI groups. There were no differences between the three groups in the GFAP immunolabelling within the dentate gyrus region of the hippocampus (Fig. 5.15D).

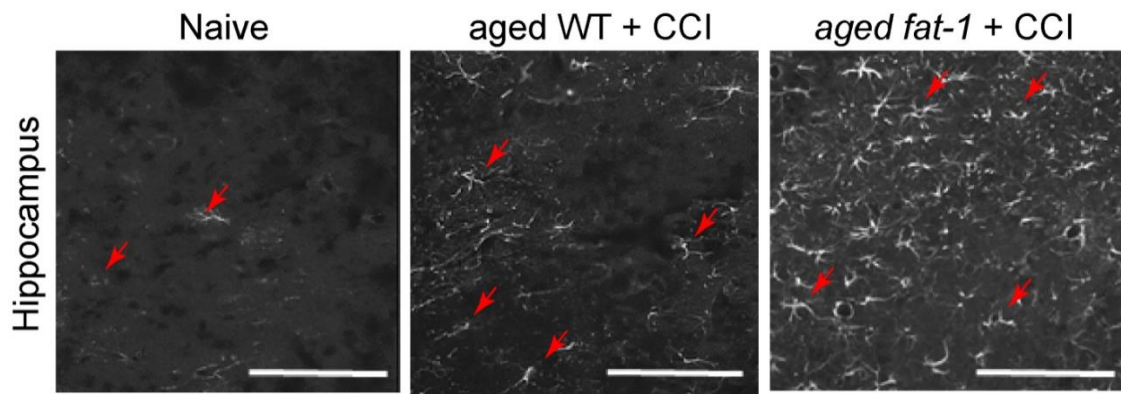


**Figure 5.14 The effect of *fat-1* gene on GFAP expression.** Immunolabelling of reactive astrocytes with GFAP in the ipsilateral cortex in the naive, aged WT+CCI and aged *fat-1*+CCI groups. Red arrows indicate a GFAP+ cell. Scale bar= 100  $\mu$ m.



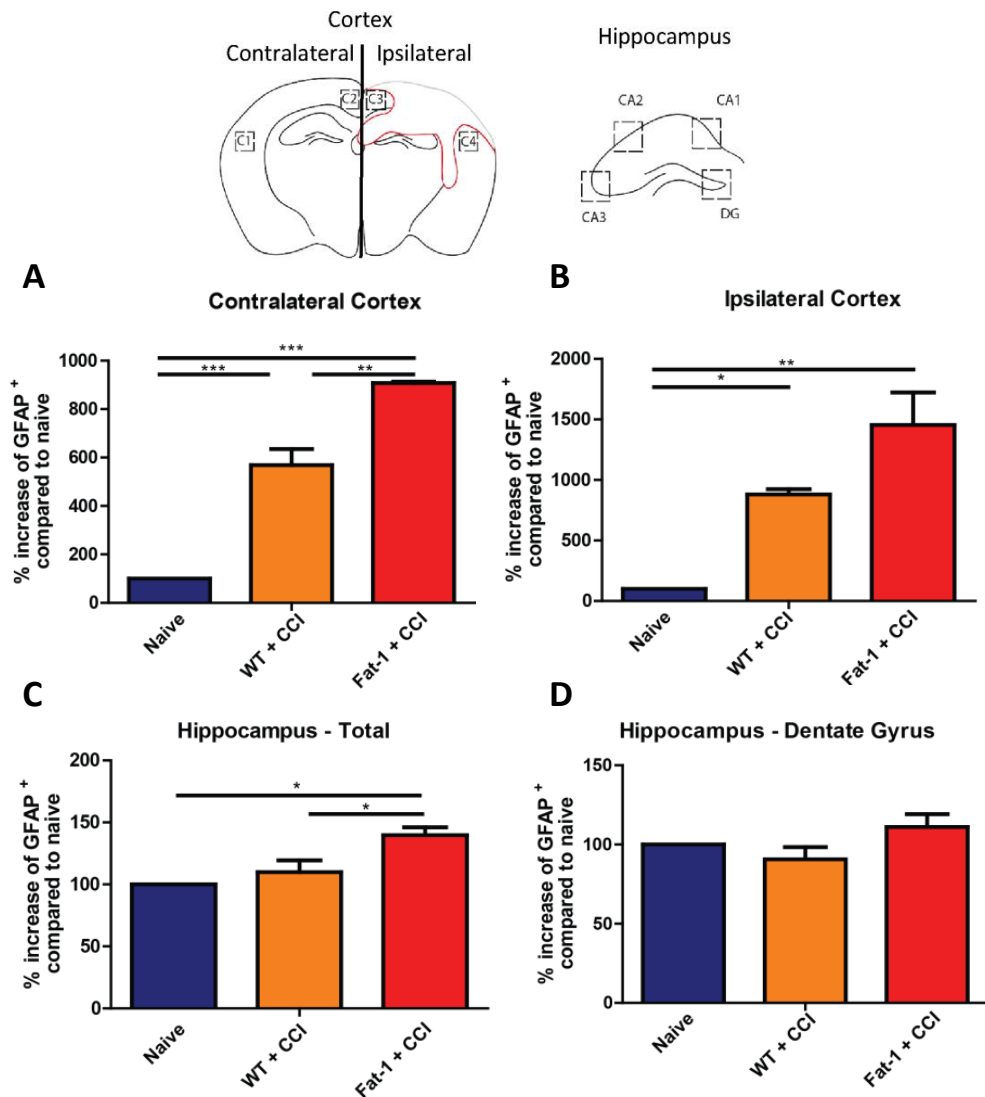


**Figure 5.15. The effect the *fat-1* gene had on reactive astrogliosis in the cortex and hippocampus of aged males.** Schematic showing the ROI in the cortex and hippocampus that were analysed for GFAP labelling (GFAP+). The percentage increase in GFAP labelling in the aged WT + CCI and *aged fat-1* + CCI groups was compared to aged naïve tissue. (A) In the contralateral cortex the aged WT + CCI (\*\*\*)  $p < 0.001$  and the *aged fat-1* + CCI (\*\*\*)  $p < 0.001$  groups had an increased amount of GFAP+ labelling compared to the naïve group. The *aged fat-1* + CCI group (\*\*  $p < 0.01$ ) also had increased GFAP+ vs naïve group. (B) In the ipsilateral cortex there was increased GFAP+ labelling in the CCI groups (aged WT + CCI vs naïve, \*  $p < 0.05$ ; *aged fat-1* + CCI vs naïve, \*\*  $p < 0.01$ ). (C) In the contralateral hippocampus the *aged fat-1* + CCI showed increased GFAP+ labelling compared to the naïve group (\*  $p < 0.05$ ) and the aged WT + CCI group (\*  $p < 0.05$ ). (D) There was no difference in GFAP+ labelling between groups in the dentate gyrus of the hippocampus. Statistical significance was determined using one-way ANOVA and post-hoc Bonferroni test. Mean  $\pm$  S.E.M. Naïve,  $n=5$ ; aged WT + CCI,  $n=5$ ; aged *Fat-1* + CCI,  $n=4$ .

#### 5.4.2.4 The effect of CCI in aged *fat-1* males – Microglia/macrophage activation

The same regions of interest (ROI) were used to analyse the number of microglia/macrophages in these mice (Fig. 5.16). The lowest number of Iba1+ cells were found in the Naïve group in all ROI. In the contralateral cortex (Fig. 5.17A) the naïve group had  $27 \pm 5$  Iba1+ cells, which was statistically fewer than the aged WT + CCI group  $45 \pm 4$  (\* $p < 0.05$ ) and the aged *fat-1* + CCI group  $49 \pm 3$  (\* $p < 0.05$ ). In the ipsilateral cortex (Fig. 5.17B) the aged *fat-1* + CCI had the highest number of Iba1+ cells  $57 \pm 1$ , which was statistically more than the naïve group (\* $p < 0.05$ ).

In the contralateral hippocampus the two injury groups had a higher number of Iba1+ cells than the naïve group (Fig. 5.17C). The aged WT + CCI group had  $195 \pm 12$  Iba1+ cells and the aged *fat-1* + CCI group had  $210 \pm 14$  cells, both of these had statistically increased number of Iba1+ cells compared to the naïve group (aged WT + CCI vs naïve, \*\* $p < 0.01$ ; aged *fat-1* + CCI vs naïve, \*\* $p < 0.01$ ).

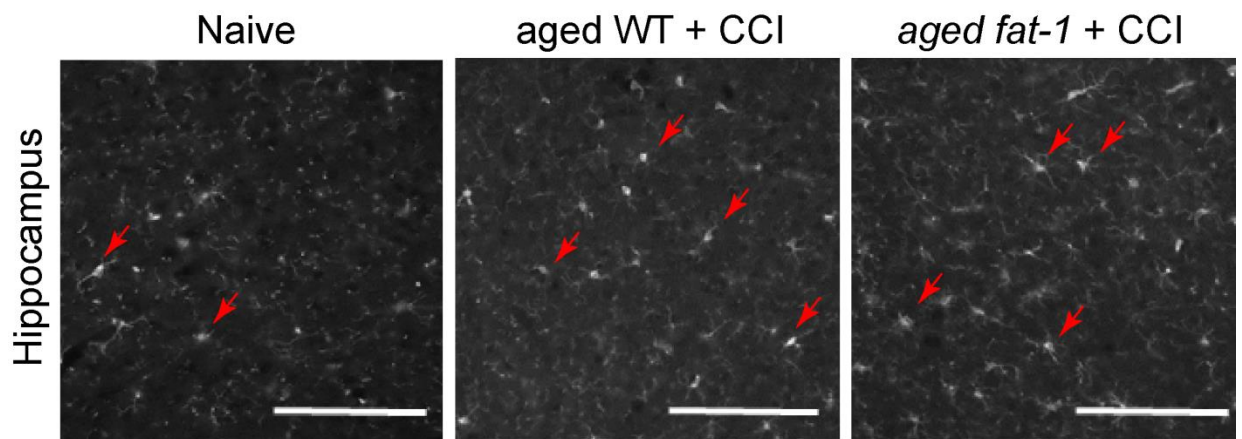


**Figure 5.16. The effect of *fat-1* gene on the no. of Iba1+ cells in aged *fat-1* males.** Immunolabelling of activated microglia/macrophages within the ipsilateral cortex in the aged naïve, aged WT + CCI and aged *fat-1* + CCI groups. Red arrows indicate Iba1+ cells. Scale bar = 100  $\mu\text{m}$ .

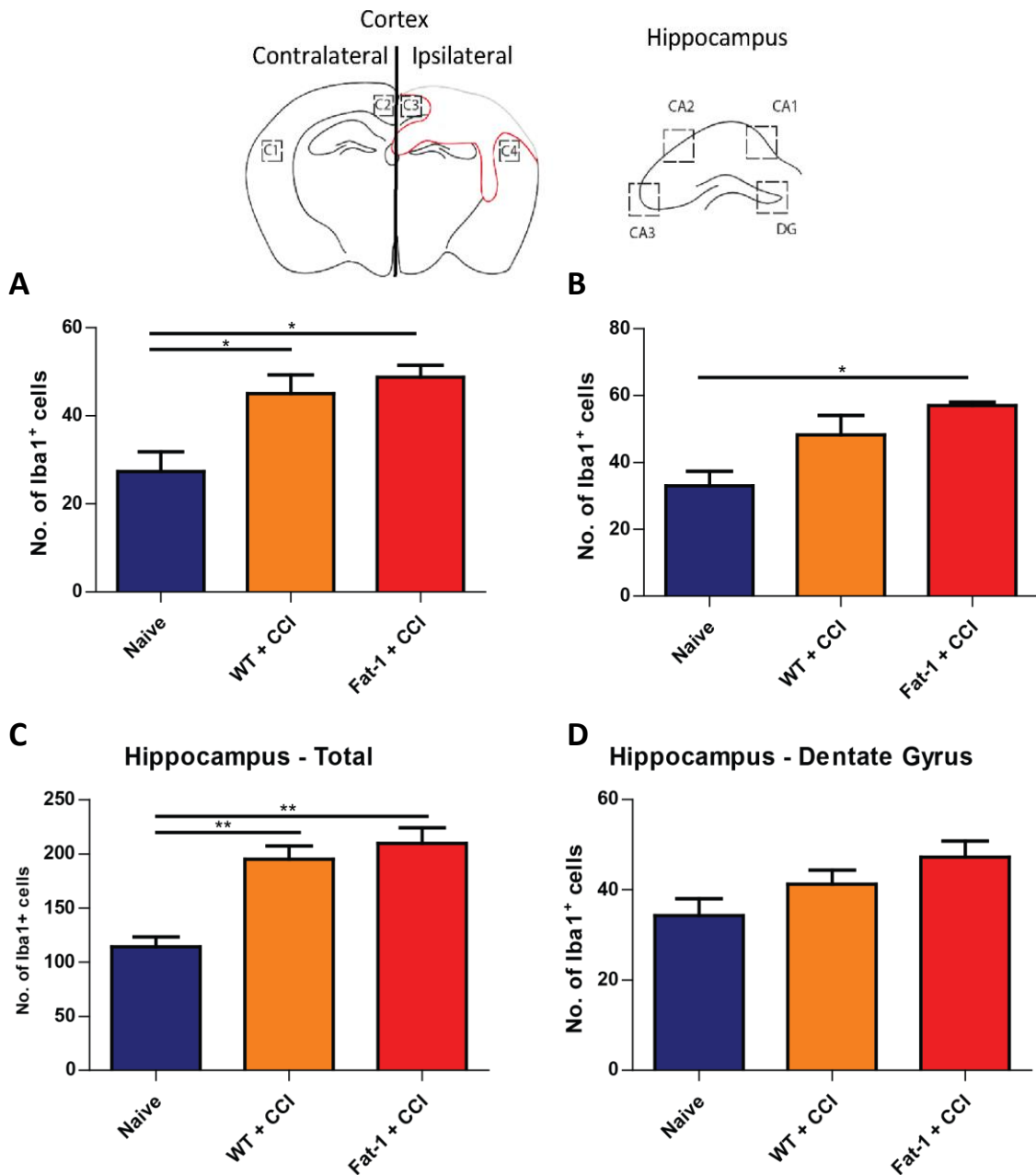


**Figure 5.17. The effect of the *fat-1* gene in aged males on the number of microglia/macrophages in the cortex and hippocampus.** Schematic showing the ROI in the cortex and hippocampus that were analysed for Iba1+ labelling. The number of Iba1+ cells were analysed in the (A) contralateral cortex, where the aged WT + CCI (\* $p < 0.05$ ) and the *aged fat-1* + CCI group (\* $p < 0.05$ ) had an increased number of Iba1+ cells compared to the naïve group. (B) In the ipsilateral cortex the *aged fat-1* + CCI (\* $p < 0.05$ ) had a higher number of Iba1+ cells compared to the naïve group. (C) In the hippocampus the aged WT + CCI (\*\* $p < 0.01$ ) and the *aged fat-1* + CCI (\*\* $p < 0.01$ ) had a higher number of Iba1+ cells compared to the naïve group. (D) There was no difference between the number of Iba1+ cells in the dentate gyrus of the hippocampus. Statistical significance was determined using one-way ANOVA and post-hoc Bonferroni test. Mean  $\pm$  S.E.M. Naïve,  $n=5$ ; aged WT + CCI,  $n=5$ ; aged *Fat-1* + CCI,  $n=4$ .

### 5.4.3 The effect of CCI on the brain lipid profile in young adult fat-1 females

Using thin layer chromatography followed by gas chromatography (section 2.1.8), the fatty acid profile of the brain tissue from young adult female *fat-1* mice and their wild-type littermates was analysed following CCI injury. A naïve group of age- and strain-matched mice were included as the control group. The changes in two selected omega-6 fatty acids (LA and AA) and two omega-3 fatty acids (DPA and DHA) were expressed as a percentage of the total fatty acids in tissue. We considered separately the effect of the diet, of the sham injury (craniotomy) and of the CCI. Figure 5.18 shows a representative chromatogram, annotated for the various fatty acids detected.

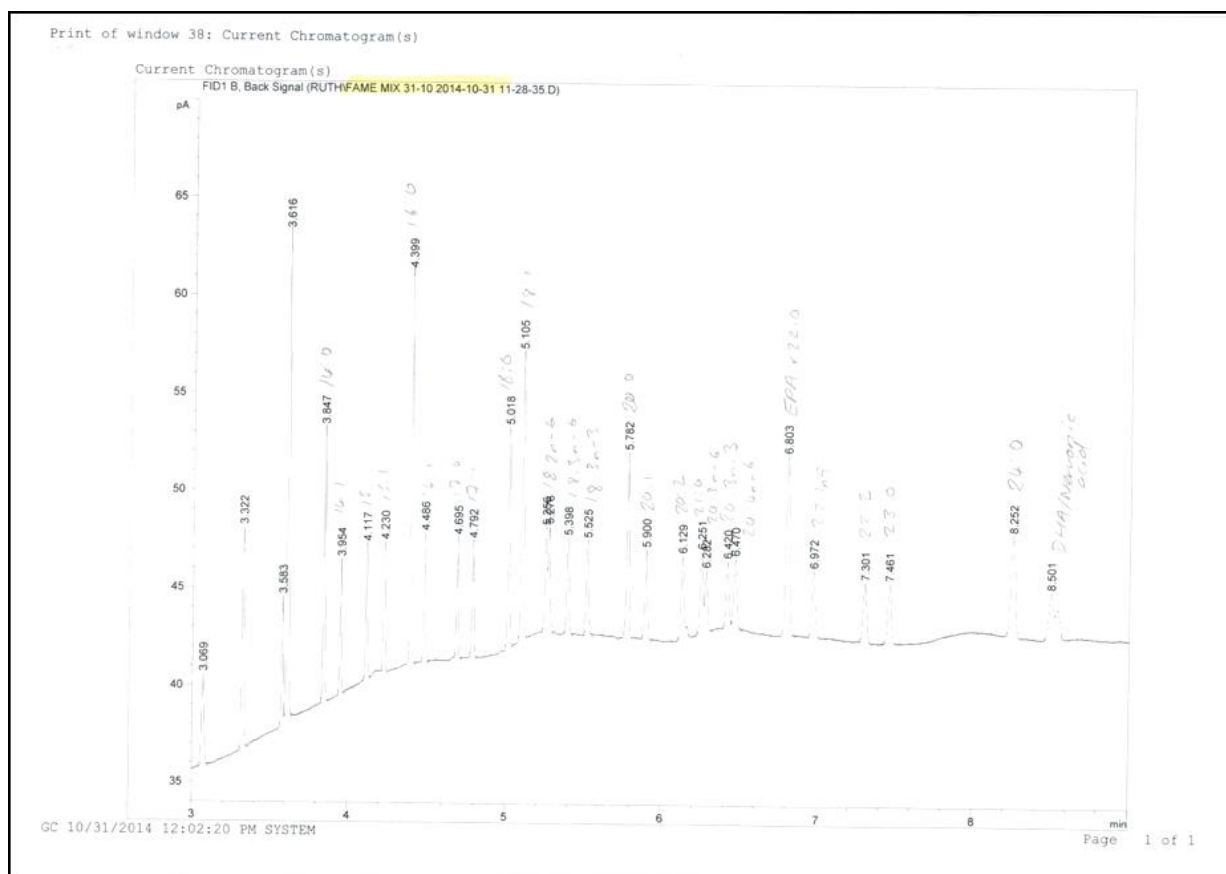
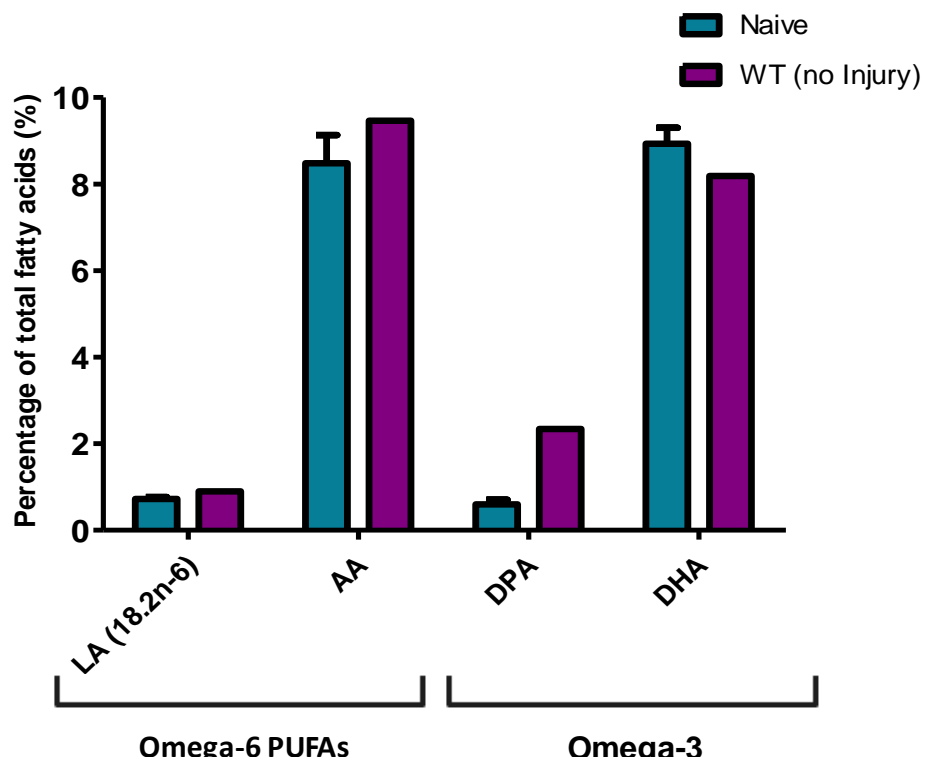


Figure 5.18 Representative gas chromatogram.

#### 5.4.3.1 Effect of the omega-6 enriched diet on the brain lipid profile

The effect of a high omega-6 diet on the lipid composition of the brain was analysed. A group of age matched C57BL/6 females was compared to WT females fed on the high omega-6 PUFA diet (Fig. 5.19). The percentage of omega-6 free fatty acids in the brains of these mice were very similar; both groups had less than 1 % LA and both had between 8 – 9 % of AA in their tissue. It may appear that the percentage of AA was higher in the WT group; however, due to an early death of a female WT mouse, there are only 2 females in this test group and therefore the N number was not high enough to apply statistical analysis.

In the omega-3 fatty acid analysis, a higher percentage of DPA and a lower percentage of DHA was observed in the WT diet fed group when compared to the naïve group fed on a normal murine chow. However, due to the low number of animals in the WT group, statistical analysis was not performed.



**Figure 5.19. The effect a high omega-6 PUFA diet has on the lipid profile of the brain tissue.** The fatty acids from naïve and WT mice, fed on a control or a high omega-6 PUFA diet, respectively, were compared. The omega-6 PUFAs LA (18:2n-6) and AA, and the omega-3 PUFAs DPA and DHA, were expressed as percentage of total fatty acids. Mean  $\pm$  SEM. Naïve, n=3; WT (no injury), n=2.

#### 5.4.3.2 Effect of the *fat-1* gene on brain lipid profile

In this section, we present the data obtained from the two groups of animals fed on the omega-6 rich diet. Since the *fat-1* group expressed the *fat-1* gene, these mice will convert exogenous omega-6 PUFAs into omega-3 PUFAs, resulting in a higher level of endogenous omega-3 PUFAs in their tissues.

The WT and *fat-1* groups both expressed similar levels of the omega-6 PUFAs LA and AA (Fig. 5.20). However, there did appear to be differences in the percentage of the omega-3 PUFAs, DPA and DHA, between the WT and *fat-1* groups. The WT mice had higher levels of the omega-3 fatty acid DPA (2 %) compared to the mice expressing the *fat-1* gene (< 1 % of total brain fatty acids). In contrast, the omega-3 fatty acid DHA was found at higher concentrations in the *fat-1* mice (12%), compared to the WT mice (8%).

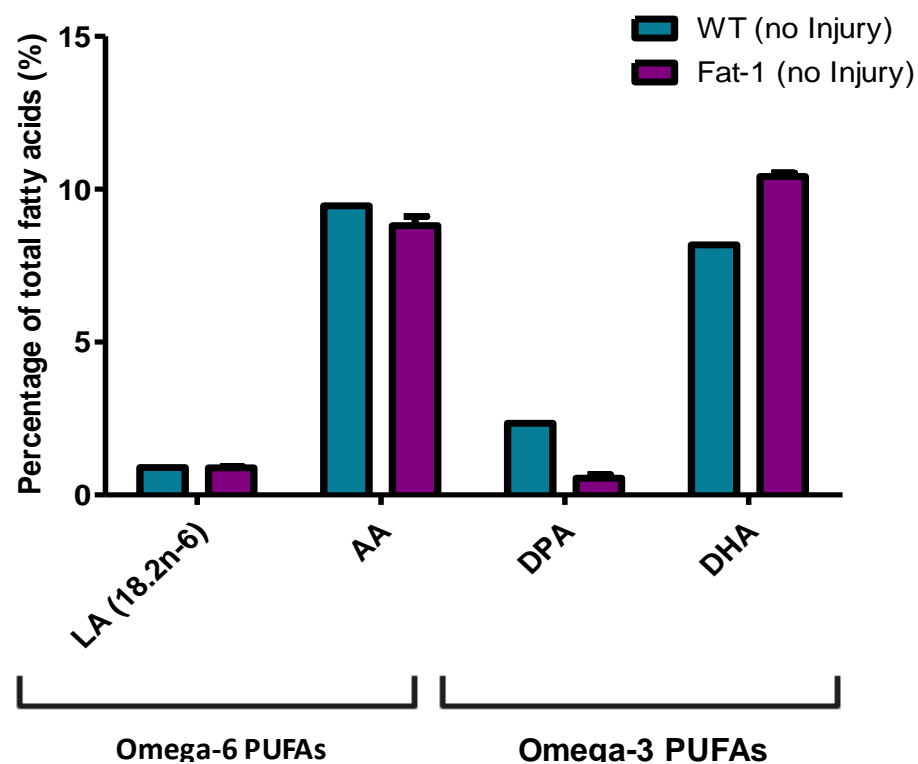


**Figure 5.20.** The effect of the *fat-1* gene has on the lipid profile of the brain tissue. The fatty acids from WT mice and *Fat-1* mice, fed on the same high omega-6 PUFA diet, were compared. The omega-6 PUFAs LA (18:2n-6) and AA, and the omega-3 PUFAs DPA and DHA, were expressed as percentage of total fatty acids. Mean  $\pm$  SEM. *Fat-1* (no injury), n=3; WT (no injury), n=2.

#### **5.4.3.3 Effect of the fat-1 gene on the lipid profile in the brain following a sham injury**

To determine if the CCI injury had any effect on the fatty acid composition of the brain, brain tissue from animals with a sham injury (craniotomy) was analysed (Fig. 5.21).

The sham injured mice showed no difference in the amount of the omega-6 fatty acid LA in comparison to the naive group, regardless of whether they expressed the *fat-1* gene. However, some differences were observed in the percentage of the omega-6 fatty acid AA. In the sham injured mice, there was a decrease in the percentage of AA in both the *fat-1* + sham group and the WT + sham group, when compared to the uninjured groups, but no statistical difference was observed.

There were some other differences noted between the percentage brain composition of the omega-3 fatty acids. The WT + no injury group had the highest percentage of DPA among all the 4 groups, at 2%. No statistically significant difference in the percentage of DHA, between the groups was observed. Interestingly, the *fat-1* + no injury group had the highest percentage of DHA; it was statistically higher than the *fat-1* with a sham injury (*fat-1* + no injury vs. WT + sham, \*\* $p < 0.01$ ; *fat-1* + no injury vs. *fat-1* + sham, \* $p < 0.05$ ). Thus, the sham injury appears to have caused a reduction in the amount of the omega-3 PUFA DHA in the brain tissue.

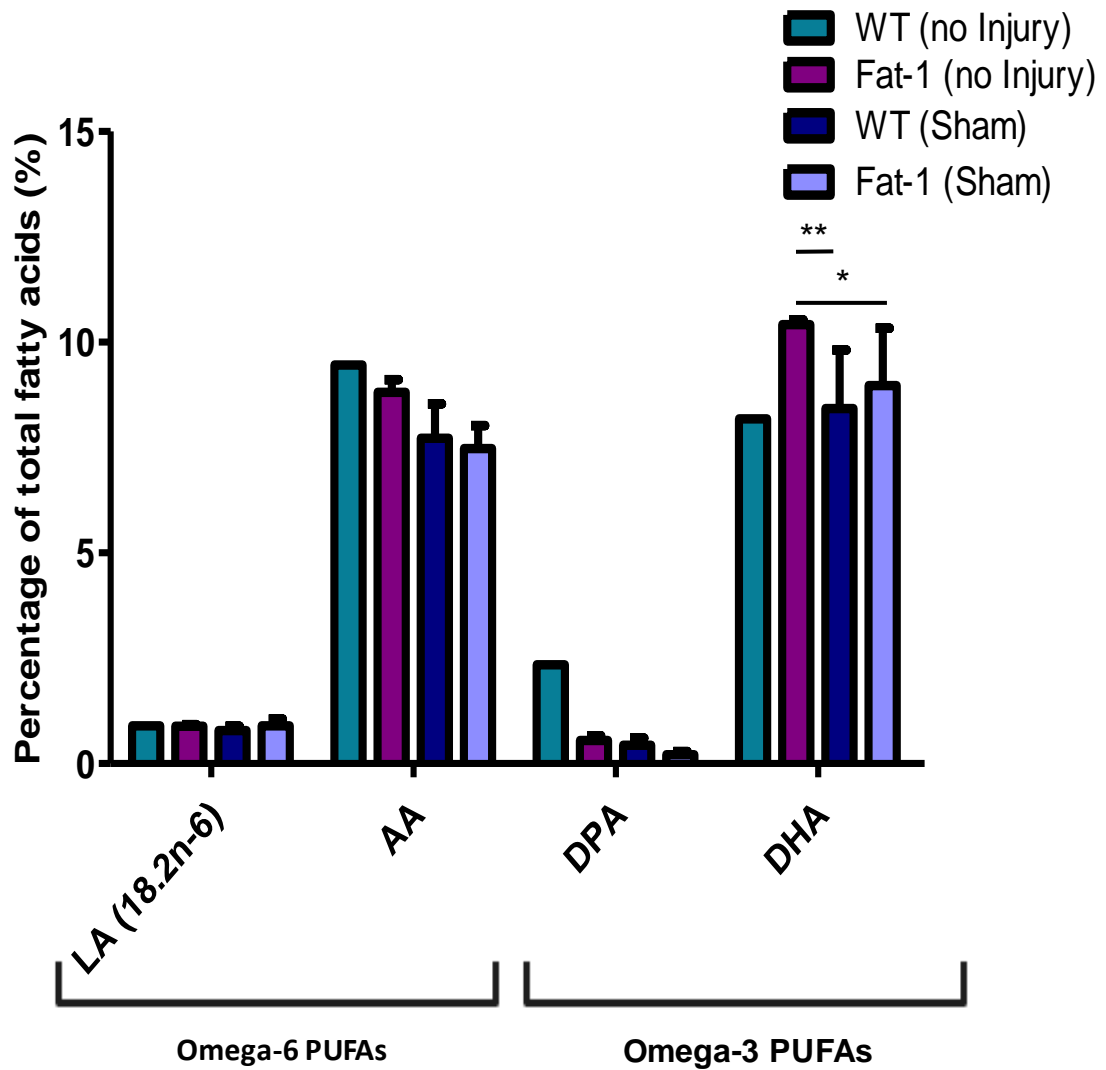


**Figure 5.21 The effect the sham injury has on the lipid profile of the brain tissue.** The fatty acids from WT mice and *Fat-1* mice, fed on the same high omega-6 PUFA diet, and with or without a sham injury, were compared. The omega-6 PUFAs LA (18:2n-6) and AA, and the omega-3 PUFAs DPA and DHA, were expressed as percentage of total fatty acids. The percentage of the omega-3 PUFA DHA was statistically significantly different between groups. The *fat-1* with no injury group had an increased percentage of DHA compared to *fat-1* with sham group (\* $p < 0.05$ ) and the WT with sham group (\*\* $p < 0.01$ ). The *fat-1* with sham group had an increased percentage of DHA compared to the WT with sham group (\* $p < 0.05$ ). Statistical analysis was performed using a two-way ANOVA with post-hoc Bonferroni tests. Mean  $\pm$  SEM. WT (no injury),  $n=2$ ; *Fat-1* (no injury),  $n=3$ ; WT (Sham),  $n=3$ ; *Fat-1* (Sham),  $n=3$ .



#### **5.4.3.4 Effect of the *fat-1* gene had on the lipid profile in the brain following a CCI injury**

To assess the effect of the CCI injury on the fatty acid composition, tissue was collected and analysed from WT + CCI and *fat-1* + CCI mice 24 hours after injury, and analysed alongside sham injured brain tissue.

The percentage of the omega-6 fatty acid AA increased in mice that received a CCI injury whether or not the *fat-1* gene was present, although this was not statistically significant.

From the omega-3 fatty acids analysed, the percentage of DHA was increased in the CCI groups when compared to the WT + sham group. Of the total fatty acids in the brain tissue, the WT + CCI had  $12.1 \pm 0.5\%$  DHA, which was significantly ( $**p < 0.01$ ) more than in the WT + sham group, which had  $8.4 \pm 1.4\%$ . The *fat-1* + CCI ( $12.6 \pm 0.7\%$ ) group also had a significantly higher ( $***p < 0.001$ ) percentage of DHA than the WT + sham group. Despite not showing any statistical significance, both CCI injured groups had an increased percentage of DHA than the *fat-1* + sham group. The CCI injury appeared to increase the percentage of DHA ( $>3\%$ ), compared to a sham injury. The WT + CCI group and the *fat-1* + CCI group have the highest total percentage of DHA among all the groups tested in this chapter.

The lipid analysis of the brain tissue suggests that there is an increased amount of DHA in the *fat-1* mice, that the sham injury causes a reduction in the percentage of DHA and that a CCI injury increases the percentage of DHA.

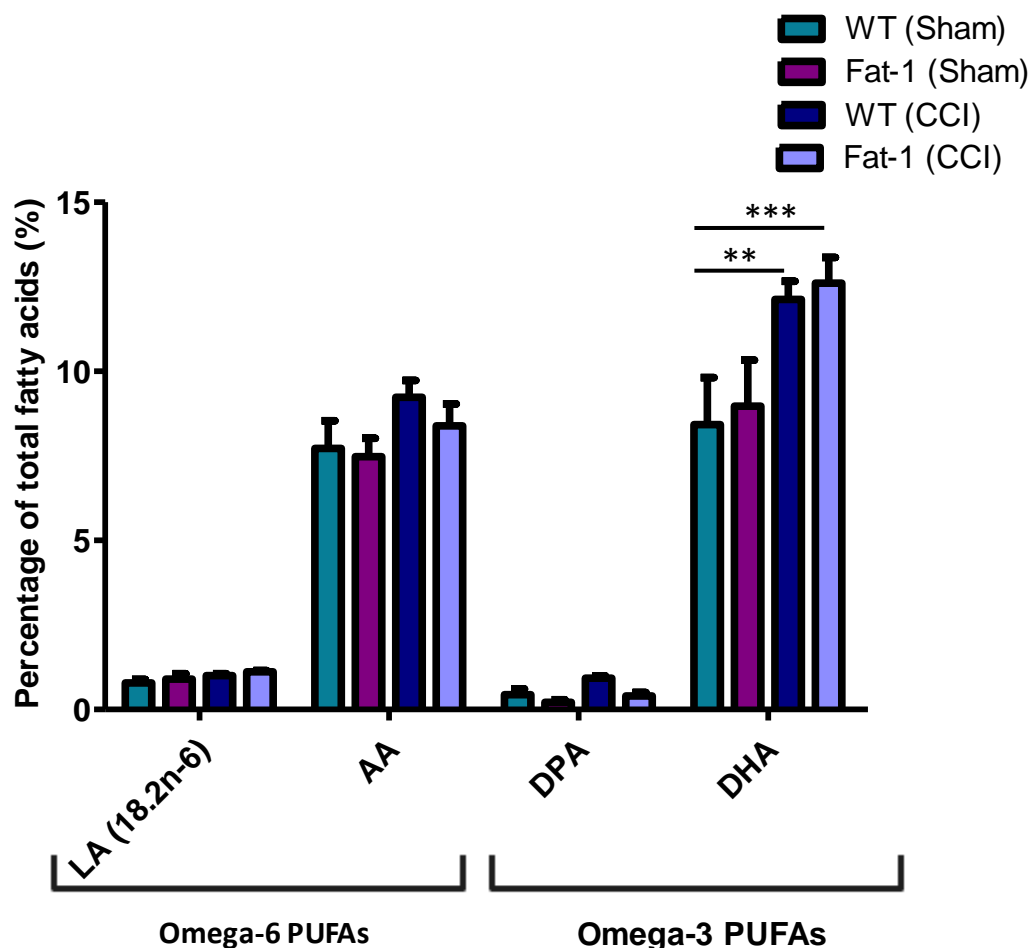


**Figure 5.22. The effect the CCI injury has on the lipid profile of the brain tissue.** The brain lipids from wild type mice with Sham injury, wild type mice with CCI injury, *fat-1* mice with Sham injury and *fat-1* mice with CCI injury, were compared. The percentage of the omega-3 PUFA DHA was statistically significantly different between groups. The *fat-1* CCI injury group had an increased percentage of DHA compared to the WT sham injury group (\*\* $p < 0.001$ ). The WT CCI injury group also had an increased percentage of DHA compared to the WT sham group (\*\* $p < 0.01$ ). Statistical analysis was performed using a two-way ANOVA with post-hoc Bonferroni tests. Mean  $\pm$  SEM. WT (Sham),  $n=3$ ; *fat-1* (Sham),  $n=3$ ; WT (CCI),  $n=3$ ; *fat-1* (CCI),  $n=5$ .

## 5.5 Discussion

The studies in this chapter investigated whether high endogenous levels of omega-3 fatty acids due to the presence of the *fat-1* gene and consumption of an omega-6 enriched diet, conferred neuroprotection in mice following CCI injury, in comparison to the impact of injury in wild-type littermates with high endogenous levels of omega-6 fatty acids. Furthermore, this aspect of response to CCI was investigated in both young and aged *fat-1* transgenic male mice. The measure used to assess cognitive outcome was the MWM test, which was performed using a one-week protocol (Fig. 5.1). To assess the effect of the *fat-1* gene on the brain following CCI, the amount of gross tissue loss, reactive astrogliosis and activated microglia were measured. Furthermore, in a pilot study focused on the acute changes in the brain fatty acid composition 24 h post-injury, we investigated the impact of the *fat-1* gene and of the CCI on the lipid composition of the brain tissue.

### 5.5.1 The fat-1 gene did not improve cognitive function following a CCI injury

Recent experimental and clinical studies have shown that omega-3 PUFA supplementation is correlated with improved cognitive outcome (Janssen et al., 2015, Abdel-Wahab et al., 2015, Bauer et al., 2014). The group that created the *fat-1* transgenic mice have also tested them in the MWM, where the adult *fat-1* mice exhibited improved acquisition when compared to the WT control mice (He et al., 2009). However, the study that He and colleagues reported used a protocol that included a five-day acquisition training phase, which was one day longer than in our study, and the improvement observed in their study was only seen on the final day of the acquisition training, therefore rather limited. Therefore, it may be suggested that we might have missed any significant improvement due to a shorter acquisition phase protocol. Interestingly, the Kang group also performed a probe trial following the acquisition training, and failed to see any difference between the *fat-1* and WT groups, as was also observed in our study. Another study by Wu and colleagues also showed that the presence of the *fat-1* gene failed to improve performance in the MWM probe trial (He et al., 2009, Wu et al., 2016a). The data we show in this chapter suggest that the presence of the *fat-1* gene does not lead to

a robustly improved performance in the MWM, either in the acquisition training or the probe trial, following a CCI injury, which is in accordance with the data reported in uninjured *fat-1* mice.

In the young adult male mice of both CCI-injured groups, animals were able to reduce their escape latency over the acquisition training, although as expected, not as quickly as the naïve group. This reduction in escape latency over the acquisition trial regardless of the moderate CCI injury, has been observed in both of the previous chapters. In the young male mice, the *fat-1* gene did not improve their performance in the acquisition training phase or the probe trial when compared to their WT littermates with CCI injury. However, we noted that in the probe trial, when the number of entries in the platform zone was considered, young adult *fat-1* mice appeared to perform after CCI at the level of the naïve mice – albeit with lack of statistical significance for this difference.

Aging has been linked to a decline in cognitive function, such as impaired memory, in both humans and animals (Harada et al., 2013, Rosenzweig and Barnes, 2003). Various diets and dietary supplements have been investigated and suggested to have an impact upon cognitive ability in the elderly (Allen et al., 2013, Oleson et al., 2016, Singh et al., 2011, Pan et al., 2010), in particular supplementation with omega-3 PUFAs preparations (Kiso, 2011, Strike et al., 2016, Pusceddu et al., 2016). However, in a study in aged mice that were fed on an omega-3 rich diet, the authors failed to demonstrate any increased cognitive ability in the MWM test, but reported some improvement in the spatial Y-maze cognitive test, when compared to age matched controls (Cutuli et al., 2014). In our study, aged mice that expressed the *fat-1* gene failed to show an improved behavioural performance following the CCI in the MWM. The aged naïve group did demonstrate some learning ability by reducing their average escape latency over the acquisition training days. However, unlike the young males that received the CCI injury, the aged CCI injured males failed to demonstrate any learning capability over the acquisition training phase. This data supports the literature that documents a worse outcome after TBI in aged patients (Rozenbeek et al., 2013, Thompson et al., 2006).

### **5.5.2 The fat-1 gene did not prevent gross tissue loss**

The presence of the *fat-1* gene failed to reduce the brain tissue loss in the ipsilateral hemisphere, cortex or hippocampus following CCI injury, whether the mice were young or aged. Interestingly, the aged animals did not show any more tissue loss than the young CCI injured mice, although the literature would suggest that aged mice would suffer a larger lesion size following TBI (Kumar et al., 2013).

### **5.5.3 The fat-1 gene did not change the microglial/macrophage activation**

The presence of the *fat-1* gene did not change the amount of activated microglial/macrophage cells in the brain tissue detected several weeks following CCI injury. The CCI injury caused an increase in the number of activated microglia/macrophage cells, as was observed in the brain tissue of the CCI injured mice in the previous chapters. In the aged mice there was an increase in activated microglia/macrophages in both the ipsilateral and contralateral cortices, as well as in the contralateral hippocampus. In a recent study by Kumar and colleagues, aged mice were more likely to have activated microglia of the detrimental 'M1-like' phenotype following a CCI injury when compared to young mice (Kumar et al., 2013). They suggested that the increased 'M1-like' microglia created an increased inflammatory response and contributed to a poorer outcome (Kumar et al., 2013). Reduction in the activated 'M1-like' microglia in mice has been shown to correlate with an improved performance following CCI injury in the MWM (Bedi et al., 2013). In our aged mice, the activated microglia in the CCI brain tissue may have had a higher proportion of the 'M1-like' phenotype compared to the 'M2-like' phenotype – this remains to be analysed further, with specific markers (e.g. arginase 1 or CD11b) (Cherry et al., 2014, Loane and Byrnes, 2010). This would make the detrimental, pro-inflammatory 'M1-like' microglia the predominant phenotype in the brain and may have contributed to the poor outcome our aged mice had in the MWM test. Recent literature suggests that categorising the microglia phenotypes may be more complex than just the 'M1-like' and 'M2-like' phenotypes (Loane and Kumar, 2016). Future studies could establish the predominant microglial phenotype in the aged mice at different stages following CCI, in the wild-type and also transgenic mice.

#### **5.5.4 The fat-1 gene causes increased reactive astrogliosis following CCI injury**

In the previous chapter, an acute injection of the omega-3 fatty acid DHA correlated with an increase in the amount of reactive astrogliosis in the brains of mice 28 days after TBI, despite not exhibiting any beneficial (or detrimental) effect on the behaviour of the mice in the MWM task. In this chapter, we show that the mice expressing the *fat-1* gene also exhibited an increase in reactive astrogliosis in selective brain regions, but with no correlation in cognition when compared to the wild-type littermates.

This increase in reactive astrogliosis was seen predominantly in the aged mice, but was also observed in the young male mice (only in the ipsilateral ROI). This data is in total contrast with previous studies that show that omega-3 PUFAs reduce astrogliosis and neuroinflammation, including studies in our group and others that have shown a reduction in astrogliosis following SCI, with acute DHA treatment (Zendedel et al., 2015, Paterniti et al., 2014).

The aged *fat-1* mice had increased reactive astrogliosis in both the ipsilateral and contralateral cortex, and in the contralateral hippocampus. Increased neuroinflammation, including increased reactive astrogliosis, has been associated with the aging brain particularly in the hippocampal region which correlates with decreased cognitive function (Lynch et al., 2010, Cowley et al., 2012). This increase in reactive astrogliosis in the hippocampus has also been seen in rats following a CCI injury (Sandhir et al., 2008). The age-related increase in astrogliosis in these *fat-1* aged mice appears to be exacerbated by the CCI injury and the presence of the *fat-1* gene.

A direct link between omega-3 administration, either via an acute injection of DHA (chapter 4) or increased endogenous levels of omega-3 PUFAs as caused by the presence of the *fat-1* gene following CCI, and the increased reactive astrogliosis has yet to be analysed in detail and this is the primary aim of the following chapter.

### 5.5.5 CCI injury altered the lipid profile of the brain tissue

To characterise the changes in lipids after TBI and in the presence of the *fat-1* gene, we investigated in a pilot study the brain lipid profiles of the *fat-1* mice and their wild-type littermates in response to CCI injury. The analysis explored changes following sham injury and CCI injury, at an acute time point, i.e. 24 hours post-injury.

Although we had samples from a limited number of animals, and overall the analysis was underpowered, we noted a few trends. The percentage of the omega-3 fatty acid DHA appeared to have changed the most with genotype and CCI injury. The wild-type mice fed an omega-6 enriched diet, in the absence of the *fat-1* gene could not convert this excess omega-6 PUFAs endogenously into omega-3 PUFAs, resulting in a lower percentage of DHA when compared to naïve controls. The *fat-1* mice, as expected, had a higher percentage of DHA in their brain lipid profile compared to their wild-type littermates (Bousquet et al., 2011, Wu et al., 2016a)..

Interestingly, in the sham animals, the fatty acid profile of the *fat-1* mice also changed, and a decrease in the percentage of DHA was observed. However, following a CCI injury the *fat-1* mice had an increase in the percentage of DHA measured in tissue. Our data supports observations in the experimental and clinical literature, whereby TBI has been shown to decrease the amount of phospholipids containing DHA around the injury site and induce an increase in the amount of DHA as a free fatty acid in cerebrospinal fluid (CSF) (Roux et al., 2016, Pilitsis et al., 2003a). In a study employing mass spectrometry in the brain of CCI injured rats, there were early changes (24 hours after injury, i.e. the same analysis time we present here) in various lipid classes, including the membrane phospholipids, and notably there was a significant reduction in the phospholipid phosphatidylethanolamine (PE) containing DHA (Roux et al., 2016). This reduction is a likely consequence of the activation of phospholipases after injury, such as phospholipase C (Wei et al, 1982, Dhillon et al, 1999). The activation is extremely rapid, with positive detection at 5 min after injury. This activation of lipases and in particular phospholipases, following excessive stimulation in the CNS, was described initially by Bazan (1970), and has come to be known as the “Bazan effect” –it reflects the very rapid deterioration of the structure of membranes following injury. In a clinical study on TBI patients, a five-fold increase

in the amount of DHA detected as a free fatty acid in their CSF when compared to control patients, was reported (Pilitsis et al., 2003a). This study also reported an increase in the amount of AA measured as a free fatty acid in the CSF, which although not significant was also increased in our mice following CCI injury, irrespectively of WT or *fat-1* background. Furthermore, the studies by Pilitsis and collaborators correlated moderately favourable GOS scores (>3) with significantly lower levels of free fatty acids in the CSF (Pilitsis et al., 2003a, Pilitsis et al., 2003b). This data suggests that free fatty acids would be a useful indicator of TBI severity. Lower levels of PE were also reported 3 months post-injury in mouse CCI, in brain tissue and plasma (Abdullah et al, 2014). A very recent study in a closed head model of TBI supports these findings and shows that abnormalities in lipids (i.e. decrease in plasma phospholipids) are long-lasting and can still be detected 3 months after injury (Emmerich et al, 2016). In our studies, the CCI injury may cause such large destruction of the brain parenchyma and complex changes in the fatty acid and phospholipid dynamics, that any neuroprotection conferred by the presence of the *fat-1* gene and the increased omega-3 PUFAs incorporated into the phospholipid membranes, may be insufficient.

### **5.5.6 Conclusion**

The data produced in this chapter suggests that the *fat-1* gene does not confer neuroprotection following a CCI injury. However, the *fat-1* gene did appear to cause an increase in reactive astrogliosis particularly in the aged mice. As expected, the aged mice fared worse in the MWM protocol than the young males. The *fat-1* mice were shown to have an increased amount of DHA in their brain tissue compared to their wild-type littermates, as expected. The CCI injury elicited a further increase in the DHA detected in the tissue, early after injury.

The lack of efficacy of the *fat-1* genetic manipulation in providing tissue protection after TBI or in improving neurological outcome is markedly different from what we previously reported after SCI or PNI, and different from observations reported in stroke models (Hu et al, 2013), but reminiscent of the negative results reported in a mouse model of Parkinson's disease (Bousquet et al., 2011). In this study, using adult mice treated with the toxin methyl-phenyl-tetra-hydropyridine (MPTP), although the *fat-1* manipulation induced an increase in the tissue omega-3: omega-6 ratio (around 28%), this was



not sufficient to confer any neuroprotection. This is in contrast with what the authors had previously reported in the same disease model, using chronic oral supplementation with omega-3 PUFA (starting before the injury, from 2 to 12 months of age, after which the MPTP exposure occurred) (Bousquet et al, 2008). In the latter study, this supplementation regime led to a much larger increase in the omega-3: omega-6 ratio (92%) and the authors reported neuroprotection in terms of higher dopamine levels detected after injury, although no data were provided to show whether this was correlated with any beneficial neurological outcome. However, it is tempting to conclude that certain forms of injury in the CNS may require much larger increases in the omega-3 fatty acid levels than those provided by the *fat-1* background, in order to confer neuroprotection. This hypothesis remains to be tested by carrying out future DHA chronic supplementation studies in our CCI model.

The observations reported in this chapter and the previous chapter also suggest that there is a link between DHA and increased reactive astrogliosis following a CCI injury. The following chapter investigates the effect DHA has directly on astrocytes in a novel *in vitro* model of focal mechanical injury.

### **5.5.7 Main outcomes**

- CCI injury in aged mice leads to a worse outcome in the MWM
- The *fat-1* gene does not confer neuroprotection following CCI injury
- The *fat-1* gene leads to an increased astrogliosis following CCI injury
- CCI injury elicits changes in brain tissue DHA levels

## **6 A novel in vitro model of focal mechanical injury in a 3D astrocytic cell culture**

### **6.1 Introduction**

In this chapter we set-up and optimized an *in vitro* model of mechanical TBI. We decided to move to an *in vitro* model so that we could focus on the reactions of astrocytes alone following a mechanical lesion. In an *in vivo* model, it is hard to see if the lesion directly causes astrogliosis or whether injury to other cells (other glial cells, the BBB or neurones) causes the increase in GFAP expression following CCI injury. Also using an *in vitro* model allowed us to study the morphology of the astrocytes in detail.

#### **6.1.1 Glial cells**

Glial cells and neurones are the two largest cell populations within the brain and spinal cord. It was previously thought that for every neurone in the human brain there were 10-50 supporting glial cells. However, in 2009 this ratio was queried and, using a novel cell counting technique, the ratio of glial to neuronal cells in the human brain was found to be closer to 1:1, therefore representing a scaled-up primate brain (Azevedo et al., 2009).

Glial cells are responsible for many functions within the brain, which include maintaining homeostasis of the brain environment through neurotransmitter regulation and synapse support, providing myelin sheaths for neuronal signalling, and involvement in the immune response during disease.

There are several subtypes of glial cells in the CNS, namely astrocytes, microglia, oligodendrocytes, and ependymal cells. Microglia and astrocytes have already been mentioned in the previous chapters in this thesis, with astrocytes displaying a reactive phenotype after injury and an increased GFAP expression in the *fat-1* mice and mice treated with DHA. Due to this change which was linked to treatment with an omega-3 PUFA or a higher level of endogenous omega-3 PUFA, astrocytes are the cell type that was chosen for further investigation *in vitro*.

## 6.1.2 Astrocytes

### 6.1.2.1 Morphology

Astrocytes have been divided into two subgroups based on their morphology and location, since they were first described in the 1870s (Papura and Verkhratsky, 2012). These two subtypes are referred to as either protoplasmic or fibrous astrocytes (Kettenmann and Verkhratsky, 2011).

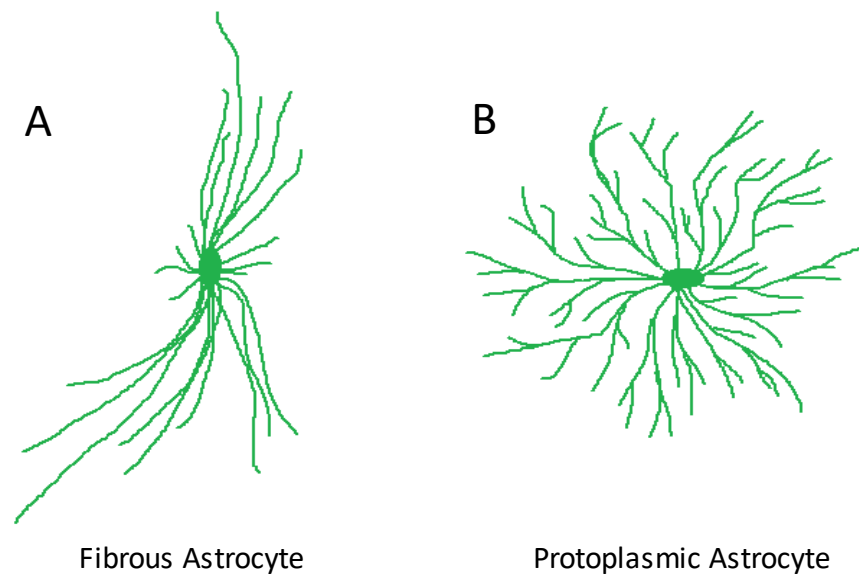


**Figure 6.1. Schematic representation of protoplasmic and fibrous astrocyte morphology.**

(A) Fibrous astrocytes found in the white matter have long bi-directional processes. (B) Protoplasmic astrocytes from the grey matter are highly ramified, with several branches and finer processes.

Protoplasmic astrocytes are found in the grey matter and have several thin processes, whereas fibrous astrocytes are located in the white matter and have fewer but much longer processes than the protoplasmic astrocytes. These two major subtypes are still valid today, and, in addition, there are several smaller populations of other astrocytic subtypes identified since the late 19<sup>th</sup> century. These are summarised in table 6.1 below:

**Table 6.1. Subtypes of astrocytes based on their location, morphology and structural characteristics.** (Kettenmann and Verkhratsky, 2011, Şovrea and Boşca, 2013, Sofroniew and Vinters, 2010).

Subtype	Location	Morphology	Structural components
Protoplasmic astrocytes	Grey matter	High numbers of complex processes	-Perivascular endfeet -Subpial endfeet
Fibrous astrocytes	White matter – Orientated longitudinally alongside nerves	Long, thin and straight processes	-Perivascular endfeet -Subpial endfeet -Perinodal endfeet
Radial glia	Embryonic brain (differentiated into Müller cells and Bergmann glia)	Bipolar – ovoid cell body with two main processes	-One process forms periventricular endfoot -One process forms subpial endfoot
Müller cells	Retina – In the sixth layer	Elongated cells with long processes that extend along the rod and cone cells	-Form limiting membranes that act as barriers
Bergmann glia	Cerebellum – Purkinje cell and granular layers	Small bodies with 3–6 long processes, that extend towards the molecular layer of the cerebellar cortex	-Perivascular endfeet -Subpial endfeet
Interlaminar astrocytes	Cerebral cortex – Layer I, adjacent to the pial surface (in higher Primates)	Spherical body with one long process (up to 1mm)	-Subpial endfeet
Pituicytes	Posterior pituitary gland	Irregular shapes with many cytoplasmic processes	-Surround neuro-secretory axons

These subtypes of astrocytes can be identified based on their location, morphology and structural characteristics. The endfeet of astrocytes are specialized foot-processes that make contact with other structures in the brain or ensheath distinct neuronal elements, in order to mediate exchange of molecules and neurotransmitters (Parpura and Verkhratsky, 2012). Astrocytic endfeet make contact with the brain vasculature (perivascular endfeet), the pia mater of the brain (subpial endfeet), the ventricles of the brain (periventricular endfeet) and the nodes of Ranvier of axons (perinodal endfeet).

### **6.1.2.2 Molecular markers**

The most frequently used immunohistological marker for astrocytes is glial fibrillary acidic protein (GFAP). This protein is an intermediate filament that is present in the cytoskeleton of astrocytes. A recent study published by a group in the Netherlands has identified 10 isoforms of the GFAP protein, that are expressed differentially in different brain regions and impose different properties onto the intermediate filament network (Kamphuis et al., 2014). The expression of this protein is increased by astrocytes in diseased tissue and is often not present at detectable levels in healthy tissue. Astrocytes that display an increased GFAP expression are referred to as 'reactive astrocytes' or as undergoing 'reactive astrogliosis'.

Despite GFAP being the 'gold standard' immunohistochemical marker for astrocytes, GFAP staining has its limitations. As mentioned above, GFAP is often not expressed at detectable levels by astrocytes unless they have become 'reactive' in response to disease or injury (Sofroniew and Vinters, 2010). Furthermore, GFAP does not label all of the astrocyte, as it is not present consistently throughout the astrocytic cytoplasm and is often not detectable in the cell body. This means that only the thicker branches and not the finer processes of the astrocyte are labelled with the GFAP marker. Therefore, GFAP labelling may only represent a small amount of the branching, and this can greatly underestimate the total astrocytic processes and cell volume (Sofroniew and Vinters, 2010). In addition, GFAP is not exclusively expressed by CNS astrocytes; it is also expressed in the brain by ependymal cells from the subventricular zone (SVZ) (Wang and Bordey, 2008). There are several peripheral cells that also express GFAP, including keratinocytes, Leydig cells, osteocytes and chondrocytes and cells within the pancreas and liver (Wang and Bordey, 2008).

There are other immunohistochemical markers that have been used to identify astrocytes, which include vimentin, S100B, GLT-1, human EAAT2, glutamine synthase, the potassium Kir4.1 channel and the aquaporin 4 channel. These markers are summarised in the table below.

**Table 6.2. Molecular markers for the identification of astrocytes and astrocytic subtypes.**

The specificity of the molecular marker, the location of the molecular target and the limitations that targeting these markers pose for the identification of astrocytes (Şovrea and Boşca, 2013, Nagelhus et al., 2004, Kalsi et al., 2004, Yang et al., 2011, Benner et al., 2013).

<b>Astrocytic Marker</b>	<b>Specificity</b>	<b>Location within Astrocytes</b>	<b>Limitations</b>
GFAP – Glial fibrillary acidic protein	Intermediate filament, part of the cytoskeleton	Standard marker for astrocytes – Up-regulated in response to CNS injury	Also present in ependymal cells of the CNS
Vimentin	Intermediate filament, part of the cytoskeleton	Up-regulated in response to CNS injury	Also present in ependymal cells
S100B	Calcium binding protein	Present on the cell membrane	Expressed by mature astrocytes and NG2-expressing astrocytes
Aquaporin 4	Water-selective channels	Present on the astrocyte cell membrane at the endfeet of astrocytic processes – Up-regulated in response to CNS injury	Also present in ependymal cells and endothelial cells
Kir4.1	Inwardly rectifying K <sup>+</sup> channels	Present on the perivascular endfeet of astrocytes	Also present on the cell bodies of oligodendrocytes
GLT-1 and GLAST (rats) or EAAT1 and EAAT2 (humans)	Glutamate transporters	Distributed along the cell membrane	Other isoforms are present in neurons
Glutamine synthase	Enzyme that catalyses the conversion of glutamate and ammonia to glutamine	Present in the cytoplasm of astrocytes	Also expressed by oligodendrocytes
Aldehyde dehydrogenase 1 family, member 1 (AldhL1)	Enzyme that catalyses the oxygenation of aldehydes	Present in the branches rather than cell body	Low expression levels in mature spinal cord
Thrombospondin 4	Thrombospondin family of glycoproteins	Present in astrocytes generated in the SVZ	Low expression levels

Transgenic mice that express a fluorescent reporter protein under promoters of astrocytic markers such as GFAP or GLT-1 can also be a useful tool to identify astrocytes *in vivo* (Nolte et al., 2001, de Vivo et al., 2010). They can be used to identify astrocytes using fluorescence microscopy within living brain slices and fixed tissue preparations. As an investigative tool, these mice can be extremely valuable; however, it is important to confirm the staining with additional immunolabelling with another astrocyte marker (Wang and Bordey, 2008).

### 6.1.3 The physiological roles of astrocytes

Astrocytes have many functions which contribute to general homeostatic mechanisms in the CNS. They play key roles within the blood-brain barrier (BBB), the maintenance of the extracellular environment, synapse formation and function, metabolic support and the regulation of blood flow.

#### 6.1.3.1 Blood-brain barrier and blood flow

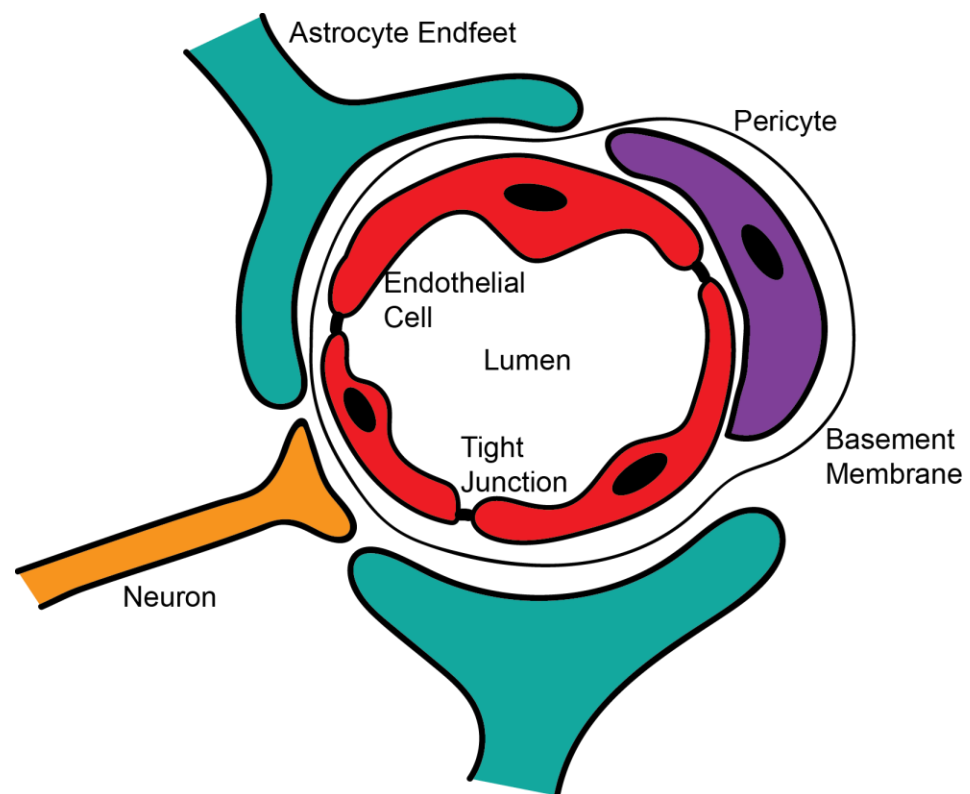


**Figure 6.2. Schematic of the blood brain-barrier (BBB).** Detailing the microvasculature of the BBB, including the basement membrane, endothelial cells, pericytes, astrocyte endfeet and neurons.

The blood-brain barrier (BBB) refers to the specialized structure of the brain's microvasculature, which comprises endothelial cells, basement membrane, pericytes and astrocyte endfeet (Fig. 6.2) (Zlokovic,

2008). The function of the BBB is to help maintain the brain microenvironment by preventing potentially harmful substances from the blood entering the brain tissue. The endfeet of astrocytes can ensheath the brain microvasculature, make contact with the neuronal cell membrane or encapsulate the synaptic cleft. In this way, the astrocytes act as a bridge between the neurones and the vasculature. Astrocytes help mediate the permeability of the BBB as well as the vasodilation or vasoconstriction of the neurovasculature through the release of mediators such as prostaglandins (e.g. PGE<sub>2</sub>) and nitric oxide (Alvarez et al., 2013, Sofroniew and Vinters, 2010).

#### **6.1.3.2 K<sup>+</sup> homeostasis**

Astrocytes help maintain ion homeostasis in the extracellular space, particularly the K<sup>+</sup> concentration. Neurotransmission leads to K<sup>+</sup> ions building up in the extracellular space, which, if not rectified, can lead to depolarization and hyperexcitability of neurones (Wang and Bordey, 2008). Inwardly rectifying K<sup>+</sup> channels (Kir) and sodium potassium pumps (Na<sup>+</sup>/K<sup>+</sup> ATPases) on the astrocyte cell membrane help to buffer this increase in extracellular K<sup>+</sup> (Wang and Bordey, 2008). Mice with a conditional knock-out of the Kir4.1 channel show motor impairment, body tremor and an increased mortality rate (Neusch et al., 2001).

#### **6.1.3.3 Neurotransmitter uptake**

A key function that astrocytes are responsible for is the uptake of the excitatory neurotransmitter glutamate from the synaptic cleft. After neurotransmission glutamate needs to be cleared, as an excess can lead to excitotoxicity and trigger neuronal cell death. Astrocytes remove the extracellular glutamate through uptake via the excitatory amino acid transporters (EAAT). There are currently five types of EAAT identified in the human brain, and the EAAT1 and EAAT2 types are expressed by astrocytes (the rodent equivalents are GLAST and GLT-1, respectively) (Bak et al., 2006, Palacín et al., 1998). GLAST transporters are found in both astrocytes and oligodendrocytes, whereas GLT-1 are found in much higher levels in astrocytes as opposed to any other types of brain cells (Rothstein et al., 1994, Robinson and Jackson, 2016). The GLT-1 transporters are responsible for the bulk of the glutamate clearance in the brain and the deletion of these transporters results in seizures and



premature death (Tanaka et al., 1997). The deletion of the GLAST transporter causes minimal abnormalities in the motor coordination (Watase et al., 1998).

The glutamate accumulated by astrocytes is converted to glutamine by the enzyme glutamine synthase, and then transported back to the pre-synaptic terminal in a process known as the glutamate-glutamine shuttle (Bak et al., 2006). This uptake of glutamate by the astrocytes prevents excitotoxicity and improves synaptic transmission through the reduction of background noise (Wang and Bordey, 2008).

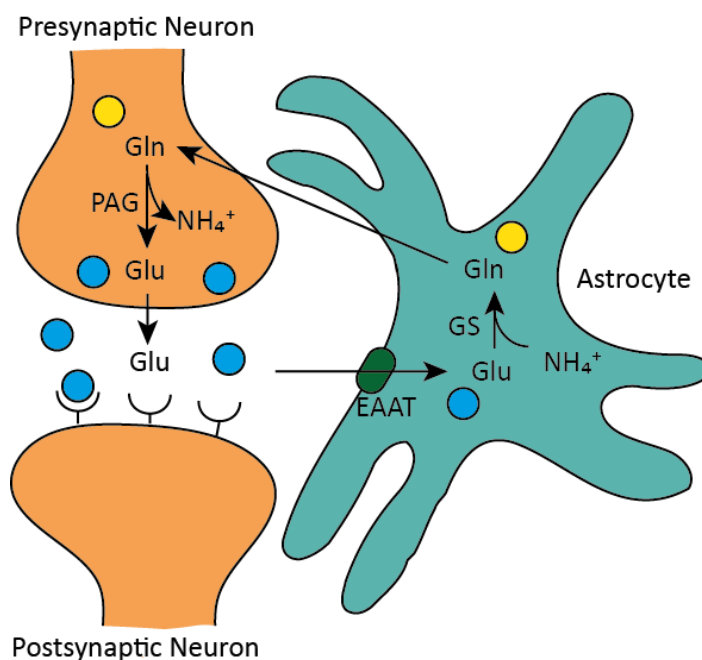


**Figure 6.3. Schematic representation of the glutamate-glutamine shuttle at a glutamatergic synapse.** Glutamate (Glu, blue filled circles) is released from the presynaptic terminal into the synaptic cleft. Glutamate diffuses across the cleft and binds to receptors of the postsynaptic membrane. Excess glutamate in the cleft is taken up by the astrocytes through the excitatory amino acid transporters (EAAT) and converted to glutamine (Gln) using free ammonia (NH<sub>4</sub><sup>+</sup>). This conversion is catalysed by the enzyme glutamine synthase (GS). The glutamine is then returned to the presynaptic neuron, where it is converted back to glutamate by phosphate-activated glutaminase (PAG), with the release of ammonia (NH<sub>4</sub><sup>+</sup>).

#### 6.1.3.4 Synaptic function

Astrocytes are involved in both the formation and maintenance of synapses. Around 60% of synapses are ensheathed by astrocytic processes (Bernardinelli et al., 2014). Astrocytes play an important role in synaptic transmission, and have been suggested to be as integral to the synapse as the pre- and post-

synaptic neuron terminals; this is referred to as the 'tripartite synapse' (Bernardinelli et al., 2014). As part of the 'tripartite synapse', astrocytes can regulate synaptic function, plasticity and transmission. Astrocytes can respond to the release of neurotransmitters from the neurones, and can, themselves, release 'gliotransmitters' into the synapse (Harada et al., 2015). Astrocytes exhibit several types of receptors including glutamatergic, GABAergic, adrenergic, purinergic, serotonergic, muscarinic and peptidergic receptors (Porter and McCarthy, 1997).

It has been shown that neuronal activity can evoke rises in intracellular calcium ( $\text{Ca}^{2+}$ ) within astrocytes and that these increases in intracellular calcium can propagate to adjacent astrocytes and even back to neurons (Parpura et al., 1994, Hamilton and Attwell, 2010, Charles et al., 1991, Cornell-Bell et al., 1990). The term 'gliotransmission' has been used to describe this phenomenon, whereby these astrocytes and neurones can communicate with each other. These  $\text{Ca}^{2+}$  waves can provoke the release of gliotransmitters, such as glutamate (Bernardinelli et al., 2014). The release of astrocytic glutamate can alter neuronal excitability (Hamilton and Attwell, 2010). Other gliotransmitters include several neuroactive molecules that can bind to receptors on neurones, including D-serine, adenosine, GABA and the cytokine tumour necrosis factor- $\alpha$  (TNF- $\alpha$ ) (Perea et al., 2009).

Astrocytes can promote synaptogenesis through the release of other factors such as cholesterol, which has been hypothesised to aid synaptogenesis by increasing the number of lipoproteins in neurones which are used to create synaptic vesicles (Mauch et al., 2001, Göritz et al., 2002). Astrocytes can also control neurotransmission by altering the density of post-synaptic receptors, including the up-regulation of AMPA receptors and down-regulation of GABA<sub>A</sub> receptors, through the release of TNF $\alpha$  (Stellwagen and Malenka, 2006, Kettenmann and Verkhratsky, 2011, Chung et al., 2015).

#### **6.1.3.5 Metabolic support**

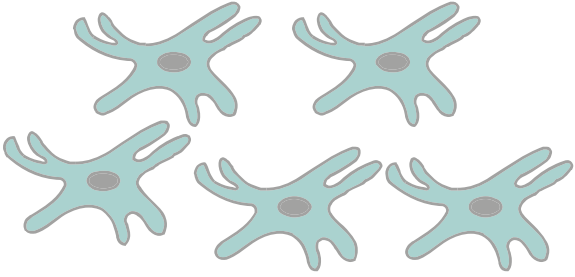
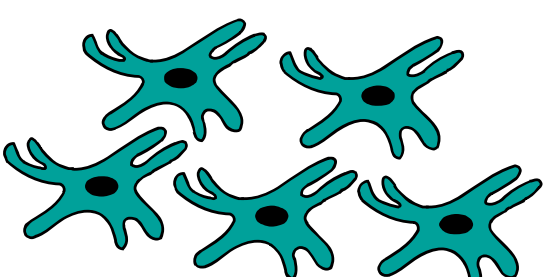
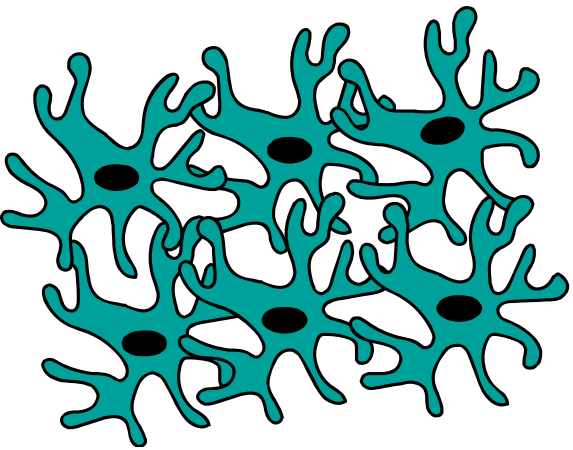
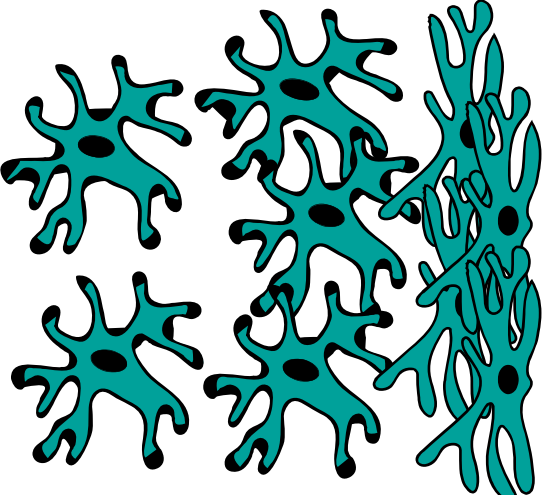
Astrocytes provide metabolic support to the neurones by acting as a glycogen store, which provides energy during periods of high neuronal activity or hypoglycemic conditions (Brown and Ransom, 2007). Astrocytes also provide neurones with the glutamate precursor glutamine, as neurones do not have the ability to synthesise glutamate. As previously mentioned, glutamate released into the synaptic

clef is uptaken into the astrocytes through EAAT1 and EAAT2 transporters and converted to glutamine via the glutamate-glutamine shuttle (Fig. 6.3). This glutamine is non-toxic and can be released back close to the pre-synaptic terminal. The pre-synaptic terminal can then convert this glutamine back into glutamate (Bak et al., 2006).

#### **6.1.4 Brain pathology**

##### **6.1.4.1 Reactive astrogliosis**

Under pathological conditions, astrocytes undergo a noticeable change in their morphology and a corresponding increase in the expression of the intermediate filament GFAP (Baldwin and Scheff, 1996). This astrocytic response is known as “reactive astrogliosis” (Sofroniew and Vinters, 2010). The main morphological changes include hypertrophy, increase in number, thickness and length of the cytoplasmic cell processes, overlapping of the processes and proliferation. The term ‘reactive gliosis’ (or astrogliosis) has been used as an umbrella term to describe any evidence of these changes seen in astrocytes. Recently however, Sofroniew and colleagues have suggested that there are categories or gradations of reactive astrogliosis, which are detailed below (Anderson et al., 2014).

	
<p>A) <u>Astrocytes under normal conditions</u></p> <ul style="list-style-type: none"> <li>• Low levels of GFAP expression</li> <li>• No overlapping</li> <li>• Little or no proliferation</li> </ul>	<p>B) Mild to moderate astrogliosis</p> <ul style="list-style-type: none"> <li>• Higher levels of GFAP expression</li> <li>• No overlapping</li> <li>• Little or no proliferation</li> </ul>
	
<p>C) <u>Severe diffuse reactive astrogliosis</u></p> <ul style="list-style-type: none"> <li>• High levels of GFAP expression</li> <li>• Overlapping of processes</li> <li>• Proliferation</li> <li>• Extension of processes</li> </ul>	<p>D) <u>Severe astrogliosis and the glial scar</u></p> <ul style="list-style-type: none"> <li>• High levels of GFAP expression</li> <li>• Substantial overlapping</li> <li>• Proliferation</li> <li>• Reorganisation of the tissue architecture – Formation of a compact glial scar surrounding an area of CNS tissue damage</li> </ul>

**Figure 6.4. Schematic representations of the gradations of reactive astrogliosis.**

(A) The characteristics of astrocytes under normal physiological conditions are the expression of low levels of GFAP and the maintenance of individual domains. (B) Mild to moderate astrogliosis is associated with higher expression levels of GFAP and maintenance of individual domains. This type of reactive astrogliosis can occur after mild TBI or in areas distal to the lesion, and it can also occur in mild infections. (C) Severe diffuse reactive astrogliosis occurs after a more severe TBI, in which astrocytes proliferate, become highly ramified, and overlap, losing individual domains. (D) Severe astrogliosis with glial scar surrounds a focal lesion after TBI. The glial scar forms a compact barrier preventing axonal regeneration. It contains highly ramified astrocytes and newly proliferated astrocytes. This type of reactive astrogliosis causes reorganisation of the tissue architecture, with the glial scar persisting for a long time. Adapted from (Anderson et al., 2014, Sofroniew and Vinters, 2010).

#### **6.1.4.2 Glial scar formation**

The glial scar as depicted in figure 6.4D, is a barrier of primarily newly proliferated astrocytes, which have elongated processes that intertwine with adjacent astrocytes at the lesion edge. This thick glial scar acts to protect the remaining healthy tissue from the damaged tissue of the primary injury site, mediates inflammatory responses and instructs wound healing (Burda et al., 2016). The glial scar contributes to the tissue reorganization that occurs following severe TBI. Originally thought to protect healthy tissue by providing a physical barrier against the injured tissue, the glial scar has now been shown to produce inhibitory molecules to provide a molecular barrier as well (Fitch and Silver, 2008). Heavily glycosylated proteins, known as proteoglycans, are released by astrocytes and have an inhibitory effect on axonal growth. The biggest group of proteoglycans up-regulated and released by astrocytes of the glial scar are the chondroitin-sulphate proteoglycans (CSPGs), which are extremely inhibitory to axonal growth (Silver and Miller, 2004). In spinal cord injury (SCI), the physical and molecular barrier of the glial scar prevents axonal regeneration across the lesion, thus making the glial scar and CSPGs a major target for SCI treatment.

There may be a specific molecular trigger for the formation of the inhibitory glial scar structure. The candidates for this function include the cytokines transforming growth factor  $\beta$  (TGF $\beta$ ) and interferon- $\gamma$  (Silver and Miller, 2004). In an experiment in rats with a brain lesion, TGF $\beta$ -1 and TGF $\beta$ -2 were attenuated with antibodies, which caused glial scar formation to be significantly reduced (Moon and Fawcett, 2001). The introduction of interferon- $\gamma$  caused an increase in proliferation of human astrocytes *in vitro* and increased glial scarring in brain lesioned adult mice (Yong et al., 1991).

#### **6.1.4.3 Molecular triggers of astrogliosis**

The molecular triggers for reactive astrogliosis are numerous and include: large polypeptide growth factors, cytokines, neurotransmitters and reactive oxygen species (Sofroniew and Vinters, 2010). Reactive astrogliosis can also be induced through deprivation of glucose, hypoxia, and the exposure to molecules linked with neurodegenerative diseases such as  $\beta$ -amyloid, which is associated with Alzheimer's disease (Sofroniew, 2009). Molecular triggers can be released by a number of CNS cell types including neurons, microglia, oligodendrocytes, endothelial cells, leukocytes and other

astrocytes. These triggers may be released by cells at the primary lesion site and trigger a chain reaction of reactive astrogliosis in the tissue surrounding the lesion and in more distal locations.

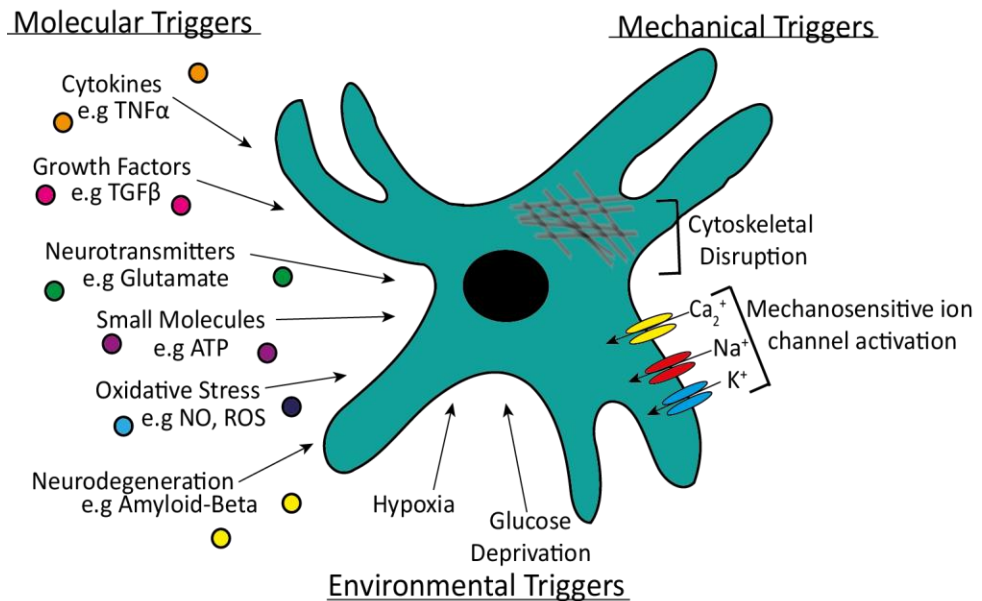


**Figure 6.5. Examples of main triggers of reactive astrogliosis.**

There are numerous molecular triggers (e.g. cytokines, growth factors, neurotransmitters, small molecules released at the time of a TBI, molecules released during oxidative stress and molecules associated with neurodegenerative diseases). Environmental changes that can trigger reactive astrogliosis include hypoxia and glucose deprivation, and the action of mechanical forces. Adapted from (Burda et al., 2016, Sofroniew and Vinters, 2010).

#### **6.1.4.4 Mechanical triggers of astrogliosis**

Molecular triggers are not the only mechanisms by which reactive astrogliosis can be initiated, since the force of the injury can also induce a phenotypic change in astrocytes. The processes and mechanisms by which a mechanical force exerted during a TBI can have a harmful effect on CNS cells are still largely unknown. There have been *in vitro* studies in co-cultures that showed reactive astrogliosis and glial scar formation after a mechanical stretch (Wanner et al., 2008). Some mechanisms have been proposed, including mechanical forces prompting plasmalemmal instability, which causes disruption to the cytoskeleton (Singleton and Povlishock, 2004). Another mechanical trigger worth considering is that plasmalemmal instability may activate mechanosensitive ion channels on the astrocyte cell membrane and trigger the phenotypic changes associated with reactive astrogliosis (Burda et al., 2016). Candidates for these mechanosensitive ion channels include the transient receptor potential cation channels, TRPV4 and TRPC1 (Maneshi et al., 2015).

#### **6.1.4.5 Time course of reactive astrogliosis**

The time course of reactive astrogliosis following TBI is dependent on numerous factors, such as the severity of TBI, location of TBI and the type of injury. After focal lesions, astrocytes in the immediate tissue surrounding the injury site display a fast response to the TBI. Studies *in vivo* have shown that following TBI, astrocytes up-regulate GFAP expression and some populations have already begun to proliferate by 24 hours post-injury (Susarla et al., 2014). The same study by Susarla et al., reported further proliferation of astrocytes at 7 days post-impact and maintenance of high levels of GFAP expression and proliferation in astrocytes at 28 days post injury (Susarla et al., 2014). Several patient studies have shown continued high levels of GFAP immunoreactivity in the brains of TBI patients from 6 months to 22 years post-injury (Levin et al., 2014).

#### **6.1.4.6 The role of astrocytes following traumatic brain injury**

Many central nervous system (CNS) disorders are associated with reactive astrogliosis, including Alzheimer's disease, encephalitis, epilepsy, multiple sclerosis, Parkinson's disease, amyotrophic lateral sclerosis, Huntington's disease, several psychiatric disorders, brain tumours, stroke and cerebrovascular disease, as well as CNS trauma including TBI. For the purpose of this thesis the astrocytic response in TBI will be the main focus of discussion.

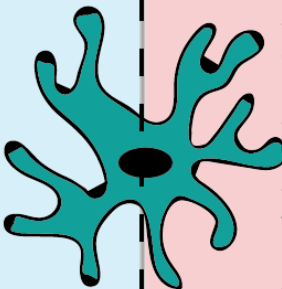
TBI triggers reactive astrogliosis and at the site of impact in a focal lesion a glial scar will form. In tissue distal to the lesion and throughout the brain tissue, there may be mild to moderate astrogliosis; this is dependent upon the severity of the TBI. This is demonstrated in the first results chapter in this thesis. It is also worth noting that the level of the GFAP-breakdown product (GFAP-BDP) in the serum of TBI patients correlates with the severity of their TBI, as measured by GCS and CT scans (Papa et al., 2012).

Whether reactive astrogliosis contributes to the damaging secondary injury sequelae following TBI, or offers some beneficial and protective support to the remaining healthy tissue, is a matter that is still largely unresolved. It has been common knowledge for almost a century that reactive astrogliosis inhibits axonal regeneration, since it was first reported by Ramon y Cajal (Ramon y Cajal, 1928).

Therefore, targeting astrogliosis has been explored as a therapeutic strategy for CNS trauma treatment

(McGraw et al., 2001). Moon et al., showed that removal of glial cells with ethidium bromide following transection of the nigrostriatal tract, allowed axons to regenerate by up to 4 mm (Moon et al., 2000). This rapid growth was lost at day 7 post-lesion, when glial cells returned to the site of the lesion to form a glial scar. Another study employed transgenic mice that expressed herpes simplex virus thymidine kinase (HSV-TK) specifically in astrocytes, so that newly divided reactive astrocytes could be ablated using the anti-viral drug ganciclovir (Bush et al., 1999). Ablation of these astrocytes resulted in the increased axonal growth following a forebrain stab injury. It is worth noting that alongside the axonal growth, ablation of astrocytes also resulted in prolonged increased leukocyte infiltration and a sustained BBB leakage (Bush et al., 1999). On the other hand, a study employing this same transgenic mouse model by Myer and colleagues, showed that a moderate CCI injury in these transgenic mice led to significantly more cortical tissue loss (60%), than the CCI in wild-type mice (18% cortical tissue loss) (Myer et al., 2006). These examples demonstrate that reactive astrogliosis may exhibit both damaging and protective effects following a TBI.

**Table 6.3. A summary of the potentially beneficial or damaging roles of astrocytes following TBI.**

<u>Beneficial Roles of Astrocytes following TBI</u>		<u>Damaging Roles of Astrocytes following TBI</u>
<ul style="list-style-type: none"> <li>- Glial scar restricts the area of tissue damage and death</li> <li>- Astrocytes help repair the BBB</li> <li>- Astrocytes may help remove the damaged tissue</li> <li>- Inflammation</li> </ul>		<ul style="list-style-type: none"> <li>- Exacerbates glutamate excitotoxicity by downregulation of the GLAST and GLT-1</li> <li>- Astrocytic swelling and brain edema</li> <li>- Prevents axonal regeneration across the glial scar</li> <li>- Inflammation</li> </ul>

In table 6.3, inflammation is listed as being both a potentially beneficial and damaging role for astrocytes following a TBI. It has been shown that astrocytes can secrete several molecules with both pro- or anti-inflammatory properties (Farina et al., 2007). Pro-inflammatory mediators released by astrocytes include cytokines (e.g. TNF- $\alpha$ ), ROS and nitric oxide (NO), all of which elicit an inflammatory response from other astrocytes (Avila-Muñoz and Arias, 2014, Sofroniew, 2014). Anti-inflammatory



interleukins released from astrocytes include IL-6 and IL-10 (Sofroniew, 2015). These conflicting actions may not happen simultaneously but instead may occur at different phases following a TBI.

### **6.1.5 3D modelling in vitro**

Various *in vitro* models have been summarised in the general introduction (section 1.7). *In vivo* modelling allows for the analysis of a whole system response to a TBI, i.e. both the tissue response and the pathophysiological changes, and the neurobehavioural consequences. The complexity of the pathophysiological response can make it difficult to distinguish the individual roles of various molecular mechanisms or cell types following a TBI. *In vitro* models of TBI have been developed to address this problem as well as to provide a model in which many factors can be tightly controlled, including the extracellular environment, and the administration of various agents (Morrison et al., 1998).

Traditional *in vitro* models utilise cell cultures that are grown on flat plastic or glass surfaces in a 2D monolayer. Under such conditions, cells adhere to the surface and only contact adjacent cells at their border (Antoni et al., 2015). This 2D arrangement *in vitro* is very different to the arrangement of cells *in vivo*; they are unable to lie on top of each other, to make multiple contacts with other cells or, in the case of astrocytes, extend their processes in a third dimension. Three-dimensional (3D) cell culture systems have been developed to address these limitations and to make the *in vitro* environment more relevant to the *in vivo* situation.

Typically, 3D culture systems comprise of a hydrogel matrix in which the chosen cell population (from immortalised cell lines to primary cells) are placed (Fig. 6.6). The cells within these gels are able to make contacts with other cells, proliferate, migrate, respond to stimuli and change morphology, which is relevant to their behaviour in a three dimensional space, *in vivo* (Abbott, 2003, Antoni et al., 2015).

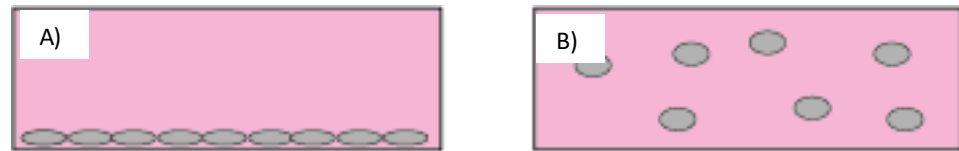


**Figure 6.6. Schematic representation of cells in *in vitro* cultures.**  
 (A) Conventional 2D monolayer culture and (B) a 3D cell culture system.

#### **6.1.5.1 Astrocytes in a 3D cell culture**

Astrocyte cell cultures have been used in *in vitro* studies to investigate astrogliosis and glial scar formation. These studies have been predominantly conducted in 2D monolayer cultures (Wanner et al., 2008, Polikov et al., 2006). Within a 2D culture system astrocytes exhibit a high level of astrogliosis without stimulus (East et al., 2009, Wang et al., 2015). This high baseline astrogliosis does not accurately reflect the *in vivo* situation and therefore makes it difficult to use GFAP up-regulation as an endpoint measurement in an *in vitro* model that would attempt to mimic TBI.

Astrocytes have been put into a 3D culture system, where the environment is closer to that of the *in vivo* situation; such studies revealed that when grown in a 3D collagen gel, astrocytes exhibit a far less reactive phenotype when compared to a 2D monolayer culture. They exhibit a less reactive morphology and a lower level of activation markers (East et al., 2009). This 3D cell culture system was also exposed to the cytokine TGF $\beta$ 1, which is known to trigger astrogliosis *in vivo*. Astrogliosis was thus simulated in the 3D gels and, by day 15 post-stimulation, astrocytes exhibited high GFAP, vimentin and aquaporin 4 (AQP4) expression (East et al., 2009). This astrocyte cell culture system offers a novel way to investigate therapeutic strategies targeted at astrogliosis, and could be used to develop a novel *in vitro* model mechanical injury relevant to TBI. This 3D astrocyte culture developed in the group led by Dr Philips is the system employed in this chapter to explore a novel *in vitro* model of focal mechanical injury.

## 6.2 Methods

Primary astrocyte cultures were prepared from P2 GFP+ rat cortices. Astrocytes were dissociated and expanded for 2 weeks before being placed in 3D collagen gels (Fig. 6.7). The GFP gene was expressed ubiquitously in the culture, which had been established as 95% astrocytes (East et al., 2009). The induction of the lesion was carried out using the computer-controlled pneumatic Hatteras PinPoint Precision Cortical Impactor™ and then cultures were fixed at 24 hours, 5 days and 10 days post-impact. DHA (1  $\mu$ M) or vehicle treatment was applied to cultures at the time of the impact. Cells were then labelled with GFAP, as an index of reactive astrogliosis within the cultures. The volume of GFP and GFAP per cell was measured in the peri-lesion ROI and in ROI distal to the lesion, using confocal microscopy and 3D image analysis software (VLOCITY), to assess the amount of reactive astrogliosis. The number of astrocytes in the peri-lesion and distal from the lesion ROI was also measured. Furthermore, the number of processes per astrocyte was analysed in the different ROI.

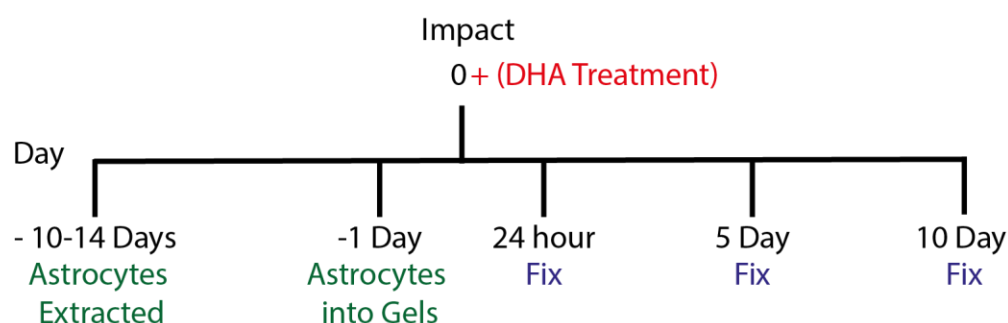


**Figure 6.7 Timeline of the in vitro studies.** Astrocytes were extracted 10-14 days prior to lesion and were placed in a 3D collagen gel 24 hours before lesion. DHA or vehicle was added to the gel directly after the lesion. Astrocytes in 3D gels were fixed 1 day, 5 days and 10 days post lesion.

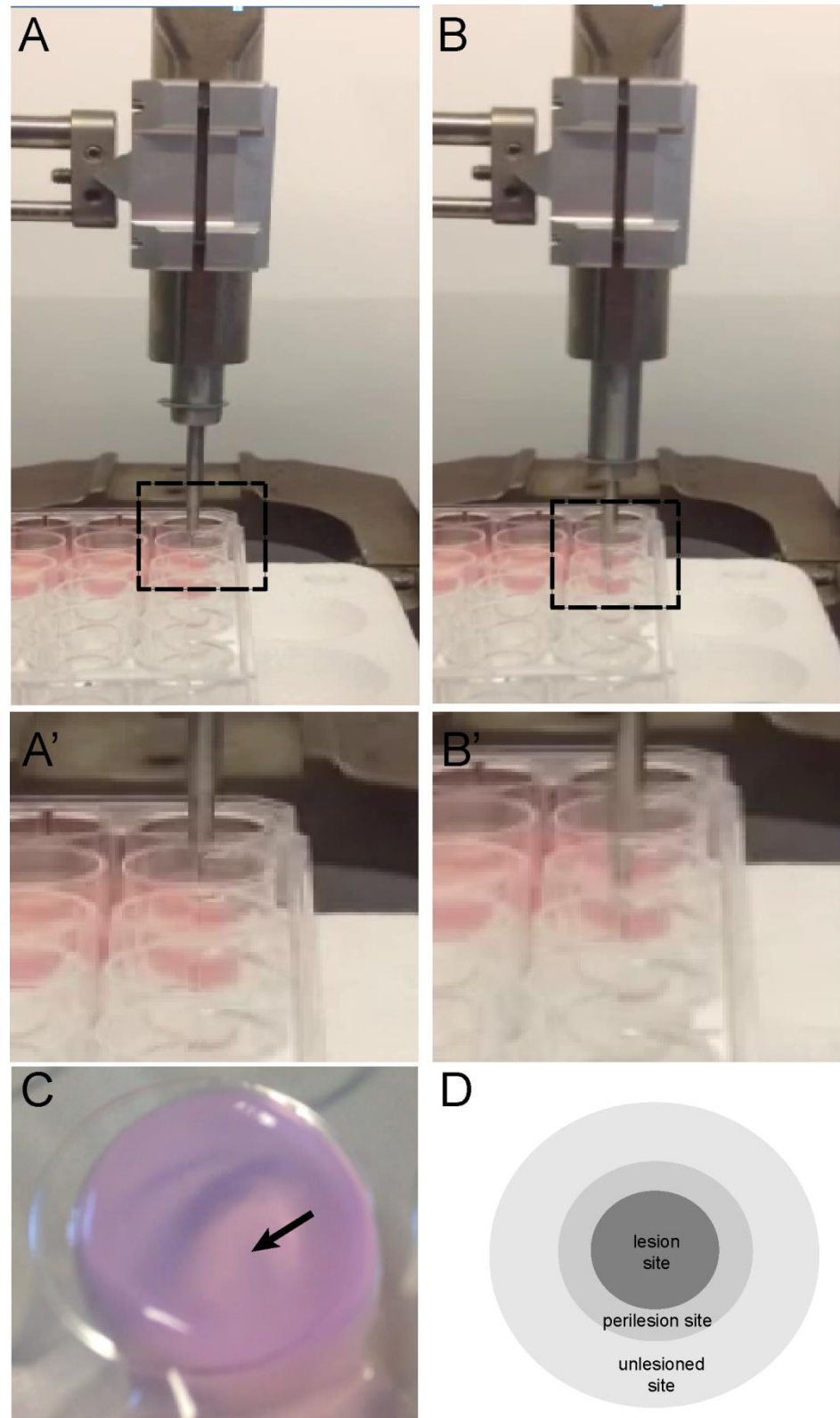


**Figure 6.8. Experimental setup for the 3D astrocytic culture.** (A-A') 3D astrocytic gel cultures were generated in 12-well plates. (B-B') Using a computer-controlled mechanical device, a mechanical impact was induced onto the gel. (C) An image of the gel post lesion (arrow indicates region of lesion). (D) A diagrammatic representation of the different regions of the lesioned 3D gel analysed.

## **6.3 Aims and hypothesis**

### **6.3.1 Aims**

The primary aim of this chapter is to develop and optimise a novel model of focal mechanical injury using the 3D astrocyte cell culture system. The pneumatically driven rigid impactor used in previous chapters to cause a CCI injury *in vivo*, was employed in this study to cause an impact injury to the 3D collagen gels. The main aim of this injury was to induce reactive astrogliosis in the astrocytes, as was seen in the astrocytes *in vivo* after CCI TBI.

Alongside the development of a novel *in vitro* model of TBI, the omega-3 PUFA DHA was tested, to identify any direct effects it had on astrocytes in culture after injury. In previous chapters, mice that received a CCI injury with DHA treatment or transgenic mice with the *fat-1* gene, exhibited reactive astrocytes with higher levels of GFAP expression.

In summary, the aims of work of in this chapter were:

- To optimise a model of focal mechanical impact injury *in vitro*.
- To assess any direct effect DHA had on astrocytes after a mechanical impact.

### **6.3.2 Hypothesis**

The hypothesis of this chapter is that a mechanical impact to a 3D astrocyte culture system will trigger reactive astrogliosis within the astrocytes at the lesion site and those further away from the lesion site. We hypothesised that the reactive astrogliosis will be evident by a distinct change in the morphology of the astrocytes and an increase in the expression of the intermediate filament GFAP.

## 6.4 Results

### 6.4.1 Effect of a mechanical injury on the cellular volume of astrocytes in the perilesional regions of interest

Astrocytes in the perilesional region of interest (Peri-ROI) showed no significant differences in the levels of GFP expression between the lesion-only, lesion + Veh and lesion + DHA (1  $\mu$ M) compared to the control group in the 3D cultures, at 24 h post lesion (Fig. 6.9E). Furthermore, there was no difference within the 4 groups in GFP expression at 5 days and 10 days post-impact (Fig. 6.9E). However, the level of GFAP staining in the peri-ROI was significantly higher per cell in the lesion-only (\* $p$ <0.05) and the lesion + Veh groups (\* $p$ <0.05), compared to the control group, on day 5 post-injury (Fig.6.9F). Interestingly, the lesion + DHA group also had higher levels of GFAP staining, but it was not statistically significant when compared to the control group on day 5.

On day 10 post-injury, the lesioned only and the lesion + Veh group, had higher levels of GFAP labelling per cell when compared to the control group, although the effect was not statistically significant (Fig. 6.9F). In regards to the lesion + DHA group, a similar level of GFAP labelling to that in the control group was observed.

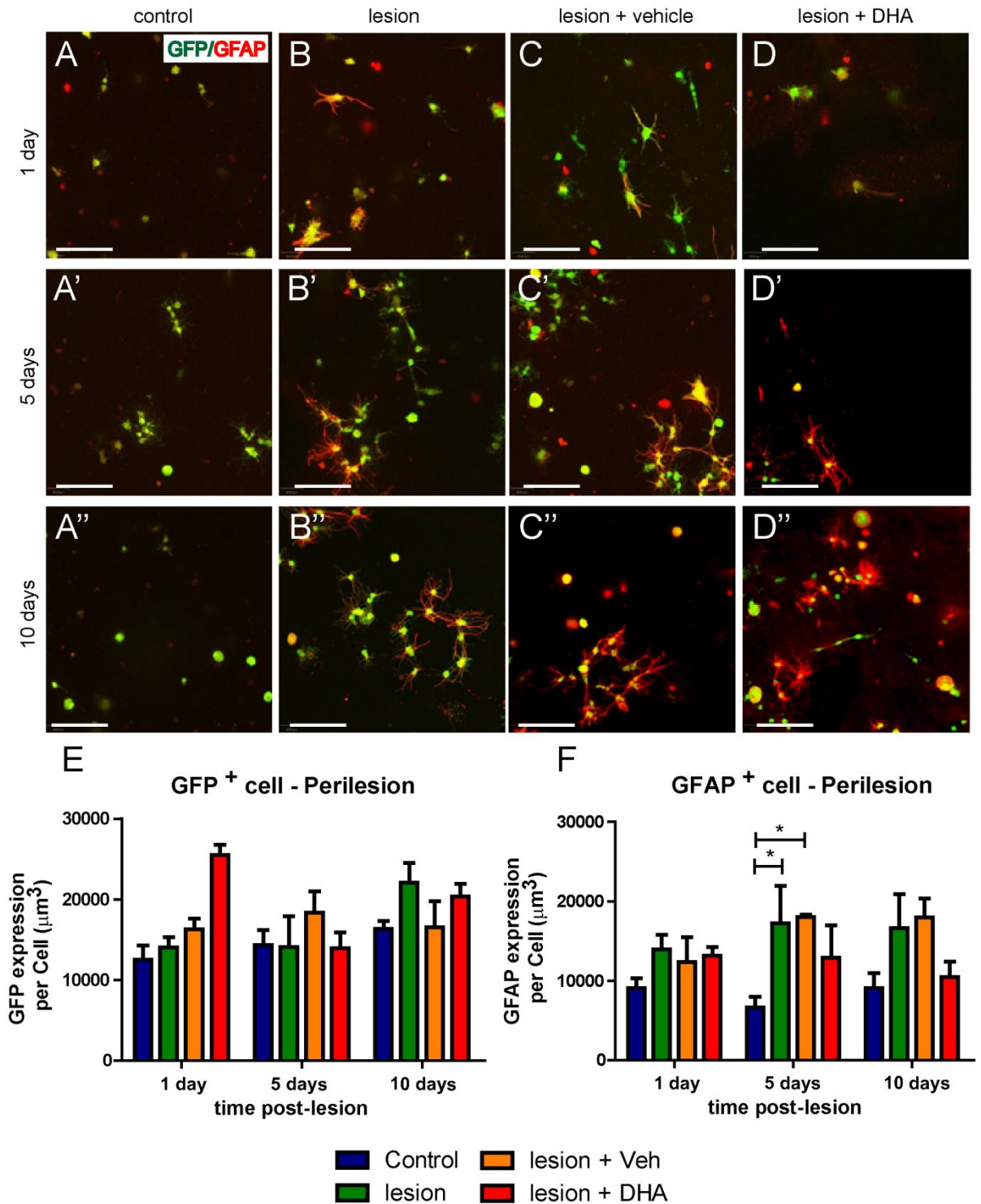


**Figure 6.9** The effect of lesion and DHA treatment on GFP expression and GFAP immunostaining in the perilesional ROI. (A, A' & A'') Control non-lesioned group, (B, B' & B'') lesion-only gels, (C, C' & C'') lesion + Veh group, (D, D' & D'') lesion + DHA group, at 1d, 5 d and 10 days post lesion, respectively. (E) GFP expression per cell and (F) GFAP expression by cell, the lesion + Veh and lesion-only groups at day 5 had statistically higher ( $*p < 0.05$ ) GFAP expression compared to the control group. Repeated measures two-way ANOVA with post-hoc Bonferroni testing used for statistical testing. Scale bar = 300  $\mu\text{m}$ . Means  $\pm$  S.E.M. N=4-5 separate gels from 2-3 separate independent experiments.

#### **6.4.2 Effect of a mechanical injury on the cellular volume of astrocytes in the distal lesion regions of interest**

Astrocytes in our *in vivo* studies showed an increase in GFAP immunolabelling in areas distal to the lesion site, termed the unlesioned site in figure 6.10. To determine if this novel *in vitro* model reflected this distal increase of astrogliosis observed *in vivo*, astrocytes in ROI distal to the lesion (Distal-ROI) site were also analysed for GFP and GFAP volume per cell.

The GFP defined volume per cell showed no statistically significant differences between the groups or the time points post-lesion. The GFAP defined volume per cell analysis also showed no statistically significant differences between the groups or time points. However, there was a trend that showed that at each time point post-injury, the lesioned groups had an increased volume of GFAP per cell, in particular at day 5.



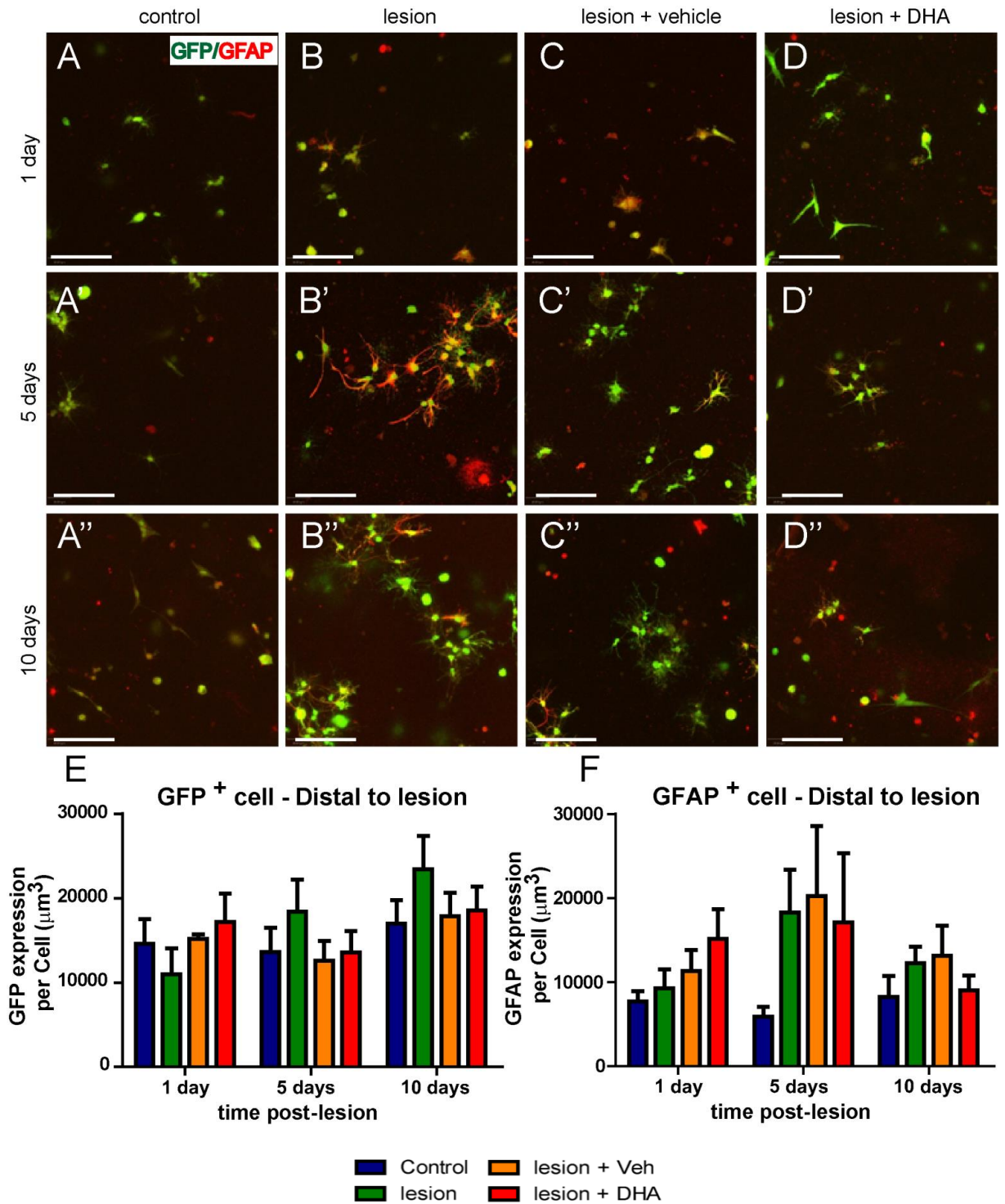


**Figure 6.10. The effect of lesion and DHA treatment on GFP expression and GFAP immunostaining in the ROI distal to the lesion.** (A, A' & A'') Control non-lesioned group, (B, B' & B'') lesion-only gels, (C, C' & C'') lesion-Veh group, (D, D' & D'') lesion+ DHA group, at 1d, 5 d and 10 days post lesion, respectively. (E) GFP expression per cell and (F) GFAP expression by cell. Scale bar = 300  $\mu\text{m}$ . Means  $\pm$  S.E.M. N=4-5 separate gels from 2-3 separate independent experiments.

### **6.4.3 The number of astrocytes in the perilesional regions of interest**

Over the course of the study, all of the groups saw an increase in the number of astrocytes in the Peri-ROI. Despite seeing increasing numbers of astrocytes over the study, the control group still had the lowest number on day 10 (day 10; Control,  $25 \pm 3$ ; lesion-only,  $41 \pm 9$ ; lesion + Veh,  $28 \pm 2$ ; lesion + DHA,  $34 \pm 2$ ).

Despite being no statistically significant differences observed between any of the groups, there was a higher number of astrocytes at day 5 and day 10 in the lesion + only (Fig. 6.11) (day 5,  $37 \pm 7$ ; day 10,  $41 \pm 9$ ) group when compared to the control non-lesioned group (day 5,  $25 \pm 3$ ; day 10,  $41 \pm 9$ ).

### **6.4.4 The number of astrocytes in the regions distal from the lesion site**

The number of astrocytes in the Distal-ROI in the lesion-only and the lesion + Veh group increased almost two-fold between day 1 post-lesion (day 1; lesion-only,  $43 \pm 9$ ; lesion + Veh,  $43 \pm 8$ ) and 10 days (day 10; lesion-only,  $22 \pm 3$ ; lesion + Veh,  $21 \pm 3$ ) post-lesion. The lesion + DHA group had an increase in the number of astrocytes between 24 hours ( $15 \pm 3$ ) and day 5 ( $30 \pm 3$ ) post-lesion, but then decreased again by day 10 ( $25 \pm 4$ ) post-lesion (Fig. 6.12).

The lesion-only group, as well as the lesion + Veh group, displayed significantly ( $*p < 0.05$ ) higher numbers of astrocytes at day 10 when compared with the control group (Fig. 6.12). There was also a significantly higher ( $*p < 0.05$ ) number of astrocytes at day 10 in the lesion-only group as well as the lesion + Veh group, when compared to the lesion + DHA group (Fig. 6.12).

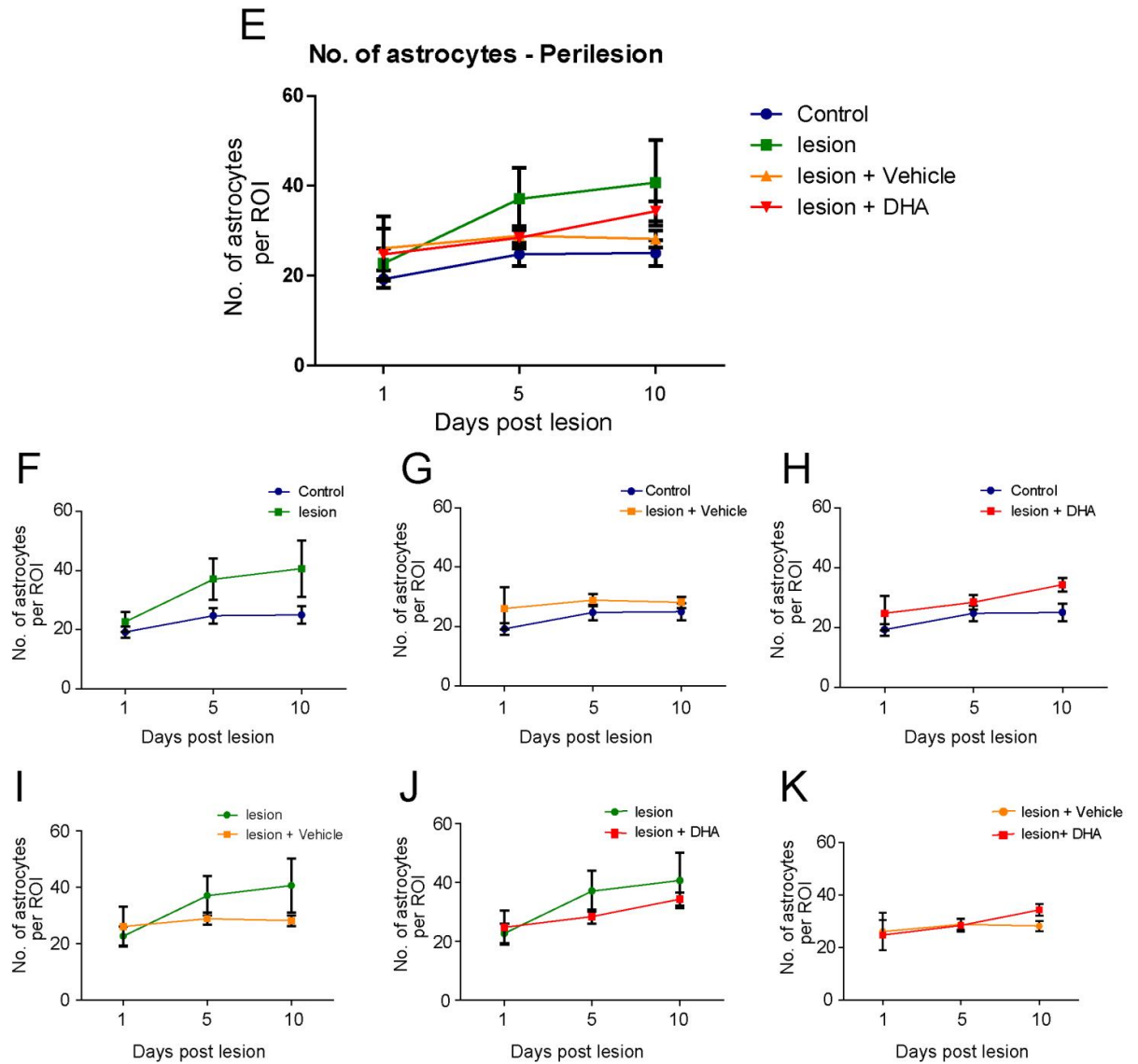
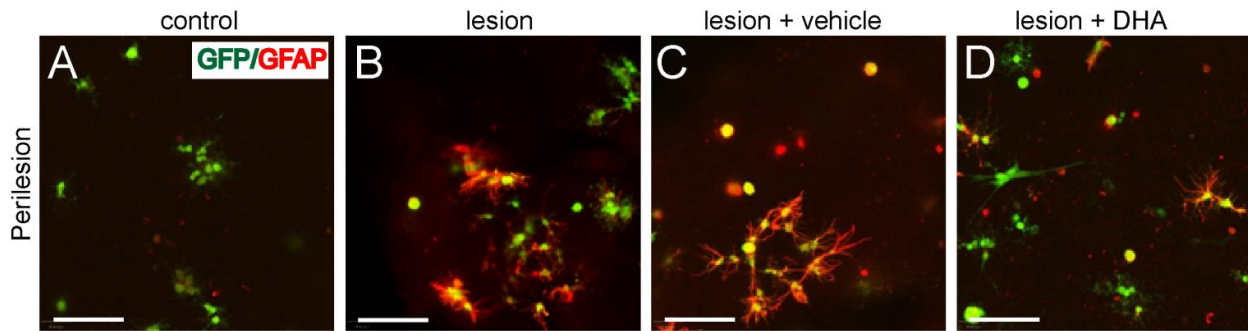


**Figure 6.11. Effect of Impact and DHA treatment on the number of astrocytes in the perilesional ROI at 1 day, 5 days and 10 days post-lesion.** (A-D) Representative images from all 4 groups. (E) Quantitative analysis of the number of astrocytes in the perilesion area, from all 4 groups. The graphs were reduced to 2 group comparison for clearer comparison; (F) Control vs. lesion-only, (G) Control vs. lesion + Veh (H) Control vs. lesion + DHA (I) lesion vs. lesion + Veh (J) lesion vs. lesion + DHA and (K) lesion + Veh vs. lesion + DHA. Data are represented as mean  $\pm$  S.E.M. N=4–5 separate gels from 2-3 independent experiments.

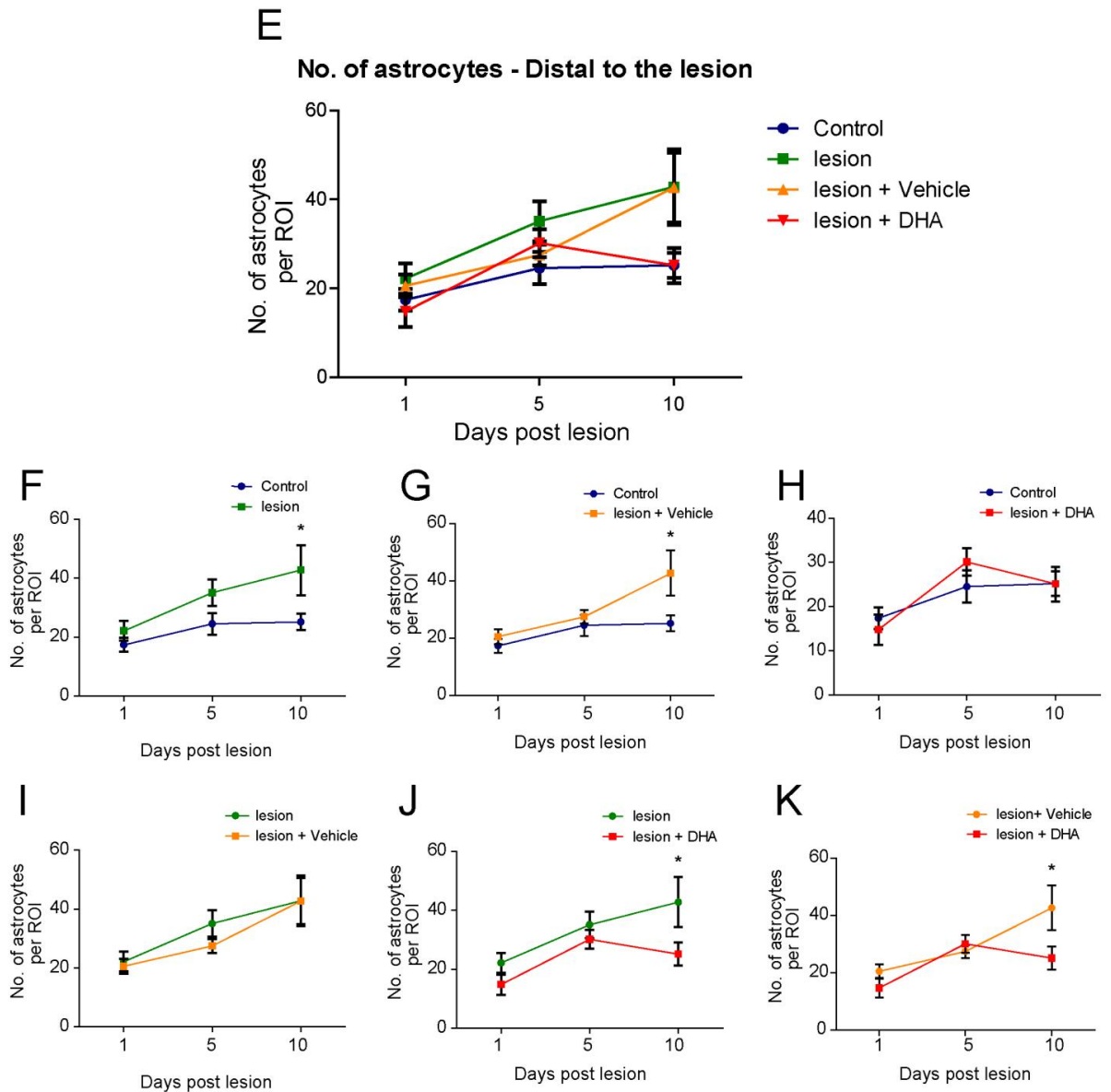
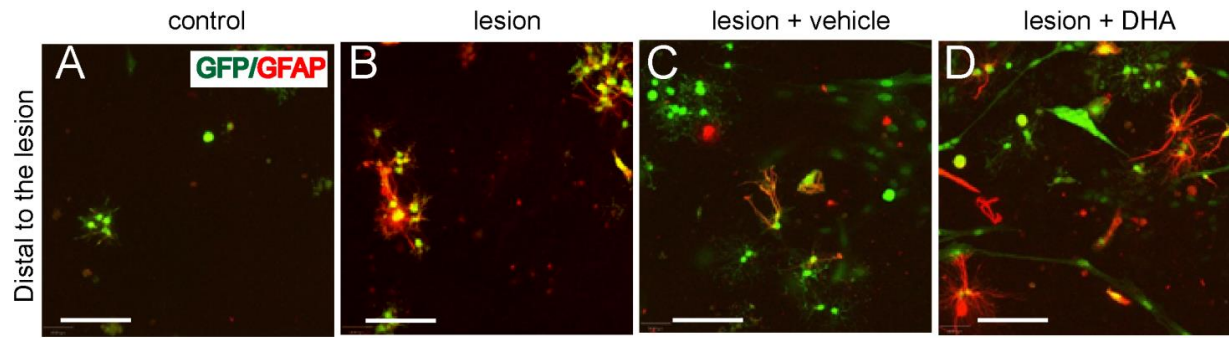


**Figure 6.12. Effect of Impact and DHA treatment on the number of astrocytes in the distal to the lesion ROI at 1 day, 5 days and 10 days post lesion.** (A-D) Representative images from all 4 groups. (E) Quantitative analysis of the number of astrocytes distal to the lesion, from all 4 groups. The graphs were reduced to 2 group comparison for clarity; (F) Control vs. lesion (day 10, \* $p < 0.05$ ), (G) Control vs. lesion + Veh (day 10, \* $p < 0.05$ ) (H) Control vs. lesion + DHA (I) lesion vs. lesion + Veh (J) lesion-only vs. lesion + DHA (day 10, \* $p < 0.05$ ) and (K) lesion + Veh vs. lesion + DHA (day 10, \* $p < 0.05$ ). Repeated measures two-way ANOVA with post-hoc Bonferroni testing used for statistical testing. Data are represented as mean  $\pm$  S.E.M. N=4 – 5 separate gels from 2-3 independent experiments.

#### **6.4.4.1 A summary of the impact injury in 3D gels as an *in vitro* model of astrogliosis after a mechanical focal injury**

This is a novel *in vitro* model to model the reactive astrogliosis that occurs similarly to that following a focal TBI. The ability of this model to induce reactive astrogliosis in response to a mechanical injury can be seen when comparing the control and lesion-only group data (Fig. 6.13).

The analysis of cell counts shows that the number of astrocytes in the Peri-ROI (Peri-ROI; Control,  $19 \pm 2$ ; lesion-only,  $23 \pm 3$ ) and the distal-ROI (distal-ROI; Control,  $17 \pm 2$ ; lesion-only,  $22 \pm 3$ ) at day 1 post-lesion is not significantly different between control non-lesioned group and the lesion-only group. However, by day 5 post-lesion the lesion-only group had a much higher number of astrocytes, although non statistically significant, in the Peri-ROI (Peri-ROI; Control,  $25 \pm 3$ ; lesion-only,  $37 \pm 7$ ) and distal-ROI (distal ROI; Control,  $25 \pm 4$ ; lesion-only,  $35 \pm 5$ ) vs. the control group. The number of astrocytes continued to increase in the distal-ROI until day 10, when the difference reached significance ( $*p < 0.05$ ; Control,  $25 \pm 3$ ; lesion-only,  $43 \pm 9$ ) when compared to the control group (Fig. 6.13B).

The GFP volume per cell did not show any significant difference between the control group and the lesion group at day 1 and 5 days post-lesion. At day 10 post-lesion, there was a more obvious, but non-significant, increase in the GFP volume per cell in the lesion-only group compared to the control group, in both the Peri-ROI and distal ROI (Fig. 6.13C, D).

The difference in GFAP volume per cell was more apparent. In the Peri-ROI the GFAP volume per cell was considerably higher in the lesion-only group compared to the control group, with a significant difference ( $*p < 0.05$ ) observed at 5 days post-lesion. In the distal-ROI the GFAP volume per cell is largest in the lesion group at day 5 post-lesion (Fig. 6.13F). At day 5, in the lesion group there was a significant ( $*p < 0.05$ ) increase, which represented almost 3-fold more GFAP per cell than that in the control group. At the 1 day and 10 day time points, the lesion group had a higher volume of GFAP than the control group, but this increase was not statistically significant.

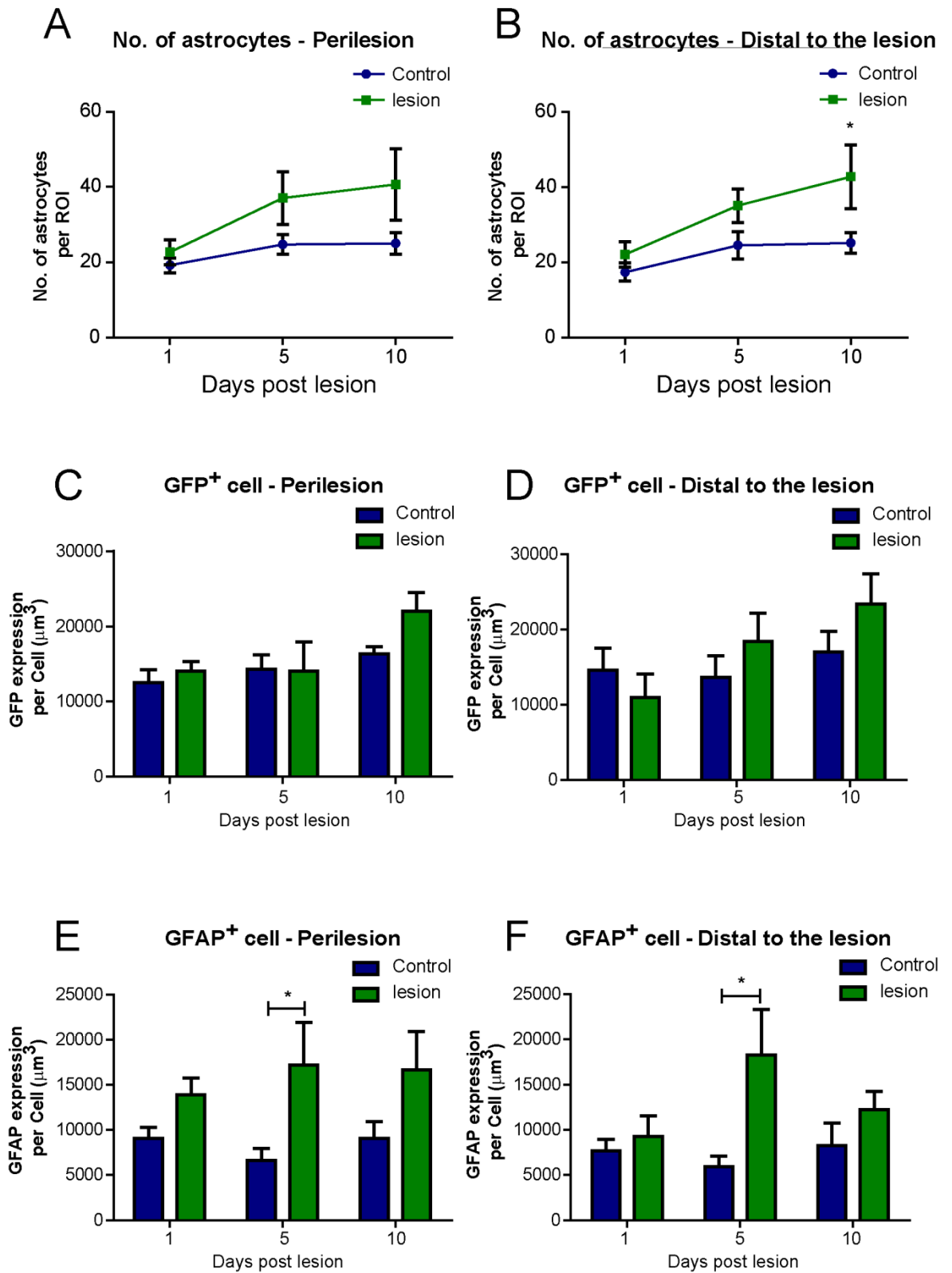


**Figure 6.13. Effect of impact on a 3D astrocyte culture in the perilesional and away from lesion ROI, at 1 day, 5 days and 10 days post-impact.** Number of astrocytes in (A) the perilesion ROI and (B) the distal to the lesion ROI. GFP volume per cell in (C) the perilesion ROI and (D) the distal to the lesion ROI. GFAP volume per cell in (E) the perilesion ROI and (F) the distal to the lesion ROI. \* $p < 0.05$ . Mean  $\pm$  S.E.M.  $N = 4 - 5$  separate gels from 2-3 independent experiments.

#### **6.4.5 Effect of a mechanical injury on the morphology of astrocytes**

The astrocytes in the lesion group displayed a much more ramified morphology, compared to those in the control group. Nevertheless, within each region of interest there are astrocytes that exhibit severe astrogliosis that are highly ramified, as well as astrocytes that display mild astrogliosis that have very few processes. In order to assess the percentage of astrocytes that displayed a highly ramified or less reactive phenotype, we used a quantitative analysis which showed that the distribution of astrocyte process number was altered after lesion (Fig. 6.14).

The control group showed a narrower range in the number of astrocytic processes, at every time point, in both the Peri-ROI and distal-ROI, when compared to the lesion only group. Furthermore, for the majority of astrocytes assessed, there were fewer than 5 processes per an astrocyte (>50%).

Interestingly, the lesion only group showed a far greater range of astrocyte process number, especially at day 5; in both the Peri-ROI and distal-ROI astrocytes have the greatest range, with a small percentage of astrocytes having over 30 processes (Fig. 6.14). At all time points and ROI, the lesion group had over 40 % of astrocytes with 5 or more processes (Fig. 6.14).

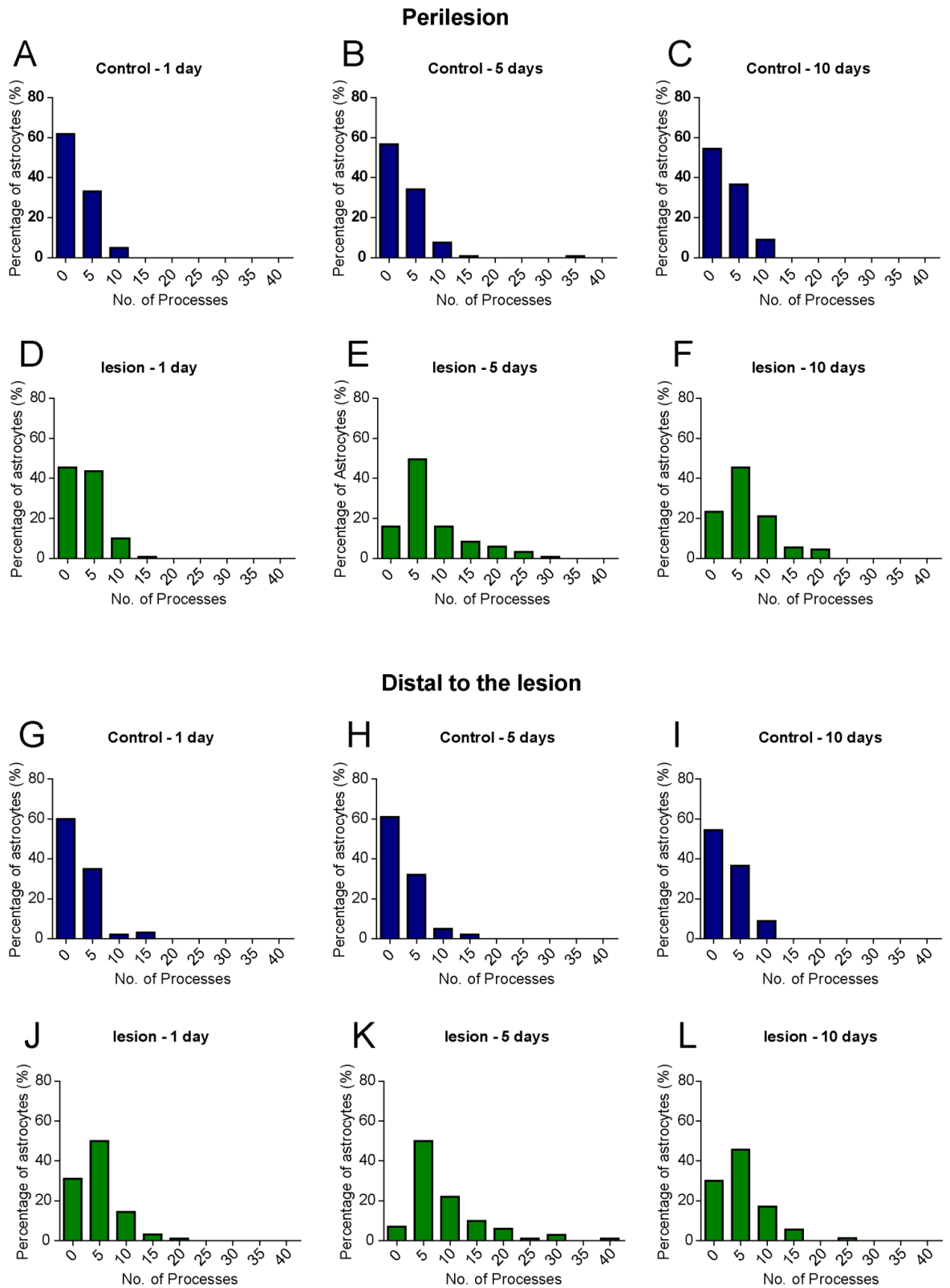


**Figure 6.14. Population analysis of the effect of impact on the number of processes per astrocyte in the perilesional and away from lesion ROI. At 1 day, 5 days and 10 days post-impact. (A, B & C) Perilesion ROI in Control group, the (D, E & F) Impact only group and distal from lesion ROI (G, H & I) in the Control and (J, K & L) Impact only group, at 1 day, 5 days and 10 days, respectively. Mean  $\pm$  S. E. M. N=3 - 4 gels, from 2-3 individual experiments.**



#### 6.4.6 Effect of the lesion on astrocytes at the lesion site

In the *in vivo* CCI model, astrocytes at the edge of the lesion site formed a thick and complex barrier, i.e. a glial scar (chapter 3, Fig 3.23F). Interestingly, in this *in vitro* model of mechanically induced injury, astrocytes immediately adjacent to the lesion site also appeared to form a structure similar to that of the glial scar (Fig. 6.15). The processes of the astrocytes at 1 day post-lesion in the lesion only group appeared to align themselves along the lesion edge. By day 5 post-impact, astrocytes at the lesion edge were highly ramified and establishing several contacts with processes from surrounding astrocytes. By day 10 post-impact the astrocytes were highly ramified, aligned with the lesion edge, and had several contacts, overlapping to form a barrier similar to the glial scar observed *in vivo*.

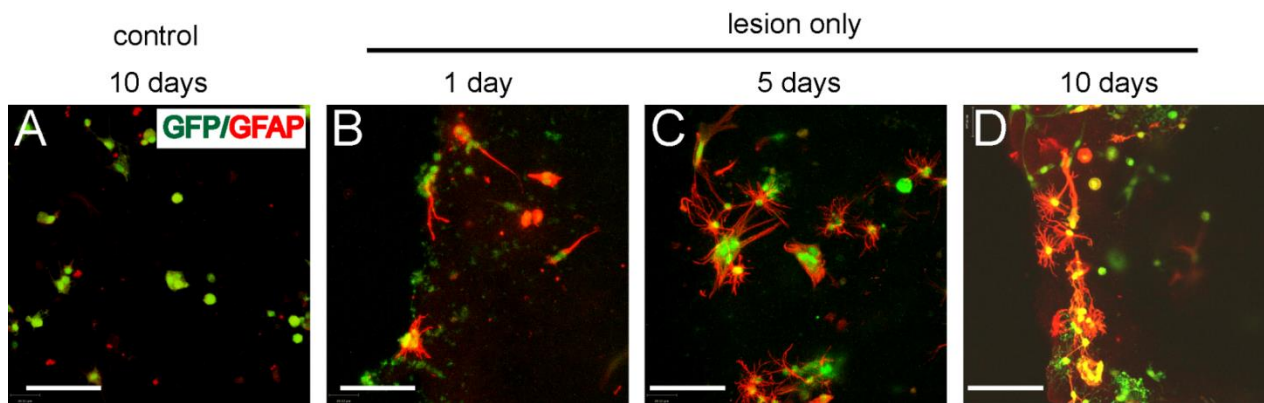


**Figure 6.15. Glial scar formation in 3D astrocytic culture.** (A) GFP- expressing cells express low GFAP immunostaining in astrocytic 3D cultures in the absence of lesion at 10 days in culture. (B-D) GFP- expressing cells express increasing levels of GFAP immunostaining in astrocytic 3D cultures after a lesion at various times in culture.

## 6.5 Discussion

### 6.5.1 A 3D culture as an in vitro model of focal mechanical injury

#### 6.5.1.1 Astrogliosis

The primary aim of this study was to develop a novel *in vitro* model of a focal mechanical injury in a 3D astrocyte cell culture system. Reactive astrogliosis was used as an outcome measure to evaluate the efficacy of this model in inducing a quantifiable response after impact. To determine reactive astrogliosis, the level of GFAP immunolabelling was measured and the changes in the astrocyte morphology were observed.

#### 6.5.1.2 GFAP expression

A hallmark of reactive astrogliosis is an up-regulation of the intermediate filament GFAP. In this study, the astrocytes in the control group had low GFAP immunolabelling. Due to the astrocytes being in a 3D collagen gel the baseline immunoreactivity was similar to that observed in healthy brain tissue. The impacted group had an increased amount of GFAP volume per cell when compared to the control group at all 3 time points after injury. This increase in GFAP indicates that the astrocytes in the lesioned gels had changed to a reactive phenotype. Therefore, this suggests that a mechanical injury at the chosen setting induced by the Hatteras™ impactor to the 3D gel was sufficient to elicit reactive astrogliosis and is therefore a valid *in vitro* model of focal mechanical injury.

The increase in GFAP volume per cell was seen in both the Peri-ROI and the distal-ROI. In the previous *in vivo* studies reported here, reactive astrogliosis was seen very distal to the lesion as well as perilesionally after injury. The astrocytes within this cell culture model appeared to have a similar response to the *in vivo* response after injury. The astrocytes in the distal-ROI displayed the greatest GFAP volume per cell at 5 days after injury. This delayed reaction could possibly be indicative of astrocyte-astrocyte communication through release of molecular mediators such as growth factors (e.g. TGFβ) and cytokines (e.g. IL-6 and TNFα) (Sofroniew and Vinters, 2010, Sofroniew, 2009). Interestingly, the significant increase in GFAP was diminished by day 10. As astrocytes are able to move through the collagen gel, those that become reactive may have migrated towards the lesion site.

It has been previously reported that astrocytes are able to migrate from different areas in the brain to the lesion site, 2-4 weeks after injury *in vivo* (Benner et al., 2013).

#### **6.5.1.3 Changes in morphology**

In combination with an increase in GFAP immunostaining, marked morphological changes were observed during development of reactive astrogliosis in this cell culture study. These changes included hypertrophy of the cell body, increase in the number of processes, thickening of the processes and elongation of the processes. Qualitatively, the astrocytes in the lesioned group exhibited these changes and also displayed several process-process contacts between astrocytes. The astrocytes in the control non-lesioned group maintained a less ramified morphology and kept their individual domains, non-over-lapping with other cells.

Changes in morphology proved difficult to quantify in detail, due to astrocytes within each ROI displaying a range of different morphologies, which may be representative of different astrocyte subtypes present in the 3D culture. However, it was possible to analyse the number of processes detected per astrocyte, to determine a change in astrocytic overall morphology. The data showed that within the control groups, a large percentage of astrocytes had fewer than 5 processes, while astrocytes in the lesioned group had a higher percentage of astrocytes, with over 5 processes, and some displaying upwards of 30 processes. This highly ramified phenotype would be described as severe astrogliosis according to Sofroniew and Vinters (Sofroniew and Vinters, 2010). The marked change in the morphology of the astrocytes in the lesioned gels provides further evidence to support this *in vitro* model as a viable model of a focal mechanical injury, relevant to focal TBI.

#### **6.5.1.4 Change in astrocyte number**

It has been observed that astrocytes migrate and proliferate in response to TBI *in vivo* (Sofroniew and Vinters, 2010, Wang and Bordey, 2008, Susarla et al., 2014). In this *in vitro* study the number of astrocytes also changed according to the group, ROI and time point after injury. The control group showed no increase in astrocyte numbers over the time course of 1-10 days. In contrast, the number of astrocytes in the lesioned group was higher than in the control group at 5 days and 10 days post

lesion. The lesion group may be displaying an increase in astrocyte number due to astrocyte proliferation. If proliferation was occurring in the Peri-ROI, this would suggest this was a severe reactive astrogliosis (Fig. 6.3), and it may be that this was driven by the need to produce more astrocytes to contribute to the formation of the glial scar. It is worth mentioning that the cell number in the Peri-ROI plateaued after day 5; this could be due to a limited capacity of proliferation being reached, or maintenance of the rate of proliferation with an increased amount of migration out of the ROI and towards the lesion edge. The cell number in the distal-ROI of the lesion group continued to increase up until day 10. This again may indicate proliferation. In a study conducted by Susarla and colleagues, proliferation of GFAP+ immunopositive cells was seen at day 1, 3, and 7 post-injury, with the highest rate of proliferation at 3 days post-injury, in a mouse model of CCI (Susarla et al., 2014). If the increase in our cell count data was due to proliferation, it would correlate with the *in vivo* data published by Susarla et al., and may explain the plateau in cell number, as seen at day 10 in our Peri-ROI.

Astrocytes could also be migrating from the outer areas of the gel towards the centre of the gel, towards the lesion site, and this could explain the increased cell numbers seen in the ROI. If migration occurred towards the lesion site this would indicate that the astrocytes can sense the location of the lesion site, possibly via release of chemicals such as cytokines from the lesion site, although there is limited data in the literature to suggest a particular mediator. Interestingly, blocking ATP signalling via the P2Y nucleotide receptor on astrocytes has been shown to reduce migration of astrocytes *in vitro* (Wang et al., 2005).

#### **6.5.1.5 Topography of the reactive astrocytes**

Astrocytes in the Peri-ROI and distal-ROI exhibited reactive astrogliosis, and this suggests that there is some form of communication between the astrocytes at different locations with reference to the impact zone. The main focus of many biological investigations is the identification of a molecular mediator or mediators that may be released from a reactive astrocyte, that could elicit a reactive phenotype in another astrocyte. This list of potential mediators is long and includes cytokines, neurotransmitters, growth factors and ROS (Sofroniew, 2009, Sofroniew and Vinters, 2010). Although

these mediators can be released by numerous CNS cell types, the high purity of our astrocyte culture suggests such mediators identified within this cell culture system would be attributed to astrocytes (East et al., 2009). A further study that could be carried out to implicate a molecular mediator as the propagator of reactive astrogliosis would be to take the media from a lesioned gel exhibiting high levels of reactive astrogliosis and introduce it to a non-lesioned gel to see if a reactive phenotype could be induced. If reactive astrogliosis was primarily propagated by molecular mediators, it could be hypothesised that in this *in vitro* model the astrocytes within the lesion site may be damaged and their cell membranes are leaky or ruptured, therefore release of the initial wave of mediators would start the chain reaction of reactive astrogliosis in the surrounding astrocytes. Mediators of reactive astrogliosis may also be released by astrocytes under stress in a controlled manner, via exocytosis (Hamilton and Attwell, 2010, Singh et al., 2015). In this model, at the earliest time point of 24 hours, the gel at the lesion site was destroyed, creating a void similar to that observed in the *in vivo* tissue after CCI injury.

The astrocytes in the gel could also be changing to a reactive phenotype in response to the mechanical force exerted by the impact. This has been referred to as mechanopathogenesis in a recent review by Burda et al. on astrocytes and TBI (Burda et al., 2016). The benefit of the 3D collagen cell culture system is the creation of a structure in which the impactor can penetrate. It also allows the inertial forces caused by the impaction to radiate out from the impaction site to be experienced by cells within the gel, similar to the cells distal to the impact in the brain after TBI. How astrocytes convert this mechanical stress into a change in phenotype is still widely unknown, although some mechanisms have been described, which include disturbing the cytoskeletal intermediate filaments or activation of mechanosensitive ion channels, such as TRPV4 or TRPC1 (Burda et al., 2016, Bowman et al., 1992, Maneshi et al., 2015). This force-induced reactive astrogliosis could be working in tandem with molecular mediators to propagate a global increase in reactive astrogliosis across the gel.

#### **6.5.1.6 Glial scar formation**

An important outcome from this study is the evidence of a glial scar-like structure formation at the lesion-edge of the gels. By day 5 in the lesioned gels, astrocytes at the edge of the lesion site became highly ramified and their domains began to overlap. By day 10 post lesion, the processes of the astrocytes intertwined and formed a thick barrier, similar to the glial scar described by Sofroniew (Sofroniew and Vinters, 2010). The formation of this scar-like structure provides further evidence to support this model as a good *in vitro* model of focal mechanical injury, with direct relevance to TBI. If the time course of this study were longer, a denser and more complex scar may form and this could be a useful *in vitro* model to investigate the glial scar formation after traumatic impact.

#### **6.5.2 DHA had no effect on GFAP expression or the morphology of astrocytes after impact**

The groups that received a lesion and vehicle or DHA treatment failed to show any significant differences between each other or the impact only group, with regards to GFAP volume per cell. This failure to see any change in astrocyte reactivity after exposure to DHA was a somewhat unexpected finding. The data in the previous thesis chapters showed an apparent increase in reactive astrogliosis after DHA treatment or in the *fat-1* gene. This *in vitro* study suggests that any effect DHA may have on astrogliosis may be through an indirect mechanism that may involve other CNS cell types. Despite not showing any significant differences, there is a noticeable decrease in the GFAP volume per cell 10 days post lesion in the DHA group compared to the other lesioned groups, in both the Peri-ROI and distal-ROI. This decrease conflicts with the *in vivo* data and contributes to the concept that the effect DHA has on astrocytes *in vivo* may be via an indirect mechanism and that were not be reproduced *in vitro*. Triggers of astrogliosis can be released by all CNS cell types, including microglia, oligodendrocytes, neurones, pericytes and endothelia cell of the BBB. These molecular mediators of astrogliosis include growth factors (e.g. TGF $\beta$ ), cytokines (e.g. IL-6), Toll-like receptor ligands, glutamate, ATP and ROS (Sofroniew and Vinters, 2010).

### **6.5.2.1 DHA treatment and astrocyte numbers**

The day 10 post lesion observation that the DHA treated group had a decrease in the GFAP volume per cell coincides with the observation that at day 10 there was a decrease in the cell number in the distal-ROI. There was a significantly lower number of astrocytes in the distal-ROI when compared to the lesion with vehicle group, or the lesion only group. The number of astrocytes at day 10 was similar to the control group. This data appears to suggest that DHA may be preventing astrocyte proliferation in these ROI, assuming that proliferation was the reason for the cell number increase seen in the lesion group.

It is worth noting that the administration of DHA to the cultures was directly into the media and at the time of the lesion. The addition of DHA to the culture media could affect cell signalling as DHA can act as a ligand to retinoid X receptors (RXR) as well as acting on ion channels such as TREK-1 (de Urquiza et al., 2000, Wu et al., 2013, Begum et al., 2012). However, as DHA was only administered once, it may have been oxidised or metabolised soon after administration without eliciting an effect. Given that the media of the cultures was changed every third day, we would presume that at 10 days post-lesion, if degraded DHA is absent from the media. The DHA group at 1 day and 5 days post-lesion behaved similarly to the lesion only group in the number of cells present, whereas at 1 day it had the highest GFAP volume per cell. The data may show that the DHA had a delayed effect that was not seen until day 10, indicating a longer mechanism of action of DHA. This is not surprising since a single bolus i.v. injection of DHA can induce neuroplasticity in an in vivo model of SCI (Liu et al., 2015). Another consideration is that the cells in the DHA group were not being protected from the lesion, but in fact were dying or dead. In either case, further *in vitro* studies are required to elucidate the effect DHA is having on astrocytes.

### **6.5.3 Limitations**

The many benefits of the 3D collagen cell culture system are detailed in the introduction of this chapter. The 3D system does have some limitations that are worth considering. Firstly, the tension created in the collagen gel at the boundaries of the system causes a high level of baseline reactive astrogliosis, similar to that seen in the 2D astrocyte cultures. Recording this baseline reactive

astrogliosis as an impact elicited response can be avoided by establishing the ROI far from the edge of the culture dish and by starting the z-stack analysis at 30  $\mu\text{m}$  from the top of the gel, as was carried out in this study.

The 3D gel culture system eradicates for the most part the baseline reactive astrogliosis which is present in 2D astrocyte cultures, but the 3D nature of the gels makes the imaging of these astrocytes difficult (East et al., 2009). A confocal microscope was used in this study for imaging these gels after fixation. As revealed by the cell count data, there is an increase in the number of astrocytes after impact at day 5 and day 10. Astrocyte migration could be a reason for this increase. Live cell imaging is a technique commonly used to monitor cell migration, however in 3D culture systems cells are able to travel in multiple directions and therefore in and out of focus, making individual cells difficult to track.

Limitations of GFAP staining are covered in the introduction and need to be considered when looking at the GFAP data from this study. GFAP immunolabelling does not label all of the branching and finer processes, therefore the true extent of the ramification of the reactive astrocytes may not be visible in the images.

The astrocytes in this culture came from the cortex of rat pups, so there may be potential differences between astrocytes derived from an immature versus an adult brain. However, the behaviour of the astrocytes in these cultures has exhibited similarity with the astrocytic behaviour observed in the previous chapters in *in vivo* experiments performed in mice. The species difference may have interfered with the DHA experiment outcomes. Cortical astrocytes are only a subpopulation of the astrocytes from the brain and therefore only partially representative of the behaviour of the total brain astrocytes after injury.



#### **6.5.4 Conclusion**

In summary, this novel *in vitro* model of focal mechanical injury within a 3D astrocyte culture system is a viable model, with clear endpoints that reflect the *in vivo* reactive astrogliosis seen following TBI. This novel model can be used as an investigative tool for the analysis of reactive astrogliosis and the screening of potential therapies targeted at astrocytes or the glial scar.

#### **6.5.5 Main outcomes**

- Astrocytes in lesioned gels had higher levels of GFAP volume per cell compared to control
- Astrocytes in lesioned gels displayed a much more ramified morphology compared to control
- In the lesioned gels there was an increase in astrocyte numbers on day 5 and day 10 post lesion compared to control non-lesioned cultures
- At day 10 post lesion, astrocytes formed a glial scar-like structure at the edge of the lesion site

## **7 General discussion**

Traumatic brain injury (TBI) is one of the leading causes of death and disability worldwide, in particular in men aged below 50 year-old (Maas et al., 2008). TBI is a condition with substantial heterogeneity and can significantly impact upon a patient's quality of life because of long-term motor, sensory and cognitive dysfunction. Currently there are no effective treatments for TBI, and there is a worldwide effort to understand better what can be improved in terms of diagnosis and of definition of relevant outcomes, through initiatives such as TRACK-TBI (Yue et al., 2013) and CENTRE-TBI (Maas et al., 2015). Although several experimental neuroprotective therapies have been taken to clinical trials, they have been unsuccessful. In this thesis, an animal model of TBI was optimised in mice, and then used to assess omega-3 PUFAs as a potential neuroprotective treatment. Omega-3 PUFAs (and in particular the long-chain DHA) are a class of compounds which have elicited much interest and research over the last decade in a variety of models of disease. Previous to the beginning of this work, data from our group and others, showed a clear therapeutic or prophylactic potential of DHA in traumatic injury in the PNS and CNS (for SCI) (King et al., 2006, Huang et al., 2007, Ward et al., 2010, Lim et al., 2013b, Lim et al., 2013a, Liu et al., 2015, Paterniti et al., 2014, Figueroa et al., 2012). The results reported in this thesis in a specific animal model of TBI, however, did not provide strong evidence to support omega-3 PUFAs as an effective treatment for TBI or protection against TBI. We will conclude this thesis with final comments on various issues raised by this work, in the general context of neurotrauma and neuroprotection.

### **7.1 Modelling TBI in vivo**

The first results chapter of this thesis details the characterization and optimisation of a CCI injury in mice, with outcome measures that reflect the cognitive dysfunction and pathophysiological changes seen in human TBI. The CCI injury caused severity-dependent deficits in the MWM test, gross brain tissue loss, and reactive astrogliosis and activated microglia within the injured brain. The main aim of the first chapter was to establish the parameters of the injury that would provide reproducible outcomes. A unilateral injury above the parietal lobe at the velocity of 3 m/s, dwell time of 100 ms, tip

diameter of 3 mm, set at 20°, with an impact depth of 2.2 mm, was finally chosen as an injury severe enough to cause behavioural deficits and histological changes, but not to lead to major behavioural disruption and impairment in mice. This injury paradigm was then used in the following chapters to investigate the efficacy of an acute single bolus DHA treatment and the neuroprotective potential of the *fat-1* gene.

The work in the model development chapter did reveal some interesting consequences of the CCI injury. Firstly, we noted the activation of glial cells on the contralateral side of the brain. Originally, the contralateral cortex was to be used as a control for the injured ipsilateral side. This phenomenon highlights the global impact a CCI injury has on the brain, despite the model being traditionally used to replicate a focal localized injury. This extended pathology has been reported in the stroke literature, i.e. increased reactive gliosis is observed on the contralateral side to the occlusion side (Patience et al., 2015). While our studies were proceeding, a report was published by Niesman, showing neuroinflammatory responses both ipsilaterally and contralaterally after CCI in mice, at 7 days post-injury, supporting the concept of a bilateral response to unilateral trauma. Furthermore, a contralateral response after injury in terms of tau pathology, has also been reported in the 3xTg model of Alzheimer's disease (Tran et al., 2011, Niesman et al., 2014). In agreement, this phenomenon was also observed throughout the rest of the *in vivo* chapters in this thesis, regardless of treatment or genetic manipulation. Possible explanations for this contralateral increase in glial cell activation were discussed in the first results chapter, which include: contralateral compression against the skull at the time of injury, chemotaxic signalling, migration of activated glial cells, or communication of damage to the contralateral side through interhemispheric functional connectivity of large brain networks such as the cortico-cortical connections. This concept of global dysfunction seen in animals is supported by observations in humans after TBI, showing global network dysfunction (Sharp et al., 2014).

Another finding from the first results chapter was the detrimental effect the sham injury had on mice, particularly on their performance in the MWM test. A sham injury control could be expected to have an outcome more comparable to a naïve control. However, due to the invasive nature of the sham injury in the case of an open skull model of TBI (craniotomy), there were behavioural and

pathophysiological consequences. This observation suggests that comparison of CCI injured groups to naïve groups alone may confound results and their interpretation, especially in the earlier period after injury, as the pathology seen in the injured animals may be a cumulative result of both the negative consequences of the surgical sham-injury and the direct brain impact-linked injury. Therefore, in order to elucidate the effect a treatment has on the focal brain injury alone, CCI injured animals using an open-skull approach, should be whenever possible compared to a sham-operated group, especially for the analysis of the early events after injury. The importance of using a sham control in studies with the CCI model is reiterated in a paper published by Cole and colleagues (Cole et al., 2011). It is interesting to note that there is evidence that different mouse strains respond differently to sham surgery, with some strains (e.g. FVB/N and 129/SvEMS) presenting a persistent impairment in cognition induced by a sham operation (Fox et al, 1999). Interestingly, in this study the authors also show that somewhat paradoxically, the resilience to CCI in the FVB/N strain is higher than in 129/SvEMS or C57BL/6 mice. In all three of the *in vivo* chapters of this thesis, our CCI injury paradigm was robust enough to cause a deficit in learning and trigger secondary injury mechanisms, which was independent of the age of the mice or their strain (CD1 and C57/BL6). The possible strain-dependent variation in the response to injury was mentioned above, and it has been documented in mice and also in rats (Fox et al., 1999, Tan et al., 2009). However, the use of this CCI model also revealed some of its limitations. Firstly, there was the extensive tissue loss at the site of the lesion. In time, the injury resulted most commonly in destruction of almost half of the ipsilateral hemisphere beneath the site of the injury and almost the entire ipsilateral hippocampus. This level of tissue loss is not comparable to the tissue pathology of human TBI patients, or at least those that survive the injury (Marklund and Hillered, 2011). Secondly, in our model we replaced the skull bone flap after the injury. Although we did not secure the bone flap in its place, this may not be sufficient enough to overcome the damaging effects from secondary brain swelling. The model is not reflecting well the surgical decompressive craniectomy which is used in the clinic to reduce ICP in TBI patients (De Bonis et al., 2010). In conjunction with this, anaesthetics have been shown to confer neuroprotection, or in the case of the anaesthetic drug used in our studies, ketamine, can cause increased neuronal cell death in the hippocampus of rats following TBI (Statler et

al., 2006). However, since ketamine is provided in prehospital care as a safe and effective option, we tried to relate our animal model to the clinical setting (Porter, 2004).

In addition to the limitations of the actual CCI surgery, the outcome measures used in this study have their disadvantages. The MWM, despite it being commonplace in the TBI literature, has limitations, such as the sensitivity of the test to the surrounding environment (D'Hooge and De Deyn, 2001). Despite keeping the experimenter, testing room and extra maze cues consistent in all the studies, environmental factors (such as noise, olfactory cues and housing details), which are sometimes beyond the experimenter's control, might have affected in some instances the performance of the mice in the MWM test – and affected differently the different groups. In our MWM protocol, the acquisition training was the most sensitive part of the protocol, since it could differentiate between the severities of the injuries, as shown in the first results chapter. However, in the probe trial, one of the two measures used to assess memory function was the number of visits to the platform zone. This measure may not have been robust enough to differentiate between test groups, due to the low frequency of visits to the zone. It is important to note that we chose a cognition test because of the importance of cognition and memory impairment after TBI, but this is only one of the possible choices; further studies could explore other equally relevant aspects, such as fatigue or depression, which could reflect for example damage to the pituitary (Zaben et al., 2013).

## **7.2 Effect of DHA and of the fat-1 genotype in CCI**

In order to assess the effect of the injury severity, treatment with DHA or genotype on the outcome and secondary injury mechanisms following CCI injury, we measured behaviours and also chose to focus in the tissue on the amount of activation detected within the astrocytes and microglia cell populations, bilaterally. Data from previous SCI studies, whether injury was induced by hemisection or compression, carried in our group and others, showed that acute i.v. treatment with DHA or the presence of the *fat-1* gene caused a significant reduction in the reactivity of these glial cell types (Paterniti et al., 2014, Lim et al., 2013a). The results we present in this thesis do not show such reduction after acute treatment with DHA in *contusion* TBI. One potential explanation may be due to

the timing of the examination of the tissue post-injury, as there are complex polyphasic temporal cellular changes which are linked to the neuroinflammatory response after CNS injury (Bowes and Yip, 2014). The brain tissues from the studies presented in this thesis on the model optimisation/severity variation and the DHA treatment were obtained at 28 days, and the tissue from the mice in the *fat-1* studies was obtained at 21 days post-injury. This means that the immunohistochemical data gathered in this thesis were from relatively delayed time points after injury (comparable though to the SCI time line examined previously). However, the general levels of activation in both astrocytes and microglia can vary at different time points following TBI, and the predominant microglial phenotype also changes at different time points post-TBI (Loane and Byrnes, 2010, Woodcock and Morganti-Kossmann, 2013). Any relevant transient changes in glial cells at earlier time points post-injury were missed, as we focused on a late evaluation of the brain tissue. In particular, DHA treatment or the *fat-1* background may have influenced earlier events affecting the glial populations. Interestingly, in a recent study in our group using acute DHA after thoracic SCI induced by contusion, it was also noticed that there was a time-dependent response of microglia (analysed using the Iba1 marker): DHA **increased** the microglia response to injury by 7 days, but in the tissue collected 28 days after injury, there was no difference between control injured and DHA-treated animals (Dr Ping Yip, personal communication). Finally, in the months preceding submission of this thesis, our group completed another DHA study in this CCI model, at the same dose of DHA shown in this thesis, and examined the tissue both 7 days after injury and 28 days after injury, to have a better grasp of the time line of events. In this latter study, there was a very significant decrease in the Iba1 perilesional post-injury reactivity at 7 days, after treatment with DHA, but this effect was not seen any more at 28 days (Dr Orli Thau-Zuchman, personal communication), which confirms the observations in contusion SCI. These time-dependent changes in the impact of DHA on the Iba1 positive cells were seen in parallel with a significant improvement in sensorimotor neurological dysfunction after injury (as assessed by a modified neurological score), which was already significant by 7 days and maintained at 28 days. Therefore, it is difficult using this general marker for microglia/macrophages, to establish a simple correlation between neurological outcome and the microglia/macrophages detected in tissue.

Microglia are cells that actively reshape circuits in development and disease, and it is necessary to be able to differentiate the various subtypes (Wake et al., 2013). Future work using histological markers for the different subtypes of microglia, and also markers which allow the assessment of the functional activity of the microglia (e.g. phagocytic activity), will help elucidate these post-injury changes. For example, in a recent PET imaging study in our group, using the 18-kDa translocator protein (TSPO) as a marker of activated microglia, we showed that acute DHA post-injury decreases the activation of this specific microglia population, at 7 days post-SCI (Tremoleda et al., 2016).

Concerning the astrocytes, in the model development chapter we showed that there was increased reactive astrogliosis with increasing injury severity, and this correlated with a poorer performance in the MWM. An amplified reactive astrogliosis was also seen in CCI injured mice after DHA treatment and in those possessing the *fat-1* gene, compared to their respective control groups. However, the further increase in reactive astrogliosis seen in these latter mice did not correlate with poorer performance in the MWM. These results suggest that increased astrogliosis may not always and necessarily correlate with decreased cognitive function. This is in direct conflict with the literature that suggests that the beneficial effects of omega-3 PUFAs are causally linked to a reduction in the glial inflammatory reaction (Zendedel et al., 2015, Orr et al., 2013). Astrogliosis has been associated with poor recovery in SCI, but in the context of injury in the brain, Harris and colleagues, have shown that the reduction of the glial scar by administration of chondroitinase ABC, and the subsequent increase in peri-contusional axonal sprouting, do not lead to robust neurological improvement (Harris et al., 2010). However, our observations do suggest a link between DHA and reactive astrogliosis following a CCI injury. The nature of this link remains elusive. In a manner similar to what we saw in terms of microglia activation, it is likely that the astrocytic response evolves in a complex manner post-injury. At very early times after injury, the glial scar may limit the injury but then become a neutral by-stander or even play a beneficial role. Indeed, in the recent repeat study in our group on acute DHA treatment in CCI, which is mentioned above, it was seen that DHA **reduced** markedly the ipsilateral perilesional GFAP reactivity at 7 days – but this effect was no longer seen at 28 days (Dr Orli-Thau-Zuchman, personal communication). Amplification of the astrocytic response contralaterally may have a positive

impact on the reported plasticity of the contralateral hemisphere after a focal TBI, which may lead to at least a partial recovery of function (Axelson et al., 2013). There is clear recognition of the positive role of astrocytes in the active remodelling of synapses and consequent brain plasticity (Jones et al., 1996). Astrocytes have gradually emerged in the last decade as key regulators of behaviour (Oliveira et al., 2015), which confirms their important roles in the “tripartite synapse” (Perea et al., 2009). They are also the only brain cells capable of synthesizing DHA (Moore, 1993). Disruption of intracellular calcium signalling in astrocytes (Petraovic et al., 2014) or disruption of the “lactate shuttle” (which provides lactate formed through anaerobic glycolysis in astrocytes and delivered to neurons) (Newman et al., 2011) can lead to significant spatial memory disruption. The ablation of astrocytes in the prefrontal cortex leads to significant cognitive impairment (Lima et al., 2014), while the engraftment of larger, human astrocytes into the murine hippocampus, enhances hippocampal LTP and hippocampal-dependent learning (Han et al., 2013). Interestingly, in contrast with a tendency to amplify astrogliosis, no amplification of the strong neurogenesis seen post-CCI was detected at 28 days after treatment with DHA, as reflected through use of a marker of immature neurones.

Due to the complexity of the secondary injury mechanisms following TBI, characterizing in detail a link between omega-3 PUFAs and reactive astrogliosis *in vivo* could be difficult. In order to simplify this investigation, a novel *in vitro* model of reactive astrogliosis in a 3D culture was developed.

### **7.3 In vitro model of TBI**

Our novel *in vitro* model of TBI was able to reproduce reactive astrogliosis and even a “glial scar” formation using only a single mechanical insult, within a 3D culture of astrocytes. The main benefits of a 3D culture system are described in the introduction of the final results chapter. Astrocytes are highly reactive and in a 2D culture system they exhibit an increased baseline level of GFAP expression, due to the stress of being restricted to growing in only one plane (East et al., 2009). In contrast, astrocytes in a 3D cell culture system exhibit much lower levels of GFAP and a reduced ramified morphology, therefore reflecting the unreactive astrocytes seen in normal uninjured brain tissue (East et al., 2009). To replicate the CCI injury in an *in vitro* model, after we optimized the *in vivo* model in mice, the same



impactor used to create the lesion *in vivo* was also used to create a focal mechanical lesion in the 3D cell culture. The 3D structure of the culture system was more similar to brain tissue architecture than a 2D system, and allowed for mechanical destruction by impaction. At the start of this work we were uncertain as to whether a mechanical insult would elicit reactive astrogliosis in astrocytes in culture. Reactive astrogliosis has been elicited in *in vitro* models through hypoglycaemia, hypoxia, or inflammation - through the introduction of lipopolysaccharide (LPS)(East et al., 2009). Surprisingly, our *in vitro* impaction model not only elicited reactive astrogliosis at the site of the lesion, but also distal to the lesion site. The reactive astrogliosis increased over the time course of the study. One of the most exciting observations following the injury was the appearance of a glial scar-like structure at the edge of the lesion. The development of this model allowed us to investigate the direct effect DHA had on astrocytes following an injury. In this study, the DHA-treated cultures did not have a significantly different response post-impact compared to injured vehicle-treated cultures. Therefore, it was not possible to further study the correlation between DHA and the modulation of increased reactive astrogliosis post-CCI. One possible explanation for the lack of significant effect may be linked to the DHA concentration used or the protocol of administration. DHA used at a higher concentration (10  $\mu$ M) has been shown in acute experiments to inhibit the endoplasmic reticulum stress response and subsequent cell death in a 2D astrocyte culture submitted to oxygen-glucose deprivation (ischaemia model) (Begum et al., 2012). The authors also showed that a similar protective effect was obtained with a metabolite of DHA which was an isomer of neuroprotectin D1. Interestingly, DHA has also been shown to increase the gap junction coupling in astrocytes and also decrease aspartate uptake (Champeil-Potokar et al., 2006, Grintal et al., 2009).

An obvious question that arises from this *in vitro* data is whether the increase in astrocyte number in the lesioned gels is due to migration of astrocytes from distal regions or proliferation of the astrocytes at the site of the lesion. The data from the *in vivo* studies shows increased reactive astrogliosis on the contralateral side 4 weeks after injury. Utilizing this novel *in vitro* model and labelling the astrocytes for proliferation markers or by employing time lapse microscopy, will allow in future to better characterize the mechanisms underlying the response of astrocytes to injury. The exact composition of

the scar formation, and its similarities with the scar formed in vivo – in particular enrichment in axon-inhibiting chondroitin sulfate proteoglycans such as NG2 (Chen et al., 2002), also remains to be determined.

This 3D astrocyte model could also be used in combination with other CNS cell types such as neurones, microglia and oligodendrocytes, to see how the focal mechanical injury affects mixed cultures.

#### **7.4 Omega-3 PUFAs and their potential in the treatment of TBI**

Several therapies have shown promise in animal models in terms of neuroprotection in TBI. However, no treatment has been successfully translated into the clinic. Therefore, there is a significant translational block in the development of new neuroprotective treatments in TBI. Despite using a similar dosing regimen of DHA to the regimen that conferred neuroprotection in models of SCI and employing the *fat-1* transgenic mice as an investigative tool, the data in this thesis did not point towards omega-3 PUFAs being a viable neuroprotective treatment for TBI – at least for the type of injury and mode of administration considered.

Evidence has accumulated which allows us to compare the data reported so far with DHA in three models of acute injury to the CNS: SCI, TBI and stroke, which have strong similarities in the pathophysiology of secondary injury. While our group has carried out numerous studies in models of SCI, where we have shown the significant neuroprotective potential of DHA, the group led by Bazan has published extensive data supporting the neuroprotective potential of acute single administration of DHA in stroke models, in adult or aged rats (Belayev et al., 2005, Belayev et al., 2009, Eady et al., 2012b). In these various studies, the i.v. fatty acid bolus was either administered at the onset of reperfusion or up to 3 h post-ischaemia onset. Interestingly, in one of their studies, the authors showed an increased astrocyte density in the lesioned hemisphere at 7 days compared to controls (Eady et al., 2012a). In a subsequent study, in which the authors used a formulation of DHA bound to albumin, the post-injury administration time window was extended up to 7 h post-ischaemia (Eady et al., 2012b). However, in this study as in previous studies, the neurological score improvement was only

monitored in the first 7 days, raising the question whether the improvement was long-lasting. Albumin has the potential to mobilize PUFAs and facilitates the delivery of DHA to the injured brain tissue (Rodriguez de Turco et al., 2002). It is interesting to note that in their most recent studies this group show that while the sensorimotor improvement induced by DHA post-ischaemia can still be seen at 3 weeks after injury, the cognitive improvement is transient and lost by 3 weeks (Hong et al., 2014). The group led by Bazan have suggested that the improvement seen after a bolus of DHA in stroke models is due to the formation of the metabolite neuroprotectin D1 (Mukherjee et al., 2007, Bazan, 2005, Eady et al., 2012a). However, it cannot be ruled out that other metabolites of DHA – and there is a wide array of possibilities of such pro-resolving and potentially protective mediators (Serhan and Chiang, 2008), could also play a role in the observed effect; thus, Harrison and colleagues, have shown that an aspirin-triggered epimer of neuroprotectin D1 (Harrison et al., 2015), AT-resolvin D1, reduced motor and cognitive deficit (Rotarod and novel object recognition test) at 7 days after a fluid percussion injury in mice; it is important to note though that the administration of the resolvin was initiated *before* the injury and continued daily during the 7 days post-TBI. Under these conditions, AT-resolvin D1 had no effect on microglial immunoreactivity post-injury.

The neuroprotective effect of an intraperitoneal administration of the long chain omega-3 PUFAs in models of neonate hypoxia-ischaemia was first reported by Williams, using the post-natal P10 mouse Rice-Vannucci model of hypoxia-ischaemia, with a time window for efficacy of 2 h post-ischaemia; the authors reported that this protective effect was seen after a DHA-containing emulsion and not EPA emulsion (Williams et al., 2013). In a very recent follow-up study, the group showed that 8 weeks after the intraperitoneal administration of a DHA-emulsion, first immediately after injury, and then a repeated injection at 1 h, the animals had a tendency to show better learning in the MWM and also a partially improved performance in the memory trial, in parallel with a reduced tissue loss (Mayurasakorn et al., 2016). Overall, all these observations suggest that there may be some potential for DHA administration in stroke/hypoxia-ischaemia, in the adult, aged and also immature brain.

Concerning the prophylactic potential of omega-3 PUFAs: the data reported by Desai and colleagues, suggest that deficiency in the PUFAs can worsen outcome, but to this date, no clear indication has

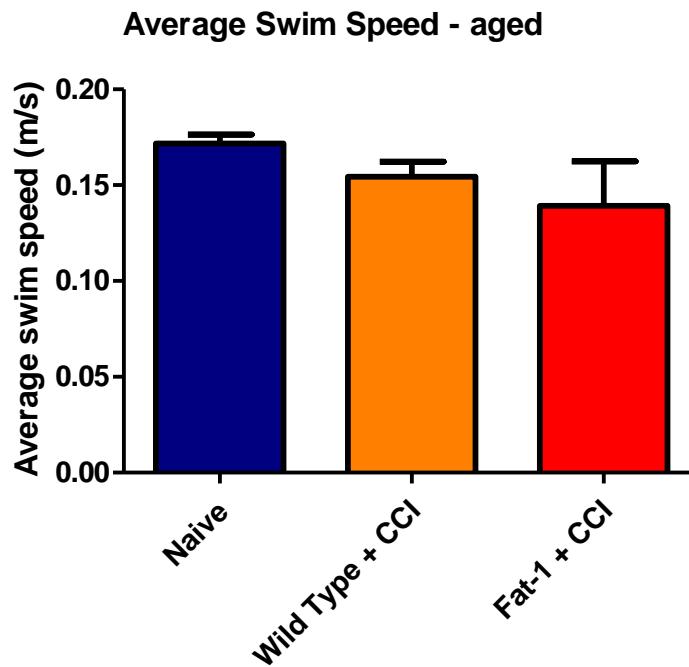
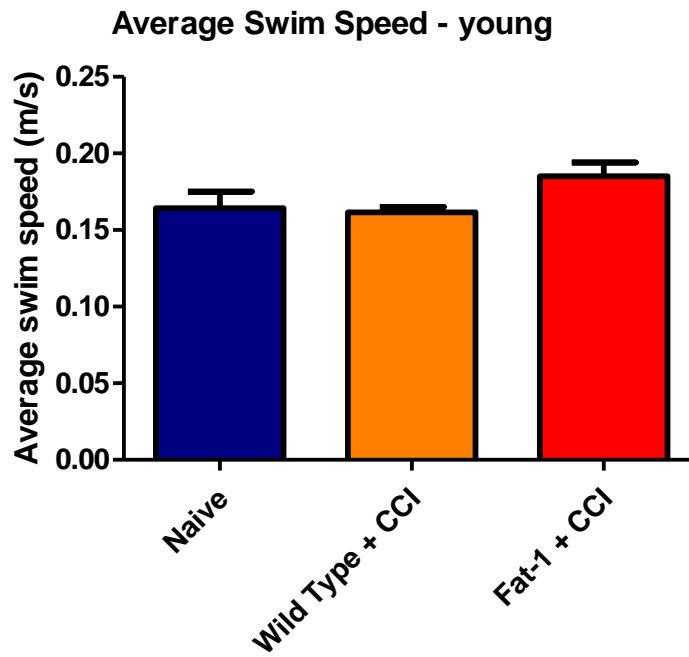
emerged that DHA has a significant long-lasting efficacy in TBI (Desai et al., 2014). While this dissertation was completed, Shi and colleagues published data which showed that the *fat-1* cortical neurones in culture had a better response to the stress of oxygen-glucose deprivation and that pre-treatment of cultures from wild-type animals with DHA, also improves resilience in this model (Shi et al., 2015). Furthermore, in the same study, the authors induced very limited focal cortical ischaemia and reported protection of the tissue and improved sensorimotor outcome 2 weeks post-injury in *fat-1* mice. Very recently, the authors showed in a model of more extensive damage, induced by transient middle cerebral artery occlusion in mice, that only a combination of intraperitoneal injections of DHA and sustained oral supplementation, leads to significant tissue protection, increased angiogenesis and improved spatial memory in the MWM (Pu et al., 2016).

## **7.5 Conclusion**

To date, there has been much promise raised by positive experimental observations using DHA or its metabolites and striking improvement reported on a single TBI case history basis, after treatment with very large doses of omega-3 PUFAs added to enteral feeding (Lewis et al., 2013). However, much more research work is necessary to establish whether significant and sustained efficacy can be induced by treatment with this type of compound post-TBI. Although there is some indication in the literature of secondary injury TBI mechanisms which could be alleviated by omega-3 PUFAs, it is still not clear which critical cellular targets, i.e. specific receptors, are the key drivers of the effects observed, and whether DHA would act more as a parent drug (therefore the efficacy is linked to specific metabolites) or as the intrinsic active compound. Furthermore, there is a need to try more varied regimes of administration (e.g. time window, duration and dose) which remain clinically relevant, and explore the long-term outcome, in several models of TBI. Considering that omega-3 PUFAs have a major potential to contribute to the resolution of persistent inflammation post-trauma, it will be important to design studies to understand better the impact of the treatment with these compounds on the systemic response to injury, e.g. the changes in the immune system which occur after trauma in general and TBI

in particular, and which are also long-lasting (Schwulst et al., 2013, Hazeldine et al., 2015). Finally, there is also much promise in the concept of using omega-3 PUFA in combination with rehabilitation after TBI (Wu et al., 2011, 2014), and this idea of support of neuroplasticity

**Appendix 1.1 - The average swim speed during the MWM probe trial for the young and aged fat-1 mice**



## Appendix 1.2 - Standard RM1 chow diet for WT mice with normal diet

### Rat and Mouse No.1 Maintenance

#### Calculated Analysis

NUTRIENTS			Total	Supp (9)	NUTRIENTS			Total	Supp (9)	
<b>Proximate Analysis</b>					<b>Glutamic Acid</b>					
Moisture (1)	%		10.00			%	3.17			
Crude Oil	%		2.71			%	1.20			
Crude Protein	%		14.38			%	0.56			
Crude Fibre	%		4.65			%				
Ash	%		6.00			%				
Nitrogen Free Extract	%		61.73			%	0.16			
<b>Digestibility Co-Efficients (7)</b>					<b>Macro Minerals</b>					
Digestible Crude Oil	%		2.47			%	0.73		0.63	
Digestible Crude Protein	%		12.92			%	0.52		0.04	
<b>Carbohydrates, Fibre and Non Starch Polysaccharides (NSP)</b>							%	0.24		
Total Dietary Fibre	%		17.05			%	0.28		0.04	
Pectin	%		1.52			%	0.25		0.19	
Hemicellulose	%		10.17			%	0.38		0.32	
Cellulose	%		4.32			%	0.67			
Lignin	%		1.68			%	0.23			
Starch	%		44.97		<b>Micro Minerals</b>					
Sugar	%		4.05				mg/kg	159.30	82.50	
<b>Energy (5)</b>							mg/kg	11.50	1.94	
Gross Energy	MJ/kg		14.74				mg/kg	72.44	19.22	
Digestible Energy (15)	MJ/kg		11.90				mg/kg	35.75		
Metabolisable Energy (15)	MJ/kg		10.74				µg/kg	634.10	550.00	
Atwater Fuel Energy (AFE)(8)	MJ/kg		13.75				µg/kg	1202.69	1085.00	
AFE from Oil	%		7.42				µg/kg	298.99	100.00	
AFE from Protein	%		17.49				mg/kg	10.49		
AFE from Carbohydrate	%		75.09		<b>Vitamins</b>					
<b>Fatty Acids</b>							mg/kg	0.16		
<b>Saturated Fatty Acids</b>							µg/kg	2566.38	2400.00	
C12:0 Lauric	%		0.02				iu/kg	8554.27	8000.00	
C14:0 Myristic	%		0.14				µg/kg	15.54	15.00	
C16:0 Palmitic	%		0.31				iu/kg	621.70	600.00	
C18:0 Stearic	%		0.04				mg/kg	76.45	56.82	
<b>Monounsaturated Fatty Acids</b>							iu/kg	84.10	62.50	
C14:1 Myristoleic	%		0.02				mg/kg	8.58	1.96	
C16:1 Palmitoleic	%		0.09				mg/kg	4.33	2.94	
C18:1 Oleic	%		0.77				mg/kg	4.81	0.98	
<b>Polyunsaturated Fatty Acids</b>							µg/kg	7.49	6.00	
C18:2(ω6) Linoleic	%		0.69				mg/kg	2.59		
C18:3(ω3) Linolenic	%		0.06				mg/kg	10.17	9.36	
C20:4(ω6) Arachidonic	%		0.13				mg/kg	0.79		
C22:5(ω3) Clupanodonic	%						mg/kg	61.32	2.45	
<b>Amino Acids</b>							mg/kg	20.17	5.80	
Arginine	%		0.91				mg/kg	1080.14	366.60	
Lysine (6)	%		0.66	0.07			mg/kg	2369.59		
Methionine	%		0.22	0.04			µg/kg	277.13		
Cystine	%		0.24		<b>Notes</b>					
Tryptophan	%		0.18		1. All values are calculated using a moisture basis of 10%.					
Histidine	%		0.35		Typical moisture levels will range between 9.5 - 11.5%.					
Threonine	%		0.49		2. a. Vitamin A includes Retinol and the Retinol equivalents of β-carotene					
Isoleucine	%		0.54		b. Retinol includes the Retinol equivalents of β-Carotene.					
Leucine	%		0.98		c. 0.48 µg Retinol = 1 µg β-carotene = 1.6 iu Vitamin A activity					
Phenylalanine	%		0.66		d. 1 µg Retinol = 3.33* iu Vitamin A activity					
Valine	%		0.69		e. 1 iu Vitamin A = 0.3 µg Retinol = 0.6 µg β-carotene					
Tyrosine	%		0.49		f. The standard analysis for Vitamin A does not detect β-carotene					
Taurine	%				3. 1 µg Cholecalciferol (D <sub>3</sub> ) = 40.0 iu Vitamin D					
Glycine	%		1.11		4. 1 mg all- <i>rac</i> -α-tocopherol = 1.1 iu Vitamin E activity					
Aspartic Acid	%		0.67		1 mg all- <i>rac</i> -α-tocopherol acetate = 1.0 iu Vitamin E activity					
					5. 1 MJ = 239.23 Kcalories = 239.23 Calories = 239,230 calories					
					6. These nutrients coming from natural raw materials such as cereals may have low availabilities due to the interactions with other compounds.					
					7. Based on in-vitro digestibility analysis.					
					8. AF Energy = Atwater Fuel Energy = ((CO%/100)*9000)+((CP%/100)*4000)+((NFE%/100)*4000)/239.23					
					9. Supplemented nutrients from manufactured and mined sources.					
					15. Calculated.					

**AIN-76A Western Diet**

**5342**

**DESCRIPTION**

AIN-76A Western Diet. Originally manufactured as D12079B.

Storage conditions are particularly critical to TestDiet® products, due to the absence of antioxidants or preservative agents. To provide maximum protection against possible changes during storage, store in a dry, cool location. Storage under refrigeration (2° C) is recommended. Maximum shelf life is six months. (If long term studies are involved, storing the diet at -20° C or colder may prolong shelf life.) Be certain to keep in air tight containers.

Product Forms Available*	Catalog #
1/2" Pellet	1810060
1/2" Pellet, Irradiated	1810061
3/16" Crumble	1811553
3/16" Short Cut Nugget, Irradiated	1811554

\*Other Forms Available On Request

INGREDIENTS (%)	
Sucrose	34.0476
Milk Fat	19.9692
Casein - Vitamin Tested	19.4700
Maltodextrin	9.9846
Corn Starch	4.9923
Powdered Cellulose	4.9923
AIN-76 Mineral Mix	3.4946
AIN-76A Vitamin Mix	0.9985
Corn Oil	0.9985
Calcium Carbonate	0.3994
DL-Methionine	0.2995
Choline Bitartrate	0.1997
Cholesterol	0.1498
Ethoxyquin (a preservative)	0.0040

**FEEDING DIRECTIONS**

Feed ad libitum. Plenty of fresh, clean water should be available at all times.

**CAUTION:**

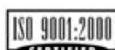
Perishable - store properly upon receipt. For laboratory animal use only; NOT for human consumption.

4/15/2013

**NUTRITIONAL PROFILE <sup>1</sup>**

<b>Protein, %</b>	<b>17.4</b>	<b>Minerals</b>	
Arginine, %	0.68	Calcium, %	0.69
Histidine, %	0.50	Phosphorus, %	0.56
Isoleucine, %	0.93	Potassium, %	0.36
Leucine, %	1.68	Magnesium, %	0.05
Lysine, %	1.42	Sodium, %	0.12
Methionine, %	0.80	Chloride, %	0.21
Cystine, %	0.07	Fluorine, ppm	0.0
Phenylalanine, %	0.93	Iron, ppm	39
Tyrosine, %	0.99	Zinc, ppm	35
Threonine, %	0.75	Manganese, ppm	58
Tryptophan, %	0.21	Copper, ppm	6.0
Valine, %	1.11	Cobalt, ppm	0.0
Alanine, %	0.54	Iodine, ppm	0.21
Aspartic Acid, %	1.25	Chromium, ppm	2.0
Glutamic Acid, %	3.98	Molybdenum, ppm	0.00
Glycine, %	0.38	Selenium, ppm	0.17
Proline, %	2.29		
Serine, %	1.07	<b>Vitamins</b>	
Taurine, %	0.00	Vitamin A, IU/g	10.2
		Vitamin D-3 (added), IU/g	1.0
<b>Fat, %</b>	<b>20.0</b>	Vitamin E, IU/kg	49.9
Cholesterol, ppm	2,027	Vitamin K, ppm	0.50
Linoleic Acid, %	1.07	Thiamin Hydrochloride, ppm	6.0
Linolenic Acid, %	0.10	Riboflavin, ppm	6.7
Arachidonic Acid, %	0.03	Niacin, ppm	30
Omega-3 Fatty Acids, %	0.21	Pantothenic Acid, ppm	16
Total Saturated Fatty A	12.09	Folic Acid, ppm	2.1
Total Monounsaturated Fatty Acids, %	4.61	Pyridoxine, ppm	5.8
Polyunsaturated Fatty Acids, %	0.58	Biotin, ppm	0.2
		Vitamin B-12, mcg/kg	14
<b>Fiber (max), %</b>	<b>5.0</b>	Choline Chloride, ppm	999
		Ascorbic Acid, ppm	0.0
<b>Carbohydrates, %</b>	<b>49.9</b>		
<b>Energy (kcal/g) <sup>2</sup></b>	<b>4.49</b>		
<b>From:</b>	<b>kcal</b>	<b>%</b>	
Protein	0.697	15.5	
Fat (ether extract)	1.804	40.1	
Carbohydrates	1.995	44.4	

1. Formulation based on calculated values from the latest ingredient analysis information. Since nutrient composition of natural ingredients varies and some nutrient loss will occur due to manufacturing processes, analysis will differ accordingly. Nutrients expressed as percent of ration on an As-Fed basis except where otherwise indicated.  
2. Energy (kcal/gm) - Sum of decimal fractions of protein, fat and carbohydrate x 4,9,4 kcal/gm respectively.





## References

- Abbott, A. (2003) 'Cell culture: biology's new dimension', *Nature*, 424(6951), pp. 870-2.
- Abdel-Wahab, B. A., Al-Qahtani, J. M. and El-Safy, S. A. (2015) 'Omega-3 polyunsaturated fatty acids in large doses attenuate seizures, cognitive impairment, and hippocampal oxidative DNA damage in young kindled rats', *Neurosci Lett*, 584, pp. 173-7.
- Abdul-Muneer, P. M., Chandra, N. and Haorah, J. (2015) 'Interactions of oxidative stress and neurovascular inflammation in the pathogenesis of traumatic brain injury', *Mol Neurobiol*, 51(3), pp. 966-79.
- Abdullah, L., Evans, J. E., Ferguson, S., Mouzon, B., Montague, H., Reed, J., Crynen, G., Emmerich, T., Crocker, M., Pelot, R., Mullan, M. and Crawford, F. (2014) 'Lipidomic analyses identify injury-specific phospholipid changes 3 mo after traumatic brain injury', *FASEB J*, 28(12), pp. 5311-21.
- Akbar, M., Calderon, F., Wen, Z. and Kim, H. Y. (2005) 'Docosahexaenoic acid: a positive modulator of Akt signaling in neuronal survival', *Proc Natl Acad Sci U S A*, 102(31), pp. 10858-63.
- Allen, V. J., Methven, L. and Gosney, M. A. (2013) 'Use of nutritional complete supplements in older adults with dementia: systematic review and meta-analysis of clinical outcomes', *Clin Nutr*, 32(6), pp. 950-7.
- Alvarez, J. I., Katayama, T. and Prat, A. (2013) 'Glial influence on the blood brain barrier', *Glia*, 61(12), pp. 1939-58.
- Anderson, D. K. and Hall, E. D. (1993) 'Pathophysiology of spinal cord trauma', *Ann Emerg Med*, 22(6), pp. 987-92.
- Anderson, M. A., Ao, Y. and Sofroniew, M. V. (2014) 'Heterogeneity of reactive astrocytes', *Neurosci Lett*, 565, pp. 23-9.
- Andrews, P. J., Sinclair, H. L., Rodriguez, A., Harris, B. A., Battison, C. G., Rhodes, J. K., Murray, G. D. and Collaborators, E. T. (2015) 'Hypothermia for Intracranial Hypertension after Traumatic Brain Injury', *N Engl J Med*, 373(25), pp. 2403-12.
- Andrews, P. J., Sinclair, L. H., Harris, B., Baldwin, M. J., Battison, C. G., Rhodes, J. K., Murray, G., De Backer, D. and collaborators, E. T. (2013) 'Study of therapeutic hypothermia (32 to 35°C) for intracranial pressure reduction after traumatic brain injury (the Eurotherm3235Trial): outcome of the pilot phase of the trial', *Trials*, 14, pp. 277.
- Antalis, C. J., Stevens, L. J., Campbell, M., Pazdro, R., Ericson, K. and Burgess, J. R. (2006) 'Omega-3 fatty acid status in attention-deficit/hyperactivity disorder', *Prostaglandins Leukot Essent Fatty Acids*, 75(4-5), pp. 299-308.
- Antoni, D., Burckel, H., Josset, E. and Noel, G. (2015) 'Three-dimensional cell culture: a breakthrough in vivo', *Int J Mol Sci*, 16(3), pp. 5517-27.
- Armario, A. and Nadal, R. (2013) 'Individual differences and the characterization of animal models of psychopathology: a strong challenge and a good opportunity', *Front Pharmacol*, 4, pp. 137.
- Avila-Muñoz, E. and Arias, C. (2014) 'When astrocytes become harmful: functional and inflammatory responses that contribute to Alzheimer's disease', *Ageing Res Rev*, 18, pp. 29-40.
- Axelsson, H. W., Winkler, T., Flygt, J., Djupsjö, A., Hånell, A. and Marklund, N. (2013) 'Plasticity of the contralateral motor cortex following focal traumatic brain injury in the rat', *Restor Neurol Neurosci*, 31(1), pp. 73-85.
- Azevedo, F. A., Carvalho, L. R., Grinberg, L. T., Farfel, J. M., Ferretti, R. E., Leite, R. E., Jacob Filho, W., Lent, R. and Herculano-Houzel, S. (2009) 'Equal numbers of neuronal and nonneuronal cells make the human brain an isometrically scaled-up primate brain', *J Comp Neurol*, 513(5), pp. 532-41.
- Bailes, J. E. and Mills, J. D. (2010) 'Docosahexaenoic acid reduces traumatic axonal injury in a rodent head injury model', *J Neurotrauma*, 27(9), pp. 1617-24.
- Bains, M. and Hall, E. D. (2012) 'Antioxidant therapies in traumatic brain and spinal cord injury', *Biochim Biophys Acta*, 1822(5), pp. 675-84.

- Bak, L. K., Schousboe, A. and Waagepetersen, H. S. (2006) 'The glutamate/GABA-glutamine cycle: aspects of transport, neurotransmitter homeostasis and ammonia transfer', *J Neurochem*, 98(3), pp. 641-53.
- Baldwin, S. A. and Scheff, S. W. (1996) 'Intermediate filament change in astrocytes following mild cortical contusion', *Glia*, 16(3), pp. 266-75.
- Bareyre, F. M., Kerschensteiner, M., Raineteau, O., Mettenleiter, T. C., Weinmann, O. and Schwab, M. E. (2004) 'The injured spinal cord spontaneously forms a new intraspinal circuit in adult rats', *Nat Neurosci*, 7(3), pp. 269-77.
- Bauer, I., Hughes, M., Rowsell, R., Cockerell, R., Pipingas, A., Crewther, S. and Crewther, D. (2014) 'Omega-3 supplementation improves cognition and modifies brain activation in young adults', *Hum Psychopharmacol*, 29(2), pp. 133-44.
- Bauman, R. A., Ling, G., Tong, L., Januszkiewicz, A., Agoston, D., Delanerolle, N., Kim, Y., Ritzel, D., Bell, R., Ecklund, J., Armonda, R., Bandak, F. and Parks, S. (2009) 'An introductory characterization of a combat-casualty-care relevant swine model of closed head injury resulting from exposure to explosive blast', *J Neurotrauma*, 26(6), pp. 841-60.
- Bazan, N. G. (2005) 'Neuroprotectin D1 (NPD1): a DHA-derived mediator that protects brain and retina against cell injury-induced oxidative stress', *Brain Pathol*, 15(2), pp. 159-66.
- Bazan, N. G. (2009a) 'Cellular and molecular events mediated by docosahexaenoic acid-derived neuroprotectin D1 signaling in photoreceptor cell survival and brain protection', *Prostaglandins Leukot Essent Fatty Acids*, 81(2-3), pp. 205-11.
- Bazan, N. G. (2009b) 'Neuroprotectin D1-mediated anti-inflammatory and survival signaling in stroke, retinal degenerations, and Alzheimer's disease', *J Lipid Res*, 50 Suppl, pp. S400-5.
- Bazinet, R. P. and Layé, S. (2014) 'Polyunsaturated fatty acids and their metabolites in brain function and disease', *Nat Rev Neurosci*, 15(12), pp. 771-85.
- Bedi, S. S., Walker, P. A., Shah, S. K., Jimenez, F., Thomas, C. P., Smith, P., Hetz, R. A., Xue, H., Pati, S., Dash, P. K. and Cox, C. S. (2013) 'Autologous bone marrow mononuclear cells therapy attenuates activated microglial/macrophage response and improves spatial learning after traumatic brain injury', *J Trauma Acute Care Surg*, 75(3), pp. 410-6.
- Begum, G., Kintner, D., Liu, Y., Cramer, S. W. and Sun, D. (2012) 'DHA inhibits ER Ca<sup>2+</sup> release and ER stress in astrocytes following in vitro ischemia', *J Neurochem*, 120(4), pp. 622-30.
- Begum, G., Yan, H. Q., Li, L., Singh, A., Dixon, C. E. and Sun, D. (2014) 'Docosahexaenoic acid reduces ER stress and abnormal protein accumulation and improves neuronal function following traumatic brain injury', *J Neurosci*, 34(10), pp. 3743-55.
- Belayev, L., Khoutorova, L., Atkins, K. D. and Bazan, N. G. (2009) 'Robust docosahexaenoic acid-mediated neuroprotection in a rat model of transient, focal cerebral ischemia', *Stroke*, 40(9), pp. 3121-6.
- Belayev, L., Marcheselli, V. L., Khoutorova, L., Rodriguez de Turco, E. B., Busto, R., Ginsberg, M. D. and Bazan, N. G. (2005) 'Docosahexaenoic acid complexed to albumin elicits high-grade ischemic neuroprotection', *Stroke*, 36(1), pp. 118-23.
- Benner, E. J., Luciano, D., Jo, R., Abdi, K., Paez-Gonzalez, P., Sheng, H., Warner, D. S., Liu, C., Eroglu, C. and Kuo, C. T. (2013) 'Protective astrogenesis from the SVZ niche after injury is controlled by Notch modulator Thbs4', *Nature*, 497(7449), pp. 369-73.
- Bermppohl, D., You, Z., Korsmeyer, S. J., Moskowitz, M. A. and Whalen, M. J. (2006) 'Traumatic brain injury in mice deficient in Bid: effects on histopathology and functional outcome', *J Cereb Blood Flow Metab*, 26(5), pp. 625-33.
- Bernardinelli, Y., Muller, D. and Nikonenko, I. (2014) 'Astrocyte-synapse structural plasticity', *Neural Plast*, 2014, pp. 232105.
- Bidmon, H. J., Jancsik, V., Schleicher, A., Hagemann, G., Witte, O. W., Woodhams, P. and Zilles, K. (1998) 'Structural alterations and changes in cytoskeletal proteins and proteoglycans after focal cortical ischemia', *Neuroscience*, 82(2), pp. 397-420.
- Bliss, T. V. and Collingridge, G. L. (1993) 'A synaptic model of memory: long-term potentiation in the hippocampus', *Nature*, 361(6407), pp. 31-9.

- Boone, M. D., Oren-Grinberg, A., Robinson, T. M., Chen, C. C. and Kasper, E. M. (2015) 'Mannitol or hypertonic saline in the setting of traumatic brain injury: What have we learned?', *Surg Neurol Int*, 6, pp. 177.
- Bousquet, M., Gue, K., Emond, V., Julien, P., Kang, J. X., Cicchetti, F. and Calon, F. (2011) 'Transgenic conversion of omega-6 into omega-3 fatty acids in a mouse model of Parkinson's disease', *J Lipid Res*, 52(2), pp. 263-71.
- Bowes, A. L. and Yip, P. K. (2014) 'Modulating inflammatory cell responses to spinal cord injury: all in good time', *J Neurotrauma*, 31(21), pp. 1753-66.
- Bowman, C. L., Ding, J. P., Sachs, F. and Sokabe, M. (1992) 'Mechanotransducing ion channels in astrocytes', *Brain Res*, 584(1-2), pp. 272-86.
- Breckenridge, W. C., Gombos, G. and Morgan, I. G. (1972) 'The lipid composition of adult rat brain synaptosomal plasma membranes', *Biochim Biophys Acta*, 266(3), pp. 695-707.
- Brenna, J. T. and Diau, G. Y. (2007) 'The influence of dietary docosahexaenoic acid and arachidonic acid on central nervous system polyunsaturated fatty acid composition', *Prostaglandins Leukot Essent Fatty Acids*, 77(5-6), pp. 247-50.
- Brizuela, M., Blizzard, C. A., Chuckowree, J. A., Dawkins, E., Gasperini, R. J., Young, K. M. and Dickson, T. C. (2015) 'The microtubule-stabilizing drug Epothilone D increases axonal sprouting following transection injury in vitro', *Mol Cell Neurosci*, 66(Pt B), pp. 129-40.
- Brody, D. L., Mac Donald, C., Kessens, C. C., Yuede, C., Parsadonian, M., Spinner, M., Kim, E., Schwetye, K. E., Holtzman, D. M. and Bayly, P. V. (2007) 'Electromagnetic controlled cortical impact device for precise, graded experimental traumatic brain injury', *J Neurotrauma*, 24(4), pp. 657-73.
- Bromley-Brits, K., Deng, Y. and Song, W. (2011) 'Morris water maze test for learning and memory deficits in Alzheimer's disease model mice', *J Vis Exp*, (53).
- Brown, A. M. and Ransom, B. R. (2007) 'Astrocyte glycogen and brain energy metabolism', *Glia*, 55(12), pp. 1263-71.
- Broxton, C. N. and Culotta, V. C. (2016) 'SOD Enzymes and Microbial Pathogens: Surviving the Oxidative Storm of Infection', *PLoS Pathog*, 12(1), pp. e1005295.
- Buccafusco JJ, e. (2009) *Methods of Behavior Analysis in Neuroscience. 2nd edition*. CRC Press/Taylor & Francis edn.: CRC Press/Taylor & Francis.
- Burckhardt, M., Herke, M., Wustmann, T., Watzke, S., Langer, G. and Fink, A. (2016) 'Omega-3 fatty acids for the treatment of dementia', *Cochrane Database Syst Rev*, 4, pp. CD009002.
- Burda, J. E., Bernstein, A. M. and Sofroniew, M. V. (2016) 'Astrocyte roles in traumatic brain injury', *Exp Neurol*, 275 Pt 3, pp. 305-15.
- Burgess, S., Abu-Laban, R. B., Slavik, R. S., Vu, E. N. and Zed, P. J. (2016) 'A Systematic Review of Randomized Controlled Trials Comparing Hypertonic Sodium Solutions and Mannitol for Traumatic Brain Injury: Implications for Emergency Department Management', *Ann Pharmacother*.
- Bush, T. G., Puvanachandra, N., Horner, C. H., Polito, A., Ostefeld, T., Svendsen, C. N., Mucke, L., Johnson, M. H. and Sofroniew, M. V. (1999) 'Leukocyte infiltration, neuronal degeneration, and neurite outgrowth after ablation of scar-forming, reactive astrocytes in adult transgenic mice', *Neuron*, 23(2), pp. 297-308.
- Butovsky, O., Ziv, Y., Schwartz, A., Landa, G., Talpalar, A. E., Pluchino, S., Martino, G. and Schwartz, M. (2006) 'Microglia activated by IL-4 or IFN-gamma differentially induce neurogenesis and oligodendrogenesis from adult stem/progenitor cells', *Mol Cell Neurosci*, 31(1), pp. 149-60.
- Calandria, J. M., Sharp, M. W. and Bazan, N. G. (2015) 'The Docosanoid Neuroprotectin D1 Induces TH-Positive Neuronal Survival in a Cellular Model of Parkinson's Disease', *Cell Mol Neurobiol*, 35(8), pp. 1127-36.
- Can, A., Dao, D. T., Arad, M., Terrillion, C. E., Piantadosi, S. C. and Gould, T. D. (2012) 'The mouse forced swim test', *J Vis Exp*, (59), pp. e3638.
- Cao, D., Kevala, K., Kim, J., Moon, H. S., Jun, S. B., Lovinger, D. and Kim, H. Y. (2009) 'Docosahexaenoic acid promotes hippocampal neuronal development and synaptic function', *J Neurochem*, 111(2), pp. 510-21.

- Carbonell, W. S., Maris, D. O., McCall, T. and Grady, M. S. (1998) 'Adaptation of the fluid percussion injury model to the mouse', *J Neurotrauma*, 15(3), pp. 217-29.
- Carey, M. E., Sarna, G. S. and Farrell, J. B. (1990) 'Brain edema following an experimental missile wound to the brain', *J Neurotrauma*, 7(1), pp. 13-20.
- Cederholm, T., Salem, N. and Palmblad, J. (2013) 'ω-3 fatty acids in the prevention of cognitive decline in humans', *Adv Nutr*, 4(6), pp. 672-6.
- Cernak, I. (2005) 'Animal models of head trauma', *NeuroRx*, 2(3), pp. 410-22.
- Cernak, I., Vink, R., Zapple, D. N., Cruz, M. I., Ahmed, F., Chang, T., Fricke, S. T. and Faden, A. I. (2004) 'The pathobiology of moderate diffuse traumatic brain injury as identified using a new experimental model of injury in rats', *Neurobiol Dis*, 17(1), pp. 29-43.
- Champeil-Potokar, G., Chaumontet, C., Guesnet, P., Lavielle, M. and Denis, I. (2006) 'Docosahexaenoic acid (22:6n-3) enrichment of membrane phospholipids increases gap junction coupling capacity in cultured astrocytes', *Eur J Neurosci*, 24(11), pp. 3084-90.
- Chang, P. K., Khatchadourian, A., McKinney, R. A. and Maysinger, D. (2015) 'Docosahexaenoic acid (DHA): a modulator of microglia activity and dendritic spine morphology', *J Neuroinflammation*, 12, pp. 34.
- Charles, A. C., Merrill, J. E., Dirksen, E. R. and Sanderson, M. J. (1991) 'Intercellular signaling in glial cells: calcium waves and oscillations in response to mechanical stimulation and glutamate', *Neuron*, 6(6), pp. 983-92.
- Chauhan, N. B., Gatto, R. and Chauhan, M. B. (2010) 'Neuroanatomical correlation of behavioral deficits in the CCI model of TBI', *J Neurosci Methods*, 190(1), pp. 1-9.
- Chen, C. T., Kitson, A. P., Hopperton, K. E., Domenichiello, A. F., Trépanier, M. O., Lin, L. E., Ermini, L., Post, M., Thies, F. and Bazinet, R. P. (2015) 'Plasma non-esterified docosahexaenoic acid is the major pool supplying the brain', *Sci Rep*, 5, pp. 15791.
- Chen, C. T., Liu, Z., Ouellet, M., Calon, F. and Bazinet, R. P. (2009) 'Rapid beta-oxidation of eicosapentaenoic acid in mouse brain: an in situ study', *Prostaglandins Leukot Essent Fatty Acids*, 80(2-3), pp. 157-63.
- Chen, W., Esselman, W. J., Jump, D. B. and Busik, J. V. (2005) 'Anti-inflammatory effect of docosahexaenoic acid on cytokine-induced adhesion molecule expression in human retinal vascular endothelial cells', *Invest Ophthalmol Vis Sci*, 46(11), pp. 4342-7.
- Chen, Y., Mao, H., Yang, K. H., Abel, T. and Meaney, D. F. (2014) 'A modified controlled cortical impact technique to model mild traumatic brain injury mechanics in mice', *Front Neurol*, 5, pp. 100.
- Chen, Z. J., Ughrin, Y. and Levine, J. M. (2002) 'Inhibition of axon growth by oligodendrocyte precursor cells', *Mol Cell Neurosci*, 20(1), pp. 125-39.
- Cheng, G., Kong, R. H., Zhang, L. M. and Zhang, J. N. (2012) 'Mitochondria in traumatic brain injury and mitochondrial-targeted multipotential therapeutic strategies', *Br J Pharmacol*, 167(4), pp. 699-719.
- Cherry, J. D., Olschowka, J. A. and O'Banion, M. K. (2014) 'Neuroinflammation and M2 microglia: the good, the bad, and the inflamed', *J Neuroinflammation*, 11, pp. 98.
- Chodobski, A., Zink, B. J. and Szmydynger-Chodobska, J. (2011) 'Blood-brain barrier pathophysiology in traumatic brain injury', *Trans Stroke Res*, 2(4), pp. 492-516.
- Chung, W. S., Allen, N. J. and Eroglu, C. (2015) 'Astrocytes Control Synapse Formation, Function, and Elimination', *Cold Spring Harb Perspect Biol*, 7(9), pp. a020370.
- Clark, R. E., Broadbent, N. J. and Squire, L. R. (2005) 'Hippocampus and remote spatial memory in rats', *Hippocampus*, 15(2), pp. 260-72.
- Clelland, C. D., Choi, M., Romberg, C., Clemenson, G. D., Fagniere, A., Tyers, P., Jessberger, S., Saksida, L. M., Barker, R. A., Gage, F. H. and Bussey, T. J. (2009) 'A functional role for adult hippocampal neurogenesis in spatial pattern separation', *Science*, 325(5937), pp. 210-3.
- Cole, J. T., Yarnell, A., Kean, W. S., Gold, E., Lewis, B., Ren, M., McMullen, D. C., Jacobowitz, D. M., Pollard, H. B., O'Neill, J. T., Grunberg, N. E., Dalgard, C. L., Frank, J. A. and Watson, W. D. (2011) 'Craniotomy: true sham for traumatic brain injury, or a sham of a sham?', *J Neurotrauma*, 28(3), pp. 359-69.

- Collard, C. D., Park, K. A., Montalto, M. C., Alapati, S., Buras, J. A., Stahl, G. L. and Colgan, S. P. (2002) 'Neutrophil-derived glutamate regulates vascular endothelial barrier function', *J Biol Chem*, 277(17), pp. 14801-11.
- Connor, W. E. (2000) 'Importance of n-3 fatty acids in health and disease', *Am J Clin Nutr*, 71(1 Suppl), pp. 171S-5S.
- Cooper, D. J., Rosenfeld, J. V., Murray, L., Arabi, Y. M., Davies, A. R., D'Urso, P., Kossmann, T., Ponsford, J., Seppelt, I., Reilly, P., Wolfe, R., Investigators, D. T. and Group, A. a. N. Z. I. C. S. C. T. (2011) 'Decompressive craniectomy in diffuse traumatic brain injury', *N Engl J Med*, 364(16), pp. 1493-502.
- Cornell-Bell, A. H., Finkbeiner, S. M., Cooper, M. S. and Smith, S. J. (1990) 'Glutamate induces calcium waves in cultured astrocytes: long-range glial signaling', *Science*, 247(4941), pp. 470-3.
- Cortez, S. C., McIntosh, T. K. and Noble, L. J. (1989) 'Experimental fluid percussion brain injury: vascular disruption and neuronal and glial alterations', *Brain Res*, 482(2), pp. 271-82.
- Cowley, T. R., O'Sullivan, J., Blau, C., Deighan, B. F., Jones, R., Kerskens, C., Richardson, J. C., Virley, D., Upton, N. and Lynch, M. A. (2012) 'Rosiglitazone attenuates the age-related changes in astrocytosis and the deficit in LTP', *Neurobiol Aging*, 33(1), pp. 162-75.
- Creed, J. A., DiLeonardi, A. M., Fox, D. P., Tessler, A. R. and Raghupathi, R. (2011) 'Concussive brain trauma in the mouse results in acute cognitive deficits and sustained impairment of axonal function', *J Neurotrauma*, 28(4), pp. 547-63.
- Crofts, J. J., Higham, D. J., Bosnell, R., Jbabdi, S., Matthews, P. M., Behrens, T. E. and Johansen-Berg, H. (2011) 'Network analysis detects changes in the contralesional hemisphere following stroke', *Neuroimage*, 54(1), pp. 161-9.
- Cunha, C., Brambilla, R. and Thomas, K. L. (2010) 'A simple role for BDNF in learning and memory?', *Front Mol Neurosci*, 3, pp. 1.
- Cutuli, D., De Bartolo, P., Caporali, P., Laricchiuta, D., Foti, F., Ronci, M., Rossi, C., Neri, C., Spalletta, G., Caltagirone, C., Farioli-Vecchioli, S. and Petrosini, L. (2014) 'n-3 polyunsaturated fatty acids supplementation enhances hippocampal functionality in aged mice', *Front Aging Neurosci*, 6, pp. 220.
- D'Hooge, R. and De Deyn, P. P. (2001) 'Applications of the Morris water maze in the study of learning and memory', *Brain Res Brain Res Rev*, 36(1), pp. 60-90.
- Dams-O'Connor, K., Gibbons, L. E., Bowen, J. D., McCurry, S. M., Larson, E. B. and Crane, P. K. (2013) 'Risk for late-life re-injury, dementia and death among individuals with traumatic brain injury: a population-based study', *J Neurol Neurosurg Psychiatry*, 84(2), pp. 177-82.
- De Bonis, P., Pompucci, A., Mangiola, A., D'Alessandris, Q. G., Rigante, L. and Anile, C. (2010) 'Decompressive craniectomy for the treatment of traumatic brain injury: does an age limit exist?', *J Neurosurg*, 112(5), pp. 1150-3.
- de Lau, L. M., Bornebroek, M., Witteman, J. C., Hofman, A., Koudstaal, P. J. and Breteler, M. M. (2005) 'Dietary fatty acids and the risk of Parkinson disease: the Rotterdam study', *Neurology*, 64(12), pp. 2040-5.
- de Urquiza, A. M., Liu, S., Sjöberg, M., Zetterström, R. H., Griffiths, W., Sjövall, J. and Perlmann, T. (2000) 'Docosahexaenoic acid, a ligand for the retinoid X receptor in mouse brain', *Science*, 290(5499), pp. 2140-4.
- de Vivo, L., Melone, M., Rothstein, J. D. and Conti, F. (2010) 'GLT-1 Promoter Activity in Astrocytes and Neurons of Mouse Hippocampus and Somatic Sensory Cortex', *Front Neuroanat*, 3, pp. 31.
- DeKosky, S. T., Blennow, K., Ikonomic, M. D. and Gandy, S. (2013) 'Acute and chronic traumatic encephalopathies: pathogenesis and biomarkers', *Nat Rev Neurol*, 9(4), pp. 192-200.
- Demar, J. C., Ma, K., Chang, L., Bell, J. M. and Rapoport, S. I. (2005) 'alpha-Linolenic acid does not contribute appreciably to docosahexaenoic acid within brain phospholipids of adult rats fed a diet enriched in docosahexaenoic acid', *J Neurochem*, 94(4), pp. 1063-76.
- Dempsey, R. J., Başkaya, M. K. and Doğan, A. (2000) 'Attenuation of brain edema, blood-brain barrier breakdown, and injury volume by ifenprodil, a polyamine-site N-methyl-D-aspartate receptor antagonist, after experimental traumatic brain injury in rats', *Neurosurgery*, 47(2), pp. 399-404; discussion 404-6.

- Desai, A., Kevala, K. and Kim, H. Y. (2014) 'Depletion of brain docosahexaenoic acid impairs recovery from traumatic brain injury', *PLoS One*, 9(1), pp. e86472.
- Desai, A., Nierenberg, D. W. and Duhaime, A. C. (2010) 'Akathisia after mild traumatic head injury', *J Neurosurg Pediatr*, 5(5), pp. 460-4.
- Dewar, D., Underhill, S. M. and Goldberg, M. P. (2003) 'Oligodendrocytes and ischemic brain injury', *J Cereb Blood Flow Metab*, 23(3), pp. 263-74.
- Dixon, C. E., Clifton, G. L., Lighthall, J. W., Yaghamai, A. A. and Hayes, R. L. (1991) 'A controlled cortical impact model of traumatic brain injury in the rat', *J Neurosci Methods*, 39(3), pp. 253-62.
- Domercq, M., Vázquez-Villoldo, N. and Matute, C. (2013) 'Neurotransmitter signaling in the pathophysiology of microglia', *Front Cell Neurosci*, 7, pp. 49.
- Drapeau, E., Mayo, W., Aourousseau, C., Le Moal, M., Piazza, P. V. and Abrous, D. N. (2003) 'Spatial memory performances of aged rats in the water maze predict levels of hippocampal neurogenesis', *Proc Natl Acad Sci U S A*, 100(24), pp. 14385-90.
- Drew, L. J., Fusi, S. and Hen, R. (2013) 'Adult neurogenesis in the mammalian hippocampus: why the dentate gyrus?', *Learn Mem*, 20(12), pp. 710-29.
- Dyall, S. C. (2015) 'Long-chain omega-3 fatty acids and the brain: a review of the independent and shared effects of EPA, DPA and DHA', *Front Aging Neurosci*, 7, pp. 52.
- Dyall, S. C., Michael, G. J., Whelpton, R., Scott, A. G. and Michael-Titus, A. T. (2007) 'Dietary enrichment with omega-3 polyunsaturated fatty acids reverses age-related decreases in the GluR2 and NR2B glutamate receptor subunits in rat forebrain', *Neurobiol Aging*, 28(3), pp. 424-39.
- Dyall, S. C. and Michael-Titus, A. T. (2008) 'Neurological benefits of omega-3 fatty acids', *Neuromolecular Med*, 10(4), pp. 219-35.
- Eady, T. N., Belayev, L., Khoutorova, L., Atkins, K. D., Zhang, C. and Bazan, N. G. (2012a) 'Docosahexaenoic acid signaling modulates cell survival in experimental ischemic stroke penumbra and initiates long-term repair in young and aged rats', *PLoS One*, 7(10), pp. e46151.
- Eady, T. N., Khoutorova, L., Atkins, K. D., Bazan, N. G. and Belayev, L. (2012b) 'Docosahexaenoic acid complexed to human albumin in experimental stroke: neuroprotective efficacy with a wide therapeutic window', *Exp Transl Stroke Med*, 4(1), pp. 19.
- East, E., Golding, J. P. and Phillips, J. B. (2009) 'A versatile 3D culture model facilitates monitoring of astrocytes undergoing reactive gliosis', *J Tissue Eng Regen Med*, 3(8), pp. 634-46.
- Edwards, P., Arango, M., Balica, L., Cottingham, R., El-Sayed, H., Farrell, B., Fernandes, J., Gogichaisvili, T., Golden, N., Hartzenberg, B., Husain, M., Ulloa, M. I., Jerbi, Z., Khamis, H., Komolafe, E., Laloë, V., Lomas, G., Ludwig, S., Mazairac, G., Muñoz Sánchez, M. e. L., Nasi, L., Ollidashi, F., Plunkett, P., Roberts, I., Sandercock, P., Shakur, H., Soler, C., Stocker, R., Svoboda, P., Trenkler, S., Venkataramana, N. K., Wasserberg, J., Yates, D., Yutthakasemsunt, S. and collaborators, C. t. (2005) 'Final results of MRC CRASH, a randomised placebo-controlled trial of intravenous corticosteroid in adults with head injury-outcomes at 6 months', *Lancet*, 365(9475), pp. 1957-9.
- Effgen, G. B., Hue, C. D., Vogel, E., Panzer, M. B., Meaney, D. F., Bass, C. R. and Morrison, B. (2012) 'A Multiscale Approach to Blast Neurotrauma Modeling: Part II: Methodology for Inducing Blast Injury to in vitro Models', *Front Neurol*, 3, pp. 23.
- Effgen, G. B., Vogel, E. W., Lynch, K. A., Lobel, A., Hue, C. D., Meaney, D. F., Bass, C. R. and Morrison, B. (2014) 'Isolated primary blast alters neuronal function with minimal cell death in organotypic hippocampal slice cultures', *J Neurotrauma*, 31(13), pp. 1202-10.
- Ellis, E. F., McKinney, J. S., Willoughby, K. A., Liang, S. and Povlishock, J. T. (1995) 'A new model for rapid stretch-induced injury of cells in culture: characterization of the model using astrocytes', *J Neurotrauma*, 12(3), pp. 325-39.
- Emmerich, T., Abdullah, L., Ojo, J., Mouzon, B., Nguyen, T., Laco, G. S., Crynen, G., Evans, J. E., Reed, J., Mullan, M. and Crawford, F. (2016) 'Mild TBI Results in a Long-Term Decrease in Circulating Phospholipids in a Mouse Model of Injury', *Neuromolecular Med*.
- Eriksson, P. S., Perfilieva, E., Björk-Eriksson, T., Alborn, A. M., Nordborg, C., Peterson, D. A. and Gage, F. H. (1998) 'Neurogenesis in the adult human hippocampus', *Nat Med*, 4(11), pp. 1313-7.
- Ernst, A. and Frisén, J. (2015) 'Adult neurogenesis in humans - common and unique traits in mammals', *PLoS Biol*, 13(1), pp. e1002045.

- Estrada, F. S., Hernandez, V. S., Medina, M. P., Corona-Morales, A. A., Gonzalez-Perez, O., Vega-Gonzalez, A. and Zhang, L. (2009) 'Astrogliosis is temporally correlated with enhanced neurogenesis in adult rat hippocampus following a glucoprivic insult', *Neurosci Lett*, 459(3), pp. 109-14.
- Everts, S. and Davis, J. H. (2000) '<sup>1</sup>H and (<sup>13</sup>C NMR of multilamellar dispersions of polyunsaturated (22:6) phospholipids', *Biophys J*, 79(2), pp. 885-97.
- Farace, E. and Alves, W. M. (2000) 'Do women fare worse? A metaanalysis of gender differences in outcome after traumatic brain injury', *Neurosurg Focus*, 8(1), pp. e6.
- Farina, C., Aloisi, F. and Meinl, E. (2007) 'Astrocytes are active players in cerebral innate immunity', *Trends Immunol*, 28(3), pp. 138-45.
- Farooqui, A. A., Horrocks, L. A. and Farooqui, T. (2007) 'Modulation of inflammation in brain: a matter of fat', *J Neurochem*, 101(3), pp. 577-99.
- Fedorova, I., Hussein, N., Di Martino, C., Moriguchi, T., Hoshiba, J., Majchrzak, S. and Salem, N. (2007) 'An n-3 fatty acid deficient diet affects mouse spatial learning in the Barnes circular maze', *Prostaglandins Leukot Essent Fatty Acids*, 77(5-6), pp. 269-77.
- Feigenbaum, J. J., Bergmann, F., Richmond, S. A., Mechoulam, R., Nadler, V., Kloog, Y. and Sokolovsky, M. (1989) 'Nonpsychotropic cannabinoid acts as a functional N-methyl-D-aspartate receptor blocker', *Proc Natl Acad Sci U S A*, 86(23), pp. 9584-7.
- Feller, S. E. (2008) 'Acyl chain conformations in phospholipid bilayers: a comparative study of docosahexaenoic acid and saturated fatty acids', *Chem Phys Lipids*, 153(1), pp. 76-80.
- Feuerstein, G. Z., Liu, T. and Barone, F. C. (1994) 'Cytokines, inflammation, and brain injury: role of tumor necrosis factor-alpha', *Cerebrovasc Brain Metab Rev*, 6(4), pp. 341-60.
- Fields, R. D. (2008) 'White matter in learning, cognition and psychiatric disorders', *Trends Neurosci*, 31(7), pp. 361-70.
- Figuroa, J. D., Cordero, K., Baldeosingh, K., Torrado, A. I., Walker, R. L., Miranda, J. D. and Leon, M. D. (2012) 'Docosahexaenoic acid pretreatment confers protection and functional improvements after acute spinal cord injury in adult rats', *J Neurotrauma*, 29(3), pp. 551-66.
- Fitch, M. T. and Silver, J. (2008) 'CNS injury, glial scars, and inflammation: Inhibitory extracellular matrices and regeneration failure', *Exp Neurol*, 209(2), pp. 294-301.
- Fleminger, S., Oliver, D. L., Lovestone, S., Rabe-Hesketh, S. and Giora, A. (2003) 'Head injury as a risk factor for Alzheimer's disease: the evidence 10 years on; a partial replication', *J Neurol Neurosurg Psychiatry*, 74(7), pp. 857-62.
- Fletcher, D. A. and Mullins, R. D. (2010) 'Cell mechanics and the cytoskeleton', *Nature*, 463(7280), pp. 485-92.
- Flierl, M. A., Stahel, P. F., Beauchamp, K. M., Morgan, S. J., Smith, W. R. and Shohami, E. (2009) 'Mouse closed head injury model induced by a weight-drop device', *Nat Protoc*, 4(9), pp. 1328-37.
- Flynn, L. M., Rhodes, J. and Andrews, P. J. (2015) 'Therapeutic Hypothermia Reduces Intracranial Pressure and Partial Brain Oxygen Tension in Patients with Severe Traumatic Brain Injury: Preliminary Data from the Eurotherm3235 Trial', *Ther Hypothermia Temp Manag*, 5(3), pp. 143-51.
- Foda, M. A. and Marmarou, A. (1994) 'A new model of diffuse brain injury in rats. Part II: Morphological characterization', *J Neurosurg*, 80(2), pp. 301-13.
- FOLCH, J., LEES, M. and SLOANE STANLEY, G. H. (1957) 'A simple method for the isolation and purification of total lipides from animal tissues', *J Biol Chem*, 226(1), pp. 497-509.
- Foley, R. N. (2008) 'Erythropoietin: physiology and molecular mechanisms', *Heart Fail Rev*, 13(4), pp. 405-14.
- Fournier, A. J., Hogan, J. D., Rajbhandari, L., Shrestha, S., Venkatesan, A. and Ramesh, K. T. (2015) 'Changes in Neurofilament and Microtubule Distribution following Focal Axon Compression', *PLoS One*, 10(6), pp. e0131617.
- Fox, G. B., Fan, L., Levasseur, R. A. and Faden, A. I. (1998) 'Sustained sensory/motor and cognitive deficits with neuronal apoptosis following controlled cortical impact brain injury in the mouse', *J Neurotrauma*, 15(8), pp. 599-614.

- Fox, G. B., LeVasseur, R. A. and Faden, A. I. (1999) 'Behavioral responses of C57BL/6, FVB/N, and 129/SvEMS mouse strains to traumatic brain injury: implications for gene targeting approaches to neurotrauma', *J Neurotrauma*, 16(5), pp. 377-89.
- Freemantle, E., Vandal, M., Tremblay-Mercier, J., Tremblay, S., Blachère, J. C., Bégin, M. E., Brenna, J. T., Windust, A. and Cunnane, S. C. (2006) 'Omega-3 fatty acids, energy substrates, and brain function during aging', *Prostaglandins Leukot Essent Fatty Acids*, 75(3), pp. 213-20.
- Furuhashi, M., Ishimura, S., Ota, H. and Miura, T. (2011) 'Lipid chaperones and metabolic inflammation', *Int J Inflamm*, 2011, pp. 642612.
- Gamoh, S., Hashimoto, M., Hossain, S. and Masumura, S. (2001) 'Chronic administration of docosahexaenoic acid improves the performance of radial arm maze task in aged rats', *Clin Exp Pharmacol Physiol*, 28(4), pp. 266-70.
- Gamoh, S., Hashimoto, M., Sugioka, K., Shahdat Hossain, M., Hata, N., Misawa, Y. and Masumura, S. (1999) 'Chronic administration of docosahexaenoic acid improves reference memory-related learning ability in young rats', *Neuroscience*, 93(1), pp. 237-41.
- Gardner, R. C., Burke, J. F., Nettiksimmons, J., Kaup, A., Barnes, D. E. and Yaffe, K. (2014) 'Dementia risk after traumatic brain injury vs nonbrain trauma: the role of age and severity', *JAMA Neurol*, 71(12), pp. 1490-7.
- Gasquoine, P. G. (1997) 'Postconcussion symptoms', *Neuropsychol Rev*, 7(2), pp. 77-85.
- Gatto, R., Chauhan, M. and Chauhan, N. (2015) 'Anti-edema effects of rhEpo in experimental traumatic brain injury', *Restor Neurol Neurosci*, 33(6), pp. 927-41.
- Gawrisch, K., Eldho, N. V. and Holte, L. L. (2003) 'The structure of DHA in phospholipid membranes', *Lipids*, 38(4), pp. 445-52.
- Gennarelli, T. A. (1994) 'Animate models of human head injury', *J Neurotrauma*, 11(4), pp. 357-68.
- Gennarelli, T. A., Thibault, L. E., Adams, J. H., Graham, D. I., Thompson, C. J. and Marcincin, R. P. (1982) 'Diffuse axonal injury and traumatic coma in the primate', *Ann Neurol*, 12(6), pp. 564-74.
- German, O. L., Insua, M. F., Gentili, C., Rotstein, N. P. and Politi, L. E. (2006) 'Docosahexaenoic acid prevents apoptosis of retina photoreceptors by activating the ERK/MAPK pathway', *J Neurochem*, 98(5), pp. 1507-20.
- Gladman, S. J., Huang, W., Lim, S. N., Dyal, S. C., Boddy, S., Kang, J. X., Knight, M. M., Priestley, J. V. and Michael-Titus, A. T. (2012) 'Improved outcome after peripheral nerve injury in mice with increased levels of endogenous  $\omega$ -3 polyunsaturated fatty acids', *J Neurosci*, 32(2), pp. 563-71.
- Gladman, S. J., Ward, R. E., Michael-Titus, A. T., Knight, M. M. and Priestley, J. V. (2010) 'The effect of mechanical strain or hypoxia on cell death in subpopulations of rat dorsal root ganglion neurons in vitro', *Neuroscience*, 171(2), pp. 577-87.
- Goldstein, F. C., Caveney, A. F., Hertzberg, V. S., Silbergleit, R., Yeatts, S. D., Palesch, Y. Y., Levin, H. S. and Wright, D. W. (2016) 'Very Early Administration of Progesterone Does Not Improve Neuropsychological Outcomes in Subjects with Moderate to Severe Traumatic Brain Injury', *J Neurotrauma*.
- Gouvier, W. D., Cubic, B., Jones, G., Brantley, P. and Cutlip, Q. (1992) 'Postconcussion symptoms and daily stress in normal and head-injured college populations', *Arch Clin Neuropsychol*, 7(3), pp. 193-211.
- Graber, R., Sumida, C. and Nunez, E. A. (1994) 'Fatty acids and cell signal transduction', *J Lipid Mediat Cell Signal*, 9(2), pp. 91-116.
- Grintal, B., Champeil-Potokar, G., Lavialle, M., Vancassel, S., Breton, S. and Denis, I. (2009) 'Inhibition of astroglial glutamate transport by polyunsaturated fatty acids: evidence for a signalling role of docosahexaenoic acid', *Neurochem Int*, 54(8), pp. 535-43.
- Groswasser, Z., Cohen, M. and Keren, O. (1998) 'Female TBI patients recover better than males', *Brain Inj*, 12(9), pp. 805-8.
- Guo, Q., Sayeed, I., Baronne, L. M., Hoffman, S. W., Guennoun, R. and Stein, D. G. (2006) 'Progesterone administration modulates AQP4 expression and edema after traumatic brain injury in male rats', *Exp Neurol*, 198(2), pp. 469-78.
- Gupta, S., Knight, A. G., Keller, J. N. and Bruce-Keller, A. J. (2012) 'Saturated long-chain fatty acids activate inflammatory signaling in astrocytes', *J Neurochem*, 120(6), pp. 1060-71.



- Gustavsson, A., Svensson, M., Jacobi, F., Allgulander, C., Alonso, J., Beghi, E., Dodel, R., Ekman, M., Faravelli, C., Fratiglioni, L., Gannon, B., Jones, D. H., Jennum, P., Jordanova, A., Jönsson, L., Karampampa, K., Knapp, M., Kobelt, G., Kurth, T., Lieb, R., Linde, M., Ljungcrantz, C., Maercker, A., Melin, B., Moscarelli, M., Musayev, A., Norwood, F., Preisig, M., Pugliatti, M., Rehm, J., Salvador-Carulla, L., Schlehofer, B., Simon, R., Steinhausen, H. C., Stovner, L. J., Vallat, J. M., Van den Bergh, P., den Bergh, P. V., van Os, J., Vos, P., Xu, W., Wittchen, H. U., Jönsson, B., Olesen, J. and Group, C. S. (2011) 'Cost of disorders of the brain in Europe 2010', *Eur Neuropsychopharmacol*, 21(10), pp. 718-79.
- Gómez Candela, C., Bermejo López, L. M. and Loria Kohen, V. (2011) 'Importance of a balanced omega 6/omega 3 ratio for the maintenance of health: nutritional recommendations', *Nutr Hosp*, 26(2), pp. 323-9.
- Gómez-Nicola, D., Fransen, N. L., Suzzi, S. and Perry, V. H. (2013) 'Regulation of microglial proliferation during chronic neurodegeneration', *J Neurosci*, 33(6), pp. 2481-93.
- Göriz, C., Mauch, D. H., Nägler, K. and Pfrieder, F. W. (2002) 'Role of glia-derived cholesterol in synaptogenesis: new revelations in the synapse-glia affair', *J Physiol Paris*, 96(3-4), pp. 257-63.
- Haddad, S. H. and Arabi, Y. M. (2012) 'Critical care management of severe traumatic brain injury in adults', *Scand J Trauma Resusc Emerg Med*, 20, pp. 12.
- Ham, T. E. and Sharp, D. J. (2012) 'How can investigation of network function inform rehabilitation after traumatic brain injury?', *Curr Opin Neurol*, 25(6), pp. 662-9.
- Hamilton, N. B. and Attwell, D. (2010) 'Do astrocytes really exocytose neurotransmitters?', *Nat Rev Neurosci*, 11(4), pp. 227-38.
- Hamm, R. J., Temple, M. D., Pike, B. R. and Ellis, E. F. (1996) 'The effect of postinjury administration of polyethylene glycol-conjugated superoxide dismutase (pegorgotein, Dismutec) or lidocaine on behavioral function following fluid-percussion brain injury in rats', *J Neurotrauma*, 13(6), pp. 325-32.
- Han, X., Chen, M., Wang, F., Windrem, M., Wang, S., Shanz, S., Xu, Q., Oberheim, N. A., Bekar, L., Betstadt, S., Silva, A. J., Takano, T., Goldman, S. A. and Nedergaard, M. (2013) 'Forebrain engraftment by human glial progenitor cells enhances synaptic plasticity and learning in adult mice', *Cell Stem Cell*, 12(3), pp. 342-53.
- Han, Y. M., Jeong, M., Park, J. M., Kim, M. Y., Go, E. J., Cha, J. Y., Kim, K. J. and Hahm, K. B. (2016) 'The  $\omega$ -3 polyunsaturated fatty acids prevented colitis-associated carcinogenesis through blocking dissociation of  $\beta$ -catenin complex, inhibiting COX-2 through repressing NF- $\kappa$ B, and inducing 15-prostaglandin dehydrogenase', *Oncotarget*.
- Hanisch, U. K. (2013) 'Functional diversity of microglia - how heterogeneous are they to begin with?', *Front Cell Neurosci*, 7, pp. 65.
- Hanisch, U. K. and Kettenmann, H. (2007) 'Microglia: active sensor and versatile effector cells in the normal and pathologic brain', *Nat Neurosci*, 10(11), pp. 1387-94.
- Harada, C. N., Natelson Love, M. C. and Triebel, K. L. (2013) 'Normal cognitive aging', *Clin Geriatr Med*, 29(4), pp. 737-52.
- Harada, K., Kamiya, T. and Tsuboi, T. (2015) 'Gliotransmitter Release from Astrocytes: Functional, Developmental, and Pathological Implications in the Brain', *Front Neurosci*, 9, pp. 499.
- Harish, G., Mahadevan, A., Pruthi, N., Sreenivasamurthy, S. K., Puttamalles, V. N., Keshava Prasad, T. S., Shankar, S. K. and Srinivas Bharath, M. M. (2015) 'Characterization of traumatic brain injury in human brains reveals distinct cellular and molecular changes in contusion and pericontusion', *J Neurochem*, 134(1), pp. 156-72.
- Harris, N. G., Mironova, Y. A., Hovda, D. A. and Sutton, R. L. (2010) 'Chondroitinase ABC enhances pericontusion axonal sprouting but does not confer robust improvements in behavioral recovery', *J Neurotrauma*, 27(11), pp. 1971-82.
- Harrison, J. L., Rowe, R. K., Ellis, T. W., Yee, N. S., O'Hara, B. F., Adelson, P. D. and Lifshitz, J. (2015) 'Resolvins AT-D1 and E1 differentially impact functional outcome, post-traumatic sleep, and microglial activation following diffuse brain injury in the mouse', *Brain Behav Immun*, 47, pp. 131-40.

- Harvey, L. D., Yin, Y., Attarwala, I. Y., Begum, G., Deng, J., Yan, H. Q., Dixon, C. E. and Sun, D. (2015) 'Administration of DHA Reduces Endoplasmic Reticulum Stress-Associated Inflammation and Alters Microglial or Macrophage Activation in Traumatic Brain Injury', *ASN Neuro*, 7(6).
- Hayes, R. L., Stalhammar, D., Povlishock, J. T., Allen, A. M., Galinat, B. J., Becker, D. P. and Stonnington, H. H. (1987) 'A new model of concussive brain injury in the cat produced by extradural fluid volume loading: II. Physiological and neuropathological observations', *Brain Inj*, 1(1), pp. 93-112.
- Hazeldine, J., Lord, J. M. and Belli, A. (2015) 'Traumatic Brain Injury and Peripheral Immune Suppression: Primer and Prospectus', *Front Neurol*, 6, pp. 235.
- He, C., Qu, X., Cui, L., Wang, J. and Kang, J. X. (2009) 'Improved spatial learning performance of fat-1 mice is associated with enhanced neurogenesis and neuritogenesis by docosahexaenoic acid', *Proc Natl Acad Sci US A*, 106(27), pp. 11370-5.
- Hellewell, S. C., Yan, E. B., Alwis, D. S., Bye, N. and Morganti-Kossmann, M. C. (2013) 'Erythropoietin improves motor and cognitive deficit, axonal pathology, and neuroinflammation in a combined model of diffuse traumatic brain injury and hypoxia, in association with upregulation of the erythropoietin receptor', *J Neuroinflammation*, 10, pp. 156.
- Helmes, E., Østbye, T. and Steenhuis, R. E. (2011) 'Incremental contribution of reported previous head injury to the prediction of diagnosis and cognitive functioning in older adults', *Brain Inj*, 25(4), pp. 338-47.
- Heras-Sandoval, D., Pedraza-Chaverri, J. and Pérez-Rojas, J. M. (2016) 'Role of docosahexaenoic acid in the modulation of glial cells in Alzheimer's disease', *J Neuroinflammation*, 13(1), pp. 61.
- Hernandez-Ontiveros, D. G., Tajiri, N., Acosta, S., Giunta, B., Tan, J. and Borlongan, C. V. (2013) 'Microglia activation as a biomarker for traumatic brain injury', *Front Neurol*, 4, pp. 30.
- Hibbeln, J. R. and Davis, J. M. (2009) 'Considerations regarding neuropsychiatric nutritional requirements for intakes of omega-3 highly unsaturated fatty acids', *Prostaglandins Leukot Essent Fatty Acids*, 81(2-3), pp. 179-86.
- Hickey, W. F. and Kimura, H. (1988) 'Perivascular microglial cells of the CNS are bone marrow-derived and present antigen in vivo', *Science*, 239(4837), pp. 290-2.
- Hill, C. S., Coleman, M. P. and Menon, D. K. (2016) 'Traumatic Axonal Injury: Mechanisms and Translational Opportunities', *Trends Neurosci*, 39(5), pp. 311-24.
- Himmelseher, S. and Durieux, M. E. (2005) 'Revising a dogma: ketamine for patients with neurological injury?', *Anesth Analg*, 101(2), pp. 524-34, table of contents.
- Hong, S. H., Belayev, L., Khoutorova, L., Obenaus, A. and Bazan, N. G. (2014) 'Docosahexaenoic acid confers enduring neuroprotection in experimental stroke', *J NeuroSci*, 338(1-2), pp. 135-41.
- Hong, S. H., Khoutorova, L., Bazan, N. G. and Belayev, L. (2015) 'Docosahexaenoic acid improves behavior and attenuates blood-brain barrier injury induced by focal cerebral ischemia in rats', *Exp Transl Stroke Med*, 7(1), pp. 3.
- Hu, X., Zhang, F., Leak, R. K., Zhang, W., Iwai, M., Stetler, R. A., Dai, Y., Zhao, A., Gao, Y. and Chen, J. (2013) 'Transgenic overproduction of omega-3 polyunsaturated fatty acids provides neuroprotection and enhances endogenous neurogenesis after stroke', *Curr Mol Med*, 13(9), pp. 1465-73.
- Huang, W., Wang, B., Li, X. and Kang, J. X. (2015) 'Endogenously elevated n-3 polyunsaturated fatty acids alleviate acute ethanol-induced liver steatosis', *Biofactors*, 41(6), pp. 453-62.
- Huang, W. L., King, V. R., Curran, O. E., Dyall, S. C., Ward, R. E., Lal, N., Priestley, J. V. and Michael-Titus, A. T. (2007) 'A combination of intravenous and dietary docosahexaenoic acid significantly improves outcome after spinal cord injury', *Brain*, 130(Pt 11), pp. 3004-19.
- Ichai, C., Armando, G., Orban, J. C., Berthier, F., Rami, L., Samat-Long, C., Grimaud, D. and Leverage, X. (2009) 'Sodium lactate versus mannitol in the treatment of intracranial hypertensive episodes in severe traumatic brain-injured patients', *Intensive Care Med*, 35(3), pp. 471-9.
- Igarashi, H., Huber, V. J., Tsujita, M. and Nakada, T. (2011) 'Pretreatment with a novel aquaporin 4 inhibitor, TGN-020, significantly reduces ischemic cerebral edema', *NeuroSci*, 32(1), pp. 113-6.
- Insua, M. F., Garelli, A., Rotstein, N. P., German, O. L., Arias, A. and Politi, L. E. (2003) 'Cell cycle regulation in retinal progenitors by glia-derived neurotrophic factor and docosahexaenoic acid', *Invest Ophthalmol Vis Sci*, 44(5), pp. 2235-44.

- Irimia, A., Wang, B., Aylward, S. R., Prastawa, M. W., Pace, D. F., Gerig, G., Hovda, D. A., Kikinis, R., Vespa, P. M. and Van Horn, J. D. (2012) 'Neuroimaging of structural pathology and connectomics in traumatic brain injury: Toward personalized outcome prediction', *Neuroimage Clin*, 1(1), pp. 1-17.
- Ito, D., Tanaka, K., Suzuki, S., Dembo, T. and Fukuuchi, Y. (2001) 'Enhanced expression of Iba1, ionized calcium-binding adapter molecule 1, after transient focal cerebral ischemia in rat brain', *Stroke*, 32(5), pp. 1208-15.
- J, B. J. (2009) *Methods of Behavior Analysis in Neuroscience. Frontiers in Neuroscience* 2nd Edition edn. Boca Raton (FL): CRC Press/Taylor & Francis.
- Jagannatha, A. T., Kamath, S., Devi, I. and Rao, U. G. (2016) '376 The Salt Versus Sugar Debate: Urinary Sodium Losses Following Hypertonic Saline Administration Curtails Its Superior Osmolar Effect in Comparison to Mannitol in Severe Traumatic Brain Injury', *Neurosurgery*, 63 Suppl 1, pp. 212.
- Janssen, C. I. and Kiliaan, A. J. (2014) 'Long-chain polyunsaturated fatty acids (LCPUFA) from genesis to senescence: the influence of LCPUFA on neural development, aging, and neurodegeneration', *Prog Lipid Res*, 53, pp. 1-17.
- Janssen, C. I., Zerbi, V., Mutsaers, M. P., de Jong, B. S., Wiesmann, M., Arnoldussen, I. A., Geenen, B., Heerschap, A., Muskiet, F. A., Jouni, Z. E., van Tol, E. A., Gross, G., Homberg, J. R., Berg, B. M. and Kiliaan, A. J. (2015) 'Impact of dietary n-3 polyunsaturated fatty acids on cognition, motor skills and hippocampal neurogenesis in developing C57BL/6J mice', *J Nutr Biochem*, 26(1), pp. 24-35.
- Jarrard, L. E. (1993) 'On the role of the hippocampus in learning and memory in the rat', *Behav Neural Biol*, 60(1), pp. 9-26.
- Jia, Q., Lupton, J. R., Smith, R., Weeks, B. R., Callaway, E., Davidson, L. A., Kim, W., Fan, Y. Y., Yang, P., Newman, R. A., Kang, J. X., McMurray, D. N. and Chapkin, R. S. (2008) 'Reduced colitis-associated colon cancer in Fat-1 (n-3 fatty acid desaturase) transgenic mice', *Cancer Res*, 68(10), pp. 3985-91.
- Jin, X., Ishii, H., Bai, Z., Itokazu, T. and Yamashita, T. (2012) 'Temporal changes in cell marker expression and cellular infiltration in a controlled cortical impact model in adult male C57BL/6 mice', *PLoS One*, 7(7), pp. e41892.
- Johnson, V. E., Stewart, J. E., Begbie, F. D., Trojanowski, J. Q., Smith, D. H. and Stewart, W. (2013a) 'Inflammation and white matter degeneration persist for years after a single traumatic brain injury', *Brain*, 136(Pt 1), pp. 28-42.
- Johnson, V. E., Stewart, W. and Smith, D. H. (2013b) 'Axonal pathology in traumatic brain injury', *Exp Neurol*, 246, pp. 35-43.
- Jones, N. C., Cardamone, L., Williams, J. P., Salzberg, M. R., Myers, D. and O'Brien, T. J. (2008) 'Experimental traumatic brain injury induces a pervasive hyperanxious phenotype in rats', *J Neurotrauma*, 25(11), pp. 1367-74.
- Jones, T. A., Hawrylak, N. and Greenough, W. T. (1996) 'Rapid laminar-dependent changes in GFAP immunoreactive astrocytes in the visual cortex of rats reared in a complex environment', *Psychoneuroendocrinology*, 21(2), pp. 189-201.
- Kabadi, S. V., Stoica, B. A., Hanscom, M., Loane, D. J., Kharebava, G., Murray Li, M. G., Cabatbat, R. M. and Faden, A. I. (2012) 'CR8, a selective and potent CDK inhibitor, provides neuroprotection in experimental traumatic brain injury', *Neurotherapeutics*, 9(2), pp. 405-21.
- Kalsi, A. S., Greenwood, K., Wilkin, G. and Butt, A. M. (2004) 'Kir4.1 expression by astrocytes and oligodendrocytes in CNS white matter: a developmental study in the rat optic nerve', *J Anat*, 204(6), pp. 475-85.
- Kamphuis, W., Middeldorp, J., Kooijman, L., Sluijs, J. A., Kooi, E. J., Moeton, M., Freriks, M., Mizee, M. R. and Hol, E. M. (2014) 'Glial fibrillary acidic protein isoform expression in plaque related astrogliosis in Alzheimer's disease', *Neurobiol Aging*, 35(3), pp. 492-510.
- Kang, J. X. (2007) 'Fat-1 transgenic mice: a new model for omega-3 research', *Prostaglandins Leukot Essent Fatty Acids*, 77(5-6), pp. 263-7.
- Kang, J. X., Wang, J., Wu, L. and Kang, Z. B. (2004) 'Transgenic mice: fat-1 mice convert n-6 to n-3 fatty acids', *Nature*, 427(6974), pp. 504.

- Karve, I. P., Taylor, J. M. and Crack, P. J. (2016) 'The contribution of astrocytes and microglia to traumatic brain injury', *Br J Pharmacol*, 173(4), pp. 692-702.
- Kawakami, M., Iwasaki, S., Sato, K. and Takahashi, M. (2000) 'Erythropoietin inhibits calcium-induced neurotransmitter release from clonal neuronal cells', *Biochem Biophys Res Commun*, 279(1), pp. 293-7.
- Kawakita, E., Hashimoto, M. and Shido, O. (2006) 'Docosahexaenoic acid promotes neurogenesis in vitro and in vivo', *Neuroscience*, 139(3), pp. 991-7.
- Kempinski, O. (2001) 'Cerebral edema', *Semin Nephrol*, 21(3), pp. 303-7.
- Kernie, S. G. and Parent, J. M. (2010) 'Forebrain neurogenesis after focal Ischemic and traumatic brain injury', *Neurobiol Dis*, 37(2), pp. 267-74.
- Kettenmann, H. and Verkhratsky, A. (2011) '[Neuroglia--living nerve glue]', *Fortschr Neurol Psychiatr*, 79(10), pp. 588-97.
- King, C., Robinson, T., Dixon, C. E., Rao, G. R., Larnard, D. and Nemoto, C. E. (2010) 'Brain temperature profiles during epidural cooling with the ChillerPad in a monkey model of traumatic brain injury', *J Neurotrauma*, 27(10), pp. 1895-903.
- King, J. T., Carlier, P. M. and Marion, D. W. (2005) 'Early Glasgow Outcome Scale scores predict long-term functional outcome in patients with severe traumatic brain injury', *J Neurotrauma*, 22(9), pp. 947-54.
- King, V. R., Huang, W. L., Dyall, S. C., Curran, O. E., Priestley, J. V. and Michael-Titus, A. T. (2006) 'Omega-3 fatty acids improve recovery, whereas omega-6 fatty acids worsen outcome, after spinal cord injury in the adult rat', *J Neurosci*, 26(17), pp. 4672-80.
- Kiso, Y. (2011) 'Pharmacology in health foods: effects of arachidonic acid and docosahexaenoic acid on the age-related decline in brain and cardiovascular system function', *J Pharmacol Sci*, 115(4), pp. 471-5.
- Knoller, N., Levi, L., Shoshan, I., Reichenthal, E., Razon, N., Rappaport, Z. H. and Biegon, A. (2002) 'Dexanabinol (HU-211) in the treatment of severe closed head injury: a randomized, placebo-controlled, phase II clinical trial', *Crit Care Med*, 30(3), pp. 548-54.
- Kotapka, M. J., Graham, D. I., Adams, J. H. and Gennarelli, T. A. (1994) 'Hippocampal pathology in fatal human head injury without high intracranial pressure', *J Neurotrauma*, 11(3), pp. 317-24.
- Krassioukov, A. V., Ackery, A., Schwartz, G., Adamchik, Y., Liu, Y. and Fehlings, M. G. (2002) 'An in vitro model of neurotrauma in organotypic spinal cord cultures from adult mice', *Brain Res Brain Res Protoc*, 10(2), pp. 60-8.
- Kuge, A., Takemura, S., Kokubo, Y., Sato, S., Goto, K. and Kayama, T. (2009) 'Temporal profile of neurogenesis in the subventricular zone, dentate gyrus and cerebral cortex following transient focal cerebral ischemia', *Neurol Res*, 31(9), pp. 969-76.
- Kumar, A., Stoica, B. A., Sabirzhanov, B., Burns, M. P., Faden, A. I. and Loane, D. J. (2013) 'Traumatic brain injury in aged animals increases lesion size and chronically alters microglial/macrophage classical and alternative activation states', *Neurobiol Aging*, 34(5), pp. 1397-411.
- Kwon, B. K., Tetzlaff, W., Grauer, J. N., Beiner, J. and Vaccaro, A. R. (2004) 'Pathophysiology and pharmacologic treatment of acute spinal cord injury', *Spine J*, 4(4), pp. 451-64.
- Lafourcade, M., Larrieu, T., Mato, S., Duffaud, A., Sepers, M., Matias, I., De Smedt-Peyrusse, V., Labrousse, V. F., Bretillon, L., Matute, C., Rodríguez-Puertas, R., Layé, S. and Manzoni, O. J. (2011) 'Nutritional omega-3 deficiency abolishes endocannabinoid-mediated neuronal functions', *Nat Neurosci*, 14(3), pp. 345-50.
- Laird, M. D., Vender, J. R. and Dhandapani, K. M. (2008) 'Opposing roles for reactive astrocytes following traumatic brain injury', *Neurosignals*, 16(2-3), pp. 154-64.
- Langham, J., Goldfrad, C., Teasdale, G., Shaw, D. and Rowan, K. (2003) 'Calcium channel blockers for acute traumatic brain injury', *Cochrane Database Syst Rev*, (4), pp. CD000565.
- Larrieu, T., Madore, C., Joffre, C. and Layé, S. (2012) 'Nutritional n-3 polyunsaturated fatty acids deficiency alters cannabinoid receptor signaling pathway in the brain and associated anxiety-like behavior in mice', *J Physiol Biochem*, 68(4), pp. 671-81.
- Lavoie, A., Ratte, S., Clas, D., Demers, J., Moore, L., Martin, M. and Bergeron, E. (2004) 'Preinjury warfarin use among elderly patients with closed head injuries in a trauma center', *J Trauma*, 56(4), pp. 802-7.

- Lawson, L. J., Perry, V. H., Dri, P. and Gordon, S. (1990) 'Heterogeneity in the distribution and morphology of microglia in the normal adult mouse brain', *Neuroscience*, 39(1), pp. 151-70.
- Lazaridis, C. and Robertson, C. S. (2016) 'Hypothermia for Increased Intracranial Pressure: Is It Dead?', *Curr Neurol Neurosci Rep*, 16(9), pp. 78.
- Lee, B. and Newberg, A. (2005) 'Neuroimaging in traumatic brain imaging', *NeuroRx*, 2(2), pp. 372-83.
- Lee, C. and Agoston, D. V. (2010) 'Vascular endothelial growth factor is involved in mediating increased de novo hippocampal neurogenesis in response to traumatic brain injury', *J Neurotrauma*, 27(3), pp. 541-53.
- Lee, J. M., Lee, H., Kang, S. and Park, W. J. (2016) 'Fatty Acid Desaturases, Polyunsaturated Fatty Acid Regulation, and Biotechnological Advances', *Nutrients*, 8(1).
- Lee, Y. K., Hou, S. W., Lee, C. C., Hsu, C. Y., Huang, Y. S. and Su, Y. C. (2013) 'Increased risk of dementia in patients with mild traumatic brain injury: a nationwide cohort study', *PLoS One*, 8(5), pp. e62422.
- Lemasters, J. J., Nieminen, A. L., Qian, T., Trost, L. C., Elmore, S. P., Nishimura, Y., Crowe, R. A., Cascio, W. E., Bradham, C. A., Brenner, D. A. and Herman, B. (1998) 'The mitochondrial permeability transition in cell death: a common mechanism in necrosis, apoptosis and autophagy', *Biochim Biophys Acta*, 1366(1-2), pp. 177-96.
- Levin, H. S. e. o. c., Shum, D. e. o. c. and Chan, R. C. K. e. o. c. (2014) *Understanding traumatic brain injury: current research and future directions*.
- Lewis, M., Ghassemi, P. and Hibbeln, J. (2013) 'Therapeutic use of omega-3 fatty acids in severe head trauma', *Am J Emerg Med*, 31(1), pp. 273.e5-8.
- Lewén, A., Fredriksson, A., Li, G. L., Olsson, Y. and Hillered, L. (1999) 'Behavioural and morphological outcome of mild cortical contusion trauma of the rat brain: influence of NMDA-receptor blockade', *Acta Neurochir (Wien)*, 141(2), pp. 193-202.
- Lewén, A., Fujimura, M., Sugawara, T., Matz, P., Copin, J. C. and Chan, P. H. (2001) 'Oxidative stress-dependent release of mitochondrial cytochrome c after traumatic brain injury', *J Cereb Blood Flow Metab*, 21(8), pp. 914-20.
- Lewén, A., Matz, P. and Chan, P. H. (2000) 'Free radical pathways in CNS injury', *J Neurotrauma*, 17(10), pp. 871-90.
- Lighthall, J. W. (1988) 'Controlled cortical impact: a new experimental brain injury model', *J Neurotrauma*, 5(1), pp. 1-15.
- Lim, G. P., Calon, F., Morihara, T., Yang, F., Teter, B., Ubeda, O., Salem, N., Frautschy, S. A. and Cole, G. M. (2005) 'A diet enriched with the omega-3 fatty acid docosahexaenoic acid reduces amyloid burden in an aged Alzheimer mouse model', *J Neurosci*, 25(12), pp. 3032-40.
- Lim, S. N., Gladman, S. J., Dyall, S. C., Patel, U., Virani, N., Kang, J. X., Priestley, J. V. and Michael-Titus, A. T. (2013a) 'Transgenic mice with high endogenous omega-3 fatty acids are protected from spinal cord injury', *Neurobiol Dis*, 51, pp. 104-12.
- Lim, S. N., Huang, W., Hall, J. C., Michael-Titus, A. T. and Priestley, J. V. (2013b) 'Improved outcome after spinal cord compression injury in mice treated with docosahexaenoic acid', *Exp Neurol*, 239, pp. 13-27.
- Lima, A., Sardinha, V. M., Oliveira, A. F., Reis, M., Mota, C., Silva, M. A., Marques, F., Cerqueira, J. J., Pinto, L., Sousa, N. and Oliveira, J. F. (2014) 'Astrocyte pathology in the prefrontal cortex impairs the cognitive function of rats', *Mol Psychiatry*, 19(7), pp. 834-41.
- Lin, M. T. and Beal, M. F. (2006) 'Mitochondrial dysfunction and oxidative stress in neurodegenerative diseases', *Nature*, 443(7113), pp. 787-95.
- Liu, Z. H., Yip, P. K., Adams, L., Davies, M., Lee, J. W., Michael, G. J., Priestley, J. V. and Michael-Titus, A. T. (2015) 'A Single Bolus of Docosahexaenoic Acid Promotes Neuroplastic Changes in the Innervation of Spinal Cord Interneurons and Motor Neurons and Improves Functional Recovery after Spinal Cord Injury', *J Neurosci*, 35(37), pp. 12733-52.
- Loane, D. J. and Byrnes, K. R. (2010) 'Role of microglia in neurotrauma', *Neurotherapeutics*, 7(4), pp. 366-77.
- Loane, D. J. and Faden, A. I. (2010) 'Neuroprotection for traumatic brain injury: translational challenges and emerging therapeutic strategies', *Trends Pharmacol Sci*, 31(12), pp. 596-604.

- Loane, D. J. and Kumar, A. (2016) 'Microglia in the TBI brain: The good, the bad, and the dysregulated', *Exp Neurol*, 275 Pt 3, pp. 316-27.
- Loane, D. J., Kumar, A., Stoica, B. A., Cabatbat, R. and Faden, A. I. (2014) 'Progressive neurodegeneration after experimental brain trauma: association with chronic microglial activation', *J Neuropathol Exp Neurol*, 73(1), pp. 14-29.
- Longhi, L., Perego, C., Ortolano, F., Aresi, S., Fumagalli, S., Zanier, E. R., Stocchetti, N. and De Si moni, M. G. (2013) 'Tumor necrosis factor in traumatic brain injury: effects of genetic deletion of p55 or p75 receptor', *J Cereb Blood Flow Metab*, 33(8), pp. 1182-9.
- Lotocki, G., de Rivero Vaccari, J., Alonso, O., Molano, J. S., Nixon, R., Dietrich, W. D. and Bramlett, H. M. (2011) 'OLIGODENDROCYTE VULNERABILITY FOLLOWING TRAUMATIC BRAIN INJURY IN RATS: EFFECT OF MODERATE HYPOTHERMIA', *Ther Hypothermia Temp Manag*, 1(1), pp. 43-51.
- Lucas, S. M., Rothwell, N. J. and Gibson, R. M. (2006) 'The role of inflammation in CNS injury and disease', *Br J Pharmacol*, 147 Suppl 1, pp. S232-40.
- Lynch, A. M., Murphy, K. J., Deighan, B. F., O'Reilly, J. A., Gun'ko, Y. K., Cowley, T. R., Gonzalez-Reyes, R. E. and Lynch, M. A. (2010) 'The impact of glial activation in the aging brain', *Aging Dis*, 1(3), pp. 262-78.
- Lyons, S. A. and Kettenmann, H. (1998) 'Oligodendrocytes and microglia are selectively vulnerable to combined hypoxia and hypoglycemia injury in vitro', *J Cereb Blood Flow Metab*, 18(5), pp. 521-30.
- Maas, A. I., Menon, D. K., Steyerberg, E. W., Citerio, G., Lecky, F., Manley, G. T., Hill, S., Legrand, V., Sorgner, A. and Investigators, C.-T. P. a. (2015) 'Collaborative European NeuroTrauma Effectiveness Research in Traumatic Brain Injury (CENTER-TBI): a prospective longitudinal observational study', *Neurosurgery*, 76(1), pp. 67-80.
- Maas, A. I., Murray, G., Henney, H., Kassem, N., Legrand, V., Mangelus, M., Muizelaar, J. P., Stocchetti, N., Knoller, N. and investigators, P. T. (2006) 'Efficacy and safety of dexamethasone in severe traumatic brain injury: results of a phase III randomised, placebo-controlled, clinical trial', *Lancet Neurol*, 5(1), pp. 38-45.
- Maas, A. I., Stocchetti, N. and Bullock, R. (2008) 'Moderate and severe traumatic brain injury in adults', *Lancet Neurol*, 7(8), pp. 728-41.
- Mahncke, H. W., Bronstone, A. and Merzenich, M. M. (2006) 'Brain plasticity and functional losses in the aged: scientific bases for a novel intervention', *Prog Brain Res*, 157, pp. 81-109.
- Maneshi, M. M., Sachs, F. and Hua, S. Z. (2015) 'A Threshold Shear Force for Calcium Influx in an Astrocyte Model of Traumatic Brain Injury', *J Neurotrauma*, 32(13), pp. 1020-9.
- Manku, M. S., Horrobin, D. F., Huang, Y. S. and Morse, N. (1983) 'Fatty acids in plasma and red cell membranes in normal humans', *Lipids*, 18(12), pp. 906-8.
- Manley, G. T., Rosenthal, G., Lam, M., Morabito, D., Yan, D., Derugin, N., Bollen, A., Knudson, M. M. and Panter, S. S. (2006) 'Controlled cortical impact in swine: pathophysiology and biomechanics', *J Neurotrauma*, 23(2), pp. 128-39.
- Mark, L. P., Prost, R. W., Ulmer, J. L., Smith, M. M., Daniels, D. L., Strottmann, J. M., Brown, W. D. and Hacein-Bey, L. (2001) 'Pictorial review of glutamate excitotoxicity: fundamental concepts for neuroimaging', *AJNR Am J Neuroradiol*, 22(10), pp. 1813-24.
- Marklund, N. and Hillered, L. (2011) 'Animal modelling of traumatic brain injury in preclinical drug development: where do we go from here?', *Br J Pharmacol*, 164(4), pp. 1207-29.
- Marmarou, A., Fatouros, P. P., Barzó, P., Portella, G., Yoshihara, M., Tsuji, O., Yamamoto, T., Laine, F., Signoretti, S., Ward, J. D., Bullock, M. R. and Young, H. F. (2000) 'Contribution of edema and cerebral blood volume to traumatic brain swelling in head-injured patients', *J Neurosurg*, 93(2), pp. 183-93.
- Marmarou, A., Signoretti, S., Fatouros, P. P., Portella, G., Aygok, G. A. and Bullock, M. R. (2006) 'Predominance of cellular edema in traumatic brain swelling in patients with severe head injuries', *J Neurosurg*, 104(5), pp. 720-30.
- Marquez de la Plata, C. D., Garces, J., Shokri Kojori, E., Grinnan, J., Krishnan, K., Pidikiti, R., Spence, J., Devous, M. D., Moore, C., McColl, R., Madden, C. and Diaz-Arrastia, R. (2011) 'Deficits in functional connectivity of hippocampal and frontal lobe circuits after traumatic axonal injury', *Arch Neurol*, 68(1), pp. 74-84.

- Martens, K. M., Vonder Haar, C., Hutsell, B. A. and Hoane, M. R. (2013) 'The dig task: a simple scent discrimination reveals deficits following frontal brain damage', *J Vis Exp*, (71).
- Mauch, D. H., Nägler, K., Schumacher, S., Göritz, C., Müller, E. C., Otto, A. and Pfrieder, F. W. (2001) 'CNS synaptogenesis promoted by glia-derived cholesterol', *Science*, 294(5545), pp. 1354-7.
- Mayer, A. R., Mannell, M. V., Ling, J., Gasparovic, C. and Yeo, R. A. (2011) 'Functional connectivity in mild traumatic brain injury', *Hum Brain Mapp*, 32(11), pp. 1825-35.
- Mayurasakorn, K., Niatsetskaya, Z. V., Sosunov, S. A., Williams, J. J., Zirpoli, H., Vlasakov, I., Deckelbaum, R. J. and Ten, V. S. (2016) 'DHA but Not EPA Emulsions Preserve Neurological and Mitochondrial Function after Brain Hypoxia-Ischemia in Neonatal Mice', *PLoS One*, 11(8), pp. e0160870.
- McGraw, J., Hiebert, G. W. and Steeves, J. D. (2001) 'Modulating astrogliosis after neurotrauma', *J Neurosci Res*, 63(2), pp. 109-15.
- McIntosh, T. K., Vink, R., Noble, L., Yamakami, I., Fernyak, S., Soares, H. and Faden, A. L. (1989) 'Traumatic brain injury in the rat: characterization of a lateral fluid-percussion model', *Neuroscience*, 28(1), pp. 233-44.
- Meyfroidt, G. and Taccone, F. S. (2015) 'Another failed attempt of neuroprotection: Progesterone for moderate and severe traumatic brain injury', *Minerva Anesthesiol.*
- Michinaga, S. and Koyama, Y. (2015) 'Pathogenesis of brain edema and investigation into anti-edema drugs', *Int J Mol Sci*, 16(5), pp. 9949-75.
- Mills, J. D., Hadley, K. and Bailes, J. E. (2011) 'Dietary supplementation with the omega-3 fatty acid docosahexaenoic acid in traumatic brain injury', *Neurosurgery*, 68(2), pp. 474-81; discussion 481.
- Miron, V. E., Boyd, A., Zhao, J. W., Yuen, T. J., Ruckh, J. M., Shadrach, J. L., van Wijngaarden, P., Wagers, A. J., Williams, A., Franklin, R. J. and ffrench-Constant, C. (2013) 'M2 microglia and macrophages drive oligodendrocyte differentiation during CNS remyelination', *Nat Neurosci*, 16(9), pp. 1211-8.
- Moon, L. D., Brecknell, J. E., Franklin, R. J., Dunnett, S. B. and Fawcett, J. W. (2000) 'Robust regeneration of CNS axons through a track depleted of CNS glia', *Exp Neurol*, 161(1), pp. 49-66.
- Moon, L. D. and Fawcett, J. W. (2001) 'Reduction in CNS scar formation without concomitant increase in axon regeneration following treatment of adult rat brain with a combination of antibodies to TGFbeta1 and beta2', *Eur J Neurosci*, 14(10), pp. 1667-77.
- Moore, S. A. (1993) 'Cerebral endothelium and astrocytes cooperate in supplying docosahexaenoic acid to neurons', *Adv Exp Med Biol*, 331, pp. 229-33.
- Morales, D. M., Marklund, N., Lebold, D., Thompson, H. J., Pitkanen, A., Maxwell, W. L., Longhi, L., Laurer, H., Maegle, M., Neugebauer, E., Graham, D. I., Stocchetti, N. and McIntosh, T. K. (2005) 'Experimental models of traumatic brain injury: do we really need to build a better mousetrap?', *Neuroscience*, 136(4), pp. 971-89.
- Moriguchi, T., Greiner, R. S. and Salem, N. (2000) 'Behavioral deficits associated with dietary induction of decreased brain docosahexaenoic acid concentration', *J Neurochem*, 75(6), pp. 2563-73.
- Moriguchi, T. and Salem, N. (2003) 'Recovery of brain docosahexaenoate leads to recovery of spatial task performance', *J Neurochem*, 87(2), pp. 297-309.
- Morishita, E., Masuda, S., Nagao, M., Yasuda, Y. and Sasaki, R. (1997) 'Erythropoietin receptor is expressed in rat hippocampal and cerebral cortical neurons, and erythropoietin prevents in vitro glutamate-induced neuronal death', *Neuroscience*, 76(1), pp. 105-16.
- Morris, R. (1984) 'Developments of a water-maze procedure for studying spatial learning in the rat', *J Neurosci Methods*, 11(1), pp. 47-60.
- Morrison, B., Saatman, K. E., Meaney, D. F. and McIntosh, T. K. (1998) 'In vitro central nervous system models of mechanically induced trauma: a review', *J Neurotrauma*, 15(11), pp. 911-28.
- Muizelaar, J. P., Marmarou, A., Young, H. F., Choi, S. C., Wolf, A., Schneider, R. L. and Kontos, H. A. (1993) 'Improving the outcome of severe head injury with the oxygen radical scavenger polyethylene glycol-conjugated superoxide dismutase: a phase II trial', *J Neurosurg*, 78(3), pp. 375-82.

- Mukherjee, P. K., Chawla, A., Loayza, M. S. and Bazan, N. G. (2007) 'Docosanoids are multifunctional regulators of neural cell integrity and fate: significance in aging and disease', *Prostaglandins Leukot Essent Fatty Acids*, 77(5-6), pp. 233-8.
- Mukherjee, P. K., Marcheselli, V. L., Serhan, C. N. and Bazan, N. G. (2004) 'Neuroprotectin D1: a docosahexaenoic acid-derived docosatriene protects human retinal pigment epithelial cells from oxidative stress', *Proc Natl Acad Sci U S A*, 101(22), pp. 8491-6.
- Murphy, M. P. (2009) 'How mitochondria produce reactive oxygen species', *Biochem J*, 417(1), pp. 1-13.
- Myer, D. J., Gurkoff, G. G., Lee, S. M., Hovda, D. A. and Sofroniew, M. V. (2006) 'Essential protective roles of reactive astrocytes in traumatic brain injury', *Brain*, 129(Pt 10), pp. 2761-72.
- Nagelhus, E. A., Mathiisen, T. M. and Ottersen, O. P. (2004) 'Aquaporin-4 in the central nervous system: cellular and subcellular distribution and coexpression with KIR4.1', *Neuroscience*, 129(4), pp. 905-13.
- Nakamura, M. T. and Nara, T. Y. (2003) 'Essential fatty acid synthesis and its regulation in mammals', *Prostaglandins Leukot Essent Fatty Acids*, 68(2), pp. 145-50.
- Narayan, R. K., Michel, M. E., Ansell, B., Baethmann, A., Biegon, A., Bracken, M. B., Bullock, M. R., Choi, S. C., Clifton, G. L., Contant, C. F., Coplin, W. M., Dietrich, W. D., Ghajar, J., Grady, S. M., Grossman, R. G., Hall, E. D., Heetderks, W., Hovda, D. A., Jallo, J., Katz, R. L., Knoller, N., Kochanek, P. M., Maas, A. I., Majde, J., Marion, D. W., Marmarou, A., Marshall, L. F., McIntosh, T. K., Miller, E., Mohberg, N., Muizelaar, J. P., Pitts, L. H., Quinn, P., Riesenfeld, G., Robertson, C. S., Strauss, K. I., Teasdale, G., Temkin, N., Tuma, R., Wade, C., Walker, M. D., Weinrich, M., Whyte, J., Wilberger, J., Young, A. B. and Yurkewicz, L. (2002) 'Clinical trials in head injury', *J Neurotrauma*, 19(5), pp. 503-57.
- Neill, A. R. and Masters, C. J. (1973) 'Metabolism of fatty acids by ovine spermatozoa', *J Reprod Fertil*, 34(2), pp. 279-87.
- Neusch, C., Rozengurt, N., Jacobs, R. E., Lester, H. A. and Kofuji, P. (2001) 'Kir4.1 potassium channel subunit is crucial for oligodendrocyte development and in vivo myelination', *J Neurosci*, 21(15), pp. 5429-38.
- Newman, L. A., Korol, D. L. and Gold, P. E. (2011) 'Lactate produced by glycogenolysis in astrocytes regulates memory processing', *PLoS One*, 6(12), pp. e28427.
- Nguyen, L. N., Ma, D., Shui, G., Wong, P., Cazenave-Gassiot, A., Zhang, X., Wenk, M. R., Goh, E. L. and Silver, D. L. (2014) 'Mfsd2a is a transporter for the essential omega-3 fatty acid docosahexaenoic acid', *Nature*, 509(7501), pp. 503-6.
- NHS (2016) *Severe head injury - Recovery*. UK: National Health Service. Available at: <http://www.nhs.uk/Conditions/Head-injury-severe-/Pages/Recovery.aspx>.
- NICE (2014) *Head injury: assessment and early management*: National Institute for Health and Care Excellence NICE Guidelines. Available at: <http://www.nice.org.uk/guidance/cg176/chapter/About-this-guideline>.
- Nichol, A., French, C., Little, L., Haddad, S., Presneill, J., Arabi, Y., Bailey, M., Cooper, D. J., Duranteau, J., Huet, O., Mak, A., McArthur, C., Pettilä, V., Skrifvars, M., Vallance, S., Varma, D., Wills, J., Bellomo, R., Investigators, E.-T. and Group, A. C. T. (2015a) 'Erythropoietin in traumatic brain injury (EPO-TBI): a double-blind randomised controlled trial', *Lancet*, 386(10012), pp. 2499-506.
- Nichol, A., French, C., Little, L., Presneill, J., Cooper, D. J., Haddad, S., Duranteau, J., Huet, O., Skrifvars, M., Arabi, Y., Bellomo, R. and Group, E.-T. I. a. t. A. a. N. Z. I. C. S. C. T. (2015b) 'Erythropoietin in traumatic brain injury: study protocol for a randomised controlled trial', *Trials*, 16, pp. 39.
- Niesman, I. R., Schilling, J. M., Shapiro, L. A., Kellerhals, S. E., Bonds, J. A., Kleschevnikov, A. M., Cui, W., Voong, A., Krajewski, S., Ali, S. S., Roth, D. M., Patel, H. H., Patel, P. M. and Head, B. P. (2014) 'Traumatic brain injury enhances neuroinflammation and lesion volume in caveolin deficient mice', *J Neuroinflammation*, 11, pp. 39.
- Nolte, C., Matyash, M., Pivneva, T., Schipke, C. G., Ohlemeyer, C., Hanisch, U. K., Kirchhoff, F. and Kettenmann, H. (2001) 'GFAP promoter-controlled EGFP-expressing transgenic mice: a tool to visualize astrocytes and astrogliosis in living brain tissue', *Glia*, 33(1), pp. 72-86.



- Norouzi Javidan, A., Sabour, H., Latifi, S., Abrishamkar, M., Soltani, Z., Shidfar, F. and Emami Razavi, H. (2014) 'Does consumption of polyunsaturated fatty acids influence on neurorehabilitation in traumatic spinal cord-injured individuals? A double-blinded clinical trial', *Spinal Cord*, 52(5), pp. 378-82.
- Nylén, K., Ost, M., Csajbok, L. Z., Nilsson, I., Blennow, K., Nellgård, B. and Rosengren, L. (2006) 'Increased serum-GFAP in patients with severe traumatic brain injury is related to outcome', *J Neurol Sci*, 240(1-2), pp. 85-91.
- O'Connor, W. T., Smyth, A. and Gilchrist, M. D. (2011) 'Animal models of traumatic brain injury: a critical evaluation', *Pharmacol Ther*, 130(2), pp. 106-13.
- Ohsawa, K., Irino, Y., Nakamura, Y., Akazawa, C., Inoue, K. and Kohsaka, S. (2007) 'Involvement of P2X4 and P2Y12 receptors in ATP-induced microglial chemotaxis', *Glia*, 55(6), pp. 604-16.
- Oleson, S., Gonzales, M. M., Tarumi, T., Davis, J. N., Cassill, C. K., Tanaka, H. and Haley, A. P. (2016) 'Nutrient intake and cerebral metabolism in healthy middle-aged adults: Implications for cognitive aging', *Nutr Neurosci*, pp. 1-8.
- Oliveira, J. F., Sardinha, V. M., Guerra-Gomes, S., Araque, A. and Sousa, N. (2015) 'Do stars govern our actions? Astrocyte involvement in rodent behavior', *Trends Neurosci*, 38(9), pp. 535-49.
- Omalu, B. I., DeKosky, S. T., Minster, R. L., Kamboh, M. I., Hamilton, R. L. and Wecht, C. H. (2005) 'Chronic traumatic encephalopathy in a National Football League player', *Neurosurgery*, 57(1), pp. 128-34; discussion 128-34.
- Onyszchuk, G., Al-Hafez, B., He, Y. Y., Bilgen, M., Berman, N. E. and Brooks, W. M. (2007) 'A mouse model of sensorimotor controlled cortical impact: characterization using longitudinal magnetic resonance imaging, behavioral assessments and histology', *J Neurosci Methods*, 160(2), pp. 187-96.
- Orr, S. K., Trépanier, M. O. and Bazinet, R. P. (2013) 'n-3 Polyunsaturated fatty acids in animal models with neuroinflammation', *Prostaglandins Leukot Essent Fatty Acids*, 88(1), pp. 97-103.
- Palacín, M., Estévez, R., Bertran, J. and Zorzano, A. (1998) 'Molecular biology of mammalian plasma membrane amino acid transporters', *Physiol Rev*, 78(4), pp. 969-1054.
- Pallier, P. N., Poddighe, L., Zbarsky, V., Kostusiak, M., Choudhury, R., Hart, T., Burguillos, M. A., Musbahi, O., Groenendijk, M., Sijben, J. W., deWilde, M. C., Quartu, M., Priestley, J. V. and Michael-Titus, A. T. (2015) 'A nutrient combination designed to enhance synapse formation and function improves outcome in experimental spinal cord injury', *Neurobiol Dis*, 82, pp. 504-15.
- Pan, Y., Larson, B., Araujo, J. A., Lau, W., de Rivera, C., Santana, R., Gore, A. and Milgram, N. W. (2010) 'Dietary supplementation with medium-chain TAG has long-lasting cognition-enhancing effects in aged dogs', *Br J Nutr*, 103(12), pp. 1746-54.
- Pangilinan (2015) **Classification and Complications of Traumatic Brain Injury** Medscape. Available at: <http://emedicine.medscape.com/article/326643-overview>.
- Paniak, C., Reynolds, S., Phillips, K., Toller-Lobe, G., Melnyk, A. and Nagy, J. (2002) 'Patient complaints within 1 month of mild traumatic brain injury: a controlled study', *Arch Clin Neuropsychol*, 17(4), pp. 319-34.
- Papa, L., Lewis, L. M., Falk, J. L., Zhang, Z., Silvestri, S., Giordano, P., Brophy, G. M., Demery, J. A., Dixit, N. K., Ferguson, I., Liu, M. C., Mo, J., Akinyi, L., Schmid, K., Mondello, S., Robertson, C. S., Tortella, F. C., Hayes, R. L. and Wang, K. K. (2012) 'Elevated levels of serum glial fibrillary acidic protein breakdown products in mild and moderate traumatic brain injury are associated with intracranial lesions and neurosurgical intervention', *Ann Emerg Med*, 59(6), pp. 471-83.
- Parekh, A. K. and Barton, M. B. (2010) 'The challenge of multiple comorbidity for the US health care system', *JAMA*, 303(13), pp. 1303-4.
- Parent, J. M. (2003) 'Injury-induced neurogenesis in the adult mammalian brain', *Neuroscientist*, 9(4), pp. 261-72.
- Parpura, V., Basarsky, T. A., Liu, F., Jęftinija, K., Jęftinija, S. and Haydon, P. G. (1994) 'Glutamate-mediated astrocyte-neuron signalling', *Nature*, 369(6483), pp. 744-7.
- Parpura, V. and Verkhratsky, A. (2012) 'Astrocytes revisited: concise historic outlook on glutamate homeostasis and signaling', *Croat Med J*, 53(6), pp. 518-28.

- Pasvogel, A. E., Miketova, P. and Moore, I. M. (2010) 'Differences in CSF phospholipid concentration by traumatic brain injury outcome', *Biol Res Nurs*, 11(4), pp. 325-31.
- Paterniti, I., Impellizzeri, D., Di Paola, R., Esposito, E., Gladman, S., Yip, P., Priestley, J. V., Michael-Titus, A. T. and Cuzzocrea, S. (2014) 'Docosahexaenoic acid attenuates the early inflammatory response following spinal cord injury in mice: in-vivo and in-vitro studies', *J Neuroinflammation*, 11, pp. 6.
- Patience, M. J., Zouikr, I., Jones, K., Clarkson, A. N., Isgaard, J., Johnson, S. J., Walker, F. R. and Nilsson, M. (2015) 'Photothrombotic stroke induces persistent ipsilateral and contralateral astrogliosis in key cognitive control nuclei', *Neurochem Res*, 40(2), pp. 362-71.
- Pekny, M. and Pekna, M. (2016) 'Reactive gliosis in the pathogenesis of CNS diseases', *Biochim Biophys Acta*, 1862(3), pp. 483-91.
- Pelinka, L. E., Kroepfl, A., Schmidhammer, R., Krenn, M., Buchinger, W., Redl, H. and Raabe, A. (2004) 'Glial fibrillary acidic protein in serum after traumatic brain injury and multiple trauma', *J Trauma*, 57(5), pp. 1006-12.
- Perea, G., Navarrete, M. and Araque, A. (2009) 'Tripartite synapses: astrocytes process and control synaptic information', *Trends Neurosci*, 32(8), pp. 421-31.
- Peterson, K., Carson, S. and Carney, N. (2008) 'Hypothermia treatment for traumatic brain injury: a systematic review and meta-analysis', *J Neurotrauma*, 25(1), pp. 62-71.
- Petravicz, J., Boyt, K. M. and McCarthy, K. D. (2014) 'Astrocyte IP3R2-dependent Ca(2+) signaling is not a major modulator of neuronal pathways governing behavior', *Front Behav Neurosci*, 8, pp. 384.
- Pettus, E. H. and Povlishock, J. T. (1996) 'Characterization of a distinct set of intra-axonal ultrastructural changes associated with traumatically induced alteration in axolemmal permeability', *Brain Res*, 722(1-2), pp. 1-11.
- Pilitsis, J. G., Coplin, W. M., O'Regan, M. H., Wellwood, J. M., Diaz, F. G., Fairfax, M. R., Michael, D. B. and Phillis, J. W. (2003a) 'Free fatty acids in cerebrospinal fluids from patients with traumatic brain injury', *Neurosci Lett*, 349(2), pp. 136-8.
- Pilitsis, J. G., Coplin, W. M., O'Regan, M. H., Wellwood, J. M., Diaz, F. G., Fairfax, M. R., Michael, D. B. and Phillis, J. W. (2003b) 'Measurement of free fatty acids in cerebrospinal fluid from patients with hemorrhagic and ischemic stroke', *Brain Res*, 985(2), pp. 198-201.
- Pleasant, J. M., Carlson, S. W., Mao, H., Scheff, S. W., Yang, K. H. and Saatman, K. E. (2011) 'Rate of neurodegeneration in the mouse controlled cortical impact model is influenced by impactor tip shape: implications for mechanistic and therapeutic studies', *J Neurotrauma*, 28(11), pp. 2245-62.
- Pohland, M., Glumm, R., Stoenica, L., Hölting, M., Kiwit, J., Ahnert-Hilger, G., Strauss, U., Bräuer, A. U., Paul, F. and Glumm, J. (2015) 'Studying Axonal Outgrowth and Regeneration of the Corticospinal Tract in Organotypic Slice Cultures', *J Neurotrauma*, 32(19), pp. 1465-77.
- Polikov, V. S., Block, M. L., Fellous, J. M., Hong, J. S. and Reichert, W. M. (2006) 'In vitro model of glial scarring around neuroelectrodes chronically implanted in the CNS', *Biomaterials*, 27(31), pp. 5368-76.
- Ponce, L. L., Navarro, J. C., Ahmed, O. and Robertson, C. S. (2013) 'Erythropoietin neuroprotection with traumatic brain injury', *Pathophysiology*, 20(1), pp. 31-8.
- Porter, J. T. and McCarthy, K. D. (1997) 'Astrocytic neurotransmitter receptors in situ and in vivo', *Prog Neurobiol*, 51(4), pp. 439-55.
- Porter, K. (2004) 'Ketamine in prehospital care', *Emerg Med J*, 21(3), pp. 351-4.
- Povlishock, J. T. (1992) 'Traumatically induced axonal injury: pathogenesis and pathobiological implications', *Brain Pathol*, 2(1), pp. 1-12.
- Prins, M., Greco, T., Alexander, D. and Giza, C. C. (2013) 'The pathophysiology of traumatic brain injury at a glance', *Dis Model Mech*, 6(6), pp. 1307-15.
- Prut, L. and Belzung, C. (2003) 'The open field as a paradigm to measure the effects of drugs on anxiety-like behaviors: a review', *Eur J Pharmacol*, 463(1-3), pp. 3-33.
- Pu, H., Jiang, X., Hu, X., Xia, J., Hong, D., Zhang, W., Gao, Y., Chen, J. and Shi, Y. (2016) 'Delayed Docosahexaenoic Acid Treatment Combined with Dietary Supplementation of Omega-3 Fatty

- Acids Promotes Long-Term Neurovascular Restoration After Ischemic Stroke', *Transl Stroke Res*.
- Pun, P. B., Lu, J. and Mochhala, S. (2009) 'Involvement of ROS in BBB dysfunction', *Free Radic Res*, 43(4), pp. 348-64.
- Pusceddu, M. M., Kelly, P., Stanton, C., Cryan, J. F. and Dinan, T. G. (2016) 'N-3 Polyunsaturated Fatty Acids Through the Lifespan: Implication for Psychopathology', *Int J Neuropsychopharmacol*.
- Raghupathi, R., Graham, D. I. and McIntosh, T. K. (2000) 'Apoptosis after traumatic brain injury', *J Neurotrauma*, 17(10), pp. 927-38.
- Ramon y Cajal, S. (1928) *Degeneration and Regeneration of the nervous system*. [S.l.]: OUP.
- Rapoport, M., McCauley, S., Levin, H., Song, J. and Feinstein, A. (2002) 'The role of injury severity in neurobehavioral outcome 3 months after traumatic brain injury', *Neuropsychiatry Neuropsychol Behav Neurol*, 15(2), pp. 123-32.
- Rapoport, M., Wolf, U., Herrmann, N., Kiss, A., Shammi, P., Reis, M., Phillips, A. and Feinstein, A. (2008) 'Traumatic brain injury, Apolipoprotein E-epsilon4, and cognition in older adults: a two-year longitudinal study', *J Neuropsychiatry Clin Neurosci*, 20(1), pp. 68-73.
- Rapoport, S. I. (1999) 'In vivo fatty acid incorporation into brain phospholipids in relation to signal transduction and membrane remodeling', *Neurochem Res*, 24(11), pp. 1403-15.
- Rapoport, S. I. (2001) 'In vivo fatty acid incorporation into brain phospholipids in relation to plasma availability, signal transduction and membrane remodeling', *J Mol Neurosci*, 16(2-3), pp. 243-61; discussion 279-84.
- Rapoport, S. I., Rao, J. S. and Igarashi, M. (2007) 'Brain metabolism of nutritionally essential polyunsaturated fatty acids depends on both the diet and the liver', *Prostaglandins Leukot Essent Fatty Acids*, 77(5-6), pp. 251-61.
- Reifschneider, K., Auble, B. A. and Rose, S. R. (2015) 'Update of Endocrine Dysfunction following Pediatric Traumatic Brain Injury', *J Clin Med*, 4(8), pp. 1536-60.
- Reilly and Bullock (1997) *Head Injury. Physiology and Management of Severe Closed Injury*. London: Chapman and Hall Medical.
- Robertson, C. S., Hannay, H. J., Yamal, J. M., Gopinath, S., Goodman, J. C., Tilley, B. C., Baldwin, A., Rivera Lara, L., Saucedo-Crespo, H., Ahmed, O., Sadasivan, S., Ponce, L., Cruz-Navarro, J., Shahin, H., Aisiku, I. P., Doshi, P., Valadka, A., Neipert, L., Waguspack, J. M., Rubin, M. L., Benoit, J. S., Swank, P. and Investigators, E. S. T. T. (2014) 'Effect of erythropoietin and transfusion threshold on neurological recovery after traumatic brain injury: a randomized clinical trial', *JAMA*, 312(1), pp. 36-47.
- Robinson, M. B. and Jackson, J. G. (2016) 'Astroglial glutamate transporters coordinate excitatory signaling and brain energetics', *Neurochem Int*, 98, pp. 56-71.
- Robson, L. G., Dyllal, S., Sidloff, D. and Michael-Titus, A. T. (2010) 'Omega-3 polyunsaturated fatty acids increase the neurite outgrowth of rat sensory neurones throughout development and in aged animals', *Neurobiol Aging*, 31(4), pp. 678-87.
- Rodriguez de Turco, E. B., Belayev, L., Liu, Y., Busto, R., Parkins, N., Bazan, N. G. and Ginsberg, M. D. (2002) 'Systemic fatty acid responses to transient focal cerebral ischemia: influence of neuroprotectant therapy with human albumin', *J Neurochem*, 83(3), pp. 515-24.
- Romine, J., Gao, X. and Chen, J. (2014) 'Controlled cortical impact model for traumatic brain injury', *J Vis Exp*, (90), pp. e51781.
- Romner, B. and Grände, P. O. (2013) 'Traumatic brain injury: Intracranial pressure monitoring in traumatic brain injury', *Nat Rev Neurol*, 9(4), pp. 185-6.
- Roof, R. L., Duvdevani, R., Heyburn, J. W. and Stein, D. G. (1996) 'Progesterone rapidly decreases brain edema: treatment delayed up to 24 hours is still effective', *Exp Neurol*, 138(2), pp. 246-51.
- Roof, R. L., Duvdevani, R. and Stein, D. G. (1993) 'Gender influences outcome of brain injury: progesterone plays a protective role', *Brain Res*, 607(1-2), pp. 333-6.
- Roof, R. L., Hoffman, S. W. and Stein, D. G. (1997) 'Progesterone protects against lipid peroxidation following traumatic brain injury in rats', *Mol Chem Neuropathol*, 31(1), pp. 1-11.
- Roozenbeek, B., Maas, A. I. and Menon, D. K. (2013) 'Changing patterns in the epidemiology of traumatic brain injury', *Nat Rev Neurol*, 9(4), pp. 231-6.

- Rosenzweig, E. S. and Barnes, C. A. (2003) 'Impact of aging on hippocampal function: plasticity, network dynamics, and cognition', *Prog Neurobiol*, 69(3), pp. 143-79.
- Rothstein, J. D., Martin, L., Levey, A. I., Dykes-Hoberg, M., Jin, L., Wu, D., Nash, N. and Kuncl, R. W. (1994) 'Localization of neuronal and glial glutamate transporters', *Neuron*, 13(3), pp. 713-25.
- Roux, A., Muller, L., Jackson, S. N., Post, J., Baldwin, K., Hoffer, B., Balaban, C. D., Barbacci, D., Schultz, J. A., Gouty, S., Cox, B. M. and Woods, A. S. (2016) 'Mass spectrometry imaging of rat brain lipid profile changes over time following traumatic brain injury', *J Neurosci Methods*.
- Rowland, J. W., Hawryluk, G. W., Kwon, B. and Fehlings, M. G. (2008) 'Current status of acute spinal cord injury pathophysiology and emerging therapies: promise on the horizon', *Neurosurg Focus*, 25(5), pp. E2.
- Royo, N. C., Conte, V., Saatman, K. E., Shimizu, S., Belfield, C. M., Soltesz, K. M., Davis, J. E., Fujimoto, S. T. and McIntosh, T. K. (2006) 'Hippocampal vulnerability following traumatic brain injury: a potential role for neurotrophin-4/5 in pyramidal cell neuroprotection', *Eur J Neurosci*, 23(5), pp. 1089-102.
- Saatman, K. E., Feeko, K. J., Pape, R. L. and Raghupathi, R. (2006) 'Differential behavioral and histopathological responses to graded cortical impact injury in mice', *J Neurotrauma*, 23(8), pp. 1241-53.
- Sahuquillo, J. and Vilalta, A. (2007) 'Cooling the injured brain: how does moderate hypothermia influence the pathophysiology of traumatic brain injury', *Curr Pharm Des*, 13(22), pp. 2310-22.
- Sanderson, D. J., Good, M. A., Skelton, K., Sprengel, R., Seeburg, P. H., Rawlins, J. N. and Bannerman, D. M. (2009) 'Enhanced long-term and impaired short-term spatial memory in GluA1 AMPA receptor subunit knockout mice: evidence for a dual-process memory model', *Learn Mem*, 16(6), pp. 379-86.
- Sanderson, D. J., Gray, A., Simon, A., Taylor, A. M., Deacon, R. M., Seeburg, P. H., Sprengel, R., Good, M. A., Rawlins, J. N. and Bannerman, D. M. (2007) 'Deletion of glutamate receptor-A (GluR-A) AMPA receptor subunits impairs one-trial spatial memory', *Behav Neurosci*, 121(3), pp. 559-69.
- Sanderson, D. J., McHugh, S. B., Good, M. A., Sprengel, R., Seeburg, P. H., Rawlins, J. N. and Bannerman, D. M. (2010) 'Spatial working memory deficits in GluA1 AMPA receptor subunit knockout mice reflect impaired short-term habituation: evidence for Wagner's dual-process memory model', *Neuropsychologia*, 48(8), pp. 2303-15.
- Sandhir, R., Onyszchuk, G. and Berman, N. E. (2008) 'Exacerbated glial response in the aged mouse hippocampus following controlled cortical impact injury', *Exp Neurol*, 213(2), pp. 372-80.
- Sarnyai, Z., Sibille, E. L., Pavlides, C., Fenster, R. J., McEwen, B. S. and Toth, M. (2000) 'Impaired hippocampal-dependent learning and functional abnormalities in the hippocampus in mice lacking serotonin(1A) receptors', *Proc Natl Acad Sci U S A*, 97(26), pp. 14731-6.
- Satz, P., Zaucha, K., Forney, D. L., McCleary, C., Asarnow, R. F., Light, R., Levin, H., Kelly, D., Bergsneider, M., Hovda, D., Martin, N., Caron, M. J., Namerow, N. and Becker, D. (1998) 'Neuropsychological, psychosocial and vocational correlates of the Glasgow Outcome Scale at 6 months post-injury: a study of moderate to severe traumatic brain injury patients', *Brain Inj*, 12(7), pp. 555-67.
- Schaar, K. L., Brenneman, M. M. and Savitz, S. I. (2010) 'Functional assessments in the rodent stroke model', *Exp Transl Stroke Med*, 2(1), pp. 13.
- Scherbel, U., Raghupathi, R., Nakamura, M., Saatman, K. E., Trojanowski, J. Q., Neugebauer, E., Marino, M. W. and McIntosh, T. K. (1999) 'Differential acute and chronic responses of tumor necrosis factor-deficient mice to experimental brain injury', *Proc Natl Acad Sci U S A*, 96(15), pp. 8721-6.
- Schober, M. E., Requena, D. F., Block, B., Davis, L. J., Rodesch, C., Casper, T. C., Juul, S. E., Kesner, R. P. and Lane, R. H. (2014) 'Erythropoietin improved cognitive function and decreased hippocampal caspase activity in rat pups after traumatic brain injury', *J Neurotrauma*, 31(4), pp. 358-69.
- Schreibelt, G., Kooij, G., Reijkerk, A., van Doorn, R., Gringhuis, S. I., van der Pol, S., Weksler, B. B., Romero, I. A., Couraud, P. O., Piontek, J., Blasig, I. E., Dijkstra, C. D., Ronken, E. and de Vries, H. E. (2007) 'Reactive oxygen species alter brain endothelial tight junction dynamics via RhoA, PI3 kinase, and PKB signaling', *FASEB J*, 21(13), pp. 3666-76.

- Schumacher, M., Denier, C., Oudinet, J. P., Adams, D. and Guennoun, R. (2015) 'Progesterone neuroprotection: The background of clinical trial failure', *J Steroid Biochem Mol Biol*.
- Schwulst, S. J., Trahanas, D. M., Saber, R. and Perlman, H. (2013) 'Traumatic brain injury-induced alterations in peripheral immunity', *J Trauma Acute Care Surg*, 75(5), pp. 780-8.
- Schöfeld, P. and Reiser, G. (2013) 'Why does brain metabolism not favor burning of fatty acids to provide energy? Reflections on disadvantages of the use of free fatty acids as fuel for brain', *J Cereb Blood Flow Metab*, 33(10), pp. 1493-9.
- Serhan, C. N. and Chiang, N. (2008) 'Endogenous pro-resolving and anti-inflammatory lipid mediators: a new pharmacologic genus', *Br J Pharmacol*, 153 Suppl 1, pp. S200-15.
- Sharp, D. J., Scott, G. and Leech, R. (2014) 'Network dysfunction after traumatic brain injury', *Nat Rev Neurol*, 10(3), pp. 156-66.
- Shear, D. A., Galani, R., Hoffman, S. W. and Stein, D. G. (2002) 'Progesterone protects against necrotic damage and behavioral abnormalities caused by traumatic brain injury', *Exp Neurol*, 178(1), pp. 59-67.
- Shi, Z., Ren, H., Luo, C., Yao, X., Li, P., He, C., Kang, J. X., Wan, J. B., Yuan, T. F. and Su, H. (2015) 'Enriched Endogenous Omega-3 Polyunsaturated Fatty Acids Protect Cortical Neurons from Experimental Ischemic Injury', *Mol Neurobiol*.
- Si, D., Yang, P., Jiang, R., Zhou, H., Wang, H. and Zhang, Y. (2014) 'Improved cognitive outcome after progesterone administration is associated with protecting hippocampal neurons from secondary damage studied in vitro and in vivo', *Behav Brain Res*, 264, pp. 135-42.
- Siedler, D. G., Chuah, M. I., Kirkcaldie, M. T., Vickers, J. C. and King, A. E. (2014) 'Diffuse axonal injury in brain trauma: insights from alterations in neurofilaments', *Front Cell Neurosci*, 8, pp. 429.
- Sieg, F., Wahle, P. and Pape, H. C. (1999) 'Cellular reactivity to mechanical axonal injury in an organotypic in vitro model of neurotrauma', *J Neurotrauma*, 16(12), pp. 1197-213.
- Sierra-Mercado, D., McAllister, L. M., Lee, C. C., Milad, M. R., Eskandar, E. N. and Whalen, M. J. (2015) 'Controlled cortical impact before or after fear conditioning does not affect fear extinction in mice', *Brain Res*, 1606, pp. 133-41.
- Silver, B. V. and Yablon, S. A. (1996) 'Akathisia resulting from traumatic brain injury', *Brain Inj*, 10(8), pp. 609-14.
- Silver, J. and Miller, J. H. (2004) 'Regeneration beyond the glial scar', *Nat Rev Neurosci*, 5(2), pp. 146-56.
- Simopoulos, A. P. (2006) 'Evolutionary aspects of diet, the omega-6/omega-3 ratio and genetic variation: nutritional implications for chronic diseases', *Biomed Pharmacother*, 60(9), pp. 502-7.
- Simopoulos, A. P. (2011) 'Evolutionary aspects of diet: the omega-6/omega-3 ratio and the brain', *Mol Neurobiol*, 44(2), pp. 203-15.
- Singh, A. V., Raymond, M., Pace, F., Certo, A., Zuidema, J. M., McKay, C. A., Gilbert, R. J., Lu, X. L. and Wan, L. Q. (2015) 'Astrocytes increase ATP exocytosis mediated calcium signaling in response to microgroove structures', *Sci Rep*, 5, pp. 7847.
- Singh, R., Kanwar, S. S., Sood, P. K. and Nehru, B. (2011) 'Beneficial effects of folic acid on enhancement of memory and antioxidant status in aged rat brain', *Cell Mol Neurobiol*, 31(1), pp. 83-91.
- Singleton, R. H. and Povlishock, J. T. (2004) 'Identification and characterization of heterogeneous neuronal injury and death in regions of diffuse brain injury: evidence for multiple independent injury phenotypes', *J Neurosci*, 24(14), pp. 3543-53.
- Skolnick, B. E., Maas, A. I., Narayan, R. K., van der Hoop, R. G., MacAllister, T., Ward, J. D., Nelson, N. R., Stocchetti, N. and Investigators, S. T. (2014) 'A clinical trial of progesterone for severe traumatic brain injury', *N Engl J Med*, 371(26), pp. 2467-76.
- Smith, D. H., Okiyama, K., Thomas, M. J., Claussen, B. and McIntosh, T. K. (1991) 'Evaluation of memory dysfunction following experimental brain injury using the Morris water maze', *J Neurotrauma*, 8(4), pp. 259-69.
- Smith, D. H., Soares, H. D., Pierce, J. S., Perlman, K. G., Saatman, K. E., Meaney, D. F., Dixon, C. E. and McIntosh, T. K. (1995) 'A model of parasagittal controlled cortical impact in the mouse: cognitive and histopathologic effects', *J Neurotrauma*, 12(2), pp. 169-78.

- Sofroniew, M. V. (2009) 'Molecular dissection of reactive astrogliosis and glial scar formation', *Trends Neurosci*, 32(12), pp. 638-47.
- Sofroniew, M. V. (2014) 'Multiple roles for astrocytes as effectors of cytokines and inflammatory mediators', *Neuroscientist*, 20(2), pp. 160-72.
- Sofroniew, M. V. (2015) 'Astrocyte barriers to neurotoxic inflammation', *Nat Rev Neurosci*, 16(5), pp. 249-63.
- Sofroniew, M. V. and Vinters, H. V. (2010) 'Astrocytes: biology and pathology', *Acta Neuropathol*, 119(1), pp. 7-35.
- Stangl, D. and Thuret, S. (2009) 'Impact of diet on adult hippocampal neurogenesis', *Genes Nutr*, 4(4), pp. 271-82.
- Starkov, A. A. (2008) 'The role of mitochondria in reactive oxygen species metabolism and signaling', *Ann N Y Acad Sci*, 1147, pp. 37-52.
- Statler, K. D., Alexander, H., Vagni, V., Dixon, C. E., Clark, R. S., Jenkins, L. and Kochanek, P. M. (2006) 'Comparison of seven anesthetic agents on outcome after experimental traumatic brain injury in adult, male rats', *J Neurotrauma*, 23(1), pp. 97-108.
- Stein, D. G. (2011) 'Is progesterone a worthy candidate as a novel therapy for traumatic brain injury?', *Dialogues Clin Neurosci*, 13(3), pp. 352-9.
- Stein, D. G. (2015) 'Embracing failure: What the Phase III progesterone studies can teach about TBI clinical trials', *Brain Inj*, 29(11), pp. 1259-72.
- Stein, S. C., Chen, X. H., Sinson, G. P. and Smith, D. H. (2002) 'Intravascular coagulation: a major secondary insult in nonfatal traumatic brain injury', *J Neurosurg*, 97(6), pp. 1373-7.
- Stellwagen, D. and Malenka, R. C. (2006) 'Synaptic scaling mediated by glial TNF- $\alpha$ ', *Nature*, 440(7087), pp. 1054-9.
- Stillwell, W., Shaikh, S. R., Zerouga, M., Siddiqui, R. and Wassall, S. R. (2005) 'Docosahexaenoic acid affects cell signaling by altering lipid rafts', *Reprod Nutr Dev*, 45(5), pp. 559-79.
- Stillwell, W. and Wassall, S. R. (2003) 'Docosahexaenoic acid: membrane properties of a unique fatty acid', *Chem Phys Lipids*, 126(1), pp. 1-27.
- Stocchetti, N., Paternò, R., Citerio, G., Beretta, L. and Colombo, A. (2012) 'Traumatic brain injury in an aging population', *J Neurotrauma*, 29(6), pp. 1119-25.
- Stocchetti, N. and Zanier, E. R. (2016) 'Chronic impact of traumatic brain injury on outcome and quality of life: a narrative review', *Crit Care*, 20(1), pp. 148.
- Stoica, B. A. and Faden, A. I. (2010) 'Cell death mechanisms and modulation in traumatic brain injury', *Neurotherapeutics*, 7(1), pp. 3-12.
- Strike, S. C., Carlisle, A., Gibson, E. L. and Dyal, S. C. (2016) 'A High Omega-3 Fatty Acid Multinutrient Supplement Benefits Cognition and Mobility in Older Women: A Randomized, Double-blind, Placebo-controlled Pilot Study', *J Gerontol A Biol Sci Med Sci*, 71(2), pp. 236-42.
- Su, E. J., Fredriksson, L., Kanzawa, M., Moore, S., Folestad, E., Stevenson, T. K., Nilsson, I., Sashindranath, M., Schielke, G. P., Warnock, M., Ragsdale, M., Mann, K., Lawrence, A. L., Medcalf, R. L., Eriksson, U., Murphy, G. G. and Lawrence, D. A. (2015) 'Imatinib treatment reduces brain injury in a murine model of traumatic brain injury', *Front Cell Neurosci*, 9, pp. 385.
- Su, H. M. (2010) 'Mechanisms of n-3 fatty acid-mediated development and maintenance of learning memory performance', *J Nutr Biochem*, 21(5), pp. 364-73.
- Sullivan, S., Friess, S. H., Ralston, J., Smith, C., Propert, K. J., Rapp, P. E. and Margulies, S. S. (2013) 'Improved behavior, motor, and cognition assessments in neonatal piglets', *J Neurotrauma*, 30(20), pp. 1770-9.
- Sun, D. (2014) 'The potential of endogenous neurogenesis for brain repair and regeneration following traumatic brain injury', *Neural Regen Res*, 9(7), pp. 688-92.
- Sun, D., Bullock, M. R., Altememi, N., Zhou, Z., Hagoood, S., Rolfe, A., McGinn, M. J., Hamm, R. and Colello, R. J. (2010) 'The effect of epidermal growth factor in the injured brain after trauma in rats', *J Neurotrauma*, 27(5), pp. 923-38.
- Sun, D., Bullock, M. R., McGinn, M. J., Zhou, Z., Altememi, N., Hagoood, S., Hamm, R. and Colello, R. J. (2009) 'Basic fibroblast growth factor-enhanced neurogenesis contributes to cognitive recovery in rats following traumatic brain injury', *Exp Neurol*, 216(1), pp. 56-65.

- Susarla, B. T., Villapol, S., Yi, J. H., Geller, H. M. and Symes, A. J. (2014) 'Temporal patterns of cortical proliferation of glial cell populations after traumatic brain injury in mice', *ASN Neuro*, 6(3), pp. 159-70.
- Taha, A. Y., Jeffrey, M. A., Taha, N. M., Bala, S. and Burnham, W. M. (2010) 'Acute administration of docosahexaenoic acid increases resistance to pentylentetrazol-induced seizures in rats', *Epilepsy Behav*, 17(3), pp. 336-43.
- Takatsuru, Y., Eto, K., Kaneko, R., Masuda, H., Shimokawa, N., Koibuchi, N. and Nabekura, J. (2013) 'Critical role of the astrocyte for functional remodeling in contralateral hemisphere of somatosensory cortex after stroke', *J Neurosci*, 33(11), pp. 4683-92.
- Talving, P., Lustenberger, T., Kobayashi, L., Inaba, K., Barmparas, G., Schnüriger, B., Lam, L., Chan, L. S. and Demetriades, D. (2010) 'Erythropoiesis stimulating agent administration improves survival after severe traumatic brain injury: a matched case control study', *Ann Surg*, 251(1), pp. 1-4.
- Tambuyzer, B. R., Ponsaerts, P. and Nouwen, E. J. (2009) 'Microglia: gatekeepers of central nervous system immunology', *J Leukoc Biol*, 85(3), pp. 352-70.
- Tan, A. A., Quigley, A., Smith, D. C. and Hoane, M. R. (2009) 'Strain differences in response to traumatic brain injury in Long-Evans compared to Sprague-Dawley rats', *J Neurotrauma*, 26(4), pp. 539-48.
- Tanabe, Y., Hashimoto, M., Sugioka, K., Maruyama, M., Fujii, Y., Hagiwara, R., Hara, T., Hossain, S. M. and Shido, O. (2004) 'Improvement of spatial cognition with dietary docosahexaenoic acid is associated with an increase in Fos expression in rat CA1 hippocampus', *Clin Exp Pharmacol Physiol*, 31(10), pp. 700-3.
- Tanaka, K., Watase, K., Manabe, T., Yamada, K., Watanabe, M., Takahashi, K., Iwama, H., Nishikawa, T., Ichihara, N., Kikuchi, T., Okuyama, S., Kawashima, N., Hori, S., Takimoto, M. and Wada, K. (1997) 'Epilepsy and exacerbation of brain injury in mice lacking the glutamate transporter GLT-1', *Science*, 276(5319), pp. 1699-702.
- Tang-Schomer, M. D., Patel, A. R., Baas, P. W. and Smith, D. H. (2010) 'Mechanical breaking of microtubules in axons during dynamic stretch injury underlies delayed elasticity, microtubule disassembly, and axon degeneration', *FASEBJ*, 24(5), pp. 1401-10.
- Tassoni, D., Kaur, G., Weisinger, R. S. and Sinclair, A. J. (2008) 'The role of eicosanoids in the brain', *Asia Pac J Clin Nutr*, 17 Suppl 1, pp. 220-8.
- Tecoma, E. S., Monyer, H., Goldberg, M. P. and Choi, D. W. (1989) 'Traumatic neuronal injury in vitro is attenuated by NMDA antagonists', *Neuron*, 2(6), pp. 1541-5.
- Thompson, H. J., Lifshitz, J., Marklund, N., Grady, M. S., Graham, D. I., Hovda, D. A. and McIntosh, T. K. (2005) 'Lateral fluid percussion brain injury: a 15-year review and evaluation', *J Neurotrauma*, 22(1), pp. 42-75.
- Thompson, H. J., McCormick, W. C. and Kagan, S. H. (2006) 'Traumatic brain injury in older adults: epidemiology, outcomes, and future implications', *J Am Geriatr Soc*, 54(10), pp. 1590-5.
- Tinoco, J. (1982) 'Dietary requirements and functions of alpha-linolenic acid in animals', *Prog Lipid Res*, 21(1), pp. 1-45.
- Towart, R. and Kazda, S. (1979) 'The cellular mechanism of action of nimodipine (BAY e 9736), a new calcium antagonist [proceedings]', *Br J Pharmacol*, 67(3), pp. 409P-410P.
- Tran, H. T., LaFerla, F. M., Holtzman, D. M. and Brody, D. L. (2011) 'Controlled cortical impact traumatic brain injury in 3xTg-AD mice causes acute intra-axonal amyloid- $\beta$  accumulation and independently accelerates the development of tau abnormalities', *J Neurosci*, 31(26), pp. 9513-25.
- Tremoleda, J. L., Thau-Zuchman, O., Davies, M., Foster, J., Khan, I., Vadivelu, K. C., Yip, P. K., Sosabowski, J., Trigg, W. and Michael-Titus, A. T. (2016) 'In vivo PET imaging of the neuroinflammatory response in rat spinal cord injury using the TSPO tracer [(18)F]GE-180 and effect of docosahexaenoic acid', *Eur J Nucl Med Mol Imaging*, 43(9), pp. 1710-22.
- Trépanier, M. O., Kwong, K. M., Domenichiello, A. F., Chen, C. T., Bazinet, R. P. and Burnham, W. M. (2015) 'Intravenous infusion of docosahexaenoic acid increases serum concentrations in a dose-dependent manner and increases seizure latency in the maximal PTZ model', *Epilepsy Behav*, 50, pp. 71-6.

- Trépanier, M. O., Taha, A. Y., Mantha, R. L., Ciobanu, F. A., Zeng, Q. H., Tchkhartichvili, G. M., Domenichiello, A. F., Bazinet, R. P. and Burnham, W. M. (2012) 'Increases in seizure latencies induced by subcutaneous docosahexaenoic acid are lost at higher doses', *Epilepsy Res*, 99(3), pp. 225-32.
- Tucker, L. B., Burke, J. F., Fu, A. H. and McCabe, J. T. (2016) 'Neuropsychiatric Symptom Modeling in Male and Female C57BL/6J Mice after Experimental Traumatic Brain Injury', *J Neurotrauma*.
- Türeyen, K., Vemuganti, R., Sailor, K. A., Bowen, K. K. and Dempsey, R. J. (2004) 'Transient focal cerebral ischemia-induced neurogenesis in the dentate gyrus of the adult mouse', *J Neurosurg*, 101(5), pp. 799-805.
- Underhill, S. M. and Goldberg, M. P. (2007) 'Hypoxic injury of isolated axons is independent of ionotropic glutamate receptors', *Neurobiol Dis*, 25(2), pp. 284-90.
- Unterberg, A. W., Stover, J., Kress, B. and Kiening, K. L. (2004) 'Edema and brain trauma', *Neuroscience*, 129(4), pp. 1021-9.
- Vajda, F. J. (2002) 'Neuroprotection and neurodegenerative disease', *J Clin Neurosci*, 9(1), pp. 4-8.
- van Bruggen, N., Thibodeaux, H., Palmer, J. T., Lee, W. P., Fu, L., Cairns, B., Tumas, D., Gerlai, R., Williams, S. P., van Lookeren Campagne, M. and Ferrara, N. (1999) 'VEGF antagonism reduces edema formation and tissue damage after ischemia/reperfusion injury in the mouse brain', *J Clin Invest*, 104(11), pp. 1613-20.
- van Landeghem, F. K., Weiss, T., Oehmichen, M. and von Deimling, A. (2006) 'Decreased expression of glutamate transporters in astrocytes after human traumatic brain injury', *J Neurotrauma*, 23(10), pp. 1518-28.
- Vandromme, M., Melton, S. M. and Kerby, J. D. (2008) 'Progesterone in traumatic brain injury: time to move on to phase III trials', *Crit Care*, 12(3), pp. 153.
- Vergouwen, M. D., Vermeulen, M. and Roos, Y. B. (2006) 'Effect of nimodipine on outcome in patients with traumatic subarachnoid haemorrhage: a systematic review', *Lancet Neurol*, 5(12), pp. 1029-32.
- Verweij, B. H., Muizelaar, J. P., Vinas, F. C., Peterson, P. L., Xiong, Y. and Lee, C. P. (2000) 'Improvement in mitochondrial dysfunction as a new surrogate efficiency measure for preclinical trials: dose-response and time-window profiles for administration of the calcium channel blocker Ziconotide in experimental brain injury', *J Neurosurg*, 93(5), pp. 829-34.
- von Oettingen, G., Bergholt, B., Gyldensted, C. and Astrup, J. (2002) 'Blood flow and ischemia within traumatic cerebral contusions', *Neurosurgery*, 50(4), pp. 781-8; discussion 788-90.
- Vorhees, C. V. and Williams, M. T. (2006) 'Morris water maze: procedures for assessing spatial and related forms of learning and memory', *Nat Protoc*, 1(2), pp. 848-58.
- Vos, P. E., Jacobs, B., Andriessen, T. M., Lamers, K. J., Borm, G. F., Beems, T., Edwards, M., Rosmalen, C. F. and Vissers, J. L. (2010) 'GFAP and S100B are biomarkers of traumatic brain injury: an observational cohort study', *Neurology*, 75(20), pp. 1786-93.
- Wakai, A., Roberts, I. and Schierhout, G. (2007) 'Mannitol for acute traumatic brain injury', *Cochrane Database Syst Rev*, (1), pp. CD001049.
- Wake, H., Moorhouse, A. J., Miyamoto, A. and Nabekura, J. (2013) 'Microglia: actively surveying and shaping neuronal circuit structure and function', *Trends Neurosci*, 36(4), pp. 209-17.
- Walcott, B. P., Kahle, K. T. and Simard, J. M. (2012) 'Novel treatment targets for cerebral edema', *Neurotherapeutics*, 9(1), pp. 65-72.
- Walker, K. R. and Tesco, G. (2013) 'Molecular mechanisms of cognitive dysfunction following traumatic brain injury', *Front Aging Neurosci*, 5, pp. 29.
- Wang, D. D. and Bordey, A. (2008) 'The astrocyte odyssey', *Prog Neurobiol*, 86(4), pp. 342-67.
- Wang, F., Franco, R., Skotak, M., Hu, G. and Chandra, N. (2014a) 'Mechanical stretch exacerbates the cell death in SH-SY5Y cells exposed to paraquat: mitochondrial dysfunction and oxidative stress', *Neurotoxicology*, 41, pp. 54-63.
- Wang, G., Zhang, J., Hu, X., Zhang, L., Mao, L., Jiang, X., Liou, A. K., Leak, R. K., Gao, Y. and Chen, J. (2013) 'Microglia/macrophage polarization dynamics in white matter after traumatic brain injury', *J Cereb Blood Flow Metab*, 33(12), pp. 1864-74.



- Wang, J., Shi, Y., Zhang, L., Zhang, F., Hu, X., Zhang, W., Leak, R. K., Gao, Y., Chen, L. and Chen, J. (2014b) 'Omega-3 polyunsaturated fatty acids enhance cerebral angiogenesis and provide long-term protection after stroke', *Neurobiol Dis*, 68, pp. 91-103.
- Wang, M., Kong, Q., Gonzalez, F. A., Sun, G., Erb, L., Seye, C. and Weisman, G. A. (2005) 'P2Y nucleotide receptor interaction with alpha integrin mediates astrocyte migration', *J Neurochem*, 95(3), pp. 630-40.
- Wang, Y., Wang, N., Cai, B., Wang, G. Y., Li, J. and Piao, X. X. (2015) 'In vitro model of the blood-brain barrier established by co-culture of primary cerebral microvascular endothelial and astrocyte cells', *Neural Regen Res*, 10(12), pp. 2011-7.
- Wanner, I. B., Deik, A., Torres, M., Rosendahl, A., Neary, J. T., Lemmon, V. P. and Bixby, J. L. (2008) 'A new in vitro model of the glial scar inhibits axon growth', *Glia*, 56(15), pp. 1691-709.
- Ward, R. E., Huang, W., Curran, O. E., Priestley, J. V. and Michael-Titus, A. T. (2010) 'Docosahexaenoic acid prevents white matter damage after spinal cord injury', *J Neurotrauma*, 27(10), pp. 1769-80.
- Washington, P. M., Forcelli, P. A., Wilkins, T., Zapple, D. N., Parsadanian, M. and Burns, M. P. (2012) 'The effect of injury severity on behavior: a phenotypic study of cognitive and emotional deficits after mild, moderate, and severe controlled cortical impact injury in mice', *J Neurotrauma*, 29(13), pp. 2283-96.
- Watase, K., Hashimoto, K., Kano, M., Yamada, K., Watanabe, M., Inoue, Y., Okuyama, S., Sakagawa, T., Ogawa, S., Kawashima, N., Hori, S., Takimoto, M., Wada, K. and Tanaka, K. (1998) 'Motor discoordination and increased susceptibility to cerebellar injury in GLAST mutant mice', *Eur J Neurosci*, 10(3), pp. 976-88.
- Watkins, P. A. (2008) 'Very-long-chain acyl-CoA synthetases', *J Biol Chem*, 283(4), pp. 1773-7.
- Wellner, N., Tsuboi, K., Madsen, A. N., Holst, B., Diep, T. A., Nakao, M., Tokumura, A., Burns, M. P., Deutsch, D. G., Ueda, N. and Hansen, H. S. (2011) 'Studies on the anorectic effect of N-acylphosphatidylethanolamine and phosphatidylethanolamine in mice', *Biochim Biophys Acta*, 1811(9), pp. 508-12.
- Werner, C. and Engelhard, K. (2007) 'Pathophysiology of traumatic brain injury', *Br J Anaesth*, 99(1), pp. 4-9.
- Whalen, M. J., Clark, R. S., Dixon, C. E., Robichaud, P., Marion, D. W., Vagni, V., Graham, S. H., Virag, L., Hasko, G., Stachlewitz, R., Szabo, C. and Kochanek, P. M. (1999) 'Reduction of cognitive and motor deficits after traumatic brain injury in mice deficient in poly(ADP-ribose) polymerase', *J Cereb Blood Flow Metab*, 19(8), pp. 835-42.
- WHO (2006) *Neurological disorders: public health challenges*, Switzerland.
- Williams, J. J., Mayurasakorn, K., Vannucci, S. J., Mastropietro, C., Bazan, N. G., Ten, V. S. and Deckelbaum, R. J. (2013) 'N-3 fatty acid rich triglyceride emulsions are neuroprotective after cerebral hypoxic-ischemic injury in neonatal mice', *PLoS One*, 8(2), pp. e56233.
- Wolfer, D. P., Stagljar-Bozicevic, M., Errington, M. L. and Lipp, H. P. (1998) 'Spatial Memory and Learning in Transgenic Mice: Fact or Artifact?', *News Physiol Sci*, 13, pp. 118-123.
- Woo, S. J., Lim, K., Park, S. Y., Jung, M. Y., Lim, H. S., Jeon, M. G., Lee, S. I. and Park, B. H. (2015) 'Endogenous conversion of n-6 to n-3 polyunsaturated fatty acids attenuates K/BxN serum-transfer arthritis in fat-1 mice', *J Nutr Biochem*, 26(7), pp. 713-20.
- Woodcock, T. and Morganti-Kossmann, M. C. (2013) 'The role of markers of inflammation in traumatic brain injury', *Front Neurol*, 4, pp. 18.
- Wright, D. W., Kellermann, A. L., Hertzberg, V. S., Clark, P. L., Frankel, M., Goldstein, F. C., Salomone, J. P., Dent, L. L., Harris, O. A., Ander, D. S., Lowery, D. W., Patel, M. M., Denson, D. D., Gordon, A. B., Wald, M. M., Gupta, S., Hoffman, S. W. and Stein, D. G. (2007) 'ProTECT: a randomized clinical trial of progesterone for acute traumatic brain injury', *Ann Emerg Med*, 49(4), pp. 391-402, 402.e1-2.
- Wright, D. W., Yeatts, S. D., Silbergleit, R., Palesch, Y. Y., Hertzberg, V. S., Frankel, M., Goldstein, F. C., Caveney, A. F., Howlett-Smith, H., Bengelink, E. M., Manley, G. T., Merck, L. H., Janis, L. S., Barsan, W. G. and Investigators, N. (2014) 'Very early administration of progesterone for acute traumatic brain injury', *N Engl J Med*, 371(26), pp. 2457-66.

- Wright, R. L. and Conrad, C. D. (2005) 'Chronic stress leaves novelty-seeking behavior intact while impairing spatial recognition memory in the Y-maze', *Stress*, 8(2), pp. 151-4.
- Wu, A., Ying, Z. and Gomez-Pinilla, F. (2008) 'Docosahexaenoic acid dietary supplementation enhances the effects of exercise on synaptic plasticity and cognition', *Neuroscience*, 155(3), pp. 751-9.
- Wu, A., Ying, Z. and Gomez-Pinilla, F. (2011) 'The salutary effects of DHA dietary supplementation on cognition, neuroplasticity, and membrane homeostasis after brain trauma', *J Neurotrauma*, 28(10), pp. 2113-22.
- Wu, K., Gao, X., Shi, B., Chen, S., Zhou, X., Li, Z., Gan, Y., Cui, L., Kang, J. X., Li, W. and Huang, R. (2016a) 'Enriched endogenous n-3 polyunsaturated fatty acids alleviate cognitive and behavioral deficits in a mice model of Alzheimer's disease', *Neuroscience*, 333, pp. 345-55.
- Wu, L., Sun, H. L., Gao, Y., Hui, K. L., Xu, M. M., Zhong, H. and Duan, M. L. (2016b) 'Therapeutic Hypothermia Enhances Cold-Inducible RNA-Binding Protein Expression and Inhibits Mitochondrial Apoptosis in a Rat Model of Cardiac Arrest', *Mol Neurobiol*.
- Wu, X., Liu, Y., Chen, X., Sun, Q., Tang, R., Wang, W., Yu, Z. and Xie, M. (2013) 'Involvement of TREK-1 activity in astrocyte function and neuroprotection under simulated ischemia conditions', *J Mol Neurosci*, 49(3), pp. 499-506.
- Wu, Y., Shang, Y., Sun, S. and Liu, R. (2007) 'Antioxidant effect of erythropoietin on 1-methyl-4-phenylpyridinium-induced neurotoxicity in PC12 cells', *Eur J Pharmacol*, 564(1-3), pp. 47-56.
- Xiao, G., Wei, J., Yan, W., Wang, W. and Lu, Z. (2008) 'Improved outcomes from the administration of progesterone for patients with acute severe traumatic brain injury: a randomized controlled trial', *Crit Care*, 12(2), pp. R61.
- Xiong, Y., Mahmood, A. and Chopp, M. (2009) 'Emerging treatments for traumatic brain injury', *Expert Opin Emerg Drugs*, 14(1), pp. 67-84.
- Xiong, Y., Mahmood, A. and Chopp, M. (2013) 'Animal models of traumatic brain injury', *Nat Rev Neurosci*, 14(2), pp. 128-42.
- Xiong, Y., Mahmood, A., Lu, D., Qu, C., Kazmi, H., Goussev, A., Zhang, Z. G., Noguchi, C. T., Schallert, T. and Chopp, M. (2008) 'Histological and functional outcomes after traumatic brain injury in mice null for the erythropoietin receptor in the central nervous system', *Brain Res*, 1230, pp. 247-57.
- Xu, J., Wang, H., Ding, K., Zhang, L., Wang, C., Li, T., Wei, W. and Lu, X. (2014a) 'Luteolin provides neuroprotection in models of traumatic brain injury via the Nrf2-ARE pathway', *Free Radic Biol Med*, 71, pp. 186-95.
- Xu, S., Jay, A., Brunaldi, K., Huang, N. and Hamilton, J. A. (2013) 'CD36 enhances fatty acid uptake by increasing the rate of intracellular esterification but not transport across the plasma membrane', *Biochemistry*, 52(41), pp. 7254-61.
- Xu, T., Fan, X., Tan, Y., Yue, Y., Chen, W. and Gu, X. (2014b) 'Expression of PHB2 in rat brain cortex following traumatic brain injury', *Int J Mol Sci*, 15(2), pp. 3299-318.
- Xuan, W., Vatanserver, F., Huang, L. and Hamblin, M. R. (2014) 'Transcranial low-level laser therapy enhances learning, memory, and neuroprogenitor cells after traumatic brain injury in mice', *J Biomed Opt*, 19(10), pp. 108003.
- Yakovlev, A. G. and Faden, A. I. (2001) 'Caspase-dependent apoptotic pathways in CNS injury', *Mol Neurobiol*, 24(1-3), pp. 131-44.
- Yang, L. Y., Huang, C. C., Chiu, W. T., Huang, L. T., Lo, W. C. and Wang, J. Y. (2016) 'Association of traumatic brain injury in childhood and attention-deficit/hyperactivity disorder: a population-based study', *Pediatr Res*, 80(3), pp. 356-62.
- Yang, Y., Vidensky, S., Jin, L., Jie, C., Lorenzini, I., Frankl, M. and Rothstein, J. D. (2011) 'Molecular comparison of GLT1+ and ALDH1L1+ astrocytes in vivo in astroglial reporter mice', *Glia*, 59(2), pp. 200-7.
- Yang, Z. and Wang, K. K. (2015) 'Glial fibrillary acidic protein: from intermediate filament assembly and gliosis to neurobiomarker', *Trends Neurosci*, 38(6), pp. 364-74.
- Yehuda, S., Rabinovitz, S., Carasso, R. L. and Mostofsky, D. I. (2002) 'The role of polyunsaturated fatty acids in restoring the aging neuronal membrane', *Neurobiol Aging*, 23(5), pp. 843-53.
- Yehuda, S., Rabinovitz, S. and Mostofsky, D. I. (2005) 'Essential fatty acids and the brain: from infancy to aging', *Neurobiol Aging*, 26 Suppl 1, pp. 98-102.

- Yi, J. H. and Hazell, A. S. (2006) 'Excitotoxic mechanisms and the role of astrocytic glutamate transporters in traumatic brain injury', *Neurochem Int*, 48(5), pp. 394-403.
- Yin, X., Yu, X. W., Zhu, P., Zhang, Y. M., Zhang, X. H., Wang, F., Zhang, J. J., Yan, W., Xi, Y., Wan, J. B., Kang, J. X., Zou, Z. Q. and Bu, S. Z. (2016) 'Endogenously synthesized n-3 fatty acids in fat-1 transgenic mice prevent melanoma progression by increasing E-cadherin expression and inhibiting  $\beta$ -catenin signaling', *Mol Med Rep*, 14(4), pp. 3476-84.
- Yong, V. W., Moumdjian, R., Yong, F. P., Ruijs, T. C., Freedman, M. S., Cashman, N. and Antel, J. P. (1991) 'Gamma-interferon promotes proliferation of adult human astrocytes in vitro and reactive gliosis in the adult mouse brain in vivo', *Proc Natl Acad Sci U S A*, 88(16), pp. 7016-20.
- You, S. W., Chen, B. Y., Liu, H. L., Lang, B., Xia, J. L., Jiao, X. Y. and Ju, G. (2003) 'Spontaneous recovery of locomotion induced by remaining fibers after spinal cord transection in adult rats', *Restor Neurol Neurosci*, 21(1-2), pp. 39-45.
- Young, B., Runge, J. W., Waxman, K. S., Harrington, T., Wilberger, J., Muizelaar, J. P., Boddy, A. and Kupiec, J. W. (1996) 'Effects of pegargotein on neurologic outcome of patients with severe head injury. A multicenter, randomized controlled trial', *JAMA*, 276(7), pp. 538-43.
- Yu, F., Wang, Z., Tchantchou, F., Chiu, C. T., Zhang, Y. and Chuang, D. M. (2012) 'Lithium ameliorates neurodegeneration, suppresses neuroinflammation, and improves behavioral performance in a mouse model of traumatic brain injury', *J Neurotrauma*, 29(2), pp. 362-74.
- Yue, J. K., Vassar, M. J., Lingsma, H. F., Cooper, S. R., Okonkwo, D. O., Valadka, A. B., Gordon, W. A., Maas, A. I., Mukherjee, P., Yuh, E. L., Puccio, A. M., Schnyer, D. M., Manley, G. T. and Investigators, T.-T. (2013) 'Transforming research and clinical knowledge in traumatic brain injury pilot: multicenter implementation of the common data elements for traumatic brain injury', *J Neurotrauma*, 30(22), pp. 1831-44.
- Zaben, M., El Ghouli, W. and Belli, A. (2013) 'Post-traumatic head injury pituitary dysfunction', *Disabil Rehabil*, 35(6), pp. 522-5.
- Zendedel, A., Habib, P., Dang, J., Lammerding, L., Hoffmann, S., Beyer, C. and Slowik, A. (2015) 'Omega-3 polyunsaturated fatty acids ameliorate neuroinflammation and mitigate ischemic stroke damage through interactions with astrocytes and microglia', *J Neuroimmunol*, 278, pp. 200-11.
- Zetterberg, H., Smith, D. H. and Blennow, K. (2013) 'Biomarkers of mild traumatic brain injury in cerebrospinal fluid and blood', *Nat Rev Neurol*, 9(4), pp. 201-10.
- Zhang, B. F., Wang, J., Liu, Z. W., Zhao, Y. L., Li, D. D., Huang, T. Q., Gu, H. and Song, J. N. (2015) 'Meta-analysis of the efficacy and safety of therapeutic hypothermia in children with acute traumatic brain injury', *World Neurosurg*, 83(4), pp. 567-73.
- Zhang, L., Liu, J., Cheng, C., Yuan, Y., Yu, B., Shen, A. and Yan, M. (2012) 'The neuroprotective effect of pyrroloquinoline quinone on traumatic brain injury', *J Neurotrauma*, 29(5), pp. 851-64.
- Zhao, S., Yu, Z., Zhao, G., Xing, C., Hayakawa, K., Whalen, M. J., Lok, J. M., Lo, E. H. and Wang, X. (2012a) 'Neuroglobin-overexpression reduces traumatic brain lesion size in mice', *BMC Neurosci*, 13, pp. 67.
- Zhao, Y., Calon, F., Julien, C., Winkler, J. W., Petasis, N. A., Lukiw, W. J. and Bazan, N. G. (2011) 'Docosahexaenoic acid-derived neuroprotectin D1 induces neuronal survival via secretase- and PPAR $\gamma$ -mediated mechanisms in Alzheimer's disease models', *PLoS One*, 6(1), pp. e15816.
- Zhao, Z., Loane, D. J., Murray, M. G., Stoica, B. A. and Faden, A. I. (2012b) 'Comparing the predictive value of multiple cognitive, affective, and motor tasks after rodent traumatic brain injury', *J Neurotrauma*, 29(15), pp. 2475-89.
- Zlokovic, B. V. (2008) 'The blood-brain barrier in health and chronic neurodegenerative disorders', *Neuron*, 57(2), pp. 178-201.
- Zweckberger, K., Hackenberg, K., Jung, C. S., Hertle, D. N., Kiening, K. L., Unterberg, A. W. and Sakowitz, O. W. (2014) 'Glibenclamide reduces secondary brain damage after experimental traumatic brain injury', *Neuroscience*, 272, pp. 199-206.
- Şovrea, A. S. and Boşca, A. B. (2013) 'Astrocytes reassessment - an evolving concept part one: embryology, biology, morphology and reactivity', *J Mol Psychiatry*, 1, pp. 18.